

FROM THE EDITOR

Lots of new this year

*Thomas Kohnen, MD, PhD, FEBO
Frankfurt, Germany*

*Nick Mamalis, MD
Salt Lake City, Utah, USA*

*William J. Dupps Jr, MD, PhD
Cleveland, Ohio, USA*

*Sathish Srinivasan, FRCSEd, FRCOph, FACS
Ayr, Scotland, UK*

This New Year brings several exciting developments to the *Journal of Cataract & Refractive Surgery*, starting with this issue. As of January 1, 2020, Wolters Kluwer, a leading global provider of information and point-of-care solutions for the healthcare industry, is the new publisher of *JCRS*. We are excited about the technical support Wolters Kluwer provides, as well as their commitment to rigorous academic publishing and serious analytics. We agree with American Society of Cataract and Refractive Surgery Executive Director Steve Speares, who said, "In collaborating with Wolters Kluwer, *JCRS* has an opportunity to amplify the scientific exchange of innovative research and breakthrough findings, enhancing surgical outcomes and ultimately improving patient care."

The journal will also have two editor transitions in 2020. Dr. Nick Mamalis, current president of the American Society of Cataract and Refractive Surgery, will be stepping down from the Editorial Board in May 2020. Dr. Mamalis has contributed greatly to the growth and development of the journal, having served as Associate Editor of *JCRS* from 2001 to 2006 and as Editor of *JCRS* since 2007, and will be certainly missed. Taking over as U.S. Editor will be current Associate Editor Dr. W.J. Dupps, Jr. Dr. Dupps is Professor of Ophthalmology and Biomedical Engineering at Cleveland Clinic Lerner College of Medicine, Case Western Reserve University, and is a refractive, corneal, and cataract surgeon at the Cole Eye Institute in Cleveland, Ohio. In addition, the Editorial Board is excited to welcome Liliana Werner, MD, PhD, from the John A. Moran Eye Center at the University of Utah in the role of U.S. Associate Editor. Dr. Werner is an outstanding laboratory scientist who specializes in pathology, intraocular lens materials, and accommodating mechanisms.

The aim of *JCRS* is to publish manuscripts of a guaranteed high academic and scientific standard of broad international relevance to the field of cataract and refractive surgery. Our accepted manuscripts will advance the science in the field by challenging and/or improving current and emerging techniques and practices and adding to the general knowledge of cataract and refractive surgery. Maintaining this high standard would not be possible without the peer-review system and the dedication and expertise of our peer reviewers. In an effort to show the value we put on our academic peer reviewers, we are

pleased to announce that together with our new publisher, Wolters Kluwer, *JCRS* will be joining the Publons community. Similar to ORCID, Publons gives peer reviewers the opportunity to track their peer reviews and research impact. *JCRS* is continually building its peer reviewer database. If you are interested in contributing to the journal as a peer reviewer, please express your interest at jcrs@ascrs.org.

We look forward to the continued involvement from you, our readers and authors. From submitted articles to letters to the editor and case reports, together we are exploring, building, and developing the field of cataract and refractive surgery. All of us from the Editorial Board wish you a prosperous New Year!



Thomas Kohnen, MD, PhD, FEBO
*Department of Ophthalmology, Goethe
University, Frankfurt am Main, Germany*



Nick Mamalis, MD
*Department of Ophthalmology and Visual
Sciences, John A. Moran Eye Center,
University of Utah, Salt Lake City, USA*



William J. Dupps Jr, MD, PhD
*Cole Eye Institute, Cleveland Clinic,
Cleveland, Ohio, USA*



Sathish Srinivasan, FRCSEd, FRCOph,
FACS
University Hospital Ayr, Ayr, Scotland, UK

Assessment of the accuracy of new and updated intraocular lens power calculation formulas in 10 930 eyes from the UK National Health Service

Kieren Darcy, BM, MRCS(Eng), CertLRS, FRCOphth, David Gunn, MBBS (Hons I), FRANZCO, Shokufeh Tavassoli, MBBS, FRCOphth, John Sparrow, DPhil, FRCS, FRCOphth, Jack X. Kane, MBBS

Purpose: To compare the accuracy of new/updated methods of intraocular lens (IOL) power calculation (Kane, Hill-RBF 2.0, and Holladay 2 with new axial length adjustment) with that of established methods (Barrett Universal II, Olsen, Haigis, Holladay 1, Hoffer Q, and SRK/T).

Setting: Bristol Eye Hospital, University Hospitals Bristol National Health Service, Foundation Trust, Bristol, UK.

Design: Retrospective consecutive case series.

Methods: Data from patients having uneventful cataract surgery with the insertion of 1 of 4 IOL types were included. Optimized IOL constants were used to calculate the predicted refraction of each formula for each patient. This was compared with the actual refractive outcome to give the prediction error. A subgroup analysis occurred based on the axial length and IOL type.

Results: The study included 10 930 eyes of 10 930 patients with the Kane formula having the lowest mean absolute prediction error (MAE), which was statistically significant ($P < .001$ in all cases) followed by the Hill 2.0, Olsen, Holladay 2, Barrett Universal 2, Holladay 1, SRK/T, Haigis, and Hoffer Q formula. The percentage of eyes predicted within ± 0.5 D was Kane, 72%; Hill 2.0, 71.2%; Olsen, 70.6%; Holladay 2, 71%; Barrett 2, 70.7%; SRK/T, 69.1%; Haigis, 69%; and Hoffer Q, 68.1%. The Kane formula had the lowest MAE for short, medium, and long axial length subgroups and for each IOL type assessed. The updated versions of the Holladay 2 and Hill 2.0 formulas have resulted in improved accuracy.

Conclusions: Overall and in each axial length subgroup, the Kane formula was more accurate than the other formulas.

J Cataract Refract Surg 2020; 46:2–7 Copyright © 2019 Published by Wolters Kluwer on behalf of ASCRS and ESCRS

Refractive accuracy is 1 of the key tenets of successful cataract surgery, with improvements in surgical technique¹ and in preoperative measurements² contributing to increasing accuracy.

Modern intraocular lens (IOL) power formulas have also contributed to the increase in accuracy. The differences in the derivation method and metrics used are summarized in Table 1. Although the Holladay 2 formula (the first “newer generation” formula) was not the most accurate in large cohort studies,^{3–5} there has been progress. The Barrett Universal 2 (Barrett) and the Olsen⁶ formulas are more accurate than both older generation formulas and the Holladay 2 formula.^{3,4} The recently developed Hill-RBF formula (version 1.0) was found to be less accurate than the Barrett and the best-performing third-generation formulas in the only large-scale study to date.⁷

Further attempts to improve the accuracy of some of these modern IOL formulas have been implemented with version 2.0 of the Hill-RBF formula (hereafter “Hill 2.0”) based on a size-increased database. Similarly, a new axial length (AL) adjustment has been incorporated into the Holladay 2 formula⁸ (Holladay 2-AL adjusted). The Kane formula^A is based on theoretical optics and incorporates both regression and artificial intelligence components to further refine its predictions. The formula was developed using approximately 30 000 cases from selected refractive cataract practices and then using high-performance cloud-based computing to create its algorithm. The Kane formula requires the AL, keratometry, anterior chamber depth, and sex to make its predictions. The addition of IOL thickness and central corneal thickness significantly improves the accuracy of the formula; however, it is optional.

Submitted: February 26, 2019 | Final revision submitted: June 26, 2019 | Accepted: August 7, 2019

From the Bristol Eye Hospital, University Hospitals Bristol NHS, Foundation Trust (Darcy, Gunn, Tavassoli, Sparrow), Bristol, United Kingdom; and Department of Ophthalmology, Alfred Health (Kane), Melbourne, Australia.

Corresponding author: Kieren Darcy, BM, MRCS(Eng), CertLRS, FRCOphth, Bristol Eye Hospital, Lower Maudlin St, Bristol BS1 2LX, UK. Email: kierendarcy@me.com.

Table 1. Summary of intraocular lens formulas.

Formula	First Publication	Metrics Used	Derivation Method
SRK/T	1990	AL, K	Theoretical
Hoffer Q	1993	AL, K	Theoretical
Haigis	1993	AL, K, ACD	Theoretical
Barrett 1	1993	AL, K, ACD	Theoretical
Holliday 1	1998	AL, K	Theoretical
Olsen	2007	AL, K, ACD, LT†, CCT†	Ray tracing
Barrett 2	2016	AL, K, ACD, LT†, WTW†	Theoretical
Hill-RBF 1.0	2016	AL, K, ACD	Regression/artificial intelligence
Hill-RBF 2.0	2018	AL, K, ACD, WTW, LT, CCT	Regression/artificial intelligence
Holliday 2	2018 current version	AL, K, ACD, LT, WTW, age, PR†	Theoretical
Kane	2018	AL, K, ACD, sex, LT†, CCT†	Theoretical/artificial intelligence

ACD = anterior chamber depth; AL = axial length; CCT = central corneal thickness; K = keratometry; LT = lens thickness; PR = preoperative refraction; WTW = white to white

† optional

The aim of the current study was to assess the accuracy of these new/updated IOL formulas in a large population to determine which is the best overall predictor of the actual postoperative refractive outcome. A subgroup analysis will also examine each AL subgroup and differing IOL types.

METHODS

A retrospective chart review was conducted on all cataract surgeries performed from May 2008 until November 2017 at 2 National Health Service trusts in the United Kingdom. Institutional review board approval was granted. Inclusion criteria were uneventful phacoemulsification cataract surgery with the insertion of 1 of the following 4 different IOL types: SA60AT (Alcon Laboratories, Inc.), Superflex Aspheric 920H, C-Flex Aspheric 970C (Rayner Intraocular Lenses Limited Akreos Adapt AO (Bausch & Lomb, Inc.), and preoperative biometry performed using partial coherence interferometry (IOLMaster; Carl Zeiss Meditec AG). Exclusion criteria were incomplete biometry using the IOLMaster, corneal astigmatism greater than 4.0 D, other corneal disease, previous vitrectomy, complicated cataract surgery, postoperative corrected distance visual acuity worse than 20/40, or postoperative complications.

All data including preoperative biometry data were collected from the electronic medical record (Medisoft; Medisoft Limited). If patients underwent bilateral phacoemulsification cataract extraction, then a randomly selected eye was chosen for inclusion in the study.

Subjective manifest refraction was performed preoperatively and postoperatively by hospital or community optometrists. Only eyes with formal refractions were included in the study. No details of crystalline lens thickness, central corneal thickness, or white-to-white measurements were used.

The Hoffer Q,⁹ Holladay 1,⁹ Haigis,¹¹ and SRK/T¹² formulas were calculated using already validated⁴ Excel spreadsheets (Microsoft Corporation) according to their original publications and errata. The Kane formula was calculated by author J.X.K. The Holladay 2-AL adjusted formula was calculated using the Holladay IOL consultant software,^B and the Olsen formula was calculated with the PhacoOptics software. The Hill 2.0^C and the Barrett^D formulas were calculated through their respective websites.

The constant for each of the formulas was optimized either within the spreadsheets or through trialing different constants for the black box formulas until the mean prediction error was zero. The Haigis formula underwent single optimization using ULIB-optimized (User Group for Laser Interference Biometry) constants for a1 and a2, as suggested by Melles et al.⁵

Some calculators limit the entry of IOL constants to only 2 decimal places, which makes it impossible to achieve a mean error of exactly zero. In these cases, the mean error was reduced to as small a value as possible by constant optimization. The mean error was then fully “zeroed” by adjusting the refractive prediction error for each eye by an amount equal to the overall mean prediction error for that formula as described by Wang et al.¹³ The prediction error was calculated as the actual postoperative refraction minus the formula-predicted refractive result.

The mean numerical prediction error, mean absolute prediction error (MAE), median absolute prediction error (MedAE), and standard deviation of prediction error (STDEV) were calculated for each formula. The percentages of eyes that had a prediction error of ± 0.25 diopter (D), ± 0.50 D, and ± 1.00 D were calculated for each formula. The subgroup analysis was performed based on the AL for short ($AL \leq 22.0$ mm), medium ($22.0 \text{ mm} < AL < 26.0$ mm), and long ($AL \geq 26.0$ mm) eyes and based on the IOL type. The mean rank score was calculated for each subgroup analysis as recommended by Cooke et al.³

The differences in the absolute error between formulas were assessed using the Friedman test, and in the event of a significant result, post hoc analysis was undertaken using the Wilcoxon test with Bonferroni correction, as suggested by Aristodemou et al.¹⁴ A *P* value less than .05 was considered statistically significant. Statistical analysis was performed in R (R Project; R Foundation).

RESULTS

A total of 13 351 eyes having uneventful cataract surgery, with the insertion of 1 of 4 IOL types and a postoperative corrected distance visual acuity of at least 20/40, were included in the study. Excluded from the initial database were 219 eyes with corneal pathology, 44 eyes with previous vitrectomy, 6 eyes with previous laser corrective surgery, and 89 eyes with anterior corneal astigmatism of greater than 4.0 D; 12 993 eyes remained. After randomly excluding 1 eye of patients who had both eyes eligible for inclusion, 10 930 eyes remained. The demographics are shown in Table 2. The optimized IOL constants used are shown in Table 3. The Friedman test on the absolute prediction error of each formula revealed a significant difference between formulas ($P < .001$), with post hoc analysis showing a significant difference between the Kane formula and all other formulas ($P < .001$ for all). Newer

Table 2. Demographics of patients.

Demographics	Mean (SD)
Female sex	58.08%
Age	75.33 (9.72)
AL	23.65 (1.34)
Average keratometry	43.79 (1.51)
Anterior chamber depth	3.07 (0.42)
IOL power	20.76 (3.72)
IOL subgroups, n (%)	
SA60AT	6516 (59.6)
B+L Akreos Adapt AO	721 (6.6)
Rayner C-Flex 970C	3067 (28.1)
Rayner Superflex 920H	626 (5.7)
AL subgroup, n (%)	
Short (≤ 22.0 mm)	766 (7.0)
Medium ($22 < AL < 26.0$ mm)	9527 (87.2)
Long (≥ 26.0 mm)	637 (5.8)

AL = axial length; IOL = intraocular lens

generation formulas (Hill 2.0, Olsen, Holladay 2-AL adjusted, and Barrett) had lower MAE compared with third-generation formulas (all $P < .05$). The Kane formula also had the lowest MedAE, STDEV, and highest percentage of eyes within 0.25 D, 0.50 D, and 1.00 D (Table 4).

Significant Results by Axial Length

The MAE for each AL subgroup is shown in Table 5. For short eyes, the Kane formula had the lowest MAE compared with all other formulas ($P < .01$). The Holladay 2-AL adjusted, Olsen, Holladay 1, and Hill 2.0 formulas were more accurate than the Barrett, SRK/T, and Haigis formulas (all $P < .05$). No significant difference existed between the Holladay 2-AL adjusted, Olsen, Holladay 1, Hill 2.0, and Hoffer Q formula. In medium eyes, the Kane formula had the lowest MAE compared with all other formulas ($P < .001$). The Hill 2.0 and Olsen formulas were more accurate than the third-generation formulas and the Haigis formula (all $P < .05$). There was no significant difference between the Barrett and Olsen formulas ($P = .28$) nor between the Barrett, Holladay 2-AL adjusted, and Holladay 1 formulas. In long AL eyes, the Kane formula had the lowest MAE compared with all other formulas ($P < .05$ compared with Barrett and $P < .001$ compared with all others). The

Barrett formula had a lower MAE compared with the remainder of the formulas ($P < .05$). The Hill, Olsen, and Holladay 2-AL adjusted formulas were more accurate than the Holladay 1 and Hoffer Q formulas ($P < .01$).

Significant Results by Intraocular Lens Type

Figure 1 shows the MAE of each formula for each IOL type. The Kane formula was more accurate compared with all other formulas for the SA60AT IOL ($P < .001$), CFlex IOL ($P < .001$), and Akreos Adapt IOL ($P < .05$) and more accurate than all formulas ($P < .01$) except the Barrett ($P = .4$) and Hill 2.0 ($P = .06$) formulas for the SuperFlex IOL. For the SA60AT IOL, the Hill 2.0, Olsen, Barrett, and Holladay 2-AL adjusted formulas performed better than the third-generation formulas (all $P < .01$). For the CFlex IOL, the Olsen, Hill 2.0, and Holladay 1 formulas performed better than the Haigis, Barrett, and SRK/T formulas (all $P < .05$). For the SuperFlex IOL, the Kane and Barrett formulas were more accurate than all formulas ($P < .01$), except for the Hill 2.0 formula. The Hill 2.0 formula was not more accurate compared with the Holladay 2-AL adjusted ($P = .31$) or the Olsen ($P = .11$) formula but was more accurate than the remainder of formulas ($P < .01$). For the Akreos Adapt IOL, the Hill, Olsen, Holladay 2-AL adjusted, and Barrett formulas were more accurate than the SRK/T formula ($P < .05$) but not more accurate than the Hoffer Q, Holladay 1, or Haigis formula.

DISCUSSION

To our knowledge, this is the first study to assess the Kane, Hill 2.0, and Holladay 2-AL adjusted formulas. In our cohort, the Kane formula was found to be the most accurate. It also had the lowest MAE, standard deviation of error, median absolute error, and highest percentage of eyes within 0.25 D, 0.50 D, and 1.00 D. In the short, medium, and long AL subgroups, the Kane formula had the lowest MAE, which was statistically significant compared with all other formulas ($P < .01$). For each IOL subgroup studied, the Kane formula had the lowest MAE, which was statistically significant compared with all other formulas, except in the SuperFlex IOL group, in which the Kane formula had the lowest MAE, which was statistically significant compared with all formulas except the Barrett and the Hill 2.0 formulas. No

Table 3. Optimized IOL constants.

Formula	Constant	SA60AT	Adapt AO	C-Flex	Superflex
Olsen	ACDConst	4.53	4.53	4.31	4.15
Barrett	SF	1.72	1.78	1.74	1.62
Hill 2.0	A-Constant	118.67	118.73	118.70	118.64
Holladay 2	ACD	5.31	5.362	5.33	5.19
Kane	A-Constant	118.71	118.82	118.73	118.52
Holladay 1	SF	1.65	1.73	1.66	1.67
Hoffer Q	pACD	5.42	5.51	5.41	5.64
SRK/T	A-Constant	118.73	118.85	118.79	118.47
Haigis	a0 (a1, a2)*	-0.137 (0.249, 0.179)	-0.517 (0.305, 0.191)	1.257 (0.4, 0.1)	1.375 (0.4, 0.1)

ACDConst = anterior chamber depth constant; IOL = intraocular lens; pACD = personalized ACD; SF = surgeon factor

*Haigis values for a1 and a2 are from the ULIB website.

Table 4. Overall outcomes for each formula sorted by the mean absolute error.

Formula	MAE	MedAE	ME	STDEV	Percentage of Eyes within PE		
					±0.25	±0.50	±1.00
Kane	0.377	0.302	0.000	0.490	42.6	72.0	95.2
Hill	0.387	0.310	0.000	0.501	41.4	71.2	94.9
Olsen	0.388	0.309	0.000	0.501	41.4	70.6	94.9
Holladay 2	0.390	0.312	0.000	0.503	41.2	71.0	94.9
Barrett	0.390	0.314	0.000	0.505	41.7	70.7	94.7
Holladay 1	0.397	0.321	0.000	0.512	40.2	69.6	94.4
SRK/T	0.403	0.323	0.000	0.522	39.9	69.1	93.9
Haigis	0.405	0.327	0.000	0.521	39.9	69.0	94.3
Hoffer Q	0.410	0.332	0.000	0.527	39.0	68.1	94.0

MAE = mean absolute prediction error; ME = mean error; MedAE = median absolute prediction error; PE = prediction error; STDEV = standard deviation of the error

published study on the Kane formula exists to compare our results.

Multiple studies³⁻⁵ have shown the Barrett Universal 2 formula is more accurate than the third-generation and Haigis formulas, which was confirmed in this study. The Holladay 2 formula has recently updated its AL adjustment method.⁵ Before its adjustment, the Holladay 2 formula was found to be less accurate than the Barrett formula before its new adjustment.^{3,4,7} In our cohort, the Holladay 2-AL adjusted formula had a similar MAE, a lower STDEV, and higher percentages of eyes within 0.50 D and 1.00 D than the Barrett formula, indicating improvement of the formula.

The Hill 2.0 formula uses a larger database for its artificial intelligence algorithm, which has improved its accuracy compared with other formulas. In the first study to assess the Hill-RBF formula (version 1.0), it was less accurate than the Barrett, Holladay 1, SRK/T, T2, and Ladas Super Formula.⁷ A study by Roberts et al.¹⁵ found the Hill-RBF formula (v1.05) to have the third lowest mean absolute numerical error of the 5 formulas studied. In our study, the Hill 2.0 formula had the second lowest MAE and STDEV, third lowest MedAE, and second highest percentage of eyes within 0.50 D, indicating improvement.

For each of the AL groups, the Kane formula had the lowest MAE, which was statistically significant in all cases

($P < .01$). In the short AL eyes, the Holladay 2-AL adjusted formula had the second lowest MAE, although there was no statistically significant difference found between it and the Olsen, Holladay 1, or Hill 2.0 formula, which is a similar finding to the study by Gökce et al.¹⁶ In the medium AL group, the Hill 2.0 formula had the second lowest MAE. Both the Hill 2.0 and the Olsen formulas were more accurate than the third-generation and Haigis formulas. In the long AL group, the Barrett formula had the second lowest MAE, which was statistically significant compared with the other formulas ($P < .05$) and is consistent with other findings.⁷

The overall predictability of the data (approximately 72.0% within 0.50 D) is lower than that of Melles et al.,⁵ which had 80.0% of eyes for the SA60AT IOL. Melles et al.⁵ used predictions made by the Lenstar 900 optical biometer (Haag-Streit) that, which would be expected to improve outcomes and may explain the differences between the 2 studies. The results in our study are similar to the results seen in the EUREQUO data, which reported 72.7% of eyes (of 282, 811 cases) as achieving a prediction error within 0.50 D.¹⁷

The different IOL models have different results with a variation in the mean absolute error between models from 0.340 for the Superflex and 0.405 for the C-Flex. This is likely explained by the ranges that these IOLs are available in. The Superflex is available from -10.0 to +22.0 D, and the C-Flex

Table 5. Mean absolute error for each formula by axial length subgroups.

Formula	Short ≤ 22.0 mm	Medium 22.0 mm, 26.0 mm	Long ≥ 26.0 mm	Mean Rank
Kane	0.441	0.375	0.329	1
Holladay 2	0.458	0.387	0.352	3.33
Olsen	0.459	0.384	0.352	3.66
Hill 2.0	0.470	0.382	0.352	3.66
Barrett	0.493	0.385	0.338	5
Holladay 1	0.461	0.387	0.475	6.33
Hoffer Q	0.478	0.401	0.454	7.33
Haigis	0.486	0.402	0.359	7.33
SRK/T	0.492	0.399	0.363	7.33

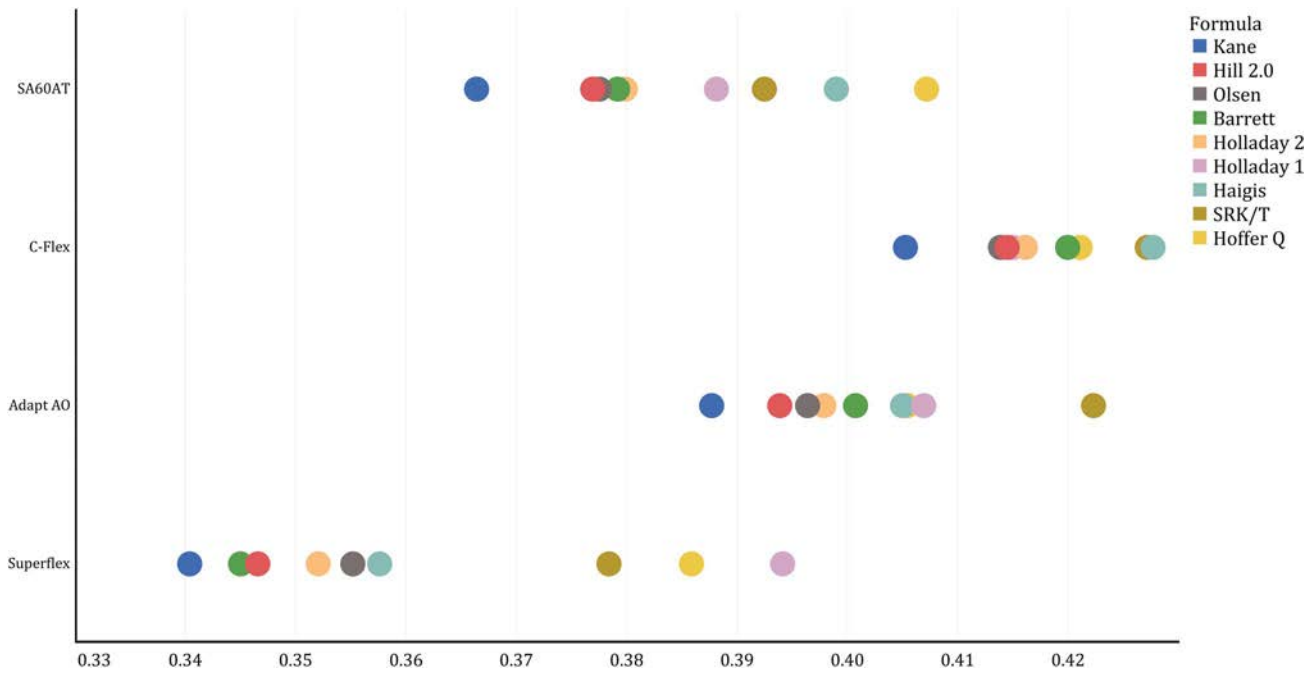


Figure 1. Mean absolute error of each formula for each intraocular lens type.

is available from +8.00 to +34.0. The worst performance of the C-Flex is explained by the C-Flex being implanted in more short AL eyes (which have a higher MAE compared with longer AL eyes).

The order of accuracy for the formulas changes in some cases depending on which IOL model is used. All IOL formulas are based on data derived from clinical practice and the IOL type that the formula is based on may lead to changes in the performance of that particular formula for that particular IOL. For example, the Hoffer Q formula performed better for the Akreos Adapt AO IOL than it did for the other IOL models. This may be because the Akreos Adapt AO IOL has a similar configuration as the JFCLRU (Alcon Laboratories, Inc.) IOL, which the Hoffer Q formula is based on. IOL manufacturers do not provide exact configurations, which makes it difficult to make further comparisons.

The absence of crystalline lens thickness, central corneal thickness, and white-to-white measurements limits our ability to draw further conclusions about formula accuracy. The Olsen formula and Kane formula both use crystalline lens thickness and central corneal thickness to make their predictions, whereas the Barrett Universal 2 and Holladay 2-AL adjusted formulas use crystalline lens thickness and white-to-white measurements. The inclusion of these extra variables may improve the accuracy of these formulas nevertheless, these additional variables are optional extras in the formulas mentioned previously, with none of them being an absolute requirement. Given many surgeons use older biometers that do not have the ability to measure the crystalline lens thickness or central corneal thickness, this study will assist in decision-making about IOL formulas.

Another potential limitation is the inclusion of data from multiple surgeons and refractions performed by different practitioners might introduce bias due to differences in operating style and technique. However, in modern surgery and optometry, this has been shown to only minimally impact results.^{18,19} Furthermore, studies with only a single surgeon and a single person performing refraction are unlikely to reach the number of cases required for significance and in themselves may be biased. The multi-center, multisurgeon approach described here might have greater generalizability and is advantageous.

This study includes a large number of short and long AL eyes and enough numbers for each IOL type to be adequately powered to detect relevant effects in all categories. The strict criteria for IOL formula studies that have been suggested by Hoffer et al.,²⁰ with statistical analysis as suggested by Aristodemou et al.,¹⁴ have been carefully followed, although we prefer to compare formulas by the MAE rather than MedAE, as per Kane et al.⁴ and Wang et al.¹³ Few studies have been able to assess the Hill-RBF formulas because of the daily entry limits and pop-up blockers; we used computer programs that assisted us gathering data.

This study shows the ongoing improvement in IOL formulas and, hence, the potential for ongoing improvement in patient refractive results. The 2 updated formulas (Hill 2.0 and Holladay 2-AL adjusted) performed better than previously, and the Hill 2.0 formula outperforming the Barrett formula, which previously was shown to be the most accurate. The new Kane IOL formula demonstrated a significant improvement over current IOL formulas overall in short and in long AL eyes and for each IOL type.

WHAT WAS KNOWN

- The Barrett Universal II formula was the most accurate predictor of postoperative refraction compared with third-generation and newer generation formulas, including the Hill-RBF formula (version 1.0).

WHAT THIS PAPER ADDS

- The Kane formula was a more accurate predictor of postoperative refraction compared with all other formulas.

REFERENCES

1. Landau IME, Laurell CG. Ultrasound biomicroscopy examination of intraocular lens haptic position after phacoemulsification with continuous curvilinear capsulorhexis and extracapsular cataract extraction with linear capsulotomy. *Acta Ophthalmologica Scand* 1999;77:394–396
2. Findl O, Drexler W, Menapace R, Heinzl H, Hitzinger CK, Fercher AF. Improved prediction of intraocular lens power using partial coherence interferometry. *J Cataract Refract Surg* 2001;27:861–867
3. Cooke DL, Cooke TL. Comparison of 9 intraocular lens power calculation formulas. *J Cataract Refract Surg* 2016;42:1157–1164
4. Kane JX, Van Heerden A, Atik A, Petsoglou C. Intraocular lens power formula accuracy: comparison of 7 formulas. *J Cataract Refract Surg* 2016;42:1490–1500
5. Melles RB, Holladay JT, Chang WJ. Accuracy of intraocular lens calculation formulas. *Ophthalmology* 2018;125:169–178
6. Olsen T. The Olsen formula. In: Shammass HJ, ed, *Intraocular Lens Power Calculations*. Thorofare, NJ, Slack, 2004; 27–38
7. Kane JX, Van Heerden A, Atik A, Petsoglou C. Accuracy of 3 new methods for intraocular lens power selection. *J Cataract Refract Surg* 2017;43:333–339
8. Wang L, Holladay JT, Koch DD. Wang-Koch axial length adjustment for the Holladay 2 formula in long eyes. *J Cataract Refract Surg* 2018;44:1291–1292
9. Hoffer KJ. The Hoffer Q formula: a comparison of theoretic and regression formulas. *J Cataract Refract Surg* 1993;19:700–712; errata, 1994; 20:677; 2007; 33:2–3
10. Holladay JT, Prager TC, Chandler TY, Musgrove KH, Lewis JW, Ruiz RS. A three-part system for refining intraocular lens power calculations. *J Cataract Refract Surg* 1988;14:17–24
11. Haigis W, Lege B, Miller N, Schneider B. Comparison of immersion ultrasound biometry and partial coherence interferometry for intraocular lens calculation according to Haigis. *Graefes Arch Clin Exp Ophthalmol* 2000;38:765–773
12. Retzlaff JA, Sanders DR, Kraff MC. Development of the SRK/T intraocular lens implant power calculation formula. *J Cataract Refract Surg* 1990;16:333–340
13. Wang L, Koch DD, Hill W, Abulafia A. Pursuing perfection in intraocular lens calculations: III. Criteria for analyzing outcomes. *J Cataract Refract Surg* 2017;43:999–1002
14. Aristodemou P, Knox Cartwright NE, Sparrow JM, Johnston RL. Statistical analysis for studies of intraocular lens formula accuracy. *Am J Ophthalmol* 2015;160:1085–1086
15. Roberts TV, Hodge C, Sutton G, Lawless M. Comparison of Hill-radial basis function, Barrett Universal and current third generation formulas for the calculation of intraocular lens power during cataract surgery. *Clin Exp Ophthalmol* 2018;46:240–246
16. Gökçe SE, Zeiter JH, Weikert MP, Koch DD, Hill W, Wang L. Intraocular lens power calculations in short eyes using 7 formulas. *J Cataract Refract Surg* 2017;43:892–897
17. Lundström M, Dickman M, Henry Y, Manning S, Rosen P, Tassignon MJ, Young D, Stenevi U. Risk factors for refractive error after cataract surgery: analysis of 282 811 cataract extractions reported to the European Registry of Quality Outcomes for cataract and refractive surgery. *J Cataract Refract Surg* 2018;44:447–452
18. Aristodemou P, Knox Cartwright NE, Sparrow JM, Johnston RL. Intraocular lens formula constant optimization and partial coherence interferometry biometry: refractive outcomes in 8108 eyes after cataract surgery. *J Cataract Refract Surg* 2011;37:50–62
19. Reinstein DZ, Yap TE, Carp GI, Archer TJ, Gobbe M; London Vision Clinic optometric group. Reproducibility of manifest refraction between surgeons and optometrists in a clinical refractive surgery practice. *J Cataract Refract Surg* 2014;40:450–459
20. Hoffer KJ, Aramberri J, Haigis W, Olsen T, Savini G, Shammass HJ, Bentov S. Protocols for studies of intraocular lens formula accuracy. *Am J Ophthalmol* 2016;160:403–405

OTHER CITED MATERIALS

- A. Kane J. Kane Formula. Available at: <https://www.iolformula.com>
- B. Holladay JT. Holladay IOL Consultant Software & Surgical Outcomes Assessment. 0120. 2018 ed. Bellaire, TX. Holladay Consulting
- C. Hill W. Hill-RBF Calculator Version 2.0. Available at: <https://rbfcalculator.com/online/index.html>
- D. Barrett G. Barrett Universal II Formula. Singapore, Asia-Pacific Association of Cataract and Refractive Surgeons. Available at: http://www.apacrs.org/barrett_universal2/

Disclosures: *Dr. Kane is the creator of the Kane formula. None of the other authors has a financial or proprietary interest in any material or method mentioned.*

Long-term follow-up and clinical evaluation of the light-adjustable intraocular lens implanted after cataract removal: 7-year results

Merita Schojai, MD, Tim Schultz, MD, Katrin Schulze, MD, Fritz H. Hengerer, MD, PhD, H. Burkhard Dick, MD, PhD

Purpose: To determine the long-term safety and effectiveness of a light-adjustable intraocular lens (LAL) over a period that is longer than reported in the literature at the time of the study.

Setting: University Eye Hospital, Bochum, Germany.

Design: Noninterventive observation.

Methods: In 445 patients, cataract surgery with LAL implantation was performed between April 2008 and December 2012. It was possible to contact 171 of these patients or their relatives through letter or telephone; 61 patients (103 eyes) agreed to participate in the long-term study and were examined.

Results: The mean time between the lock-in (final light treatment) and long-term visit was 7.2 years; 61 patients were included and

examined. Corrected and uncorrected distance visual acuity was and remained good ($n = 93$). The refractive outcome was stable with minimal deviation. There were no significant changes in corneal thickness. In 2 patients, there were slight opacities of the IOL material without impact on visual acuity. Other eye diseases were within the normal range of the patients' age.

Conclusion: Seven years after implantation and refractive adjustment, eyes with an LAL had stable refraction, good visual acuity, and no IOL-associated pathologies. The findings suggest that LAL technology is a safe and efficient method to achieve good visual results without long-term complications.

J Cataract Refract Surg 2020; 46:8–13 Copyright © 2019 Published by Wolters Kluwer on behalf of ASCRS and ESCRS

Cataract surgery has become increasingly safe and efficient over the past decades. Owing to elevated patient expectations, the achievement of the desired refraction has become a major challenge in modern cataract surgery.

Several trials have demonstrated that the target refraction is missed in a significant percentage of patients. In a multicenter data study with a high number of cases, Lundström et al.¹ reported that the biometry prediction error of ± 0.5 D was only achieved in 72.7% of the cases. Similar results were measured by Simon et al.² in a retrospective study with 94% of the cases within ± 1.0 D of the target refraction. Furthermore, many patients who have undergone corneal refractive surgery are now reaching the typical age for cataract surgery, with intraocular lens (IOL) power determination being particularly challenging in these eyes.³ In addition to advanced preoperative biometry devices, IOL calculation formulas, and intraoperative aberrometry, IOL technologies

that allow for postoperative adjustments of the refractive power have also been developed. Although in the past most of these adjustable technologies required an invasive procedure, the light-adjustable intraocular lens (LAL; RxSight, Inc.) uses profiled doses of ultraviolet (UV) light to adjust for residual refractive errors after cataract surgery. This technology received Conformité Européenne Mark approval in Europe in 2007 and U.S. Food and Drug Administration (FDA) approval in the United States in 2017. In a trial published by Hengerer et al.,⁴ the deviation from the targeted refraction with the LAL was better than ± 0.5 D in 98% of the cases 18 months postoperatively and in 91.8% of the cases 6 months postoperatively in the FDA-approved trial.⁵ However, during the procedure, a significant amount of energy is sent through the eye and no long-term data are available in terms of refractive stability and safety. Our trial aimed at investigating the long-term safety and effectiveness of the LAL over a longer

Submitted: April 30, 2019 | Final revision submitted: July 16, 2019 | Accepted: August 6, 2019

From the Ruhr University Eye Hospital (Schojai, T. Schultz, K. Schulze, Dick), Bochum, and Bürgerhospital (Hengerer), Frankfurt, Germany.

M. Schojai and T. Schultz contributed equally to this work.

Corresponding Author: Merita Schojai, MD, Ruhr University Eye Hospital, In der Schornau 23-25, 44892 Bochum, Germany. Email: merita.schojai@kk-bochum.de.

period than was reported in the literature at the time of this study.

METHODS

In this noninterventive observation trial, all patients who had been treated with an LAL at Ruhr University Eye Hospital in Bochum (Germany) between April 2008 and December 2012 were contacted. Through letter or telephone call, patients were invited to a follow-up examination, conducted in 2016 and 2017.

In total, 445 patients were contacted. Of these, 274 (62%) were not reached by phone and did not respond to the letter sent. In total, 171 patients or their relatives (38%) were reached, and 61 (14%) were able and willing to participate in the long-term trial, which consisted of 1 follow-up visit/examination. The trial received ethical committee approval from Ruhr University, and all aspects of the Declaration of Helsinki were observed. All patients signed an informed consent form.

Light-Adjustable Intraocular Lens

The LAL technology has been described in detail in earlier publications.⁶⁻⁹ Briefly, it is a foldable, 3-piece, silicone IOL with an overall diameter of 13.0 mm; the optic is 6.0 mm in diameter. The IOL has squared posterior optic edges, round anterior edges, and blue poly(methyl methacrylate) modified-C haptics with a posterior optic-haptic 10-degree angulation. The IOL is manufactured in the range of +10.00 to +30.0 D, in 0.50 D increments from +16.00 to +24.0 D and in 1.00 D increments from +10.00 to +15.00 D and +25.00 to +30.0 D. The silicone contains macromers that are sensitive to UV light (365 nm). Two to 3 weeks after routine implantation of the IOL, the light delivery device is used to induce a controlled polymerization of the contained silicone macromers, which results in a predictable spherical and/or cylindrical power change. If further refinement of the refractive outcome is desired, the IOL power can be modified again, up to a total of 3 D of cylinder and 2 D of sphere. Owing to the distribution of the photosensitive silicone macromers, UV irradiation of the central segment of the LAL is performed in cases of hyperopic correction, whereas the periphery of the IOL is irradiated to treat residual postoperative myopia.¹⁰ If the desired refractive state has been achieved, a final lock-in is then performed to permanently fix the refractive power of the IOL. This lock-in does not affect the final dioptric power of the IOL. Patients are required to wear special UV protective spectacles after LAL implantation until the final light treatment is completed to protect the eye from any unscheduled UV light exposure, which might severely influence the IOL power in a desirable way.

Surgical Technique

From 2008 to 2012, all included patients were operated on with the same surgical technique by two experienced surgeons (F.H.H. and H.B.D.). In most cases, paralytic anesthesia was administered by either injecting 2 mL to 6 mL of anesthetics (lidocaine hydrochloride 2% in combination with tetracaine hydrochloride at equal volumes), or applying topical anesthesia (oxybuprocaine hydrochloride eyedrops, Conjucaïn EDO 0.4%). After pharmacological mydriasis (0.5% tropicamide eyedrops, Mydriaticum; 5.0% phenylephrine eyedrops, Neo-Synephrine), a clear corneal incision at the 12 o'clock position using a 2.75 mm steel keratome (Alcon Laboratories, Inc.) was made. The side-port incisions were positioned at 3 o'clock and 9 o'clock. After instillation of the ophthalmic viscosurgical device (sodium hyaluronate 1.0%) into the anterior chamber, a continuous curvilinear anterior capsulorhexis between 4.5 mm and 5.5 mm was created. This was followed by phacoemulsification with the stop-and-chop technique (Stellaris; Bausch & Lomb, Inc.). The residual cortex was removed with irrigation/aspiration. The 3-piece silicone LAL was implanted directly in the capsular bag. After ophthalmic

viscosurgical device removal, corneal wounds were closed with a balanced salt solution for watertightness, and antibiotic (ofloxacin, Floxal) and steroidal ointments (prednisolone, Ultracortenol) were applied.

Postoperative Treatment

Postoperative medication consisted of topical antibiotic (ofloxacin, Floxal) and steroid eyedrops (Dexa EDO), which were administered 4 times daily for the first week, after which the dosage was gradually tapered over 6 weeks. All patients were required to wear UV light-filtering spectacles during waking hours after cataract surgery until the final lock-in treatment was completed. All irradiation procedures were performed with the pupil fully dilated and the patient fixating on a flashing target light. The treatment exposures were delivered in a continuous dose. One to 2 days after the adjustment, the patient returned to the clinic for clinical examination. If the desired refraction had been achieved, the LAL was locked in. If further refinement of the residual refractive error was required, the IOL was adjusted again.

Long-Term Visit

In all cases, data from the original 1-year postoperative visit were available. This included subjective refraction (spherical equivalent [SE]) and uncorrected distance visual acuity (UDVA) and corrected distance visual acuity (CDVA) under photopic light conditions. Furthermore, preoperative and 1-year pachymetry data were available in 54 (52%) of 103 eyes.

During the long-term follow-up visit, subjective refraction, UDVA and CDVA under photopic light conditions, pachymetry, optical coherence tomography of the macula, and slitlamp examination of the anterior and posterior segment were performed by experienced investigators.

Statistics

The statistics were made using IBM SPSS Statistics for Windows software (version 19.0, IBM Corp.). A *P* value less than .05 was considered statistically significant.

RESULTS

This study enrolled 103 eyes of 61 patients. The mean age of the study group was 75 years \pm 6.8 (SD) (range 54 to 88 years) with a sex ratio of 20 men (33%) and 41 women (67%). The median time between LAL implantation and the last follow-up was 7.2 years \pm 0.9 (SD). All planned measurements were performed successfully in all patients.

Ten eyes were excluded from the refraction and visual acuity analyses because of the following pathologies: 1 case of retinal detachment, 3 cases of epiretinal gliosis, and 1 case each of central retinal vein occlusion and branch arterial occlusion. Two eyes each developed wet age-related macular degeneration with anti-vascular endothelial growth factor therapy. One eye showed a decompensated Fuchs endothelial dystrophy and 1 eye developed vitreomacular traction.

The box plots in [Figure 1](#) demonstrate the UDVA for the remaining 93 eyes. One year postoperatively, UDVA was 0.2 logarithm of the minimum angle of resolution (logMAR) (median \pm 0.2; range 1.2 to 0.1), and 7 years postoperatively, it was 0.28 logMAR (median \pm 0.21; range 1.2 to 0.2) (*n* = 93; *P* = .001). There was a minor change in CDVA from 0.07 logMAR (median \pm 0.12; range 0.6 to 0.1) 1 year postoperatively to 0.12 logMAR (median \pm 0.18; range 1

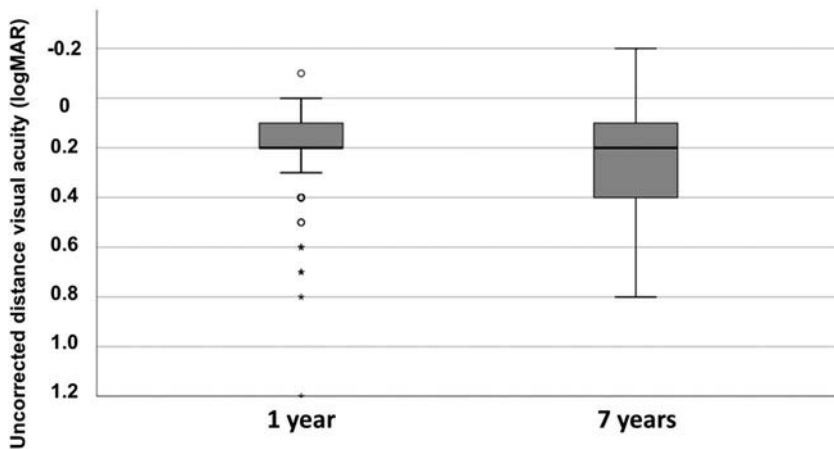


Figure 1. Uncorrected distance visual acuity after 1 year and 7 years (logMAR = logarithm of the minimum angle of resolution).

to -0.2) 7 years postoperatively ($n = 93$; $P = .005$) (Figure 2). Refraction was also stable (Figure 3). The refraction after 1 year was 0.04 D (median ± 0.68 ; range -3.13 to 1.5) and 0.23 D (median ± 0.73 ; range -3.13 to 1.88) after 7 years ($n = 93$; $P = .005$). The average central corneal thickness (CCT) remained unchanged from 550 μm (median ± 29 ; range 485 to 612) preoperatively to 555 μm (median ± 29 ; range 475 to 605) after 1 year ($n = 53$, $P = .58$) and 553 μm (median ± 28 ; range 489 to 610) after 7 years ($n = 54$, $P = .12$) (Figure 4).

In 2 eyes, slight IOL opacities were found (after a history of chronic uveitis over years in 1 eye and multiple anti-vascular endothelial growth factor injections and a vitrectomy in the other). Both patients had a good visual acuity. They were asked whether they had photic phenomena. No photic phenomena were reported.

DISCUSSION

Refractive outcomes after cataract surgery are an important factor for determining the patient's satisfaction or, rather, disappointment after postoperative recovery and rehabilitation are completed. Residual refractive errors are common, even for the most experienced cataract surgeons. While treating these residual ametropias with corneal refractive procedures such as laser in situ keratomileusis or photorefractive keratectomy being a well-established approach, they may introduce new issues such as dry eye and other complications that can be avoided with an adjustable IOL.¹¹

In addition, an increasing number of former refractive patients will undergo cataract surgery with remnants of earlier procedures on the eye's surface, potentially making further corneal procedures problematic.

A number of adjustable IOLs have been developed to address these shortcomings, described in a 2014 review by Ford et al.¹⁰ Some of these technologies require a second invasive intervention, such as the multicomponent IOL, the mechanically adjustable IOL, and the repeatedly adjustable IOL. Other technologies allow for an external adjustment, such as the magnetically adjustable IOL and the liquid-crystal IOL with wireless control. These authors suggest that IOLs permitting noninvasive postoperative adjustment may become a mainstay of cataract treatment in the future.¹⁰ The most clinically advanced of these is the LAL, first described by Schwartz in 2003.⁶

In our series, we have documented long-term results that confirm the refractive stability, good visual outcomes, and high safety profile of the LAL. Of the 445 operated patients, 274 (62%) were not reached by phone and did not respond to the letter sent. Most likely, the patients moved to a retirement home or are deceased. Similarly, 73.9% of the patients died 10 years after cataract surgery in the Blue Mountains Eye Study Cohort.¹² Therefore, the number of patients reached in our trial can be classified as valid. The results extend the observations published previously by Hengerer et al., which demonstrated favorable results after

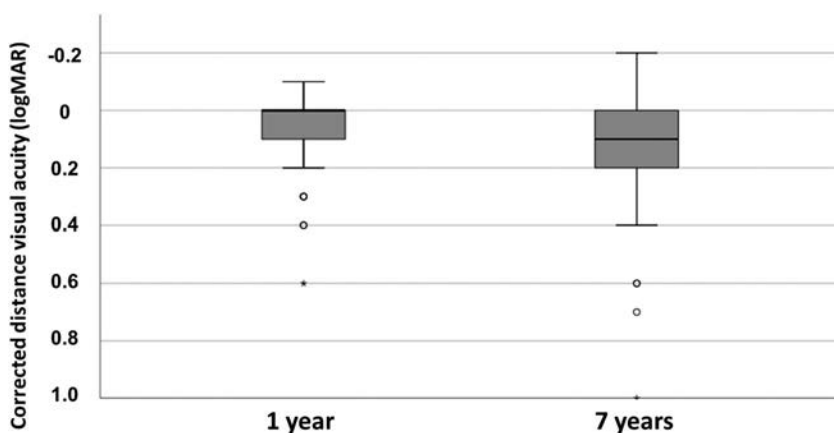


Figure 2. Corrected distance visual acuity after 1 year and 7 years (logMAR = logarithm of the minimum angle of resolution). (The bottom and top of the box are the 25th percentile and 75th percentile, respectively, and the bands near the center are the 50th percentile. The bars outside the box indicate the maximum and minimum of all data. A minor outlier (denoted by a small circle) is an observation 1.5 interquartile range outside the central box. An extreme outlier (denoted by an asterisk) is an observation 3 interquartile range outside the central box.)

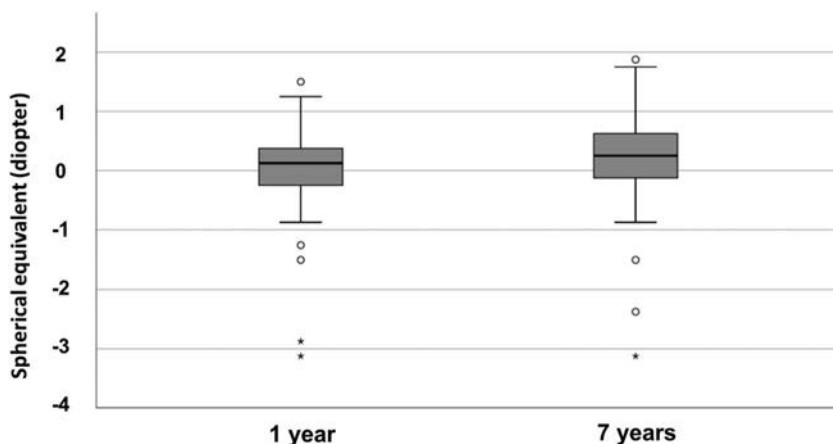


Figure 3. Subjective refraction preoperatively, after 1 and 7 years.

18-month follow-up.⁴ That study included 122 eyes of 91 patients with residual postoperative refractive errors of $+0.96 (\pm 0.85)$ D of sphere and $-0.98 (\pm 0.50)$ D of cylinder. At the 18-month post-lock-in visit, the mean SE refraction was 0.03 ± 0.17 D with a mean residual sphere of 0.10 ± 0.22 D and a mean residual cylinder of -0.25 ± 0.22 D. In that study, 98% of eyes were within ± 0.50 D of the targeted refractive outcome, 97% were within ± 0.25 D, and 100% were within ± 1.00 D of the intended outcome.⁴ We also studied the technology in a group of 21 eyes with myopia because of an axial length of greater than 24.5 mm.¹³ Twelve months postoperatively, 20 (96%) of the 21 eyes were within ± 0.50 D of the intended refractive outcome and 17 (81%) were within ± 0.25 D.¹³ The efficacy of LAL technology had been demonstrated earlier in a number of pilot studies by Chayet et al.⁷ on correcting postoperative myopia, hyperopia, and astigmatism. In the myopia study, for example, 14 eyes of 14 patients had residual refractive errors between -0.25 D and -1.50 D. Adjustment by irradiation was performed 10 to 21 days after implantation, followed by lock-in. After that, 93% of the eyes were within ± 0.25 D of the intended refraction and 100% were within ± 0.5 D. Refraction was stable for the 9-month follow-up, with a mean rate of change of 0.006 D per month, which was deemed to be about 6 times more stable than after corneal refractive procedures. The results in eyes with residual hyperopia and astigmatism were similar; in

a small group of 5 eyes needing adjustment for astigmatism, all patients achieved a SE refraction within ± 0.25 D of emmetropia and a UDVA of 20/25 or better at the 9-month follow-up.^{8,14} The irradiation of the LAL may not only eliminate hyperopia, myopia, and astigmatism but may also—as Sandstedt et al.¹⁵ have shown in vitro—have the potential to change the optical design of the IOL from monofocality to multifocality.

A retrospective trial by Brierley³ focused on the performance of LAL technology in postrefractive ametropic pseudophakic patients, a group of patients that regularly pose problems in preoperative biometry and IOL calculation. The 34 eyes of 21 patients had a very precise refractive outcome: after the final lock-in, 74% of eyes were within ± 0.25 D, 97% of eyes were within ± 0.50 D, and 100% were within ± 1.00 D of the target refraction. The mean absolute refractive error in the Brierley³ cohort was 0.19 D. There are also a number of studies on the safety profile of LAL technology, following pioneering publications by Werner et al.¹⁶ who demonstrated in an animal model that therapeutic dosages of UV light administered during lock-in do not cause corneal damage.

We therefore evaluated the potential effect of UV irradiation on the macula. Results showed that there was no significant difference in the mean macular thickness between preoperative and postoperative measurements. Preoperative mean center macular thickness measurements

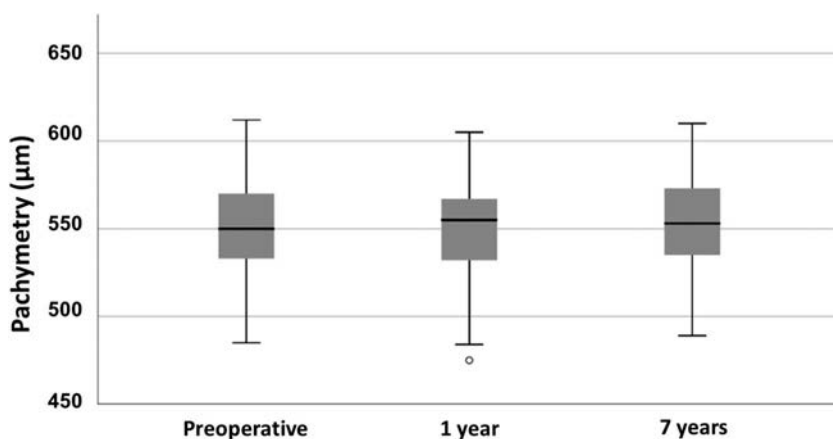


Figure 4. Corneal thickness preoperatively, and after 1 and 7 years.

were $210 \pm 21 \mu\text{m}$ (range 166 to $278 \mu\text{m}$). Postoperatively, the mean central macular thickness was $209 \pm 23 \mu\text{m}$ (range 171 to $320 \mu\text{m}$) before adjustments, $210 \pm 18 \mu\text{m}$ (range 170 to $265 \mu\text{m}$) 1 week after adjustments, $212 \pm 31 \mu\text{m}$ (range 171 to $271 \mu\text{m}$) 1 month after lock-in, $218 \pm 28 \mu\text{m}$ (range 171 to $274 \mu\text{m}$) 3 months after lock-in, and $213 \pm 17 \mu\text{m}$ (range 172 to $268 \mu\text{m}$) at the 1-year follow-up visit. We therefore concluded that UV light exposure during LAL adjustments did not influence the incidence of postoperative macular edema and did not induce any changes in the macular layers.¹⁷

Werner et al.¹⁸ conducted a trial in which no signs of retinal toxicity after near-UV light exposure up to 5 times the expected maximum treatment dosage used during adjustment and lock-in irradiation were evident. We have evaluated quantitative changes in endothelial cell loss and corneal thickness in 122 eyes with an LAL; the UV light exposure for adjustment and lock-in procedures did not add to the endothelial damage caused by cataract surgery. Two weeks postoperatively, before UV light exposure, the mean endothelial cell loss was $6.91\% \pm 3.66\%$, recovering to $6.57\% \pm 3.84\%$ 12 months after the final lock-in. The decrease in the endothelial cell count was statistically significant from preoperatively to postoperatively before adjustment ($P < .05$) but not from postoperatively to 1 year after lock-in ($P > .05$). This indicates that endothelial cell loss was caused by cataract surgery, not the UV light exposure, because no additional cell loss was observed after the application of UV light for adjustments and lock-ins. These results were considerably better than the mean endothelial cell loss of 12.6% and 9.1% from preoperative values in 10 eyes 1 week postoperatively before the adjustment of the LAL and at 6 months, respectively, reported by Lichtinger et al.¹⁹ The mean CCT increased from $548 \pm 34 \mu\text{m}$ preoperatively to $563 \pm 43 \mu\text{m}$ 2 weeks postoperatively before UV light exposure; at 12 months, the mean CCT was $544 \pm 35 \mu\text{m}$. These results suggest that UV light administered for adjustments and lock-ins is a safe and stable procedure for the human cornea.²⁰

As mentioned previously, 10 eyes were excluded from the trial because of the development of ocular pathologies with major impact on visual acuity 7 years after IOL implantation; occurrence of these retinal conditions were consistent with the rate reported in the literature. One eye with an axial length of 25 mm developed rhegmatogenous retinal detachment (0.9%). As Gariano and Kim²¹ described, the lifetime risk in this case is 1/300 (0.33%). Three patients (1%) had severe epiretinal membranes on both eyes. According to Fraser-Bell et al.,²² the risk to develop epiretinal membranes after 5 years is 9.1%. Two patients (2%) were excluded because of wet macular degeneration. The lifetime risk was described as 1.6% by Klein et al.²³ In 1 eye (1%), a retinal artery occlusion occurred, which is described to have an incidence of 1/100 000.²⁴ One eye (1%) had a vitreomacular traction syndrome. The lifetime risk of this pathology is 1.5%.²⁵ Furthermore, 2 patients (4%) with Fuchs endothelial dystrophy were excluded. The risk of the development of Fuchs endothelial dystrophy in patients

older than 40 years is 4%.²⁶ Our 7-year results add to the growing literature on LAL technology that demonstrates an excellent safety and effectiveness profile. It remains to be seen how this method will develop, now that it is FDA-approved and therefore increasingly used in the United States.

WHAT WAS KNOWN

- In cataract surgery, the refractive outcome can differ from the preoperatively calculated target refraction.
- In short-term trials, excellent postoperative refraction was reached with the light-adjustable intraocular lens (LAL).

WHAT THIS PAPER ADDS

- In this trial, for the first time to our knowledge, the long-term stability and safety of the LAL was investigated.
- Seven years after the implantation and adjustment of the LAL, stable refraction, good visual acuity, and no IOL-associated pathologies were measured.

REFERENCES

1. Lundström M, Dickman M, Henry Y, Manning S, Rosen P, Tassignon MJ, Young D, Stenevi U. Risk factors for refractive error after cataract surgery: Analysis of 282 811 cataract extractions reported to the European Registry of Quality Outcomes for cataract and refractive surgery. *J Cataract Refract Surg* 2018;44:447–452
2. Simon SS, Chee YE, Haddadin RI, Veldman PB, Borboli-Gerogiannis S, Brauner SC, Chang KK, Chen SH, Gardiner MF, Greenstein SH, Kloek CE, Chen TC. Achieving target refraction after cataract surgery. *Ophthalmology* 2014;121:440–444
3. Brierley L. Refractive results after implantation of a light-adjustable intraocular lens in postrefractive surgery cataract patients. *Ophthalmology* 2013;120:1968–1972
4. Hengerer FH, Dick HB, Conrad-Hengerer I. Clinical evaluation of an ultraviolet light adjustable intraocular lens implanted after cataract removal: Eighteen months follow-up. *Ophthalmology* 2011;118:2382–2388
5. FDA approves first implanted lens that can be adjusted after cataract surgery to improve vision without eyeglasses in some patients. 2017. Available at: <https://www.fda.gov/NewsEvents/Newsroom/PressAnnouncements/ucm586405.htm>. Accessed March 2, 2019
6. Schwartz DM. Light-adjustable lens. *Trans Am Ophthalmological Soc* 2003;101:417–436
7. Chayet A, Sandstedt C, Chang S, Rhee P, Tsuchiyama B, Grubbs R, Schwartz D. Correction of myopia after cataract surgery with a light-adjustable lens. *Ophthalmology* 2009;116:1432–1435
8. Chayet A, Sandstedt CA, Chang SH, Rhee P, Tsuchiyama B, Schwartz D. Correction of residual hyperopia after cataract surgery using the light adjustable intraocular lens technology. *Am J Ophthalmol* 2009;147:392–397.e391
9. Hengerer FH, Conrad-Hengerer I, Buchner SE, Dick HB. Evaluation of the Calhoun Vision UV light adjustable lens implanted following cataract removal. *J Refract Surg* 2010;26:716–721
10. Ford J, Werner L, Mamalis N. Adjustable intraocular lens power technology. *J Cataract Refract Surg* 2014;40:1205–1223
11. Sales CS, Manche EE. Managing residual refractive error after cataract surgery. *J Cataract Refract Surg* 2015;41:1289–1299
12. Fong GS, Mitchell P, Rochtchina E, Teber ET, Hong T, Wang JJ. Correction of visual impairment by cataract surgery and improved survival in older persons: The Blue Mountains Eye Study cohort. *Ophthalmology* 2013;120:1720–1727
13. Hengerer FH, Hutz WW, Dick HB, Conrad-Hengerer I. Combined correction of sphere and astigmatism using the light-adjustable intraocular lens in eyes with axial myopia. *J Cataract Refract Surg* 2011;37:317–323
14. Chayet A, Sandstedt C, Chang S, Rhee P, Tsuchiyama B, Grubbs R, Schwartz D. Use of the light-adjustable lens to correct astigmatism after cataract surgery. *Br J Ophthalmol* 2010;94:690–692
15. Sandstedt CA, Chang SH, Grubbs RH, Schwartz DM. Light-adjustable lens: Customizing correction for multifocality and higher-order aberrations. *Trans Am Ophthalmological Soc* 2006;104:29–39
16. Werner L, Yeh O, Haymore J, Haugen B, Romaniv N, Mamalis N. Corneal endothelial safety with the irradiation system for light-adjustable intraocular lenses. *J Cataract Refract Surg* 2007;33:873–878

17. Hengerer FH, Muller M, Dick HB, Conrad-Hengerer I. Clinical Evaluation of macular thickness changes in cataract Surgery using a light-adjustable intraocular lens. *J Refract Surg* 2016;32:250–254
18. Werner L, Chang W, Haymore J, Haugen B, Romaniv N, Sandstedt C, Chang S, Mamalis N. Retinal safety of the irradiation delivered to light-adjustable intraocular lenses evaluated in a rabbit model. *J Cataract Refract Surg* 2010;36:1392–1397
19. Lichtinger A, Sandstedt CA, Padilla K, Schwartz DM, Chayet AS. Corneal endothelial safety after ultraviolet light treatment of the light-adjustable intraocular lens. *J Cataract Refract Surg* 2011;37:324–327
20. Hengerer FH, Dick HB, Buchwald S, Hutz WW, Conrad-Hengerer I. Evaluation of corneal endothelial cell loss and corneal thickness after cataract removal with light-adjustable intraocular lens implantation: 12-month follow-up. *J Cataract Refract Surg* 2011;37:2095–2100
21. Gariano RF, Kim CH. Evaluation and management of suspected retinal detachment. *Am Fam Physician* 2004;69:1691–1698
22. Fraser-Bell S, Guzowski M, Rohtchina E, Wang JJ, Mitchell P. Five-year cumulative incidence and progression of epiretinal membranes: The Blue Mountains Eye Study. *Ophthalmology* 2003;110:34–40
23. Klein R, Klein BE, Linton KL, De Mets DL. The Beaver Dam Eye Study: Visual acuity. *Ophthalmology* 1991;98:1310–1315
24. Varma DD, Cugati S, Lee AW, Chen CS. A review of central retinal artery occlusion: Clinical presentation and management. *Eye* 2013;27:688–697
25. Jackson TL, Nicod E, Simpson A, Angelis A, Grimaccia F, Kanavos P. Symptomatic vitreomacular adhesion. *Retina* 2013;33:1503–1511
26. Musch DC, Niziol LM, Stein JD, Kamyar RM, Sugar A. Prevalence of corneal dystrophies in the United States: Estimates from claims data. *Invest Ophthalmol Vis Sci* 2011;52:6959–6963

Disclosures: *Drs. Hengerer and Dick own stock options of RxSight. None of the other authors have a financial or proprietary interest in any material or method mentioned.*

Clinical factors affecting operating room utilization in cataract surgery: Results from the PCIOL study

K. Matthew McKay, MD, Durga S. Borkar, MD, Giannis A. Moustafa, MD, Miriam J. Haviland, MSPH, Carolyn E. Kloek, MD, The PCIOL Study Group

Purpose: To identify preoperative clinical characteristics affecting cataract surgery operative time.

Setting: Academic center.

Design: Large-scale retrospective cohort study.

Methods: All cases of cataract extraction by phacoemulsification and intraocular lens insertion performed by Comprehensive Ophthalmology at Massachusetts Eye and Ear between January 1, 2014, and December 31, 2014, were reviewed. Clinically relevant predictors of operative time were identified a priori, and a multivariate analysis was used to identify which predictors were associated with operative time. To quantify the surgeon effect, 2 regression models were built, one inclusive of surgeon identity and the other with years of experience and the training level of the supervised resident instead of identity.

Results: Overall, 1349 cataract surgeries in 1072 patients were included. The mean operative time was 22.1 ± 7.8 minutes. Multiple

clinical factors were significantly associated with operative time, with attending surgeon identity being the most important. In the multivariate model with surgeon identity, longer operative time was associated with male sex, increased body mass index, first-eye surgery, left operative eye, advanced cataract, use of iris hooks, use of Malyugin ring, use of trypan blue, history of diabetic retinopathy, short axial length, and shallow anterior chamber depth. The R^2 value for the model inclusive of attending identity was 0.42, significantly higher than the R^2 value of 0.23 for the model exclusive of identity.

Conclusion: Preoperative clinical characteristics, such as patient demographics, biometry data, and cataract severity, significantly correlate with operative time. Surgeon identity is highly correlated with operative time. Incorporating these results into predictive algorithms may allow for more predictable surgical scheduling and more efficient use of operative resources.

J Cataract Refract Surg 2020; 46:14–19 Copyright © 2019 Published by Wolters Kluwer on behalf of ASCRS and ESCRS

Although cataract surgery is a safe¹ and cost-effective² surgical procedure, it still poses a significant burden on the healthcare system in terms of cost and operative resources due to the frequency with which it is performed.³ Cataract prevalence is predicted to increase dramatically in the coming decades, which will further increase the burden of this procedure on the healthcare system.⁴ Operating room (OR) time in particular is a scarce and valuable resource, with case delays, complications, and scheduling inefficiency having a direct impact on the revenue generated for the institution. OR time cost per minute in cataract surgery has been estimated at \$11.24 USD⁵; thus, even minor delays can have a substantial financial impact.

Recently, increasing attention has been paid to improving the efficiency of cataract surgery with the goal of

decreasing unit cost per surgery and optimizing the use of OR time.^{6–9} Efforts thus far have primarily focused on the preoperative identification of cataract surgeries at high risk for intraoperative complications. These complications are potentially devastating in terms of visual outcome for the patient and costly in terms of OR delays and requirements for secondary surgeries. Established preoperative cataract surgery risk-stratification systems may correlate with operative time.⁷ There is also evidence that surgeon-related factors are an important determinant of operative time.¹⁰ A number of studies have explored the potential to predict operative time in various surgical procedures.^{8,11–13} However, to our knowledge, there have been no specific large-scale efforts to predict operative time in cataract surgery.

Submitted: May 15, 2019 | Final revision submitted: July 7, 2019 | Accepted: August 5, 2019

From the Department of Ophthalmology, Massachusetts Eye and Ear Infirmary (McKay, Borkar, Moustafa, Kloek), Department of Epidemiology, Boston University School of Public Health (Haviland), Boston, Massachusetts, and Wills Eye Hospital Retina Service (Borkar), Philadelphia, Pennsylvania, USA.

Funded by a research grant from the American Society of Cataract and Refractive Surgery, Fairfax, VA, USA (D.S. Borkar, C.E. Kloek).

Corresponding author: Carolyn E. Kloek, MD, Department of Ophthalmology, Massachusetts Eye and Ear Infirmary, 243 Charles St, Boston, MA 02114. Email: carolyn-kloek@dmei.org.

Predictive modeling of cataract surgery duration may help improve operative scheduling, thereby promoting the efficient use of OR time. The current strategy for operative scheduling relies on surgeon prediction for case duration, a method of unknown accuracy, and a high degree of intersurgeon variability. The objective of this study was to identify relevant patient-related factors and clinical features that are strongly correlated with operative time for cataract surgery using a large-scale retrospective cohort of patients.

METHODS

Institutional review board approval was obtained through the Massachusetts Eye and Ear Human Studies Committee, and a waiver of patient consent was obtained given its retrospective nature.

Patient Selection

All cases of phacoemulsification were reviewed with intraocular lens insertion performed by 10 Massachusetts Eye and Ear attending cataract surgeons in the Comprehensive Ophthalmology Service between January 1, 2014, and December 31, 2014. *Current Procedural Terminology* codes 66982 (extracapsular cataract extraction with the insertion of intraocular lens prosthesis, complex) and 66984 (extracapsular cataract extraction with the insertion of intraocular lens prosthesis) were used to identify eligible cases. We only included cases in which phacoemulsification was used for intraocular lens extraction.

We excluded all cases which were primarily attended by resident physicians, because of the association of these cases with longer operative times. The Accreditation Council for Graduate Medical Education case log was reviewed and cross-referenced for cases performed by resident surgeons. Cases marked by residents as primary were considered to be resident-performed cases, whereas cases not logged as resident primary surgeries were considered to be attending cases. Combined cataract surgery cases with planned additional procedures (Descemet stripping endothelial keratoplasty, glaucoma procedures, or pars plana vitrectomy [PPV]) were also eliminated from the analysis.

Data Collection

Four members of the study team reviewed the medical records of all eligible cases. To ensure that data were extracted in a standardized way, all 4 reviewers received training from a study investigator. Baseline data were collected at the preoperative visit closest to the date of surgery.

Operative time data recorded by OR staff at the time of surgery included the date of the surgical case, the time of the day of the beginning and end of the case, operative time (excluding time under direct control of the anesthesiologist), and the total time the patient spent in the OR. Scheduled case duration was provided as standard practice preoperatively by attending surgeons for OR scheduling. Predicted case duration was provided in 15-minute increments as 30, 45, or 60 minutes. Operative time data were merged with the existing clinical data from chart review. The order of the surgical case in the OR schedule was determined using the start time of the case compared with other surgical cases performed that day by the same attending surgeon.

Predictor Selection

Patient-related, surgeon-related, and other clinical factors were identified that could potentially be associated with operative time based on the previously published reports and experience of our group. Variables included in the analysis were as follows: age (greater than or less than 90 years),^{14,15} sex,¹⁴ body mass index (greater than or less than 30),¹⁶ first or second eye, operative eye, advanced cataract,¹⁷⁻²⁰ iris hooks/Malyugin ring (Microsurgical Technology) (poor pupillary dilation), use of trypan blue, diabetic retinopathy,¹⁴ presence of pseudoexfoliation (PXF),^{21,22} axial length (≤ 22.4 , 22.5 to 25.9, or ≥ 26 mm),¹⁵ anterior chamber (AC) depth (≤ 2.4 , 2.5 to 3.9, or ≥ 4 mm),²¹ history of alpha-blocker use,²³⁻²⁷

prior PPV,²⁸ history of glaucoma,¹⁴ prior ocular surgery, post-graduate year (PGY) level of the assisting resident trainee (PGY2, PGY3, or PGY4),²⁹ years of attending surgeon experience after residency training,¹⁰ attending surgeon identity (coded as a unique numerical identifier),^{10,30} and order of surgery in the OR schedule.³¹

Statistical Analysis

All statistical analyses were performed using R (R Core Team, 2017) and SAS 9.4 (SAS Institute). Owing to the highly right-skewed distribution of operative time, the analysis was restricted to cases with operative times within 2 standard deviations above the mean operative time (≤ 46 minutes).

Bivariate analyses were conducted using the *t* test and analysis of variance to determine which factors were independently associated with the mean operative time. Multivariate linear regression with backward elimination was then used to identify factors that were significantly associated with operative time, after adjusting for other factors included in the model. A liberal threshold was set for statistical significance ($P < .2$) to include predictors that were found to be both strongly and moderately associated with operative time in the initial model. Variables were removed from the model one at a time, until all but 2 variables were significantly associated with the outcome at $\alpha = 0.20$. Although not significantly associated with operative time after adjusting for other predictors, we retained presence of PXF and history of PPV in the final model because of their generally accepted association with case complexity and increased risk for complication.^{21,22,32-34}

Two independent models were developed with respect to the surgeon performing the surgery: excluding the identity of the attending surgeon but replaced with the surgeon's years of experience and PGYs of training of the surgeon's trainee (Model 1) and using surgeon identity (Model 2). These models were developed for 2 primary reasons. First was the ability to generalize the model to other institutions in which surgeons will differ. Second was to quantify the effect of the surgeon independent of their or their trainee's experience.

RESULTS

Of the 1931 cataract surgeries reviewed, 1349 cataract surgeries in 1072 unique patients were included in the final analysis. Case characteristics are summarized in Table 1. The mean operative time was 22.1 ± 7.8 minutes. The range of mean operative times associated with each attending surgeon spanned nearly 10 minutes, from 17.2 to 27 minutes for the surgeon with the shortest and longest operative times, respectively. Of the included patients, 5 experienced posterior capsular tear and 4 of these underwent anterior vitrectomy. One additional patient underwent anterior vitrectomy in which no posterior capsular violation was noted intraoperatively.

Preoperative and intraoperative clinical characteristics associated with operative time in the bivariate analysis are

Table 1. Case characteristics.

	<i>n</i> = 1349
Age (y)	68.6 \pm 10.7
Operative time (min)	22.1 \pm 7.8
Sex	
Male	601 (44.6)
Female	748 (55.4)
Operative eye	
Right eye	675 (50.0)
Left eye	674 (50.0)

Data are presented as mean \pm SD or *n* (%)

Table 2. Unadjusted mean operative time by predictors and adjusted change in operative time by predictors from 2 prediction models.

	Bivariate Analysis		Model 1*		Model 2†	
	Mean ± SD	P Value	Mean Change	95% CI	Mean Change	95% CI
Sex		.005				
Female	21.6 ± 7.8		-0.70	-1.5, 0.07	-0.81	-1.5, -0.14
Male	22.8 ± 7.8		0.0	REF	0.0	REF
BMI > 30		.11				
Yes	22.7 ± 8.6		0.95	0.13, 1.8	0.82	0.11, 1.5
No	21.9 ± 7.5		0.0	REF	0.0	REF
Second eye		.003				
No	22.7 ± 7.9		0.0	REF	0.0	REF
Yes	21.4 ± 7.8		-1.4	-2.2, -0.64	-1.0	-1.7, -0.33
Operative eye		.06				
Right eye	21.7 ± 7.5		0.0	REF	0.0	REF
Left eye	22.5 ± 8.1		0.84	0.10, 1.6	0.90	0.26, 1.5
Advanced cataract		<.0001				
Yes	28.4 ± 8.1		4.4	2.1, 6.6	3.0	1.0, 4.9
No	21.9 ± 7.7		0.0	REF	0.0	REF
Iris hooks		<.0001				
Yes	30.7 ± 5.8		8.9	7.4, 10.4	7.8	6.5, 9.2
No	21.3 ± 7.5		0.0	REF	0.0	REF
Malyugin ring		<.0001				
Yes	26.6 ± 9.4		4.5	2.7, 6.3	4.7	3.2, 6.3
No	21.9 ± 7.7		0.0	REF	0.0	REF
Trypan blue		<.0001				
Yes	26.3 ± 8.2		3.1	2.0, 4.1	2.8	1.9, 3.8
No	21.3 ± 7.5		0.0	REF	0.0	REF
Diabetic retinopathy		.0002				
Yes	25.1 ± 6.5		2.5	0.80, 4.2	1.04	-0.43, 2.5
No	22.0 ± 7.7		0.0	REF	0.0	REF
PXF		.006				
Yes	24.6 ± 7.6		0.14	-1.5, 1.8	-0.44	-1.9, 1.0
No	22.0 ± 7.8		0.0	REF	0.0	REF
AL		.03				
0-22.4	23.6 ± 7.8		1.9	0.64, 3.1	0.99	-0.11, 2.1
22.5-25.9	22.1 ± 7.8		0.0	REF	0.0	REF
≥26.0	21.1 ± 7.7		-0.29	-1.5, 0.91	-0.33	-1.4, 0.73
AC depth‡		.04				
0-2.4	24.7 ± 9.7		—	—	2.7	0.73, 4.7
2.5-3.9	22.2 ± 7.7		—	—	0.0	REF
≥4	21.0 ± 8.2		—	—	-0.30	-1.5, 0.91
Prior PPV		.11				
Yes	23.6 ± 7.9		0.34	-1.4, 2.05	-0.62	-2.11, 0.87
No	22.1 ± 7.8		0.0	REF	0.0	REF
Resident PGY		<.0001				
4	23.2 ± 7.6		7.1	5.3, 8.9	—	—
3	21.7 ± 8.3		0.94	-0.32, 2.2	—	—
2	20.3 ± 6.2		0.0	REF	—	—
Years of attending experience		.006				
<4	23.2 ± 7.2		0.0	REF	—	—

(continued on next page)

summarized in Table 2. Clinical characteristics associated with longer operative time in both Model 1 and Model 2 were male sex, body mass index greater than 30, first-eye surgery, left operative eye, advanced cataract, use of iris hooks, use of Malyugin ring, use of trypan blue, history of diabetic retinopathy, and shorter axial length (<22.5 mm).

Additional significant predictors of longer operative time in Model 1 were more advanced level of trainee experience and less attending experience after residency training. Additional significant predictors of longer operative time in Model 2 were shallow AC depth (<2.5 mm) and inter-surgeon variability.

Table 2. Continued

	Bivariate Analysis		Model 1*		Model 2†	
	Mean ± SD	P Value	Mean Change	95% CI	Mean Change	95% CI
4–11	21.5 ± 8.2	<.0001	−2.8	−4.0, −1.7	—	
>11	22.5 ± 7.5		−8.6	−10.6, −6.7	—	
Attending						
1	26.5 ± 7.1		—		7.1	5.7, 8.6
2	23.9 ± 5.6		—		3.7	1.9, 5.4
3	17.3 ± 5.7		—		−1.5	−3.0, −0.03
4	27.0 ± 7.2		—		7.7	5.9, 9.4
5	25.4 ± 6.7		—		4.0	2.7, 5.4
6	17.2 ± 4.9		—		−6.3	−7.9, −4.7
7	24.5 ± 8.3		—		−2.1	−3.8, −0.44
8	23.0 ± 6.9	—		5.0	2.8, 7.26	
9	19.0 ± 5.0	—		0.0	REF	

AC = anterior chamber; AL = axial length; BMI = body mass index; PGY = postgraduate year; PPV = pars plana vitrectomy; PXF = pseudoexfoliation

*Model 1: Model includes variables for years of experience and resident PGY, but not attending name

†Model 2: Model includes a variable for attending name, but not years of experience or resident PGY

‡Dropped from model 1 during the backward selection process

Scheduled case duration provided by the surgeon was compared with the operative time and total time in the OR (Table 3). Most cases were scheduled for 30, 45, or 60 minutes. The analysis of variance demonstrated a significant difference in the operative time and total case time based on scheduled case duration ($P < .001$ for both). The shorter operative time and total OR time were associated with cases scheduled for 30 minutes compared with 45 or 60 minutes ($P < .001$). There was no significant difference between 45-minute and 60-minute scheduled cases.

The R^2 value for Model 2 ($R^2 = 0.42$) was significantly higher than that calculated for Model 1 ($R^2 = 0.23$), that is, more of the variability in operative time was accounted for in Model 2. The most significant difference between these models was attending and resident experience in Model 1 replaced with surgeon identity in Model 2, suggesting intersurgeon variability independent of experience is an important predictor of operative time.

Variables not significant enough for inclusion in the regression models or dropped from the models during backward selection are presented in Table 4. History of alpha-blocker use, although significantly correlated with longer operative time in the bivariate analysis, was dropped from both Model 1 and Model 2 during the selection process. Advanced age and case number of the day were not independently associated with operative time.

Table 3. Comparison of surgeon-predicted case duration and actual operative time.

	Scheduled Case Time (min)		
	30	45	60
Cases (n)	90	1110	144
Operative time (mean ± SD)	16.7 ± 8.8	22.3 ± 7.6	23.2 ± 6.9
Time in OR (mean ± SD)	30.0 ± 9.0	36.0 ± 9.4	36.9 ± 9.03

OR = operating room

Notably, although PXF and history of PPV were associated with prolonged case time in the bivariate analysis, neither reached significance in the multivariate analysis. A high degree of correlation was found between PXF and use of ancillary devices including trypan blue, Malyugin ring, and iris hooks. Thus, when we controlled for these factors, PXF was no longer significantly associated with increased operative time. Both prior PPV and history of PXF were forced into the final models because of their generally accepted association with complicated cataract surgery.

DISCUSSION

In this study, bivariate and multivariate analyses were used to identify preoperative clinical characteristics affecting operative time in cataract surgery and to build a predictive model of cataract surgery operative time. Although much of the published literature has examined risk factors for complications in cataract surgery, there is only limited information on factors affecting operative time.^{7,10,30,31,35,36} More accurate prediction of operative time for cataract surgery has the potential to save OR resources and efficiently use surgeon and patient time.

There was a limited correlation between surgeon-planned and actual utilization of OR time. We found no significant difference in the operative time or total OR time between cases with the scheduled duration of 45 minutes and 60 minutes. This contrasted with a significantly shorter operative time and total OR time (both by a mean difference of approximately 6 minutes) for cases scheduled for 30 minutes. These differences in the total case length, albeit small on a case-by-case basis, can cause significant cumulative delays over the course of the full day in the OR.

Perhaps not surprisingly, the strongest predictor of operative time in our analysis was related to the identity of the attending surgeon. Furthermore, a large degree of the overall variability in operative time was explained by the

Table 4. Mean operative time for predictors not included in the final prediction models.

	Mean ± SD	P Value
Age > 90 y		.76
Yes	22.7 ± 6.3	
No	22.1 ± 7.8	
Alpha blocker*		.005
Yes	23.7 ± 6.9	
No	22.0 ± 7.9	
Glaucoma*		.04
Yes	24.2 ± 8.6	
No	22.0 ± 7.8	
Prior ocular surgery*		.19
Yes	21.1 ± 7.4	
No	22.2 ± 7.8	
Surgery of the day		.71
1st	22.5 ± 7.6	
2nd	22.1 ± 7.5	
3rd	22.0 ± 7.7	
4th or more	21.9 ± 8.4	

*Dropped from the prediction model during the manual backward selection process

identity of the surgeon as evidenced by the increased R^2 value in Model 2 ($R^2 = 0.42$) as compared with Model 1 ($R^2 = 0.23$). This suggests that nearly 20% of the variability in operative time is accounted for by a “surgeon factor” (ie, surgeon identity alone) and that this variability is not accounted for by the surgeon’s years of experience or by the level of the surgeon’s trainee. Although the inclusion of attending surgeon identity lessens this model’s generalizability to other institutions, we have included an alternative analysis with variables applicable to all centers.

In Model 1, both attending years of experience and PGY level of the resident serving as the first assistant in the surgery were significantly associated with operative time. Attending surgeons had a significantly and progressively shorter operative time with greater years of experience. Resident trainees demonstrated the opposite effect with increasing PGY associated with longer operative times. This is likely due to the greater involvement of more senior residents in cataract cases. Although primary resident surgeries were excluded from the analysis, assistant cases were not. Whether a case was resident assisted, and the degree to which it was, is not reliably recorded in our institution. Therefore, this variable was not included in the analysis but likely has an impact on operative times.

Predictably, ancillary instruments (iris hooks, Malyugin ring, or trypan blue) used during surgery were highly correlated with longer operative time in both models. For the management of poor pupillary dilation, use of iris hooks was associated with longer operative time than Malyugin ring. Nderitu et al.³⁶ similarly reported longer operative time with pupillary expansion devices with additional operative time of 14 minutes for iris hooks and 4 minutes for pupil expansion ring. Usefulness of these data is dependent on the predictability of their use preoperatively and the identification of

poor pupillary dilation as a preoperative factor. Poor pupillary dilation is often but not always noted in the preoperative period. Similarly, an obscured anterior capsule necessitating the use of trypan blue may be noted in the preoperative period. Intraoperative use of trypan blue is a technically facile procedure, which itself is unlikely to add a significant amount of time to the surgical procedure. The obscuration of the anterior capsule complicating capsulorhexis is likely the true operative time predictor in this instance. Circumstances in which use of ancillary instruments is not predictable, some unforeseen variability in operative time is unavoidable.

Advanced cataract defined as brunescant, mature, Morgagnian, or white was associated with prolonged operative time. Mature and hypermature cataracts are known risk factors for complicated surgery. The Muhtaseb et al.,¹⁷ Buckinghamshire,¹⁸ and Habib et al.¹⁹ criteria all include advanced cataract in their scoring systems for risk of complication in cataract surgery. Achiron et al.⁷ correlated higher risk surgeries by the Muhtaseb scoring system with increased operative time. It is reasonable to suspect that more advanced cataracts would therefore be associated with longer operative times because of increased case difficulty. Although not a direct measure of operative time, there is also a reported association of nuclear density with the total phacoemulsification time.^{37,38}

Interestingly, left operative eye was associated with longer operative time in both models. Although we are not certain of the reason for this difference, it may be due to the anatomical difficulty of a right-handed surgeon operating through superior wounds having to cross the nasal bridge for access. All surgeons in this cohort were right handed, so the subgroup analysis could not be conducted.

Limitations of this study were its retrospective nature and inclusion of cases from a single academic center. Owing to the inclusion of cases with assisting residents, there was a variable degree of trainee involvement, which we could not control for. Factors that are difficult to measure, such as day-to-day variation in surgeon performance, degree of patient cooperation, and equipment malfunctions, were not taken into account. The inclusion of cases such as patients with PXF syndrome and eyes with a history of PPV undoubtedly injected a degree of variability in operative time that may limit the accuracy of the predictive model. However, we aimed to include variables that are commonly collected in clinical practice, making our model practical and applicable in an average operative suite. Furthermore, there is a great deal of coordination at the system level and efforts by the OR staff, which contribute to the efficient utilization of operative resources. This study did not examine these factors, although they are likely an important element to predicting operative time in any surgical procedure. We would predict these factors to be highly institution dependent and, therefore, may require institution-specific data to be addressed.

Strengths of this study include the identification of factors affecting operative time from raw clinical data and limiting reliance on the previously published risk factors for

complication. Future work is necessary to validate the operative time factors and to test the models prospectively.

There is a limited correlation between surgeon-planned and actual utilization of OR time. Surgeon factors, iris challenges, and advanced cataract were most strongly correlated with longer cataract surgery duration. The identification of these and other risk factors may assist surgeons in accurate case scheduling and contribute to more efficient utilization of operative resources.

WHAT WAS KNOWN

- A number of studies have sought to identify preoperative risk factors for complications in cataract surgery.
- Far less is known about the factors affecting operative time in cataract surgery and what preoperative clinical features affect operative time.

WHAT THIS PAPER ADDS

- There was a limited correlation between surgeon-planned and actual utilization of operating room time.
- This is the first large-scale effort to identify the patient-related factors that affect operative time in cataract surgery.
- Two predictive models are presented that may inform more accurate utilization of operating room time.

REFERENCES

1. Shaw AD, Ang GS, Eke T. Phacoemulsification complication rates. *Ophthalmology* 2007;114:2101–2102
2. Lansingh VC, Carter MJ, Martens M. Global cost-effectiveness of cataract surgery. *Ophthalmology* 2007;114:1670–1678
3. Rein DB, Zhang P, Wirth KE, Lee PP, Hoerger TJ, McCall N, Klein R, Tielsch JM, Vijan S, Saaddine J. The economic burden of major adult visual disorders in the United States. *Arch Ophthalmol* 2006;124:1754–1760
4. Congdon N, Vingerling JR, Klein BE, West S, Friedman DS, Kempen J, O'Colmain B, Wu SY, Taylor HR; Eye Diseases Prevalence Research Group. Prevalence of cataract and pseudophakia/aphakia among adults in the United States. *Arch Ophthalmol* 2004;122:487–494
5. Taravella MJ, Davidson R, Erlanger M, Guiton G, Gregory D. Time and cost of teaching cataract surgery. *J Cataract Refract Surg* 2014;40:212–216
6. De Regge M, Gemmel P, Duyck P, Claerhout I. A multilevel analysis of factors influencing the flow efficiency of the cataract surgery process in hospitals. *Acta Ophthalmologica* 2016;94:31–40
7. Achiron A, Haddad F, Gerra M, Bartov E, Burgansky-Eliash Z. Predicting cataract surgery time based on preoperative risk assessment. *Eur J Ophthalmol* 2016;26:226–229
8. Edelman ER, van Kuijk SMJ, Hamaekers AEW, de Korte MJM, van Merode GG, Buhre WFFA. Improving the prediction of total surgical procedure time using linear regression modeling. *Front Med* 2017;4:85
9. Jones JJ, Chu J, Graham J, Zalusk S, Rocha G. The impact of a preloaded intraocular lens delivery system on operating room efficiency in routine cataract surgery. *Clin Ophthalmol* 2016;10:1123–1129
10. Strum DP, Sampson AR, May JH, Vargas LG. Surgeon and type of anesthesia predict variability in surgical procedure times. *Anesthesiology* 2000;92:1454–1466
11. Eijkemans MJ, van Houdenhoven M, Nguyen T, Boersma E, Steyerberg EW, Kazemier G. Predicting the unpredictable: a new prediction model for operating room times using individual characteristics and the surgeon's estimate. *Anesthesiology* 2010;112:41–49
12. Wright IH, Kooperberg PC, Bonar BA, Bashein G. Statistical modeling to predict elective surgery time comparison with a computer scheduling system and surgeon-provided estimates. *Anesthesiology* 1996;85:1235–1245
13. Laskin DM, Abubaker AO, Strauss RA. Accuracy of predicting the duration of a surgical operation. *J Oral Maxill Surg* 2013;71:446–447
14. Narendran N, Jaycock P, Johnston RL, Taylor H, Adams M, Tole DM, Asaria RH, Galloway P, Sparrow JM. The Cataract National Dataset electronic multicentre audit of 55,567 operations: risk stratification for posterior capsule rupture and vitreous loss. *Eye* 2009;23:31–37
15. Fesharaki H, Peyman A, Rowshandel M, Peyman M, Alizadeh P, Akhlaghi M, Ashtari A. A comparative study of complications of cataract surgery with phacoemulsification in eyes with high and normal axial length. *Adv Biomed Res* 2012;1:67
16. Mansour AM, Al-Dairy M. Modifications in cataract surgery for the morbidly obese patient. *J Cataract Refract Surg* 2004;30:2265–2268
17. Muhtaseb M, Kalhoro A, Ionides A. A system for preoperative stratification of cataract patients according to risk of intraoperative complications: a prospective analysis of 1441 cases. *Br J Ophthalmol* 2004;88:1242–1246
18. Butler TK. Risk stratification and assessment in cataract surgery. *J Cataract Refract Surg* 2012;38:184
19. Habib MS, Bunce CV, Fraser SG. The role of case mix in the relation of volume and outcome in phacoemulsification. *Br J Ophthalmol* 2005;89:1143–1146
20. Chakrabarti A, Singh S. Phacoemulsification in eyes with white cataract. *J Cataract Refract Surg* 2000;26:1041–1047
21. Kuchle M, Viestenz A, Martus P, Handel A, Junemann A, Naumann GO. Anterior chamber depth and complications during cataract surgery in eyes with pseudoexfoliation syndrome. *Am J Ophthalmol* 2000;129:281–285
22. Drolsum L, Haaskjold E, Sandvig K. Phacoemulsification in eyes with pseudoexfoliation. *J Cataract Refract Surg* 1998;24:787–792
23. Oshika T, Ohashi Y, Inamura M, Ohki K, Okamoto S, Koyama T, Sakabe I, Takahashi K, Fujita Y, Miyoshi T, Yasuma T. Incidence of intraoperative floppy iris syndrome in patients on either systemic or topical alpha(1)-adrenoceptor antagonist. *Am J Ophthalmol* 2007;143:150–151
24. Chang DF, Campbell JR. Intraoperative floppy iris syndrome associated with tamsulosin. *J Cataract Refract Surg* 2005;31:664–673
25. Chadha V, Borooah S, Tey A, Styles C, Singh J. Floppy iris behaviour during cataract surgery: associations and variations. *Br J Ophthalmol* 2007;91:40–42
26. Gani J, Perlis N, Radomski SB. Urologic medications and ophthalmologic side effects: a review. *Can Urol Assoc J* 2012;6:53–58
27. Haridas A, Syrimi M, Al-Ahmar B, Hingorani M. Intraoperative floppy iris syndrome (IFIS) in patients receiving tamsulosin or doxazosin—a UK-based comparison of incidence and complication rates. *Graefes Arch Clin Exp Ophthalmol* 2013;251:1541–1545
28. Diaz Lacalle V, Orbegozo Garate FJ, Martinez Alday N, Lopez Garrido JA, Aramberri Agesta J. Phacoemulsification cataract surgery in vitrectomized eyes. *J Cataract Refract Surg* 1998;24:806–809
29. Randleman JB, Wolfe JD, Woodward M, Lynn MJ, Cherwek DH, Srivastava SK. The resident surgeon phacoemulsification learning curve. *Arch Ophthalmol* 2007;125:1215–1219
30. Thanigasalam T, Reddy SC, Zaki RA. Factors associated with complications and postoperative visual outcomes of cataract surgery; a study of 1,632 cases. *J Ophthalmic Vis Res* 2015;10:375–384
31. Gupta D, Taravati P. Effect of surgical case order on cataract surgery complication rates and procedure time. *J Cataract Refract Surg* 2015;41:594–597
32. Scorolli L, Scorolli L, Campos EC, Bassein L, Meduri RA. Pseudoexfoliation syndrome: a cohort study on intraoperative complications in cataract surgery. *Ophthalmologica* 1998;212:278–280
33. Ahfat FG, Yuen CH, Groenewald CP. Phacoemulsification and intraocular lens implantation following pars plana vitrectomy: a prospective study. *Eye* 2003;17:16–20
34. Braunstein RE, Airiani S. Cataract surgery results after pars plana vitrectomy. *Curr Opin Ophthalmol* 2003;14:150–154
35. Hosler MR, Scott IU, Kunselman AR, Wolford KR, Oltra EZ, Murray WB. Impact of resident participation in cataract surgery on operative time and cost. *Ophthalmology* 2012;119:95–98
36. Nderitu P, Ursell P. Iris hooks versus a pupil expansion ring: operating times, complications, and visual acuity outcomes in small pupil cases. *J Cataract Refract Surg* 2019;45:167–173
37. Gupta M, Ram J, Jain A, Sukhija J, Chaudhary M. Correlation of nuclear density using the lens opacity classification system III versus Scheimpflug imaging with phacoemulsification parameters. *J Cataract Refract Surg* 2013;39:1818–1823
38. Davison JA, Chylack LT. Clinical application of the lens opacities classification system III in the performance of phacoemulsification. *J Cataract Refract Surg* 2003;29:138–145

Disclosures: None of the authors has a financial or proprietary interest in any material or method mentioned.

Reasons for explantation, demographics, and material analysis of 200 intraocular lens explants

Tabitha Neuhaan, MD, Timur M. Yildirim, MD, Hyeck-Soo Son, MD, Patrick R. Merz, PhD, Ramin Khoramnia, MD, PhD, Gerd U. Auffarth, MD, PhD

Purpose: To report demographics, reasons for explantation, and material changes in explanted intraocular lenses (IOLs).

Setting: The David J. Apple International Laboratory for Ocular Pathology, Department of Ophthalmology, University of Heidelberg, Germany.

Design: Retrospective study laboratory investigation.

Methods: IOL explants that were sent consecutively to the laboratory were assessed for demographics (patient sex and age), duration of implant, IOL type, model, power, and reason for IOL explantation. In opacified lenses histological staining, scanning electron microscopy, and energy-dispersive X-ray spectroscopy was performed.

Results: The analysis included 200 IOLs that were explanted in median after 5.8 years. The median time the IOL was in the eye was

5.8 years. IOL opacification was the main cause for explantation in 153 (76.5%) cases. Only 27 (13.5%) were explanted due to dislocation. Evaluation of IOL type showed that 167 (83.5%) were made from hydrophilic acrylic material, with 125 (62%) from hydrophilic acrylic material with a hydrophobic surface coating. Analysis of opacities revealed superficial and subsurface deposits of calcium phosphate in most of the opacified lenses (152/153). In total, 22 different manufacturers were represented, with 119 (59.5%) lenses from a single manufacturer.

Conclusion: In this cross-sectional study, late IOL calcification was the main reason for IOL explantation. The second most common reason was IOL dislocation. Most explants were lenses from a single manufacturer exchanged due to primary IOL calcification.

J Cataract Refract Surg 2020; 46:20–26 Copyright © 2019 Published by Wolters Kluwer on behalf of ASCRS and ESCRS

Cataract surgery with implantation of an intraocular lens (IOL) is a safe and cost-effective procedure that usually leads to long-lasting visual rehabilitation. Nevertheless, in some cases, the IOL needs to be explanted. There is no single register for explanted IOLs today, but some laboratories have specialized in registering, storing, and analyzing explanted IOLs. Evaluation of such databases might lead to a better understanding of current problems in IOL surgery, thus leading to improvements in IOL technology.

In the 1990s, IOL dislocation, incorrect IOL power, and inflammation were the main reasons for explantation in the David J. Apple Laboratory.¹ Several recent studies reported on IOL explantation due to lens opacities.^{2–4} The

reasons lens opacification develops can depend on the IOL's material. IOLs made from hydrophobic acrylic material can develop liquid-filled vacuoles that can lead to a loss of clarity of the lens.^{3,5} In silicone and hydrophilic acrylic lenses, deposition of calcium phosphate can degrade the optical quality to a point requiring IOL exchange.^{4,6–8}

The reasons for IOL explantation have varied over time, depending on the IOL design, its material, power calculation, and changes in implantation techniques.^{1,9–13}

This study aimed to analyze the demographics, the reasons for explantation, and material changes in a recently explanted group of 200 explants received at our laboratory.

Submitted: July 1, 2019 | Final revision submitted: August 8, 2019 | Accepted: August 26, 2019

From the Department of Ophthalmology, The David J. Apple International Laboratory for Ocular Pathology, University of Heidelberg, Heidelberg, Germany.

T. Neuhaan and T. Yildirim contributed equally to this work.

Supported by Klaus Tschira Stiftung, Heidelberg, Germany. The funding organization had no role in the design or conduct of this research.

Presented at the ASCRS•ASOA Annual Meeting, Washington, DC, April 2018.

The authors thank all ophthalmologists who donated explanted IOLs and provided information about the cases. D.J. Munro made a contribution to the review of the prepublication report.

Corresponding Author: Gerd U. Auffarth, MD, PhD, Department of Ophthalmology, University of Heidelberg, Im Neuenheimer Feld 400, 69120 Heidelberg, Germany. Email: auffarth@aol.com.

METHODS

This was a retrospective cross-sectional study of 200 explanted IOLs that were sent to the David J. Apple International Laboratory for Ocular Pathology in the Department of Ophthalmology of Heidelberg University Hospital. We received the lenses mainly from clinics in Germany and the United Kingdom within a 12-month period (March 2016 to February 2017). Explantation surgery was performed between September 2015 and February 2017. Information about each case was obtained from the donating surgeon using a standard questionnaire form that requested patient data (age and sex), date of IOL implantation/explantation, IOL manufacturer, IOL type, model, power, and reason for explantation. As the standard protocol of our laboratory requires, every IOL explanted from a German surgical center was notified to the Bundesinstitut für Arzneimittel und Medizinprodukte (BfArM—the German Federal Institute for Drugs and Medical Devices).

Handling of the Explants

On receipt, all the information provided by the explanting surgeon was recorded in a data sheet, and the lens was examined under an Olympus BX50 light microscope (Olympus Optical Co., Ltd.). If gross microscopic examination revealed abnormalities, material analysis was performed using a standard protocol as described in several former studies, including histological staining.^{4,6} Where cases required further analysis, part of the lens was sent to the Max Planck Institute for Polymer Research in Mainz, Germany, to perform scanning or transmission electron microscopy, local elementary analysis using energy-dispersive X-ray spectroscopy, or diffraction pattern analysis.^{4,6}

Data Analysis

Descriptive statistics were entered in an Excel data sheet (Excel v14.7.7, Microsoft). Numerical data are presented as mean (\pm SD), median (range), or number (percentage) as appropriate.

RESULTS

Lenses were explanted from 194 patients, 108 female and 83 male. In 3 cases, the patient's sex could not be determined, as only their initials were provided. The mean age of patients at the time of IOL explantation was 74 years (range 19 to 94 years). The mean time the lens was in the eye was 5.8 years \pm 4.5 (SD). The median IOL power was 21.5 D (range 5.0–31.0 D).

Reasons for IOL Explantation

The reasons for IOL explantation are presented in Figure 1. In 4 (2%) cases with a phakic lens, explantation of an

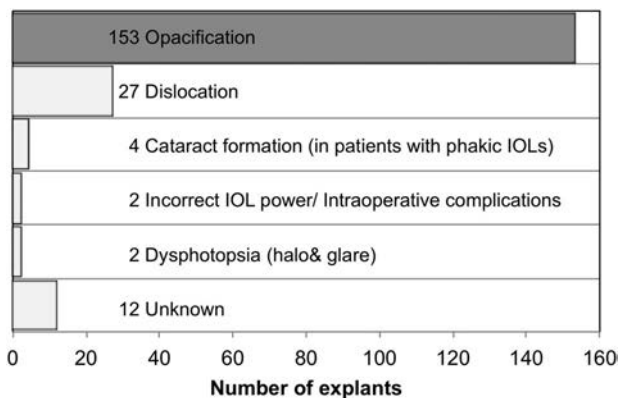


Figure 1. Reasons for IOL explantation. The main reason for explantation in this series of 200 lenses was IOL calcification (76.5%) (IOL = intraocular lens).

anterior chamber IOL was necessary due to development of cataract with subsequent cataract surgery. We recorded no cases of IOLs explanted because of inflammation. Opacification of the IOL mainly occurred within the first 7 years after implantation. The prevalence of dislocation increased with the time the IOL was in the eye (Figure 2).

Gross examination of opacified lenses showed a whitish blurred appearance of the whole lens (optics and haptics) in 134 (67.0%) cases. In 132 (66.0%) cases, histological staining with von Kossa stains (which reveals calcium in subsurface deposits) revealed primary calcification as the reason for the opacity. A band of granular calcium phosphate crystals was found under the whole surface of the IOL including the haptics. In two hydrophobic acrylic IOLs, small vacuoles (glistenings) within the bulk of the lens were identified as the reason for opacification.

In 19 (9.5%) cases, the pattern of secondary IOL calcification was observed as a small circular area of granular deposits on the surface of the lens optic. Alizarin red staining (which reveals calcium in superficial deposits) confirmed central calcification that spared the haptics in these cases. Local energy-dispersive X-ray spectroscopy elementary analysis identified that deposits consist of calcium and phosphorus (Figure 3).

IOL Characteristics

The IOLs analyzed comprised of 188 (94%) posterior chamber lenses and seven (3.5%) anterior chamber lenses. Five IOLs could not be categorized. Distribution of the lens material is shown in Figure 4. Of the 125 hydrophilic lenses with a hydrophobic surface coating, 123 were explanted due to opacification, 1 due to dislocation, and 1 due to dysphotopsia. In total, 21 manufacturers were represented in this study. Twenty-three of the explants could not be allocated to a manufacturer. One company (Oculentis GmbH) represented the largest subgroup, with 119 (59.5%) explants. Lenses from Rayner and Alcon Laboratories, Inc. were represented with 10 IOLs each, followed by Carl Zeiss Meditec AG with 8 lenses, Argonoptics with 6, and J&J

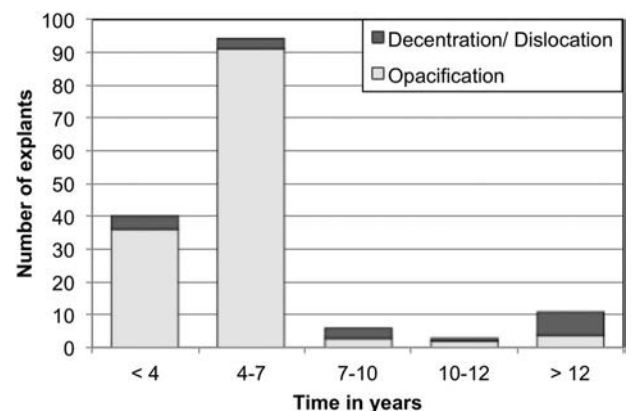


Figure 2. IOL calcification vs IOL dislocation in dependence of the time of IOL explantation. Up to 7 years after initial IOL implantation, calcification was by far the main cause for IOL explantation. In later years (>7 years), IOL dislocation becomes more prevalent (IOL = intraocular lens).

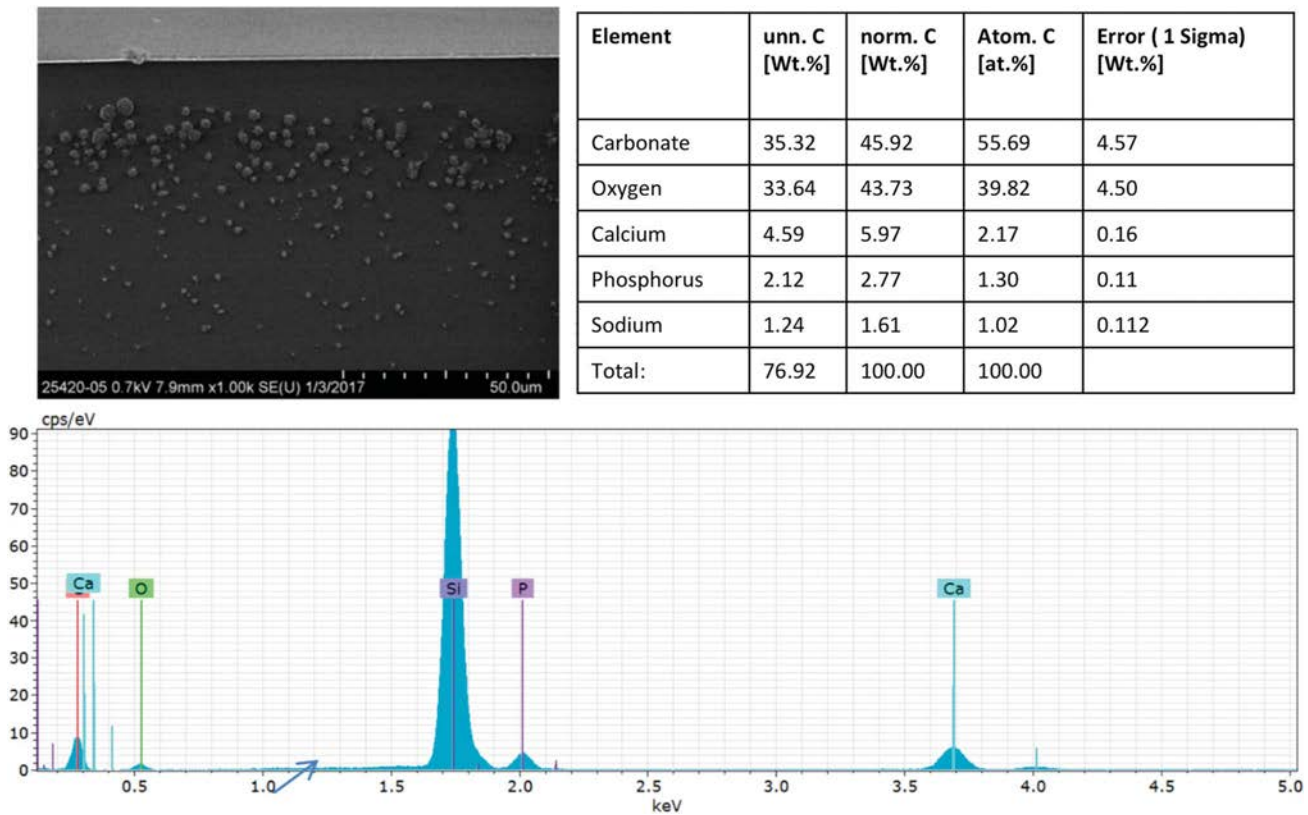


Figure 3. Material analysis of opacified explanted IOLs. Upper left: scanning electron microscopy image showing granular deposits underneath the surface of the IOL. Upper right: deposits mainly consist of calcium and phosphorus. Lower graph shows peaks for the elements found. From left to right: Na, sodium; Ca, calcium; O, oxygen; Si, silicon; P, phosphorus; Ca, calcium. The large silicon peak (Si) is an artifact caused by the silicon wafer used for analysis (IOL = intraocular lens).

Vision and 1stQ with 5 IOLs each. Other manufacturers were represented with 1 IOL each (Table 1). Nine of 10 Rayner lenses were explanted due to secondary IOL calcification and 1 due to IOL dislocation. Six of 10 Alcon lenses were explanted due to dislocation. One lens was explanted due to glistenings, and 1 trifocal IOL model due

to dysphotopsia. In 2 cases, the reason for explanting the Alcon lens could not be determined.

Subgroup Analysis

Apart from 2 lenses, all 119 Oculentis lenses were explanted due to late primary IOL calcification. One LS-313 MF15 was explanted 1 month after implantation due to IOL dislocation, and 1 LS-313 was explanted due to dysphotopsia (halos/glare). Table 2 summarizes the characteristics of the largest subgroup of explanted IOLs including 8 different models: LS-502-1 (43), LS-313 MF30 (39), LS-312 MF30 (11), LS-402 (15), LS-313 MF15 (1), Lentis L-303 (1), LS-313 (1), and LS-312 (5). Three IOLs made from HydroSmart material could not be allocated to a specific IOL model number. All lenses from this subgroup were made from hydrophilic acrylic material with a hydrophobic surface coating. Regarding the IOL design, 104 IOLs had a 1-piece design, and 15 had a three-piece design.

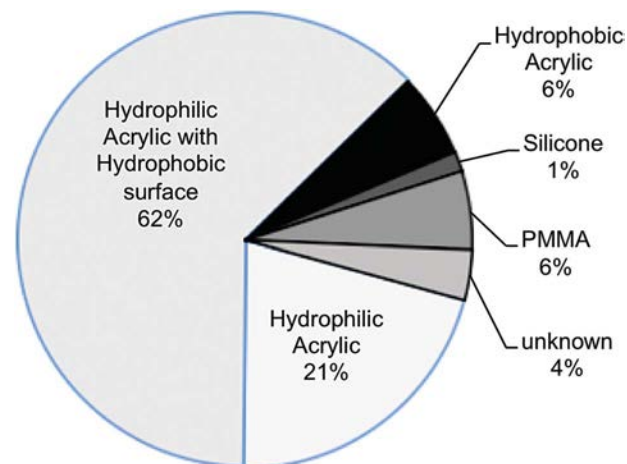


Figure 4. Material distribution of explanted lenses. Most of the explants were classified as hydrophilic acrylic lenses with a hydrophobic surface coating (62%) [PMMA = poly(methyl methacrylate)].

DISCUSSION

The reasons for IOL explantation have changed over time. This is due to a continuous evolution of IOL designs and materials, as well as in surgical techniques and lens power calculation. Our retrospective cross-sectional analysis of 200 lens explantations in the period 2016 to 2017 revealed that the main reason for IOL explantation was late

Table 1. Distribution of IOL manufacturers.

Manufacturer	IOLS (n)
Oculentis GmbH	119
Rayner	10
Alcon Laboratories, Inc.	10
Carl Zeiss Meditec AG	8
Argonoptics	6
1stQ	5
J&J Vision	5
Other manufacturers: Adatomed, Appasamy, Bausch & Lomb, Inc., Croma-Pharma, Hoya Surgical, HumanOptics, Lenstec, Medennium, Mentor Ophthalmics (Ciba Vision), Morcher, Ophtec, Pharmacia, PhysIOL, and W20	1 each
Unknown	23

IOL = intraocular lens

postoperative primary calcification of hydrophilic acrylic IOLs, whereas the second most common reason was IOL dislocation. The high proportion of primary calcification in this group reflects a recent epidemic series of primary IOL calcification in different lens models by Oculentis.

Between 1986 and 1990, the most common reasons for IOL replacement were IOL luxation (36%) and implantation of an IOL with incorrect refractive power (25%).¹⁴ In 100 silicone lenses explanted between 1984 and 1994, IOL dislocation (42%) was the most common reason for explantation, and inflammation (27.7%) and incorrect IOL power (8%) were the second and third most common reasons, respectively.¹ From 1998 to 2004, incorrect IOL power (41.2%), IOL dislocation (37.3%), and dysphotopsia (7.8%) were described as the main reasons.¹⁵ Leysen et al.¹⁶ reported on 128 lens explants from 2002 to 2007: IOL dislocation (37%), IOL opacification (31%), and capsular bag contraction (14%) were the chief reasons for explantation.

A survey from 2003 reported the reasons for IOL explantation according to the lens material and design categories. In accordance with the most commonly used IOLs at that time, three-piece silicone IOLs provided the largest group, with 27% of all IOL explants and the most common reason for silicone IOLs was dislocation (34%).⁹ Fernandez-Buenaga et al.¹⁷ reported on 257 IOLs explanted in Spain. Overall, dislocation was the main reason (56.3%), and incorrect lens power (12.8%) and IOL calcification (11.3%) were the second and third most common reasons, respectively.

In general, IOL opacification can lead to increased light scattering, decreased contrast sensitivity, and deterioration

Table 2. Characteristics of the largest subgroup of explanted IOLs.

Optic Design	IOL Model	Explants (n)	Implantation Time Frame	Explantation Time Frame	Reason for Explantation	IOL Material
Segmented bifocal IOLs	LS-313 MF30	39	April 2010– March 2014	September 2015–June 2016	Calcification	Hydrophilic acrylate with a hydrophobic surface coating
	LS-312 MF30	11	April 2010– October 2014	April 2016–August 2016	Calcification	Hydrophilic acrylate with a hydrophobic surface coating
	LS-313 MF 15	1	May 2016	July 2016	Luxation	Hydrophilic acrylate with a hydrophobic surface coating
Monofocal IOLs	LS-402	15	November 2005– March 2016	March 2016– December 2016	Calcification	Hydrophilic acrylate with a hydrophobic surface coating
	LS-502-1	43	July 2010–July 2012	February 2016–January 2017	Calcification	Hydrophilic acrylate with a hydrophobic surface coating
	LS-312	5	July 2010–May 2012	February 2016– November 2016	Calcification	Hydrophilic acrylate with a hydrophobic surface coating
	LS-303	1	—	November 2016	Calcification	Hydrophilic acrylate with a hydrophobic surface coating
	LS-313	1	—	November 2016	Dysphotopsia	Hydrophilic acrylate with a hydrophobic surface coating
	Unknown HydroSmart	3	September 2010	August 2016–October 2016	Calcification	Hydrophilic acrylate with a hydrophobic surface coating

IOL = intraocular lens

in visual acuity.⁴⁻⁶ Depending on the lens material, IOL opacification has different causation: In lenses made from hydrophobic acrylic material, liquid-filled vacuoles, the so-called glistenings, that develop within the bulk of the lens can opacify the lens material.⁵ In our group, we found only 2 hydrophobic acrylic lenses (one Alcon and one Medennium) that were exchanged because of glistening formation. Generally, surgeons should be careful when deciding to perform an IOL exchange for glistening, as they only cause a decrease in visual performance when present in a very large amount.^{5,18}

IOL calcification is a complication observed in silicone and hydrophilic acrylic lenses. First cases of brown discoloration with central haze in silicone IOLs and nodular geographic calcifications within hydrophilic lenses were reported in the early 1990s.^{19,20} As foldable hydrophilic acrylic IOLs became more popular, on account of the advantages in handling and biocompatibility, reports on IOL calcification became more frequent.

In 2008, David J. Apple and his group proposed a classification of the major types of IOL calcification according to the assumed underlying pathomechanism.²¹ Calcification relating to the IOL itself, they suggested, should be referred to as primary calcification. Eyes and patients are presumed healthy, without comorbidities. The origin of the calcification can be found in the IOL polymer itself, its manufacturing processes, or in its packaging and storage.^{2,6,21-24} On the other hand, secondary calcification described an opacification induced by environmental factors.

Factors considered to increase the risk for secondary IOL calcification include some surgical procedures, such as Descemet membrane endothelial keratoplasty and pars plana vitrectomy; also, ocular or systemic comorbidities, such as diabetes, are linked to calcification.^{4,7,25-27} Tertiary calcification or pseudocalcification refers to a misdiagnosis or false-positive histological staining.²¹

In our study, primary IOL calcification was identified only in lenses from Oculentis, Argonoptics, and Mentor Ophthalmic (Ciba Vision). All calcified lenses from other manufacturers showed the pattern of secondary IOL calcification.

Primary IOL calcification has been reported in different hydrophilic IOL models in the epidemic series in the 2000s: Hydroview (Bausch & Lomb), MemoryLens (Ciba Vision), SC60B-OUV (Medical Developmental Research), and AquaSense (Ophthalmic Innovations International) IOLs.^{22-24,28}

There are also recent, single-incident reports about isolated cases of IOL calcification in Lentis IOL models.²⁹⁻³¹ Gurabardhi et al.² presented a larger series of 71 Lentis IOLs including 6 different models: LS-312/-1Y, LS-402/-1Y, LS-313-1Y, and LS-502-1, showing the pattern of primary IOL calcification. In accordance with their findings, we also found the pattern of primary calcification in all the 123 opacified Oculentis IOLs. Opacification consisted of deposits of calcium phosphate that had accumulated underneath the surface of the whole of both IOL surfaces (Figure 3). To our knowledge, we present the largest series of explanted Oculentis HydroSmart lenses, including IOL

models that have not yet been reported as problematic, including a large number of segmented refractive bifocal premium lenses such as the LS-313/LS-312 MF30. In 2012 and 2014, Oculentis GmbH released urgent field safety notifications about the HydroSmart yellow IOL material, which had been presented sealed in glass vials. It was suggested that the interaction between phosphate crystals originating from the hydration process of the IOL material and the fluctuating batch-related presence of silicone residues on some IOLs promoted the calcification process.^{32,33} In 2017, another urgent field safety notification was released by the company, in which a voluntary recall was offered for all IOL models starting with L, LU, or LS, expiring between January 2017 and May 2020 and that have been manufactured between January 2012 and May 2015. In this notification, it was suggested that calcification might result from phosphate residuals from a detergent used in the cleaning process of the lens.³⁴ As there is a large population of patients who have been treated with hydrophilic IOL models that still might be affected by primary IOL calcification, clinicians should be aware of this complication.

In 19 (9.5%) cases, the pattern of secondary IOL calcification was observed. It should be noted that the high amount of Rayner IOLs in this group (9/20) is predominantly owing to the circumstance that Rayner routinely sends their IOLs to our laboratory for pathological analysis, whereas IOLs from other manufacturers only reach us through the cooperation of individual ophthalmic surgeons. Schrittenlocher et al.³⁵ found in 564 patients who underwent a Descemet membrane endothelial keratoplasty procedure that IOL calcification occurred in 2.5% overall. The incidence was associated with the number of rebubbings patients had received. In a previous study from our laboratory, secondary IOL calcification was found in 10 explanted lenses after pars plana vitrectomy with instillation of gas with similar calcification patterns irrespective of the IOL manufacturer.⁴ In general, secondary IOL calcification can be said to be a rare complication in lenses made of hydrophilic acrylic material, rather than a specific problem of one or more IOL manufacturers.

As stated above, IOL dislocation has always been one of the main causes for lens explantation. This complication not only depends on the surgical technique and IOL design used but also on patient-dependent factors such as the constitution of intraocular anatomical structures. Fernandez-Buenaga and Alio¹² and Pueringer et al.³⁶ suggest that the risk for IOL dislocation increases the longer the IOL is inside of the eye. Similarly, our results show that as the time inside of the eye increases, IOL dislocation becomes more prevalent (Figure 2). Thus, because of an increasing patient age and as a result of a growing pseudophakic population, this complication can be expected to remain a major reason for IOL explantation in the future.¹²

The proportion of explantation due to iatrogenic anisometropia varies from about one third to a tenth of cases.^{14,17} In our 200 explants, only one case was explanted for this reason. One may speculate that it has become less common

because of progress in the use of IOL power calculation formulas, refinements in IOL biometry equipment, improved measuring, and labeling procedures at IOL manufacturing facilities—all or some of that plus the possibility of postoperative power correction (enhancement with laser refractive surgery or implantation of a supplementary IOL).

Intraocular inflammation used to be a major reason for IOL explantation in early studies on explanted lenses, making up one third of all explanted IOLs (27.7%).¹ Presumably, through advances in IOL biocompatibility and surgical techniques, and improved pharmaceutical control, this complication has decreased, making inflammation a less common reason for IOL explantation. Recent literature rarely reports on inflammation as a reason for IOL explantation, and in this group of 200 lenses, no IOL was removed because of intraocular inflammation.

Postoperative photic phenomena depend on a large variety of factors including IOL material, optical design, ocular surface, and retinal function. Although introduction of complex optics that allocate light to more than one focal points can lead to an increased potential for dysphotopsia, IOL explantation due to this reason still is rarely reported. In our study, only one monofocal and one trifocal IOL model required to be removed because of unbearable dysphotopsia.

The retrospective character of this study does not permit conclusions about absolute numbers of explanted IOLs and does not reveal pathomechanism for any of the complications mentioned. Furthermore, it is possible that some reasons for explantation (eg, incorrect IOL power or IOL dislocation) might be underrepresented in this study, as they might be sent for analysis less frequently to our laboratory. Nevertheless, we believe that this cross-sectional report provides important information about trends and changes in the rationale for IOL explantation. This might serve in directing IOL technology to an even safer and more efficient procedure.

This study describes a large series of primary IOL calcification and reports on a shift over time in reasons for IOL explantation. Lenses made from hydrophilic acrylic material (especially Lentis IOL models) bear the risk for late postoperative calcification. The leading cause for IOL opacification (primary IOL calcification) could be avoided if greater care is taken in the production of IOL.

WHAT WAS KNOWN

- Complications and reasons for IOL explantation have changed depending on the IOL design, material, power calculation, and surgical techniques used at a certain period and in a region of the world.
- IOL opacification used to be a rare reason for IOL explantation.

WHAT THIS PAPER ADDS

- In Europe, the main reason for IOL exchange has shifted toward IOL calcification.
- A large number of recent hydrophilic IOL models, including modern refractive bifocal IOLs, required explantation due to primary IOL calcification.

REFERENCES

1. Auffarth GU, Wilcox M, Sims JC, McCabe C, Wesendahl TA, Apple DJ. Analysis of 100 explanted one-piece and three-piece silicone intraocular lenses. *Ophthalmology* 1995;102:1144–1150
2. Gurabardhi M, Haberle H, Aurich H, Werner L, Pham DT. Serial intraocular lens opacifications of different designs from the same manufacturer: clinical and light microscopic results of 71 explant cases. *J Cataract Refract Surg* 2018;44:1326–1332
3. van der Mooren M, Steinert R, Tyson F, Langeslag MJ, Piers PA. Explanted multifocal intraocular lenses. *J Cataract Refract Surg* 2015;41:873–877
4. Yildirim TM, Auffarth GU, Labuz G, Bopp S, Son HS, Khoramnia R. Material analysis and optical quality assessment of opacified hydrophilic acrylic intraocular lenses after Pars plana vitrectomy. *Am J Ophthalmol* 2018;193:10–19
5. Labuz G, Knebel D, Auffarth GU, Fang H, van den Berg T, Yildirim TM, Son HS, Khoramnia R. Glistening formation and light scattering in six hydrophobic-acrylic intraocular lenses. *Am J Ophthalmol* 2018;196:112–120
6. Khoramnia R, Salgado JP, Auffarth GU, Schmidt S, Wegner A, Kobuch KA, Winkler von Mohrenfels C. Opacification of a hydrophilic intraocular lens 4 years after cataract surgery. A biomaterial analysis [in German]. *Ophthalmologie* 2012;109:483–486
7. Kim CJ, Choi SK. Analysis of aqueous humor calcium and phosphate from cataract eyes with and without diabetes mellitus. *Korean J Ophthalmol* 2007;21:90–94
8. Stringham J, Werner L, Monson B, Theodosis R, Mamalis N. Calcification of different designs of silicone intraocular lenses in eyes with asteroid hyalosis. *Ophthalmology* 2010;117:1486–1492
9. Mamalis N, Davis B, Nilson CD, Hickman MS, LeBoyer RM. Complications of foldable intraocular lenses requiring explantation or secondary intervention—2003 survey update. *J Cataract Refract Surg* 2004;30:2209–2218
10. Jones JJ, Jones YJ, Jin GJ. Indications and outcomes of intraocular lens exchange during a recent 5-year period. *Am J Ophthalmol* 2014;157:154–162.e151
11. Chai F, Ma B, Yang XG, Li J, Chu MF. A pilot study of intraocular lens explantation in 69 eyes in Chinese patients. *Int J Ophthalmol* 2017;10:579–585
12. Fernandez-Buenaga R, Alio JL. Intraocular lens explantation after cataract surgery: indications, results, and explantation techniques. *Asia Pac Journal Ophthalmol* 2017;6:372–380
13. Szigiato AA, Schlenker MB, Ahmed IJK. Population-based analysis of intraocular lens exchange and repositioning. *J Cataract Refract Surg* 2017;43:754–760
14. Lyle WA, Jin JC. An analysis of intraocular lens exchange. *Ophthalmic Surg* 1992;23:453–458
15. Jin GJ, Crandall AS, Jones JJ. Changing indications for and improving outcomes of intraocular lens exchange. *Am J Ophthalmol* 2005;140:688–694
16. Leysen I, Bartholomeeusen E, Coeckelbergh T, Tassignon MJ. Surgical outcomes of intraocular lens exchange: five-year study. *J Cataract Refract Surg* 2009;35:1013–1018
17. Fernandez-Buenaga R, Alio JL, Munoz-Negrete FJ, Barraquer Compte RI, Alio-Del Barrio JL. Causes of IOL explantation in Spain. *Eur J Ophthalmol* 2012;22:762–768
18. Weindler JN, Labuz G, Yildirim TM, Tandogan T, Khoramnia R, Auffarth GU. The impact of glistenings on the optical quality of a hydrophobic acrylic intraocular lens. *J Cataract Refract Surg* 2019;45:1020–1025
19. Milauskas AT. Silicone intraocular lens implant discoloration in humans. *Arch Ophthalmol* 1991;109:913–915
20. Bucher PJ, Buchi ER, Daicker BC. Dystrophic calcification of an implanted hydroxyethylmethacrylate intraocular lens. *Arch Ophthalmol* 1995;113:1431–1435
21. Neuhann IM, Kleinmann G, Apple DJ. A new classification of calcification of intraocular lenses. *Ophthalmology* 2008;115:73–79
22. Habib NE, Freegard TJ, Gock G, Newman PL, Moate RM. Late surface opacification of Hydroview intraocular lenses. *Eye* 2002;16:69–74
23. Tehrani M, Mamalis N, Wallin T, Dick HB, Stoffels BM, Olson R, Fry LL, Clifford WS. Late postoperative opacification of MemoryLens hydrophilic acrylic intraocular lenses: case series and review. *J Cataract Refract Surg* 2004;30:115–122
24. Frohn A, Dick HB, Augustin AJ, Grus FH. Late opacification of the foldable hydrophilic acrylic lens SC60B-OUV. *Ophthalmology* 2001;108:1999–2004
25. Giers BC, Tandogan T, Auffarth GU, Choi CY, Auerbach FN, Sel S, Mayer C, Khoramnia R. Hydrophilic intraocular lens opacification after posterior lamellar keratoplasty—a material analysis with special reference to optical quality assessment. *BMC Ophthalmol* 2017;17:150
26. Labuz G, Yildirim TM, van den Berg T, Khoramnia R, Auffarth GU. Assessment of straylight and the modulation transfer function of intraocular lenses with centrally localized opacification associated with the intraocular injection of gas. *J Cataract Refract Surg* 2018;44:615–622

27. Marcovich AL, Tandogan T, Bareket M, Eting E, Kaplan-Ashiri I, Bukelman A, Auffarth GU, Khoramnia R. Opacification of hydrophilic intraocular lenses associated with vitrectomy and injection of intraocular gas. *BMJ Open Ophthalmol* 2018;3:e000157
28. Dargès E, Khan MA, Kyle GM, Clark D. Perioperative complications of intraocular lens exchange in patients with opacified Aqua-Sense lenses. *J Cataract Refract Surg* 2004;30:2569–2573
29. Cavallini GM, Volante V, Campi L, De Maria M, Fornasari E, Urso G. Postoperative diffuse opacification of a hydrophilic acrylic intraocular lens: analysis of an explant. *Int Ophthalmol* 2018;38:1733–1739
30. Bompastor-Ramos P, Povoja J, Lobo C, Rodriguez AE, Alió JL, Werner L, Murta JN. Late postoperative opacification of a hydrophilic-hydrophobic acrylic intraocular lens. *J Cataract Refract Surg* 2016;42:1324–1331
31. Gartaganis SP, Prahs P, Lazari ED, Gartaganis PS, Helbig H, Koutsoukos PG. Calcification of hydrophilic acrylic intraocular lenses with a hydrophobic surface: laboratory analysis of 6 cases. *Am J Ophthalmol* 2016;168:68–77
32. Oculentis. Field Safety Notice from Oculentis GmbH: Recall for LENTIS HydroSmart foldable intraocular lenses in glass vials. 2014. Accessed January 3, 2019
33. Oculentis. Field Safety Notice from Oculentis GmbH: Recall of several LENTIS IOL models (in glass vials). 2012. Accessed January 3, 2019
34. Oculentis. Field Safety Notice from Oculentis GmbH: Recall for Lentis L or LS or LU. 2017. Accessed January 3, 2019
35. Schrittenlocher S, Penier M, Schaub F, Bock F, Cursiefen C, Bachmann B. Intraocular lens calcifications after (triple-) Descemet Membrane endothelial keratoplasty. *Am J Ophthalmol* 2017;179:129–136
36. Pueringer SL, Hodge DO, Erie JC. Risk of late intraocular lens dislocation after cataract surgery, 1980-2009: a population-based study. *Am J Ophthalmol* 2011;152:618–623

Disclosures: Dr. Auffarth and Dr. Khoramnia report grants, personal fees, and nonfinancial support from Alcon Laboratories, Inc., Johnson & Johnson Vision Care, Inc., Oculentis GmbH, Hoya, Kowa, Rayner, Siff, Presbia, Oculus, Ursapharm, Glaukos, and Carl Zeiss Meditec AG; grants and personal fees from Bausch & Lomb, Inc. and Biotech; grants and nonfinancial support from Santen and Alimera; and grants from Acufocus, Physiol, Anew, and Contamac, outside the submitted work. Dr. Yildirim and Dr. Son report nonfinancial support from Alcon Laboratories, Inc., outside the submitted work. None of the authors has a financial or proprietary interest in any material or method mentioned.



First author:

Tabitha Neuhann, MD

Department of Ophthalmology, The David J. Apple International Laboratory for Ocular Pathology, University of Heidelberg, Heidelberg, Germany.

ARTICLE

Comparison of formula accuracy for intraocular lens power calculation based on measurements by a swept-source optical coherence tomography optical biometer

Giacomo Savini, MD, Kenneth J. Hoffer, MD, FACS, Nicole Balducci, MD, Piero Barboni, MD, Domenico Schiano-Lomoriello, MD

Purpose: To analyze the results of intraocular lens (IOL) power calculation using measurements by a swept-source optical coherence tomography (SS-OCT) optical biometer.

Setting: IRCCS G.B. Bietti Foundation, Rome, Italy.

Design: Evaluation of a diagnostic test instrument.

Methods: Preoperative measurements by the OA-2000 (Tomey Inc.) were taken in a consecutive series of patients undergoing cataract surgery with one IOL model (AcrySof SN60WF; Alcon Laboratories, Inc.). Measurements were entered into the following formulas: Barrett Universal II, Emmetropia Verifying Optical (EVO), Haigis, Hoffer Q, Holladay 1, Holladay 2, Holladay 2 with axial length adjustment, Kane, Olsen, Panacea, SRK/T, T2, and VRF. When refraction was measured at 1 month postoperatively, the mean arithmetic prediction error, the median absolute error (MedAE), and the percentage of eyes with a error of ± 0.50 D or less were calculated after constant optimization.

Results: We enrolled 150 eyes. All formulas yielded excellent outcomes. The MedAE ranged between 0.200 D and 0.259 D, with a statistically significant difference among formulas ($P = .0004$). The lowest MedAE values were obtained with the Barrett, EVO, Kane, Olsen_{standalone}, Radial Basis Function (RBF), and T2 formulas. The percentage of eyes with a prediction error of ± 0.50 D or less ranged between 80.00% and 90.67%, with a statistically significant difference ($P < .0001$). The Barrett, EVO, Holladay 2 with axial length adjustment, Kane, RBF, and T2 achieved the highest percentages ($\geq 88\%$).

Conclusions: Measurements provided by the SS-OCT optical biometer enable accurate IOL power calculation because all formulas yielded a prediction error within 0.50 D in at least 80% of eyes.

J Cataract Refract Surg 2020; 46:27–33 Copyright © 2019 Published by Wolters Kluwer on behalf of ASCRS and ESCRS

The OA-2000 (Tomey Corp.) is an optical biometer based on swept-source optical coherence tomography (SS-OCT). Previous studies have shown that it provides repeatable and reproducible measurements that are similar to those of the main benchmark for comparison, the IOLMaster 500 (Carl Zeiss Meditec).¹ We have shown that such measurements lead to accurate intraocular lens (IOL) power calculation when entered into standard theoretical thin-lens vergence formulas,² such as the Hoffer Q, Holladay 1, and SRK/T.^{3–5} Recently, however, several new formulas have been introduced, and authors using either the IOLMaster 500 or the Lenstar (Haag-Streit AG), have found that some of them are more accurate than the older standard

formulas.^{6–8} The aim of this study was to investigate the refractive outcomes of older and new formulas using the measurements provided by the OA-2000.

METHODS

This was a prospective interventional study. Consecutive patients having cataract surgery and implanted with nontoric, nonmultifocal IOLs were enrolled between March 2016 and December 2018 at Fondazione G.B. Bietti. Exclusion criteria were previous corneal or intraocular surgery, keratoconus and other corneal disease, contact lens usage during the previous month, and postoperative corrected distance visual acuity lower than 0.8 (20/25). Patients were also excluded when optical biometry measurements were not possible because of lens opacities (graded using Lens Opacities Classification System III).⁹ Before being included in the study, all patients were informed of its purpose and gave their written consent. The

Submitted: June 4, 2019 | Final revision submitted: July 11, 2019 | Accepted: August 26, 2019

IRCCS-G.B. Bietti Foundation (Savini, Balducci, Schiano-Lomoriello), Rome, Studio Oculistico d'Azeglio (Barboni), Bologna, San Raffaele Hospital (Barboni), Milan, Italy; Stein Eye Institute (Hoffer), University of California, Los Angeles, St. Mary's Eye Center (Hoffer), Santa Monica, California, USA.

The IRCCS -G.B. Bietti Foundation was supported by the Italian Ministry of Health and Fondazione Roma.

Corresponding Author: Giacomo Savini, MD, IRCCS -G.B. Bietti Foundation, Via Livenza, 3 -Rome, Italy. Email: giacomo.savini@alice.it.

study protocol was approved by the Ethics Committee of the G.B. Bietti Foundation, and the study complied with the tenets of the Declaration of Helsinki.

Phacoemulsification was performed through a 2.75 mm temporal incision under topical anesthesia. All patients received the same IOL (AcrySof SN60WF; Alcon Laboratories, Inc.) so that formula constant optimization could be performed according to the protocols recommended by Hoffer et al.¹⁰

Before surgery, all patients underwent optical biometry with the OA-2000. This instrument combines an optical biometer, based on SS-OCT, and a Placido ring topographer. It can measure axial length (AL), keratometry (K), anterior chamber depth (ACD, measured from the epithelium to the lens), lens thickness (LT), corneal diameter, central corneal thickness, and pupil diameter. The SS-OCT uses a wavelength of 1060 nm. Placido disk corneal topography can simultaneously measure the radius of curvature of the cornea (r) at diameters of 2.5 mm and 3.0 mm, and K is calculated using the keratometric index of $n = 1.3375$. For the purposes of this study, the 2.5 mm diameter was selected, and the mean (K_m) of the flattest (K_f) and steepest (K_s) meridian was recorded.

Intraocular lens power was calculated according to the following formulas:

- Barrett Universal II (hereafter simply referred to as the “Barrett”): this formula is included in the current software of the optical biometer and its constant, known as the Lens Factor, is calculated from the A-constant. Because the formula is not published and cannot be entered into an Excel (Microsoft Corporation) file, it is difficult to optimize its constant. Optimization and data analysis, therefore, were performed for us by Dr. Barrett himself.¹¹
- Emmetropia Verifying Optical (EVO) formula: this unpublished formula, developed by Tun Kuan Yeo, MD, is available at www.evoiolcalculator.com (accessed on May 3, 2019). Because the formula is not published and cannot be entered into an Excel file, it is difficult to optimize its constant. Optimization and data analysis, therefore, were performed for us by Dr. Yeo himself.
- Haigis: the original formula was computed in Excel, and triple optimization was performed according to the method described by Haigis, that is, using multiple linear regression to correlate d (dependent variable) with preoperative ACD and AL (independent variables).^{12,13}
- Hoffer Q: the formula was computed on Excel, and constant optimization was performed using the Excel “goal/seek” tool.^{3,10}
- Holladay 1: the original formula was computed on Excel, and constant optimization was performed using the Excel goal/seek tool.^{4–10}
- Holladay 2: this formula, which is unpublished, was accessed on Holladay software (version 2019.0302; Holladay Consultant Software & Surgical Outcomes Assessment), whose latest version contains, as an option, a nonlinear AL adjustment for eyes longer than 24.0 mm. The following parameters were entered into the software: age, AL, K_f , K_s , ACD, corneal diameter, and LT. Calculations were performed with and without AL adjustment, and the constant was optimized by the software itself.¹⁴
- Kane: this unpublished formula, developed by Jack Kane, MD, is available at www.iolformula.com (accessed on May 3, 2019). According to the author, it “is based on theoretical optics and also incorporates regression and artificial intelligence components.”¹⁵ It uses AL, K , ACD, and patient sex along with optional variables of LT and central corneal thickness to predict the refractive outcome. Because the formula is not published and cannot be entered into an Excel file, it is difficult to optimize its constant. Optimization and data analysis, therefore, were performed for us by Dr. Kane himself.
- Olsen: the version of this formula included in the optical biometer software (Olsen_{SS-OCT}) is the one based on the C-constant,¹⁶ where the IOL position is predicted from the

ACD and LT. We analyzed this version and the one available in PhacoOptics software (version 1.10.100.2032; IOL innovations), which can predict the IOL position from 4 parameters: AL, K , ACD, and LT (Olsen_{standalone}).

- Panacea: this unpublished formula, developed by David Flikier, MD, is available for free at www.panaceaiolandtoriccalculator.com (accessed on May 3, 2019). It is a thin-lens vergence formula that features the unique possibility of including the anterior-to-posterior corneal curvature ratio and the asphericity (Q value) of the anterior corneal surface. These values were obtained from a rotating Scheimpflug camera combined with Placido disk topography (Sirius, Schwind eye-tech-solutions GmbH & Co. KG). Because the formula is not published and cannot be entered into an Excel file, the value of the optimized A-constant had to be empirically derived by reiteration with multiple attempts until a zero mean prediction error (PE) was obtained.
- Radial Basis Function (RBF): version 2.0, available at www.rbfcalculator.com (accessed on May 3, 2019), was used. The optimized A-constant calculated from the SRK/T formula was entered into the online calculator.
- SRK/T: the original formula was programmed on Excel, and constant optimization was performed using the goal/seek tool.^{5,10}
- T2: this formula was published as an improvement over the SRK/T.¹⁷ The formula was computed on Excel, and constant optimization was performed using the Excel goal/seek tool.¹⁰
- VRF-IOL: the results of this formula, developed by Oleksiy V. Voytsekhivskyy, MD,¹⁸ were obtained after entering the biometric measurements in the specific software (VIOL Commander V.2.0.0.0.). Optimization and data analysis were performed for us by Dr. Voytsekhivskyy himself.

A final evaluation was performed by assessing the postoperative subjective refractive outcomes 1 month postoperatively, which is when refractive stability can be expected with small-incision clear corneal surgery and this type of IOL.¹⁹ Postoperative subjective refraction was measured at 4 m and then adjusted to infinity by subtracting 0.25 D, as recommended by Simpson and Charman.²⁰ The PE was calculated as the difference between the measured and predicted postoperative refractive spherical equivalent for the IOL power implanted (measured refraction – predicted refraction). A negative PE value indicates that the result achieved was more myopic than the predicted refraction, whereas a positive refractive prediction error represents a more hyperopic result. A calculation was made of the mean error, the median absolute error (MedAE), and the mean absolute error, as well as the rate of eyes with a PE $\leq \pm 0.50$ D.^{10,21}

Predictions made using each formula were optimized in retrospect by adjusting the respective constants to give an arithmetic PE of zero in the average case. As a result of constant optimization, it was possible to evaluate the statistical error as representing the optimum prediction error rather than offset errors related to incorrect lens constants or systematic errors in the measuring environment.

Statistical Analysis

Normality of data distribution was assessed by means of the Kolmogorov–Smirnov test. Comparison of the arithmetic PEs was performed by repeated-measures analysis of variance (ANOVA). Comparison of the absolute errors was performed by means of the Friedman test (nonparametric ANOVA) with the Dunn post-test. The Cochran Q test was used to compare the percentage of eyes within ± 0.50 D of the predicted refraction. A P value less than .05 was considered statistically significant. For patients who had bilateral surgery, only the first eye operated on was considered for statistical analysis. All statistical analyses were performed using GraphPad software (version 3.1; Instat) and MedCalc (version 12.3.0; MedCalc Software Inc.).

The distribution of the absolute PEs was graphically shown by means of box-and-whisker plots, where the central box represents the values from the lower to the upper quartile (25th to 75th percentile), the middle line represents the median value, and the horizontal lines represent the minimum and maximum values, excluding outliers and far out values, which are displayed as separate points. An outlier is defined as a value that is smaller than the lower quartile minus 1.5 times the interquartile range or larger than the upper quartile plus 1.5 times the interquartile range. A far out value is defined as a value that is smaller than the lower quartile minus three times the interquartile range or larger than the upper quartile plus three times the interquartile range.

Based on power and sample size calculations performed using the PS program (version 3.0.12; Dupont WD, Plummer WD Jr. PS: Power and Sample Size Calculation, version 3.0. Nashville, TN, Department of Biostatistics, Vanderbilt University, 2012. Available at: <http://biostat.mc.vanderbilt.edu/wiki/bin/view/Main/PowerSampleSize>), it was estimated that a sample size of 21 eyes would be necessary to detect a difference in median absolute error of 0.05 D with a power of 95% at a significance level of 5%, given a within-subject SD for simulated keratometry equal to 0.06 D.¹

RESULTS

We enrolled 155 eyes of 155 patients; 4 cases subsequently had to be excluded because the target refraction was too myopic for the RBF formula (between -3.25 D and -5.00 D) and 1 eye because of impossibility to achieve a correct AL measurement (in this case, the eye was classified as NO5, NC5, C5, and P5 according to the Lens Opacities Classification System III). Thus, the final analysis was performed on 150 eyes of 150 patients [mean age: 77.2 ± 10.0 years; men: 88 (58.7%)]. Table 1 contains the mean values of the measured parameters. Based on AL, 3 (2.00%) eyes were classified as short (<22.00 mm), 100 (66.67%) as medium (22.00 to 24.50 mm), 29 (19.33%) as medium long (24.51 to 26.00 mm), and 19 (12.67%) as long (>26.00 mm).

Table 2 shows the optimized constants and the refractive outcomes of all formulas for the 150 eyes investigated in the present study. The optimized constants with the OA-2000 are slightly higher than those available on the User Group for Laser Interference Biometry website (<http://ocusoft.de/ulib/c1.htm>, accessed on May 3, 2019), where the pACD of the Hoffer Q is 5.64, the Surgeon Factor of the Holladay 1 is 1.84, and the A-constant of the SRK/T is 119.0.

Repeated-measures ANOVA did not reveal any statistically significant difference for the mean PE ($P = .2728$), which was close to zero with all formulas due to constant optimization. Comparison of the absolute prediction errors, on the other hand, revealed a statistically significant difference ($P = .0004$). The lowest MedAE values were achieved with the following formulas: Kane (0.200 D), T2 (0.200 D), Barrett (0.202 D), EVO (0.205 D), RBF (0.205 D), Olsen_{standalone} (0.209 D), and VRF (0.215 D). Dunn post-test analysis showed that only the following paired comparison had statistically significant differences ($P < .005$): EVO vs Haigis, EVO vs Hoffer Q, and RBF vs Haigis.

Figure 1 shows the box-and-whisker plots and the distribution around the MedAE for the investigated formulas.

Table 1. Mean values of the parameters measured by the optical biometer.

	Mean (\pm SD)	Range
AL (mm)	24.23 \pm 1.72	20.49 to 30.62
Corneal power (D)	43.52 \pm 1.40	40.37 to 47.97
Corneal astigmatism (D)	0.56 \pm 0.33	0.05 to 1.81
CD (mm)	11.96 \pm 0.48	9.48 to 13.15
ACD (mm)	3.18 \pm 0.42	2.19 to 4.08
LT (mm)	4.69 \pm 0.42	3.29 to 5.54

ACD = anterior chamber depth (measured from the corneal epithelium to the lens); AL = axial length; CD = corneal diameter; LT = lens thickness

The most interesting finding is the lack of far outliers for most of the recent formulas: Barrett, EVO, Kane, Olsen_{standalone}, T2, and VRF. The Holladay 2 (with and without AL adjustment) and the SRK/T, although they do not belong to the last generation formulas, similarly did not show far outliers. In contrast, a few far outliers were produced by older formulas such as the Haigis, Hoffer Q, and Holladay 1 and newer formulas such as the RBF and Panacea.

With all formulas, the PE was ± 0.50 D or less in at least 80% of eyes (Table 2 and Figure 2). The highest percentages were achieved with the EVO and RBF (90.67%), followed by the Kane (90.00%), Holladay 2 with AL adjustment and Olsen_{standalone} (89.33%), T2 (88.67%), and Barrett (88%) formulas. Interestingly, good outcomes were also obtained with more traditional vergence formulas (Haigis, Hoffer Q, Holladay 1, and SRK/T), which generated a PE within 0.50 D in a percentage of eyes between 84.67% and 85.33%. According to the Cochran Q test, the proportion of eyes with a PE within 0.50 D was statistically significantly different ($P < .0001$) among the investigated formulas. Table 3 shows the results of post-test multiple comparisons. Interestingly, we found that nine formulas yielded a percentage of eyes with a PE within 0.25 D higher than 55%.

We also investigated the subgroup of long eyes (AL > 26.0 mm). Their outcomes are reported in Table 4, which shows that many formulas were able to achieve more than 80% of eyes with a PE of ± 0.50 D or less. These include the Barrett (84.21%), EVO (89.47%), Haigis (84.21%), Holladay 2 with AL adjustment (84.21%), Kane (94.74%), Olsen_{SS-OCT} (84.21%), Olsen_{standalone} (89.47%), RBF (94.74%), SRK/T (84.21%), and T2 (89.47%).

DISCUSSION

The present investigation was designed to assess the refractive outcomes of IOL power calculation using the measurements provided by the SS-OCT optical biometer and the newest and older formulas. The outcomes we obtained exceeded our expectations because all formulas, including the older ones (ie, the Haigis, Hoffer Q, Holladay 1, and SRK/T), achieved a PE of ± 0.50 D or less in at least 80% of eyes. With 11 formulas out of 15, the percentage was even higher than 85%, and with two formulas, it was higher than 90%. To our knowledge, only

Table 2. Refractive outcomes obtained with the formulas investigated and the biometric measurements obtained with the SS-OCT optical biometer.

	Optimized Constant	PE \pm SD	MedAE	MAE	PE \leq 0.25 D	PE \leq 0.50 D	PE \leq 0.75 D	PE \leq 1.00 D
Barrett	1.92	0.005 \pm 0.323	0.202	0.253	62.00	88.00	95.33	100.00
EVO	118.95	0.000 \pm 0.306	0.205	0.240	59.33	90.67	98.00	100.00
Haigis	-1.89	0.002 \pm 0.400	0.254	0.307	52.00	84.67	93.33	98.00
	0.14							
	0.28							
Hoffer Q	5.67	0.000 \pm 0.395	0.248	0.307	52.67	85.33	94.67	97.33
Holladay 1	1.91	0.000 \pm 0.407	0.249	0.306	52.00	85.33	93.33	96.67
Holladay 2	5.52	-0.020 \pm 0.417	0.228	0.279	54.67	86.67	95.33	98.00
Holladay 2 (adjusted AL)	5.52	-0.076 \pm 0.325	0.225	0.266	56.00	89.33	97.33	99.33
Kane	119.05	0.000 \pm 0.342	0.200	0.257	62.00	90.00	97.33	100.00
Olsen _{SS-OCT}	Not available	0.013 \pm 0.378	0.240	0.294	53.33	84.00	95.33	98.67
Olsen _{standalone}	Not available	-0.010 \pm 0.326	0.209	0.256	60.67	89.33	90.00	100.00
Panacea	118.90	-0.006 \pm 0.413	0.248	0.314	51.33	80.00	95.33	96.67
RBF	119.12	0.037 \pm 0.335	0.205	0.252	59.33	90.67	96.00	99.33
SRK/T	119.12	0.001 \pm 0.344	0.221	0.262	59.33	84.67	97.33	100.00
T2	119.04	0.001 \pm 0.328	0.200	0.257	61.33	88.67	96.00	100.00
VRF	5.58	0.000 \pm 0.340	0.210	0.262	59.33	86.00	96.66	99.33

AL = axial length; EVO = Emmetropia Verifying Optical; MAE = mean absolute error; MedAE = median absolute error; PE = prediction error; RBF = Radial Basis Function; SS-OCT = swept-source optical coherence tomography

rarely have similar results been reported before.^{22,23} Even more interestingly, with 9 formulas, more than 55% of eyes had a PE within 0.25 D: we should remember that according to the benchmark established by the National Health Service of the United Kingdom, this percentage should be reached for eyes with a PE within 0.50 and not 0.25 D.²⁴ This finding demonstrates the improved accuracy of IOL power calculation because the standards were published 10 years ago.

In a previous multicenter study with the same optical biometer and the same IOL model, we obtained lower

percentages with the older formulas, as the PE of ± 0.50 D or less was reached in a percentage of eyes ranging between 67.1% (SRK/T) and 71.5% (Hoffer Q).² The improvement between the previous and the current study can be related to at least two factors: first, because in this study, all eyes were operated on by the same surgeon, constant optimization did not have to compensate for different surgical techniques, such as different capsulorhexis size, which influence the postoperative IOL position; second, the postoperative refraction was assessed by the same surgeon, who measured it with the maximum attention.

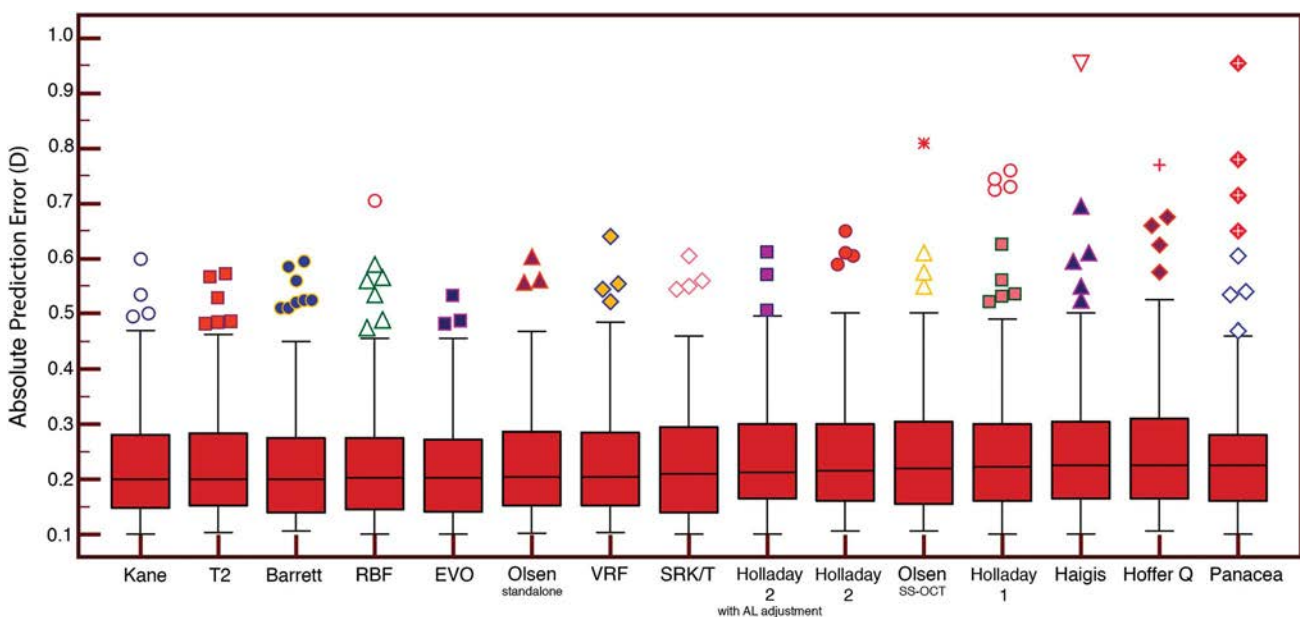


Figure 1. Distribution of the absolute prediction errors. Formulas are ranked according to the median absolute error, increasing from left to right (EVO = Emmetropia Verifying Optical; RBF = Radial Basis Function).

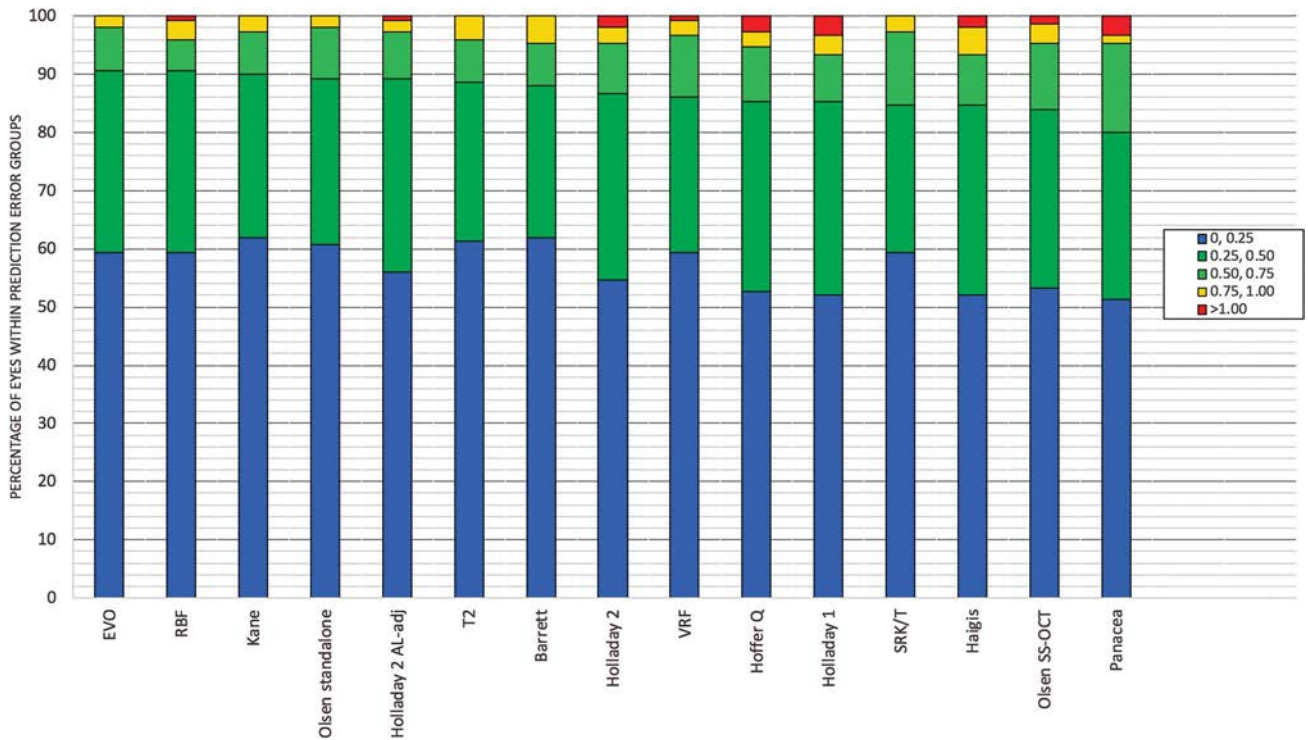


Figure 2. Stacked histogram comparing the percentage of cases with a given prediction error. Formulas are ranked according to the higher percentage for the prediction error within 0.50 D (EVO = Emmetropia Verifying Optical; RBF = Radial Basis Function; SS-OCT = swept-source optical coherence tomography).

Our results are considerably better also when compared with those previously reported by several authors, who investigated the accuracy of IOL power calculation with different formulas, different biometers, and the same IOL model as in our study.⁶⁻⁸ Table 5 clearly reveals the better

outcomes obtained with the SS-OCT optical biometer compared with those previously reported. Possible explanations for such a difference include the fact that both surgery and the assessment of postoperative refraction were performed in all cases by the same surgeon, as noted above. Moreover, our sample included only a small fraction of eyes with an AL shorter than 22.0 mm: short eyes are known to have poorer refractive outcomes,⁶ which can influence the results in the whole sample. It is likely that a larger proportion of short eyes would lead to worse results.

To our knowledge, the studies with the results most similar to the ones reported here were published in 2017 and 2018 by our own group, when we analyzed the results of IOL power calculation with two different optical biometers: the Aladdin (Topcon Europe) and the Galilei G6 (Ziemer Ophthalmology GmbH). In both studies, all patients received the same type of surgery and IOL model as in this investigation. In the first study, the percentage of eyes with a PE of ± 0.50 D or less, as calculated by the Hoffer Q, Holladay 1, and SRK/T formulas, was even higher, as it ranged between 87.67% and 89.04%. The MedAE was 0.25 D for all formulas.²² In the second study, we found that the MedAE was 0.19 D for the Barrett formula and ranged between 0.23 D and 0.26 D for older formulas. Similarly, the percentages of eyes with a PE of ± 0.50 D or less were also close to the ones found in the current study, as they ranged between 80.88% and 83.82%.²³ The good results reported by our group are likely to be due to the factors explained above.

Table 3. Multiple comparisons according to the Cochran Q test.	
Formula	Different ($P < .05$) from Formula Number
Barrett Universal II	(11)
EVO	(3), (4), (5), (9), (11), (13)
Haigis	(2), (8), (12)
Hoffer Q	(2), (11), (12)
Holladay 1	(2), (11), (12)
Holladay 2	(11)
Holladay 2 with AL adjustment	(9), (11)
Kane	(3), (9), (11), (13)
Olsen _{SS-OCT}	(2), (7), (8), (10), (12)
Olsen _{standalone}	(9), (11)
Panacea	(1), (2), (4), (5), (6), (7), (8), (10), (12), (14), (15)
RBF	(3), (4), (5), (9), (11), (13)
SRK/T	(2), (8), (12)
T2	(11)
VRF	(11)

AL = axial length; EVO = Emmetropia Verifying Optical; RBF = Radial Basis Function; SS-OCT = swept-source optical coherence tomography. The second column shows for each formula which differences were statistically significant ($P < .05$).

Table 4. Refractive outcomes obtained in eyes with AL >26.0 mm.

	PE ± SD	MedAE	MAE	PE ≤ 0.25 D	PE ≤ 0.50 D	PE ≤ 0.75 D	PE ≤ 1.00 D
Barrett	-0.011 ± 0.323	0.202	0.253	47.37	84.21	89.47	94.74
EVO	0.042 ± 0.306	0.168	0.211	68.42	89.47	100.00	100.00
Haigis	-0.017 ± 0.382	0.253	0.298	52.63	84.21	94.74	100.00
Hoffer Q	0.346 ± 0.439	0.248	0.397	52.63	73.68	78.95	89.47
Holladay 1	0.567 ± 0.454	0.436	0.582	21.05	57.89	68.42	78.95
Holladay 2	0.428 ± 0.672	0.260	0.483	54.67	73.68	73.68	78.95
Holladay 2 (adjusted AL)	-0.142 ± 0.345	0.265	0.296	56.00	84.21	94.74	100.00
Kane	-0.075 ± 0.310	0.200	0.220	52.63	94.74	100.00	100.00
Olsen _{SS-OCT}	0.194 ± 0.509	0.205	0.338	68.42	84.21	89.47	94.74
Olsen _{standalone}	-0.076 ± 0.308	0.209	0.256	47.37	89.47	100.00	100.00
Panacea	-0.331 ± 0.385	0.345	0.415	31.58	63.16	94.74	94.74
RBF	0.068 ± 0.301	0.230	0.244	57.89	94.74	100.00	100.00
SRK/T	0.173 ± 0.371	0.313	0.312	42.11	84.21	94.74	100.00
T2	-0.049 ± 0.378	0.270	0.311	47.37	89.47	89.47	100.00
VRF	-0.240 ± 0.387	0.196	0.344	57.89	68.42	94.74	94.74

AL = axial length; EVO = Emmetropia Verifying Optical; MAE = mean absolute error; MedAE = median absolute error; PE = prediction error; RBF = Radial Basis Function; SS-OCT = swept-source optical coherence tomography

The present study shows some interesting findings about the latest formulas. The Kane and EVO formulas provided outstanding outcomes, as their MedAE was ≤0.205 D and both yielded at least 90% of eyes with a PE of ±0.50 D or less. Our data for the Kane formula mirror those recently reported by its author.^{15,25} Because neither the Kane nor the EVO formulas have been published and little is known about their structure, it is not possible to discuss the reasons for their excellent performance. However, they look promising and deserve our attention.

Barrett formula confirmed its reputation as being one of the most accurate, as previously found by many researchers.⁶⁻⁸ Good results are also achieved with the RBF version 2.0, as recently reported by Connell and Kane,²⁵ the T2 formula, as previously reported by Cooke and Cooke and Kane et al.,^{6,7} the VRF formula, as previously reported by its author,¹⁸ and the Holladay 2 formula with AL adjustment (for eyes with AL > 24.0 mm). With 89.33% of eyes showing a PE of ±0.50 D or less, the Holladay 2 can now be considered one of the most accurate formulas, with a clear improvement over previous versions and

studies.^{6,7,21} Such improvement was confirmed by a direct comparison with the standard Holladay 2, as we can see in Table 2.

As regards the Olsen formula, we observed more accurate results with the standalone version, which includes K and AL among the IOL position predictors, compared with the version installed on the SS-OCT, which adopts the C-constant and thus relies only on LT and ACD to predict the IOL position. This finding is in good agreement with the data reported by Cooke and Cooke.⁷

One of the most interesting findings of this study was the good performance of older formulas, which enabled us to have more than 84% of eyes with a PE of ±0.50 D or less. This percentage is considerably higher than the corresponding values of previous studies with large samples⁶⁻⁸; the good outcomes suggest that caution should be used before abandoning these formulas, which are still accurate and have one big advantage: the possibility of optimizing their constants independently, as they can be entered into Excel. With unpublished formulas, this is not possible.

Table 5. Comparison between refractive outcomes achieved with different formulas in the current and previous studies.

Study	MedAE (D)					PE ≤ 0.50 D (%)				
	Current	Cooke* OLCR ⁷	Cooke* PCI ⁷	Kane ^{6,*}	Melles ^{8,*}	Current	Cooke* OLCR ⁷	Cooke* PCI ⁷	Kane ^{6,*}	Melles ^{8,*}
Barrett	0.202	0.230	0.255	0.305	0.252	88.00	82.9	80.6	72.3	80.8
Haigis	0.254	0.268	0.271	0.337	0.275	84.67	80.4	79.8	68.3	77.1
Hoffer Q	0.248	0.285	0.281	0.347	0.303	84.00	77.8	77.0	67.2	73.0
Holladay 1	0.249	0.268	0.270	0.326	0.287	85.33	79.1	79.5	69.4	75.0
Olsen _{SS-OCT/OLCR}	0.240	0.245	NA	NA	0.258	82.0	82.0	NA	NA	78.7
Olsen _{standalone}	0.209	0.225	0.285	NA	NA	88.67	83.7	75.1	NA	NA
SRK/T	0.221	0.289	0.290	0.335	0.292	84.67	75.7	75.1	69.6	74.0
T2	0.200	0.262	0.265	0.330	NA	88.67	79.6	79.0	70.0	NA

NA = not available; OLCR = optical low-coherence reflectometry; PCI = partial coherence interferometry; PE = prediction error; SS-OCT = swept-source optical coherence tomography

*First author.

On the other hand, Panacea performed slightly worse than the other formulas, although its results still have to be considered good. In this case, a role is played by the Scheimpflug camera measuring the Q value and the A/P ratio. We used a rotating Scheimpflug camera combined with Placido corneal topography, but other devices may offer different measurements and improve the results of Panacea.

As regards myopic eyes with AL >26.0 mm, this subgroup revealed interesting results, as many formulas achieved excellent results (ie, more than 80% of eyes with a PE of ± 0.50 D or less). These include some traditional formulas (Haigis and SRK/T) and most of the newer formulas. A larger sample is needed to confirm our preliminary data.

As a potential limitation, a smaller number of eyes were analyzed in this study than in other recent investigations, which included more than 1000 eyes.^{6–8,15} Although our sample size was sufficient to detect a statistically significant difference in the MedAE (on the basis of sample size calculation), we acknowledge that big data can provide us with additional information and therefore will go on enrolling patients. Because of the relatively small sample size, we did not investigate the influence of each biometric parameter on the outcomes of all formulas, as larger subgroups (eg, short eyes) would have been required.

In conclusion, our data suggest that all formulas can be successfully used to calculate the IOL power using the measurements provided by the SS-OCT. In most cases, newer formulas show higher accuracy because of the lack of far outliers. Older formulas, however, are still a valid option.

WHAT WAS KNOWN

- Optical biometry leads to accurate intraocular lens (IOL) power calculation, with 70% to 80% of eyes showing a prediction error within 0.50 D.
- The swept-source optical coherence tomography (SS-OCT) optical biometer investigated in this study provides repeatable measurements that, according to a previous multicenter study, lead to a prediction error of ± 0.50 D or less in about 70% of eyes, using older formulas.

WHAT THIS PAPER ADDS

- Using data from a single surgeon and a large variety of newer and older formulas, measurements by the SS-OCT optical biometer enabled us to improve the refractive outcomes of IOL power calculation compared with previous studies because we were able to achieve a prediction error within 0.50 D in at least 80% of eyes with all formulas.

REFERENCES

- Huang J, Savini G, Hoffer KJ, Chen H, Lu W, Hu Q, Bao F, Wang Q. Repeatability and interobserver reproducibility of a new optical biometer based on swept-source optical coherence tomography and comparison with IOLMaster. *Br J Ophthalmol* 2017;101:493–498
- Savini G, Hoffer KJ, Shammas HJ, Aramberri J, Huang J, Barboni P. Accuracy of a new swept-source optical coherence tomography biometer for IOL power calculation and comparison to IOLMaster. *J Refract Surg* 2017;33:690–695
- Hoffer KJ. The Hoffer Q formula: a comparison of theoretic and regression formulas. *J Cataract Refract Surg* 1993;19:700–712; errata, 1994;20:677; 2007;33:2–3
- Holladay JT, Prager TC, Chandler TY, Musgrove KH, Lewis JW, Ruiz RS. A three-part system for refining intraocular lens power calculations. *J Cataract Refract Surg* 1988;14:17–24
- Retzlaff JA, Sanders DR, Kraff MC. Development of the SRK/T intraocular lens power calculation formula. *J Cataract Refract Surg* 1990;16:333–340; erratum, 528
- Kane JX, Van Heerden A, Atik A, Petsoglou C. Intraocular lens power formula accuracy: comparison of 7 formulas. *J Cataract Refract Surg* 2016;42:1490–1500
- Cooke DL, Cooke TL. Comparison of 9 intraocular lens power calculation formulas. *J Cataract Refract Surg* 2016;42:1157–1164
- Melles RB, Holladay JT, Chang WJ. Accuracy of intraocular lens calculation formulas. *Ophthalmology* 2018;125:169–178
- Chylack LT Jr, Wolfe JK, Singer DM, Leske MC, Bullimore MA, Bailey IL, Friend J, McCarthy D, Wu SY. The lens opacities classification system III. *Arch Ophthalmol* 1993;111:831–836
- Hoffer KJ, Aramberri J, Haigis W, Olsen T, Savini G, Shammas HJ, Bentow S. Protocols for studies of intraocular lens formula accuracy. *Am J Ophthalmol* 2015;160:403–405
- Barrett GD. Barrett Universal II Formula. Singapore, Asia-Pacific Association of Cataract and Refractive Surgeons. Available at: http://www.apacrs.org/barrett_universal2/
- Haigis W, Lege B, Miller N, Schneider B. Comparison of immersion ultrasound biometry and partial coherence interferometry for intraocular lens calculation according to Haigis. *Graefes Arch Clin Exp Ophthalmol* 2000;238:765–773
- Haigis W. The thin lens formula. In: Shammas HJ, ed. *Intraocular Lens Power Calculations*. Thorofare, NJ, Slack; 2004, chapter 5:41–57
- Holladay JT. Holladay IOL Consultant User's and Reference Manual. Houston, TX, Holladay Lasik Institute, 1999
- Melles RB, Kane JX, Olsen T, Chang WJ. Update on intraocular lens power calculation formulas. *Ophthalmology* 2019;126:1334–1335
- Olsen T, Hoffmann P. C constant: new concept for ray tracing-assisted intraocular lens power calculation. *J Cataract Refract Surg* 2014;40:764–773
- Sheard RM, Smith GT, Cooke DL. Improving the prediction of the SRK/T formula: the T2 formula. *J Cataract Refract Surg* 2010;36:1829–1834
- Voytsekhivskyy OV. Accuracy of the VRF IOL power calculation formula. *Am J Ophthalmol* 2018;185:56–67
- Masket S, Tennen DG. Astigmatic stabilization of 3.0 mm temporal clear corneal cataract incisions. *J Cataract Refract Surg* 1996; 22:1451–1455
- Simpson MJ, Charman WN. The effect of testing distance on intraocular lens power calculation. *J Refract Surg* 2014;30:726
- Hoffer KJ. Clinical results using the Holladay 2 intraocular lens power formula. *J Cataract Refract Surg* 2000;26:1233–1237
- Savini G, Hoffer KJ, Barboni P, Balducci N, Schiano-Lomoriello D, Ducoli P. Accuracy of optical biometry combined with Placido disc corneal topography for intraocular lens power calculation. *PLoS One* 2017;12:e0172634
- Savini G, Negishi K, Hoffer KJ, Schiano Lomoriello D. Refractive outcomes of intraocular lens power calculation using different corneal power measurements with a new optical biometer. *J Cataract Refract Surg* 2018;44:701–708
- Gale RP, Saidana M, Johnston RL, Zuberbuhler B, McKibbin M. Benchmark standards for refractive outcomes after NHS cataract surgery. *Eye (Lond)* 2009;23:149–152
- Connell BJ, Kane JX. Comparison of the Kane formula with existing formulas for intraocular lens power selection. *BMJ Open Ophthalmol* 2019;4:e000251

Disclosures: Dr. Savini is a consultant of CSO and received speaker honoraria from Alcon Laboratories, Inc. and Oculus. Dr. Hoffer licenses the registered trademark name Hoffer® to ensure accurate programming of his formulas to Carl Zeiss Meditec (IOLMaster), Haag-Streit (LenStar/EyeStar), Heidelberg Engineering, Inc. (Anterior), Oculus (Pentacam AXL), Movu (Argos), Nidek (AL-Scan), Tomey Inc. (OA-2000), Topcon EU/Visia Imaging (Aladdin), Ziemer Ophthalmology GmbH (Galilei G6) [except Alcon Laboratories, Inc. (Verion)], and all A-scan biometer manufacturers. None of the other authors has a financial or proprietary interest in any material or method mentioned.

Complications of cosmetic iris implants: French series of 87 eyes

Hussam El Chehab, MD, Damien Gatineau, MD, PhD, Christophe Baudouin, MD, PhD, Marc Muraine, MD, PhD, Louis Hoffart, MD, PhD, Pascal Rozot, MD, Chadi Mehanna, MD, Clémence Bonnet, MD, Jean-Philippe Nordmann, MD, PhD, Pierre-Yves Santiago, MD, Carole Burillon, MD, PhD, Stéphanie Baillif, MD, PhD, Pierre Jean Pisella, MD, PhD, Michel Weber, MD, PhD, Antoine Robinet-Perrin, MD, Danielle Deidier, MD, Aurélien Hay, MD, Max Villain, MD, PhD, Georges Baïkoff, MD, Anne Sophie Gauthier, MD, Thibaud Mathis, MD, Corinne Dot, MD, PhD

Purpose: Iris intraocular implants were developed to manage congenital or traumatic iris defects. However, they are also used to change the color of patient eyes. The aim of this retrospective series was to report complications in patients managed in France after cosmetic implantation.

Setting: Ophthalmological institutions and private ophthalmologists in France.

Design: Multicenter retrospective observational study.

Methods: Questionnaires were sent to all ophthalmology departments in university hospitals and to private ophthalmologists. This questionnaire listed demographic and clinical data for each implanted eye with a focus on safety, the description of ocular complications (corneal edema, endothelial cell loss, increased intraocular pressure, and intraocular inflammation), and the therapeutic management implemented.

Results: Forty-four questionnaires (87 eyes) were collected, and ultimately, 33 questionnaires (65 eyes) were considered

complete and analyzed. Two types of implants were identified. Of the 65 eyes analyzed, only 5 eyes (7.7%) did not experience any complication and 60 eyes (92.3%) had at least 1 complication. The most commonly reported complication was corneal decompensation (78.5%). The diagnosis of glaucoma was made in over half (52.3%) of the cases. Explantation was needed in 81.5% of cases. The mean final visual acuity was 0.45 ± 0.08 logarithm of the minimum angle of resolution (logMAR) (0 to 2 logMAR).

Conclusions: Several ocular complications with a decreased mean visual acuity were described in a young healthy population. In addition, patient information on the safety of this procedure appeared insufficient.

J Cataract Refract Surg 2020; 46:34–39 Copyright © 2019 Published by Wolters Kluwer on behalf of ASCRS and ESCRS

 [Online Video](#)

Different iris implants have been developed since the first implantation of an intraocular lens (IOL) for managing iris defects by Choyce in 1956.^{1,2} They are intended to correct congenital (coloboma, ocular albinism, etc.) or traumatic iris defects to reduce glare and light sensitivity.^{3–5} Some recent studies in the literature have reported

an esthetical use of iris IOLs in young patients without ophthalmologic history to change the color of their eyes.^{6,7}

Two medical devices are used cosmetically, without Conformité Européenne (CE) marking or U.S. Food and Drug Administration (FDA) approval. The NewColorIris implant (Kahn Medical Devices), patented in 2006,⁸ is a silicone

Submitted: July 9, 2019 | Final revision submitted: August 7, 2019 | Accepted: August 9, 2019

Military Hospital of Desgenettes, Lyon, France (El Chehab and Dot); Rothschild Foundation, Paris, France (Gatineau); Quinze-Vingts National Ophthalmology Hospital, Paris, France (Baudouin); Charles-Nicolas Hospital, CHU de Rouen, Rouen, France (Muraine); Clinique Monticelli-Vélodrome, Marseille, France (Hoffart); Clinique Juge, Marseille, France (Rozot and Baïkoff); Hôtel-Dieu-Cochin Hospital, Paris, France (Mehanna and Bonnet); Clinique Sourville, Nantes, France (Santiago); Édouard Herriot Hospital, Hospices Civils de Lyon, Lyon, France (Burillon); Pasteur Hospital, Nice, France (Baillif); Bretonneau Hospital, Tours, France (Pisella); Nantes University Hospital, Nantes, France (Weber); Pellegrin Hospital, Bordeaux France (Robinet-Perrin); Private center, Toulon, France (Deidier); Private center, Nancy, France (Hay); Gui de Chauliac Hospital, Montpellier, France (Villain); Besançon University Hospital, Besançon, France (Gauthier); Croix Rousse Hospital, Hospices Civils de Lyon, Lyon, France (Mathis); and French Military Health Service Academy of Val de Grâce, Paris, France (Dot).

Presented at the ASCRS•ASOA Annual Meeting, Washington, DC, USA, April 13–17, 2018.

The authors thank Dr. Bernshaber, Prof. Bourges, Dr. Brasnu, Prof. Brézin, Prof. Daen, Prof. Delbosc, Prof. Denis, Dr. Flores, Dr. Fortoul, Dr. Janin-Magnificat, Dr. Kocaba, Dr. Landman, Dr. Le Du, Dr. Marty, Dr. Meziani, Dr. Saad, Prof. Saleh, Prof. Touboul, Dr. Trinh, Dr. Vandermeer, and Dr. Zanlonghi.

Corresponding author: Hussam El Chehab, MD, Department of Ophthalmology, Military Hospital of Desgenettes, 108, Boulevard Pinel, Lyon 69003, France. Email: elchehab_hussam@hotmail.fr.

implant 11.0 mm to 13.0 mm in diameter with a pupillary aperture of 3.5 mm and a thickness of 0.16 mm. To hold it in place in the anterior segment, 6 rounded flaps are present at the periphery. The BrightOcular (Stellar Devices LLC), patented in 2012,⁹ presents slightly different characteristics (11.5 to 13.5 mm in diameter and 0.16 to 0.18 mm in thickness). It is held in place by 5 peripheral triangular flaps. Finally, its posterior face presents grooves to theoretically allow an easier flow of the aqueous humor.¹⁰

A recent literature review has reported a significant number of ocular complications in patients in Panama who underwent an esthetic procedure with these implants.¹¹ In this study, we reported the French experience based on a single questionnaire of patients managed in 2017 after esthetic implantation performed mostly abroad, with a focus on safety.

METHODS

This was a multicenter, retrospective, observational study based on data collection through a questionnaire sent to the French College of Academic Ophthalmologists and to ophthalmologists who were members of the Société de l'Association Française des Implants et de la Chirurgie Réfractive. This questionnaire collected demographic and clinical data of patients implanted for esthetic purposes. Anonymized identification data (date of birth, sex, first 3 letters of the last name, and first names) allowed for excluding patients who consulted several ophthalmologists. Implantation data were collected (age at the time of implantation, locations, date, type of implant used, and associated surgical procedures). The other data analyzed were visual acuity (VA) at the time of the first and last consultations in

France, endothelial cell density by specular microscopy, maximal intraocular pressure (IOP), number of IOP-lowering treatments if used, presence of anterior chamber inflammation, date of the first complication, type of complication (corneal edema, intraocular inflammation, high IOP, cataract, or retinal complications), and surgical procedures performed (explantation, keratoplasty, filtering surgery, and cataract surgery). Comments were also allowed to provide information on the patients, especially on the follow-up difficulties. Only the questionnaires containing identification data and with 80% of information completed were selected for the analysis to present the most accurate data possible.

The Ethics Committee of the French Society of Ophthalmology approved the study (IRB 00008855 Société Française d’Ophtalmologie IRB#1). It was conducted in accordance with the law on data protection (no. 2004-801, August 6, 2004).

The statistical analysis was performed using IBM SPSS Statistics for Windows software (version 22.0, IBM Corp.). Data are presented as means with standard deviations and the minimum and maximum values. The difference between the initial VA and the final VA (end of follow-up) was analyzed using a *t* test for paired values. The significance threshold used was .05.

RESULTS

Forty-four questionnaires were collected, and 11 questionnaires were excluded because the reported data were either redundant or insufficient. Finally, 33 questionnaires from 33 different patients (65 eyes) were analyzed.

Patient Characteristics

The patient mean age at the time of implantation was 34.2 ± 10.9 years (Table 1). The youngest and oldest patients were

Table 1. Comparative reports of complications after cosmetic iris implantation.

	Current Study (n = 65)	Galvis et al. ¹¹ (n = 128)
Age, yrs (range)	34.2 ± 10.9 (19–57)	32.6 (19–65)
Implantation location (eyes, n)	Tunisia (37) France (8) India (6) Dubai (2) Egypt (2) Lebanon (2) Panama (2) Turkey (2) 2 NA eyes	Panama (78) Lebanon (12) India (9) Turkey (7) Tunisia (6) Jordan (4) Mexico (2) France (2) 8 NA eyes
Complication rate at first consultation (eyes, n)	92.3% (60)	91.4% (117)
Implant type	10	86
NewColorIris	12	39
BrighOcular	43 NA	3 NA
Complication rate (eyes, n)	92.3% (60)	91.4% (117)
Explantation rate (eyes, n)	81.5% (53)	68.8% (88)
Final VA	0.45 ± 0.08 logMAR 25.4% VA >1 logMAR	9.3% VA <20/200
Corneal complication (eyes, n)	78.5% (51)	33.6% (43)
Mean endothelial density	1484.9 ± 126 cells/mm ²	1224 ± 571 cells/mm ²
Keratoplasty (eyes, n)	20% (13)	20.3% (29)
Mean maximal IOP	26.1 ± 1.6 mm Hg	40 mm Hg
Glaucoma (eyes, n)	52.3% (34)	46.1% (59)
Glaucoma surgery (eyes, n)	23.1% (15)	22.7% (29)
Cataract (eyes, n)	15.4% (10)	14.8% (19)
Inflammation (eyes, n)	38.5% (25)	30.5% (39)

IOP = intraocular pressure; logMAR = logarithm of the minimum angle of resolution; NA = not available; VA = visual acuity

19 and 57 years old, respectively. Most patients were women ([26/33 78.8%]). No patient had a history of significant ocular disease other than refractive errors. No information about potential procedure-related complications was provided to 31 (93.4%) of 33 patients. Only 1 patient had unilateral surgery; all others had bilateral surgery on the same day. Some patients had iris implant combined with other refractive procedures such as laser in situ keratomileusis or photorefractive keratectomy laser (4 eyes) or phacoemulsification (6 eyes including 2 eyes with the implantation of multifocal implants).

The implant brand was identified in 22 eyes (33.9%), of which 10 eyes were implanted with NewColorIris and 12 with BrightOcular. Table 1 reports the country where procedures were performed; more than half of the procedures were performed in Europe and the north of Africa (37 eyes in Tunisia [56.9%], 8 eyes in France [12.3%], and 2 eyes in Egypt [3.1%]). In 2 patients, the origin of the implantation was not specified in the questionnaire. One patient underwent revision surgery with a second implantation and change of the first implants because she was not satisfied by the initial esthetic outcome.

Patients were implanted between July 2005 and May 2017. The mean time before the first consultation with an ophthalmologist in France was 1.5 ± 0.3 years. At the time of this first consultation, 92.3% of eyes had at least 1 complication and some patients had several complications. Only 5 eyes did not experience any complication; their implantations were performed recently, 84.4 ± 38.3 days before consultation.

The initial VA was 0.62 ± 0.09 logarithm of the minimum angle of resolution (logMAR) (0 to 2 logMAR).

Complications and Management

Corneal Complications Edematous endothelial decompensation was present in 51 (78.5%) of 65 eyes (Table 1 and Figure 1, A). Specular microscopy was performed in 51 eyes (78.4%). The result was uninterpretable in 6 eyes due to corneal edema. The mean initial endothelial density was 1484.9 ± 126 cells/mm².

Keratoplasty was performed in 13 (20%) of 65 eyes. Eleven eyes had Descemet membrane endothelial keratoplasty, and 2 eyes (of 1 patient) had bilateral penetrating keratoplasty (Figure 1, B).

IOP-Related Complications The mean maximal IOP during the follow-up was 26.1 ± 1.6 mm Hg (8.0 to 50.0 mm Hg).

Maximal ocular hypertension higher than 21 mm Hg was reported in 54.1% of patients. Initiating IOP-lowering treatment was needed in 39 (60%) of 65 eyes. Eleven eyes received a fixed dual therapy, 3 eyes received triple therapy, 15 eyes received quadritherapy, and 4 eyes received systemic treatment in addition to quadritherapy. Filtering surgery was needed in 15 eyes (23.1%). Finally, the diagnosis of glaucoma defined by a structural and functional impairment was reported in 34 eyes (52.3%). The examination of the iridocorneal angle showed a contact between the flaps of the implant and the angle (Figure 2).

Cataracts Six of the 65 eyes underwent lens surgery associated with the initial cosmetic iris implantation.

During follow-up, 10 eyes (15.4%) underwent cataract surgery. Two patients experienced unilateral retinal detachment after their cataract surgery.

Since their initial implantation (1.5 years), nearly a quarter of patients (16/65) with a mean age of 34.2 years were pseudophakic.

Intraocular Inflammation Signs of anterior uveitis were reported in 25 eyes (38.5%) and of posterior inflammation (pseudophakic cystoid macular edema [CME], CME without cataract surgery, and epiretinal membrane) in 6 eyes (9.2%) (Figure 3). One patient with CME subsequently developed bilateral macular atrophy responsible for a decrease in VA.

Iris Peripheral iridocorneal synechiae were reported in six eyes (9.2%), and 2 eyes had a corectopia. One eye had a nevus that was only discovered after explantation.

Explantation Of all eyes, 53 (81.5%) had explantation, of which 51 eyes had a complication and 2 eyes were explanted preventively (Figure 4). The other patients refused explantation (12 eyes, 6 patients). Explantation was performed on average 2.3 ± 0.4 years after implantation (Supplemental Digital Content, Video 1, <http://links.lww.com/JRS/A9>).

At the end of the follow-up, the mean VA was 0.45 ± 0.08 logMAR (0 to 2 logMAR) and the improvement in VA was statistically significant ($P = .007$); however, the VA did not reach the theoretical VA corresponding to this age range. Only half (33/65) of the patients had a VA at 0 logMAR at the end of their follow-up. At the end of this follow-up, 16 of the 33 patients presented a binocular VA less than 0.3 logMAR, which was not compatible with driving in France, and 8 patients presented criteria of blindness (binocular VA less than 1 logMAR).

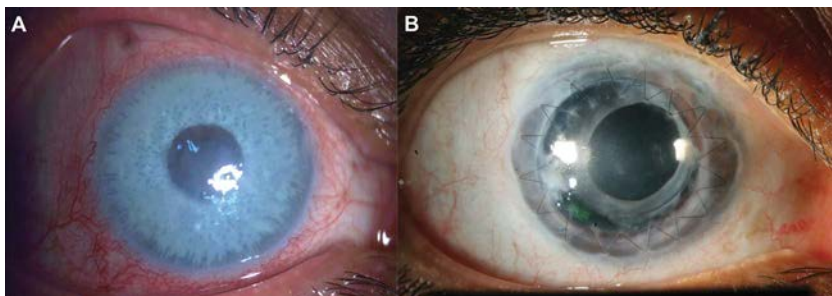


Figure 1. A: Corneal decompensation in an eye with a BrightOcular cosmetic implant (Courtesy of Dr. A. Robinet-Perrin, Bordeaux, France). B: Penetrating keratoplasty for managing decompensation, this eye underwent a cataract surgery after the implantation and before the penetrating keratoplasty (Courtesy of Prof. M. Muraine, Rouen, France).

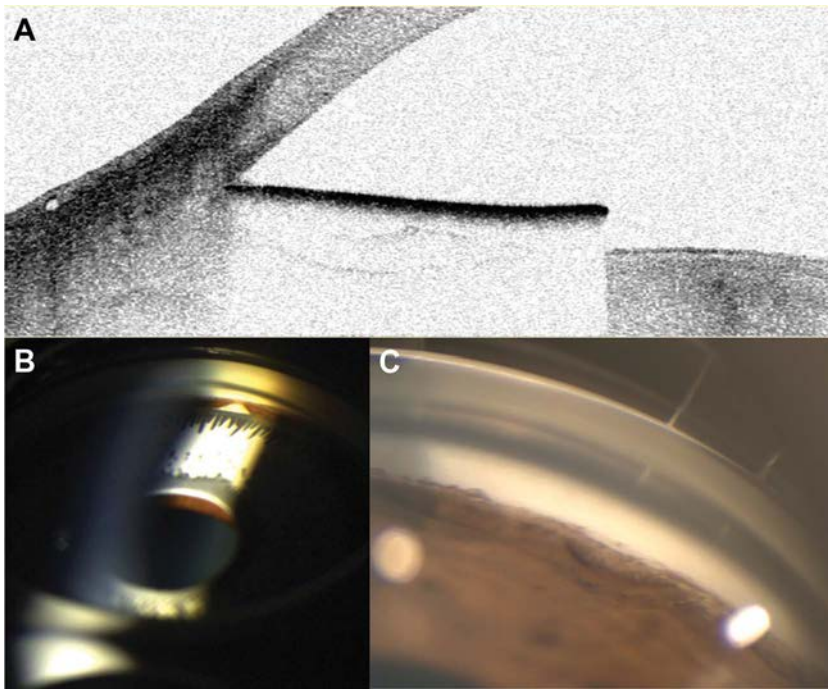


Figure 2. Angular flaps of the anterior segment implant on optical coherence tomography (A) and on gonioscopy B: showing a contact between the flaps of the implant and the apex of the angle. In this eye, the contact between the implant and the iridocorneal angle caused synechiae and pigment deposition (C) (Courtesy of Dr. E. Landman, Paris, France (A) and Dr. A. Hay, Nancy, France (B and C)).

DISCUSSION

We report here a series of patients managed in France after cosmetic iris implantation. These implants were diverted from their original use for esthetic purposes. To our knowledge, this is the largest series published to date. A review of the literature conducted by Galvis et al.¹¹ has reported a total of 128 cases in 8 countries (Table 1).

Our series did not allow for determining the incidence of complications following this procedure because the total number of implanted French patients is not known. However, 92.3% of eyes examined had at least 1 complication after a relatively short mean postoperative period of 1.5 ± 0.3 years. This figure is similar to that reported by Galvis et al.¹¹ In this review, the complication rate is estimated in 117 (91.4%) of 128 eyes. This esthetic procedure can be responsible for serious complications and cause loss of VA in patients. A final decrease in VA was observed in more than half of the patients in our series (the mean VA at the end of the management: 0.45 ± 0.08 logMAR). In 25.4% of cases, the final VA was less than 1 logMAR in these young active patients who had no significant history of ocular disease and

who likely had an initial normal VA. In more than half of the patients (16 of 33), the binocular VA was not compatible with driving according to the French law.

In addition, our study reports a lack of information provided to patients; 93.4% did not receive any information from their surgeon. The websites for these implants compare them to surgical procedures where IOLs are implanted (ie, cataract surgery).¹¹ These implants have no CE marking or FDA approval. Although there is a specific ISO standard (11979) governing the production of IOLs (anterior and posterior) and their clinical assessment, only the manufacturing standards (ISO 13485) are provided on the websites. However, obtaining CE marking is yet another certification step, which is essential for guaranteeing the safety of medical devices. Despite the absence of CE marking, some patients in Europe had implants inserted (8 eyes [12.3%] 12.3% of cases implanted in France), without being able to identify from where cosmetic iris implant was ordered.

In our series, 1 patient had an iris nevus that was discovered only after explantation. The implant made its observation and

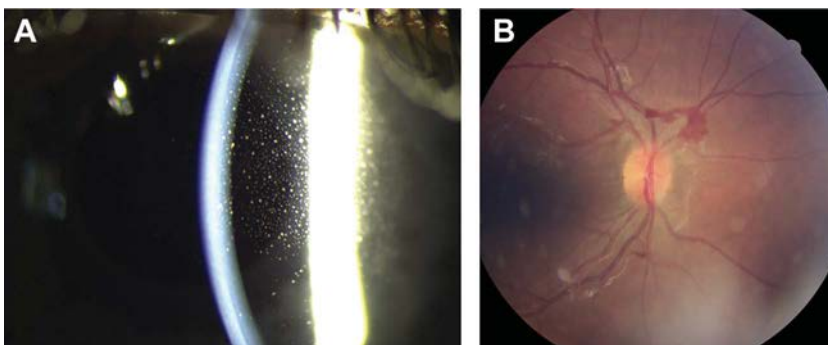


Figure 3. Anterior uveitis and posterior complications in an eye with a cosmetic implant (Courtesy of Dr. A. Hay, Nancy, France). The patient presented peripapillary hemorrhages with a papillary edema on the left eye and an anterior uveitis on the right eye.

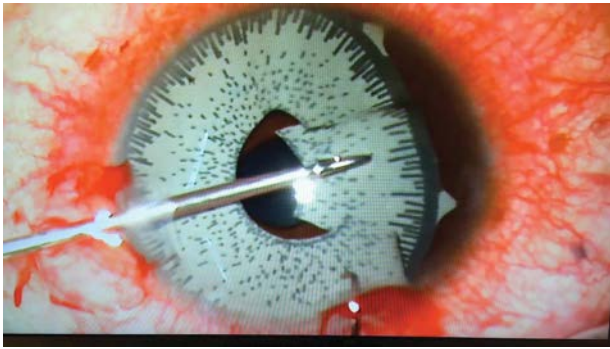


Figure 4. Surgical image of the explantation procedure of a BrightOcular cosmetic implant (Courtesy of Prof. Muraine, Rouen, France.).

follow-up impossible, so that if signs of malignancy appeared, they would not be discovered. In 1 patient, implant exchange involving a new bilateral procedure was reported for esthetic dissatisfaction, which exposed the patient to the risks of a second intraocular surgery for only cosmetic purposes. Galvis et al.¹¹ described severe iris atrophy in 3.9% of the eyes; our questionnaire was not designed for this information.

Our series reports a balanced distribution between the two different implants currently used. Data on material tolerance and implant stability in the anterior segment are limited.¹² But the case studies reviewed by Galvis et al.¹¹ and this study are consistent in reporting many complications related to this procedure. Despite these data, patients in our series had almost no postoperative follow-up after surgery in other countries and all but 1 underwent bilateral implantation on the same day despite the potential risk for infection. No cases of endophthalmitis were reported.

Corneal complications appear to be the most common.^{11,13,14} They were related to edematous decompensation because of the loss of endothelial cells as shown by the reduced corneal density (1450 cells/mm²) in this group of young patients with a mean age of 34 years. As it is known, *in vivo* mitosis of corneal endothelial cells in humans is very limited,¹⁵ and therefore, any factor causing a persistent loss of these cells may eventually lead to irreversible corneal edema. This endothelial loss could be related to several factors: a mechanical loss secondary to the implantation procedure, an endothelial contact of the implant, a mechanism that has been reported with intraocular anterior chamber implants with angular support (the absence of customized sizing of iris implants makes this assumption plausible) worsened by implant irregularities,⁶ and a biochemical toxicity of the material (shown by the presence in some cases of macrophages at the implant surface after explantation).¹ Their management required keratoplasty, especially endothelial keratoplasty, in 1 of 5 cases in this series.

Ocular hypertension was also common. More than half of the eyes showed signs of glaucomatous neuropathy. In some patients, gonioscopy revealed the presence of peripheral anterior synechiae that have previously been reported in the literature.¹⁶ These synechiae develop as a result of the trauma related to the implant flaps. These flaps could also lead to direct trauma to the trabecular

meshwork aggravating the resistance to the flow of the aqueous humor. Finally, the contact of the implant on the iris may lead to pigment dispersion, which in turn can increase the IOP.¹⁷ This hypertension is difficult to control even after explantation. Indeed, in our series, although IOP-lowering treatment was initiated, more than 2 local treatments were needed in over half of the cases (22/39 eyes). The use of filtering surgery was reported in nearly a quarter of patients (29/128 eyes [22.7%]), and this result is comparable with that reported by Galvis et al.¹¹

These implants could also be associated with posterior segment complications, including inflammation. They are probably underestimated because the analysis of the posterior segment remains difficult when the implants are positioned, because of the absence of pupillary dilation for the examination of the peripheral retina and also because of the lack of corneal transparency in some cases. We found 2 cases of retinal detachment after cataract surgery. This confirms the need for several surgical procedures in some patients during their postimplantation management, including after explantation (mean number of 2.4 ± 0.9 procedures per eye), as previously reported by Hoguet et al.¹⁷

During patient management, that is, 1.5 ± 0.3 years after implantation, all ophthalmologists proposed explantation for managing or preventing complications. This procedure might also be invasive, and different techniques are proposed to reduce this trauma.^{16,18} Explantation was performed in 81.5% of patients; several patients refused explantation. It is worth noting that explantation was performed after a mean time of 2.3 ± 0.4 years after implantation, that is, almost 1 year elapsed between the first visit and this procedure. This stresses the difficulty to convince these patients to explant the device. They accept this procedure when complications are symptomatic. Among the patients in our study some had a high level of education (ie, lawyer). Most patients were poorly observant, and there were cases of medical nomadism confirmed by cross-identification of the questionnaires.

Our study has some limitations, mainly related to the small number of cases its retrospective design. The prevalence of complications cannot be analyzed because the total number of implantations remains unknown. The identification of the implant brand was possible only in 33.9% of cases. This low rate can bias the results. The BrightOcular implant might pose less risk than the NewColorIris implant.¹⁹ Scanning electron microscopy showed surface irregularities in the NewColorIris implant, that might contribute to uveitis and trabecular meshwork damage.²⁰ BrightOcular has grooves that might have partially corrected the surface irregularities.¹⁰

The strength of our study was the use of a single questionnaire sent to anterior segment surgeons, which helped us to identify nomadic patients who were therefore included only once. We also excluded almost 1 of 5 questionnaires (18%) to ensure a satisfactory response completeness rate (>80%).

This study of French patients provides data from Europe that are consistent with those published by Galvis et al.,¹¹ of

which most data was from the Americas. Our study shows the risks of cosmetic implants, which might be vision-threatening and lead to disability. Management of the complications might require several surgical procedures, and the follow-up is difficult because of the poor compliance among these young, poorly informed patients.

WHAT WAS KNOWN

- Iris intraocular implants are used to correct iris defects, and some ophthalmologists use them for esthetical purposes. In these conditions, the implant causes different eye complications.

WHAT THIS PAPER ADDS

- The implants are used in the European Union without the CE mark or FDA approval.
- Complications lead to a decrease in visual acuity, to the extent of blindness in some patients, and loss of the professional or driving license.
- Follow-up of these patients remains difficult because of poor observance.

REFERENCES

1. Anderson JE, Grippo TM, Sbeity Z, Ritch R. Serious complications of cosmetic NewColorIris implantation. *Acta Ophthalmol (Copenh)* 2010;88:700–704
2. Pandey SK, Apple DJ. Professor Peter Choyce: an early pioneer of intraocular lenses and corneal/refractive surgery. *Clin Exp Ophthalmol* 2005;33:288–293
3. Mamalis N. Cosmetic iris implants. *J Cataract Refract Surg* 2012;38:383
4. Sundmacher T, Reinhard T, Althaus C. Black diaphragm intraocular lens in congenital aniridia. *Ger J Ophthalmol* 1994;3:197–201
5. Srinivasan S, Ting DSJ, Snyder ME, Prasad S, Koch HR. Prosthetic iris devices. *Can J Ophthalmol* 2014;49:6–17
6. Mathis T, Fortoul V, Kodjikian L, Denis P. Ocular complications of the NewColorIris(®) colored cosmetic implant [in French]. *J Fr Ophthalmol* 2015;38:e107–e109
7. Le Dù B, Boukhrissa M, Nordmann JP. Acute angle-closure attack secondary to BrightOcular(®) cosmetic iris implant and subsequent subluxation of contralateral iris implant [in French]. *J Fr Ophthalmol* 2016;39:e141–e144
8. Khan DA, original assignee, Artificial iris diaphragm implant. US patent 7025781 2B. Filed January 31, 2003; date of patent April 11, 2006
9. Basoglu A, Vaneagas RA, Ocular implant iris diaphragm. US patent 8197540. Filed April 26, 2010; date of patent June 12, 2012
10. Mansour AM, Ahmed IIK, Eadie B, Chelala E, Saade JS, Slade SG, Mearza AA, Parmar D, Ghabra M, Luk S, Kelly A, Kaufman SC. Iritis, glaucoma and corneal decompensation associated with BrightOcular cosmetic iris implant. *Br J Ophthalmol* 2016;100:1098–1101
11. Galvis V, Tello A, Corrales MI. Postoperative results of cosmetic iris implants. *J Cataract Refract Surg* 2016;42:1518–1526
12. Thiagalingam S, Tarongoy P, Hamrah P, Lobo AM, Nagao K, Barsam C, Bellows R, Pineda R. Complications of cosmetic iris implants. *J Cataract Refract Surg* 2008;34:1222–1224
13. Kazerounian S, Tsirkinidou I, Kynigopoulos M, Müller M. "Blue eyes"-case report about the risks of cosmetic iris implants [in German]. *Ophthalmol Z Dtsch Ophthalmol Ges* 2019;116:669–672
14. Mednick Z, Betsch D, Boutin T, Einan-Lifshitz A, Sorkin N, Slomovic A. Bilateral BrightOcular iris implants necessitating explantation and subsequent endothelial keratoplasty. *Am J Ophthalmol Case Rep* 2018;12:1–4
15. Galvis V, Tello A, Gutierrez AJ. Human corneal endothelium regeneration: effect of ROCK inhibitor. *Invest Ophthalmol Vis Sci* 2013;54:4971–4973
16. Bore M, Choudhari N, Chaurasia S. Management of complications of cosmetic iris implants in a phakic eye: a case report and literature review. *Int Ophthalmol* 2019;39:1141–1146
17. Hoguet A, Ritterband D, Koplin R, Wu E, Raviv T, Aljian J, Seedor J. Serious ocular complications of cosmetic iris implants in 14 eyes. *J Cataract Refract Surg* 2012;38:387–393
18. Arjmand P, Gooi P, Ahmed IIK. Surgical technique for explantation of cosmetic anterior chamber iris implants. *J Cataract Refract Surg* 2015;41:18–22
19. Koaik MK, Mansour AM, Saad A, Farah SG. BrightOcular® cosmetic iris implant: a spectrum from tolerability to severe morbidity. *Case Rep Ophthalmol* 2018;9:395–400
20. Castanera F, Fuentes-Páez G, Ten P, Pinalla B, Guevara O. Scanning electron microscopy of explanted cosmetic iris implants. *Clin Exp Ophthalmol* 2010;38:648–651

Disclosures: None of the authors has a financial or proprietary interest in any material or method mentioned.

Posterior chamber phakic intraocular lens for the correction of presbyopia in highly myopic patients

Pavel Stodulka, MD, PhD, Martin Slovak, ME, PhD, Martin Sramka, ME, Jaroslav Polisenky, MD, Karel Liska, MSc

Purpose: To report the initial experience with a new presbyopic phakic intraocular lens (pIOL) in the correction of high myopia and presbyopia.

Setting: Gemini Eye Clinic, Zlin, Czech Republic.

Design: Prospective cohort study.

Methods: Presbyopic eyes with moderate to high myopia were implanted with a presbyopic posterior chamber pIOL (IPCL). The visual acuities at near and distance, endothelial cell density, and ocular condition were examined 1 week, 3 months, 1 year and 2 years postoperatively.

Results: The mean uncorrected distance visual acuity improved significantly from 1.25 logarithm of the minimum angle of resolution (logMAR) (1.15 to 1.35 95% confidence interval [CI]) to 0.11 logMAR (95% CI, 0.03 to 0.17) ($P < .0001$). No eye lost 1 or more lines of corrected distance visual acuity. The mean distance refraction improved significantly from -6.9

diopters (D) (range -8.6 to -5.3 D) preoperatively to -0.35 D (range -0.55 to -0.15 D, $P < .0001$) with less than -0.5 D residual refraction in 11 of 17 eyes. Fifteen of 17 eyes had improved uncorrected near visual acuity to J1 (Jaeger chart) at the 2-year follow-up. The near addition at the 2-year follow-up decreased from preoperatively $+1.26$ D (range 0.19 to 2.34 D) to $+0.39$ D (range 0.18 to 0.60 D). The mean endothelial cell density was reduced from 2552 cells/mm² (range 2421 to 2682 cells/mm²) to 2299 cells/mm² (range 2108 to 2490 cells/mm²) after 2 years. All patients were subjectively satisfied with the outcomes.

Conclusions: The new pIOL provided good visual outcomes in near and far distances in an initial case series of patients.

J Cataract Refract Surg 2020; 46:40–44 Copyright © 2019 Published by Wolters Kluwer on behalf of ASCRS and ESCRS

 [Online Video](#)

Presbyopia is the most frequent refractive error worldwide in people older than 40 years.^{1,2} It is estimated that by 2050, the prevalence of high myopia will significantly increase globally.³ There are several surgical options to correct myopia in presbyopic eyes.⁴ However, none of them, with the exception of refractive lens, exchange with a bifocal, trifocal, and extended depth-of-focus intraocular lens, corrects both myopia and presbyopia in both eyes.^{5,6} Refractive lens exchange in myopic eyes is controversial because of the risk for retinal complications.^{7,8}

We report our results of the first posterior chamber phakic intraocular lens (pIOL) correcting presbyopia. For the first time, a pIOL with a diffractive trifocal pattern on its refractive optic can correct both distance refractive error and presbyopia. This study evaluated the first series of patients with moderate to high myopia and presbyopia.

METHODS

Study Design and Setting

This was a prospective single-center case series of implantations of the presbyopic pIOL. The surgical procedure was performed by a single surgeon (P.S.) at Gemini Eye Clinic (Zlin, Czech Republic) during 2016, and patients were followed for 2 years. The institutional ethics committee approved the study at Gemini Eye Clinic (Zlin, Czech Republic) The study was registered with the National Institutes of Health clinical trials (Clinicaltrial.gov NCT03836898).

Participants

Presbyopic patients with moderate to high myopia aiming to surgically correct both myopia and presbyopia with a corrected distance visual acuity (CDVA) less than 0.3 logarithm of the minimum angle of resolution (logMAR) and aged 38 to 50 years were included. Patients with a corneal endothelial cell density below 2000 cells/mm², corneal dystrophies, an anterior chamber depth less than 2.8 mm, glaucoma, history of or current uveitis, acute ocular inflammation, previous intraocular or refractive surgery, or pre

Submitted: February 20, 2019 | Final revision submitted: June 5, 2019 | Accepted: August 22, 2019

From the Gemini Eye Clinic, Zlin, (Stodulka, Slovak, Sramka, Polisenky, Liska) Czech Republic; Department of Ophthalmology, Third Faculty of Medicine, Charles University, (Stodulka) Prague, Czech Republic; and Department of Circuit Theory, Faculty of Electrical Engineering, Czech Technical University in Prague (Liska), Prague, Czech Republic.

Corresponding Author: Pavel Stodulka, MD, PhD, Gemini Eye Clinic, U Gemini 360, Zlin 760 01, Czech Republic. Email: stodulka@lasik.cz.

existing ocular pathology that might affect postoperative results, were excluded.

Presbyopic pIOL

The presbyopic posterior chamber pIOL (IPCL, EyeOL UK) (Figure 1) has a refractive optic and diffractive trifocal pattern on its anterior optical surface (Figure 2) to correct distance and near refractive errors (Video 1, see Supplemental Digital Content 1, <http://links.lww.com/JRS/A10>). The available presbyopic addition ranges +1.0 to +4.0 D in 0.5 D steps. The IOL is made of hydrophilic acrylic. The IOL has 6 thin soft haptics to ensure atraumatic contact with the eye at the ciliary sulcus. There are 8 holes to facilitate aqueous flow from the posterior to anterior chamber. Two holes are at the periphery of the optic, and 4 holes are in the body of the haptic plate. Two more holes are at the contraclockwise haptic ends to indicate proper upside-down lens orientation. The IOL used in this study did not have the hole in the center of its optic, which started to be manufactured later and is labeled as V2.0 type by the manufacturer. A distributor or manufacturer provided the IOL size calculation. The IOL size is determined by the horizontal corneal diameter (white to white).

Surgical Technique

Surgery started with 2 side-port incisions. A single-use metal trapezoidal slit knife was used for the main 1.8 mm incision. The anterior chamber was filled with hydroxypropyl methylcellulose 2% solution (OcuCoat). A drop of Ringer's solution provided in the IOL package was placed inside the cartridge, and the presbyopic pIOL was positioned along its longitudinal axis inside. The cartridge was then carefully closed with the pIOL bending upward and put into the single-use injector. The eye was stabilized using irrigating cannula through 1 of the side ports, and the pIOL was injected in the anterior chamber or with a leading edge under the iris opposite the main incision. The trailing haptic was deployed from the main incision into the anterior chamber. The leading haptic of the IOL was manipulated under the iris (in case it was not there straight after the injection), and the trailing haptic was manipulated behind the iris into the posterior chamber. An ophthalmic viscosurgical device was aspirated using biaxial cannulas from both above and below the pIOL. The pupil was pharmacologically constricted. An iridectomy was performed using a 23-gauge vitrectome at the periphery of the iris at a 12 o'clock position. Pigment epithelial cells were carefully aspirated by the vitrectomy probe during the iridectomy process to minimize pigment dispersion. Finally, the corneal incisions were closed by stromal hydration with a balanced salt solution or Ringer's solution and cefuroxime solution at the conclusion of the surgery. Video 2 (see Supplemental Digital Content 2, <http://links.lww.com/JRS/A13>) shows the complete surgery. Postoperatively, tobramycin-dexamethasone eyedrops (Tobradex;



Figure 1. Presbyopic phakic intraocular lens with six thin and soft haptic ends for atraumatic contact with the eye at the ciliary sulcus.



Figure 2. Detail of the lens diffractive trifocal pattern on its anterior optical surface.

Alcon Laboratories, Inc.) were administered 3 times a day for 3 weeks in a gradual tapering regimen.

Outcome Measures

The uncorrected distance visual acuity (UDVA), CDVA, uncorrected near visual acuity (UNVA), distance refraction, and near refraction were recorded preoperatively and 1 week, 3 months, 1 year and 2 years postoperatively. Distance visual acuities were measured using Early Treatment Diabetic Retinopathy Study charts under photopic condition projected on a 22-inch LED liquid crystal display at 6 m. Near visual acuities were assessed using the Jaeger chart at approximately 50 cm. Subjective refraction was performed with both of these charts. The endothelial cell density (ECD) EM-3000 Specular Microscope (Nidek, Inc.), intraocular pressure (IOP) (Tonoref II; Nidek, Inc.), and distance between the posterior side of the pIOL and the anterior side of the crystalline lens (vault) by anterior segment optical coherence tomography (Casia SS-1000; Tomey GmbH) were also recorded at each visit. The ECD was determined using the automated cell count algorithm in 1 image for each eye.

Subjective satisfaction was recorded verbally or using a questionnaire sent electronically to the participants' email addresses at the 2-year follow-up. The questions were as follows: Are you satisfied with the outcomes? Do you use spectacles for either distance or near vision? Are you aware of halo and glare effects and are these bothersome for you? Do you have any difficulty to see in dim light conditions? Please name activities when you struggle.

Statistical Analysis

All values are expressed as mean and 95% confidence intervals unless otherwise indicated. Owing to a small sample, datasets are not normally distributed; thus, Wilcoxon matched-pair signed-rank tests were used for the comparison of outcome measures before the surgery and at 2-year follow-up. All statistical data analyses were performed using GraphPad Prism 7 software (version 7.7.0; GraphPad Software).

RESULTS

Of the 14 included patients (25 eyes), 4 were lost to follow-up. Altogether, 17 eyes (9 right eyes) of 10 patients (5 men)

Table 1. Mean (\pm) visual acuities and SE over time.

Parameter	Preoperative	1 Week	3 Months	1 Year	2 Years
UDVA (logMAR)	1.25 \pm 0.18	0.05 \pm 0.08	0.06 \pm 0.07	0.06 \pm 0.09	0.10 \pm 0.14
CDVA (logMAR)	0.02 \pm 0.05	-0.006 \pm 0.02	0.008 \pm 0.03	0.017 \pm 0.04	0.02 \pm 0.04
UNVA (J)	11.3 \pm 4.8	2.2 \pm 1.8	1.6 \pm 1.5	1.6 \pm 1.8	1.4 \pm 1.7
SE (D)	-6.94 \pm 3.21	-0.29 \pm 0.33	-0.06 \pm 0.51	-0.26 \pm 0.30	-0.35 \pm 0.38
Near addition (D)	1.26 \pm 2.09	0.48 \pm 0.36	0.24 \pm 0.4	0.39 \pm 0.42	0.36 \pm 0.38

CDVA = corrected distance visual acuity; J = Jaeger; logMAR = logarithm of the minimum angle of resolution; SE = spherical equivalent; UDVA = uncorrected distance visual acuity; UNVA = uncorrected near visual acuity

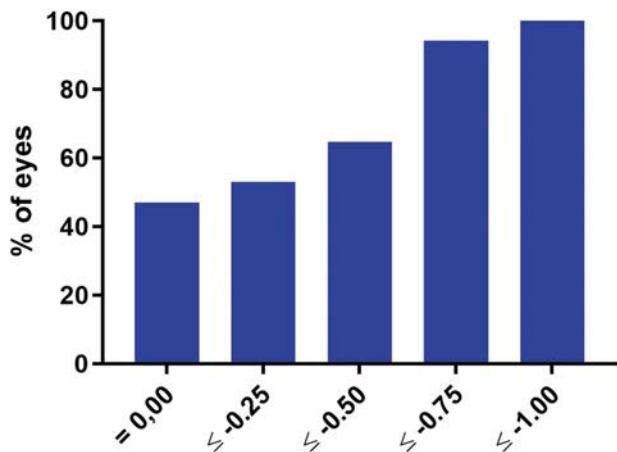


Figure 3. Cumulative distance spherical refraction at the 2-year follow-up.

with a mean age of 42.6 ± 3.5 years were included in the study analysis. All surgeries were uneventful. The mean anterior chamber depth preoperatively was 3.44 ± 0.24 mm.

Visual Acuity and Refraction

Uncorrected distance visual acuity improved significantly ($P < .0001$) from 1.25 logMAR (1.15 to 1.35, mean and 95% confidence interval) to 0.11 logMAR (0.03 to 0.17), and 16 of 17 achieved UDVA at least 0.2 logMAR at 2-year follow-up. Corrected distance visual acuity did not change significantly ($P > .999$), and all eyes achieved CDVA better than 0.15 logMAR at 2-year follow-up (Table 1). No eye lost one or more lines of CDVA and one eye has improved by 0.15 logMAR. Distance refraction improved significantly from -6.9 D (-8.6 to -5.3) preoperatively to -0.35 D (-0.55 to -0.15 , $P < .0001$) with less than -0.5 D residual refraction in 11 of 17 eyes (Figure 3). Fifteen of 17 eyes

showed UNVA improvement to J1 (Jaeger chart, Figure 4) at 2-year follow-up. The remaining 2 eyes read J1 already in the baseline. There was no mean UNVA decrease over the 2-year follow-up period at any of the follow-ups. Near addition at 2-year follow-up decreased from preop. $+1.26$ D (0.19 to 2.34) to $+0.39$ D (0.18 to 0.60).

Throughout the whole follow-up period, there were only four minor IOP spikes of IOP higher than 22 mm Hg recorded with no intervention required (Figure 5). Three of these events were in the 1-week follow-up and one at 2-year follow-up. The mean endothelial cell density was reduced from 2552 cells/mm² (2421 to 2682) to 2299 cells/mm² (2108 to 2490) after 2 years (on average 9.9% cell loss). None of the IOLs developed postoperatively any opacity detectable on the slitlamp as cataract, and no eye lost one line in CDVA. Six (40%) of 15 eyes showed minor pigment deposits on the pIOL surface. The mean lens vault was 464.7 ± 180.8 μ m (mean \pm SD) at 2-year follow-up.

All patients were subjectively satisfied with the outcomes and were spectacle independent. Forty percent of patients noticed some difficulties in dim light condition and required good light conditions, for example, had to switch the light on for reading. Surprisingly, only one patient noticed halos and glare at night, which they would rate as bothersome. One patient did not fill in the questionnaire.

DISCUSSION

Posterior chamber pIOLs have gained widespread popularity. Here, we present the first long-term case series, to our knowledge, experience with presbyopic diffractive pIOL technology for the correction of myopia and presbyopia. The visual acuity outcomes were excellent at distance and near. Sixteen of the 17 studied eyes achieved a UDVA of at least 0.2 logMAR and a UNVA of at least J1 at the 2-year

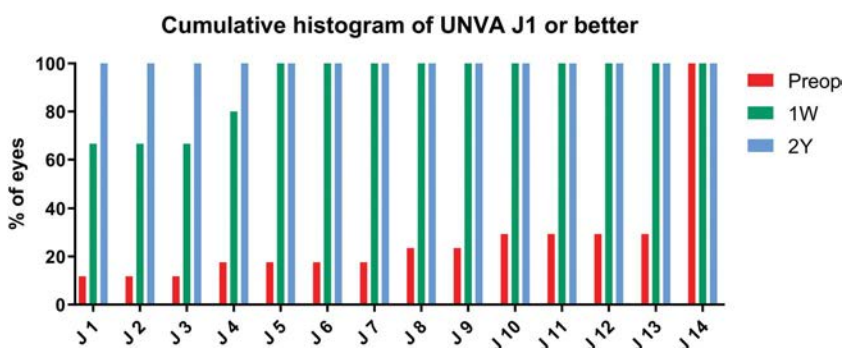


Figure 4. Cumulative uncorrected near visual acuity at 1-week and 2-year follow-up (J = Jaeger chart).

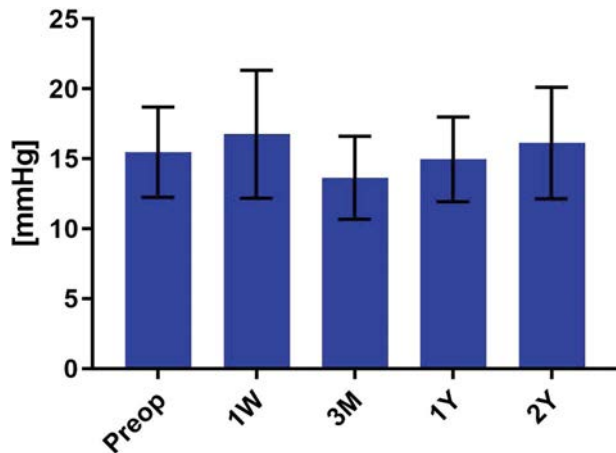


Figure 5. Stability of mean intraocular pressure throughout the study period.

follow-up. The CDVA did not significantly change from preoperatively. In this presbyopic myopic group of patients, we targeted for low myopia rather than low hyperopia with the pIOL power calculation. Therefore, distance refraction achieved good predictability because all eyes were within ± 1.0 D at 2-year follow-up (Figure 3). The UDVA was stable at the 2-year follow-up, despite that presbyopia is a progressive entity. Previously, attempts to develop the pIOL for presbyopia were made, but adequate safety was not achieved.⁹ Our visual outcomes are in line with those obtained after multifocal IOL implantation.¹⁰ Unlike laser refractive surgery, in which the results are irreversible, pIOLs offer the possibility of easy explantation with the intact cornea. Therefore, in a case of future cataract extraction, the absence of corneal surgery does not confer an additional risk to IOL calculation and the potential to cause a refractive surprise.

Phakic intraocular lens implantation is less invasive than refractive lens exchange with IOL implantation and confers less risk for retinal complications in the myopic population.¹¹ True microincision (1.8 mm) surgery is a significant advantage of the pIOL used in this study over the 3.0 mm incision needed for another pIOL available for myopia correction.¹² A 1.8 mm incision decreases the risk for surgically induced astigmatism and should also lower the risk for endophthalmitis, in which incision size is a factor.

The pigment dispersion on the anterior pIOL surface was observed in 6 (40%) of 15 eyes, which is similar to the previously reported incidence of 43.5%.¹³ There seem to be discrepancies in how this is being reported as minimum incidence was noted in some studies of the same IOLs (Visian Implantable Collamer lens; STAAR Surgical).^{13,14} In cases of pigment dispersion on the pIOL surface, no further procedure is usually required as visual acuity is not affected.¹⁵ A longer follow-up and comparison with a standard myopic pIOL without a presbyopic diffractive pattern should be performed to determine whether the diffractive pattern on the anterior pIOL surface might be causing more long-term pigment dispersion. The mean ECD loss in this study after a 2-year follow-up was perhaps on a higher end (9.9%) in comparison with a number of previously reported

trials in which, for example, the cell loss was 3.6% at 1 year and 6.6% at 2 years.^{16,17} Usually, the most significant cell loss is associated with the surgical procedure, and the trauma associated with the surgery could cause prolonged corneal endothelial remodeling.¹⁸ We have also noticed that there could be some variability in our measurements as these were only single values and not multiple measurements. We have therefore implemented and recommended further studies with a more robust endothelial density measurement processes based on the recommended guidelines for specular microscopy for pIOLs by the American Academy of Ophthalmology Task Force.¹⁹

To prevent the occurrence of pupillary block, a pre-operative or an intraoperative iridectomy must be performed when using the new pIOL. A new IPCL model (V 2.0) with a central hole in both the myopia and myopic presbyopia versions was released to eliminate the need for iridectomy. However, previously published studies show that the central hole design may not have substantial advantages in endothelial cell loss.^{20,21} The mean vault in our series at 2-year follow-up was considerably higher than that in previously reported studies,¹² although further monitoring is needed as the vault is decreasing over time, probably because of increasing crystalline lens thickness.²²

In conclusion, our results indicate the phakic trifocal posterior chamber IOL successfully corrects near and far vision in most cases of myopic patients.

WHAT WAS KNOWN

- Posterior chamber phakic lens can correct refractive error.
- Intraocular lens with diffractive structure can correct distance and near refraction.

WHAT THIS PAPER ADDS

- Phakic intraocular lens with diffractive structure corrects both distance and near refraction.
- For the first time patients can be implanted with diffractive presbyopia correcting phakic lens.
- Two-year results show high quality uncorrected distance and near visual acuity after presbyopic phakic lens implantation.

REFERENCES

1. Fricke TR, Tahhan N, Resnikoff S, Pappas E, Burnett A, Ho SM, Naduvilath T, Naidoo KS. Global prevalence of presbyopia and vision impairment from uncorrected presbyopia: systematic review, meta-analysis, and modelling. *Ophthalmology* 2018;125:1492–1499
2. Holden BA, Fricke TR, Ho SM, Wong R, Schlenker G, Cronjé S, Burnett A, Pappas E, Naidoo KS, Frick KD. Global vision impairment due to uncorrected presbyopia. *Arch Ophthalmol* 2008;126:1731–1739
3. Holden BA, Fricke TR, Wilson DA, Jong M, Naidoo KS, Sankaridurg P, Wong TY, Naduvilath TJ, Resnikoff S. Global prevalence of myopia and high myopia and temporal trends from 2000 through 2050. *Ophthalmology* 2016;123:1036–1042
4. Bilbao-Calabuig R, Llovet-Osuna F. Non-lens-based surgical techniques for presbyopia correction [in Spanish]. *Arch la Soc Española Oftalmol* 2017;92:426–435
5. Breyer DRH, Kaymak H, Ax T, Kretz FTA, Auffarth GU, Hagen PR. Multifocal intraocular lenses and extended depth of focus intraocular lenses. *Asia-Pacific J Ophthalmol* 2017;6:339–349
6. Akella SS, Juthani VV. Extended depth of focus intraocular lenses for presbyopia. *Curr Opin Ophthalmol* 2018;29:318–322
7. Horgan N, Condon PI, Beatty S. Refractive lens exchange in high myopia: long term follow up. *Br J Ophthalmol* 2005;89:670–672

8. Alió JL, Grzybowski A, Romaniuk D. Refractive lens exchange in modern practice: when and when not to do it? *Eye Vis* 2014;1:10
9. Ferraz CA, Allemann N, Chamon W. Phakic intraocular lens for presbyopia correction [in Portuguese]. *Arq Bras Oftalmol* 2007;70:603–608
10. Wolfsohn JS, Davies LN. Presbyopia: effectiveness of correction strategies. *Prog Retin Eye Res* 2019;68:124–143
11. Nanavaty MA, Daya SM. Refractive lens exchange versus phakic intraocular lenses. *Curr Opin Ophthalmol* 2012;23:54–61
12. Lee J, Kim Y, Park S, Bae J, Lee S, Park Y, Lee J, Lee JE. Long-term clinical results of posterior chamber phakic intraocular lens implantation to correct myopia. *Clin Exp Ophthalmol* 2016;44:481–487
13. Kocova H, Vlkova E, Michalcova L, Rybarova N, Motyka O. Incidence of cataract following implantation of a posterior-chamber phakic lens ICL (Implantable Collamer Lens)—long-term results. *Cesk Slov Oftalmol* 2017;73:87–93
14. Bhandari V, Karandikar S, Reddy JK, Relekar K. Implantable Collamer Lens V4b and V4c for correction of high myopia. *J Curr Ophthalmol* 2016;27:76–81
15. Kohnen T. Phakic intraocular lenses: where are we now? *J Cataract Refract Surg* 2018;44:121–123
16. Jiménez-Alfaro I, Benítez del Castillo JM, García-Feijóo J, Gil de Bernabé JG, Serrano de La Iglesia JM. Safety of posterior chamber phakic intraocular lenses for the correction of high myopia: anterior segment changes after posterior chamber phakic intraocular lens implantation. *Ophthalmology* 2001;108:90–99
17. Yasa D, Urdem U, Agca A, Yildirim Y, Kepez Yildiz B, Kandemir Beşek N, Yiğit U, Demirok A. Early results with a new posterior chamber phakic intraocular lens in patients with high myopia. *J Ophthalmol* 2018;2018:1329874
18. Edelhauser HF, Sanders DR, Azar R, Lamielle H; ICL in Treatment of Myopia Study Group. Corneal endothelial assessment after ICL implantation. *J Cataract Refract Surg* 2004;30:576–583
19. MacRae S, Holladay JT, Hilmantel G, Calogero D, Masket S, Stark W, Glasser A, Rorer E, Tarver ME, Nguyen T, Eydelman M. Special report: American Academy of Ophthalmology Task Force recommendations for specular microscopy for phakic intraocular lenses. *Ophthalmology* 2017;124:141–142
20. Goukon H, Kamiya K, Shimizu K, Igarashi A. Comparison of corneal endothelial cell density and morphology after posterior chamber phakic intraocular lens implantation with and without a central hole. *Br J Ophthalmol* 2017;101:1461–1465
21. Shimizu K, Kamiya K, Igarashi A, Kobashi H. Long-term comparison of posterior chamber phakic intraocular lens with and without a central hole (hole ICL and conventional ICL) implantation for moderate to high myopia and myopic astigmatism. *Medicine (Baltimore)* 2016;95:e3270
22. Schmidinger G, Lackner B, Pieh S, Skorpik C. Long-term changes in posterior chamber phakic intraocular collamer lens vaulting in myopic patients. *Ophthalmology* 2010;117:1506–1511

Disclosures: *None of the authors has a financial or proprietary interest in any material or method mentioned.*



First author:

Pavel Stodulka, MD, PhD

Gemini Eye Clinic, Zlin, Czech Republic

ARTICLE

Association between cataract and cotinine-verified smoking status in 11 435 Korean adults using Korea National Health and Nutrition Examination Survey data from 2008 to 2016

Hae Jeong Lee, MD, Cheol Hong Kim, MD, Ju Suk Lee, MD, Sung Hoon Kim, MD, PhD

Purpose: To investigate the association between cataract and cotinine-verified smoking status.

Setting: Samsung Changwon Hospital, Sungkyunkwan University School of Medicine, South Korea.

Design: Retrospective study.

Methods: Participants were randomly selected using data collected by the Korea National Health and Nutrition Examination Survey from 2008 to 2016. Participants completed a questionnaire to self-report smoking status and a history of cataract, among other variables. To identify the relationship between cataract and smoking, a new variable was used to define smoking status, survey-cotinine-verified smoking status (SCS)—the combination of self-reported smoking status and cotinine-verified smoking status—and thus identify hidden smokers.

Results: In total, 11 435 participants were eligible for final analysis. The study comprised 4925 men and 6510 women; the mean age

was 52.86 ± 16.83 years (median: 54 years). Of 2292 SCS smokers, 382 (16.7%) were nonsmokers according to their self-report. Notably, the ratio of the cotinine-verified to self-reported smoking rate of women was greater than that of men, 1.60 and 1.06, respectively. This indicated that female hidden smokers may affect the results of studies based on self-reported questionnaires. Multivariate logistic regression analysis showed that smoking was correlated with cataract (odds ratio [OR], 1.37 [95% CI, 1.07-1.76]; OR, 1.35 [CI, 1.12-1.64]; and OR, 1.36 [CI, 1.10-1.69]) for self-reported, cotinine-verified, and SCS, respectively. No statistically significant sex difference was found.

Conclusion: Smoking was associated with cataract, but it did not vary by sex. Female hidden smoking must be considered when investigating the association between smoking and cataract based on self-reported questionnaires.

J Cataract Refract Surg 2020; 46:45–54 Copyright © 2019 Published by Wolters Kluwer on behalf of ASCRS and ESCRS

Age-related cataract (ARC) is the leading cause of blindness.^{1,2} With the proportional increase in the elderly population, the prevalence of ARC will rapidly increase and will present a serious future public health concern.^{1,2} Although the etiology and mechanisms of ARC are complex, smoking is thought to contribute to the risk of developing ARC.¹ However, one study demonstrated no association between smoking status and ARC, and there are few studies that examine the quantitative effect of smoking on ARC.³ We assume that these inconsistent results may be influenced by misclassification bias. Because the identification of smoking status is entirely based on participants' reliability of responses to self-reported questionnaires, urine cotinine testing was used

in a recent study to verify smoking status to reduce misclassification bias.⁴ We previously reported that smoking was associated with hypertension using survey-cotinine-verified smoking status (SCS).⁵

Therefore, the aim of the present study was to investigate the effects of hidden smokers on ARC occurrence using the previously reported method. These smokers, mostly women, were identified as nonsmokers on self-response questionnaires but were subsequently found to be cotinine-verified smokers. We also wanted to investigate the relationship of all types of smoking habits, including hidden smoking, with ARC by using Korea National Health and Nutrition Examination Survey (KNHANES) data.

Submitted: March 12, 2019 | Final revision submitted: July 18, 2019 | Accepted: August 8, 2019

Department of Pediatrics, Samsung Changwon Hospital, Sungkyunkwan University School of Medicine, South Korea.

Corresponding Author: Sung Hoon Kim, MD, PhD, Department of Pediatrics, Samsung Changwon Hospital, Sungkyunkwan University School of Medicine, 158 Paryong-ro, Masanhoewon-gu, Changwon, 51353, South Korea. Email: hee7307@skku.edu.

Copyright © 2019 Published by Wolters Kluwer on behalf of ASCRS and ESCRS
Published by Wolters Kluwer Health, Inc.

0886-3350/\$ - see frontmatter
<https://doi.org/10.1016/j.jcrs.2019.08.035>

Copyright © 2020 Published by Wolters Kluwer on behalf of ASCRS and ESCRS. Unauthorized reproduction of this article is prohibited.

METHODS

Study Population

This study was approved by the IRB of Samsung Changwon Hospital (IRB No. 2019–01-006). The need to obtain informed consent was waived by the board. This retrospective study was conducted using 2008 to 2016 KNHANES data (<http://knhanes.cdc.go.kr>). The 2012 to 2013 data were excluded because the urinary cotinine level was not investigated as part of the survey at that time. KNHANES is a nationwide, population-based, cross-sectional survey designed to examine the health and nutritional status of the Korean population and is conducted by the Division of Chronic Disease Surveillance at the Korea Centers for Disease Control and Prevention. Participants were randomly selected using stratified sampling by population, sex, age, regional area, and type of residential area. The KNHANES health records are based on household interviews, physical examinations, laboratory tests, and nutritional surveys. This study was approved by the IRB of Samsung Changwon Hospital (IRB No. 2019–01-006). The need to obtain informed consent from patients was waived by the board. All survey protocols were approved by the Korea Centers for Disease Control and Prevention Institutional Review Board, and written informed consent was obtained for all initial research conducted from 2018 to 2016, before the survey began.

Data Collection

To determine the demographic and socioeconomic characteristics of the participants, well-established questions were used. Each participant completed a questionnaire providing information on sex, age, marital status, employment status, education level, monthly family income, number of household members, residence area, smoking habits, alcohol use, body mass index, and medical history. Marital status was divided into 3 groups as married, formerly married (separated or divorced), and never married. Body mass index was categorized into 3 groups in accordance with the Asian-Pacific guideline: normal weight (<23 kg/m²); overweight (23 to 25 kg/m²); and obese (≥25 kg/m²).⁶ For cataract, participants were asked whether a diagnosis of cataract had ever been made by a physician. Owing to the study design, there was no information about accurate diagnosis based on the actual eye examination, history of cataract surgery, and presence of visual impairments.

Self-reported smoking status was divided into smoker, ex-smoker, and never-smoker according to their response to the question, “Do you smoke cigarettes now?” Smokers were identified as respondents who reported having consumed 100 or more cigarettes in their lifetime with a “Yes” response to the previously mentioned question. Ex-smokers were those who have consumed 100 or more cigarettes in their lifetime and answered “No” to the same question. Never-smokers were defined as respondents who have consumed less than 100 cigarettes in their lifetime. The level of urinary cotinine was measured by tandem mass spectrometry with an API 4000 Tandem mass spectrometer (Applied Biosystems) and by gas chromatography and mass spectrometry with a PerkinElmer Clarus 600T (PerkinElmer). Cotinine-verified smokers were defined as participants with urinary cotinine levels 50 ng/ml or higher, whereas cotinine-verified nonsmokers were identified as those with urinary cotinine levels less than 50 ng/ml.⁷

To better identify the relationship between cataract and smoking, a new variable was used to define smoking-status (Table 1) according to the previously reported study.⁵ We hypothesized that inclusion of this variable indicated that any of the smoking habit types, including light, intermittent, passive, and hidden smoking, may have been present.

Statistical Analysis

All statistical analyses were conducted using SPSS complex sample procedures with SPSS Statistics for Windows software (version 21.0, IBM Corp.). For more accurate statistical comparisons, χ^2 analysis was conducted to select significant covariates. Multivariate logistic regression was used, and the respective odds ratio (OR) was estimated to identify the relationships between risk factors and the prevalence of cataract. For all analyses, *P* values were two-tailed, and *P* values less than .05 were considered statistically significant.

RESULTS

Participant Characteristics

Initially, 76 909 individuals who participated in KNHANES were considered. A flow diagram of the inclusion and exclusion procedure is shown in Figure 1. Ultimately, 11 435 participants (4925 men and 6510 women) were eligible for inclusion in the final analysis. The mean age was 52.86 ± 16.83 years (median: 54 years). The majority of participants were married (67.2%), unemployed (61.6%), had an education level of high school or higher (72.4%), and lived in urban areas (83.5%) Table 2 shows patient characteristics.

Smoking Status

The prevalence of self-reported smokers was 21.1%, whereas that of cotinine-verified smokers in the overall population was 23.8% (Table 2). Table 3 shows prevalence rates of smoking status both by self-report and by urine cotinine verification. The prevalence of self-reported and cotinine-verified smokers was 37.1% and 39.2% in men and 5.5% and 8.8% in women, respectively. The cotinine-verified smoking prevalence was greater than the self-reported smoking prevalence rate was 2.1% and 3.3% in men and women, respectively. Notably, the ratio of cotinine-verified to self-reported smoking in women was greater than that in men, 1.60 and 1.06, respectively. Of the total of 2292 cotinine-verified male and female smokers, 382 (16.7%) were nonsmokers according to their self-reported smoking status (ie, never-smokers plus ex-smokers) (Table 1). This underreporting differed markedly by sex. Of the male cotinine-verified smokers, 8.5% were self-reported nonsmokers (1.6% never-smokers and 6.9% ex-smokers), whereas of the female cotinine-verified smokers, 42.2% were self-reported nonsmokers (33.3% never-smokers and 8.9% ex-smokers); and 0.41% of cotinine-verified male and female nonsmokers, respectively, were smokers by self-reported status (Table 3).

Association Between Cataract and Smoking

Univariate analysis did not reveal any statistically significant differences in marital status and residential area between participants with and without cataract (Table 4). As compared with patients without cataract, those with cataract were more likely to be female, older, married or single (separated or divorced), unemployed, less educated, and obese; to have a lower monthly family income and a lower number of household members; and to live in a rural area (Table 4). Although the univariate statistical analysis of self-

Table 1. Definition of survey-cotinine-verified smoking status.

Self-reported Smoking Status (n)	Cotinine-verified Smoking Status	
	Nonsmoker (≤ 50 ng/mL)	Smoker (> 50 ng/mL)
Nonsmoker	6949	206
Ex-smoker	2123	176
Smoker	71	1910

reported, cotinine-verified, and SCS smoking showed that there was no statistically significant relationship between smoking and cataract, the multivariate logistic regression analysis showed that smoking was correlated with cataract (OR, 1.37 [95% CI, 1.07-1.76]; OR, 1.35 [CI, 1.12-1.64]; and OR, 1.36 [CI, 1.10-1.69]) (Table 5). When sex was considered, the adjusted OR of the association of smoking with cataract in men was 1.22 (CI, 0.90-1.66), 1.29 (CI, 1.03-1.62), and 1.33 (CI, 0.98-1.79), whereas in female smokers, it was 1.70 (CI, 1.15-2.49), 1.33 (CI, 0.95-1.86), and 1.40 (CI, 0.99-1.94) for self-reported smoking status, cotinine-verified smoking status, and SCS, respectively (Tables 6 and 7). Therefore, the results indicate that although the adjusted OR of female sex was higher than that of male sex in all survey forms, there was no statistical significance. Sex did not affect the incidence of cataract in this study.

DISCUSSION

In our study, smoking was positively associated with cataract, and this did not vary by sex. Cigarette smoke is a complex mixture of over 7000 compounds, including particles (eg, nicotine), gases (eg, carbon monoxide), and volatile chemicals (eg, formaldehyde).⁸ Smoking adversely affects human health through direct toxic

influence and indirect mechanisms. These affect apoptosis and depress the immune system, decreasing the body's protection from illness and the ability to heal or repair tissues.⁸⁻¹⁰

Smoking is associated with many ocular diseases, which have a significant impact on the quality of life, and smoking is also one of many established or putative risk factors for cataract.^{8,11-15} Cataract, the opacification of the lens, is divided anatomically into nuclear, cortical, and posterior subcapsular types.⁸ There is a study revealing strong association of smoking with nuclear cataract and weaker association with cortical cataract.⁸ Although the mechanism is very complex and multifactorial and little is known about the etiology of cataract, many studies have confirmed the risk of cataract to be elevated in smokers.¹¹⁻¹⁷ Smokers have a significantly higher prevalence of ARC compared with never-smokers.^{17,18} Also, current smokers have a higher risk of ARC than ex-smokers because of longer exposure time and higher total cumulative dose of smoking than ex-smokers.^{11,17} Similarly, heavy smokers are at a higher risk of ARC than light smokers.¹⁶ Smoking impairs lenticular function and causes lens opacification through many mechanisms. Increased activity of free

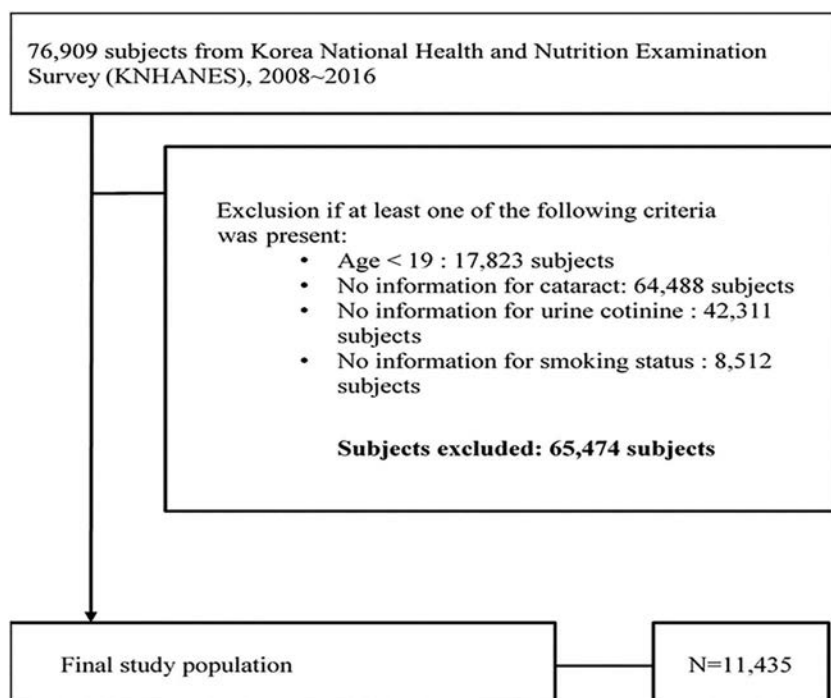
**Figure 1.** Flow chart of targeted participants.

Table 2. Participant characteristics.		
Characteristics	Sample Size	Estimate % (95% CI)
Sex (n = 11 435)		
Male	4925	49.42 (48.53-50.31)
Female	6510	50.58 (49.69-51.47)
Age (n = 11 435)		
<40s	2863	34.00 (32.45-35.58)
40-49	1934	19.88 (18.85-20.95)
50-59	2173	19.92 (18.90-20.98)
60-69	2228	13.74 (12.90-14.62)
≥70	2237	12.47 (11.67-13.31)
Marital status (n = 11 415)		
Married	8078	67.18 (65.71-68.62)
Formerly married (separated or divorced)	1743	11.71 (10.90-12.59)
Never married	1594	21.10 (19.83-22.43)
Employment status (n = 11 392)		
Employed	6543	38.38 (37.14-39.63)
Unemployed	4849	61.62 (30.37-62.86)
Education level (n = 11 382)		
<High school	4208	27.64 (26.13-29.21)
High school	3545	35.55 (34.23-36.90)
>High school	3629	36.80 (34.97-38.67)
Monthly family income (n = 11 360)		
<25th	2411	17.11 (15.76-18.54)
25 to 50th	2816	23.36 (21.98-24.79)
50 to 75th	3001	29.08 (27.45-30.78)
≥75th	3132	30.45 (28.27-32.73)
No. of household members (n = 11 434)		
1	1303	9.01 (8.06-10.05)
2	3483	25.04 (23.78-26.33)
3	2754	27.20 (25.80-28.65)
4	2730	27.88 (26.34-29.47)
≥5	1164	10.88 (9.88-11.97)
Residence area (n = 11 435)		
Urban	9079	83.51 (79.92-86.57)
Rural	2356	16.49 (13.43-20.08)
Smoking status		
Self-reported (n = 11 435)		
Nonsmoker	7155	59.31 (58.19-60.43)
Ex-smoker	2299	19.61 (18.81-20.43)
Current smoker	1981	21.08 (19.99-22.20)
Cotinine-verified (n = 11 435)		
Nonsmoker/ex-smoker	9143	76.20 (75.05-77.31)
Smoker	2292	23.80 (22.69-24.95)
Survey-cotinine-verified (n = 11 435)		
Nonsmoker	6949	57.53 (56.40-58.65)
Ex-smoker	2123	17.87 (17.10-18.67)
Current smoker	2363	24.60 (23.48-25.76)
BMI (n = 11 418)		
<23	4720	42.03 (40.82-43.24)
23 to 25	2704	23.33 (22.42-24.26)
≥25	3994	34.64 (33.46-35.85)
Cataract (n = 11 415)		
No	9139	85.67 (84.71-86.57)
Yes	2296	14.33 (13.43-15.29)

BMI = body mass index

radicals, oxidative stress, and lipid peroxidation causes direct oxidative lens damage, and the accumulation of cadmium, lead, and copper in the lens causes direct lens toxicity.^{19,20} Also, smokers have significant

reduction in the endogenous antioxidant levels of vitamins C and E and beta carotene when compared with nonsmokers.²⁰ This is associated with indirect oxidative lens damage.²⁰

Table 3. Self-reported and cotinine-verified smoking status in men and women.

Self-reported Smoking Status	Total	Cotinine-verified Smoking Status	
		Nonsmoker (≤ 50 ng/mL)	Smoker (> 50 ng/mL)
Male (n = 4925)			
Total		60.84 (59.10, 62.55)	39.16 (37.45, 40.90)
Nonsmoker	27.70 (26.17, 29.28)	27.08 (25.59, 28.63)	0.61 (0.38, 0.99)
Ex-smoker	35.25 (33.68, 36.84)	32.52 (31.01, 34.06)	2.72 (2.18, 3.41)
Smoker	37.06 (35.34, 38.81)	1.24 (0.93, 1.64)	35.82 (34.10, 37.58)
Female (n = 6510)			
Total		91.21 (90.23, 92.10)	8.79 (7.90, 9.77)
Nonsmoker	90.21 (89.24, 91.11)	87.28 (86.19, 88.30)	2.93 (2.48, 3.46)
Ex-smoker	4.33 (3.77, 4.97)	3.55 (3.06, 4.13)	0.78 (0.55, 1.09)
Smoker	5.46 (4.77, 6.25)	0.37 (0.21, 0.68)	5.09 (4.42, 5.85)

The current adolescent smoking rate is high and increasing despite globally designed preventative actions; this will induce serious health problems when they are elderly. According to the Korean Youth Risk Behavior Web-based Survey (<http://www.cdc.go.kr/search/search.es?mid=a20101000000>) 2018, the current smoking rate of male adolescents in South Korea is higher than that of female adolescents (9.4% vs 3.7%); however, there has been a significant increase in the female adolescent smoking rate during the 3 most recent survey years (2.7%, 3.1%, and 3.7%). There has been no change in the male adolescent smoking rate (9.6%, 9.5%, and 9.4%). The increased rate of female adolescent smoking will be associated with not only ARC but also prenatal and maternal smoking problems. This phenomenon will induce several health problems for fetuses or offspring;^{21–25} the survey was started by began as pediatricians to identify the actual state of female hidden smokers by using new variables. Because the reliability of smoking status in the previously conducted cross-sectional studies was based on the fidelity of participants' responses to self-reported questionnaires, there is a possibility of having misclassification bias. To reduce this misclassification bias, urine cotinine testing was used to measure smoking status in a recent study.⁴ In addition to urine cotinine test use, we used SCS to better understand the association between cataract and smoking and to consider the effects of hidden smoking in this study. We found that the ratio of the cotinine-verified to self-reported smoking rate of women was greater than that of men, 1.60 and 1.06, respectively. Of the male cotinine-verified smokers, 8.5% were self-reported nonsmokers, whereas of the female cotinine-verified smokers, 42.2% were self-reported nonsmokers. Thus, this new variable showed that female hidden smoking should be considered as a risk factor when investigating the association between smoking and cataract based on self-reported questionnaires. We believe that this underestimated self-reported smoking prevalence in Korean women may be the result of a patriarchal culture in which female smoking is stigmatized among people under the influence of conservative Confucianism.²⁶ Conversely,

there was no sex difference in regard to the response reliability of smoking history in a study from the United States.²⁷

Because previous studies have found that passive smoking increases the risk for cataract,^{14,28} we also wanted to investigate the effects of the smoking type on cataract by using SCS. Passive smoking, also known as second-hand smoke or environmental tobacco exposure, is the combination of 15% mainstream smoke exhaled by the smoker and 85% side-stream smoke from the burning end of a cigarette.⁷ Light and intermittent smokers often remain undetected; because these smokers may consider themselves not current smokers, they may deny their smoking habits when they answer the questionnaire.²⁹ Our new variable showed similar results as those of self-reported and cotinine-verified smoking status. Passive and light smoking may have a similar effect on the development of cataract as active smoking, and the KNHANES data were reliable when considering smoking status. From a preventive measure point of view, among ex-smokers, the risk of ARC decreases with the number of abstinent years, but not to the level of never-smokers, even 25 or more years after smoking cessation.²⁰ Therefore, nonsmoking or smoking cessation education should be emphasized in schools for preventing ARC.

There are several limitations to our study. First, we could not confirm the causal relationship between smoking and cataract because of its cross-sectional design. Second, although this study was based on the data of the national survey, our results may be influenced by selection bias or recall bias of participants. Third, we could not exclude respondents using nicotine replacement therapy during the survey. Fourth, other recognized risk factors for cataract could not be assessed with our study design. These risk factors include ultraviolet radiation exposure, genetic factors, supplement and selected drug use, trauma, diabetes mellitus, hypoparathyroidism, and prolonged corticosteroid administration.^{11–15} Fifth, we know that an eye examination is crucial to the diagnosis of cataract from the perspective of an ophthalmologist. We have removed

Table 4. Crude ORs and associated 95% CIs for the prevalence of cataract.						
Characteristics	Total		Male		Female	
	OR (95% CI)	P Value	OR (95% CI)	P Value	OR (95% CI)	P Value
Sex						
Male	Reference		—		—	
Female	1.57 (1.41, 1.75)	<.001	—		—	
Age						
<40s	Reference		Reference		Reference	
40–49	2.63 (1.60, 4.30)	<.001	3.23 (1.74, 5.96)	<.001	1.87 (0.95, 3.66)	.068
50–59	6.51 (4.24, 9.99)	<.001	6.03 (3.47, 10.49)	<.001	7.22 (4.28, 12.19)	<.001
60–69	25.14 (16.70, 37.85)	<.001	17.11 (10.09, 29.01)	<.001	35.82 (21.75, 58.97)	<.001
≥70	84.12 (55.54, 127.40)	<.001	54.20 (32.12, 91.45)	<.001	119.79 (72.22, 198.68)	<.001
Marital status						
Married	22.59 (12.11, 42.15)	<.001	21.99 (9.45, 51.15)	<.001	24.40 (10.74, 55.43)	<.001
Formerly married	95.25 (50.23, 180.62)	<.001	46.36 (18.91, 113.68)	<.001	124.97 (53.89, 289.78)	<.001
Never married	Reference		Reference		Reference	
Employment status						
Employed	Reference		Reference		Reference	
Unemployed	3.28 (2.90, 3.71)	<.001	3.07 (2.56, 3.70)	<.001	3.21 (2.75, 3.75)	<.001
Education						
<High school	10.65 (8.80, 12.90)	<.001	6.09 (4.84, 7.66)	<.001	18.33 (13.67, 24.59)	<.001
High school	1.76 (1.43, 2.16)	<.001	1.61 (1.24, 2.10)	<.001	2.14 (1.54, 2.97)	<.001
>High school	Reference		Reference		Reference	
Monthly family income						
<25th	6.16 (5.01, 7.58)	<.001	4.53 (3.41, 6.02)	<.001	7.45 (5.84, 9.52)	<.001
25 to 50th	2.44 (1.99, 3.01)	<.001	2.11 (1.58, 2.81)	<.001	2.74 (2.15, 3.49)	<.001
50 to 75th	1.22 (0.99, 1.51)	.068	1.18 (0.88, 1.59)	.268	1.25 (0.97, 1.62)	.083
≥75th	Reference		Reference		Reference	
No. of household members						
1	2.32 (1.80, 2.99)	<.001	1.25 (0.82, 1.92)	.294	3.22 (2.44, 4.25)	<.001
2	1.78 (1.44, 2.20)	<.001	1.94 (1.38, 2.74)	<.001	1.72 (1.34, 2.20)	<.001
3	0.69 (0.55, 0.88)	.003	0.78 (0.52, 1.16)	.219	0.65 (0.49, 0.87)	.003
4	0.50 (0.40, 0.63)	<.001	0.66 (0.45, 0.97)	.035	0.41 (0.31, 0.55)	<.001
≥5	Reference		Reference		Reference	
Residence area						
Urban	Reference		Reference		Reference	
Rural	1.60 (1.26, 2.03)	<.001	1.45 (1.09, 1.93)	.011	1.74 (1.35, 2.24)	<.001
Smoking status						
Self-reported						
Nonsmoker	Reference		Reference		Reference	
Ex-smoker	1.13 (0.99, 1.28)	.066	2.27 (1.82, 2.83)	<.001	0.90 (0.66, 1.22)	.489
Current smoker	0.64 (0.54, 0.77)	<.001	1.13 (0.87, 1.48)	.364	1.02 (0.73, 1.43)	.897
Cotinine-verified						
Nonsmoker/ex-smoker	Reference		Reference		Reference	
Smoker	0.69 (0.59, 0.81)	<.001	0.76 (0.63, 0.93)	.007	0.96 (0.73, 1.27)	.786
Survey-cotinine-verified						
Nonsmoker	Reference		Reference		Reference	
Ex-smoker	1.14 (0.99, 1.30)	.051	2.32 (1.86, 2.91)	<.001	0.99 (0.71, 1.38)	.945
Current smoker	0.71 (0.60, 0.83)	<.001	1.26 (0.97, 1.63)	.079	0.95 (0.73, 1.24)	.716
BMI (n = 11 418)						
<23	Reference		Reference		Reference	
23 to 25	1.26 (1.10, 1.45)	.001	0.78 (0.62, 0.98)	.036	1.94 (1.63, 2.32)	<.001
≥25	1.27 (1.13, 1.44)	<.001	0.67 (0.55, 0.81)	<.001	2.26 (1.93, 2.65)	<.001

BMI = body mass index; OR = odds ratio; Reference = when unable to distinguish or define a normal state, ie, social economic state and environmental state, the reference was established for variables where the adjusted odds ratio is more than 1.

Table 5. Adjusted ORs and associated 95% CIs for the prevalence of cataract.

Characteristics	Self-reported		Cotinine-verified		Survey-cotinine-verified	
	OR (95% CI)	P Value	OR (95% CI)	P Value	OR (95% CI)	P Value
Sex						
Male	Reference		Reference		Reference	
Female	1.11 (0.91, 1.34)	.304	1.09 (0.94, 1.26)	.271	1.08 (0.89, 1.30)	.454
Age						
<40s	Reference		Reference		Reference	
40–49	2.20 (1.27, 3.82)	.005	2.21 (1.28, 3.84)	.005	2.22 (1.28, 3.84)	.004
50–59	4.79 (2.92, 7.85)	<.001	4.83 (2.95, 7.93)	<.001	4.86 (2.97, 7.97)	<.001
60–69	14.52 (8.93, 23.62)	<.001	14.69 (9.02, 23.94)	<.001	14.81 (9.10, 24.10)	<.001
≥70	37.74 (22.92, 62.13)	<.001	38.16 (23.09, 63.04)	<.001	38.53 (23.36, 63.56)	<.001
Marital status						
Married	3.82 (1.87, 7.79)	<.001	3.81 (1.87, 7.77)	<.001	3.82 (1.87, 7.78)	<.001
Formerly married	4.88 (2.31, 10.28)	<.001	4.87 (2.31, 10.26)	<.001	4.87 (2.31, 10.27)	<.001
Never married	Reference		Reference		Reference	
Employment status						
Employed	Reference		Reference		Reference	
Unemployed	1.49 (1.29, 1.73)	<.001	1.49 (1.29, 1.73)	<.001	1.49 (1.29, 1.73)	<.001
Education						
<High school	1.57 (1.23, 2.00)	<.001	1.56 (1.22, 1.99)	<.001	1.56 (1.22, 1.99)	<.001
High school	1.18 (0.93, 1.49)	.177	1.18 (0.93, 1.49)	.173	1.18 (0.93, 1.49)	.177
>High school	Reference		Reference		Reference	
Monthly family income						
<25th	1.33 (1.03, 1.71)	.029	1.32 (1.03, 1.71)	.030	1.32 (1.03, 1.71)	.031
25 to 50th	1.33 (1.05, 1.68)	.017	1.33 (1.05, 1.67)	.018	1.33 (1.05, 1.67)	.018
50 to 75th	1.03 (0.81, 1.31)	.799	1.03 (0.81, 1.31)	.795	1.03 (0.82, 1.31)	.788
≥75th	Reference		Reference		Reference	
No. of household members						
1	0.79 (0.58, 1.08)	.134	0.79 (0.58, 1.07)	.130	0.79 (0.58, 1.07)	.132
2	0.76 (0.59, 0.98)	.033	0.76 (0.59, 0.98)	.032	0.76 (0.59, 0.98)	.033
3	0.74 (0.56, 0.98)	.034	0.74 (0.56, 0.98)	.033	0.74 (0.56, 0.98)	.034
4	0.87 (0.65, 1.17)	.365	0.88 (0.65, 1.18)	.378	0.88 (0.65, 1.18)	.382
≥5	Reference		Reference		Reference	
Residence area						
Urban	Reference		Reference		Reference	
Rural	1.10 (0.86, 1.39)	.444	1.10 (0.86, 1.39)	.454	1.10 (0.86, 1.39)	.453
Smoking status						
Self-reported						
Nonsmoker	Reference		—		—	
Ex-smoker	1.03 (0.84, 1.27)	.794	—		—	
Current smoker	1.37 (1.07, 1.76)	.013	—		—	
Cotinine-verified						
Nonsmoker/ex-smoker	—		Reference		—	
Smoker	—		1.35 (1.12, 1.64)	.002	—	
Survey-cotinine-verified						
Nonsmoker	—		—		Reference	
Ex-smoker	—		—		0.97 (0.79, 1.20)	.786
Current smoker	—		—		1.36 (1.10, 1.69)	.005
BMI						
<23	Reference		Reference		Reference	
23 to 25	0.97 (0.82, 1.15)	.757	0.97 (0.82, 1.15)	.750	0.97 (0.82, 1.15)	.746
≥25	0.97 (0.84, 1.12)	.674	0.97 (0.84, 1.12)	.678	0.97 (0.84, 1.12)	.680

BMI = body mass index; CI = confidence interval; OR = odds ratio; Reference = when unable to distinguish or define a normal state, ie, social economic state and environmental state, the reference was established for variables where the adjusted odds ratio is more than 1.

some of the confounding effects of underreporting of the smoking variable by use of the cotinine test, but we could not remove that problem from the cataract variable. Owing to the study design as a self-reporting

questionnaire, we could not determine how many participants who had a history of cataract actually had a diagnosis based on an eye examination, whether they had cataract surgery, or whether they had any

Table 6. Adjusted ORs and associated 95% CIs for the prevalence of cataract in men.						
Characteristics	Self-reported		Cotinine-verified		Survey-cotinine-verified	
	OR (95% CI)	P Value	OR (95% CI)	P Value	OR (95% CI)	P Value
Age						
<40s	Reference		Reference		Reference	
40–49	2.61 (1.23, 5.56)	.013	2.66 (1.25, 5.64)	.011	2.66 (1.25, 5.64)	.011
50–59	4.40 (2.16, 8.98)	<.001	4.52 (2.22, 9.18)	<.001	4.53 (2.23, 9.20)	<.001
60–69	10.78 (5.31, 21.90)	<.001	11.19 (5.52, 22.70)	<.001	11.23 (5.54, 22.77)	<.001
≥70	27.83 (13.50, 57.36)	<.001	29.29 (14.23, 60.30)	<.001	29.37 (14.28, 60.44)	<.001
Marital status						
Married	4.50 (1.64, 12.39)	.004	4.53 (1.65, 12.46)	.003	4.49 (1.64, 12.33)	.004
Formerly married	5.86 (2.03, 16.91)	.001	5.86 (2.02, 16.96)	.001	5.81 (2.01, 16.73)	.001
Never married	Reference		Reference		Reference	
Employment status						
Employed	Reference		Reference		Reference	
Unemployed	1.48 (1.16, 1.89)	.002	1.49 (1.17, 1.90)	.001	1.49 (1.17, 1.90)	.001
Education						
<High school	1.36 (0.99, 1.86)	.052	1.35 (0.99, 1.84)	.058	1.35 (0.99, 1.84)	.059
High school	1.22 (0.89, 1.68)	.224	1.22 (0.88, 1.68)	.230	1.21 (0.88, 1.67)	.236
>High school	Reference		Reference		Reference	
Monthly family income						
<25th	1.45 (0.98, 2.13)	.063	1.43 (0.97, 2.12)	.069	1.44 (0.97, 2.12)	.068
25 to 50th	1.38 (0.99, 1.92)	.056	1.37 (0.98, 1.91)	.062	1.37 (0.99, 1.91)	.059
50 to 75th	1.16 (0.83, 1.61)	.381	1.16 (0.83, 1.62)	.378	1.16 (0.83, 1.62)	.373
≥75th	Reference		Reference		Reference	
No. of household members						
1	0.71 (0.41, 1.22)	.212	0.70 (0.41, 1.22)	.207	0.70 (0.41, 1.21)	.203
2	0.76 (0.52, 1.11)	.160	0.77 (0.52, 1.12)	.167	0.76 (0.52, 1.11)	.158
3	0.76 (0.49, 1.17)	.206	0.76 (0.49, 1.17)	.213	0.76 (0.49, 1.17)	.207
4	1.01 (0.66, 1.57)	.947	1.02 (0.66, 1.58)	.924	1.02 (0.66, 1.58)	.938
≥5	Reference		Reference		Reference	
Residence area						
Urban	Reference		Reference		Reference	
Rural	1.04 (0.77, 1.41)	.788	1.04 (0.77, 1.41)	.802	1.04 (0.77, 1.41)	.797
Smoking status						
Self-reported						
Nonsmoker	Reference		—		—	
Ex-smoker	1.06 (0.82, 1.38)	.636	—		—	
Current smoker	1.22 (0.90, 1.66)	.204	—		—	
Cotinine-verified						
Nonsmoker/ex-smoker	—		Reference		—	
Smoker	—		1.29 (1.03, 1.62)	.026	—	
Survey-cotinine-verified						
Nonsmoker	—		—		Reference	
Ex-smoker	—		—		1.03 (0.80, 1.34)	.814
Current smoker	—		—		1.33 (0.98, 1.79)	.066
BMI						
<23	Reference		Reference		Reference	
23, 25	0.79 (0.61, 1.03)	.086	0.79 (0.61, 1.03)	.086	0.79 (0.61, 1.03)	.086
≥25	0.80 (0.64, 0.99)	.048	0.80 (0.64, 1.01)	.053	0.80 (0.64, 1.01)	.054

BMI = body mass index; OR = odds ratio; Reference = when unable to distinguish or define a normal state, ie, social economic state and environmental state, the reference was established for variables where the adjusted odds ratio is more than 1.

visual impairment. Further study based on eyesight examination and refractive testing by ophthalmologists needs to be performed. Sixth, we need to further research other possible sources of nicotine exposure, such as nicotine patch or gum use, in addition to second-

hand smoke. Finally, the amount and duration of smoking were not considered. Further prospective and collaborative global studies are needed to clarify the effect of smoking status on the onset or aggravated degree of cataract. However, the worthwhile aspect of

Table 7. Adjusted ORs and associated 95% CIs for the prevalence of cataract in women.

Characteristics	Self-reported		Cotinine-verified		Survey-cotinine-verified	
	OR (95% CI)	P Value	OR (95% CI)	P Value	OR (95% CI)	P Value
Age						
<40s	Reference		Reference		Reference	
40–49	1.48 (0.70, 3.15)	.305	1.48 (0.70, 3.14)	.307	1.48 (0.70, 3.15)	.305
50–59	4.62 (2.44, 8.75)	<.001	4.62 (2.44, 8.75)	<.001	4.64 (2.44, 8.81)	<.001
60–69	16.61 (8.72, 31.65)	<.001	16.49 (8.67, 31.37)	<.001	16.63 (8.70, 31.76)	<.001
≥70	43.30 (22.45, 83.51)	<.001	42.50 (22.07, 81.87)	<.001	42.92 (22.18, 83.07)	<.001
Marital status						
Married	3.70 (1.53, 8.99)	.004	3.66 (1.51, 8.90)	.004	3.66 (1.51, 8.90)	.004
Single (separated or divorced)	4.19 (1.64, 10.69)	.003	4.20 (1.65, 10.73)	.003	4.19 (1.64, 10.70)	.003
Never married	Reference		Reference		Reference	
Employment status						
Employed	Reference		Reference		Reference	
Unemployed	1.60 (1.33, 1.93)	<.001	1.60 (1.33, 1.93)	<.001	1.60 (1.33, 1.93)	<.001
Education						
<High school	1.89 (1.30, 2.75)	.001	1.91 (1.31, 2.77)	.001	1.90 (1.31, 2.76)	.001
High school	1.27 (0.88, 1.84)	.197	1.29 (0.89, 1.86)	.174	1.28 (0.89, 1.85)	.181
>High school	Reference		Reference		Reference	
Monthly family income						
<25th	1.18 (0.87, 1.60)	.293	1.18 (0.87, 1.60)	.297	1.18 (0.86, 1.60)	.302
25 to 50th	1.26 (0.94, 1.70)	.119	1.27 (0.94, 1.70)	.117	1.27 (0.94, 1.70)	.118
50 to 75th	0.90 (0.66, 1.21)	.473	0.89 (0.66, 1.21)	.472	0.89 (0.66, 1.21)	.472
≥75th	Reference		Reference		Reference	
No. of household members						
1	0.88 (0.60, 1.29)	.517	0.88 (0.60, 1.29)	.513	0.88 (0.60, 1.29)	.513
2	0.80 (0.57, 1.12)	.194	0.81 (0.58, 1.13)	.21	0.80 (0.57, 1.13)	.206
3	0.77 (0.53, 1.11)	.165	0.77 (0.53, 1.12)	.169	0.77 (0.53, 1.12)	.166
4	0.74 (0.50, 1.08)	.121	0.74 (0.50, 1.09)	.128	0.74 (0.50, 1.09)	.129
≥5	Reference		Reference		Reference	
Residence area						
Urban	Reference		Reference		Reference	
Rural	1.16 (0.88, 1.52)	.282	1.16 (0.88, 1.52)	.283	1.16 (0.88, 1.52)	.282
Smoking status						
Self-reported						
Nonsmoker	Reference		—		—	
Ex-smoker	0.92 (0.62, 1.37)	.687	—		—	
Current smoker	1.70 (1.15, 2.49)	.007	—		—	
Cotinine-verified						
Nonsmoker/ex-smoker	—		Reference		—	
Smoker	—		1.33 (0.95, 1.86)	0.093	—	
Survey-cotinine-verified						
Nonsmoker	—		—		Reference	
Ex-smoker	—		—		0.97 (0.64, 1.47)	.869
Current smoker	—		—		1.40 (0.99, 1.94)	.051
BMI						
<23	Reference		Reference		Reference	
23 to 25	1.11 (0.89, 1.38)	.369	1.11 (0.89, 1.38)	.369	1.11 (0.89, 1.38)	.364
≥25	1.02 (0.83, 1.27)	.825	1.02 (0.83, 1.27)	.827	1.03 (0.83, 1.27)	.819

BMI = body mass index; OR = odds ratio; Reference = when unable to distinguish or define a normal state, ie, social economic state and environmental state, the reference was established for variables where the adjusted odds ratio is more than 1.

our study is the use of large quantities of widely sampled data. Also, we analyzed various results that derived from interviews, physical examinations, and laboratory tests such as urine cotinine levels. To our knowledge, this study is the first report to consider the effects of all types of smoking, including hidden smoking, on cataract.

Consistent with other studies, this study found that smoking was associated with cataract in the overall population, but no significant sex difference was noted. Female hidden smoking should be considered when investigating the association between smoking and cataract based on self-reported questionnaires.

WHAT WAS KNOWN

- Cataract is the leading cause of blindness worldwide.
- Although the etiology and mechanisms of cataract are complex, smoking is thought to contribute to the risk of developing cataract.

WHAT THIS PAPER ADDS

- When a new variable was used to define smoking status (survey-cotinine-verified smoking status), smoking was associated with cataract, but this relationship did not vary by sex.
- Female hidden smoking should be considered when investigating the association between smoking and cataract based on self-reported questionnaires.

REFERENCES

1. Ellwein LB, Kupfer C. Strategic issues in preventing cataract blindness in developing countries. *Bull World Health Organ* 1995;73:681–690
2. Kar T, Ayata A, Aksoy Y, Kaya A, Unal M. The effect of chronic smoking on lens density in young adults. *Eur J Ophthalmol* 2014;24:682–687
3. Klein BE, Klein R, Linton KL, Franke T. Cigarette smoking and lens opacities: the Beaver Dam Eye Study. *Am J Prev Med* 1993;9:27–30
4. Kim BJ, Han JM, Kang JG, Kim BS, Kang JH. Association between cotinine-verified smoking status and hypertension in 167,868 Korean adults. *Blood Press* 2017;26:303–310
5. Inoue S, Zimmet P, Caterson I, Chen C, Ikeda Y, Khalid AK, Kim YS, Bassett J. The Asia-Pacific perspective: redefining obesity and its treatment. 2000. Available at: <http://otforg/>. Accessed February 19, 2002
6. Haufroid V, Lison D. Urinary cotinine as a tobacco-smoke exposure index: a minireview. *Int Arch Occup Environ Health* 1998;71:162–168
7. Nita M, Grzybowski A. Smoking and eye pathologies. A systemic review. Part II. Retina diseases, uveitis, optic neuropathies, thyroid-associated orbitopathy. *Curr Pharm Des* 2017;23:639–654
8. Zeidler R, Albermann K, Lang S. Nicotine and apoptosis. *Apoptosis* 2007;12:1927–1943
9. Kode A, Yang SR, Rahman I. Differential effects of cigarette smoke on oxidative stress and proinflammatory cytokine release in primary human airway epithelial cells and in a variety of transformed alveolar epithelial cells. *Respir Res* 2006;7:132
10. Theodoropoulou S, Theodossiadi P, Samoli E, Vergados I, Lagiou P, Tzonou A. The epidemiology of cataract: a study in Greece. *Acta Ophthalmol* 2011;89:e167–e173
11. West S. Epidemiology of cataract: accomplishments over 25 years and future directions. *Ophthalmic Epidemiol* 2007;14:173–178
12. Lu ZQ, Sun WH, Yan J, Jiang TX, Zhai SN, Li Y. Cigarette smoking, body mass index associated with the risks of age-related cataract in male patients in northeast China. *Int J Ophthalmol* 2012;5:317–322
13. Cheng AC, Pang CP, Leung AT, Chua JK, Fan DS, Lam DS. The association between cigarette smoking and ocular diseases. *Hong Kong Med J* 2000;6:195–202
14. Beltrán-Zambrano E, García-Lozada D, Ibáñez-Pinilla E. Risk of cataract in smokers: a meta-analysis of observational studies. *Arch Soc Esp Ophthalmol* 2019;94:60–74
15. Wu R, Wang JJ, Mitchell P, Lamoureux EL, Zheng Y, Rochtchina E, Tan AG, Wong TY. Smoking, socioeconomic factors, and age-related cataract: the Singapore Malay Eye Study. *Arch Ophthalmol* 2010;128:1029–1035
16. Ye J, He J, Wang C, Wu H, Shi X, Zhang H, Xie J, Lee SY. Smoking and risk of age-related cataract: a meta-analysis. *Invest Ophthalmol Vis Sci* 2012;53:3885–3895
17. Krishnaiah S, Vilas K, Shamanna BR, Rao GN, Thomas R, Balasubramanian D. Smoking and its association with cataract: results of the Andhra Pradesh Eye Disease Study from India. *Invest Ophthalmol Vis Sci* 2005;46:58–65
18. Weintraub JM, Willett WC, Rosner B, Colditz GA, Seddon JM, Hankinson SE. Smoking cessation and risk of cataract extraction among US women and men. *Am J Epidemiol* 2002;155:72–79
19. Lindblad BE, Håkansson N, Svensson H, Philipson B, Wolk A. Intensity of smoking and smoking cessation in relation to risk of cataract extraction: a prospective study of women. *Am J Epidemiol* 2005;162:73–79
20. Harris HR, Willett WC, Michels KB. Parental smoking during pregnancy and risk of overweight and obesity in the daughter. *Int J Obes (Lond)* 2013;37:1356–1363
21. Niemelä S, Räisänen A, Koskela J, Taanila A, Miettunen J, Ramsay H, Veijola J. The effect of prenatal smoking exposure on daily smoking among teenage offspring. *Addiction* 2017;112:134–143
22. Mistry R, Jones AD, Pednekar MS, Dhimal G, Dasika A, Kulkarni U, Gomare M, Gupta PC. Antenatal tobacco use and iron deficiency anemia: integrating tobacco control into antenatal care in urban India. *Reprod Health* 2018;15:72
23. Thacher JD, Gehring U, Gruzieva O, Standl M, Pershagen G, Bauer CP, Berdel D, Keller T, Koletzko S, Koppelman GH, Kull I, Lau S, Lehmann I, Maier D, Schikowski T, Wahn U, Wijga AH, Heinrich J, Bousquet J, Anto JM, von Berg A, Melén E, Smit HA, Keil T, Bergström A. Maternal smoking during pregnancy and early childhood and development of asthma and rhinoconjunctivitis—a MeDALL project. *Environ Health Perspect* 2018;126:047005
24. Leybovitz-Haleluya N, Wainstock T, Landau D, Sheiner E. Maternal smoking during pregnancy and the risk of pediatric cardiovascular diseases of the offspring: a population-based cohort study with up to 18-years of follow up. *Reprod Toxicol* 2018;78:69–74
25. Jung-Choi KH, Khang YH, Cho HJ. Hidden female smokers in Asia: a comparison of self-reported with cotinine-verified smoking prevalence rates in representative national data from an Asian population. *Tob Control* 2012;21:536–542
26. Park M, Chesla C. Revisiting Confucianism as a conceptual framework for Asian family study. *J Fam Nurs* 2007;13:293–311
27. Caraballo RS, Giovino GA, Pechacek TF, Mowery PD. Factors associated with discrepancies between self-reports on cigarette smoking and measured serum cotinine levels among persons aged 17 years or older: Third National Health and Nutrition Examination Survey, 1988–1994. *Am J Epidemiol* 2001;153:807–814
28. Lois N, Abdelkader E, Reglitz K, Garden C, Ayres JG. Environmental tobacco smoke exposure and eye disease. *Br J Ophthalmol* 2008;92:1304–1310
29. Chan-Yeung M, Dimich-Ward H. Respiratory health effects of exposure to environmental tobacco smoke. *Respirology* 2003;8:131–139

Disclosures: None of the authors has a financial or proprietary interest in any material or method mentioned.



First author:

Hae Jeong Lee, MD

Department of Pediatrics, Samsung Changwon Hospital, Sungkyunkwan University School of Medicine, South Korea

ARTICLE

Anterior vitreous detachment: risk factor for intraoperative complications during phacoemulsification

Natalia S. Anisimova, MD, PhD, Lisa B. Arbisser, MD, Natalya F. Shilova, MD, Maria A. Melnik, MD, Alexandra V. Belodedova, MD, Boris Knyazer, MD, Boris E. Malyugin, MD, PhD

Purpose: To confirm the presence of incomplete vitreolenticular adhesion via microscope-integrated intraoperative optical coherence tomography (iOCT) during cataract surgery and via diagnostic spectral-domain OCT (SD-OCT) postoperatively.

Setting: S. Fyodorov Eye Microsurgery Complex State Institution, Moscow, Russia.

Design: Prospective noninterventional single-center study.

Methods: Clinical characteristics and surgical videos of 27 patients (28 eyes) who had cataract surgery were documented. Real-time iOCT integrated into the surgical microscope was directed to view the retrolenticular anatomy at the end of the surgery. Postoperatively, SD-OCT was also performed.

Results: This study comprised 28 eyes of 27 patients. Berger space was identified in 21 cases (75%) intraoperatively via iOCT and in 23 cases (82%) postoperatively via stationary OCT. Depth dimensions varied from $33.5 \pm 87.0 \mu\text{m}$ to $383.1 \pm 226.3 \mu\text{m}$. Hyperreflective dots and particles of different shapes and sizes

were documented within Berger space in 16 cases (57%) intraoperatively and in 9 cases (32%) postoperatively. Capsular rupture occurred in 1 case due to excessive posterior capsular movement anteriorly. The posterior capsular rupture was converted into a posterior capsulorhexis, leaving the anterior hyaloid membrane intact.

Conclusions: iOCT confirmed the penetration of crystalline lens microfragments, cellular material, or medical suspension (triamcinolone) into the space between the posterior lens capsule and the anterior hyaloid membrane. This occurs due to discontinuity of both lenticular zonules and Wieger ligament attachment. A Wieger ligament rupture can also allow excessive Berger space hydration during phacoemulsification leading to anterior displacement of the posterior lens capsule increasing the risk of instrument touch and posterior capsule rupture.

J Cataract Refract Surg 2020; 46:55–62 Copyright © 2019 Published by Wolters Kluwer on behalf of ASCRS and ESCRS

 [Online Video](#)

Modern technologies allow visualization of intraocular structures in vivo in a noninvasive fashion, providing valuable insight into anatomic configuration.^{1,A} Intraoperative optical coherence tomography (iOCT) may elucidate vitreolenticular anatomy, resulting in a better understanding of changes associated with complicated cataract surgery.^{2–4}

Direct intraoperative communication between the anterior chamber (AC) and Berger space due to Wieger ligament detachment combined with zonular insufficiency has not yet been unequivocally proven. The exact intraoperative alteration remains debatable because of the challenge of simultaneous direct visualization of the lenticular zonules and vitreolenticular

interface in the presence of the iris.^{5,6} Lenticular zonular insufficiency potentially provides an avenue to the Berger space from the AC during phacoemulsification or irrigation and aspiration resulting in residual lens material,^A blood cells, or medication into this usually optically clear, real or potential space. Moreover, excessive fluids flow through channels formed by insufficient vitreolenticular adhesion (also known as partial or total anterior vitreous detachment^A), normally prevented by the complete 360-degree attachment of the Wieger ligament, and might displace the posterior capsule anteriorly, creating a sudden increase in vitreous pressure, and elevating the risk for posterior capsular rupture and iris prolapse. To our knowledge, this is the first prospective

Submitted: April 20, 2019 | Final revision submitted: August 1, 2019 | Accepted: August 4, 2019

From the S. Fyodorov Eye Microsurgery Complex State Institution (Anisimova, Belodedova, Shilova, Malyugin), Moscow, A.I. Yevdokimov Moscow State University of Medicine and Dentistry (Anisimova, Malyugin), Russia; John A. Moran Eye Center (Arbisser), University of Utah, USA; and Ophthalmology Department, Soroka University Medical Center (Knyazer), Be'er-Sheva, Israel.

Presented at the 23rd Winter Meeting of the European Society of Cataract and Refractive Surgeons, Athens, Greece, February 2019.

Corresponding Author: Boris Malyugin, MD, PhD, Professor of Ophthalmology, Department of Cataract and Implant Surgery, S. Fyodorov Eye Microsurgery Complex State Institution, Beskudnikovskiy Boulevard 59A, Moscow 127486, Russia. E-mail: boris.malyugin@gmail.com.

study of intraoperative and postoperative Berger space size and consistency variations. The study identifies the presence of microfragments of different origin migrated from the AC into the Berger space and that potentially serves as a clinical biomarker of the increased mobility of the posterior capsule.

METHODS

Patients with bilateral age-related nuclear cataracts who consented to surgery were included in the study. Twelve patients (13 eyes) underwent conventional phacoemulsification, and 15 patients (15 eyes) opted for femtosecond laser-assisted cataract surgery (FLACS) with a Femto LDV Z8 (Ziemer Ophthalmic Systems AG) laser. Phacoemulsification was performed with a Stellaris (Bausch & Lomb, Inc.) using a quick-chop technique.

FLACS included anterior capsulotomy (4.7 to 5.0 mm) and lens fragmentation (4.7 to 5.0 mm). Chang-modified MST capsule retractors (MicroSurgical Technology Inc.) were used to stabilize the lens during surgery in 2 cases with significant zonular weakness; a capsular tension ring (Reper-NN) and a hydrophobic

acrylic monofocal intraocular lens (IOL) were implanted into the capsular bag after the AC was filled with an ophthalmic viscosurgical device (OVD).

All patients had cataract surgery with a similar OVD with aspheric ($n = 23$), multifocal ($n = 1$), and toric ($n = 4$) IOL implantation; 6 required a capsular tension ring to stabilize the bag; in 3 cases, a 6.25 mm ring 2.0 (MicroSurgical Technology Inc.) was used to achieve sufficient pupil diameter during surgery (Table 1).

Phacoemulsification parameters were customized by subjective cataract grading and capsular stability and were set up as follows. Pulse mode was used with ultrasound (US) power up to 40% (160 pps, 50% duty cycle), vacuum was linear to 400 mm Hg, and bottle height to provide passive infusion was set at 100 cm above eye level and reduced to 50 cm in cases of capsular instability or posterior capsular rupture. Dual lineal foot pedal control allowing the surgeon to separate the control of vacuum and US power was used in all cases. During all surgical procedures, special attention was focused on avoiding excessive AC depth fluctuation, especially at the moment irrigation or phacoemulsification handpieces were

Table 1. Main baseline, intraoperative, and postoperative characteristics.

Preoperative Condition and Ocular Comorbidities	Age (yr)/Sex	Operated Eye	ACD/LT/AL (mm)	Surgery	IOL	MR/CH/CTR	Comments
Iridodonesis, PEX	82/F	RE	3.1/5.0/22.7	FLACS	Monofocal	-/+/+	—
PEX	71/F	RE	3.1/5.0/23.4	FLACS	Monofocal	-/-/+	—
PEX	76/F	RE	2.4/4.4/21.6	CPE	Monofocal	-/-/-	—
—	64/F	RE	3.4/4.7/24.5	CPE	Monofocal	-/-/-	—
PEX	89/M	LE	2.6/4.4/23.0	CPE	Monofocal	-/-/-	—
Lens subluxation, posterior synechiae >250°	77/F	RE	2.4/4.4/22.7	FLACS	Monofocal	+/-/-	Posterior capsular rupture followed by PCCC
—	78/M	LE	3.2/4.6/22.9	CPE	Monofocal	-/-/-	—
—	71/M	RE	2.5/5.1/21.9	CPE	Multifocal	-/-/-	—
Postkeratotomy	63/F	LE	3.5/3.9/26.0	CPE	Toric	-/-/-	—
Glaucoma, PEX, iridodonesis	61/M	RE	3.4/4.5/24.3	CPE	Monofocal	-/-/-	—
Glaucoma, PEX	78/F	RE	2.4/5.6/23.1	CPE	Monofocal	-/-/+	Postoperative transient IOP rise
Postkeratotomy	51/F	RE	3.4/4.3/27.5	CPE	Monofocal	-/-/+	—
Postkeratotomy	62/M	RE	3.3/4.6/28.4	CPE	Toric	-/-/-	—
Traumatic cataract	44/M	RE	2.9/4.6/22.6	CPE	Toric	-/-/-	Postoperative transient corneal edema
PEX	78/F	LE	3.3/4.7/27.7	CPE	Monofocal	-/-/-	—
PEX	78/F	RE	3.4/4.4/26.5	FLACS	Monofocal	+/+/-	—
PEX	78/F	LE	2.5/5.6/23.0	CPE	Monofocal	-/-/-	Postoperative transient IOP rise
PEX, AMD	71/M	RE	2.7/4.7/23.5	FLACS	Monofocal	-/-/+	—
PEX	62/F	LE	3.4/3.7/25.6	FLACS	Toric	-/-/-	—
—	65/F	RE	3.5/4.5/23.6	FLACS	Monofocal	-/-/-	—
PEX	70/M	RE	3.5/4.6/24.9	FLACS	Monofocal	+/-/-	—
PEX, AMD	85/F	RE	2.9/4.6/23.9	FLACS	Monofocal	-/-/-	—
PEX	71/M	RE	3.4/4.1/24.8	FLACS	Monofocal	-/-/-	—
PEX	77/M	LE	3.4/4.2/23.9	FLACS	Monofocal	-/-/-	—
—	86/M	RE	2.8/4.9/23.3	FLACS	Monofocal	-/-/-	Postoperative transient IOP rise
PEX	70/M	LE	3.8/4.4/24.7	FLACS	Monofocal	-/-/+	—
PEX, AMD	60/M	RE	3.2/4.5/26.4	FLACS	Monofocal	-/-/-	—
—	80/F	LE	2.5/5.1/23.1	FLACS	Monofocal	-/-/-	—

ACD = anterior chamber depth; AL = axial length; AMD = age-related macular degeneration; CH = capsular hook; CPE = conventional phacoemulsification; CTR = capsular tension ring; F = female; FLACS = femtosecond laser-assisted cataract surgery; IOL = intraocular lens; IOP = intraocular pressure; LE = left eye; M = male; LT = lens thickness; MR = Malyugin ring; PEX = pseudoexfoliation syndrome; PCCC = posterior continuous circular capsulorhexis; RE = right eye

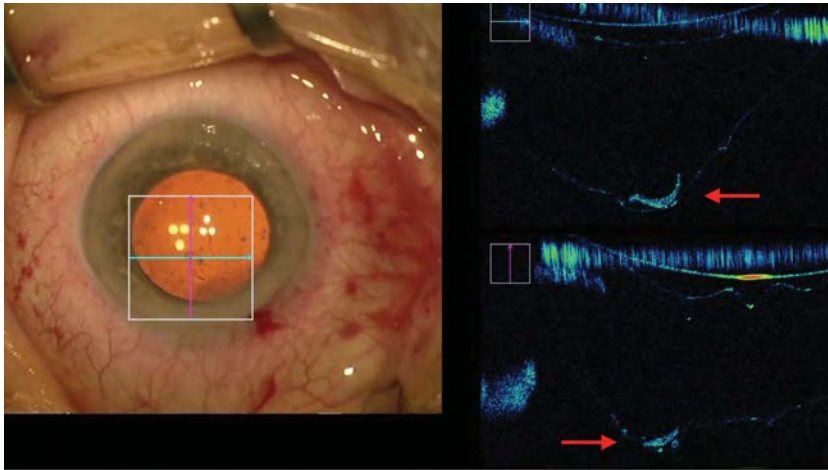


Figure 1. Screenshot from intraoperative optical coherence tomography immediately after intraocular lens in-the-bag implantation. Dislocation of the lens cortex material into the Berger space is seen (red arrows). The hyperreflective microfragment is visualized in proximity to the outer side of the anterior hyaloid.

withdrawn from the eye. The AC was immediately refilled and stabilized with a balanced salt solution or OVD to minimize the risk of anterior vitreous detachment.

In all cases, immediately after IOL implantation and irrigation/aspiration of OVD, real-time iOCT integrated into the surgical microscope (Rescan 700; Carl Zeiss Meditec AG) was recorded on video, and screenshots were acquired. The control scans of iOCT in 10 cases were performed in different time points of the surgery (immediately after lens removal, capsular bag homogeneously filled with an OVD, immediately after IOL implantation, and at the end of the surgery) that verified the absence of the visible change in the quality of iOCT scans of the retrolenticular space.

In the early postoperative period, OCT of the vitreolenticular interface was performed with the RTVue XR 100 (OptoVue, Inc.) in the three-dimensional cornea, cross, and line scan mode.

RESULTS

A wavy configuration of the posterior capsule and anterior hyaloid membrane associated with mild AC hydration was noted in most cases. Extensive hydration of the AC resulted in a concave arcuate shape of both the posterior capsule and the anterior hyaloid membrane. In some cases, for better identification of the vitreolenticular structures, the AC was depressurized, which made it possible to visualize the anterior hyaloid within the iOCT scan depth with reasonable intraoperative intraocular pressure (IOP).

In the pupil projection, incomplete adhesion of the posterior lens capsule (represented by a hyperreflective line directly under the IOL scan) to anterior vitreous layers (represented by a hyperreflective line behind the posterior

lens capsule) was also the most frequently seen anatomy ($n = 20$; 71%). Complete adhesion of the posterior capsule to the posterior IOL surface was identified in only 2 cases as a hyperreflective line extending in the plane of the IOL optic.

Dislocation of lens microfragments into the retrolenticular area was observed through the surgical microscope intraoperatively in only 10 cases (Figure 1), whereas the more sensitive iOCT demonstrated hyperreflective planar formations or focal dots in direct contact or in proximity to the superior side of the anterior hyaloid membrane in 16 cases (57%) (Supplemental Digital Content, Video 1, available at <http://links.lww.com/JRS/A7>). Of these, 13 were identified as lens cortex, 1 as cellular material, and 2 as triamcinolone suspension particles (used to exclude vitreous prolapse after IOL implantation and irrigation/aspiration of OVD in these cases). After none was visualized, despite subsequent irrigation/aspiration, the hyperreflective dots were identified in the Berger space without penetration into the vitreous body. This was interpreted as an anterior vitreous detachment from the lens with an intact hyaloid membrane (Figure 2 and Supplemental Digital Content, Video 2, available at <http://links.lww.com/JRS/A8>).

The posterior capsule remained intact in 27 (96%) cases. One case was notable for extensive preoperative iridodonesis and pseudoexfoliation syndrome. There was spontaneous forward bowing of the posterior capsule during phacoemulsification resulting in a paracentral capsular tear

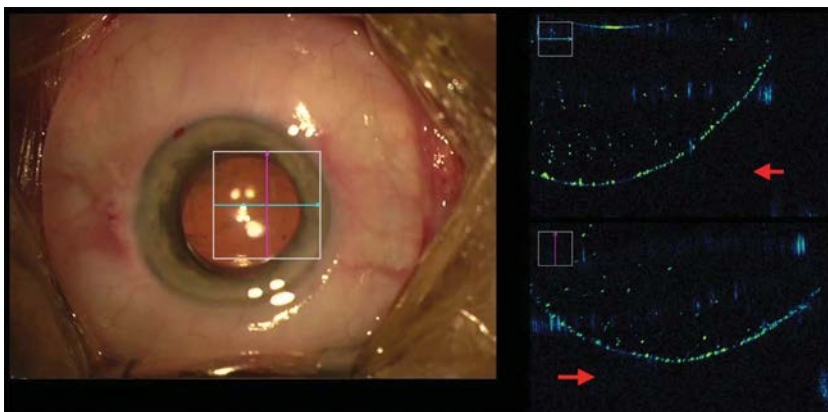


Figure 2. Postoperative screenshot from 3D cornea scan mode on the second day of follow-up. The wavy configuration of the lens capsule remains. The hyaloid-capsular interspace is reduced in length. The hyperreflective focal area is identified in the Berger space (red arrows).

subsequently converted to a continuous curvilinear capsulorhexis. Because of the small pupil size and iris rigidity in this case, a pupillary expansion ring (Malyugin Ring 2.0; Micro-Surgical Technology Inc.) had been injected before phacoemulsification causing minimal bleeding from abnormal iris edge vessels. After emulsification of the cataract, red blood cells were observed and identified just below the posterior capsule. The blood spontaneously resorbed within 2 weeks postoperatively.

All patients had uneventful postoperative courses, except for 3 with transient medically controlled ocular hypertension and 1 with mild corneal edema after intraoperative dissection of posterior synechiae. All patients improved in

clinical and functional parameters. The vitreolenticular interface was scanned in maximal mydriatic conditions during follow-up. The posterior capsule was partially or fully separated from the IOL in 25 (89%) cases. The presence of hyperreflective microfragments in the Berger space was confirmed in 9 (56%) cases (Table 2 and Figure 3).

The 1 case with intraoperative bleeding showed partial hyaloid-capsular adhesion on OCT on the first postoperative day (Figure 4); its thickening confirmed the accumulation of blood cells in the Berger space with its partial collapse presumably due to the sticky healing ability of fibrin blood components.

Table 2. Vitreolenticular interface patient characteristics in the intra- and early postoperative period.

Intraoperative OCT			Follow-up Day (OCT)	Postoperative OCT		
Berger Space	Residual hyperreflective material			Berger space		Residual Hyperreflective Material in Berger Space (μm)
	Between IOL and PC	In Berger Space		Min (μm)	Max (μm)	
+	–	+	2	0	353	+ (46 × 183)
+	+	–	–	ND	ND	ND
–	+	–	6	0	146	+ (25 × 24; 20 × 10; 24 × 16)
+	+	+	2	0	272	+ (70 × 70)
+	+	–	2	0	366	–
+	–	+Multiple hyperreflective focal points (hemorrhage features)	2	0	20	Increased hyperreflectivity of the hyaloid-capsular interspace, extended adhesion
–	–	–	1	0	347	–
+	+	+	1	0	100	–
+	–	+	1	0	1020	+ (105 × 79; 47 × 47; 63 × 63)
ND	–	+	1	0	463	+ (106 × 58)
–	–	–	2	0	418	–
+	–	+	1	40	279	+
+	+	–	1	0	321	–
+	+	–	1	LQ	LQ	LQ
+	+	+(After TA injection – multiple hyperreflective focal points)	1	0	829	Multiple hyperreflective focal points
+	+	+	1	0	471	–
+	+	+(After TA injection – multiple hyperreflective focal points)	1	0	410	Multiple hyperreflective focal points
+	+	+	1	104	471	–
–	+	–	1	–	–	–
+	+	+	1	0	469	–
+	–	–	1	362	572	–
+	+	–	1	0	391	–
+	+	+	1	50	270	–
+	+	+	1	215	413	–
+	+	+	2	0	406	–
–	–	–	1	–	–	–
–	–	–	1	–	–	–
+	+	+	1	0	4	–
21	18	16	1.4 ± 1.0	33.5 ± 87.0 μm	383.1 ± 226.3 μm	9

IOL = intraocular lens; LQ = low-quality scan; ND = no data; TA = triamcinolone acetonide

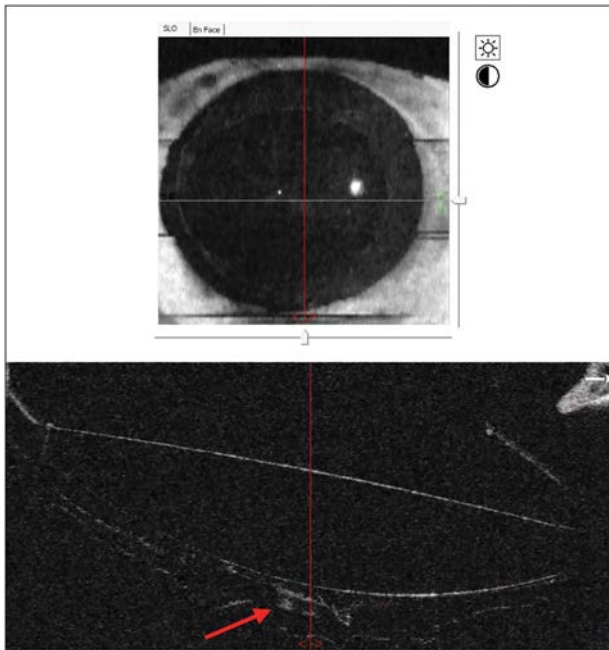


Figure 3. Screenshot from intraoperative optical coherence tomography immediately after intraocular lens in-the-bag implantation. Accumulation of the triamcinolone acetonide suspension into the Berger space is visualized as multiple hyperreflective discrete dots in proximity to the outer side of the anterior hyaloid. The vitreous is free of triamcinolone (red arrow).

DISCUSSION

The unique nature of the anterior vitreous has garnered the interest of researchers for more than a century.^{5,6,B,C} Complex anatomy, unusual embryogenesis, high level of transparency, paucity of cells, complete avascularity, abundant meshwork of collagen fibrils, distinct consistency, and peculiar biomechanical properties comprise vitreous characteristics.^{7-9,D} Its connection with the crystalline lens structure makes it extremely important to understand its influence on anterior segment surgery.^A

The vitreolenticular interface was first described by Joseph von Hasner in 1851 as the “tellerförmige Grube”^E (plate-shaped pit) and meticulously studied by Germain Wieger in 1883.^B Some years later, the interface was verified by anatomist Emil Berger in postmortem specimens,^C and is now well known as the Berger space; however, it is undisclosed who adopted the term. Other terms, such as hyaloid-capsular interspace, vitreolenticular interface, or patellar fossa, are also used to describe this anterior hyaloid depression site. The Berger space is delimited by the lens hyaloid-capsular adhesion, the Wieger ligament (named by G. Wieger as “ligamentum hyaloideo-capsulare”); it is also known as Egger line. It is seen biomicroscopically as an annular structure inserted into the posterior lens capsule from 4.0 to 5.0 mm from the lens center to within 1.0 mm of the lens periphery.^{10,C}

The older concept of the membranous structures’ adhesion^C to the posterior capsule within the vitreolenticular interface was confirmed by a recent study performed in cadaver eyes by using barium sulfate contrast.¹¹

The crossing zonular fiber, (the anterior vitreous zonular fibers extending from the ciliary structures to the Wieger ligament, and the posterior insertion zone-to-lens equator zonular fibers,¹² not only have significant impact on the complex mechanism of lens accommodation¹³ but also stabilize, shape, and act as a scaffold to the vitreolenticular complex. Fluid within the annular Wieger ligament likely functions as a lubricant, contributing to the change in lens configuration during accommodation.³ Aqueous humor in the retrolenticular space might provide less resistance than does vitreous gel with its higher viscosity and filamentary structure. The hydrodynamic flow in the Berger space is considered to function as a relatively closed chamber.

The rare occurrence of Berger space-AC barrier breakdown is described in terms of pigment accumulation after trauma¹⁴ or localized hemorrhage within this structure. This is likely to be associated with alteration in the

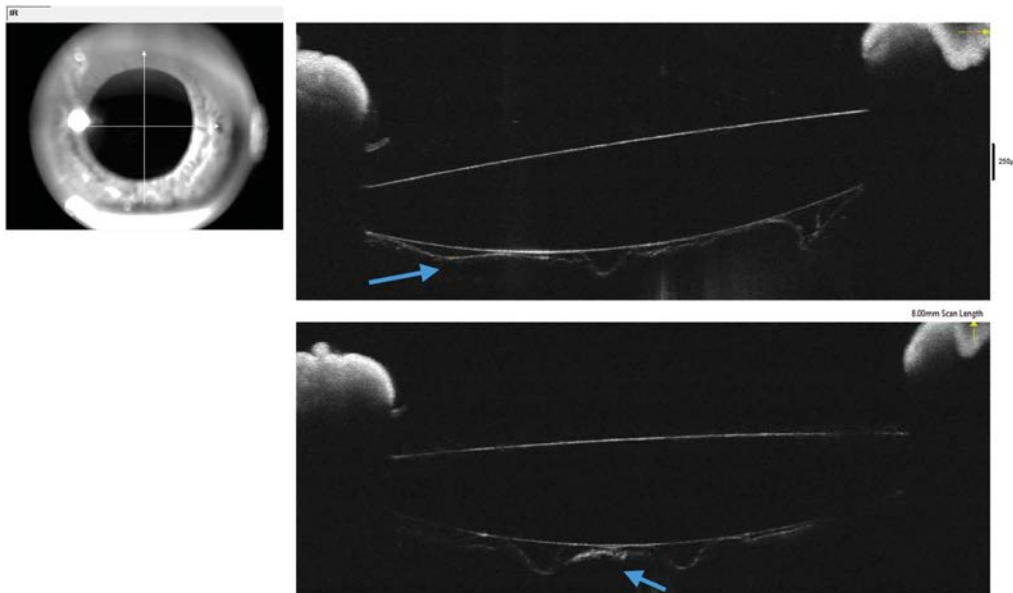


Figure 4. Anterior segment optical coherence tomography scans. Partial hyaloid-capsular adhesion visualized on the first postoperative day of a case with iris bleed; collapse of the Berger space with thickening of the hyaloid-capsular interface with increased hyperreflectivity is seen (blue arrows).

Wieger ligament resulting in a partial crevice in vitreolenticular adhesion.

There is limited information regarding the vitreolenticular interface in pediatric cases. Recently, anterior vitreolenticular dysgenesis was described to be associated with unilateral pediatric cataract, particularly in cases with a posterior capsule plaque composed of mesenchymal proteins, firmly adherent to the inside of the posterior lens capsule.¹⁵ It remains unknown whether the alteration in the Berger space is primary or secondary to cataract development or whether both pathologies occur independently.

Wieger ligament is most adherent in the mid-peripheral region of the lens in young individuals and loses its adherence with aging. Progressive vitreous liquefaction with architectonic collapse of the vitreous body occurs in the elderly.¹⁶ Great anatomical variability of the vitreolenticular interface was reported clinically while performing primary posterior continuous curvilinear capsulorhexis but was not confirmed using diagnostic tools.¹⁷ Advanced ligament adhesion degradation during the course of aging and zonular insufficiency in pseudoexfoliation syndrome might be the main causative factors promoting intraoperative fluid flow through the zonular network, causing both expansion of the hyaloid-capsular interspace and providing access to the lens material subsequently visualized in the Berger space during and after cataract surgery.

Intraoperative hydrodynamics during phacoemulsification or during irrigation/aspiration, especially when associated with chamber collapse and expansion on irrigation removal and reintroduction as well as the high parameters of the irrigation, may result in excessive flow to the Berger space through weakened zonules and incomplete attachment of the Wieger ligament. It may cause or extend ligament dislocation leading to anterior vitreous detachment. The exact intraoperative alteration is currently unknown because of the difficulty of visualization. Dick and Schultz¹⁸ reported the ability to visualize the Berger space immediately after FLACS with the femtosecond laser-integrated OCT in 81% of cases, allowing femtosecond laser posterior capsulotomy with immediate redocking. Tassignon et al. visualized vitreolenticular space after complete crystalline lens and OVD removal from the capsular bag when the total collapse of the capsular bag was observed. The only patient presented with anterior vitreous detachment was myopic.^A Theoretically, multiple factors might influence the frequency of this finding. There were only 2 cases reported with identified residual lens material in the retrolenticular space visualized by iOCT in myopic eyes with no detailed description of the patient and no postoperative confirmation via stationary OCT in the postoperative period.^A

More recently, continuous iOCT has become increasingly popular as a noninvasive, high-resolution, precise tool for detailed studies of the anterior and posterior segments.^{2,3,19} To enhance intraoperative visualization, the transzonular capsulo-hyaloidal hydroseparation with optional triamcinolone augmentation was proposed to improve the safety and feasibility of the primary posterior laser capsulotomy.²⁰ However, unfortunately, image penetration depth

of OCT is determined by optical scattering and is thereby limited to tissues with high optical density (iris and corneal opacities).²¹

In the present study, we confirm the hypothesis that with age-related or pathologic weakening of the retrolenticular apparatus, possibly precipitated or worsened by the hydrodynamic fluctuations during cataract surgery, the normal vitreolenticular interface adhesion of the anterior hyaloid membrane to the peripheral zone of the lens is violated, causing an anterior vitreous detachment.^A The presence of this pathological pathway during phacoemulsification results in the migration of crystalline remnants, cellular material, or medication into the space between the posterior capsule and anterior cortical layers of the vitreous humor intraoperatively. The Berger space in the presence of the crystalline lens is too narrow to be recognized even with modern diagnostic tools in its native state. However, it is transformed into a true space of varying depth when the lens is extracted from the capsular bag and the posterior capsule is moved forward. In some circumstances, the retrolenticular space is no longer limited by the Wieger ligament and can extend to the periphery, forming one compartment.¹⁷

In such cases, the direct connection to the periphery forms a single chamber that is defined anteriorly only by lenticular structures and the zonular network of Zinn peripherally by the pars plicata and posteriorly by the anterior hyaloid membrane. Intraoperative misdirected aqueous might predispose some of these cases to postoperative malignant glaucoma. The other potential negative consequence of Wieger ligament detachment and increased mobility of the anterior vitreous hyaloid is traction at the vitreous base, which is closely connected with the peripheral retina. Excessive vitreous traction, especially in long eyes, is a well-established risk factor for retinal detachment.²²

In our study, we had 1 posterior capsule rupture during lens cortical material evacuation. It resulted from anterior displacement of the posterior capsule that occurred despite the continuous irrigation of the AC. This capsular displacement is in sharp contrast to the concave shape of the posterior capsule usually observed in uneventful cataract surgery. In that case, iOCT verified anterior hyaloid detachment from the posterior capsule. Although our posterior capsular rupture rate in this study was limited, we do believe that Wieger ligament detachment associated with increased zonular permeability is the additional risk factor for posterior chamber rupture during the irrigation/aspiration step of the cataract procedure. To our knowledge, this risk factor for cataract surgery has not been previously identified.

Rosen⁶ showed that detachment of the anterior hyaloid membrane from the posterior lens capsule can be observed with biomicroscopy in relatively young patients with myopia and sufficiently transparent crystalline lenses. In our study, it was not possible to identify any of these conditions at the preoperative examination.

We have shown that the absence of adhesion of the anterior hyaloid membrane to the posterior capsule of the lens (ie, Wieger ligament lysis) accompanies the penetration of lens

fragments into the hyaloid-capsular interspace confirmed via iOCT. Because of the effects of gravity and weight, the microfragments of various origins mostly accumulate on the surface of the anterior hyaloid without penetrating the vitreous cavity in the supine position during surgery. The effect of gravity is also observed in the early postoperative period with slitlamp examination and postoperative OCT, showing that the Berger space has reduced depth superiorly.

Several studies have indicated that primary posterior capsulorhexis performed at the end of cataract surgery is safe and effective in adults²³ and in pediatric populations alike.^{17,24} Viscoseparation of the posterior capsule from the anterior portion of the vitreous body performed with a needle seems to be effective in assuring space for safe optic capture into the Berger space with haptics remaining in the bag, thus eliminating the potential for secondary cataract formation. Although in cases of Wieger ligament detachment, the maneuver to delineate the posterior capsule from the anterior hyaloid membrane may be superfluous, providing a cushion of OVD between the capsule and the anterior hyaloid remains prudent to avoid breaching the hyaloid membrane with the capsulorhexis forceps or subsequent optic capture. During this viscodissection maneuver, one can often visualize the OVD conforming to a circular margin delimited by the Wieger ligament, especially in pediatric cases in which attachment remains complete. We believe that iOCT performed before posterior rhexis may potentially enhance the safety of the primary posterior capsulorhexis procedure and help avoid unnecessary maneuvers.⁴

We found no evidence of iOCT data in the literature on the migration of lens microfragments, triamcinolone, or cellular material into the Berger space in emmetropic and hypermetropic eyes. It is hoped that the above-described anatomical and topographic changes of the retrolenticular space will help improve understanding of anterior segment

compartment connections with retrolenticular structures in the complete or partial absence of the Wieger ligament. This may be key to elucidating the poorly understood mechanism of acute aqueous misdirection syndrome also known as acute rock-hard eye syndrome (AIRES) (Figure 5). There was no AIRES case in our study, although we assume that the complex nature of this condition may not be solely based on the changes in the anterior vitreolenticular interface but might also involve the accumulation of a balanced salt solution behind the detached posterior vitreous hyaloid. Better understanding of the vitreolenticular interface configuration during AIRES might lead to changes in the surgical approach, avoiding the need for invasive techniques of pars plana anterior vitrectomy²⁵ or blind vitreous tap.²⁶ In some cases, a less traumatic iOCT-controlled transzonular drainage of the vitreolenticular interface might suffice. This new technique may reduce complications associated with vitreoretinal traction or inadvertent posterior capsule damage.^A The effectiveness and safety of such surgical approaches requires testing in large clinical studies.

Elimination of IOP spikes intraoperatively reduces the disruption of the posterior chamber–anterior hyaloid membrane barrier during cataract operations in ex vivo porcine eyes.²⁷ Dynamic pressure–assisted hydrodissection allows improved posterior chamber–anterior hyaloid membrane barrier integrity compared with manual hydrodissection due to the resultant absence of uncontrolled IOP spikes.²⁸ The IOP control systems integrated into the infusion line of phacoemulsification machines might reduce the misdirected flow of aqueous humor containing lenticular remnants toward the posterior segment. Theoretically, the pressurized infusion systems available on some phacoemulsification machines and/or constant AC irrigation with AC maintainers may predispose to a higher incidence of lens particles in the Berger space. This theory has yet to be proven in the clinical setting. Alternatively, allowing the chamber to alternately collapse and then dramatically deepen

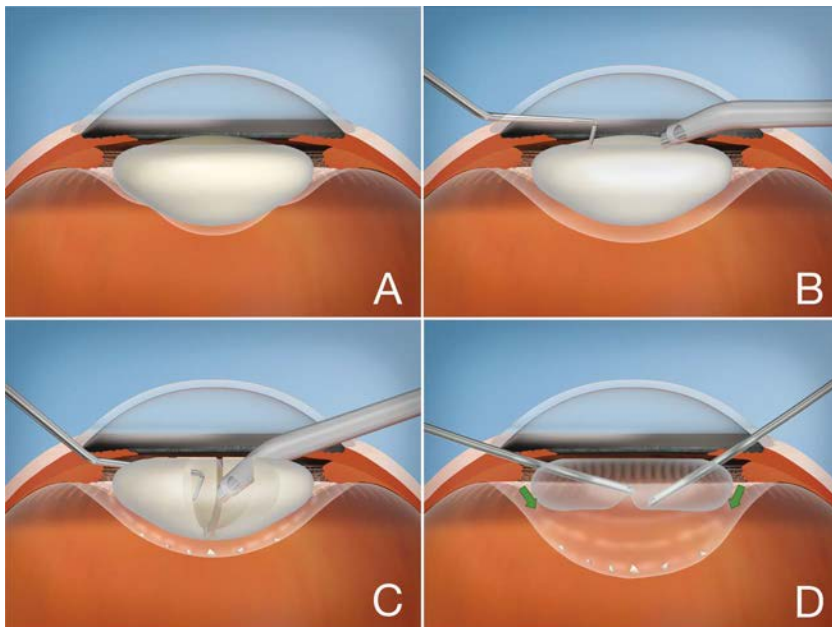


Figure 5. Schematic conceptual 3D drawing of the cross-sectional anterior segment view of the human eye. **A:** Normal structure of the vitreolenticular interface. The Berger space is delimited by the lens hyaloid-capsular adhesion (Wieger ligament). **B:** Wieger ligament insufficiency during phacoemulsification. **C:** Migration of crystalline lens remnants into the retrolenticular space. **D:** Acute aqueous misdirection syndrome resulting in extensive hydration of the Berger space and consequent posterior capsule movement anteriorly (greens arrows indicate the direction of fluid flow).

on removal of irrigation and its reintroduction may also predispose to intraoperative aqueous misdirection syndrome.

Our study demonstrated visualization of hyperreflective particles in the Berger space via iOCT, which correlated with the localization of these microfragments of the lens cortex, triamcinolone acetonide, and cellular material by the surgeon's direct visualization via the operative microscope. We believe that this confirms the presence of the previously unproven intraoperative direct communication of the Berger space with the AC through an insufficient Wieger ligament.

WHAT WAS KNOWN

- The anterior vitreous is firmly attached to the posterior lens capsule. This adhesion is denoted as the Wieger ligament.
- The Berger space is the hyaloid-capsular interspace located within the circular Wieger ligament.

WHAT THIS PAPER ADDS

- Intraoperative optical coherence tomography verification of the presence of microfragments of the crystalline lens, cellular material, or medical suspension in the space between the posterior capsular lens and the anterior hyaloid membrane serves as a biomarker of anterior vitreous detachment (as a result of Wieger ligament rupture) in specific cases.
- The defect in the Wieger ligament can be a source of intraoperative aqueous misdirection syndrome, specifically due to excessive hydration of the Berger space during phacoemulsification, leading to displacement of the lens posterior capsule anteriorly, thereby significantly increasing the risk of capsular aspiration and rupture.

REFERENCES

- Ehlers JP, Modi YS, Pecan PE, Goshe J, Dupps WJ, Rachitskaya A, Sharma S, Yuan A, Singh R, Kaiser PK, Reese JL, Calabrise C, Watts A, Srivastava SK. The DISCOVER study 3-year results: feasibility and usefulness of microscope-integrated intraoperative OCT during ophthalmic surgery. *Ophthalmology* 2018;125:1014–1027
- Haeussler-Sinangin Y, Schultz T, Holtmann E, Dick HB. Primary posterior capsulotomy in femtosecond laser-assisted cataract surgery: in vivo spectral-domain optical coherence tomography study. *J Cataract Refract Surg* 2016;42:1339–1344
- Tassignon MJ, Dhuhghaill SN. Real-time intraoperative optical coherence tomography imaging confirms older concepts about the Berger space. *Ophthalmic Res* 2016;56:222–226
- Looveren JV, Vael A, Ideler N, Sillen H, Mathysen D, Tassignon MJ. Influence of the vitreolenticular interface in pediatric cataract surgery. *J Cataract Refract Surg* 2018;44:1203–1210
- Rosen E. Anterior hyaloid membrane. *Am J Ophthalmol* 1965;59:1069–1079
- Rosen E. Detachment of anterior hyaloid membrane. *Am J Ophthalmol* 1966;62:1185–1194
- Sebag J. Seeing the invisible: the challenge of imaging vitreous. *J Biomed Opt* 2004;9:38–47
- Fine BS, Tousimis AJ. The structure of the vitreous body and the suspensory ligaments of the lens. *Arch Ophthalmol* 1961;65:95–110
- Lütjen-Drecoll E, Kaufman PL, Wasielewski R, Ting-Li L, Croft MA. Morphology and accommodative function of the vitreous zonule in human and monkey eyes. *Invest Ophthalmol Vis Sci* 2010;51:1554–1564
- Egger A. Die Zonula Zinnii des Menschen nach Untersuchungen von Leichenaugen am Spaltlampenmikroskop. *Graefes Arch Clin Exp Ophthalmol* 1924;113:1–15
- Kisiltsyna NM, Novikov SV, Kolesnik SV, Veselkova MP. Anatomical and topographical features of anterior vitreous cortex. *Oftal'mokhirurgiya* 2017;1:66–71
- Croft MA, Nork TM, McDonald JP, Katz A, Lütjen-Drecoll E, Kaufman PL. Accommodative movements of the vitreous membrane, choroid, and sclera in young and presbyopic human and nonhuman primate eyes. *Invest Ophthalmol Vis Sci* 2013;54:5049–5058

- Goldberg D. Computer-animated model of accommodation and theory of reciprocal zonular action. *Clin Ophthalmol* 2011;5:1559–1566
- Campanella PC, Aminlari A, DeMaio R. Traumatic cataract and Wiegers ligament. *Ophthalmic Surg Lasers* 1997;28:422–423
- Looveren JV, Gerwen VV, Schildermans K, Laukens K, Baggerman G, Tassignon MJ. Proteomic analysis of posterior capsular plaques in congenital unilateral cataract. *Acta Ophthalmol* 2018;96:e963–e969
- Teng CC, Chi HH. Vitreous changes and the mechanism of retinal detachment. *Am J Ophthalmol* 1957;44:335–356
- Menapace R. Posterior capsulorhexis combined with optic buttonholing: an alternative to standard in-the-bag implantation of sharp-edged intraocular lenses? A critical analysis of 1000 consecutive cases. *Graefes Arch Clin Exp Ophthalmol* 2008;246:787–801
- Dick HB, Schultz T. Primary posterior laser-assisted capsulotomy. *J Refract Surg* 2014;30:128–134
- Ehlers JP, Dupps WJ, Kaiser PK, Goshe J, Singh RP, Petkovsek D, Srivastava SK. The prospective intraoperative and perioperative ophthalmic imaging with optical coherence tomography (PIONEER) study: 2-year results. *Am J Ophthalmol* 2014;158:999–1007
- Menapace R. Transzonular capsulo-hyaloidal hydroseparation with optional triamcinolone enhancement: a technique to detect or induce anterior hyaloid membrane detachment for primary posterior laser capsulotomy. *J Cataract Refract Surg* 2019;45:903–909
- Hoerauf H, Wirbelauer C, Scholz C, Engelhardt R, Koch P, Laqua H, Birngruber R. Slit-lamp-adapted optical coherence tomography of the anterior segment. *Graefes Arch Clin Exp Ophthalmol* 2000;238:8–18
- Mitry D, Fleck BW, Wright AF, Campbell H, Charteris DG. Pathogenesis of rhegmatogenous retinal detachment. *Retina* 2010;30:1561–1572
- Menapace R. Routine posterior optic buttonholing for eradication of posterior capsule opacification in adults. *J Cataract Refract Surg* 2006;32:929–943
- Tassignon MJ, Veuster ID, Godts D, Kosec D, Dooren KVD, Gobin L. Bag-in-the-lens intraocular lens implantation in the pediatric eye. *J Cataract Refract Surg* 2007;33:611–617
- Grzybowski A, Prasad S. Acute aqueous misdirection syndrome: pathophysiology and management. *J Cataract Refract Surg* 2014;40:2167
- Lau OC, Montfort JM, Sim BW, Lim CH, Chen TS, Ruan CW, Agar A, Francis IC. Acute intraoperative rock-hard eye syndrome and its management. *J Cataract Refract Surg* 2014;40:799–804
- Kawasaki S. Influence of elevated intraocular pressure on the posterior chamber–anterior hyaloid membrane barrier during cataract operations. *Arch Ophthalmol* 2011;129:751–757
- Kato N, Masuda Y, Oki K, Iwaki H, Tsuneoka H. Influence of irrigation dynamic pressure-assisted hydrodissection on intraocular pressure and the posterior chamber–anterior hyaloid membrane barrier during cataract surgery. *Jpn J Ophthalmol* 2019;63:221–228

OTHER CITED MATERIALS

- Tassignon MJ, Ni Dhuhghaill S, Van Os L. *Innovative Implantation Technique. Bag-in-the-Lens Cataract Surgery*. Springer Nature Switzerland, 2019.
- Wieger G. Ueber den Canalis Petitii und ein "Ligamentum hyaloideo-capsulare" [thesis]. Strassburg, 1883.
- Berger E. *Beiträge zur Anatomie des Auges in Normalem und Pathologischem Zustande*. Wiesbaden, Bergmann, 1887.
- Worst JGF, Los LI. *Cisternal Anatomy of the Vitreous*. Amsterdam/New York, Kugler Publications, 1995.
- Hasner. Ueber das anatomische Verhältnis der Linsenkapsel zum Glaskörper, in *Deutsche Klinik*. III, 1851.

Disclosures: Dr. Malyugin has financial interest in the Malyugin ring (MicroSurgical Technology Inc.). None of the other authors has a financial or proprietary interest in any material or method mentioned.



First author:

Natalia S. Anisimova, MD, PhD

S. Fyodorov Eye Microsurgery Complex
State Institution, Moscow, Russia

ARTICLE

Comparison of outcome between small incision lenticule extraction and FS-LASIK in eyes having refractive error greater than negative 10 diopters

Xiaonan Yang, PhD, Quan Liu, PhD, Fang Liu, PhD, Jiping Xu, PhD, Yi Xie, PhD

Purpose: To compare small incision lenticule extraction (SMILE) and femtosecond laser-assisted laser in situ keratomileusis (FS-LASIK) in terms of safety, refractive outcomes, visual quality, and biomechanical responses in correcting myopia with maximum myopic meridian exceeding 10 diopters (D).

Setting: Zhongshan Ophthalmic Center, Sun Yat-sen University.

Design: Prospective, randomized, comparative study.

Methods: The study comprised 60 eyes (60 patients) with a maximum myopic meridian exceeding 10 D; 30 eyes were corrected using SMILE and 30 eyes were corrected using FS-LASIK. Patients received preoperative and 6-month postoperative examinations, including refractive outcomes, corneal curve, contrast sensitivity, ocular aberrometry, and corneal biomechanical responses.

Results: At 6 months postoperatively, the uncorrected distance visual acuity was -0.01 ± 0.06 and -0.05 ± 0.10 in the SMILE and LASIK eyes, respectively ($P = .08$). The corrected distance

visual acuity was -0.07 ± 0.07 and -0.08 ± 0.08 ($P = .624$), respectively. The postoperative spherical equivalent (SE) was -0.20 ± 0.25 D and -0.03 ± 0.20 D, respectively ($P = .008$). The posterior corneal curvature was unchanged after SMILE and FS-LASIK ($P > .05$). The measured corneal thickness was reduced by 137.40 ± 15.01 μm and 155.06 ± 17.43 μm ($P < .001$). The change in the SE was -0.01 ± 0.26 and -0.13 ± 0.30 from 1 week ($P = .103$). Only the peak distance (the distance between the highest points of the nondeformed corneal parts) differed between the groups (1.06 ± 1.44 mm vs -0.26 ± 1.16 mm, $P = .007$). In the SMILE patients, changes in higher-order aberration ($P = .018$) and spherical aberration ($P = .011$) were smaller than in LASIK patients.

Conclusions: Compared with LASIK, SMILE might offer superior safety and objective visual quality, comparable stability and efficacy, and a little inferior predictability in correcting maximum myopic meridian exceeding 10 D.

J Cataract Refract Surg 2020; 46:63–71 Copyright © 2019 Published by Wolters Kluwer on behalf of ASCRS and ESCRS

Corneal refractive surgery has improved significantly over the past decade with the introduction of new lasers, procedures such as small incision lenticule extraction (SMILE), and ablation algorithms.^{1–3} The SMILE procedure is a popular technique because it is flapless and requires only a femtosecond laser.⁴ Furthermore, myopic correction greater than 10 diopters (D) is possible in SMILE.⁵ However, laser in situ keratomileusis (LASIK) nomograms for high myopia have undergone more than 2 decades of development.^{6,7} The advent of the femtosecond flap cut brought additional improvements to LASIK.⁸ The Amaris excimer laser system (Schwind eye-tech-solutions GmbH & Co. KG) is equipped with a good eye tracking system, a high repetition rate,

SmartPulse (SCHWIND AMARIS) technology, and a small laser spot size to reduce the induction of higher-order aberrations (HOAs) and obtain better postoperative visual acuity.^{2,9,10} Thus, a prospective comparison of outcomes between SMILE and femtosecond laser-assisted LASIK (FS-LASIK) in eyes having high myopia (greater than -10 D) is of immense interest.

A number of studies compared the outcomes between SMILE and FS-LASIK on correcting myopia less than -10 D.^{11–15} The SMILE procedure caused less damage to the subbasal nerve plexus of the cornea and less effect on the ocular surface parameters than FS-LASIK.¹⁶ Correcting high myopia using any corneal refractive surgery is still a challenge for refractive

Submitted: January 25, 2019 | Final revision submitted: August 4, 2019 | Accepted: August 8, 2019

Zhongshan Ophthalmic Center, State Key Laboratory of Ophthalmology, Sun Yat-sen University, Guangzhou, China.

Supported by the National Natural Science Foundation of China (grant no. 81371051).

Corresponding Author: Quan Liu, PhD, Zhongshan Ophthalmic Center, State Key Laboratory of Ophthalmology, Sun Yat-sen University, No. 54, Xianlie Rd (South), Guangzhou, Guangdong, China 510000. Email: drliuquan@163.com.

surgeons. The induced HOA, very thin residual stromal bed, small optical zone, subjective visual quality, refractive regression, and risk of iatrogenic ectasia need careful preoperative examination. Thus, this study aimed to prospectively evaluate the outcomes of SMILE and FS-LASIK in terms of visual quality, refractive outcomes, corneal power, and corneal biomechanical changes in eyes having myopia in excess of -10 D.

METHODS

The inclusion criteria were a minimum age of 18 years, stable refraction for more than 1 year, a sum of manifest sphere and cylinder exceeding -10 D (sphere: -5.00 to -10.00 D; cylinder: 0.0 to -5.00 D), no ocular conditions other than myopia (with or without astigmatism), and a minimum theoretical residual stromal thickness exceeding 260 μm . The exclusion criteria were history of keratoconus, previous corneal lesions, prior corneal surgery, cataracts, glaucoma, or posterior abnormalities (eg, choroidal neovascularization, retinoschisis, retinal detachment, or macular holes). The benefits and known complications of refractive surgery were explained to the patients, who were found suitable for refractive surgery. The current study was conducted in line with the tenets of the Declaration of Helsinki. This single-center, prospective, randomized study was approved by the ethics board of the Zhongshan Ophthalmic Center of Sun Yat-sen University, China. The study included 60 eyes from 60 patients. Only 1 eye per patient was included, although both eyes of the patient underwent surgery. A computer randomly assigned the eyes to either SMILE ($n = 30$ eyes) or FS-LASIK surgery ($n = 30$ eyes).

Surgical Procedures

Small Incision Lenticule Extraction All SMILE surgeries were performed by a single surgeon (Q.L.). SMILE was performed with the VisuMax 500-kHz laser system (Carl Zeiss Meditec AG). A pulse energy and spot spacing of 140 nJ and 4.50 μm were used, respectively. The lenticule diameter ranged from 6.0 to 6.6 mm. The lenticule side cut was 10 μm . The cap diameter varied from 6.8 to 7.6 mm. The intended cap thickness ranged from 110 to 130 μm .

Femtosecond Laser-Assisted Laser In Situ Keratomileusis The FS-LASIK procedure was performed by the same experienced refractive surgeon (Q.L.). The flap was created using the VisuMax laser. The Amaris 750S excimer laser was used for stromal ablation. The optical zone varied from 6.0 to 6.8 mm. The intended

flap diameter varied from 7.9 to 8.2 mm. The flap thickness was 95 μm .

Examination The clinical examinations were recorded preoperatively and at 6 months postoperatively. The uncorrected distance visual acuity (UDVA) and corrected distance visual acuity (CDVA), measured by the Snellen chart, were converted to logarithm of the minimum angle of resolution units. The Oculyzer (OCULUS Optikgeräte GmbH) was used preoperatively and at 6 months postoperatively. Only the scans graded as "OK" by the instrument were used for further analyses. The simulated keratometry (K_1 and K_2), mean keratometry (K_m), and minimum corneal thickness were noted. The contrast sensitivity (CS) was measured at a distance of 2.5 m under CDVA and 4 different lighting conditions (CSV 1000E, Vector Vision). These included photopic CS with or without glare and scotopic CS with or without glare at spatial frequencies of 3, 6, 12, and 18 cycles per degree. The amount of contrast sensitivity function (CSF) improvement was quantified by computing the change in the area under the log CSF between the preoperative and the 6-month postoperative period. The WASCA (Carl Zeiss Meditec AG) aberrometer was used to measure aberrations preoperatively and at 6 months postoperatively. The root mean square (in micrometer) was used to analyze the HOAs for 6.0 mm analysis diameters. The Corvis ST (OCULUS Optikgeräte GmbH) was used to evaluate corneal biomechanical deformations and corneal thickness preoperatively and at 6 months postoperatively. The Corvis data that were analyzed included the time, length, and velocity of the first applanation (A1), the highest concavity, and the second applanation (A2), along with deformation amplitude (ie, deformation of the corneal apex in the vertical direction) and the peak distance (ie, the distance between the highest points of the nondeformed parts of the cornea).

Statistical Analyses

All statistical analyses were performed using IBM SPSS Statistics for Windows software (version 21.0, IBM Corp.). The normality of distribution was checked using the Kolmogorov-Smirnov test. Continuous variables were reported as mean \pm standard deviation. A paired-samples t test was used to compare preoperative and postoperative data within the SMILE and FS-LASIK groups. A 2-tailed Student t test was used to compare data between the SMILE and FS-LASIK groups. The significance level was set to $P < .05$.

RESULTS

Preoperatively, SMILE and FS-LASIK eyes were similar in terms of age, CDVA, sphere, cylinder, corneal thickness, and corneal curvature ($P > .05$). The preoperative features

Table 1. Demographics and preoperative data of the study population.

	SMILE	LASIK	P Value
Age (yrs)	25.0 \pm 6.6 (18–38)	27.5 \pm 5.7 (18–36)	.143
CDVA (logMAR)	-0.02 ± 0.07 (-0.18 to 0.10)	-0.05 ± 0.09 (-0.18 to 0.22)	.242
Maximum myopic meridian (D)	-10.74 ± 0.55 (-10.25 to -12.00)	-10.84 ± 0.64 (-10.25 to -12.25)	.517
Sphere refraction (D)	-9.06 ± 0.62 (-7.75 to -10)	-9.02 ± 0.73 (-7.25 to -10)	.813
Cylinder refraction (D)	-1.68 ± 0.75 (-4.25 to -0.25)	-1.83 ± 0.88 (-3.75 to -0.25)	.507
Spherical equivalent (D)	-9.90 ± 0.45 (-11.00 to -9.25)	-9.93 ± 0.53 (-11.13 to -9.00)	.818
Central corneal thickness (μm)	550.3 \pm 28.4 (506 to 629)	551.2 \pm 32.8 (500 to 625)	.913
Flat keratometry (K_1 , D)	43.03 \pm 1.18 (39.90 to 45.20)	42.57 \pm 1.09 (40.70 to 44.60)	.140
Steep keratometry (K_2 , D)	44.96 \pm 1.53 (41.40 to 48.30)	44.43 \pm 1.34 (41.60 to 47.10)	.181
Mean keratometry (K_m , D)	43.96 \pm 1.31 (40.60 to 46.70)	43.49 \pm 1.16 (41.40 to 45.40)	.169

CDVA = corrected distance visual acuity; LASIK = laser in situ keratomileusis; logMAR = logarithm of the minimum angle of resolution; SMILE = small incision lenticule extraction

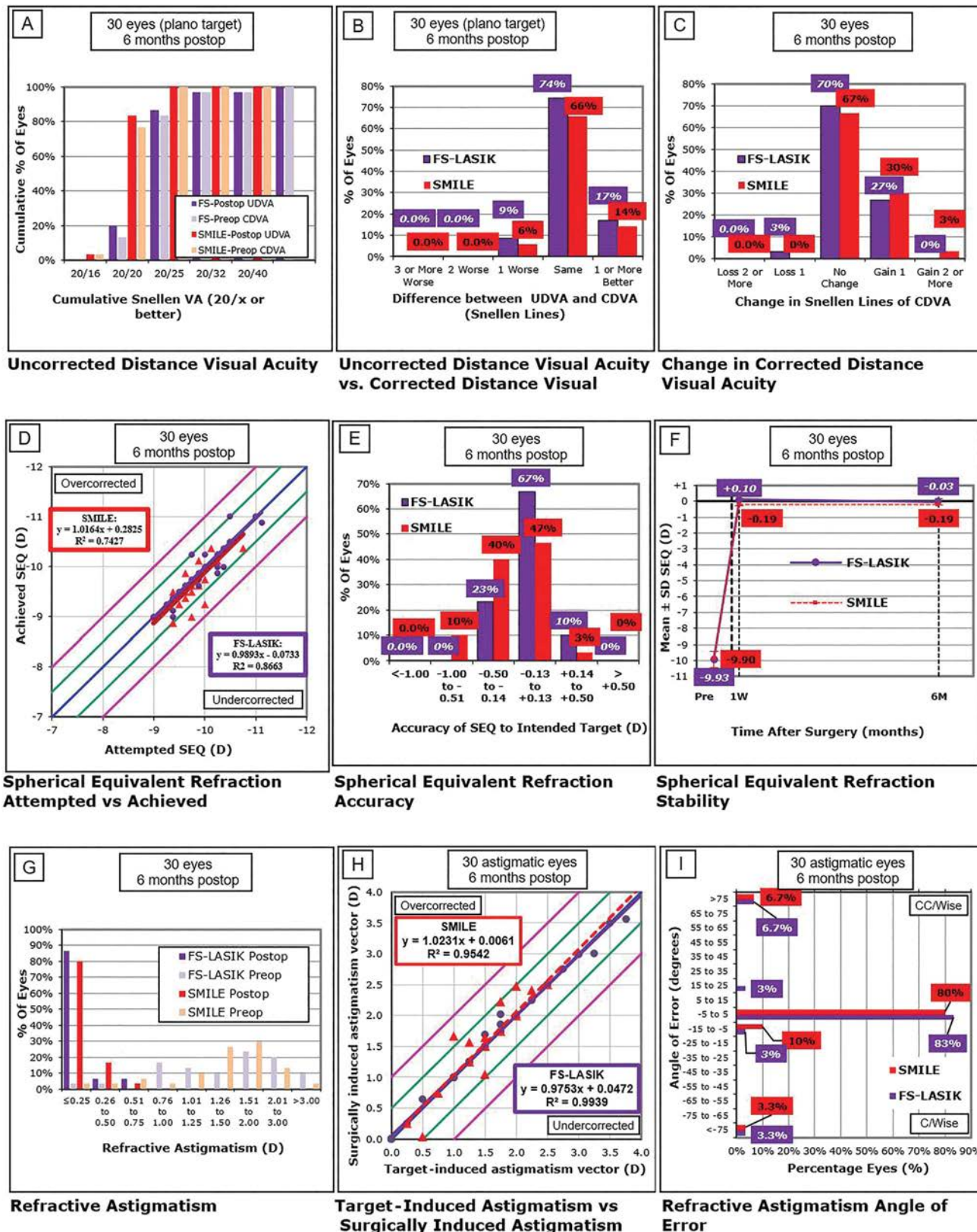


Figure 1. Nine standard graphs for reporting refractive surgery showing the visual and refractive outcomes for 60 eyes at 6 months after SMILE (30 eyes from 30 patients) and LASIK (30 eyes from 30 patients). A: UDVA; B: difference between UDVA and CDVA; C: changes in CDVA; D: SE refraction Attempted vs. Achieved; E: accuracy of SE refraction; F: SE refraction stability; G: refractive astigmatism; H: TIA vs. SIA; I: refractive astigmatism angle of error (CDVA = corrected distance visual acuity; FS = femtosecond; LASIK = laser in situ keratomileusis; postop = postoperative; preop = preoperative; SEQ = spherical equivalent refraction; SIA = surgically induced astigmatism; SMILE = small incision lenticule extraction; TIA = target-induced astigmatism; UDVA = uncorrected distance visual acuity; VA = visual acuity).

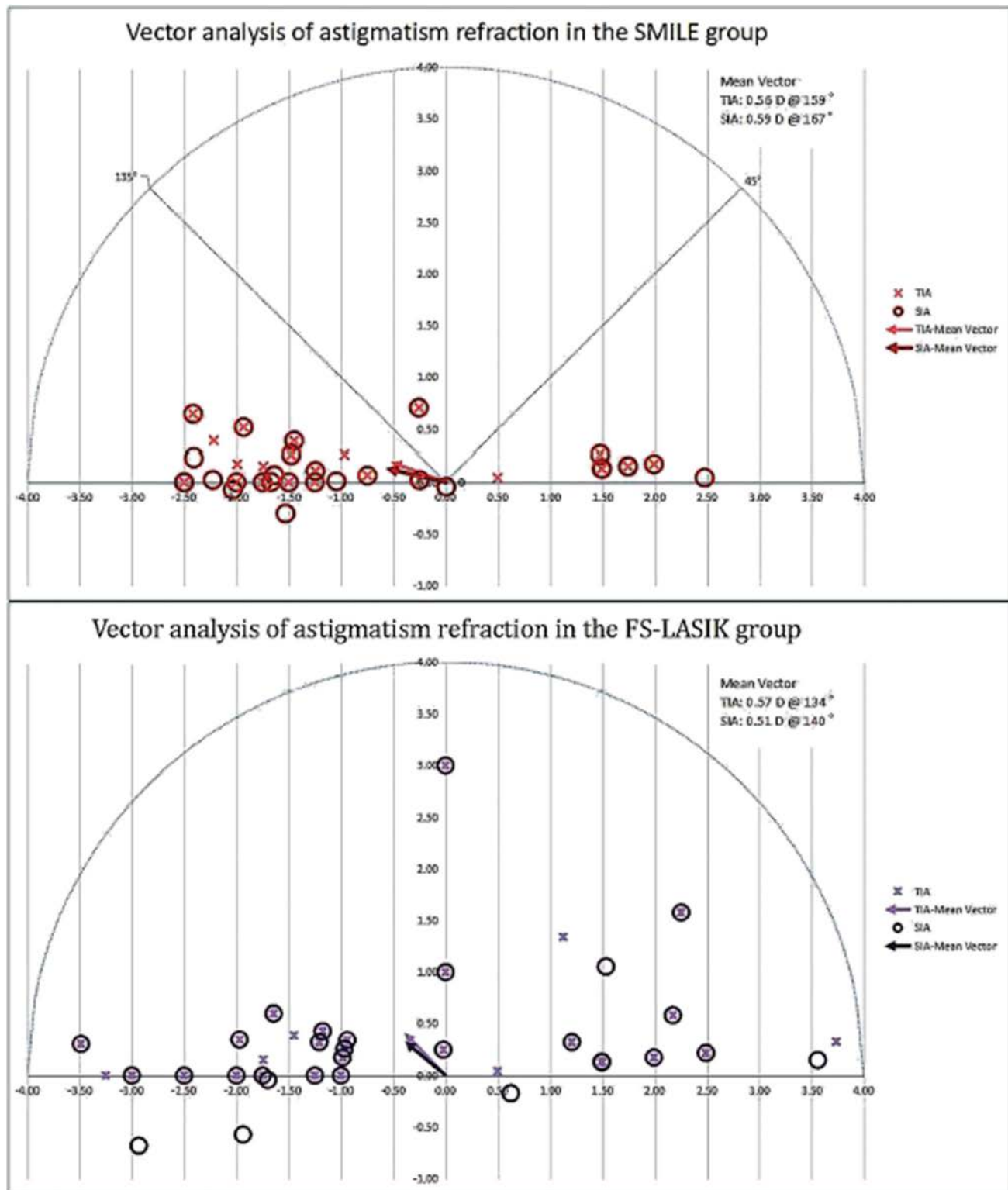


Figure 2. Vector analysis of TIA and 6-month SIA in the SMILE group and in the FS-LASIK group (FS-LASIK = femtosecond-assisted laser in situ keratomileusis; SIA = surgically induced astigmatism; SMILE = small incision lenticule extraction; TIA = targeted-induced astigmatism).

are summarized in Table 1. Figures 1, A–I show the visual quality and refractive outcomes between the two groups.

Efficacy

At 6 months postoperatively, UDVA was -0.01 ± 0.06 and -0.05 ± 0.10 in the SMILE and FS-LASIK group,

respectively ($P = .080$). One week postoperatively, the UDVA (logarithm of the minimum angle of resolution) was 0.01 ± 0.11 in the SMILE group and -0.02 ± 0.09 in the FS-LASIK group. Figure 1, A shows the cumulative distribution of Snellen UDVA. The efficacy index was 0.99 ± 0.13 and 1.03 ± 0.18 in the SMILE and FS-LASIK group,

Table 2. Posterior corneal power.

	SMILE		LASIK	
	Pre	Post	Pre	Post
Flat keratometry (K_1 , D)	-6.05 ± 0.21	-6.07 ± 0.18	-6.02 ± 0.24	-6.02 ± 0.23
Steep keratometry (K_2 , D)	-6.53 ± 0.28	-6.53 ± 0.27	-6.50 ± 0.30	-6.51 ± 0.28
Mean keratometry (K_m , D)	-6.27 ± 0.23	-6.29 ± 0.20	-6.24 ± 0.24	-6.25 ± 0.21
Astigmatism	0.48 ± 0.16	0.46 ± 0.15	0.48 ± 0.26	0.48 ± 0.25

LASIK = laser in situ keratomileusis; SMILE = small incision lenticule extraction

respectively ($P = .332$). Figure 1, B shows the difference between the 6-month postoperative UDVA and the pre-operative CDVA.

Safety

Figure 1, C shows the changes in CDVA on Snellen lines. At 6 months postoperatively, the safety index was 1.14 ± 0.2 and

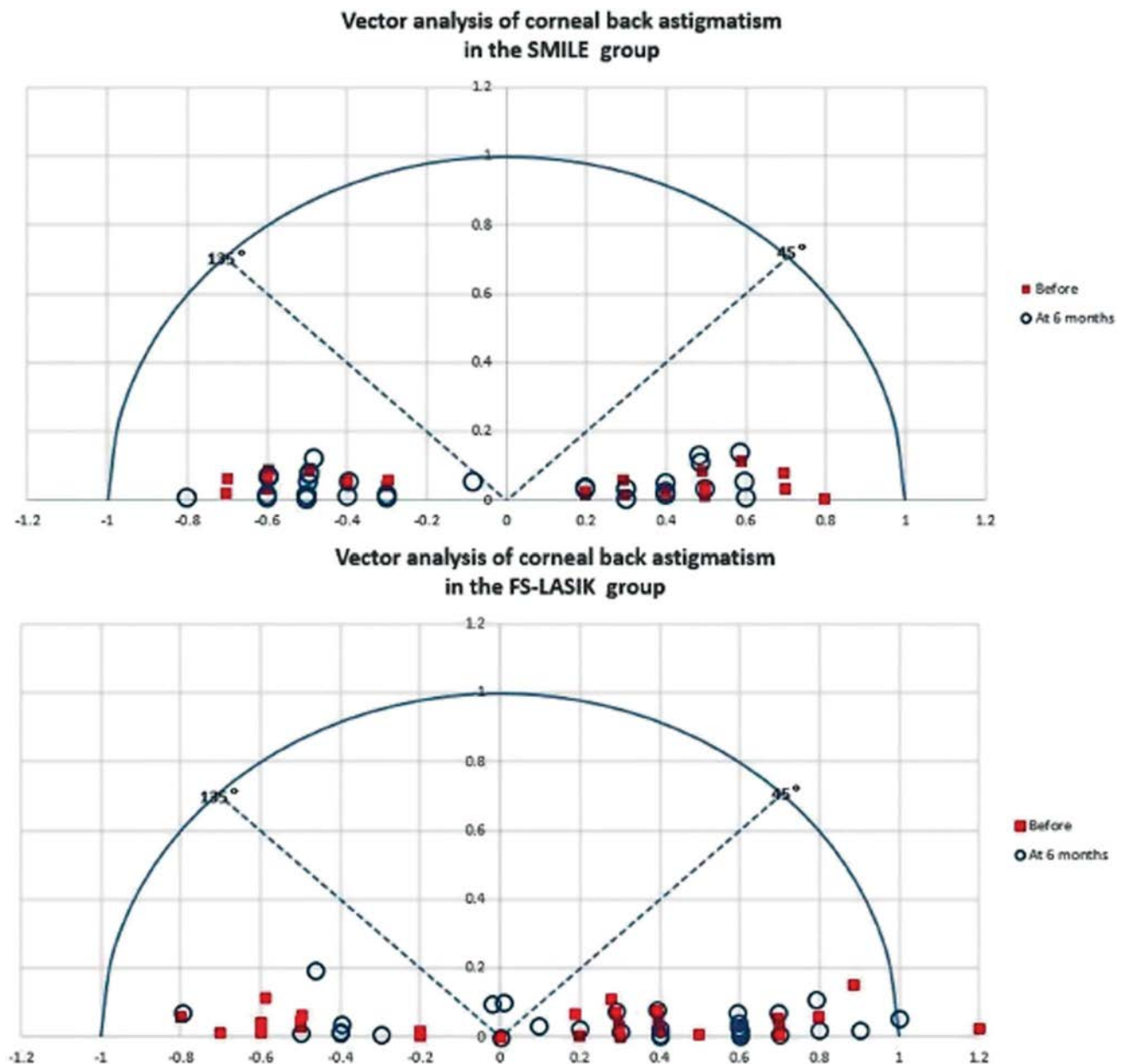


Figure 3. Corneal back astigmatism power (FS-LASIK = femtosecond-assisted laser in situ keratomileusis; SIA = surgically induced astigmatism; SMILE = small incision lenticule extraction; TIA = targeted-induced astigmatism).

Table 3. Change in subjective visual quality from the preoperative to 6-month postoperative period for the AULCSF.

	Photopic	Photopic and Glare	Scotopic	Scotopic and Glare
SMILE	0.017 ± 0.260	0.043 ± 0.230	0.042 ± 0.211	0.005 ± 0.209
LASIK	-0.020 ± 0.254	-0.022 ± 0.196	0.110 ± 0.195	0.142 ± 0.228
<i>P</i> value	.646	.629	.841	.327

AULCSF = area under the log contrast sensitivity function; LASIK = laser in situ keratomileusis; SMILE = small incision lenticule extraction

1.10 ± 0.17 in the SMILE and FS-LASIK group, respectively ($P = .431$). The CDVA was -0.07 ± 0.07 and -0.08 ± 0.08 in the SMILE and FS-LASIK group, respectively ($P = .624$).

Predictability

Figure 1, D shows the scatter plot of attempted vs achieved refractive correction in the SMILE and FS-LASIK group. Figure 1, E shows the spherical equivalent refraction accuracy of the two groups. The difference in the attempted vs achieved spherical equivalent was -0.20 ± 0.25 D and -0.03 ± 0.20 D in the SMILE and FS-LASIK group, respectively ($P = .008$).

Stability

Figure 1, F shows the changes in the manifest spherical equivalent from 1 week to 6 months. After SMILE, the manifest spherical equivalent was -0.19 ± 0.26 D and -0.20 ± 0.25 D at 1 week and 6 months, respectively. After FS-LASIK, the manifest spherical equivalent was 0.10 ± 0.37 D and -0.03 ± 0.20 D at 1 week and 6 months, respectively. From 1 week to 6 months, the changes in the spherical equivalent was -0.01 ± 0.26 and -0.13 ± 0.30 in the SMILE and FS-LASIK group, respectively ($P = .868$).

Refractive Astigmatism

Figure 1, G–I shows outcomes of refractive astigmatism in the SMILE and FS-LASIK group. The postoperative cylinder was -0.13 ± 0.22 D and -0.10 ± 0.22 D in the SMILE and FS-LASIK group, respectively ($P = .567$). Line regression of the targeted-induced astigmatism vector vs the surgically induced astigmatism vector (Figure 1, G) was equivalent between the two groups ($P = .928$). The vector analysis of surgically induced astigmatism and targeted-induced astigmatism was shown in Figure 2.

Corneal Curvature

None of the postoperative posterior surface curvatures differed from the preoperative curvatures in the SMILE and

FS-LASIK group ($P > .05$; Table 2 and Figure 3). In SMILE and FS-LASIK groups, the 6-month posterior corneal astigmatism vector (x, y) was $(-0.05 \pm 0.49, 0.04 \pm 0.04)$ and $(0.26 \pm 0.48, 0.04 \pm 0.04)$, respectively. Likewise, the preoperative posterior corneal astigmatism was $(0.02 \pm 0.51, 0.04 \pm 0.03)$ and $(0.10 \pm 0.53, 0.04 \pm 0.04)$, respectively. No significant difference was observed between the postoperative and the preoperative posterior corneal astigmatism vector in the SMILE ($p_x = 0.483$ and $p_y = 0.972$, respectively) and in the FS-LASIK ($p_x = 0.240$ and $p_y = 0.776$, respectively) group. At 6 months postoperatively, ΔK_m was 6.70 ± 0.55 D (5.70 to 8.30 D) and 7.86 ± 0.70 D (6.40 to 9.00 D) in the SMILE and FS-LASIK group, respectively ($P < .001$).

Visual Quality

Table 3 shows the change in subjective visual quality from the preoperative to 6-month postoperative period in terms of the area under the log CSF. Also, no significant difference was found between the SMILE and LASIK groups ($P > .05$). Table 4 summarizes HOAs in the two groups. Greater HOAs and spherical aberration were found postoperatively in the LASIK than the SMILE group ($P = .018$ and $P = .011$, respectively).

Corneal Thickness

The predicted ablation depth was 161.57 ± 8.54 μm (141.00 to 175.00 μm) and 142.90 ± 9.21 μm (123.22 to 163.58 μm) in the SMILE and FS-LASIK group ($P < .001$), respectively (Table 5). The measured reduction in thickness was 138.00 ± 15.01 μm and 156.78 ± 17.42 μm in the SMILE group and FS-LASIK group, respectively ($P < .001$). Meanwhile, the postoperative minimum corneal thickness was 426.97 ± 27.88 μm and 395.58 ± 29.12 μm in the SMILE and FS-LASIK group ($P < .001$). In addition, the thickness changes measured by Corvis was -149.13 ± 12.42 μm in the SMILE group and -163.81 ± 9.72 μm in the FS-LASIK group ($P < .001$).

Table 4. Induced aberrations in the SMILE group and LASIK group.

	SMILE	LASIK	<i>P</i> value
HOA	0.25 ± 0.15	0.35 ± 0.13	.018
Trefoil	-0.01 ± 0.30	0.10 ± 0.23	.148
Coma	0.33 ± 0.84	0.47 ± 0.50	.476
SA	0.44 ± 0.33	0.72 ± 0.42	.011
Astig.	0.30 ± 0.30	0.14 ± 0.28	.056
Clover	0.05 ± 0.10	0.00 ± 0.14	.209

Astig. = astigmatism; HOA = higher-order aberration; LASIK = laser in situ keratomileusis; SA = spherical aberration; SMILE = small incision lenticule extraction
Italic entries are statistically significant.

Table 5. Surgical parameters of the FS-LASIK and SMILE groups.

	SMILE	FS-LASIK	P Value
Intended optical zone	6.32 ± 0.19 (6.0 to 6.6)	6.38 ± 0.19 (6.0 to 6.8)	.176
Intended optical zone/scotopic pupil diameter	1.07 ± 0.10 (0.90 to 1.28)	1.05 ± 0.14 (0.83 to 1.30)	.501
Intended ablation depth/lenticular thickness	161.57 ± 8.54 (141.00 to 175.00)	142.90 ± 9.21 (123.22 to 163.58)	<.001
Actual reduced central corneal thickness	137.40 ± 17.33 (104.00 to 170.00)	156.78 ± 17.42 (126.00 to 183.00)	<.001

FS-LASIK = femtosecond-assisted laser in situ keratomileusis; SMILE = small incision lenticule extraction

Corneal Biomechanical Responses

Table 6 summarizes the postoperative minus preoperative changes in corneal biomechanical properties. The preoperative intraocular pressure was 14.67±1.18 mm Hg and 15.50±1.57 mm Hg in the SMILE and FS-LASIK group ($P = .107$). The postoperative intraocular pressure was 9.90 ± 2.05 mm Hg and 10.25 ± 1.45 mm Hg in the SMILE and LASIK groups, respectively ($P = .208$). Only the changes in the peak distance differed significantly between the SMILE and LASIK groups (SMILE: 1.06 ± 1.44 mm; LASIK: -0.26 ± 1.16 mm; $P = .007$).

DISCUSSION

To our knowledge, this study was the first to compare the safety, refractive outcomes, visual quality, and biomechanical responses between SMILE and LASIK in eyes having a sum of manifest sphere and cylinder exceeding -10 D. A recent review concluded that SMILE was a promising alternative to LASIK for the correction of myopia.⁴ However, our results showed that both procedures had their own strengths. This

study evaluates the safety, efficacy, posterior corneal power, and corneal thickness after both procedures comprehensively in high myopia eyes because marked increase in ocular aberration and decrease in thickness could affect the postoperative CDVA and lead to iatrogenic corneal ectasia.¹⁷⁻¹⁹ In our study, both procedures were equivalent in terms of the change in CDVA, posterior corneal power, and UDVA. Thus, both SMILE and LASIK appeared to be safe and efficacious in correcting high myopia of patients with normal preoperative tomography. However, long-term stability should be assessed in further studies.

The LASIK eyes had lower residual corneal thickness than the SMILE eyes (Table 3). In other words, more tissue was removed from LASIK than SMILE eyes. Thus, the underlying assumption that LASIK preserved more corneal tissue than SMILE appeared to be invalid. All LASIK eyes were operated with the sixth-generation Amaris 750S excimer laser in our study. A study claimed that Amaris 750S excimer laser has the smallest laser spot, a high repetition rate, and a very short

Table 6. Comparison between SMILE and LASIK in terms of changes in corneal biomechanical response.

	SMILE	LASIK	P Value
ΔIOP	-4.77 ± 2.00	-5.25 ± 1.46	.208
ΔPachy	-149.13 ± 12.42	-163.81 ± 9.72	<.001
ΔDef. amp. max (mm)	0.11 ± 0.10	0.15 ± 0.08	.266
ΔA1 time (ms)	-0.48 ± 0.19	-0.62 ± 0.31	.139
ΔA1 length (mm)	-0.05 ± 0.22	0.04 ± 0.19	.217
ΔA1 velocity (m/s)	-0.02 ± 0.01	-0.01 ± 0.03	.224
ΔA2 time (ms)	0.11 ± 1.50	0.47 ± 0.38	.353
ΔA2 length (mm)	-0.50 ± 0.64	-0.60 ± 0.58	.359
ΔA2 velocity (m/s)	-0.14 ± 0.09	-0.13 ± 0.08	.795
ΔHC time (ms)	-0.06 ± 0.57	-0.01 ± 0.64	.884
ΔPeak dist. (mm)	1.06 ± 1.44	-0.26 ± 1.16	.007
ΔRadius (mm)	-1.46 ± 0.80	-1.77 ± 1.16	.348
ΔA1 deformation amp. (mm)	-0.02 ± 0.01	-0.02 ± 0.01	.971
ΔHC deformation amp. (mm)	0.11 ± 0.10	0.15 ± 0.08	.266
ΔA2 deformation amp. (mm)	-0.07 ± 0.12	-0.02 ± 0.04	.186
ΔDeformation amp. ratio	1.74 ± 0.37	1.54 ± 0.53	.223
ΔIntegrated radius	3.63 ± 0.61	3.59 ± 0.93	.894
ΔARTH	-396.84 ± 81.30	-390.46 ± 131.57	.870
ΔSP-A1	-44.83 ± 13.40	-50.33 ± 16.16	.262

ARTH = Ambrósio rational thickness; HC = highest concavity; IOP = intraocular pressure; LASIK = laser in situ keratomileusis; SMILE = small incision lenticule extraction; SP-A1 = stiffness parameter at the first applanation
Italic entries are statistically significant.

treatment time.¹⁰ High repetition rates and shorter treatment times reduce the thermal damage and dehydration in the cornea, which are enhanced in part by the use of excimer ablation.⁷ In SMILE, the exposure of stroma to ambient air and dehydration was probably lower than FS-LASIK. Consequently, no obvious excessive stromal extraction was observed in SMILE compared with FS-LASIK eyes. This could be one of the significant advantages of SMILE over FS-LASIK, when treating high myopia refractive errors.

In this study, the predictability was slightly inferior in the SMILE group than the FS-LASIK group (Figure 1). Compared to FS-LASIK, SMILE is a relatively newer technology and requires further improvements to the nomograms for better predictability, safety, and efficacy for high myopia. The nomogram for low and moderate myopia is not advisable for high myopia treatment. In fact, studies on nomogram development are very few in number. In our study, the 6-month postoperative spherical equivalent was -0.20 ± 0.25 D in the SMILE group. However, the accuracy of cylinder correction was similar between SMILE and LASIK eyes. Thus, the unprecise correction of the spherical power may be the main reason for the inferior predictability. Although the added magnitude of -0.25 D sphere refraction had been used in our study, it could be implied that the added magnitude we used was not enough for high myopia over 10 D. Also, we observed that the postoperative anterior corneal curvature was flatter in the FS-LASIK group than the SMILE group. In an earlier study, SMILE and FS-LASIK produced distinct changes in the anterior corneal shape and postoperative corneal curvatures, which could be attributed to the differential residual corneal thickness difference between the two procedures.¹⁴ In our study, SMILE and LASIK provided stable results in the short term. However, an earlier study showed more stable outcomes after SMILE than LASIK in the long term.²⁰ Consequently, further follow-up to assess long-term stability between SMILE and LASIK would be required. The increase in HOA and spherical aberration is an unwanted outcome of refractive surgery, which could lead to halos, glare, starbursts, and night vision problems.¹⁰ Interestingly, the induced HOA and spherical aberration were still higher in the FS-LASIK group than in the SMILE group. Consequently, the subjective visual quality displayed by CSF was also evaluated in our study. However, no significant difference was observed between SMILE and LASIK.

Theoretical predictions suggested that SMILE preserved the anterior stroma better than LASIK and has less biomechanical impact on the cornea.^{21,22} However, the conclusions of the previous clinical studies were not unanimous in terms of biomechanical differences between SMILE and LASIK.^{23–25} In our study, the peak distance was the only index, which showed differential changes after surgery between SMILE and FS-LASIK eyes (SMILE: 1.06 ± 1.44 mm; LASIK: -0.26 ± 1.16 mm; $P = .007$). The peak distance is the distance between the highest points of the

nondeformed parts of the cornea when the air puff forces the cornea inward.²⁴ In our study, the deformed parts of the cornea were larger in the SMILE group than those in the LASIK group, which was contradictory with that the reduced corneal thickness was less in the SMILE group than that in the LASIK group. However, it helps to explain this result with that SMILE had been proved to induce less proliferation and inflammation of the peripheral surgery region compared with FS-LASIK.²⁶ Meanwhile, Bowman layer distortions returned to preoperative magnitudes in the SMILE eyes within 6 months postoperatively but were greater than preoperative magnitudes in the LASIK eyes postoperatively.²⁷ The better elasticity of the cornea could be implied after SMILE vs LASIK, but no significant difference was found in the corneal stiffness change between these two groups, because of the comparable change in SP-A1 after SMILE vs LASIK. However, in a recent study, the flap and cap biomechanical differences were present only intraoperatively but not after wound healing.²⁸ In light of this new information, it will be highly speculative to conclude that just 1 index out of several Corvis-ST indices is indicative of biomechanical differences between the two surgeries. We feel that advanced methods may be required to assess true biomechanical differences such as Brillouin optical microscopy, optical coherence tomography elastography, and ultrasound shear wave velocity.^{29–31}

This study also has some limitations. First, a mature nomogram for SMILE to correct high myopia exceeding 10 D was not provided directly but with the suggestion that the added magnitude of -0.50 D sphere refraction would be more proper than -0.25 D. This needs to be evaluated in our future research. Second, the long-term comparison between SMILE and LASIK in correcting myopia astigmatism exceeding 10 D needs to be performed. Furthermore, the corneal biomechanical changes need to be studied more intensively, and the wound healing process after refractive surgery should be taken into consideration.

Compared with LASIK, SMILE might offer superior safety and objective visual quality, comparable efficacy and stability, but inferior predictability in correcting maximum myopic meridian exceeding 10 D.

WHAT WAS KNOWN

- Small incision lenticule extraction (SMILE) and femtosecond laser-assisted laser in situ keratomileusis (FS-LASIK) had comparable refractive outcomes when correcting myopia errors with maximum myopic meridian less than 10 D.

WHAT THIS PAPER ADDS

- To our knowledge, this is the first study to compare the refractive outcomes, visual quality, and corneal biomechanical responses between SMILE and FS-LASIK when correcting myopia errors with maximum myopic meridian exceeding 10 D. More corneal tissue was ablated in FS-LASIK than SMILE eyes.

REFERENCES

- Shah R, Shah S, Sengupta S. Results of small incision lenticule extraction: all-in-one femtosecond laser refractive surgery. *J Cataract Refract Surg* 2011;37:127–137
- Vega-Estrada A, Alio JL, Arba Mosquera S, Moreno LJ. Corneal higher order aberrations after LASIK for high myopia with a fast repetition rate excimer laser, optimized ablation profile, and femtosecond laser-assisted flap. *J Refract Surg* 2012;28:689–696
- Han DC, Chen J, Htoon HM, Tan DT, Mehta JS. Comparison of outcomes of conventional WaveLight(RR) Allegretto Wave(RR) and Technolas(RR) excimer lasers in myopic laser in situ keratomileusis. *Clin Ophthalmol* 2012;6:1159–1168
- Doane JF, Cauble JE, Rickstrew JJ, Tuckfield JQ. Small incision lenticule extraction SMILE—the future of refractive surgery is here. *MO Med* 2018;115:82–84
- Qin B, Li M, Chen X, Sekundo W, Zhou X. Early visual outcomes and optical quality after femtosecond laser small-incision lenticule extraction for myopia and myopic astigmatism correction of over –10 dioptres. *Acta Ophthalmol* 2018;96:e341–e346
- Pallikaris IG, Siganos DS. Excimer laser in situ keratomileusis and photorefractive keratectomy for correction of high myopia. *J Refract Corneal Surg* 1994;10:498–510
- Khoramnia R, Salgado JP, Wuellner C, Donitzky C, Lohmann CP, Winkler von Mohrenfels C. Safety, efficacy, predictability and stability of laser in situ keratomileusis (LASIK) with a 1000-Hz scanning spot excimer laser. *Acta Ophthalmol* 2012;90:508–513
- Rosa AM, Neto Murta J, Quadrado MJ, Tavares C, Lobo C, Van Velze R, Castanheira-Dinis A. Femtosecond laser versus mechanical microkeratomers for flap creation in laser in situ keratomileusis and effect of post-operative measurement interval on estimated femtosecond flap thickness. *J Cataract Refract Surg* 2009;35:833–838
- Ziaei M, Mearza AA, Allamby D. Wavefront-optimized laser in situ keratomileusis with the Allegretto Wave Eye-Q excimer laser and the FEMTO LDV Crystal Line femtosecond laser: 6 month visual and refractive results. *Cont Lens Anterior Eye* 2015;38:245–249
- Piao J, Li YJ, Whang WJ, Choi M, Kang MJ, Lee JH, Yoon G, Joo CK. Comparative evaluation of visual outcomes and corneal asphericity after laser-assisted in situ keratomileusis with the six-dimension Amaris excimer laser system. *PLoS One* 2017;12:e0171851
- Han T, Xu Y, Han X, Zeng L, Shang J, Chen X, Zhou X. Three-year outcomes of small incision lenticule extraction (SMILE) and femtosecond laser-assisted laser in situ keratomileusis (FS-LASIK) for myopia and myopic astigmatism. *Br J Ophthalmol* 2019;103:565–568
- Khalifa MA, Ghoneim A, Shafik Shaheen M, Aly MG, Pinero DP. Comparative analysis of the clinical outcomes of SMILE and wavefront-guided LASIK in low and moderate myopia. *J Refract Surg* 2017;33:298–304
- Yu CQ, Manche EE. Subjective quality of vision after myopic LASIK: prospective 1-year comparison of two wavefront-guided excimer lasers. *J Refract Surg* 2016;32:224–229
- Gyldenkerne A, Ivarsen A, Hjortdal JO. Comparison of corneal shape changes and aberrations induced by FS-LASIK and SMILE for myopia. *J Refract Surg* 2015;31:223–229
- Teus MA, Garcia-Gonzalez M. Comparison of the visual results after small incision lenticule extraction and femtosecond laser-assisted LASIK for myopia. *J Refract Surg* 2014;30:582
- Kobashi H, Kamiya K, Shimizu K. Dry eye after small incision lenticule extraction and femtosecond laser-assisted LASIK: meta-analysis. *Cornea* 2017;36:85–91
- Alio JL, Vega-Estrada A, Pinero DP. Laser-assisted in situ keratomileusis in high levels of myopia with the Amaris excimer laser using optimized aspherical profiles. *Am J Ophthalmol* 2011;152:954–963 e951
- Gavrilov JC, Atia R, Borderie V, Laroche L, Bouheraoua N. Unilateral corneal ectasia after small-incision lenticule extraction in a 43-year-old patient. *J Cataract Refract Surg* 2018;44:403–406
- Taneri S, Kiessler S, Rost A, Dick HB. Corneal ectasia after LASIK combined with prophylactic corneal cross-linking. *J Refract Surg* 2017;33:50–52
- Kobashi H, Kamiya K, Igarashi A, Takahashi M, Shimizu K. Two-years results of small-incision lenticule extraction and wavefront-guided laser in situ keratomileusis for Myopia. *Acta Ophthalmol* 2018;96:e119–e126
- Shetty R, Francis M, Shroff R, Pahuja N, Khamar P, Giris M, Nuijts R, Sinha Roy A. Corneal biomechanical changes and tissue remodeling after SMILE and LASIK. *Invest Ophthalmol Vis Sci* 2017;58:5703–5712
- Reinstein DZ, Archer TJ, Randleman JB. Mathematical model to compare the relative tensile strength of the cornea after PRK, LASIK, and small incision lenticule extraction. *J Refract Surg* 2013;29:454–460
- Raevdal P, Grauslund J, Vestergaard AH. Comparison of corneal biomechanical changes after refractive surgery by noncontact tonometry: small-incision lenticule extraction versus flap-based refractive surgery—a systematic review. *Acta Ophthalmol* 2019;97:127–136
- Sefat SMM, Wilfang R, Bechmann M, Mayer WJ, Kampik A, Kook D. Evaluation of changes in human corneas after femtosecond laser-assisted LASIK and small-incision lenticule extraction (SMILE) using non-contact tonometry and ultra-high-speed camera (Corvis ST). *Curr Eye Res* 2016;41:917–922
- Wang D, Liu M, Chen Y, Zhang X, Xu Y, Wang J, To CH, Liu Q. Differences in the corneal biomechanical changes after SMILE and LASIK. *J Refract Surg* 2014;30:702–707
- Dong Z, Zhou X, Wu J, Zhang Z, Li T, Zhou Z, Zhang S, Li G. Small incision lenticule extraction (SMILE) and femtosecond laser LASIK: comparison of corneal wound healing and inflammation. *Br J Ophthalmol* 2014;98:263–269
- Francis M, Khamar P, Shetty R, Sainani K, Nuijts R, Haex B, Sinha Roy A. In vivo prediction of air-puff induced corneal deformation using LASIK, SMILE, and PRK finite element simulations. *Invest Ophthalmol Vis Sci* 2018;59:5320–5328
- Khamar P, Shetty R, Vaishnav R, Francis M, Nuijts R, Sinha Roy A. Biomechanics of LASIK flap and SMILE cap: a prospective, clinical study. *J Refract Surg* 2019;35:324–332
- Scarcelli G, Pineda R, Yun SH. Brillouin optical microscopy for corneal biomechanics. *Invest Ophthalmol Vis Sci* 2012;53:185–190
- Larin KV, Sampson DD. Optical coherence elastography—OCT at work in tissue biomechanics [Invited]. *Biomed Opt Express* 2017;8:1172–1202
- Kijanka P, Urban MW. Local phase velocity based imaging: a new technique used for ultrasound shear wave elastography. *IEEE Trans Med Imaging* 2019;38:894–908

Disclosures: None of the authors has a financial or proprietary interest in any material or method mentioned.

**First author:**

Xianan Yang, PhD

Zhongshan Ophthalmic Center, State Key Laboratory of Ophthalmology, Sun Yat-sen University, Guangzhou, China.

Prospective 3-arm study on pain and epithelial healing after corneal crosslinking

Nienke Soeters, PhD, Iris Hendriks, MD, Daniël A. Godefrooij, MD, PhD, Maarten O. Mensink, MD, Robert P.L. Wisse, MD, PhD

Purpose: To investigate the effect of 3 regimes on pain and wound healing after corneal crosslinking (CXL).

Setting: Tertiary academic referral center, Utrecht, the Netherlands.

Design: Prospective cohort study.

Methods: Consecutive progressive keratoconus patients who underwent 9 mW/cm² epithelium-off CXL were included. Patients received a bandage contact lens (n = 20), occlusive patch (n = 20), or antibiotic ointment (n = 20) after treatment. Pain scores and quality of life, measured by the McGill Pain Questionnaire and Visual Analogue Scale (VAS), were analyzed. Epithelial healing after 2 days, correlations between pain and psychological factors that influence pain perception (depression anxiety stress score and pain catastrophizing score), and oral pain medication were evaluated.

Results: Sixty eyes of 52 patients were analyzed. On average, patients experienced considerable pain after CXL (median VAS

score 6.2, range 0 to 10). The postoperative regimen did not significantly affect pain scores, although the antibiotic ointment group reported a higher VAS score (median VAS score 7.2 vs 6.7 and 6.0; $P = .57$). Occlusive patching showed a trend to quicker resolution of epithelial defects (85% completely healed vs 65% with lenses and 70% with antibiotic ointment; $P = .43$). Correlations with pain-modulating psychological factors were weak ($R^2 < 0.3$) and not significant. The use of pain medication corresponded poorly to the prescribed use.

Conclusion: This study demonstrated clinical equivalence of 3 regimes in combating postoperative pain after routine CXL. Wound healing appeared quicker in the occlusive patch group and therefore might be the best standard of care after CXL. The clinical tradition of using bandage contact lenses should be reevaluated.

J Cataract Refract Surg 2020; 46:72–77 Copyright © 2019 Published by Wolters Kluwer on behalf of ASCRS and ESCRS

Corneal crosslinking (CXL) was introduced in 1998, and the original Dresden protocol consists of epithelial removal, admission of riboflavin eye drops, and irradiation with ultraviolet A (UVA) light.^{1,2} There are many known techniques for CXL, the most proven being the epithelium-off (epi-off) technique.^{3,4} Epi-off CXL has satisfactory potential in freezing the progression of keratoconus. The technique starts with removal of the corneal epithelial cells and their tight junctions, which results in improved penetration of the major molecule riboflavin into the corneal stroma. However, the epithelial erosion persists for several days. This causes discomfort and significant pain in patients, especially during the first 24 postoperative hours.⁵ A thorough knowledge of the

pathophysiological and psychological processes that dictate our perception of corneal pain aids in better understanding the burden of this side effect.

The intense corneal CXL-related pain is orchestrated by the neuroanatomy and the photochemical process of the treatment. First, regarding the neuroanatomy, the cornea is the most highly innervated part of the vertebrate body. The density of small nerve fibers is estimated 300 to 400 times higher than the human skin, and the cornea contains approximately 600 nerve terminals per square millimeter including myelinated A δ and unmyelinated C-fibers.⁶ The nerves derive from the ophthalmic branch of the trigeminal nerve and divide into the subepithelial nerve plexus in the anterior part of the stroma. This plexus directs pain signals

Submitted: May 22, 2019 | Final revision submitted: July 19, 2019 | Accepted: August 8, 2019

Utrecht Cornea Research Group, Department of Ophthalmology, University Medical Center, Utrecht, the Netherlands.

Sophie Looijen contributed to this study.

Presented at the following meetings: (1) Oral presentation at the annual meeting of The Optometry Association Meeting, 's-Hertogenbosch, the Netherlands, February 2019; and (2) Oral presentation at the annual meeting of Dutch Ophthalmological Society (Nederlands Oogheelkundig Gezelschap), Maastricht, the Netherlands, March 2019.

Corresponding author: Nienke Soeters, PhD, University Medical Center Utrecht, Heidelberglaan 100, 3584 CX Utrecht, the Netherlands. Email: nsoeters@umcutrecht.nl.

to the central nervous system.⁶ Second, the photochemical reaction of UVA and riboflavin releases free oxygen radicals through the Bowman layer into the corneal stroma. The Bowman layer and stroma are not disrupted. Because of the high density of nerves in those layers, the free oxygen radicals could damage the intact subepithelial nerve plexus and inflict intense pain, unrelated to the size of the epithelial defect.⁷ In addition, these free radicals contribute to lipid peroxidation and production of prostaglandins and neuropeptides. As a result, symptoms such as tearing, foreign body sensation, burning, and photophobia are common during epithelialization.^{8,9}

The perception of corneal pain is a multidimensional creation of the human brain, mediated by a wide range of pathways such as sensory perceptions, emotions, thoughts, and feelings. Corneal pain starts with the nociceptors, which respond to the mechanical and chemical stimuli of the CXL treatment. Because of rapid conduction velocities of the myelinated A δ -fibers in the corneal stroma, the pain is highly localized and sharp. The slow conduction velocity of the unmyelinated C-fibers projects a delayed burning sensation. The intensity and location of pain are directed from the trigeminal to the somatosensory cortex. The affective and cognitive dimensions are projected to the amygdala, anterior cingulate cortex, insula, and hypothalamus, which result in feelings of anxiety, stress, and avoidance of pain.^{6,10} Reactive to these sensations, the brain releases neurotransmitters, which create an algescic effect called the interoception of pain. The potency of interoception depends on the strength of the associative network between the brain structures, particularly the prefrontal cortex, hippocampus, and orbitofrontal cortex. This potency could be expressed in the amount of stress, anxiety, and the phenomenon called catastrophizing.¹¹

The major downside of the effective epi-off CXL is the corneal postoperative pain. Therefore, different strategies to circumvent epithelial removal are well studied. Notwithstanding, epi-off CXL is still the gold standard for effective treatment for its stabilizing potential.^{3,12,13} The pain experienced by patients prompted us to question the clinical convention to routinely treat patients with bandage contact lenses after CXL.⁷ Numerous studies have demonstrated the need of the use of analgesics and antibiotic eye drops.^{5,14} However, currently, there are no evidence-based guidelines for topical treatment of epithelial defects and postoperative care. Creating a protocol to deal with the inevitable postoperative pain should take the aforementioned knowledge about neurophysiology into account. Based on an existing Cochrane review on the treatment of corneal erosions, 3 postoperative regimens were considered: bandage contact lenses, occlusive patching, or topical antibiotic ointment only.¹⁵

The aim of this study was to investigate which method of postoperative treatment (bandage lens vs occlusive patching vs antibiotic ointment only) delivers the best results in terms of pain control. Secondary outcomes were epithelial healing, adverse events, and adjuvant pain medication use in a clinical

crosslinking setting. In addition, we were interested in investigating the correlation between the physiological state and the experience of pain after a CXL treatment to potentially predict reactions to pain.

METHODS

Study Group and Protocol

This prospective study included patients diagnosed with progressive keratoconus. Patients were scheduled for a routine epi-off CXL procedure under local anesthesia at a tertiary academic center (University Medical Centre, Utrecht) from March 2018 through July 2018. The study was prospectively approved by the University Medical Centre Utrecht Ethics Review Board (no. 15-157). All procedures complied with the Declaration of Helsinki and local laws regarding research on humans. Informed consent was obtained from all patients. Inclusion criteria for this prospective study were an age greater than or equal to 16 years and the ability to understand and fill in Dutch-language questionnaires. General inclusion criteria for CXL were a diagnosis of clinically progressive keratoconus and a clear central cornea. Exclusion criteria were allergy for topical antibiotics or bandages, conditions that impede normal re-epithelialization such as previous corneal ulcer, ocular herpetic disease, laser in situ keratomileusis, glaucoma, or severe dry eye disease, and previous use of analgesics. Progressive keratoconus was diagnosed after a full ophthalmological examination, including Scheimpflug corneal topography (Pentacam HR; OCULUS Optikgeräte GmbH), by a corneal specialist.

Pain-Specific Questionnaires

Two standardized and validated questionnaires were used to measure factors concerning the potency of patients' interoception for post-surgical pain in general: the Pain Catastrophizing Scale (PCS) score and the Depression Anxiety Stress Score (DASS-42).^{16,17} One questionnaire was used to assess perceived pain and pain-related quality of life after the crosslinking treatment: the McGill Pain Questionnaire–Dutch Language Version (MPQ-DLV).¹⁶

The PCS score consists of 13 statements assessing 3 dimensions: rumination, magnification, and helplessness.¹⁸ The dimensions have, respectively 4, 3, and 6 items scored on 5-point Likert scales from "not at all" (0) to "all the time" (4). The PCS score instructions ask patients to reflect on past painful experiences by indicating the degree of 13 thoughts or feelings when they experience pain. The PCS total score is computed by the sum of responses to all 13 items. PCS total scores range from 0 to 52 with an estimated score of 19.9 ± 8.9 in healthy adults and 24.3 ± 9.6 in patients with pain.

The DASS-42 was used to evaluate the level of depression, anxiety, and stress, with a total of 42 questions with 14 items for each scale. The depression scale assesses hopelessness, dysphoria, devaluation, lack of interest, and anhedonia. The anxiety scale evaluates autonomic arousal, skeletal muscle effects, and situational anxiety. The final stress scale is sensitive to levels of chronic nonspecific arousal. The answers are scored on a 4-point Likert scale ranging from "did not apply to me at all" (0) to "applied to me very much" (3).¹⁹

After the CXL treatment (before the first follow-up visit), all patients were requested to fill in the MPQ-DLV.¹⁶ The validity and reliability of the MPQ-DLV has been confirmed in numerous Dutch publications.¹⁶ The MPQ-DLV consists of 3 different questionnaires. The first questionnaire consists of 78 words that describe distinctly different aspects of the experience of pain and their effect on quality of life. The words are categorized in 3 dimensions: sensory aspects, affective qualities in terms of fear, tension, and autonomic reactions, and evaluative words that define the subjective overall intensity of the total pain experience. The second questionnaire consists of the quality of life score, in which postoperative usage of analgesics

was also documented. In the final questionnaire, patients were asked to report their pain peak during the two postoperative days using the visual analogue scale (VAS) score: a number between 0 (no pain) and 100 (worst possible pain).²⁰

Surgical Technique

Epi-off CXL was performed in all patients. After topical anesthesia with oxybuprocaine (4 mg/mL) and tetracaine (5 mg/mL), the erosion with a standard diameter of 6 mm was created using a blunt knife.² With pachymetry measurements >400 μm , isotonic riboflavin 0.1% solution with 20% dextran (Collagex) was applied every 3 minutes for 30 minutes. When pachymetry was <400 μm , hypo-osmolar riboflavin was applied until >400 μm was achieved. Accelerated 9 mW/cm² UVA irradiation was performed during 10 minutes. During irradiation, NaCl 0.9% drops were instilled every 5 minutes to hydrate the cornea.

Postoperative Regimen

After treatment, all patients received 1000 mg paracetamol and 50 mg diclofenac. All eyes received preservative-free antibiotic eye drops for 2 weeks (chloramphenicol 0.4%, Thea Pharma BV), and preservative-free artificial tears were administered (Celluvisc 0.1%, Allergan, Inc.) for 4 weeks. According to the World Health Organization (WHO) analgesic ladder, the postoperative analgesics, paracetamol (1000 mg, 1 to 4 per day) and diclofenac (50 mg, 1 to 2 per day), were prescribed.²¹ When this resulted in insufficient reduction of pain, oxycodone (10 mg, 1 to 3 per day) was prescribed as rescue medication. Patients were instructed to avoid tap water in their eye until the epithelium has healed, to avoid rubbing their eye, and to rest for 24 hours.

Patients were consecutively assigned to 1 of the 3 therapeutic modalities. The first 20 patients received a bandage lens (Purevision, Bausch & Lomb, Inc.). The bandage lens covered the entire surface of the cornea and limbus. The second group of 20 patients received an occlusive patch using two pieces of sterile gauze after insertion of antibiotic ointment (ofloxacin, 3 mg/mL, Bausch & Lomb, Inc.). The first gauze was placed folded in half, and the second horizontally over it, and they were fixed with adhesive antiallergic medical tape. The advised duration of occlusive patching was 24 hours. Topical treatment was started after removal of the occlusive patch. The third group of 20 patients received chloramphenicol-POS 1% ointment (Ursapharm) 4 times

a day for 48 hours. All patients repeatedly received oral and written instructions on the preferred use of analgesics.

Follow-up Evaluation

A routine follow-up visit was scheduled 2 days postoperatively. The follow-up visit started with removal of the bandage lens in the first group. In all groups, the use of analgesics was recorded. Consecutively, a slitlamp examination assessed corneal wound healing. Two distinctive outcomes were used for classification: complete reepithelization or an epithelial defect. In case of a closed epithelium, the patients started application of topical steroids (fluorometholone 0.1% drops, Allergan, Inc.) 2 times a day for 1 month. A persistent epithelial defect was treated with an occlusive patch.

Statistical Analysis

The distributions of all variables were checked for normality by visually assessing histograms. None of the variables were normally distributed, except for VAS, Quality of Life Scale, and Pain Rating Index–Total. Differences between the 3 treatment groups were compared using a nonparametric Kruskal–Wallis test. The Pearson correlation test was used to measure strength of relation between baseline characteristics of the potency of interoception and postoperative pain and quality of life. Snellen decimal visual acuity was converted to the logarithm of the minimum angle of resolution for analysis. A *P* value of less than .05 was considered statistically significant. Data were recorded as median \pm interquartile range. All of the tests were performed using SPSS Statistics for Windows software (version 25.0, IBM Corp.). A post hoc power analysis was performed using a specific power analysis tool.²²

RESULTS

This study comprised 60 eyes of 52 patients (37 men and 15 women) with progressive keratoconus. The median age was 24 years, ranging from 16 to 50 years. No patients were lost to follow-up. Information about epithelial healing and pain scores of 2 patients who scheduled their follow-up visit in a hospital closer by was requested. The 3 groups were comparable at baseline. Baseline characteristics and level of catastrophizing, depression, anxiety, and stress before the crosslinking treatment are listed in Table 1. All baseline

Table 1. Bandage lenses vs occlusive patching vs antibiotic ointment for postoperative pain management after epi-off CXL for keratoconus, baseline characteristics (n = 60).

Baseline Parameter	Bandage Lenses	Occlusive Patching	Antibiotic Ointment	<i>P</i> Value*
Eyes (n)	20	20	20	NA
Median age (yrs) (range)	25 (17-43)	25 (16-50)	20.5 (16-34)	.05
Male/female (n)	13/7	16/4	14/6	.56
Right/left (n)	10/10	8/12	11/9	.63
CDVA (logMAR) (median \pm IQR)	0.19 \pm 0.29	0.14 \pm 0.29	0.10 \pm 0.33	.43
Pachymetry thinnest point (μm) (median \pm IQR)	438 \pm 72	446 \pm 94	446 \pm 60	.31
Maximal keratometry (D) (median \pm IQR)	59.2 \pm 14.1	56.2 \pm 20.4	57.3 \pm 9.8	.82
Amsler-Krumeich Classification [†] (median \pm IQR)	4 \pm 2	3.5 \pm 3	3.5 \pm 2	.56
PCS score (0-50) (median \pm IQR)	12 \pm 12	13 \pm 10	5.5 \pm 11	.10
Depression [‡] (0-28) (median \pm IQR)	0.5 \pm 3	0.0 \pm 3	0.5 \pm 4	.92
Anxiety [§] (0-20) (median \pm IQR)	3.0 \pm 5	1.0 \pm 1	1.0 \pm 4	.11
Stress (0-34) (median \pm IQR)	6.0 \pm 5	3.0 \pm 6	3.0 \pm 5	.18

CDVA = corrected distance visual acuity; CXL = corneal crosslinking; epi-off = epithelium-off; IQR = interquartile range; logMAR = logarithm of the minimum angle of resolution; NA = not applicable; PCS = pain catastrophizing scale

**P* values are not corrected for multiple testing

[†]Amsler-Krumeich Classification based on K_{max}

[‡]Depression: normal (0-9), mild (10-13), moderate (14-20), severe (21-27), and extremely severe (28+)

[§]Anxiety: normal (0-7), mild (8-9), moderate (10-14), severe (15-19), and extremely severe (20+)

^{||}Stress: normal (0-14), mild (15-18), moderate (19-25), severe (26-33), and extremely severe (34+)

Table 2. Bandage lenses vs occlusive patching vs antibiotic ointment for postoperative pain management after epi-off CXL for keratoconus: pain scores and pain medication use after CXL.

Parameter*	Bandage Lenses	Occlusive Patching	Antibiotic Ointment	P Value
Eyes (n)	20	20	20	NA
MPQ-DLV				
VAS score (0-10) (median ± IQR)	6.0 ± 4.6	6.7 ± 3.4	7.2 ± 3.6	.57
Pain Rating Index–Total (0-120) (median ± IQR)	65.8 ± 34.4	65.7 ± 27.6	64.4 ± 49.8	.86
Quality of Life Scale (0-27) (median ± IQR)	13.5 ± 6.5	17.0 ± 10.0	15.0 ± 9.0	.41
Pain medication use				
Paracetamol (mg)	3000 ± 2000	4000 ± 2000	4000 ± 6000	.09
Diclofenac (mg)	150 ± 188	150 ± 250	100 ± 300	.92
Oxycodone (mg)	0 ± 18	0 ± 20	10 ± 30	.20

CXL = corneal crosslinking; epi-off = epithelium-off; IQR = interquartile range; MPQ-DLV = McGill Pain Questionnaire–Dutch Language Version; VAS = visual analogue scale; NA = not applicable.

*For outcomes of the Pain Rating Index and Quality of Life Scale: the higher the score, the more pain-related complaints patients experienced during the 2 postoperative days.

parameters except for pachymetry were not normally distributed.

Table 2 shows the outcomes of the MPQ-DLV and postoperative pain medication use in milligrams. There was no significant difference in the VAS, Pain Rating Index–Total, Quality of Life Scale, and paracetamol, diclofenac, and oxycodone use between the groups. The median VAS score of all patients was 6.2, range 0 to 10. Figure 1 illustrates the VAS pain score after crosslinking.

The status of the corneal surface 2 days after CXL treatment is shown in Figure 2. A trend of faster corneal healing seemed to be present in the occlusive patch group, although these effects were not statistically significant ($P = .43$). All correlations between catastrophizing, depression, anxiety, and stress vs primary outcomes were not significant; R square (R^2) is shown in Table 3.

Figure 3 shows the words patients used to describe their pain during the 2 postoperative days and the difference of reports between the groups. All patients in the occlusive patch group used one of the following words: “pricking”, “stabbing”, or “lancinating.”

The post hoc power analysis showed that 21 patients per group was sufficient to demonstrate a statistically significant difference ($P = .05$) with a power of 0.8 and an effect size of 0.4.

DISCUSSION

Our study demonstrated a high score of pain intensity post-CXL and an overall adequate epithelization of the corneal epithelium. Although this study was not able to show a statistically significant difference in postoperative pain

between the bandage lens, occlusive patch, and antibiotic ointment groups, the latter group reported on average more pain. Furthermore, epithelial healing seemed slightly better in the occlusive patch group, whereas perceived quality of life was equal in the groups.

A major strength of this study was the standard size of the corneal erosion. The standard size aided the comparability between the 3 treatment cohorts, in contrast to other studies in which traumatic corneal erosions are investigated with erosions that differ in size and depth.^{23,24} In addition, bias as a result of time delay in examining the patient after the erosion occurred, as is the case with traumatic erosions, was avoided because all patients received the same postoperative follow-up schedule. A second strength was the accurately reported analgesic use. The use was both documented by the patient and later orally verified and updated by the investigator. We used comprehensive questionnaires in this study, which provided insight in all factors concerning the pain experience. This facilitated assessing the potency of interoception and cerebral cortex modulation of pain.²⁵ In addition, there were no missing data in all the questionnaires, which aided in reliable results. The last strength was the young age of our sample with very little comorbidity, which otherwise could have influenced the outcomes of pain or epithelial healing. In addition, because of our relatively healthy and young population, the results correspond to the average keratoconus population and therefore are well generalizable.

A limitation of this study was the consecutive design without randomization. In addition, smoking status was

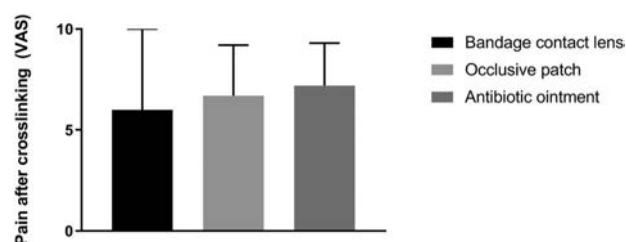


Figure 1. Median VAS scores, measured at the peak moment after corneal crosslinking in the 3 groups (VAS = visual analogue scale).

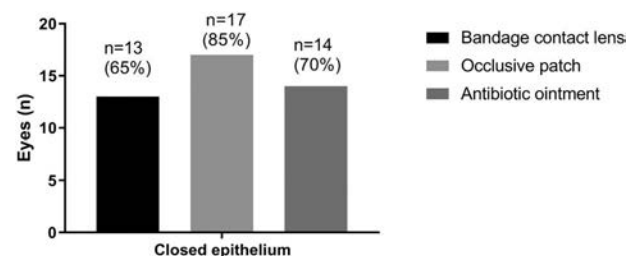


Figure 2. Status of the corneal surface 2 days after corneal crosslinking treatment in the 3 groups.

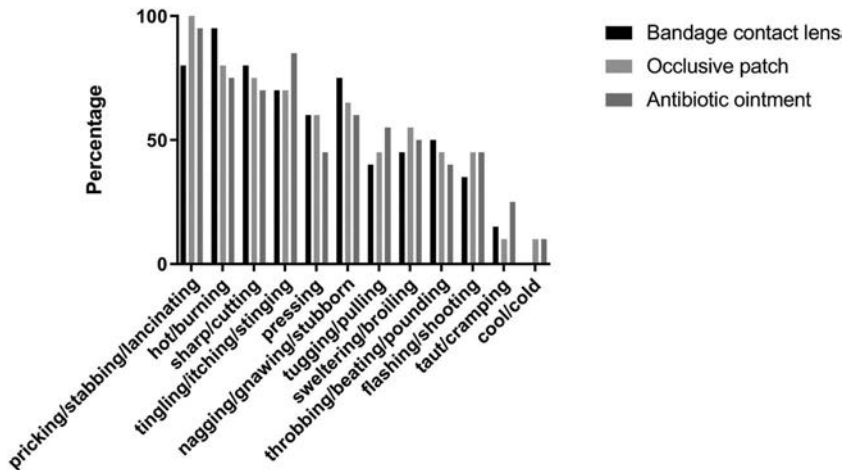


Figure 3. Characteristics of post-corneal crosslinking pain—% patients using words.

not documented, which is correlated with worse wound healing.²⁶ An ordinal scale was used to describe the status of epithelial healing after 2 days. Statistical tests with more power could have been used when the size of the epithelial defect was measured on a continuous scale. Furthermore, information about the cultural diversity of the patients was not available in this sample. Different cultures have varying ways of perceiving, labeling, and expression of pain.²⁷

Although no statistically significant difference in pain was found between treatments, it was notable that all patients scored a high intensity of pain, even with an aggressive postoperative analgesia regime. This might be explained by the young median age of our participants. The younger the patients, the higher the sensibility of the subepithelial nerve plexus in the cornea.¹⁰ In general, older patients report lower pain scores; the reason is still unknown but might be related to a decreased neurological or cognitive processing capacity. The same result was reported by Ghanem et al.⁵ in 2013; they found a significant correlation between pain and age, the younger the patient, the greater the pain after epi-off CXL. It is known that the corneal erosion by itself causes intense pain. However, the intensity of pain seems to be worse after crosslinking than after photorefractive keratectomy, suggesting that there are more factors that play a role during the riboflavin/UVA treatment.⁷ The authors hypothesize that “UVA-generated free radicals could also attribute to lipid peroxidation and prostaglandin production in CXL.⁷ This additive source for peroxidation might cause greater pain after CXL. Direct chemo-mediated stimulation of the corneal nerves could lead to severe pain unrelated to the size of epithelial defects.”

No correlations were found between the moderating psychological parameters (catastrophizing, depression, anxiety, and stress) and the level of pain or postoperative quality of life. Correlations were weak ($\rho < 0.3$) and not significant, which means that there was little linear relation between all variables. The young keratoconus group in this study was in general happy and not catastrophizing their pain.

Based on the study of Pavlin et al.,¹¹ associations between higher catastrophizing, pain scores, and poorer quality of life are expected. The lack of correlations could be declared by the relatively low PCS and DAS scores in our study population, which were comparable to a healthy adolescence population.

The one depressive patient in our study showed a normal VAS pain score of 5.9 and no increased catastrophizing score.

In the first article that describes what is currently the most used CXL procedure in humans, by Wollensak et al.² in 2003, an antibiotic ointment only was used after treatment. In 2007, Spoerl et al.²⁸ used antibiotic ointment and added a bandage contact lens that was soaked with antibiotic drops. The randomized controlled trials that included the epi-off CXL procedure mostly used bandage contact lenses.²⁹ Although bandage contact lenses are in general a safe treatment for patients with epithelial defects,³⁰ there is a risk of developing microbial keratitis while wearing the lenses. One study has reported bacterial growth on bandage contact lenses has been reported in almost 30% of patients.³¹ On the other hand, in the trials with comparisons of bandage contact lenses and patching of the erosion (Triharpini et al.²³ and Menghini et al.²⁴), no complications were described in any group with traumatic erosions.

Based on this relatively small study, a study with an adequate sample size can be initiated in the future. For further research, we advise a range of post-CXL pain score measurements to provide insight into the course of the pain. With time-based patient reporting of analgesic usage, it could be possible to capture the effect of different analgesic regimes. With the knowledge that the free oxygen radicals and prostaglandins could contribute to the intensity of postoperative pain, it may be valuable to invent a mechanism to prevent or reduce the release of both. A notable outcome in our study was a very low pain protocol adherence and relatively frequent usage of opiates. These outcomes were used to improve the instructions about the use of pain medication according to the WHO analgesic ladder in our information folder for patients.²¹ We advise the clinician to inform patients orally about the effects of different painkillers, with the aim to optimize use and minimize side effects.

Epi-off crosslinking was associated with significant postoperative pain, with no significant difference in the pain score between 3 regimes (bandage contact lens, occlusive patch, or antibiotic ointment). Wound healing appeared quicker in the occlusive patch group. Therefore, occlusive patching might be the best standard of care after CXL, and the clinical tradition of using bandage contact lenses should be reevaluated.

Table 3. Overview of correlation between catastrophizing, depression, anxiety, and stress vs the VAS pain peak score.

Variables	VAS Score	P Value
PCS score	0.055	.68
Depression	0.020	.88
Anxiety	-0.018	.89
Stress	0.043	.75

VAS score ranged from 0 (no pain) to 100 (worst possible pain).
PCS = pain catastrophizing scale; VAS = visual analogue scale.

In addition, the psychological factors that influence pain introception (catastrophizing, depression, anxiety, and stress) were not correlated with postoperative pain. Adhesion to the prescribed analgesics was suboptimal. Our recommendation to alleviate the burden of epi-off CXL is to dedicate time and effort to a proper explanation of the use of postoperative analgesics.

WHAT WAS KNOWN

- Patients experience significant pain after epithelium-off corneal crosslinking (epi-off CXL).
- Standard postoperative care after CXL consists of the placement of a bandage contact lens and pain medication.
- Currently, there are no evidence-based guidelines for topical treatment of epithelial defects and postoperative care.

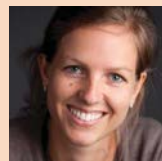
WHAT THIS PAPER ADDS

- Three regimes were evaluated to give insight in pain after epi-off CXL, duration of epithelial healing, and to assess the amount of pain medication.
- Differences in pain scores between 3 regimes (bandage contact lens, occlusive patch, or antibiotic ointment) were not statistically significant.
- Wound healing appeared quicker in the occlusive patch group.
- Occlusive patching might be the best standard of care after CXL, and the clinical tradition of using bandage contact lenses should be reevaluated.

REFERENCES

1. Spoerl E, Huhle M, Seiler T. Induction of cross-links in corneal tissue. *Exp Eye Res* 1998;66:97–103
2. Wollensak G, Spoerl E, Seiler T. Riboflavin/ultraviolet-A-induced collagen crosslinking for the treatment of keratoconus. *Am J Ophthalmol* 2003;135:620–627
3. Soeters N, Wisse RP, Godefrøoij DA, Imhof SM, Tahzib NG. Transepithelial versus epithelium-off corneal cross-linking for the treatment of progressive keratoconus: a randomized controlled trial. *Am J Ophthalmol* 2015;159:821–828
4. Liu Y, Liu Y, Zhang YN, Li AP, Zhang J, Liang QF, Jie Y, Pan ZQ. Systematic review and Meta-analysis comparing modified cross-linking and standard cross-linking for progressive keratoconus. *Int J Ophthalmol* 2017;10:1419–1429
5. Ghanem VC, Ghanem RC, de Oliveira R. Postoperative pain after corneal collagen cross-linking. *Cornea* 2013;32:20–24
6. Marfurt CF, Cox J, Deek S, Dvorscak L. Anatomy of the human corneal innervation. *Exp Eye Res* 2010;90:478–492
7. Zarei-Ghanavati S, Jafarpour S, Radyn-Majid A, Hosseinihah-Manshadi H. Evaluation of early postoperative ocular pain after photorefractive keratectomy and corneal crosslinking. *J Cataract Refract Surg* 2018;44:566–570
8. Mazzotta C, Traversi C, Baiocchi S, Caporossi O, Bovone C, Sparano MC, Balestrazzi A, Caporossi A. Corneal healing after riboflavin ultraviolet-A collagen cross-linking determined by confocal laser scanning microscopy in vivo: early and late modifications. *Am J Ophthalmol* 2008;146:527–533
9. Mazzotta C, Hafezi F, Kymionis G, Caragiuli S, Jacob S, Traversi C, Barabino S, Randleman JB. In Vivo confocal microscopy after corneal collagen crosslinking. *Ocul Surf* 2015;13:298–314
10. Belmonte C, Acosta MC, Gallar J. Neural basis of sensation in intact and injured corneas. *Exp Eye Res* 2004;78:513–525
11. Pavlin DJ, Sullivan MJL, Freund PR, Roesen K. Catastrophizing: a risk factor for postsurgical pain. *Clin J Pain* 2005;21:83–90
12. Li W, Wang B. Efficacy and safety of transepithelial corneal collagen crosslinking surgery versus standard corneal collagen crosslinking surgery for keratoconus: a meta-analysis of randomized controlled trials. *BMC Ophthalmol* 2017;17:262
13. Rush SW, Rush RB. Epithelium-off versus transepithelial corneal collagen crosslinking for progressive corneal ectasia: a randomised and controlled trial. *Br J Ophthalmol* 2017;101:503–508
14. Bakke EF, Stojanovic A, Chen X, Drolsum L. Penetration of riboflavin and postoperative pain in corneal collagen crosslinking: excimer laser superficial versus mechanical full-thickness epithelial removal. *J Cataract Refract Surg* 2009;35:1363–1366
15. Lim CH, Turner A, Lim BX. Patching for corneal abrasion. *Cochrane Database Syst Rev* 2016;7:CD004764
16. Verkes R, Vanderiet K, Vertommen H, van der Kloot WA, van der Meij J. De MPQ-DLV, een standaard Nederlandstalige versie van de McGill Pain Questionnaire voor België en Nederland. Lisse, Netherlands: Swets & Zeitlinger; LUMC; Faculteit der Sociale Wetenschappen; et al; 1989.
17. Van Damme S. Catastroferen over pijn: Pain Catastrophizing Scale-Dutch Version (PCS-DV). Gent: Universiteit Gent; 2002. Available at: <http://www.bsw.ugent.be/VWGP/fichePCS.pdf>.
18. Sullivan M, Bishop S, Pivik J. The pain catastrophizing scale: development and validation. *Psychol Assess* 1995;7:524–532
19. Beurs E, Dyck R, Marquenie LA, Lange A, Blonk RWB. De DASS; een vragenlijst voor het meten van depressie, angst en stress. *Gedragtherapie* 2001;34:35–53
20. Langley GB, Sheppard H. The visual analogue scale: its use in pain measurement. *Rheumatol Int* 1985;5:145–148
21. Jadad AR, Browman GP. The WHO analgesic ladder for cancer pain management. Stepping up the quality of its evaluation. *JAMA* 1995;274:1870–1873
22. Power calculation for One-way independent ANOVA. Available at: <https://www.anzmtg.org/stats/PowerCalculator/PowerANOVA>. Accessed July 12, 2019
23. Triharjini NN, Gede Jayanegara IW, Handayani AT, Widiani IGR. Comparison between bandage contact lenses and pressure patching on the erosion area and pain scale in patients with corneal erosion. *J Ophthalmol* 2015;4:97–100
24. Menghini M, Knecht PB, Kaufmann C, Kovacs R, Watson SL, Landau K, Bosch MM. Treatment of traumatic corneal abrasions: a three-arm, prospective, randomized study. *Ophthalmic Res* 2013;50:13–18
25. Xie Y, Huo F, Tang J. Cerebral cortex modulation of pain. *Acta Pharmacol Sin* 2009;30:31–41
26. Sorensen LT. Wound healing and infection in surgery. *Ann Surg* 2012;255:1069–1079
27. Rahim-Williams B, Riley JL, Williams AKK, Fillingim RB. A quantitative review of ethnic group differences in experimental pain response: do biology, psychology, and culture matter? *Pain Med* 2012;13:522–540
28. Spoerl E, Mrochen M, Sliney D, Trokel S, Seiler T. Safety of UVA-riboflavin cross-linking of the cornea. *Cornea* 2007;26:385–389
29. Wittig-Silva C, Chan E, Islam FM, Wu T, Whiting M, Snibson GR. A randomized, controlled trial of corneal collagen cross-linking in progressive keratoconus: three-year results. *Ophthalmology* 2014;121:812–821
30. Donnenfeld ED, Selkin Ba, Perry HD, Moadeel K, Selkin GT, Cohen AJ, Sperber LT. Controlled evaluation of a bandage contact lens and a topical nonsteroidal anti-inflammatory drug in treating traumatic corneal abrasions. *Ophthalmology* 1995;102:979–984
31. Feizi S, Masoudi A, Hosseini SB, Kanavi MR, Javadi MA. Microbiological evaluation of bandage soft contact lenses used in management of persistent corneal epithelial defects. *Cornea* 2019;38:146–150

Disclosures: None of the authors has a financial or proprietary interest in any material or method mentioned.



First author:

Nienke Soeters, PhD

Department of Ophthalmology, University Medical Center Utrecht, the Netherlands.

Clinical outcomes after femtosecond laser-assisted implantation of an intrastromal corneal ring segment with a 340-degree arc length in postkeratoplasty patients: 12-month follow-up

Patrick F. Tzelikis, MD, PhD, Antônio Helbert G.M. Jácome, MD, Guilherme Andrade N. Rocha, MD, Wilson Takashi Hida, MD, Luciene Barbosa de Souza, MD, PhD

Purpose: To assess the clinical outcomes after implantation of a new 340-degree arc length intrastromal corneal ring segment (ICRS) aided by the femtosecond laser in postkeratoplasty patients after a 12-month follow-up.

Setting: Private practice, Brasília, Brazil.

Design: Prospective case series.

Methods: Eyes with previous keratoplasty had ICRS implantation assisted by femtosecond laser. The primary outcome measure was the change in the uncorrected distance visual acuity (UDVA) 12 months postoperatively. The secondary outcome measures were the corrected distance visual acuity (CDVA), refraction, and corneal tomography 1, 3, 6, and 12 months postoperatively. The astigmatism results were analyzed using vector analysis through the double-angle polar plot.

Results: Of the 18 patients, 7 (38.9%) were men, and 11 (61.1%) were women. The mean UDVA was 20/250 (1.15 logarithm of the minimum angle of resolution [logMAR]) before implantation and 20/70 (0.54 logMAR) at the last follow-up ($P < .001$). The mean CDVA improved from 20/35 (0.26 logMAR) to 20/25 (0.10 logMAR) ($P < .001$). The mean spherical equivalent and astigmatism components were significantly reduced after ICRS implantation. The mean corneal astigmatism decreased from 5.55 ± 2.29 D preoperatively to 3.92 ± 1.82 D postoperatively ($P < .001$). The CDVA remained the same or improved in 19 of 20 eyes and decreased by 1 line in 1 patient. There were no surgical complications.

Conclusion: A new ICRS with a 340-degree arc length was effective in treating postkeratoplasty eyes, improving visual acuity and reducing corneal astigmatism.

J Cataract Refract Surg 2020; 46:78–85 Copyright © 2019 Published by Wolters Kluwer on behalf of ASCRS and ESCRS

Even after successful corneal transplantation, ametropia, astigmatism, and anisometropia can compromise a patient's final visual outcome and rehabilitation. Refractive unpredictability after corneal transplantation is common, with many articles reporting mean cylinders of 4 to 5 diopters (D) and spherical equivalents (SEs) in the range of -2 D to 12 D.^{1–5}

Postkeratoplasty astigmatism and ametropia can be managed with nonsurgical options such as spectacles and contact lenses. Contact lenses are extremely effective in those patients who cannot tolerate spectacles. The incidence of contact lens wear after penetrating keratoplasty (PKP) for keratoconus is 25% to 50%, with successful use in more than 80% of cases.^{6,7} However, contact lens wear is

not always effective in patients requiring visual correction after corneal transplantation and surgical alternatives might be the only choice.

Several surgical options have been reported for the treatment of ametropia after corneal transplantation, including manual astigmatic keratotomy,⁸ femtosecond laser astigmatic keratotomy,⁹ limbal relaxing incisions,¹⁰ wedge resection,¹¹ excimer laser-based photorefractive procedures,¹² repeat keratoplasty,¹³ and intrastromal corneal ring segments (ICRS) implantation.¹⁴

Intrastromal corneal rings segments have been used to correct ectatic corneal diseases by reducing corneal steepening, decreasing astigmatism, and improving visual acuity, with the advantage of being reversible without affecting the

Submitted: February 15, 2019 | Final revision submitted: July 24, 2019 | Accepted: August 3, 2019

Department of Ophthalmology, Hospital Oftalmológico de Brasília–HOB, DF, Brazil.

Corresponding Author: Patrick F. Tzelikis, MD, PhD, Department of Ophthalmology, Hospital Oftalmológico de Brasília–HOB, SQN 203, Block K, Apt 502, Brasília, DF 70833-110, Brazil. Email: tzelikis@gmail.com.

central corneal visual axis.¹⁴⁻¹⁷ This study assessed the outcomes of 340-degree arc length ICRS implantation for the correction of residual ametropia and corneal irregularity after corneal transplantation performed at the Brasilia Ophthalmologic Hospital, Brazil.

METHODS

Study Design

A prospective noncomparative, single-center study was conducted between February 1, 2016, and December 31, 2017, in accordance with the tenets of the Declaration of Helsinki and the principles of current Good Clinical Practices. The study protocol was approved by the Institutional Review Board of Hospital Oftalmológico de Brasilia. All patients provided written informed consent.

Patient Enrollment

Patients were enrolled at 1 site in Brasilia. Inclusion criteria were 18 years of age or older, corneal transplantation performed at least 12 months previously, graft suture removal at least 6 months before ICRS implantation, contact lens intolerance, post-keratoplasty topographic astigmatism greater than 2.0 D, and a normal ophthalmologic examination other than ametropia. Exclusion criteria were glaucoma or intraocular pressure greater than 21 mm Hg, amblyopia, a central endothelial cell count less than 1000 cells/mm², cataract, retinal abnormalities, uveitis, diabetes mellitus, connective tissue disease, trauma, or steroid or immunosuppressive treatment. Enrolled patients who had surgical complications (eg, corneal perforation through the endothelium) were subsequently excluded. The investigator also selected patients who were likely to be compliant (eg, no scheduled vacation) and to understand what was involved in participating in a clinical study.

Preoperative Evaluation

Preoperatively, patients had an extensive ophthalmologic examination, including the measurement of uncorrected distance visual acuity (UDVA), corrected distance visual acuity (CDVA), refraction, slitlamp biomicroscopy, intraocular pressure, dilated fundus examination, corneal tomography (Pentacam, OCULUS Optikgeräte GmbH), and an endothelial cell count. The UDVA and CDVA were assessed with the Early Treatment Diabetic Retinopathy Study eye meter chart under standardized conditions. The visual acuity measurements were recorded using logarithm of the minimum angle of resolution (logMAR) UDVA and CDVA notation.

Intrastromal Corneal Ring Segment

All eyes received an ICRS comprising a single poly(methyl methacrylate) noncontinuous ring with a 340-degree arc length, 5.0 mm internal diameter, 6.4 mm outer diameter, 700 μm base width, and 200 μm thickness (Keraring, Mediphacos).

Surgical Technique

All operations were performed under topical anesthesia in a standard way by the same experienced surgeon (PFT). In brief, a radial incision was created on the steep meridian with a femtosecond laser (IntraLase FS 60 kHz, Abbott Medical Optics, Inc.). The laser software was programmed to create a channel inner diameter of 4.9 mm and outer diameter of 6.4 mm. The ring energy used for channel creation was 1.20 J, and the entry cut energy was 1.10 J. The 340-degree arc length ICRS was implanted after channel creation using a modified McPherson forceps and properly positioned with the aid of a Sinsky hook that engaged the two positioning holes. The depth of the tunnel was set at 75% of the thinnest corneal thickness on the tunnel location.

Postoperative Evaluation

Postoperatively, patients were instructed to instill 1 drop of artificial tear substitute 4 times a day and prednisolone 1% drops 4 times a day for 1 week, 3 times a day for 1 week, 2 times a day for 1 week, and 1 time a day for 1 week. In addition, patients received gatifloxacin 0.3% drops (Zymar) 4 times a day for 7 days postoperatively. All patients had a thorough examination postoperatively after 1 day and then at 1, 3, 6, and 12 months. All preoperative measurements were repeated at 1, 3, 6, and 12 months.

Outcome Measures

The primary outcome measure was the change in the mean UDVA 12 months postoperatively compared with preoperative values. The secondary outcome measures were the changes in the mean CDVA, SE, corneal topographic astigmatism, minimum (K_1) and steep (K_2) keratometry values, and the percentage of patients who had a loss or gain of lines of CDVA at 3, 6, and 12 months after ICRS implantation compared with the preoperative baseline. The investigator questioned each patient about compliance at each visit and informed patients regarding the importance of follow-up adherence.

The presurgery and postsurgery refraction findings were assessed using the Thibos and Horner¹⁸ power vector method. With this notation, any spherocylindrical refractive error can be expressed as a power vector that can be plotted in a 3-dimensional space whose 3 axes represent dioptric powers M , J_0 , and J_{45} where M is the power of a spherical lens equal to the SE of the given refractive error, and J_0 and J_{45} are the powers of two Jackson cross-cylinders equivalent to a conventional cylinder. The length of the power vector defined by the distance from the origin to the point in this 3-dimensional dioptric space provides a measure of the overall blurring strength (B) of a given spherocylindrical refractive error. Conventional script notation parameters, S (sphere), C (cylinder), and α (axis) for manifest refraction, were converted to power vector coordinates and (B) using the following formulas:

$$M = S + C/2; J_0 = (-C/2) \cos(2\alpha); \\ J_{45} = (-C/2) \sin(2\alpha); B = (M^2 + J_0^2 + J_{45}^2)$$

Statistical Analysis

Data were entered into an Excel spreadsheet (Microsoft Corp.) and analyzed using SPSS Statistics for Windows software (version 17.0, SPSS, Inc.). All data were analyzed preoperatively and 3, 6, and 12 months postoperatively. The primary null hypothesis was no difference between the values of preoperative and postoperative UDVA. The alternative hypothesis was that after the implantation of ICRS, the eyes would have better UDVA than preoperatively.

Quantitative variables are described using mean \pm SD or median as well as minimum and maximum values where appropriate. The normality of data was assessed with the Shapiro-Wilks test. The paired-samples t test was used to investigate differences in preoperative and postoperative measures when the data normally distributed and the Wilcoxon test when continuous but not normally distributed. Outcomes were compared using repeated-measures analysis of variance with multiple comparisons. The qualitative variables were described with frequency distributions and compared using the Fisher exact test. Any differences with P value less than .05 (ie, at the 5% level) were considered to be statistically significant. The analyses were performed using the full analysis set, which included all patients who had at least 2 postoperative visits (3 months and 6 months).

RESULTS

Of the 24 patients screened, 2 did not meet the inclusion criteria (1 glaucoma and 1 cataract), 1 decided not to participate, and 1 fulfilled an exclusion criterion. Thus, 18 participants were included in the full analysis set. There were no complications.

Seven patients (38.9%) were men, and 11 (61.1%) were women. The mean age of the patients was 39.3 ± 11.3 years (range). They all had a corneal transplantation at presentation. Six eyes (30.0%) had PKP and 14 eyes (70.0%), deep anterior lamellar keratoplasty (DALK). The median interval between corneal keratoplasty and ICRS implantation was 5.7 years (range 2.1 to 11.3 years). All patients had follow-up to 12 months. Table 1 shows the baseline patient characteristics.

Table 2 shows the preoperative and 12-month postoperative results. By 12 months postoperatively, 1 eye (5%) had lost 1 line of CDVA, 2 eyes (10%) remained unchanged, 7 eyes (35%) gained 1 line, and 10 eyes (50%) gained 2 or more lines of CDVA. No eye lost more than 2 lines. The percentage of eyes with a CDVA of 0.3 logMAR (20/40) or better increased from 75% preoperatively to 95% 12 months postoperatively ($P = .04$). All visual parameters analyzed (K_{avg} and corneal cylinder) were stable

over the follow-up period (Figures 1 and 2). The change in K_1 , K_2 , corneal astigmatism, K_{avg} , K_{max} , central corneal thickness, and Q value (corneal asphericity) was statistically significant.

Table 3 shows the manifest distribution of the refractive error before and 12 months after ICRS implantation. There was a significant reduction in blur strength postoperatively ($P < .001$). Figure 3 shows the double-angle plots of the preoperative and postoperative keratometric astigmatism. The astigmatism component of the power vector, represented as a 2-dimensional vector (J_0 and J_{45}), is plotted in Figure 4. The coordinates at the origin (0, 0) represent an astigmatism-free eye.

Table 4 shows the UDVA and CDVA values before ICRS implantation and after 12 months of follow-up in the PKP and DALK groups. Because the number of patients in this study was small and the DALK and PKP groups were of unequal size. There was inadequate power to detect any difference between the two types of keratoplasty. Figure 5 shows the keratometric map of one of the patients before surgery and 12 months postoperatively with improvements in all parameters including 2 lines of CDVA. Figure 6 shows the same

Table 1. Patient demographics.

Characteristics	Mean \pm SD	Median	Range
Refractive sphere (D)	-2.52 ± 2.81	-2.00	-8.00, 1.00
Refractive cylinder (D)	-5.36 ± 1.72	-5.50	-8.00, -1.50
SE (D)	-5.22 ± 2.96	-5.00	-11.00, -1.50
K_1 (D)	45.49 ± 3.25	44.90	36.50, 50.60
K_2 (D)	51.05 ± 3.57	50.70	43.70, 58.10
Corneal astigmatism (D)	5.55 ± 2.29	5.04	2.80, 10.40
K_{avg} (D)	47.96 ± 3.32	47.50	39.70, 53.50
K_{max} (D)	58.53 ± 6.91	58.35	49.60, 74.30
CCT (μ m)	482.40 ± 56.19	477.00	383.00, 597.00
Q value	-0.29 ± 0.73	-0.54	-1.15, 1.33

CCT = central corneal thickness; K_1 = flat keratometry; K_2 = steep keratometry; K_{avg} = average keratometry; K_{max} = maximum keratometry; Q value = asphericity of the anterior surface of the cornea; SE = spherical equivalent

Table 2. Preoperative and 12-month postoperative evaluated parameters.

Parameter	Mean \pm SD		P Value
	Preoperative	Postoperative	
UDVA	1.15 ± 0.41	0.54 ± 0.31	<.001
CDVA	0.26 ± 0.12	0.10 ± 0.10	<.001
Sphere (D)	-2.52 ± 2.81	-1.23 ± 2.56	.005
Cylinder (D)	-5.36 ± 1.72	-2.60 ± 1.19	<.001
SE (D)	-5.22 ± 2.96	-2.52 ± 2.83	<.001
K_1 (D)	45.49 ± 3.25	42.84 ± 3.47	<.001
K_2 (D)	51.05 ± 3.57	46.77 ± 4.03	<.001
Corneal astigmatism (D)	5.55 ± 2.29	3.92 ± 1.82	<.001
K_{avg} (D)	47.96 ± 3.32	44.91 ± 3.69	<.001
K_{max} (D)	58.53 ± 6.91	56.38 ± 6.38	.016
CCT (μ m)	482.40 ± 56.19	497.35 ± 54.57	.03
Q value	-0.29 ± 0.73	0.32 ± 0.59	<.001

CCT = central corneal thickness; CDVA = corrected distance visual acuity; K_1 = flat keratometry; K_2 = steep keratometry; K_{avg} = average keratometry; K_{max} = maximum keratometry; Q value = asphericity of anterior surface of cornea; SE = spherical equivalent; UDVA = uncorrected distance visual acuity

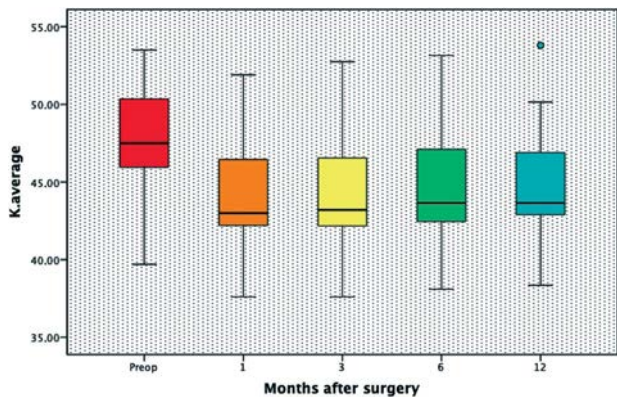


Figure 1. Average keratometry (K) before intrastromal corneal ring segment implantation and over the postoperative period.

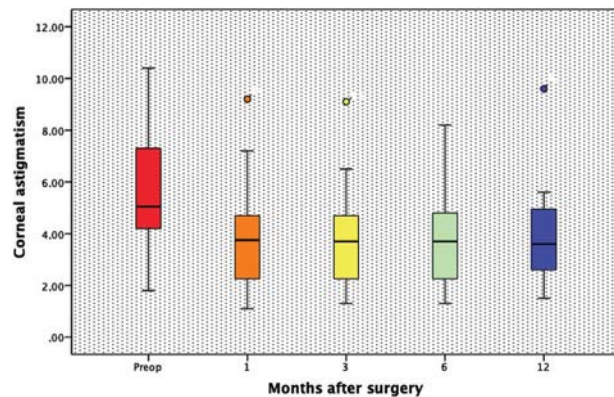


Figure 2. Corneal astigmatism before intrastromal corneal ring segment implantation and over the postoperative period.

Table 3. Distribution of the manifest refractive errors before and 12 months after ICRS implantation following the power vector method.

Parameter	Mean ± SD		P Value
	Preoperative	Postoperative	
M (D)	-5.22 ± 2.96	-2.52 ± 2.83	<.001
J ₀ (D)	0.34 ± 0.42	0.08 ± 0.23	.52
J ₄₅ (D)	-0.69 ± 2.02	0.07 ± 1.02	.15
B (D)	6.03 ± 2.72	3.40 ± 2.16	<.001

B = overall blurring strength; ICRS = intrastromal corneal ring segment; M = spherical equivalent of the given refractive error

maps before and after surgery of the only patient who lost 1 line of CDVA.

DISCUSSION

The purpose of ICRS implantation for visual rehabilitation after corneal transplantation is a sufficient reduction in myopia and astigmatism to allow for spectacle correction of the residual refractive error. Preliminary studies found ICRS implantation to be

an effective treatment for astigmatism and myopia.¹ A few recent studies reported the efficacy of ICRS implantation for astigmatism correction in eyes that previously underwent corneal keratoplasty.^{15,19-21}

We evaluated the 12-month visual acuity, refractive, and corneal topographic outcomes after ICRS implantation (340-degree arc length) in patients with astigmatism who had previous corneal keratoplasty. We observed a significant improvement and stability

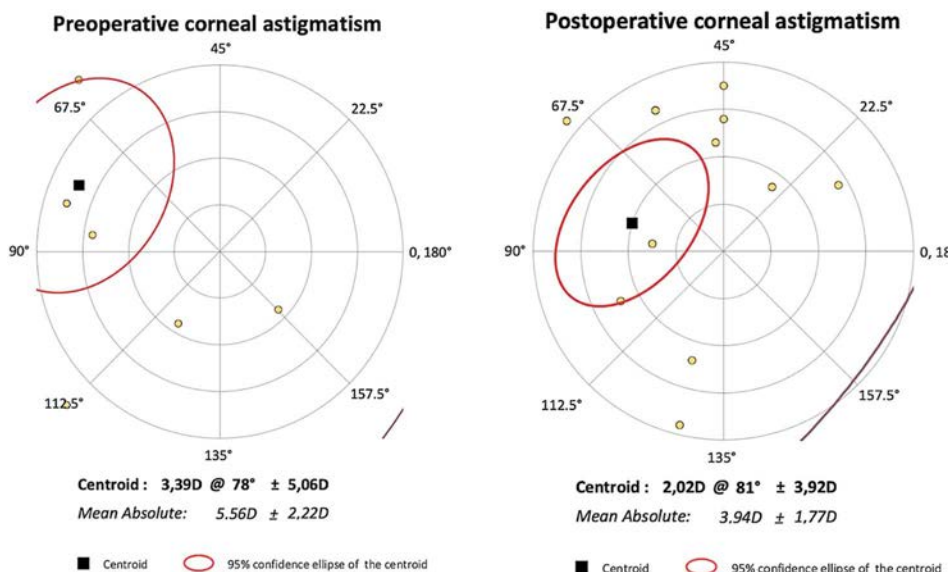


Figure 3. Double-angle plot of the preoperative and postoperative keratometric astigmatism at the corneal plane.

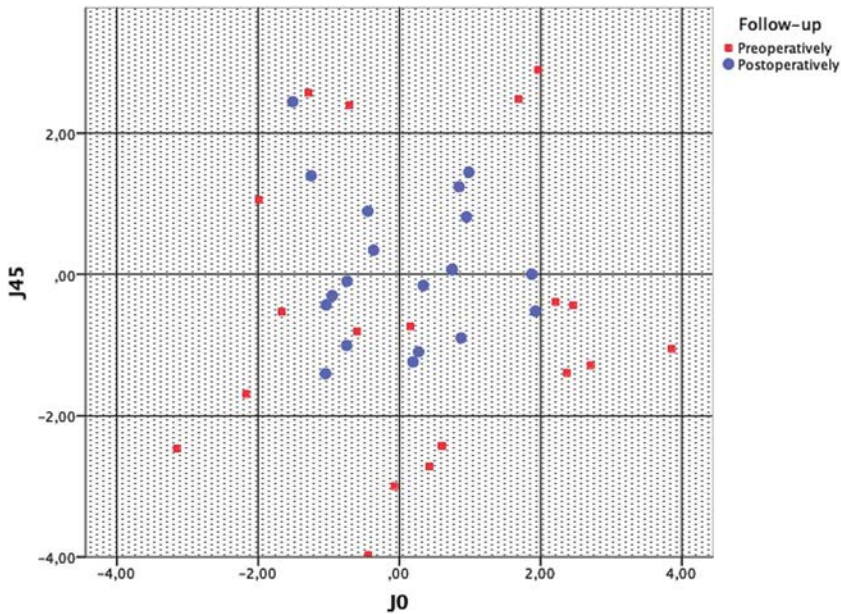


Figure 4. Astigmatic power vector (J_0 and J_{45}) before and 12 months after intrastromal corneal ring segment implantation.

in almost all variables measured during the follow-up period. To our knowledge, this is the first study to report the results of using the 340-degree arc length ICRS in the treatment of postkeratoplasty patients.

These initial clinical results with the 340-degree arc length ICRS indicate a significant improvement in UDVA and CDVA compared with preoperative values. The percentage of eyes with a CDVA of 0.3 logMAR

(20/40) or better increased from 75% preoperatively to 95% 12 months postoperatively. Lisa et al.¹⁵ conducted a prospective study in which 32 eyes of 30 patients with previous PKP had ICRS implantation and were followed for 6 months. By 6 months postoperatively, the CDVA was better than 20/40 in 96.9% of eyes. In a study by Coscarelli et al.,¹⁹ the percentage of eyes with a CDVA of 0.3 logMAR or better increased from 32.2%

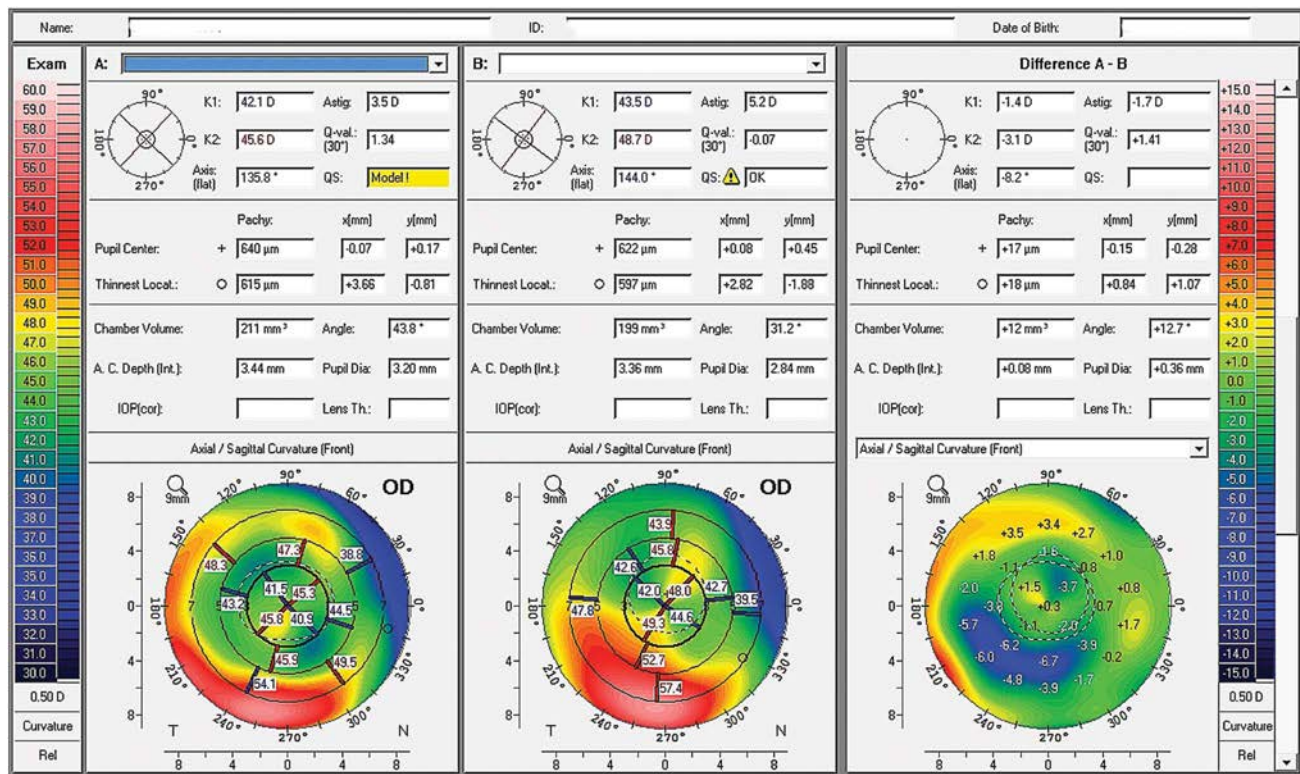


Figure 5. Comparison of corneal tomography of the right eye before and after femtosecond-assisted implantation of an intrastromal corneal ring segment with a 340-degree arc length in a postkeratoplasty patient.

Table 4. Preoperative and 12-month postoperative evaluated parameters by type of keratoplasty.

Parameter	Mean \pm SD		P Value
	Preoperative	Postoperative	
UDVA			
PKP (6 eyes)	1.25 \pm 0.29	0.76 \pm 0.38	.31
DALK (12 eyes)	1.15 \pm 0.48	0.45 \pm 0.24	.10
CDVA			
PKP	0.33 \pm 0.10	0.17 \pm 0.11	.13
DALK	0.22 \pm 0.12	0.06 \pm 0.07	.06
Refractive sphere (D)			
PKP	-2.33 \pm 2.78	-2.04 \pm 2.90	.96
DALK	-3.04 \pm 2.92	-0.89 \pm 2.43	.31
Refractive cylinder (D)			
PKP	-5.83 \pm 1.21	-3.50 \pm 1.26	.49
DALK	-4.93 \pm 1.87	-2.21 \pm 0.96	.06
SE (D)			
PKP	-5.25 \pm 2.92	-3.58 \pm 3.17	.90
DALK	-5.54 \pm 3.14	-2.07 \pm 2.67	.35
K ₁ (D)			
PKP	43.88 \pm 4.44	42.06 \pm 5.08	.17
DALK	45.95 \pm 2.28	43.15 \pm 2.60	.23
K ₂ (D)			
PKP	49.97 \pm 4.56	45.83 \pm 5.40	.31
DALK	51.27 \pm 3.19	47.15 \pm 3.42	.24
Corneal astigmatism (D)			
PKP	6.08 \pm 1.85	3.75 \pm 1.44	.54
DALK	5.39 \pm 2.58	4.00 \pm 2.01	.90
K _{avg} (D)			
PKP	46.45 \pm 4.57	43.95 \pm 5.33	.31
DALK	48.38 \pm 2.51	45.11 \pm 2.86	.24
K _{max} (D)			
PKP	59.35 \pm 8.95	56.30 \pm 6.74	.84
DALK	56.78 \pm 4.64	56.42 \pm 6.48	.96
CCT (μ m)			
PKP	469.20 \pm 49.30	485.16 \pm 74.32	.96
DALK	486.00 \pm 57.56	502.57 \pm 46.15	.84
Q value			
PKP	-0.36 \pm 0.92	0.51 \pm 0.53	.82
DALK	-0.59 \pm 0.62	0.23 \pm 0.61	.39

CCT = central corneal thickness; CDVA = corrected distance visual acuity; DALK = deep anterior lamellar keratoplasty; K₁ = flat keratometry; K₂ = steep keratometry; K_{avg} = average keratometry; K_{max} = maximum keratometry; PK = penetrating keratoplasty; Q value = asphericity of anterior surface of cornea; SE = spherical equivalent; UDVA = uncorrected distance visual acuity

preoperatively to 79.7% after ICRS implantation. Prazeres et al.¹⁴ described the outcomes of 14 eyes of 14 patients with high astigmatism after PKP. The percentage of eyes with a CDVA of 0.3 logMAR or better increased from 7.14% preoperatively to 50% postoperatively.

In our study, 7 eyes (35%) gained 1 line of CDVA, and 10 eyes (50%) gained 2 or more lines of CDVA. Only 1 eye (5%) lost 1 line of CDVA. Our findings are in agreement with the results in other studies.^{14,15,19-21} Arantes et al.²¹ found similar results. In their study, 9 eyes (36%) gained 1 line of CDVA and 9 eyes (36%) gained 2 or more lines; no eye lost lines of CDVA. Prazeres et al.¹⁴ reported that all eyes gained at least 1 line of CDVA at 6 months postoperatively, and Coscarelli et al.¹⁹ reported a gain of at least 1 line of CDVA in 72.8% of the cases.

Most published studies of the use of ICRS to treat astigmatism after corneal keratoplasty found a significant change in the topographic pattern with a reduction in the K values.^{14,15,19} In our study, the decreases in K₁, K₂, K_{avg}, K_{max}, and corneal astigmatism from preoperatively to postoperatively were statistically significant. However, when we transformed each refraction from the conventional sphere, cylinder, and axis format into the 3-dimensional vector space (*M*, *J*₀, and *J*₄₅), where the 3 components were orthogonal, the astigmatism component of the power vector did not reach statistical significance. Arriola-Villalobos et al.²⁰ also found that the decrease in refractive astigmatism did not reach statistical significance. One possible explanation is the small sample size presented in both studies. In contrast, Lisa et al.¹⁵ and Prazeres et al.¹⁴

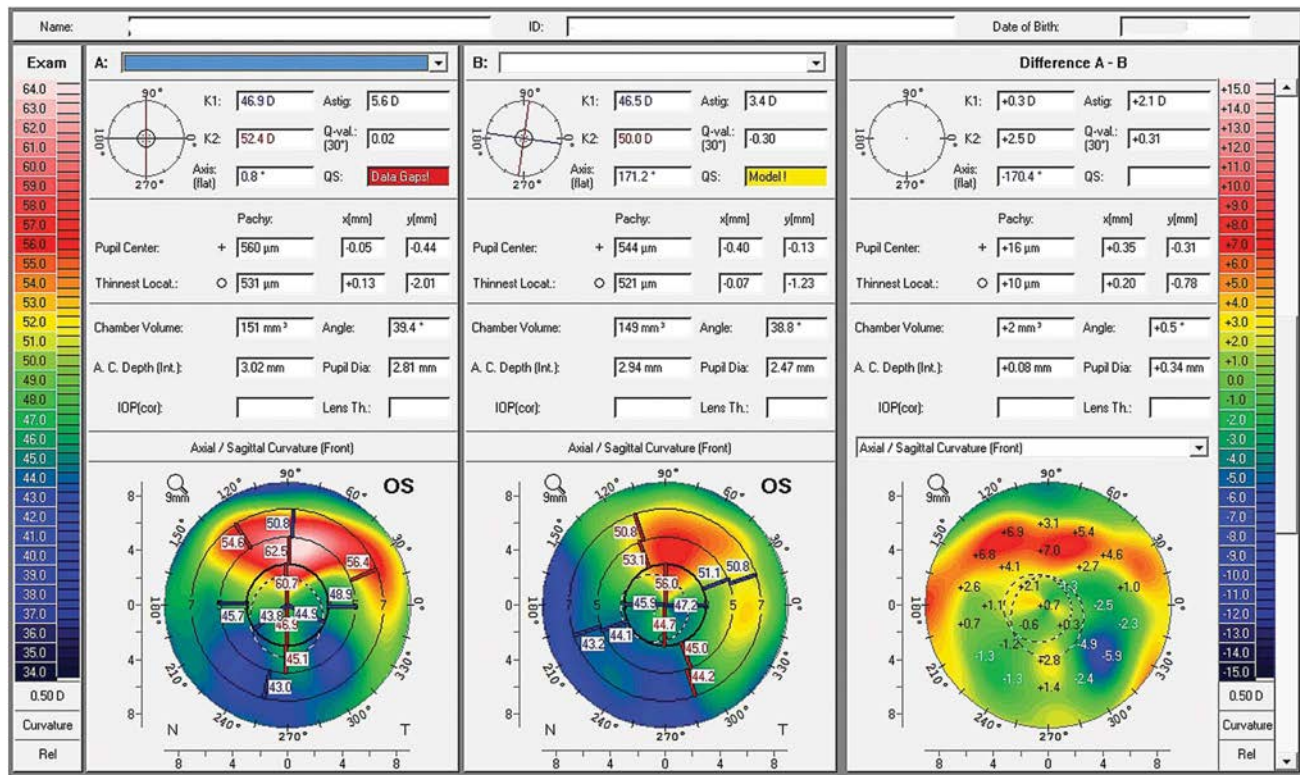


Figure 6. Comparison of corneal tomography of the left eye before and after femtosecond-assisted implantation of an intrastromal corneal ring with a 340-degree arc length in a postkeratoplasty patient; in this case, the patient lost 1 line of corrected distance visual acuity.

found a significant reduction in refractive cylinder after femtosecond laser-assisted ICRS implantation, although the last author did not consider astigmatism as a vector.

Our study has limitations. First, is the small sample. Further analysis should include more patients and possibly elucidate the real benefit of this surgery in correcting astigmatism in eyes with previous corneal transplantation. Second, we included both eyes of some patients because of the small sample, which is not ideal. However, we adjusted for dependence using repeated-measures analysis of variance to account for the potentially correlated errors. Third, we included a range of different types of corneal astigmatism (regular, irregular, asymmetric, and oblique), which makes analysis and generalization more difficult. Last, despite the prospective study design, data were collected for 12 months only. Long-term follow-up is essential to establish whether the effect of ICRS remains stable over time. The strengths of our study are that only one observer took postoperative measurements, all surgeries were performed by the same surgeon with the same technique, and the variety of corneal topographies observed in this study is representative of what is seen in clinical practice.

In conclusion, we found that the visual acuity and the refractive results improved by the implantation of a 340-degree arc length ICRS using the femtosecond laser in patients who had previous corneal transplantation.

WHAT WAS KNOWN

- Implantation of an intrastromal corneal ring segment (ICRS) can improve corneal topography and favorably modify the corneal sphere and cylinder in keratoconic and postkeratoplasty eyes.
- One study evaluated the short-term outcomes of a 340-degree arc length ICRS in patients with keratoconus; however, there have been no studies of 340-degree arc length ICRS in patients who previously underwent corneal keratoplasty.

WHAT THIS PAPER ADDS

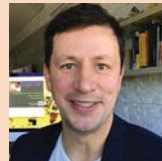
- The new ICRS with a 340-degree arc length was effective in the management of postkeratoplasty eyes with improvement in topographic and refractive parameters.

REFERENCES

1. Perlman EM. An analysis and interpretation of refractive errors after penetrating keratoplasty. *Ophthalmology* 1981;88:39–45
2. Binder PS. The effect of suture removal on postkeratoplasty astigmatism. *Am J Ophthalmol* 1988;105:637–645
3. Assil KK, Zarnegar SF, Schanzlin DJ. Visual outcome after penetrating keratoplasty with double continuous or combined interrupted and continuous suture wound closure. *Am J Ophthalmol* 1992;114: 63–71
4. Webber SK, Lawless MA, Sutton GL, Rogers CM. LASIK for post penetrating keratoplasty astigmatism and myopia. *Br J Ophthalmol* 1999;83: 1013–1018
5. Donnenfeld ED, Kornstein HS, Amin A, Speaker MD, Seedor JA, Sforza PD, Landrio LM, Perry HD. Laser in situ keratomileusis for correction of myopia and astigmatism after penetrating keratoplasty. *Ophthalmology* 1999;106: 1966–1974

6. Speaker MG, Cohen EJ, Edelhauser HF, Clemons CS, Arentsen JJ, Laibson PR, Raskin EM. Effect of gas-permeable contact lenses on the endothelium of corneal transplants. *Arch Ophthalmol* 1991;109:1703–1706
7. Lopatynsky MO, Cohen EJ. Post-keratoplasty fitting for visual rehabilitation. In: Kastl PR, ed. *Contact Lenses: the CLAO Guide to Basic Science and Clinical Practice*. Dubuque, IA: Kendall/Hunt Pub. Co., 1995; 79–90
8. Hoffart L, Touzeau O, Borderie V, Laroche L. Mechanized astigmatic arcuate keratotomy with the Hanna arcitome for astigmatism after keratoplasty. *J Cataract Refract Surg* 2007;33:862–868
9. Kymiosis GD, Yoo SH, Ide T, Culbertson WW. Femtosecond-assisted astigmatic keratotomy for post-keratoplasty irregular astigmatism. *J Cataract Refract Surg* 2009;35:11–13
10. Feizi S, Javadi MA. Corneal graft curvature change after relaxing incisions for post-penetrating keratoplasty astigmatism. *Cornea* 2012;31:1023–1027
11. Ezra DG, Hay-Smith G, Mearza A, Falcon MG. Corneal wedge excision in the treatment of high astigmatism after penetrating keratoplasty. *Cornea* 2007;26:819–825
12. Chang DH, Hardten DR. Refractive surgery after corneal transplantation. *Curr Opin Ophthalmol* 2005;16:251–255
13. Szentmáry N, Seitz B, Langenbucher A, Naumann GO. Repeat keratoplasty for correction of high or irregular postkeratoplasty astigmatism in clear corneal grafts. *Am J Ophthalmol* 2005;139:826–830
14. Prazeres TMB, Souza ACL, Pereira NC, Ursulino F, Grubenmacher L, Souza LB. Intrastromal corneal ring segment implantation by femtosecond laser for the correction of residual astigmatism after penetrating keratoplasty. *Cornea* 2011;30:1293–1297
15. Lisa C, García-Fernández M, Madrid-Costa D, Torquetti L, Merayo-Llodes J, Alfonso JF. Femtosecond laser-assisted intrastromal corneal ring segment implantation for high astigmatism correction after penetrating keratoplasty. *J Cataract Refract Surg* 2013;39:1160–1167
16. Torquetti L, Cunha P, Luz A, Kwitko S, Carrion M, Rocha G, Signorelli A, Coscarelli S, Ferrara G, Bicalho F, Neves R, Ferrara P. Clinical outcomes after implantation of 320°-arc length intrastromal corneal ring segments in keratoconus. *Cornea* 2018;37:1299–1305
17. Rocha GADN, Ferrara de Almeida Cunha P, Torquetti Costa L, Barbosa de Sousa L. Outcomes of a 320-degree intrastromal corneal ring segment implantation for keratoconus: results of a 6-month follow-up. *Eur J Ophthalmol* 2018 [epub ahead of print]
18. Thibos LN, Horner D. Power vector analysis of the optical outcome of refractive surgery. *J Cataract Refract Surg* 2001;27:80–85
19. Coscarelli S, Ferrara G, Alfonso JF, Ferrara P, Merayo-Llodes J, Araújo LP, Machado AP, Lyra JM, Torquetti L. Intrastromal corneal ring segment implantation to correct astigmatism after penetrating keratoplasty. *J Cataract Refract Surg* 2012;38:1006–1013
20. Arriola-Villalobos P, Díaz-Valle D, Güell JL, Iradier-Urrutia MT, Jiménez-Alfaro I, Cuina-Sardiña R, Benítez-del-Castillo JM. Intrastromal corneal ring segment implantation for high astigmatism after penetrating keratoplasty. *J Cataract Refract Surg* 2009;35:1878–1884
21. Arantes JCD, Coscarelli S, Ferrara P, Araújo LPN, Ávila M, Torquetti L. Intrastromal corneal ring segment for astigmatism correction after deep anterior lamellar keratoplasty. *J Ophthalmol* 2017;2017:8689017

Disclosures: None of the authors has a financial or proprietary interest in any material or method mentioned.



First author:

Patrick F. Tzelikis, MD, PhD

Department of Ophthalmology, Hospital Oftalmológico de Brasília–HOB, Brasília, DF, Brazil

Repeatability and reproducibility of corneal deformation response parameters of dynamic ultra-high-speed Scheimpflug imaging in keratoconus

Robert Herber, MSc, Riccardo Vinciguerra, MD, Bernardo Lopes, MD, PhD, Frederik Raiskup, MD, PhD, Lutz E. Pillunat, MD, Paolo Vinciguerra, MD, Renato Ambrósio Jr, MD, PhD

Purpose: To assess the repeatability and reproducibility of dynamic corneal response (DCR) parameters obtained by ultra-high-speed Scheimpflug imaging (Corvis ST); in keratoconic patients.

Setting: Clinics in Germany, Italy, and Brazil.

Design: Prospective, observational study.

Methods: Patients were examined 3 times using 2 different dynamic Scheimpflug analyzers (Corvis ST) to obtain repeatability and reproducibility. The reliability of intraocular pressure (IOP), biomechanically corrected IOP (bIOP), pachymetry, and DCR parameters were assessed by the coefficient of repeatability, coefficient of variation (CoV), intraclass correlation coefficient (ICC), and within-subject standard deviation (s_w).

Results: Ninety-eight eyes from 98 KC patients were included. The s_w of the IOP and bIOP did not exceed 1.1 mm

Hg. A CoV less than 10% was found in all DCR parameters and had a good to excellent accordance regarding the ICC. The Corvis Biomechanical Index showed an excellent repeatability and interdevice reproducibility of 0.918 and 0.827, respectively. Also, the tomographic biomechanical index showed an excellent repeatability of 3 Corvis ST and Pentacam measurements (ICC = 0.997). With regard to keratoconic severity, a significant increase in the CoV was found between mild and moderate stages compared with the advanced stage. Nevertheless, it did not exceed 10% of the CoV in severe keratoconic eyes.

Conclusion: Corvis ST measurements in keratoconic eyes were highly repeatable and reproducible.

J Cataract Refract Surg 2020; 46:86–94 Copyright © 2019 Published by Wolters Kluwer on behalf of ASCRS and ESCRS

In vivo corneal biomechanical assessment has gained increased importance in recent years. The most common applications are in refractive surgery,^{1,2} the early diagnosis of keratoconus,^{3,4} and the compensation of intraocular pressure (IOP) measurements.^{5,6}

The commercially available devices to measure corneal biomechanics (ie, the Ocular Response Analyzer⁷ [ORA] Reichert Ocular Instruments); Corvis ST dynamic Scheimpflug analyzer (Oculus Optikgeräte GmbH) are based on noncontact tonometry techniques. The newer Corvis ST version includes dynamic corneal response (DCR) parameters and the Corvis Biomechanical Index (CBI), which are known to facilitate discrimination

between normal eyes and keratoconic eyes,^{3,8} even in a subclinical stage.⁴

Subsequently, ectasia screening improved by combining biomechanical measurements with topographic and tomographic data.⁹ Recently, it was shown that the DCR parameters provided by Corvis ST can detect significant changes after corneal crosslinking (CXL).¹⁰ Nevertheless, for diagnosis and more important for follow-up purposes, the reliability of these measurements is of foremost importance, and its evaluation is carried out by analyzing repeatability and reproducibility. Repeatability indicates the accuracy of measurements on the same subject within a short period of time without changing external influencing

Submitted: February 27, 2019 | Final revision submitted: July 18, 2019 | Accepted: August 8, 2019

From the Department of Ophthalmology (Herber, Raiskup, Pillunat), University Hospital Carl Gustav Carus, TU Dresden, Germany; Humanitas San Pio X Hospital (R. Vinciguerra), Milan, Italy; School of Engineering (R. Vinciguerra, Lopes), University of Liverpool, United Kingdom; Rio de Janeiro Corneal Tomography and Biomechanics Study Group (Lopes, Ambrósio) and the Departments of Ophthalmology, Federal University of São Paulo (Lopes, Ambrósio), and Federal University of the State of Rio de Janeiro (Ambrósio), Brazil; Humanitas Clinical and Research (P. Vinciguerra), Rozzano, and Humanitas University (P. Vinciguerra), Department of Biomedical Sciences, Milan, Italy.

R. Herber and R. Vinciguerra contributed equally to this work.

Corresponding author: Robert Herber, MSc, Department of Ophthalmology, University Hospital Carl Gustav Carus, TU Dresden, Fetscherstraße 74, 01307 Dresden, Germany. Email: robert.herber@uniklinikum-dresden.de.

factors.¹¹ Similarly, the definition of reproducibility is similar to repeatability, with the difference that external factors are changeable, such as time or observer.^{11,12} The repeatability and reproducibility describe how reliable the measurements of the devices are.¹²

A study by Lopes et al.¹³ evaluated the reliability of the new DCR parameters of the Corvis ST that were introduced with the latest software release (1.3r1469 and later) in normal patients; however, given the irregularity of keratoconic corneas, the repeatability and reproducibility in this cohort of patients are expected to be worse. Conversely, the reliability of old DCR parameters (release1.00r28) was observed in several studies of keratoconic and glaucoma eyes.^{14,15}

The aim of the current study was to evaluate the repeatability and reproducibility of the new DCR parameters in keratoconic patients in the multicenter study.

METHODS

This prospective multicenter observational study included keratoconic patients enrolled at the Department of Ophthalmology, University Hospital Carl Gustav Carus, TU Dresden, Germany; Humanitas Clinical and Research, Rozzano, Italy; Rio de Janeiro Corneal Tomography and Biomechanics Study Group, Brazil; and Department of Ophthalmology, Federal University of São Paulo, Brazil, between January 2017 and January 2019.

The study protocol was approved by the ethics committee of the particular study sites following the tenets of the Declaration of Helsinki. Inclusion criteria were diagnosis of keratoconic and age younger than 18 years. Exclusion criteria were pellucid marginal corneal degeneration, undefined corneal ectasia, other ocular diseases, previous intraocular surgeries, and CXL procedures. The assessment of keratoconic was supported by topographic and tomographic data (maximum keratometry [Kmax], thinnest corneal thickness, and Belin/Ambrósio total deviation value⁹), as well as the topographic keratoconus classification (TKC) from the Pentacam Scheimpflug system (Oculus Optikgeräte GmbH, software version v1.21r33)¹⁶ and comprehensive eye examination. The diagnosis of keratoconic was approved by an experienced clinician (F.R., R.V., P.V., or R.A.).

Repeatability and Reproducibility

Each eye was examined 3 times by experienced technicians or physicians to determine the intraobserver repeatability. Between the measurements, a break of 1 to 2 minutes was taken to allow the cornea to recover from the air puff. To assess the interdevice reproducibility, a subgroup of 20 patients was analyzed separately. The measurements were performed using 2 different devices with identical technical features. The first session of measurements was taken between 9:00 AM to 10:00 AM and the second session between 11:00 AM and noon. This period between each session provides optimal starting conditions (eg, IOP and central corneal thickness) for the next measurement and eliminated measurement bias.^{17–19}

Corneal DCR Parameters Provided by the Scheimpflug Analyzer

The Corvis ST allows measures the response of the cornea induced by a calibrated air puff. Through a piston, the air puff induces a corneal deformation process, which is recorded in 2 dimensions by an ultra-high-speed Scheimpflug camera.^{20–22} The patient's head is positioned in a forehead and chin rest. The Corvis ST is movable in the *x*-, *y*-, and *z*-axes to align it in front of the eye while the patient is focusing the red light. The instrument automatically releases the air puff, when the Purkinje

reflex of the anterior corneal surface of the patient's eye is correctly adjusted.²³

All DCR parameters are derived from the different phases of corneal deformation. The first is the ongoing phase, which forces the cornea inward through the first applanation (A1), which is followed by a concavity phase until it reaches the highest concavity. Afterward, the cornea shows a second applanation (outward applanation) before going back to its natural shape.

In the first version of the Corvis ST software (1.00r28), the DCR parameters produced were IOP, central corneal thickness, time and velocity at the first (A1) and second (A2) applanation, and deformation amplitude (DA). These parameters are well described in several studies.^{3,21,22,24,25}

In the latest release of the software new DCR parameters were introduced⁶ together with a new IOP estimate (biomechanically corrected IOP [bIOP]). It is based on the numerical model, and it was proved to be less affected by age, corneal thickness, and main corneal stiffness parameters.^{5,6,26} The inverse integrated radius is the integrated sum of the reciprocal of the radius between the first and second applanation events.⁶

The deformation amplitude at 1.0 mm and 2.0 mm (DA_{ratio}) measures the ratio between the central deformation and the average of peripheral deformation determined at 1.0 mm and 2.0 mm zones.⁵ Furthermore, 2 parameters were introduced, aimed to estimate out of the plane corneal stiffness, stiffness parameter at applanation 1 (SPA1) is defined as the resultant pressure (adjusted pressure at A1 minus bIOP) divided by the deflection amplitude at applanation 1.⁸ Furthermore, a new combined parameter (Corvis Biomechanical Index [CBI]) to differentiate healthy eyes from keratoconic eyes was recently developed; it was shown to have high sensitivity and to distinguish between healthy eyes and keratoconic eyes even at a subclinical stage.^{3,4,27} Finally, Ambrósio et al.⁹ began to integrate tomographic data from Scheimpflug-based topography and tomography to the biomechanical measurements using artificial intelligence. The tomographic and biomechanical index (TBI) is the result of combined DCR parameters and tomographic data calculated by the machine learning algorithm when both datasets are available in the software.^{9,28}

Statistical Analysis

The data were collected using Excel 2016 software (Microsoft Corp.) and analyzed using IBM SPSS Statistics for Windows software (version 25.0, IBM Corp.) and *R* statistics (R Foundation for Statistical Computing).

Repeatability (intraobserver) and reproducibility (interdevice) were determined by the analysis of variance model based on 3 consecutive measurements of the same patient's eye. In particular, reproducibility was derived from the following 3 factors: random subject, random device, and random interactions between the subject and device. This analysis was based on the Gage R&R procedure (gauge repeatability and reproducibility) that quantifies the repeatability and reproducibility of the measurement system in a random way.

Different statistical coefficients are used to describe the reliability. The coefficient of repeatability (CoR) indicates the reliability of short consecutive measurements from the same subject without changing external factors (eg, observer, device, and the time of day) and is calculated from the within-subject standard deviation (*s_w*). The result of the CoR is represented in the same unit of the measuring device.²⁹

$$\text{CoR} = \sqrt{2} \times 1.96 \times s_w = 2.77 \times s_w$$

The coefficient of variation (CoV) represents the measurement error in percentage.¹¹ The variance is standardized, which allows for comparisons between different units. A CoV value less than 20% are considered highly repeatable, whereas values above 20% are considered acceptable.³⁰ The statistical significance of the

CoV was proved by the Levene test, which examines the differences in variances of 2 or more groups. A *P* value less than 0.05 was considered significant.

$$\text{CoV}[\%] = 100 \times \text{standard deviation}/\text{mean}$$

Quantifying the accordance of measurements was performed with the intraclass correlation coefficient (ICC) using SPSS. Intraclass correlation coefficient values less than 0.4, between 0.41 and 0.6, between 0.61 and 0.8, and greater than 0.8 show poor, moderate, good, and excellent accordance, respectively.³¹

Repeatability was also evaluated with regard to the keratoconic stage. Furthermore, patients were divided into 3 groups based on the TKC Pentacam classification as follows: Group 1 (KC1) included TKC 1 and 1 to 2, Group 2 (KC2) included TKC 2 and 2 to 3, and Group 3 (KC3) included TKC 3 and 3 to 4.

In addition, the dependency of the *z*-alignment was evaluated by creating 2 subgroups. Group 1 included all cases that had an alignment error of less than +0.5 mm, whereas Group 2 included cases with an error of greater than +0.5 mm.

RESULTS

Demographics

The study evaluated 98 eyes of 98 patients. The mean age of the 75 (66%) men and 33 (34%) women was 34.8 years (SD) ± 11.8 years. Fifty-three right eyes (54%) and 45 left eyes (46%) were examined. The entire cohort had a mean

bIOP, thinnest corneal thickness, K_{max} , and Belin/Ambrósio total deviation value of 14.2 ± 1.9 mm Hg, 481 ± 41 μm, 53.3 ± 5.1 D, and 6.6 ± 3.3 , respectively. In Table 1 shows the demographic data and keratoconic severity classification with regard to the clinic. Except for the inhomogeneous distribution of sex, selected eyes, and the classification of keratoconic, the other demographic parameters describing the condition of keratoconic were not significantly different between the cohorts of the clinics.

Repeatability

Table 2 shows the repeatability in the entire cohort. There was an excellent accordance (ICC > 0.8) for uncorrected IOP (CVS-IOP), pachymetry, deflection amplitude, DA_{ratio} (2.0 mm/1.0 mm), Ambrósio's relational thickness (ARTh), SPA1, integrated radius, and CBI. Biomechanically corrected IOP showed good accordance (ICC 0.6 to 0.8) and was close to the other DCR parameters. A CoV less than 10% was found for all DCR parameters. In particular, pachymetry, deflection amplitude, DA_{ratio} (2.0 mm/1.0 mm), ARTh, and integrated radius were highly reliable (CoV < 5%). The SD (s_w) of the IOP and bIOP did not exceed 1.0 mm Hg, and the CoR was 2.77 mm Hg for the IOP and 2.6 mm Hg for the bIOP. Dynamic corneal response parameters with higher

Table 1. Patient demographics overall and by clinic.

Parameter	Overall	Clinic			P Value		
		Dresden	Milan	Rio	Dresden–Milan	Dresden–Rio	Milan–Rio
Age (y)							
Mean ± SD	34.8 ± 11.8	36.3 ± 10.1	34.8 ± 13.5	32.7 ± 13.8	1.0	.170	1.0
Range	—	18, 60	18, 55	18, 60			
Sex, n (%)							
Male	65 (66)	46 (71)	8 (12)	11 (17)	.173*	.173*	.173*
Female	33 (34)	18 (55)	4 (12)	11 (33)			
Eye, n (%)							
Right	53 (54)	40 (75)	3 (6)	10 (19)	.037*†	.037*†	.037*†
Left	45 (46)	24 (53)	9 (20)	12 (27)			
bIOP (mm Hg)							
Mean ± SD	14.2 ± 1.9	13.9 ± 1.8	15.0 ± 2.6	14.7 ± 1.8	.223	.224	1.0
Range	—	9.7, 18.8	11.5, 21.1	11.7, 18.3			
TCT (Pentacam) (μm)							
Mean ± SD	481 ± 41	477 ± 44	482 ± 37	493 ± 30.6	1.0	.363	1.0
Range	—	311, 580	411, 547	432, 552			
Kmax (D)							
Mean ± SD	53.3 ± 5.1	54.2 ± 5.0	52.1 ± 5.5	51.3 ± 4.5	.520	.064	1.0
Range	—	44.9, 65.9	45.7, 64.1	46.3, 59.2			
BAD D							
Mean ± SD	6.6 ± 3.3	7.0 ± 3.6	6.6 ± 3.3	5.5 ± 2.1	1.0	.233	1.0
Range	—	0.6, 21.0	1.1, 13.8	2.0, 9.8			
Keratoconus, n (%)							
Stage 1	23	9 (39)	4 (18)	10 (44)	.028*†	.028*†	.028*†
Stage 2	41	31 (76)	3 (7)	7 (17)			
Stage 3	22	17 (77)	4 (18)	1 (5)			

BAD D = Belin/Ambrósio deviation total value; bIOP = biomechanically corrected intraocular pressure; Kmax = maximum keratometry; TCT = thinnest corneal thickness

*Significant tested using χ^2 test.

†Statistically significant (χ^2 test).

Table 2. Repeatability of all included patients.

Parameter	Mean ± SD	Range	s _w	CoR	CoV (%)	ICC	CI (ICC)	
CVS-IOP (mm Hg)	13.28 ± 2.28	7, 22.5	0.989	2.739	6.638	0.814	0.75	0.866
Pachymetry (µm)	496.67 ± 38.4	327, 589	5.311	14.713	0.717	0.981	0.974	0.987
Deflection amp. max (mm)	1.02 ± 0.11	0.721, 1.349	0.037	0.103	3.246	0.887	0.846	0.919
DA _{ratio} max (2.0 mm)	5.54 ± 0.96	3.925, 9.044	0.274	0.760	3.902	0.919	0.888	0.943
DA _{ratio} Max (1.0 mm)	1.69 ± 0.08	1.526, 1.967	0.028	0.077	1.339	0.866	0.819	0.903
ARTh	277.08 ± 130.65	42.6, 952.6	24.808	68.718	4.760	0.964	0.95	0.975
biOP (mm Hg)	14.23 ± 2.06	9.3, 23.5	0.937	2.594	5.765	0.794	0.725	0.851
Integrated radius (mm ⁻¹)	11.34 ± 2.05	6.663, 18.293	0.537	1.488	3.793	0.932	0.907	0.952
SPA1 (mm Hg/mm)	70.27 ± 18.1	24.09, 110.43	5.916	16.386	7.241	0.894	0.856	0.924
CBI	0.84 ± 0.32	0, 1	NA	NA	NA	0.918	0.887	0.942
TBI	0.92 ± 0.24	0, 1	NA	NA	NA	0.997	0.995	0.998

A1 = first applanation; Amp = amplitude; ARTh = Ambrósio’s relational thickness; biOP = biomechanically corrected intraocular pressure; CBI = Corvis Biomechanical Index; CI (ICC) = confidence interval (of interclass correlation coefficient); CoR = coefficient of repeatability; CoV = coefficient of variation; CVS = uncorrected; DA = deformation amplitude; ICC = interclass correlation coefficient; IOP = intraocular pressure; NA = not applicable; SPA1 = stiffness parameter at applanation 1; s_w = within-subject standard deviation; TBI = tomographic and biomechanical index

nominal values, such as pachymetry, ARTh, and SPA1, showed a higher CoR of 14.7 µm, 68.7, and 16.4 mm Hg/mm, respectively.

The repeatability of DCR parameters with regard to keratoconic severity is presented in Table 3 and Figure 1. As expected, the CoR and CoV were increased for CVS-IOP, biOP, DA_{ratio} (2.0 mm/1.0 mm), and integrated radius the higher the stage of keratoconic. The CoV was significantly higher for CVS-IOP and biOP between KC2 and KC3 (*P* < .001). For KC1 and KC3, the CoV was significantly increased for CVS-IOP, biOP, DA_{ratio} (2.0 mm), integrated radius, and SPA1 (all *P* < .05). However, they did not exceed 10% of the CoV in eyes with severe keratoconic.

Repeatability by the z-alignment is presented in Table 4. The CoR and CoV of DCR parameters were increased when one of the 3 measurements had an alignment error greater than +0.5 mm. The CoV of CVS-IOP, pachymetry, deflection amplitude, ARTh, biOP, and SPA1 was significantly higher in groups of alignment error greater than +0.5 mm with an alignment error less than +0.5 mm (all *P* < .05).

Reproducibility

Table 5 shows the reproducibility results in the TKC subgroups. Table 5. These patients were classified as TKC 2 (13 cases), TKC 1 (2 cases) and TKC 3 (5 cases). An excellent accordance was found for all DCR parameters

Table 3. Comparison of repeatability dependence of the severity of KC.

Parameter	KC1 (n = 23)		KC2 (n = 41)		KC3 (n = 22)		P Value of CoV		
	CoR	CoV (%)	CoR	CoV (%)	CoR	CoV (%)	KC1 – KC2	KC1 – KC3	KC2 – KC3
CVS-IOP (mm Hg)	2.21	5.25	2.38	5.79	3.13	8.17	.496	.001*	<.001*
Pachymetry (µm)	9.45	0.54	12.45	0.64	11.80	0.72	.281	.386	.922
Deflection amp. max (mm)	0.11	3.29	0.09	2.90	0.11	3.55	.302	.700	.127
DA _{ratio} max (2.0 mm)	0.49	2.88	0.72	3.84	1.12	5.81	.093	.006*	.059
DA _{ratio} max (1.0 mm)	0.06	1.07	0.08	1.33	0.09	1.70	.248	.288	.891
ARTh	50.70	4.04	41.08	4.24	56.44	5.07	.797	.404	.445
biOP (mm Hg)	2.13	4.61	2.24	5.09	2.99	6.77	.363	.001*	<.001*
Integrated radius (mm ⁻¹)	0.83	2.76	1.36	3.46	1.82	4.48	.152	.014*	.261
SPA1 (mm Hg/mm)	14.81	5.88	14.69	6.84	17.87	9.29	.443	.023*	.083

A1 = first applanation; Amp = amplitude; ARTh = Ambrósio’s relational thickness; biOP = biomechanically corrected intraocular pressure; CoR = coefficient of repeatability; CoV = coefficient of variation; CVS = uncorrected; DA = deformation amplitude; IOP = intraocular pressure; KC = keratoconus; Max = maximal; SPA1 = stiffness parameter at applanation 1

*Statistically significant (*P* < .05)

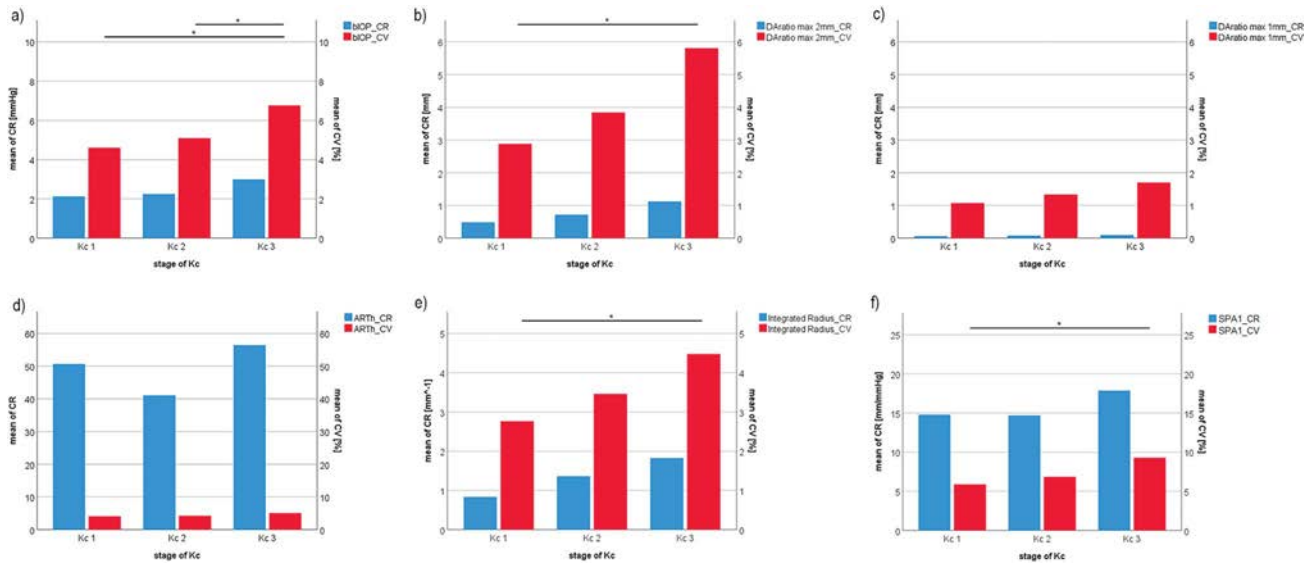


Figure 1. The CoR and CoV in dependence of the severity of KC: KC1 (n = 23), KC2 (n = 41), and KC3 (n = 22) including all cases with TKC 1 and 1 to 2, TKC 2 and 2 to 3, and TKC 3 and 3 to 4, respectively. Significance is marked with * ($P < .05$); (a) bIOP, (b) DA_{ratio} at 2.0 mm, (c) DA_{ratio} at 1.0 mm, (d) ARTh, (e) integrated radius, and (f) SPA1 (* = Statistically significant [$< .05$]; ARTh = Ambrósio’s relational thickness; bIOP = biomechanically corrected IOP; CoR = coefficient of repeatability; CoV = coefficient of variation; DA = deformation amplitude; IOP = intraocular pressure; KC = keratoconus; SPA1 = stiffness parameter at applanation 1; TKC = topographic keratoconus classification).

(ICC > 0.8) except bIOP, which was close to excellence (ICC = 0.791). The CoV was comparable to repeatability but showed overall slightly higher values (Table 5).

Also, the CoR of CVS-IOP, bIOP, deflection amplitude, DA_{ratio} (2.0 mm/1.0 mm), integrated radius, and SPA1 showed values similar as to the repeatability data.

Bland-Altman graphs of each first measurement showed that the 95% limits of agreements of the DA_{ratio} (2.0 mm), integrated radius, ARTh, and SPA1 ranged from -0.75 to 0.667 (-0.041) mm, -1.46 to 1.82 (0.18) mm^{-1} , -68.1 to 37.1 (-15.5) (unitless), -10.3 to 6.5 (-1.9) mmHg/mm, respectively (Figure 2).

Corvis Biomechanical Index and TBI

The CBI showed an excellent repeatability and inter-device reproducibility of 0.918 and 0.827, respectively. The mean SD of 3 measurements for the CBI classified

into 3 subgroups (CBI < 0.5, CBI 0.5 to 0.9, and CBI > 0.9) was 0.09, 0.15, and 0.015, respectively (Figure 3). Also, the TBI showed excellent repeatability of 3 Corvis ST and Pentacam measurements (ICC = 0.997) in a subgroup of 36 cases. In Figure 4, SDs are plotted as datapoints for the TBI less than 0.5 and TBI greater than 0.5. The majority in this subgroup had a TBI of 1.0 (mean SD = 0.0001). Only one case showed a TBI of less than 0.5.

DISCUSSION

The Corvis ST dynamic Scheimpflug analyzer was shown as useful in examining in vivo biomechanics in human corneas.^{8,10,14,15,24,32} However, to be useful in clinical practice, an instrument needs to provide valuable information and be highly reliable, particularly if it aims to show changes over time, such as in CXL. There are several reasons repeatability is

Parameter	z-Alignment <0.5 mm (n = 85)		z-Alignment >0.5 mm (n = 13)		P Value of CoV
	CoR	CoV (%)	CoR	CoV (%)	
CVS-IOP (mm Hg)	2.60	6.31	3.51	8.79	<.001*
Pachymetry (µm)	13.13	0.61	22.46	1.40	.011*
Deflection amp. max (mm)	0.10	3.10	0.14	4.20	.022*
DA_{ratio} max (2.0 mm)	0.74	3.76	0.90	4.83	.409
DA_{ratio} max (1.0 mm)	0.08	1.31	0.09	1.56	.733
ARTh	65.84	4.41	85.20	7.05	.004*
bIOP (mm Hg)	2.47	5.49	3.29	7.58	.002*
Integrated radius (mm^{-1})	1.38	3.56	2.08	5.33	.663
SPA1 (mm Hg/mm)	14.88	6.73	24.03	10.61	<.001*

A1 = first applanation; Amp = amplitude; ARTh = Ambrósio’s relational thickness; bIOP = biomechanically corrected intraocular pressure; CoR = coefficient of repeatability; CoV = coefficient of variation; CVS = uncorrected; DA = deformation amplitude; IOP = intraocular pressure; SPA1 = stiffness parameter at applanation 1

*Statistically significant ($P < .05$ Levene test)

Table 5. Interdevice reproducibility in the TKC subgroup (n = 20).

Parameter	Mean	s_w	CoR	CoV (%)	ICC	CI (ICC)	
CVS-IOP (mm Hg)	13.042	1.08	2.99	8.277	0.852	0.635	0.941
Pachymetry (μm)	489.525	8.198	22.708	1.675	0.982	0.91	0.994
Deflection amp. max (mm)	1.014	0.073	0.202	3.56	0.946	0.795	0.982
DA _{ratio} max (2.0 mm)	5.813	0.321	0.89	5.528	0.971	0.928	0.989
DA _{ratio} max (1.0 mm)	1.713	0.035	0.097	2.034	0.874	0.687	0.95
ARTh	241.031	25.089	69.500	10.409	0.969	0.899	0.989
bIOP (mm Hg)	14.098	0.997	2.763	7.075	0.791	0.485	0.916
Integrated radius (mm^{-1})	11.977	0.668	1.85	5.576	0.936	0.842	0.975
SPA1 (mm Hg/mm)	70.926	6.46	17.895	9.109	0.98	0.946	0.992
CBI	NA	NA	NA	NA	0.827	0.563	0.932

A1 = first applanation; Amp = amplitude; ARTh = Ambrósio’s relational thickness; bIOP = biomechanically corrected intraocular pressure; CBI = Corvis Biomechanical Index; CoR = coefficient of repeatability; CoV = coefficient of variation; CVS = uncorrected; DA = deformation amplitude; ICC = intraclass correlation coefficient; IOP = intraocular pressure; NA = not applicable; SPA1 = stiffness parameter at applanation 1; s_w = within-subject standard deviation; TKS = topographic keratoconus classification

low in keratoconic patients than in normal patients, namely shape abnormalities, difficulty in obtaining automated release of the air puff due to the change in keratometric reflexes that trigger the release, and fixation and centration that is not stable due to the irregular cornea.³³

To our knowledge, no study has evaluated the repeatability and reproducibility of the new Corvis ST DCR

parameters together with the CBI and TBI in keratoconic patients.

We found that the DCR parameters had excellent repeatability even in keratoconic patients. Also, the deflection amplitude showed excellent accordance (ICC > 0.8). The CoV was 3.2% and comparable to that in healthy eyes shown by Lopes et al.¹³ (3.8%). Miki et al.³⁴ published higher CoV values

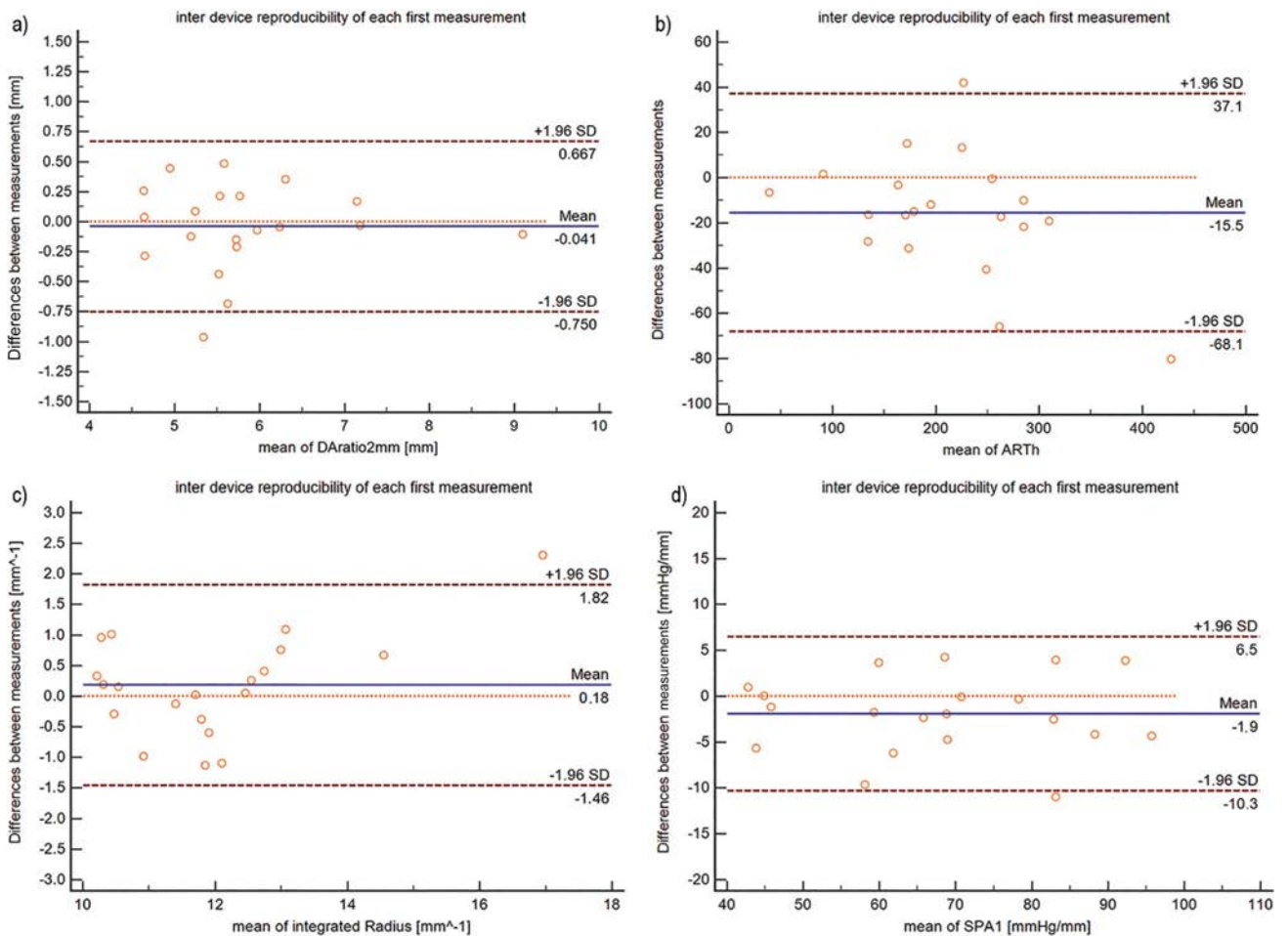


Figure 2. Interdevice reproducibility of each first measurement: limits of agreement (± 1.96 SD), (a) DA_{ratio} at 2.0 mm, (b) ARTh, (c) integrated radius, and (d) SPA1 (ARTh = Ambrósio’s relational thickness; DA = deformation amplitude; SPA1 = stiffness parameter at applanation 1).

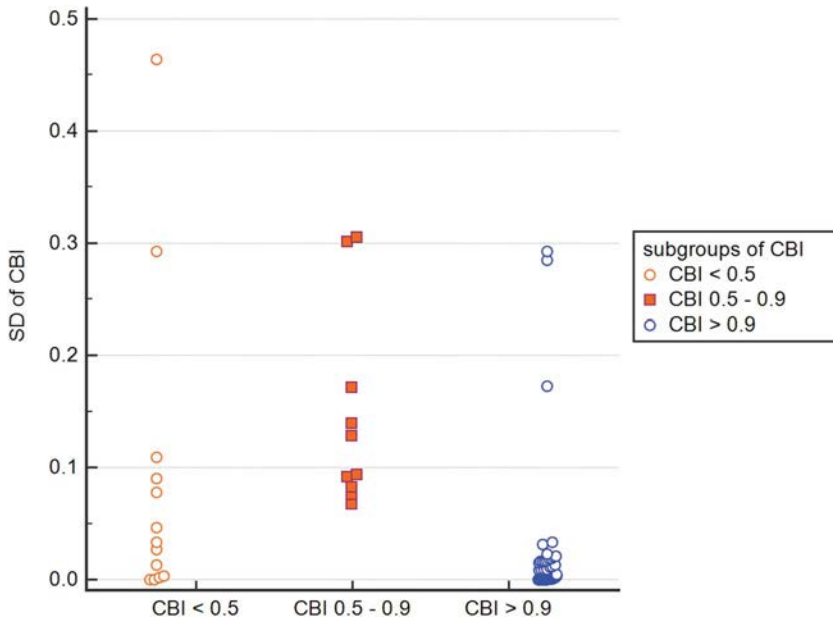


Figure 3. Standard deviation (SD) of 3 consecutive measurements separated by CBI measurement outcomes (CBI = Corvis Biomechanical Index).

(8.7%). In this study, we found a CoR of 0.103 mm, which is higher than that published for healthy eyes, which ranged from 0.065 to 0.08 mm.^{13,34}

The recently introduced DCR parameters^{3,8} had high accordance (ICC > 0.8), especially the CoV of the DA_{ratio} (2.0 mm/1.0 mm) and integrated radius, which was below 5% in our cohort, and similar to values in healthy eyes.¹³ SPA1 showed a CoV greater than 5%, which can still be considered highly repeatable.³⁰

Repeatability with regard to the keratoconic stage based on TKC showed that the higher the stage of keratoconic, the less reliable the measurement of DCR parameters. That became apparent in a slight increase in CoR and CoV for most DCR parameters between mild (KC1) and moderate (KC2) keratoconic stages, for which no significance was observed. Considering the differences between mild and advanced keratoconic stages, we observed a significant

increase of CoV in the CVS-IOP, bIOP, and most DCR parameters. Nevertheless, our study showed highly reliable results with an increase in the CoR and CoV, where CoV remained below 10%. This information is important, particularly in defining clinically significant changes in corneal biomechanics in keratoconic patients based on the repeatability of the device.

In addition, we observed the dependency of *z*-alignment errors. We found a significant increase in the CoR and CoV for CVS-IOP, bIOP, pachymetry, deflection amplitude, ARTh, and SPA1 if one of the 3 measurements had an alignment error in the *z*-axis greater than +0.5 mm. The SPA1 was significantly worse and showed a CoV of 10.6%, whereas the other DCR parameters remained below 10%. To avoid worsening repeatability and measurements, accurate alignment in the *z*-direction is important and should be considered in clinical practice.

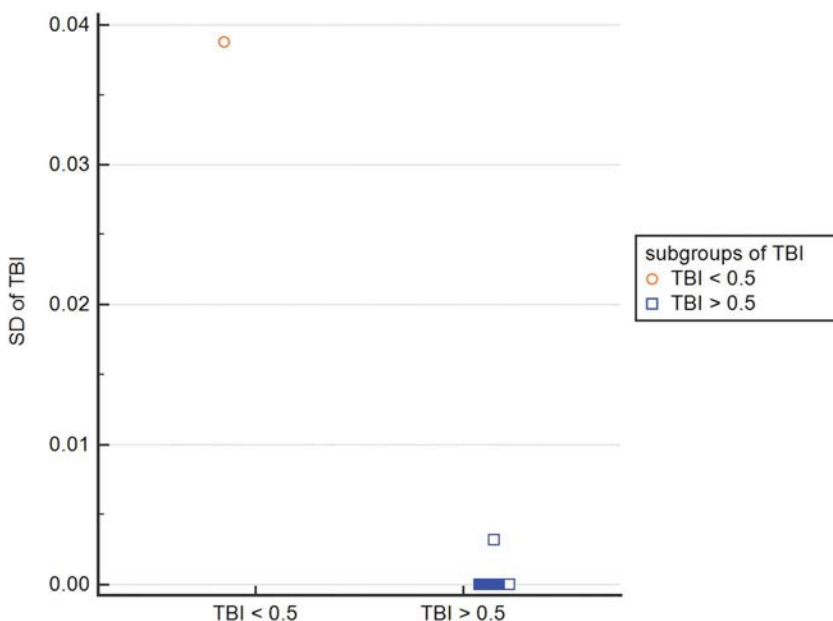


Figure 4. Standard deviation (SD) of 3 consecutive measurements separated by TBI measurement outcomes (TBI = tomographic and biomechanical index).

The CVS-IOP showed excellent accordance (ICC > 0.8) in repeatability, with a CoR and CoV of 2.74 mm Hg and 6.6%, respectively. These values are slightly higher than those in healthy eyes found by Lopes et al.,¹³ Ali et al.,³⁰ and Nemeth et al.³⁵ Instead, when considering the more advanced bIOP algorithm, the results in the present study were comparable with those in healthy eyes. The CoR and CoV were 2.6 mm Hg and 5.8% compared with 2.4 mm Hg and 6.1%, respectively in another study.¹³ However, the bIOP algorithm is not designed for eyes with abnormal topography a study is in progress to develop a bIOP modification specifically for keratoconic patients.

Pachymetry has the highest precision, with an ICC of 0.981 and CoV of 0.72% and is comparable to measurements in healthy eyes by Ali et al.³⁰ (ICC > 0.8; CoV = 1.8%) and Bak-Nielsen et al.²⁴ (CoV = 0.9%). The CoV was greater than that in other DCR parameters because of the higher nominal values.

These findings regarding the dependency of the keratoconus stage, might allow further modifications to software to allow comparison of the temporal changes in DCR parameters with the repeatability of healthy patients or keratoconus patients with the same severity based on the biomechanical response as the currently measured patient.

Reproducibility was determined by the random combination of factors such as subject, device, and interactions between the subject and device. The subgroup of 20 patients was examined using 2 different devices. Lopes et al.¹³ compared the reproducibility using 3 different devices and found that reproducibility was as good as repeatability. In our study, DCR parameters, such as the deflection amplitude max, DA_{ratio} (2.0 mm/1.0 mm), integrated radius, and SPA1, were nearly equal to repeatability data and comparable to results in healthy eyes. The CoV was below 10% for reproducibility for all DCR parameters except ARTh.

With regard to the CVS-IOP and bIOP, we estimated a CoR and CoV of 2.99 mm Hg and 8.3%, respectively, and 2.7 mm Hg and 7.1%, respectively. These results are comparable to those in healthy eyes.¹³ Bak-Nielsen et al.²⁴ investigated the interday reproducibility in the same device and obtained a CoV of 5.6% for CVS-IOP. Also, pachymetry is a reproducible parameter with an ICC of 0.982 and a CoV of 1.7%.

The equation to determine the CBI includes several DCR parameters (eg, DA_{ratio} [1.0 mm], DA_{ratio} [2.0 mm] ARTh, and SPA1).³ Overall, these DCR parameters showed good to excellent repeatability and reproducibility. The CBI itself had excellent accordance in repeatability and reproducibility. With regard to the TBI, we found an excellent accordance in repeatability. The calculation of CoR and CoV is not suitable for the nonlinear scale (logarithmic scale). For this reason, we analyzed the SD of the CBI and TBI. The SD in cases with a CBI greater than 0.9 was very low, which indicates a high reliability in moderate and advanced keratoconic eyes. The SD of the CBI was increased in lower stages of CBI because of its logit function behavior. For the TBI, the SD was very low in all cases, which indicates high reliability.

Another noncontact tonometer, the ORA, also measures the biomechanical behavior of the cornea after an air puff is replied. There are few studies in the literature describing the repeatability of these measurements in a normal population and none in keratoconic patients. The CoV of the ORA IOP and corneal-compensated IOP ranged from 7.8% to 8.2%.³⁶ The reproducibility between observers was 9.0% and 9.9%.³⁶ Other publications revealed good repeatability of ORA parameters such as corneal hysteresis and the corneal resistance factor.^{37,38}

In conclusion, we found that Corvis ST measurements were highly reliable and reproducible in a large keratoconic cohort. The measurements were as good as were those in healthy eyes but with a slight decrease in advanced cases. This indicates that the measurement of Scheimpflug-based tonometry is precise and represents the basis for clinical diagnosis and follow-up examinations. For accurate measurement results, we suggest dark room conditions, trained technicians, automatic release of the air puff, and updated software, if available.

WHAT WAS KNOWN

- Dynamic corneal response parameters provided by Corvis ST are useful in evaluation before refractive surgery, the early diagnosis of keratoconus, and the corneal biomechanical compensation of intraocular pressure measurements.
- Dynamic corneal response parameters are repeatable and reproducible in healthy patients.

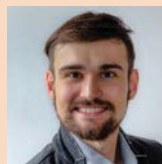
WHAT THIS PAPER ADDS

- Corvis ST measurements were highly reliable and reproducible in a keratoconus cohort.
- The repeatability of Corvis ST measurements was marginally influenced by the severity of keratoconus.

REFERENCES

1. Seiler T, Quurke AW. Iatrogenic keratectasia after LASIK in a case of forme fruste keratoconus. *J Cataract Refract Surg* 1998;24:1007–1009
2. Roberts CJ, Dupps WJ Jr. Biomechanics of corneal ectasia and biomechanical treatments. *J Cataract Refract Surg* 2014;40:991–998
3. Vinciguerra R, Ambrósio R, Elsheikh A, Roberts CJ, Lopes B, Morengi E, Azzolini C, Vinciguerra P. Detection of keratoconus with a new biomechanical index. *J Refract Surg* 2016;32:803–810
4. Vinciguerra R, Ambrósio R Jr, Roberts CJ, Azzolini C, Vinciguerra P. Biomechanical characterization of subclinical keratoconus without topographic or tomographic abnormalities. *J Refract Surg* 2017;33:399–407
5. Joda AA, Shervin MMS, Kook D, Elsheikh A. Development and validation of a correction equation for Corvis tonometry. *Comput Methods Biomech Biomed Engin* 2016;19:943–953
6. Vinciguerra R, Elsheikh A, Roberts CJ, Ambrósio R, Kang DSY, Lopes BT, Morengi E, Azzolini C, Vinciguerra P. Influence of pachymetry and intraocular pressure on dynamic corneal response parameters in healthy patients. *J Refract Surg* 2016;32:550–561
7. Luce DA. Determining in vivo biomechanical properties of the cornea with an ocular response analyzer. *J Cataract Refract Surg* 2005;31:156–162
8. Roberts CJ, Mahmoud AM, Bons JP, Hossain A, Elsheikh A, Vinciguerra R, Vinciguerra P, Ambrósio R. Introduction of two novel stiffness parameters and interpretation of air puff-induced biomechanical deformation parameters with a dynamic Scheimpflug analyzer. *J Refract Surg* 2017;33:266–273
9. Ambrósio R Jr, Lopes BT, Faria-Correia F, Salomao MQ, Bühren J, Roberts CJ, Elsheikh A, Vinciguerra R, Vinciguerra P. Integration of Scheimpflug-based corneal tomography and biomechanical assessments for enhancing ectasia detection. *J Refract Surg* 2017;33:434–443

10. Vinciguerra R, Romano V, Arbabi EM, Brunner M, Willoughby CE, Battersbury M, Kaye SB. In vivo early corneal biomechanical changes after corneal cross-linking in patients with progressive keratoconus. *J Refract Surg* 2017; 33:840–846
11. Everitt BS, Skrondal A. *The Cambridge Dictionary of Statistics*. Cambridge, United Kingdom: Cambridge University Press; 2011
12. McAlinden C, Khadka J, Pesudovs K. Precision (repeatability and reproducibility) studies and sample-size calculation. *J Cataract Refract Surg* 2015;41:2598–2604
13. Lopes BT, Roberts CJ, Elsheikh A, Vinciguerra R, Vinciguerra P, Reisdorf S, Berger S, Koprowski R, Ambrósio R Jr. Repeatability and reproducibility of intraocular pressure and dynamic corneal response parameters assessed by the Corvis ST. *J Ophthalmol* 2017;2017:8515742
14. Ye C, Yu M, Lai G, Jhanji V. Variability of corneal deformation response in normal and keratoconic eyes. *Optom Vis Sci* 2015;92:e149–e153
15. Salvetat ML, Zeppleri M, Tosoni C, Felletti M, Grasso L, Brusini P. Corneal deformation parameters provided by the Corvis-ST pachy-tonometer in healthy subjects and glaucoma patients. *J Glaucoma* 2015;24:568–574
16. Duncan JK, Belin MW, Borgstrom M. Assessing progression of keratoconus: novel tomographic determinants. *Eye Vis (Lond)* 2016;3:6
17. Recept OF, Hasiripi H, Vayisoglu E, Kalayci D, Sarikatipoglu H. Accurate time interval in repeated tonometry. *Acta Ophthalmol Scand* 1998;76:603–605
18. Kida T, Liu JH, Weinreb RN. Effect of 24-hour corneal biomechanical changes on intraocular pressure measurement. *Invest Ophthalmol Vis Sci* 2006;47:4422–4426
19. Loewen NA, Liu JH, Weinreb RN. Increased 24-hour variation of human intraocular pressure with short axial length. *Invest Ophthalmol Vis Sci* 2010;51:933–937
20. Ambrósio R Jr, Ramos I, Luz A, Faria FC, Steinmueller A, Krug M, Belin MW, Roberts CJ. Dynamic ultra high speed Scheimpflug imaging for assessing corneal biomechanical properties. *Rev Bras Oftalmol* 2013;72:99–102
21. Hon Y, Lam AK. Corneal deformation measurement using Scheimpflug noncontact tonometry. *Optom Vis Sci* 2013;90:e1–e8
22. Hong J, Xu J, Wei A, Deng SX, Cui X, Yu X, Sun X. A new tonometer—the Corvis ST tonometer: clinical comparison with noncontact and Goldmann applanation tonometers. *Invest Ophthalmol Vis Sci* 2013;54:659–665
23. Valbon BF, Ambrosio R Jr, Fontes BM, Alves MR. Effects of age on corneal deformation by non-contact tonometry integrated with an ultra-high-speed (UHS) Scheimpflug camera. *Arq Bras Oftalmol* 2013;76:229–232
24. Bak-Nielsen S, Pedersen IB, Ivarsen A, Hjortdal J. Repeatability, reproducibility, and age dependency of dynamic Scheimpflug-based pneumotonometer and its correlation with a dynamic bidirectional pneumotonometer device. *Cornea* 2015;34:71–77
25. Miki A, Maeda N, Ikuno Y, Asai T, Hara C, Nishida K. Factors associated with corneal deformation responses measured with a dynamic Scheimpflug analyzer. *Invest Ophthalmol Vis Sci* 2017;58:538–544
26. Eliasy A, Chen KJ, Vinciguerra R, Maklad O, Vinciguerra P, Ambrósio R Jr, Roberts CJ, Elsheikh A. Ex-vivo experimental validation of biomechanically-corrected intraocular pressure measurements on human eyes using the CorVis ST. *Exp Eye Res* 2018;175:98–102
27. Vinciguerra R, Ambrosio R Jr, Roberts CJ, Elsheikh A, Lopes B, Vinciguerra P. Should the Corvis biomechanical index (CBI) include corneal thickness parameters? *J Refract Surg* 2018;34:213–216
28. Lopes BT, Ramos IC, Salomao MQ, Guerra FP, Schallhorn SC, Schallhorn JM, Vinciguerra R, Vinciguerra P, Price FW Jr, Price MO, Reinstein DZ, Archer TJ, Bellin MW, Machado AP, Ambrosio R Jr. Enhanced tomographic assessment to detect corneal ectasia based on artificial intelligence. *Am J Ophthalmol* 2018;195:223–232
29. Vaz S, Falkmer T, Passmore AE, Parsons R, Andreou P. The case for using the repeatability coefficient when calculating test-retest reliability. *PLoS One* 2013;8:e73990
30. Ali NQ, Patel DV, McGhee CN. Biomechanical responses of healthy and keratoconic corneas measured using a noncontact Scheimpflug-based tonometer. *Invest Ophthalmol Vis Sci* 2014;55:3651–3659
31. Fleiss JL. *The Design and Analysis of Clinical Experiments*. New York, NY, Wiley; 1986
32. Sefat SM, Wiltfang R, Bechmann M, Mayer WJ, Kampik A, Kook D. Evaluation of changes in human corneas after femtosecond laser-assisted LASIK and small-incision lenticule extraction (SMILE) using non-contact tonometry and ultra-high-speed camera (Corvis ST). *Curr Eye Res* 2016;41:917–922
33. Chan JS, Mandell RB. Alignment effects in videokeratography of keratoconus. *CLAO J* 1997;23:23–28
34. Miki A, Maeda N, Asai T, Ikuno Y, Nishida K. Measurement repeatability of the dynamic Scheimpflug analyzer. *Jpn J Ophthalmol* 2017;61:433–440
35. Nemeth G, Hassan Z, Csutak A, Szalai E, Berta A, Modis L Jr. Repeatability of ocular biomechanical data measurements with a Scheimpflug-based noncontact device on normal corneas. *J Refract Surg* 2013; 29:558–563
36. Sullivan-Mee M, Gerhardt G, Halverson KD, Qualls C. Repeatability and reproducibility for intraocular pressure measurement by dynamic contour, ocular response analyzer, and Goldmann applanation tonometry. *J Glaucoma* 2009;18:666–673
37. Goebels SC, Seitz B, Langenbacher A. Precision of ocular response analyzer. *Curr Eye Res* 2012;37:689–693
38. David VP, Stead RE, Vernon SA. Repeatability of ocular response analyzer metrics: a gender-based study. *Optom Vis Sci* 2013;90: 691–699



First author:

Robert Herber, MSc

Department of Ophthalmology, University Hospital Carl Gustav Carus, TU Dresden, Germany

ARTICLE

Anterior chamber lens sizing: Comparison of white-to-white and scleral spur-to-scleral spur methods

Cameron Bruner, BS, David F. Skanchy, MD, John P. Wooten, MD, Alice Z. Chuang, PhD, Gene Kim, MD

Purpose: To determine the most accurate method of estimating scleral-spur-to-scleral-spur (STS) distance for ophthalmologists without access to an anterior chamber optical coherence tomography (AS-OCT) instrument when selecting an anterior chamber intraocular lens (AC IOL).

Setting: Robert Cizik Eye Clinic, Houston, TX.

Design: Prospective cohort study.

Methods: The eyes of 65 participants aged 18 years or older were imaged by the Lenstar LS 900 optical biometer and CASIA SS-1000 swept-source Fourier-domain AS-OCT. Eyes were excluded if the anterior segment anatomy was significantly altered and the angle could not be visualized. When both eyes were eligible, 1 eye was randomly selected. The white-to-white (WTW) distance, STS distance, and axial length were recorded and compared. The difference between STS and horizontal WTW was calculated for each meridian. The mean (\pm SD) differences, 95%

limits of agreement, and Bland-Altman agreement were computed for each pair of STS and WTW measurements.

Results: The study comprised 65 eyes of 65 participants. In nearly every case, WTW + 0.5 and WTW + 1 overestimated STS. The horizontal WTW without adjustment was the best predictor of STS. The WTW best corresponded to the vertical STS meridian (6 to 12 o'clock) and not the horizontal meridian (3 to 9 o'clock), along which AC IOLs are traditionally placed.

Conclusions: The horizontal WTW method without an adjustment factor most accurately estimated STS distance and should be used to select AC IOL size when AS-OCT is not available. If AS-OCT is available, it should be used instead. In addition, AC IOLs should be placed in a vertical orientation rather than the traditional horizontal orientation to minimize sizing errors.

J Cataract Refract Surg 2020; 46:95–101 Copyright © 2019 Published by Wolters Kluwer on behalf of ASCRS and ESCRS

Cataracts affect more than 24 million people in the United States, making cataract surgery 1 of the most common surgeries nationwide.^A For visually symptomatic cataracts, the current standard of treatment is phacoemulsification with intraocular lens (IOL) placement in the capsular bag. However, many conditions can compromise the integrity of the capsule, rendering it incapable of supporting an IOL. These include trauma, congenital malformations (eg, Marfan syndrome and homocystinuria), secondary causes of zonular fiber instability (eg, pseudoexfoliation syndrome and chronic uveitis), and surgical complications.^{1,2} When these situations arise, extracapsular IOL fixation, such as an anterior chamber IOL (AC IOL), scleral-fixed, or iris-fixed posterior chamber IOL, may be considered.

Among the options for patients with compromised capsules, open-loop angle-supported AC IOLs have become more popular because of the simpler surgical technique, shorter operating times, and reduction in postsurgical complications.^{1–6} Open-loop AC IOLs are preferred over closed-loop AC IOLs because of the increased incidence of pseudophakic bullous keratopathy associated with closed-loop designs.⁷ In a review of 43 well-designed prospective and retrospective studies, Wagoner et al.⁶ concluded that in the absence of capsular support, open-loop AC IOLs were as safe and effective as other therapies, such as scleral-sutured or iris-sutured posterior chamber IOLs.

Despite the advantages of open-loop designs, AC IOL sizing still poses a challenge. Oversized lenses can compress

Submitted: March 28, 2019 | Final revision submitted: July 8, 2019 | Accepted: August 26, 2019

From the Ruiz Department of Ophthalmology and Visual Science, McGovern Medical School, The University of Texas Health Science Center at Houston (Bruner, Skanchy, Wooten, Chuang, Kim), and Robert Cizik Eye Clinic (Kim), Houston, Texas, USA.

Supported in part by National Eye Institute Vision Core Grant P30EY028102 and the Hermann Eye Fund.

Corresponding author: Gene Kim, MD, Robert Cizik Eye Clinic, 6400 Fannin St, Suite 1800, Houston, TX 77030, USA. Email: gene.kim@uth.tmc.edu.

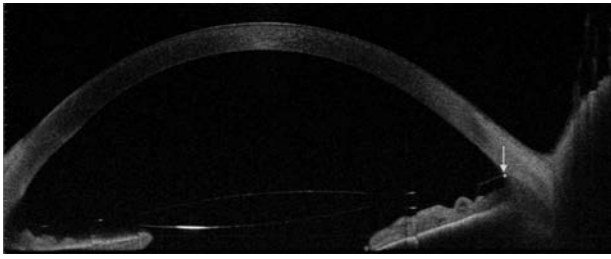


Figure 1. Anterior chamber intraocular lens footplates resting on the scleral spur. Asterisk indicates the scleral spur. Arrow indicates the point of contact between the footplate and scleral spur.

and erode structures near the angle recess, whereas undersized lenses can become mobile and damage the corneal endothelium.^{4,8,9} Ideally, the AC IOL footplates should rest on the relatively inert scleral spur (Figure 1). Therefore, the size of the AC IOL should be based on the scleral–spur–to–scleral–spur (STS) distance. However, obtaining STS measurements requires the use of an anterior chamber optical coherence tomography (AS-OCT) instrument, which is not widely available in all clinical practices. Thus, other methods have often been used to estimate the STS distance. Because the scleral spur lies posterolateral to the corneal limbus, several studies propose estimating the STS distance by adding a small constant (1 or 0.5 mm) to the white-to-white (WTW) corneoscleral diameter.^{10–14}

Conventionally, the WTW method of estimating STS uses only horizontal measurements, with the assumption that the anterior chamber is circular. Multiple studies, however, have measured STS along both the horizontal and vertical meridians and found that the anterior chamber is in fact ellipsoid, not circular.^{14–16} Furthermore, many studies have shown the anterior chamber to have a larger vertical than horizontal diameter.^{14,15,17–19} The above is further complicated as AC IOL sizing can vary based on the surgeon’s meridian of insertion.

The purpose of our study was to assess the accuracy of the traditional WTW method of estimating STS. We measured the STS distances typically encountered by AC IOL footplates using AS-OCT and compared them with horizontal WTW measurements obtained by optical biometry. This relationship between STS and WTW was then used to determine the accuracy of commonly used WTW adjustment factors and the applicability of the traditional method of estimating STS.

METHODS

This prospective cohort study was conducted at the Robert Cizik Eye Clinic of the Ruiz Department of Ophthalmology and Visual Science at the McGovern Medical School, University of Texas Health Science Center at Houston. Institutional Review Board approval was obtained from The University of Texas Committee for the Protection of Human Subjects before study commencement. All research adhered to the tenets of the Declaration of Helsinki and was U.S. Health Insurance Portability and Accountability Act compliant. Informed consent was obtained from all study participants before the initiation of study data collection and procedures.

Participants

Participants aged at least 18 years were recruited from visitors to the Robert Cizik Eye Clinic. After obtaining informed consent, the patient demographics, ocular history, and current ocular medications were recorded. Eyes with a history of ocular pathology, ocular surgery, or anterior segment abnormality that might have significantly altered the anterior segment anatomy or affected visualization of the angle of the eye (eg, significant corneal opacity and pterygium) were excluded. When both eyes were eligible, 1 eye was randomly selected for this study.

Optical Biometry

The Lenstar LS 900 optical biometer (Haag-Streit) was used to measure the WTW distance and axial length. Participants were instructed to focus on the internal fixation light. After adjusting the participant’s position, 5 consecutive scans were performed, and the results were averaged to obtain the horizontal WTW distance and axial length.

Anterior Chamber Optical Coherence Tomography Imaging

All participants had their anterior chambers imaged by the CASIA SS-1000 swept-source Fourier-domain AS-OCT device (Tomey) in a dark room. After their position was adjusted, participants were instructed to open their eyes wide and focus on the internal fixation light. If the eyelids obstructed the image, the operator was asked to hold open the participant’s lids without pressing on the globe. The eyes were scanned in “3D Angle Analysis” mode using the auto-alignment function. The AS-OCT device then took 128 cross-sectional radial scan images, 1 image per 1.41 degrees.

Anterior Chamber Optical Coherence Tomography Image Reading

Six cross-sectional images corresponding to the 1 to 7 o’clock, 2 to 8 o’clock, 3 to 9 o’clock (horizontal), 4 to 10 o’clock, 5 to 11 o’clock, and 6 to 12 o’clock (vertical) meridians were read by a reader (C.B.) using the built-in CASIA software. The scleral spurs were identified in each image based on the following criteria²⁰:

1. The point where there is a change in curvature in the corneoscleral–aqueous interface, often appearing as an inward protrusion of the sclera.
2. If the scleral spur was not clearly visible based on criterion 1, the most posterior end of the trabecular meshwork on the posterior corneoscleral–aqueous interface was chosen.

After identifying both scleral spurs on each image, the distance from 1 scleral spur to the other was measured by built-in digital calipers and recorded.

Sample-Size Calculation

The purpose of this study was to assess the accuracy (bias and precision) of the traditional WTW method of estimating STS. The accuracy was evaluated by the mean difference (bias) and its confidence interval (precision). Because AC IOL sizes are in increments of 0.5 mm, the sample size was calculated to obtain the 95% confidence width of estimated bias within ± 0.1 mm (20% of 0.5 mm). Shajari et al.²¹ reported that the mean horizontal WTW measured by the Lenstar was $12.3 \text{ mm} \pm 0.4$ (SD), and our study²² showed that the mean horizontal STS measured by the CASIA SS-1000 was 11.7 ± 0.4 mm (SD) in narrow angle eyes. Because STS and WTW are highly correlated ($R^2 \sim 1$), the SD of the bias was assumed to be 0.4 mm. Thus, a sample size of 63 was required to achieve a 95% confidence width of 0.1 mm.

Statistical Analysis

Collected data were summarized by the mean (\pm SD) for continuous variables or by the frequency (%) for discrete variables. The difference between STS and horizontal WTW was calculated for each meridian of each eye. The mean (\pm SD) differences and 95% limits of agreement (LoAs) ie, mean difference \pm 1.96 SD, were computed for each pair of STS and WTW measurements. The agreement of each pair was evaluated with a Bland–Altman plot. The Bland–Altman plot is a scatter plot $x=y$, in which the y -axis shows the difference between the 2 paired measurements (STS–WTW), and the x -axis represents the average of these measures [(STS + WTW)/2]. In other words, the difference between the 2 paired measurements is plotted against the mean of the 2 measurements. If 2 measurements are in a good agreement, the mean difference should be near 0 with narrow LoA length and 95% of the data points should lie within \pm 1.96 SD of the mean difference.

The differences between STS and horizontal WTW, as well as WTW + 0.5 mm and WTW + 1.0 mm, were calculated and categorized into the following groups: <-1.00 mm, -1.00 to -0.51 mm, -0.50 to 0.50 mm, 0.51 to 1.00 mm, and >1.00 mm. The frequencies of WTW, with and without the adjustment factor, were calculated to estimate the frequency and magnitude of WTW in over- and underestimating STS.

All statistical analyses were performed using SAS for Windows software (version 9.4, SAS, Inc.). Bland–Altman agreement statistics and plots were generated using `bland.altman.stats()` in `BlandAltmanLeh` package and `blandr.draw()` in `blandr` package, respectively, using R x64 version 3.01.

RESULTS

Sixty-five participants (65 eyes) were included in this study. There were 48 women (74%), and the mean age was 43.1 years \pm 16.4 (SD) (range 20–78 years). The study included 29 Hispanic (45%), 15 white (23%), 12 black (18%), and 9 Asian (14%) participants. Forty-two eyes (65%) had no ocular pathology, 8 (12%) had cataract, 4 (6%) had dry eye, 4 (6%) had drusen, and 1 eye (1.5%) each had 1 of the following: allergic conjunctivitis, congenital hypertrophy of the retinal pigment epithelium, episcleritis, lattice degeneration, blepharitis, bullous keratopathy, choroidal nevus, retinal tear, and non-proliferative diabetic retinopathy without diabetic macular edema. Ten eyes (15%) had previously undergone an ocular surgery, including 6 (9%) cataract surgeries, 2 (3%) laser-assisted in situ keratomileusis, 1 (1.5%) photorefractive keratectomy, and 1 (1.5%) globe repair. Demographics and ocular characteristics are summarized in Table 1.

Biometric parameters are in Table 2. AS-OCT images in 2 eyes were not analyzed because of poor image quality. The mean difference between horizontal STS and vertical STS was -0.24 ± 0.21 mm (SD), with a range of -0.78 to 0.35 mm. There were 13 (20%) eyes in which the horizontal and vertical STS difference fell within 0.1 mm, whereas 48 eyes (76%) had a difference greater than 0.1 mm. Only 2 (3%) eyes had a horizontal STS that exceeded the vertical STS by more than 0.1 mm.

Agreement

Table 3 shows the mean difference (bias) and LoAs for each studied meridian. The Bland–Altman agreement plots showing the distribution of the differences between each

Table 1. Demographics and ocular characteristics.

Variable	Value
Mean age (y) \pm SD	43.14 \pm 16.41
Female sex, n (%)	48 (74)
Race/ethnicity, n (%)	
Hispanic	29 (45)
White	15 (23)
Black	12 (18)
Asian	9 (14)
Ocular pathology, n (%)	
None	42 (65)
Cataract	8 (12)
Dry eye	4 (6)
Drusen	4 (6)
Previous ocular surgery, n (%)	
Phaco/IOL	6 (9)
LASIK	2 (3)
PRK	1 (2)
Globe repair	1 (2)

IOL = intraocular lens; LASIK = laser in situ keratomileusis; Phaco = phacoemulsification; PRK = photorefractive keratectomy

STS meridian and WTW are given in Figure 2. The bias between the STS distance and WTW distance was less than 0.25 mm for all studied meridians. The smallest bias was observed at the vertical meridian. The largest bias was at the 4 to 10 o'clock meridian followed by the horizontal meridian. The LoAs were similar across all studied meridians, ranging from 0.55 mm at the 1 to 7 o'clock to 0.59 mm at the vertical position. No outliers, linear trends, or patterns were observed on the Bland–Altman plots.

Comparing horizontal WTW distance with horizontal STS distance, 52 (83%) eyes had a bias within 0.5 mm. At this position, WTW overestimated STS by ± 0.5 to 1.0 mm in 10 eyes (16%) and underestimated STS by 0.5 to 1.0 mm in 1 eye (1.6%). Comparing horizontal WTW with vertical STS distance, 58 eyes (92%) had a bias within ± 0.5 mm. At this position, WTW overestimated STS by 0.5 to 1.0 mm in 2 eyes (3%) and underestimated STS by 0.5 to 1.0 mm in 3 eyes (5%). The vertical STS, compared with horizontal STS, resulted in significantly less over- and underestimation of WTW ($P = .004$). In

Table 2. Optical biometric measurements and STS distances.

Variable	Mean (\pm SD)	Range
Optical biometrics		
Axial length (mm)	23.98 (1.31)	(21.37, 28.16)
WTW (mm)	12.11 (0.40)	(11.03, 13.09)
STS distance		
3–9 o'clock (horizontal)	11.87 (0.33)	(11.17, 12.74)
6–12 o'clock (vertical)	12.11 (0.33)	(11.42, 13.26)
1–7 o'clock	12.07 (0.33)	(11.35, 13.00)
2–8 o'clock	11.91 (0.35)	(11.17, 12.96)
4–10 o'clock	11.87 (0.35)	(11.17, 12.87)
5–11 o'clock	11.98 (0.34)	(11.32, 13.03)
4–10 o'clock	11.87 (0.35)	(11.17, 12.87)

STS = scleral-spur-to-scleral-spur; WTW = white-to-white

Table 3. Mean Difference (bias) between WTW and STS and 95% LoAs.			
Meridian	Lower LoA	Mean Difference (Bias = WTW – STS)	Upper LoA
3–9 o'clock (horizontal)	–0.343	0.240	0.823
6–12 o'clock (vertical)	–0.584	0.005	0.593
1–7 o'clock	–0.518	0.037	0.591
2–8 o'clock	–0.368	0.196	0.759
4–10 o'clock	–0.323	0.243	0.810
5–11 o'clock	–0.449	0.133	0.714

LoA = limits of agreement; STS = scleral–spur–to–scleral–spur; WTW = white-to-white

addition, WTW overestimated at least 1 of the 6 STS meridians in 18 eyes (29%). WTW also underestimated at least 1 of the STS meridians in 5 eyes (8%). At the 4 to 10 o'clock meridian, WTW did not underestimate STS by more than 0.5 mm in any eye but overestimated STS by more than 0.5 mm in 11 eyes (17%) (Table 4).

The frequency and magnitude of bias increased as the WTW adjustment factor increased. When 0.5 or 1.0 mm was added to horizontal WTW, WTW did not underestimate STS in any eye. However, when 0.5 mm was added to horizontal WTW, WTW overestimated STS by more than 0.5 mm in 36 (57%) to 53 (84%) eyes. Furthermore, when 1.0 mm was added to horizontal WTW, WTW overestimated STS by more than 0.5 mm in 60 (95%) to 63 (100%) of eyes.

DISCUSSION

In this study, we compare WTW and STS to determine the most accurate method of estimating STS for ophthalmologists without access to AS-OCT. We show that in nearly every case of our traditional adjustments, WTW + 0.5 and WTW + 1 overestimated STS. Consequently, by using current conventions when selecting an AC IOL, ophthalmologists risk selecting a model that is oversized, exposing patients to potential complications. We found that horizontal WTW without adjustment is the best predictor of STS.

We also demonstrated that WTW best corresponds to the vertical STS meridian (6 to 12 o'clock) and not the horizontal meridian (3 to 9 o'clock), along which AC IOL are traditionally placed. In our study, 92% of eyes had

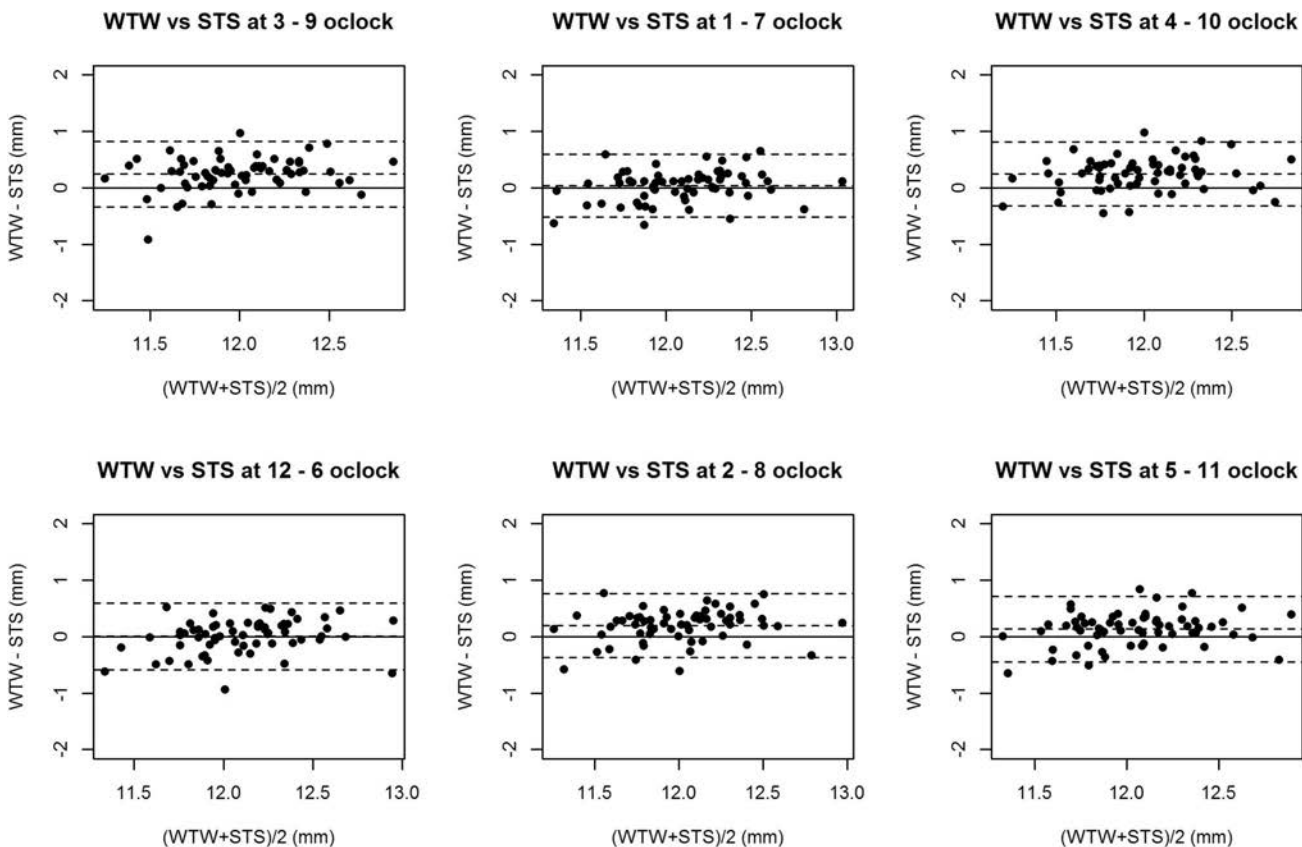


Figure 2. Bland–Altman plots showing the distribution of the differences between each STS meridian and WTW distance (STS = scleral–spur–to–scleral–spur; WTW = white-to-white).

Table 4. Frequency of bias between STS and WTW with and without adjustment constants for each meridian.

Meridian	Bias Category (n, %*)			
	-1.00 to -0.51 mm	-0.50 to 0.50 mm	0.51 to 1.00 mm	>1.00 mm
3–9 o'clock (horizontal)				
WTW to STS	1 (2%)	52 (83%)	10 (16%)	0 (0%)
WTW + 0.5 to STS	0 (0%)	10 (16%)	43 (68%)	10 (16%)
WTW + 1.0 to STS	0 (0%)	1 (2%)	9 (14%)	53 (84%)
6–12 o'clock (vertical)				
WTW to STS	3 (5%)	58 (92%)	2 (3%)	0 (0%)
WTW + 0.5 to STS	0 (0%)	27 (43%)	34 (54%)	2 (3%)
WTW + 1.0 to STS	0 (0%)	3 (5%)	24 (38%)	36 (57%)
1–7 o'clock				
WTW to STS	3 (5%)	56 (89%)	4 (6%)	0 (0%)
WTW + 0.5 to STS	0 (0%)	26 (41%)	33 (52%)	4 (6%)
WTW + 1.0 to STS	0 (0%)	3 (5%)	23 (37%)	37 (59%)
2–8 o'clock				
WTW to STS	2 (3%)	54 (86%)	7 (11%)	0 (0%)
WTW + 0.5 to STS	0 (0%)	12 (19%)	44 (70%)	7 (11%)
WTW + 1.0 to STS	0 (0%)	2 (3%)	10 (16%)	51 (81%)
4–10 o'clock				
WTW to STS	0 (0%)	52 (83%)	11 (17%)	0 (0%)
WTW + 0.5 to STS	0 (0%)	13 (21%)	39 (62%)	11 (17%)
WTW + 1.0 to STS	0 (0%)	0 (0%)	13 (21%)	50 (79%)
5–11 o'clock				
WTW to STS	2 (3%)	55 (87%)	6 (10%)	0 (0%)
WTW + 0.5 to STS	0 (0%)	15 (24%)	42 (67%)	6 (10%)
(WTW + 1.0) to STS	0 (0%)	2 (3%)	13 (21%)	48 (76%)

STS = scleral-spur-to-scleral-spur; WTW = white-to-white; WTW + 1.0 = WTW + 1.0 mm; WTW + 0.5 = WTW + 0.5 mm
 * < -1.00 mm zero (0%) for all meridians

a vertical STS bias within ±0.5 mm of WTW, whereas only 83% of eyes has a horizontal STS bias within ±0.5 mm of WTW ($P = .004$). Therefore, by placing AC IOLs in a vertical rather than horizontal orientation, ophthalmologists can theoretically reduce AC IOL sizing complications from 17% to 8%.

Evidence of ocular damage due to improperly sized AC IOLs is well documented and in many cases, is due to improper placement relative to the scleral spur.^{9,23} Currently, commercially available AC IOLs exist with different lengths to accommodate different STS lengths for different eyes. Alcon Laboratories, Inc. AC IOLs (MT3-5U0) range from 12.5 to 13.5 mm in length and increase by 0.5 mm gradations. The Bausch & Lomb L-S122UV AC IOL is only available in two lengths of 12.5 mm and 13.75 mm and a wider gradation. Based on the STS measurements, the AC IOL that is the next gradation larger should be placed based on the meridian. For example, if the vertical STS is 12.7 mm, an Alcon MTA4U0 (13.0 mm) should be placed. Undersized AC IOLs will be mobile in the eye and cause complications.

Goldsmith et al.²⁴ performed a misfit probability calculation and found that WTW alone in the selection of an AC IOL yielded a 22% chance of the lens being over- or undersized. However, when computer-automated AS-OCT analysis was used instead, the misfit probability decreased to 9%, demonstrating the greater accuracy of AS-OCT STS in sizing AC IOLs. Therefore, clinicians should judiciously select the AC IOL size when available

that best approximates AS-OCT STS. However, when unavailable, one should consider our finding of an accurate and precise correlation between horizontal WTW and vertical STS measurements. Horizontal WTW had a poorer correlation with horizontal STS, resulting in a 17.5% chance of over- or underestimating horizontal STS by more than 0.5 mm.

To assess the reproducibility of our WTW measurements with other instruments, we searched the literature for comparisons between the Lenstar and other biometric devices. Several well-designed studies showed that there was no significant difference between WTW measured by the Lenstar, Pentacam HR (Oculus Optikgeräte GmbH), IOLMaster 500 (Carl Zeiss Meditec AG), and Visante OCT (Carl Zeiss Meditec AG).^{15,21} Huang et al.²⁴ conducted a meta-analysis to further compare the Lenstar LS900 device with the gold standard IOLMaster optical biometer. They found that the mean Lenstar WTW ranged from 11.56 (±0.55) to 12.21 ±0.38 mm, whereas the mean IOLMaster WTW ranged from 11.85 ±0.44 mm to 12.19 ±0.37 mm.²⁶ The mean WTW in our study was 12.11 ± 0.4 mm, which falls within the range of the aforementioned meta-analysis. The congruency between our data and that of the meta-analysis led us to conclude that our findings can be applied to other common clinical devices that measure WTW.

The ellipsoid shape of the eye, with a larger vertical diameter, is well documented.^{14,15,17–19} Baikoff et al.¹⁵ observed that 74% of 107 normal eyes possessed a vertical diameter that

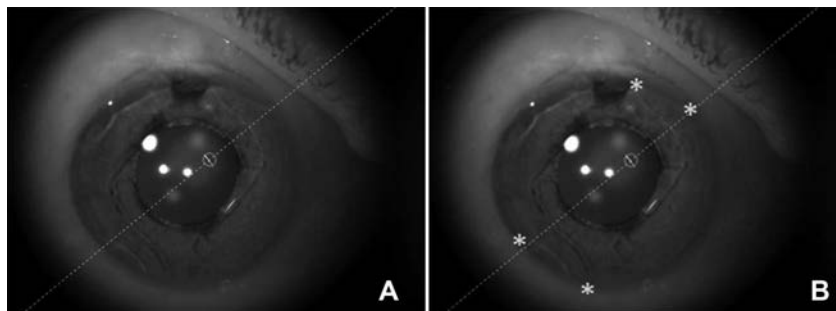


Figure 3. (A): Orientation of the AC IOL footplates. (B): Dotted line indicates the resting position of the AC IOL footplate at 39 degrees. Asterisks indicate points of contact between the footplates and scleral spur (AC IOL = anterior chamber intraocular lens).

was at least 0.1 mm larger than the horizontal diameter. Other well-designed studies have shown the vertical diameter to be 0.32 to 0.67 mm larger than the horizontal diameter.^{17–19} In our study, the mean vertical STS was 12.11 ± 0.33 mm and the mean horizontal STS was 11.87 ± 0.33 mm, with a mean difference of 0.24 ± 0.21 mm. Similar to the findings of Baikoff et al.,¹⁵ 48 (76%) of the 63 eyes in our study had a vertical diameter at least 0.1 mm larger than the horizontal diameter. Additional studies should be performed to further elucidate the relationship between the horizontal and vertical anterior chamber diameters.

To our knowledge, this is the first study to compare horizontal WTW with various STS meridians. We compared multiple STS meridians because open-loop AC IOL footplates do not rest exactly at the axis of insertion (Figure 3). Instead, they straddle the primary meridian of alignment. Thus, AC IOL size depends on the distance of multiple meridians that are not measured by traditional horizontal or vertical single-axis WTW methods. Our study showed that the vertical meridians tended to have less bias (0.005 mm) than the horizontal meridians (0.240 mm) when comparing WTW with STS. Larger studies might be necessary to confirm whether horizontal WTW is indeed a better estimate of vertical STS than horizontal STS, in which case vertical placement of AC IOLs may lead to more accurate sizing and improved outcomes.

Our study is also the first to compare WTW with adjustment to STS using AS-OCT. Our data show that WTW without adjustment is the most accurate estimate of STS along all meridians (Table 4). Yet in our study, even WTW without adjustment overestimated STS in some cases. Adding any constant to WTW might result in significant oversizing of AC IOLs and put patients at an increased risk for adverse outcomes. Several limitations exist in our study, most of which revolve around the relatively young age (mean 43 years) of our study population. This population might be younger and have healthier eyes than those typically requiring AC IOLs. In addition, nearly 75% of our study population consisted of women, and 45% consisted of Hispanics.

Previous studies have shown that there are sex and racial differences in anterior chamber parameters, with males and whites possessing wider anterior chambers.^{27–30} Asian eyes were also found to have a smaller STS diameter than white eyes.²⁸ Most of the anterior chamber biometry

studies come from the glaucoma literature in assessing the risk for angle-closure glaucoma and accordingly do not directly compare the relationship between STS and WTW. Although there are significant differences in STS based on race and sex, the difference in the WTW might correlate, allowing our relationship between STS and WTW to still hold true. However, to our knowledge, as our study is the first to study the relationship between WTW and STS, further studies should be conducted to see whether this relationship changes based on race and sex.

Horizontal WTW without an adjustment factor most accurately estimated STS, although the correlations were not always the same. Our study shows that horizontal WTW without adjustment should be used to estimate STS when selecting an AC IOL size when AS-OCT is not available. Based on our study, we recommend that AC IOLs be placed in a vertical orientation (6 to 12 o'clock) rather than a horizontal orientation (3 to 9 o'clock) to minimize sizing errors.

WHAT WAS KNOWN

- Improperly sized anterior chamber intraocular lenses (AC IOLs) can result in long-term ocular complications.
- There is no definite consensus on how to properly size an AC IOL, with current methods ranging from using the white-to-white (WTW) distance with an adjustment factor of zero to 1.0 mm to estimate the scleral-spur-to-scleral-spur (STS) distance.

WHAT THIS PAPER ADDS

- Vertical (12-6 o'clock) placement of an ACIOL using WTW + 0 mm result in less likelihood of sizing error (8%) compared to a horizontal (3-9 o'clock) placement of an ACIOL (17%).
- Traditional measures of WTW + 0.5 mm and WTW + 1.0 mm led to sizing errors in 57-84% and 95-100% of eyes, respectively.

REFERENCES

1. Holt DG, Young J, Stagg B, Ambati BK. Anterior chamber intraocular lens, sutured posterior chamber intraocular lens, or glued intraocular lens: where do we stand? *Curr Opin Ophthalmol* 2012;23:62–67
2. Por YM, Lavin MJ. Techniques of intraocular lens suspension in the absence of capsular/zonular support. *Surv Ophthalmol* 2005;50:429–462
3. Budoff G, Fine HF, Prenner JL. Secondary intraocular lens placement techniques and applications. *Ophthalmic Surg Lasers Imaging Retina* 2015;46:900–904
4. Dajee KP, Abbey AM, Williams GA. Management of dislocated intraocular lenses in eyes with insufficient capsular support. *Curr Opin Ophthalmol* 2016;27:191–195

5. Dick HB, Augustin AJ. Lens implant selection with absence of capsular support. *Curr Opin Ophthalmol* 2001;12:47–57
6. Wagoner MD, Cox TA, Ariyasu RG, Jacobs DS, Karp CL; American Academy of Ophthalmology. Intraocular lens implantation in the absence of capsular support: a report by the American Academy of Ophthalmology. *Ophthalmology* 2003;110:840–859
7. Kormmehl EW, Steinert RF, Odrich MG, Stevens JB. Penetrating keratoplasty for pseudophakic bullous keratopathy associated with closed-loop anterior chamber intraocular lenses. *Ophthalmology* 1990;97:407–412; discussion 13–4
8. Apple DJ, Brems RN, Park RB, Norman DK, Hansen SO, Tetz MR, Richards SC, Letchinger SD. Anterior chamber lenses. Part I: complications and pathology and a review of designs. *J Cataract Refract Surg* 1987;13:157–174
9. Apple DJ, Mamalis N, Loftfield K, Googe JM, Novak LC, Kavka-Van Norman D, Brady SE, Olson RJ. Complications of intraocular lenses. A historical and histopathological review. *Surv Ophthalmol* 1984;29:1–54
10. Heslin KB. Is “white-to-white” right? *J Am Intraocul Implant Soc* 1979;5: 50–51
11. Karickhoff JR. Instruments and techniques for anterior chamber implants. *Arch Ophthalmol* 1980;98:1265–1267
12. Piñero DP, Plaza Puche AB, Alió JL. Corneal diameter measurements by corneal topography and angle-to-angle measurements by optical coherence tomography: evaluation of equivalence. *J Cataract Refract Surg* 2008; 34:126–131
13. Roberts JC. A method for anterior chamber lens size determination. *J Am Intraocul Implant Soc* 1981;7:171
14. Werner L, Izak AM, Pandey SK, Apple DJ, Trivedi RH, Schmidbauer JM. Correlation between different measurements within the eye relative to phakic intraocular lens implantation. *J Cataract Refract Surg* 2004;30: 1982–1988
15. Baikoff G, Jitsuo Jodai H, Bourgeon G. Measurement of the internal diameter and depth of the anterior chamber: IOLMaster versus anterior chamber optical coherence tomographer. *J Cataract Refract Surg* 2005;31:1722–1728
16. Nemeth G, Hassan Z, Szalai E, Berta A, Modis L Jr. Comparative analysis of white-to-white and angle-to-angle distance measurements with partial coherence interferometry and optical coherence tomography. *J Cataract Refract Surg* 2010;36:1862–1866
17. Biermann J, Bredow L, Boehringer D, Reinhard T. Evaluation of ciliary sulcus diameter using ultrasound biomicroscopy in emmetropic eyes and myopic eyes. *J Cataract Refract Surg* 2011;37:1686–1693
18. Gao J, Liao RF, Li N. Ciliary sulcus diameters at different anterior chamber depths in highly myopic eyes. *J Cataract Refract Surg* 2013;39: 1011–1016
19. Oh J, Shin HH, Kim JH, Kim HM, Song JS. Direct measurement of the ciliary sulcus diameter by 35-megahertz ultrasound biomicroscopy. *Ophthalmology* 2007;114:1685–1688
20. Cumba RJ, Radhakrishnan S, Bell NP, Nagi KS, Chuang AZ, Lin SC, Mankiewicz KA, Feldman RM. Reproducibility of scleral spur identification and angle measurements using fourier domain anterior segment optical coherence tomography. *J Ophthalmol* 2012;2012:487309
21. Shajari M, Lehmann UC, Kohnen T. Comparison of corneal diameter and anterior chamber depth measurements using 4 different devices. *Cornea* 2016;35:838–842
22. Crowell EL, Gold ME, Chuang AZ, Baker L, Feldman RM, Bell NP, Blieden LS. Characterizing angle landmarks with anterior segment optical coherence tomography. *Invest Ophthalmol Vis Sci* 2014;55:929
23. Hauff W. Calculating the diameter of the anterior chamber before implanting an artificial lens [in German]. *Wien Klin Wochenschr Suppl* 1987;171: 1–19
24. Goldsmith JA, Li Y, Chalita MR, Westphal V, Patil CA, Rollins AM, Izatt JA, Huang D. Anterior chamber width measurement by high-speed optical coherence tomography. *Ophthalmology* 2005;112:238–244
25. Huang J, McAlinden C, Su B, Pesudovs K, Feng Y, Hua Y, Yang F, Pan C, Zhou H, Wang Q. The effect of cycloplegia on the lenstar and the IOLMaster biometry. *Optom Vis Sci* 2012;89:1691–1696
26. Huang J, McAlinden C, Huang Y, Wen D, Savini G, Tu R, Wang Q. Meta-analysis of optical low-coherence reflectometry versus partial coherence interferometry biometry. *Sci Rep* 2017;7:43414
27. Orucoglu F, Akman M, Onal S. Analysis of age, refractive error and gender related changes of the cornea and the anterior segment of the eye with Scheimpflug imaging. *Cont Lens Anterior Eye* 2015;38:345–350
28. Qin B, Tang M, Li Y, Zhang X, Chu R, Huang D. Anterior segment dimensions in Asian and Caucasian eyes measured by optical coherence tomography. *Ophthalmic Surg Lasers Imaging* 2012;43:135–142
29. Siguan-Bell CS, Chansangpetch S, Perez CI, Kutzscher A, Wang D, He M, Oldenburg C, Hee MR, Lin SC. Anterior segment parameters of Filipino-Americans compared to Chinese-Americans and Caucasian Americans using anterior segment optical coherence tomography. *Transl Vis Sci Technol* 2019;8:11
30. Wang D, Huang G, He M, Wu L, Lin S. Comparison of anterior ocular segment biometry features and related factors among American Caucasians, American Chinese and mainland Chinese. *Clin Exp Ophthalmol* 2012; 40:542–549

OTHER CITED MATERIALS

- A. National Eye Institute. 2010 U.S. Prevalent Cases of Cataract (in thousands) by Age, and Race/Ethnicity. Cataracts Defined Tables. <https://nei.nih.gov/eyedata/cataracts/tables#3>. Accessed March 27, 2019.

Disclosures: *None of the authors has a financial or proprietary interest in any material or method mentioned.*

Posterior capsule opacification prevention by an intraocular lens incorporating a micropatterned membrane on the posterior surface

Nathan Ellis, MD, Liliana Werner, MD, PhD, Vaishnavi Balendiran, MD, Caleb Shumway, MD, Bill Jiang, Nick Mamalis, MD

Purpose: To evaluate posterior capsule opacification (PCO) with a new hydrophobic acrylic intraocular lens (IOL) featuring a new micropatterned membrane, in comparison with a commercially available 1-piece hydrophobic acrylic IOL.

Setting: John A. Moran Eye Center, University of Utah, Salt Lake City, Utah, USA.

Study Design: Experimental study.

Methods: Twelve New Zealand rabbits had bilateral phacoemulsification and implantation of a ClearSight unpatterned IOL (Group 1), a ClearSight Sharklet-patterned IOL (Group 2), or a control, commercially available IOL (Group 3) (8 IOLs in each group). Slit-lamp examination was performed weekly for 4 weeks. The rabbits were then killed humanely, and their globes enucleated. Capsular bag opacification was assessed from the Miyake-Apple view, and the eyes underwent histopathology.

Results: The mean postmortem central PCO was 1.87 ± 1.35 in Group 1, 1.06 ± 1.23 in Group 2, and 3.14 ± 0.89 in Group 3. Peripheral PCO was 2.18 ± 1.36 in Group 1, 1.5 ± 1.03 in Group 2, and 3.57 ± 0.53 in Group 3. When comparing central and peripheral PCO between Groups 1 and 3, the difference was not statistically significant, but it was statistically significant between Groups 2 and 3 ($P = .003$ and $P = .0003$, t test with Bonferroni correction).

Conclusions: Unique discontinuous features comprising the micropattern allow for focal adhesions to be precisely guided and therefore controlling cell migration. The patterned membrane incorporated on the posterior surface of the IOL significantly reduced capsular bag opacification compared with a commercially available control IOL.

J Cataract Refract Surg 2020; 46:102–107 Copyright © 2019 Published by Wolters Kluwer on behalf of ASCRS and ESCRS

Opacification within the capsular bag may involve the anterior or posterior capsules and can have a significant impact on visual function. Posterior capsule opacification (PCO) is the most common long-term complication of cataract surgery, resulting in visual impairment and necessitating additional procedures.^{1–3} Incorporation of features for the prevention of capsular bag opacification has become one of the goals of intraocular lens (IOL) and endocapsular device development. It has been hypothesized that an open or expanded capsular bag is associated with the longer retention of bag clarity.⁴ This might be due to mechanisms that include mechanical stretch of the bag, maintaining the overall bag contour and allowing a constant flow of aqueous fluid throughout the device.⁵

However, opacification prevention may also be enhanced through the modification of the surface of the IOL itself.

Engineered surface topographies, specifically geometries of ordered features designed with unique roughness properties such as the one seen in the Sharklet micropattern (Sharklet Technologies, Inc. and ClearSight LLC), elicit specific predictable biological responses and have been shown to control bioadhesion. Previous studies have shown this sharkskin-inspired microtopography inhibits bioadhesion more effectively than other ordered topographies (eg, pillars, channels, and other geometries).^{6–8}

We have recently evaluated the outcome of capsular bag opacification with a new patterned protective membrane implanted in the bag with the secondary placement of an IOL

Submitted: April 19, 2019 | Final revision submitted: July 30, 2019 | Accepted: August 1, 2019

Department of Ophthalmology and Visual Sciences, John A. Moran Eye Center, University of Utah, Salt Lake City, USA.

Supported in part by an unrestricted grant from Research to Prevent Blindness, Inc, New York, NY, USA, to the Department of Ophthalmology and Visual Sciences, University of Utah, and by a research grant from ClearSight LLC.

Corresponding Author: Liliana Werner, MD, PhD, Department of Ophthalmology and Visual Sciences, John A. Moran Eye Center, University of Utah, 65 Mario Capecchi Dr, Salt Lake City, UT 84132, USA. Email: liliana.werner@hsc.utah.edu.

in the rabbit eye for 4 weeks.⁹ This endocapsular device was shown to be effective in preventing postoperative capsular bag opacification; however, the study was unable to conclude whether the micropattern had any effect toward the outcome. To our knowledge, this is the first in vivo study evaluating an IOL incorporating the previously reported micropattern on the posterior surface and its ability to prevent postoperative capsular bag opacification in the rabbit model.

METHODS

Twelve New Zealand white rabbits of the same sex and weighing between 2.4 kg and 3.2 kg were acquired from the approved vendors and treated in accordance with the guidelines set forth by the Association for Research in Vision and Ophthalmology. Eight rabbit eyes received the unpatterned ClearSight IOL (Group 1), the Sharklet-patterned ClearSight IOL (Group 2),^{6–8} or the control, commercially available AcrySof IOL, SA60AT, Alcon Laboratories, Inc.) (Group 3). Figure 1 shows a schematic drawing of the IOL design in Groups 1 and 2. This is a 1-piece monofocal IOL with two haptics, manufactured from a proprietary glistening-free hydrophobic acrylic polymer (nanohybrid polymer). The IOL has a diameter of 13.5 mm haptic-to-haptic. The optic zone has a diameter of 5.5 mm, with a peripheral element referred to as a membrane, extending an additional 0.75 mm beyond the optic zone for a total optic membrane diameter of 7.0 mm and also featuring a lateral wall with a height of 0.59 mm. The IOL has a 7-degree posterior optic-haptic angulation. The IOL in Group 2 featured the new micropatterned design (Sharklet pattern), only on the posterior surface of the membrane, with no extension onto the optic zone and a slight extension to the optic-haptic junctions (Figure 2).

The placement of each IOL was distributed among the rabbit eyes in 2-by-2 combinations so that 4 animals had each combination. All surgeries were performed by the same surgeon (N.M.). The rabbit model was chosen for its accelerated development of PCO, in which 1 month of implant time is approximately equivalent to 1 to 2 years in humans for PCO development.^{10–13}

Anesthesia, surgical preparation, and bilateral phacoemulsification with IOL implantation were performed as described in previous studies.^{10–13} Briefly, a fornix-based conjunctival flap was fashioned. A corneoscleral incision was then made using a crescent blade, and the anterior chamber was entered with a 3.0 mm keratome. A capsulorhexis forceps was used to create a well-centered continuous curvilinear capsulorhexis with a diameter of approximately 5.0 mm. After hydrodissection, the phacoemulsification handpiece (Alcon Infiniti System) was inserted into the posterior chamber for the removal of the IOL nucleus and cortical material. One-half milliliter of epinephrine 1:1000 and 0.5 ml of heparin (10 000 USP units/mL) were added to each 500 mL of irrigation solution to facilitate pupil dilation and control inflammation. The residual cortex was then removed with

the irrigation/aspiration handpiece. An ophthalmic viscosurgical device (sodium hyaluronate 1.6% [Amvisc Plus]) was used to expand the capsular bag. The IOLs were then injected into the capsular bag using the corresponding recommended injection systems (AccuJet 3.0 BL Injector set for IOLs in Groups 1 and 2 and Monarch III system with “C” cartridges for control Group 3). The wound was closed with a 10-0 monofilament nylon suture after the removal of the ophthalmic viscosurgical device using irrigation/aspiration.

Postoperative topical therapy included the combination of neomycin-polymyxin B sulfates-dexamethasone ointment during the first postoperative week and prednisolone acetate drops during the second postoperative week.

The eyes were dilated and evaluated by slitlamp examination for ocular inflammatory response at 1, 2, 3, and 4 weeks (± 2 days) postoperatively. Clinical color photographs of each eye at each time point were obtained with a digital camera attached to the slitlamp. A standard scoring method in 11 categories was used at each examination, including the assessment of corneal edema and the presence of cells and flare in the anterior chamber according to the previously described methods.^{10–13} Anterior capsule opacification (ACO) and PCO were also evaluated at each time point and scored from 0 to 4. Retroillumination images with the pupil fully dilated were obtained for photographic documentation.

After the final clinical examination at 4 weeks, the animals were anesthetized and then killed humanely with a 1 mL intravenous injection of pentobarbital sodium-phenytoin sodium. Their globes were enucleated and placed in 10% neutral buffered formalin for at least 24 hours. The globes were then bisected coronally just anterior to the equator. Gross examination and photographs from the posterior aspect (Miyake-Apple view) were performed to assess the ACO and PCO development as well as IOL fixation. The extent and severity of ACO and PCO were scored according to the methods established at the Intermountain Ocular Research Center. After gross examination and photographs, all globes were sectioned and the anterior segments including the capsular bags processed for standard light microscopy and stained with hematoxylin-eosin.

RESULTS

All surgical procedures were overall uneventful, with the exception of 1 eye in the AcrySof control group, which exhibited a posterior capsule tear leading to decentration of the IOL at the end of the surgical procedure. Data from this eye were not included in capsular bag opacification evaluation.

Slitlamp examination at 1 week postoperatively showed a mild inflammatory reaction composed of aqueous cells in all rabbit eyes. Most eyes in the 3 IOL groups also exhibited mild fibrin formation either at the rhexis edge or in front of the IOL. The above-mentioned findings essentially subsided

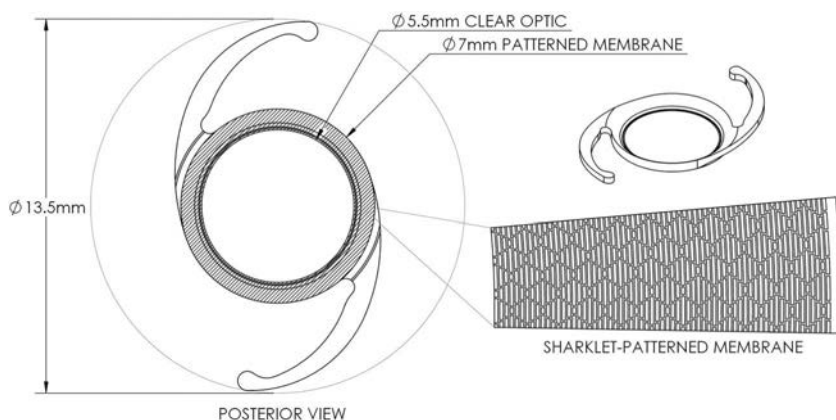


Figure 1. Schematic drawing showing the 1-piece IOL design in Group 2 with the patterned membrane on the posterior surface. The design of the IOL in Group 1 was the same, without the pattern (IOL = intraocular lens).

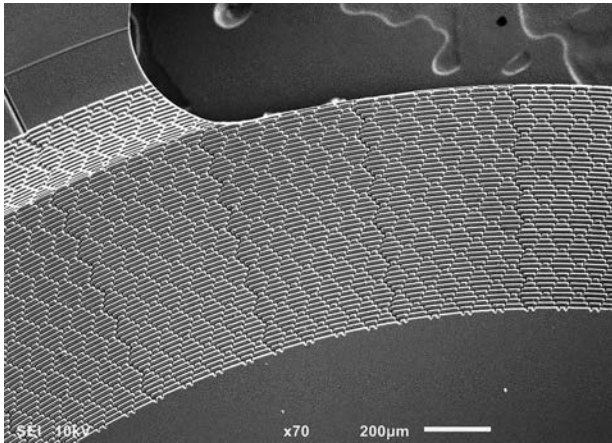


Figure 2. Scanning electron photomicrograph of an intraocular lens in Group 2 showing the details of the Sharklet-patterned membrane.

by the week 2 examination. At this time point, mild amounts of PCO started to be observed in some eyes of all IOL groups. Anterior proliferative pearl formation started to be observed in some eyes of Groups 1 and 2. At the week 3 examination, anterior proliferative pearl formation also started to be observed in the control group, Group 3. This anterior proliferation led to synechia formation in some eyes of all 3 groups, without any statistically significant difference among the groups ($P = .77$, one-way analysis of variance [ANOVA]).

Posterior capsule opacification was scored as follows at the week 4 examination: 1.93 ± 1.29 in Group 1, 1.07 ± 1.20 in Group 2, and 2.83 ± 0.93 in Group 3 ($P = .11$; one-way ANOVA) (Figure 3). It is noteworthy that the clinical assessment of PCO is limited to what can be observed behind the IOL optic through the pupil. Anterior capsule opacification was found to be mild in this study, scored as 0 to 1, with the exception of 1 eye in Group 3, with ACO scored as 2 also showing the contraction of the capsulorhexis opening (phimosis). Overall, there was statistically more ACO in Group 3, in comparison with Groups 1 and 2 ($P = .01$; one-way ANOVA).

Posterior capsule opacification formation was best assessed postmortem through the posterior or Miyake-Apple view. The mean postmortem central PCO was 1.87 ± 1.35 in Group 1, 1.06 ± 1.23 in Group 2, and 3.14 ± 0.89 in Group 3. When comparing central PCO between Groups 1 and 3, the difference was not statistically significant (Bonferroni-adjusted one-sided P -value = .05329). When comparing central PCO between Groups 2 and 3, the difference was statistically significant (Bonferroni-adjusted one-sided P -value = .00304). The mean postmortem peripheral PCO was 2.18 ± 1.36 in Group 1, 1.5 ± 1.03 in Group 2, and 3.57 ± 0.53 in Group 3. When comparing peripheral PCO between Groups 1 and 3, the difference was not statistically significant ($P = .025$, t test with Bonferroni correction). When comparing peripheral PCO between Groups 2 and 3, the difference was statistically significant ($P = .0003$, t test with Bonferroni correction). Soemmerring's ring formation was 5.12 ± 2.64 in Group 1, 5 ± 1.85 in Group 2, and 8.87 ± 3.52 in Group 3. When comparing

Soemmerring's ring formation between Groups 1 and 3, the difference was not statistically significant ($P = .03$, t test with Bonferroni correction). When comparing Soemmerring's ring formation between Groups 2 and 3, the difference was statistically significant ($P = .01$, t test with Bonferroni correction) (Figure 4).

Histopathological evaluation showed distinct difference in the amount of PCO as well as Soemmerring's ring formation and anterior cortical proliferation, with Elschnig pearl formation noted significantly more in Group 3 when

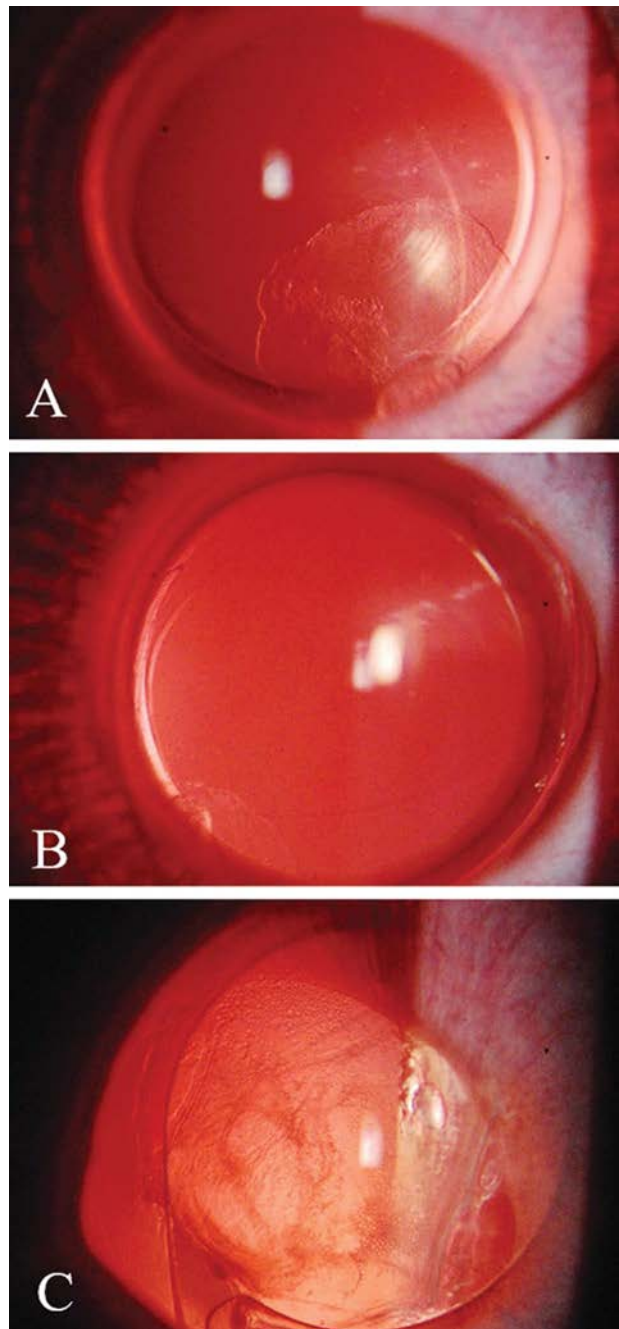


Figure 3. Slitlamp photographs of eyes from all 3 groups taken 4 weeks postoperatively (A through C: Groups 1 through 3, respectively). The eye with the patterned IOL (B: Group 2) shows significantly less posterior capsule opacification than the unpatterned IOL (A: Group 1) and the control eye (C: Group 3) (IOL = intraocular lens).

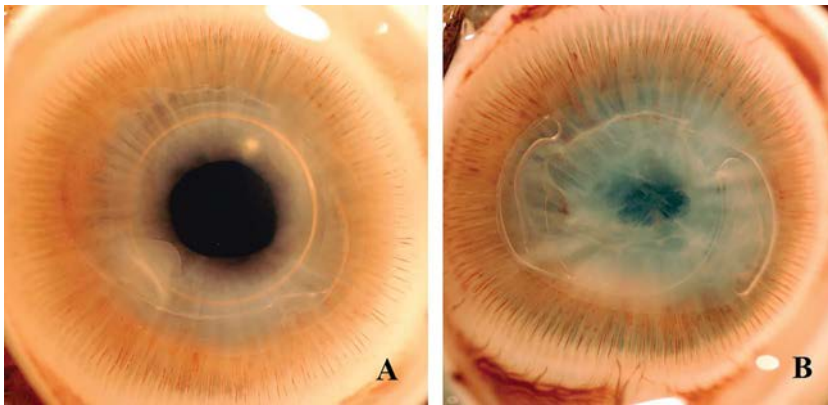


Figure 4. Miyake-Apple view of the anterior segment of rabbit eyes from Group 2 (A) and Group 3 (B). The eye with the patterned membrane (A) showed less central and peripheral posterior capsule opacification as well as less Soemmerring's ring formation than the control eye (B).

compared with both Groups 1 and 2. There was no sign of untoward inflammation nor toxicity on all 3 groups (Figure 5).

DISCUSSION

Posterior capsule opacification or secondary cataract is a well-recognized complication of cataract surgery that dates to the first IOL.² Although research has elucidated surgical and IOL-related mechanisms that are effective in its prevention, PCO remains the most common long-term postoperative complication of cataract surgery.¹⁻³

The Sharklet pattern was previously described as a patterned silicone protective membrane implanted in the bag with the secondary placement of an IOL within it.⁹ The circular geometry of the protective membrane led to the expansion of the capsular bag and appeared to prevent capsular bag opacification according to an *in vivo* rabbit study performed in our laboratory. The same study, however, was unable to determine whether the pattern on the posterior surface of the protective membrane had a role in enhancing the prevention of PCO by limiting the posterior migration of residual lens epithelial cell (LEC), as some of the membranes were injected in an inverted position within the rabbit eye.

Engineered surface topographies, particularly geometries of ordered features designed with unique roughness properties, elicit specific predictable biological responses and have been shown to control bioadhesion in medical devices such as the endotracheal tube.⁶⁻⁸ The Sharklet micropattern used in this study and a previous rabbit study is one example of such surface topographies. Other studies

in other medical specialties have shown this sharkskin-inspired microtopography inhibits bioadhesion more effectively than other ordered topographies (eg, pillars, channels, other geometries).

Cells interact with biomaterial interfaces through focal adhesions—protein assemblies embedded in the cell membrane.¹⁴ Micropatterns act to control cell migration by directing the placement of focal adhesions.¹⁴ The unique discontinuous features that comprise the Sharklet micropattern allow for focal adhesions to be precisely guided and, therefore, provide a high level of control over the migration orientation for a cell population. It was thus hypothesized that micropatterns could be optimized through altering dimensions of the pattern to the size scale of LECs to inhibit LEC migration. More recently, patterned protective membrane prototypes were tested in an *in vitro* PCO model for the reduction of cell migration behind an IOL vs unpatterned prototypes and IOLs with no membrane. Cell migration was analyzed with fluorescent microscopy, showing significant LEC migration reduction with patterned membranes.

This is the first study in which the Sharklet pattern has been directly placed on the posterior surface of the IOL, specifically onto a membrane (peripheral optic element) that surrounds the optic zone. Eyes that received the patterned IOL were associated with significantly less postmortem central and peripheral PCO than the control IOLs; however, PCO reduction related to IOLs without the pattern was not statistically significant when compared with the control IOL. This difference was not seen clinically at the week 4 slitlamp examination because of the limitation

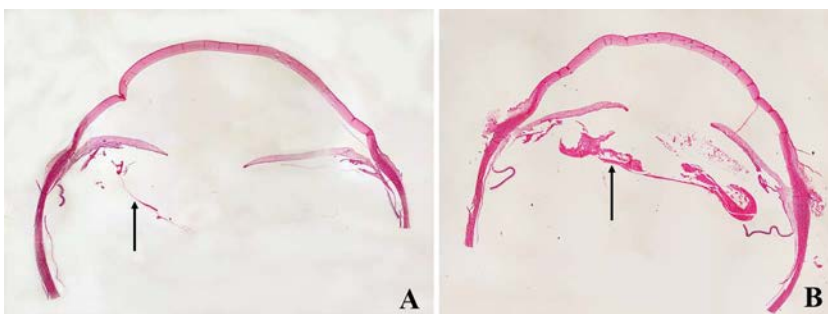


Figure 5. Light photomicrographs of histopathological sections cut from eyes in Group 2 (A) and Group 3 (B). A: Eye with the patterned IOL, showing minimal proliferative material along the posterior capsule (arrow). B: Eye with the control IOL, showing considerable Soemmerring's ring formation and posterior capsule opacification originating at the optic-haptic junctions (arrow). A and B: Composite of light photomicrographs; H&E staining; original magnification $\times 20$ (IOL = intraocular lens).

of the view through the pupil; therefore, PCO was best assessed postmortem through the posterior view of the anterior segment. When comparing postmortem Soemmerring's ring formation between groups, both patterned and unpatterned IOLs showed statistically less ring formation than the control IOL. This is likely due to the fact that the IOL design configuration in Groups 1 and 2 promotes a slight capsular bag expansion. Also, ACO was statistically higher in the control IOL when compared with the patterned and unpatterned IOLs, due to the fact that the lateral wall of IOLs in Groups 1 and 2 limited any contact between the anterior surface of the IOL and the inner surface of the anterior capsule.

The prevention of ACO and PCO and Soemmerring's ring formation with IOLs or devices maintaining the capsular bag open and/or expanded has been demonstrated in other studies by us and other groups. This can be seen in capsular tension ring-type devices, including the E-ring by Hara et al.,^{15–19} the capsular bending ring by Nishi et al.,^{20,21} and the capsular adhesion preventing ring by Nagamoto et al.²² The prevention of postoperative capsular opacification has been described in association with different IOLs as well, including the Concept 360 IOL (Corneal Laboratoire),²³ the Synchrony IOL (Abbott Medical Optics, Inc.),^{24–28} the FluidVision IOL (Powervision, Inc.),^{12,13} and the disk-shaped 1-piece hydrophilic acrylic IOL suspended between two haptic rings connected by a pillar of haptic material (Zephyr, Anew Optics Inc.).^{11,12} It is noteworthy that PCO is a multifactorial factor, and the IOL optic diameter may play a role in its outcome. In a study with 3-piece AcrySof IOLs, PCO was less with the 6.0 mm optic IOL vs the 5.5 mm IOL.²⁹ However, in another study using 1-piece AcrySof IOLs, PCO was less with the 5.5 mm optic IOL, in comparison with an experimental 7.0 mm optic IOL.³⁰ In the current study, the total optic membrane diameter of the ClearSight IOL was 7.0 mm, whereas the optic diameter of the control IOL was 6.0 mm. Posterior capsule opacification was similar between the unpatterned ClearSight IOL and the control AcrySof SA60AT. It is however difficult to draw conclusions based on the optic size alone, as other design differences exist between the ClearSight IOLs and the AcrySof SA60AT. Our study nonetheless shows that the addition of the micropattern improved PCO prevention. Although not the objective of this report, studies are underway to ensure that the design features of the test IOL are not associated with dysphotopsia, considering the optic zone of 5.5 mm in diameter with the membrane peripheral element and the lateral wall with a height of 0.59 mm.

In conclusion, the implantation of an IOL with a Sharklet pattern incorporated on its posterior surface, on a membrane surrounding the optic, resulted in less PCO compared with a commercially available control IOL, whereas the implantation of an IOL with the same membrane design but without a micropattern did not. This is the first in vivo study, to our knowledge, demonstrating that the Sharklet pattern likely has a role in enhancing PCO prevention through the limitation of the posterior migration of residual LECs.

WHAT WAS KNOWN

- A Sharklet micropattern used in medical devices allows for focal cell adhesions to be guided or inhibited, providing control over the migration orientation for a cell population.

WHAT THIS PAPER ADDS

- The presence of the Sharklet micropattern on the posterior membrane surface of a new hydrophobic acrylic intraocular lens resulted in significantly less postoperative capsular bag opacification in comparison with control eyes in the rabbit model.

REFERENCES

1. Apple DJ, Solomon KD, Tetz MR, Assia EI, Holland EY, Legler UF, Tsai JC, Castaneda VE, Hoggatt JP, Kostick AM. Posterior capsule opacification. *Surv Ophthalmol* 1992;37:73–116
2. Schmidbauer JM, Vargas LG, Peng Q, Escobar-Gomez M, Werner L, Arthur SN, Apple DJ. Posterior capsule opacification. *Int Ophthalmol Clin* 2001;41:109–131
3. Findl O, Buehl W, Bauer P, Sycha T. Interventions for preventing posterior capsule opacification. *Cochrane Database Syst Rev* 2010;2:CD003738
4. Kramer GD, Werner L, Mamalis N. Prevention of postoperative capsular bag opacification using intraocular lenses and endocapsular devices maintaining an open or expanded capsular bag. *J Cataract Refract Surg* 2016;42:469–484
5. Floyd A, Werner L, Mamalis N. PCO prevention with IOLs maintaining an open or expanded capsular bag. In: *Lens Epithelium and Posterior Capsular Opacification*. Tokyo, Japan: Springer; 2014:357–372
6. Chung KK, Schumacher JF, Sampson EM, Burne RA, Antonelli PJ, Brennan AB. Impact of engineered surface microtopography on biofilm formation of *Staphylococcus aureus*. *Biointerphases* 2007;2:89–94
7. May RM, Hoffman MG, Sogo MJ, Parker AE, O'Toole GA, Brennan AB, Reddy ST. Micro-patterned surfaces reduce bacterial colonization and biofilm formation in vitro: potential for enhancing endotracheal tube designs. *Clin Transl Med* 2014;3:8
8. Magin CM, May RM, Drinker MC, Cuevas KH, Brennan AB, Reddy ST. Micropatterned protective membranes inhibit lens epithelial cell migration in posterior capsule opacification model. *Transl Vis Sci Technol* 2015;4:9
9. Kramer GD, Werner L, MacLean K, Farukhi A, Gardiner GL, Mamalis N. Evaluation of stability and capsular bag opacification with a foldable intraocular lens coupled with a protective membrane in the rabbit model. *J Cataract Refract Surg* 2015;41:1738–1744
10. Kavoussi SC, Werner L, Fuller SR, Hill M, Burrow MK, McIntyre JS, Mamalis N. Prevention of capsular bag opacification with a new hydrophilic acrylic disk-shaped intraocular lens. *J Cataract Refract Surg* 2011;37:2194–2200
11. Leishman L, Werner L, Bodnar Z, Ollerton A, Michelson J, Schmutz M, Mamalis N. Prevention of capsular bag opacification with a modified hydrophilic acrylic disk-shaped intraocular lens. *J Cataract Refract Surg* 2012;38:1664–1670
12. Floyd AM, Werner L, Liu E, Stallings S, Ollerton A, Leishman L, Bodnar Z, Morris C, Mamalis N. Capsular bag opacification with a new accommodating intraocular lens. *J Cataract Refract Surg* 2013;39:1415–1420
13. Kohl JC, Werner L, Ford JR, Cole SC, Vasavada SA, Gardiner GL, Noristani R, Mamalis N. Long-term uveal and capsular biocompatibility of a new accommodating intraocular lens. *J Cataract Refract Surg* 2014;40:2113–2119
14. Walczysko P, Rajniecek AM, Collinson JM. Contact-mediated control of radial migration of corneal epithelial cells. *Mol Vis* 2016;22:990–1004
15. Hara T, Hara T, Yamada Y. "Equator ring" for maintenance of the completely circular contour of the capsular bag equator after cataract removal. *Ophthalmic Surg* 1991;22:358–359
16. Hara T, Hara T, Sakanishi K, Yamada Y. Efficacy of equator rings in an experimental rabbit study. *Arch Ophthalmol* 1995;113:1060
17. Hashizoe M, Hara T, Ogura Y, Sakanishi K, Honda T, Hara T. Equator ring efficacy in maintaining capsular bag integrity and transparency after cataract removal in monkey eyes. *Graefes Arch Clin Exp Ophthalmol* 1998;236:375–379
18. Hara T, Hara T, Hara T. Preventing posterior capsular opacification with an endocapsular equator ring in a young human eye. *Arch Ophthalmol* 2007;125:483
19. Hara T, Hara T, Narita M, Hashimoto T, Motoyama Y, Hara T. Long-term study of posterior capsular opacification prevention with endocapsular equator rings in humans. *Arch Ophthalmol* 2011;129:855
20. Nishi O, Nishi K, Menapace R. Capsule-Bending ring for the prevention of capsular opacification: a preliminary report. *Ophthalmic Surgery* 1998;29:749–753

21. Nishi O, Nishi K, Menapace R, Akura J. Capsular bending ring to prevent posterior capsule opacification: 2 year follow-up. *J Cataract Refract Surg* 2001;27:1359–1365
22. Nagamoto T, Tanaka N, Fujiwara T. Inhibition of posterior capsule opacification by a capsular adhesion-preventing ring. *Arch Ophthalmol* 2009;127:471
23. Werner L, Hickman MS, LeBoyer RM, Mamalis N. Experimental evaluation of the corneal concept 360 intraocular lens with the Miyake-Apple view. *J Cataract Refract Surg* 2005;31:1231–1237
24. Werner L, Pandey SK, Izak AM, Pandey SK, Izak AM, Vargas LG, Trivedi RH, Apple DJ, Mamalis N. Capsular bag opacification after experimental implantation of a new accommodating intraocular lens in rabbit eyes. *J Cataract Refract Surg* 2004;30:1114–1123
25. Werner L, Mamalis N, Stevens S, Hunter B, Chew JLL, Vargas LG. Interlenticular opacification: dual-optic versus piggyback intraocular lenses. *J Cataract Refract Surg* 2006;32:655–661
26. McLeod SD, Portney V, Ting A. A dual optic accommodating foldable intraocular lens. *Br J Ophthalmol* 2003;87:1083–1085
27. McLeod SD. Optical principles, biomechanics, and initial clinical performance of a dual-optic accommodating intraocular lens (an American Ophthalmological Society thesis). *Trans Am Ophthalmol Soc* 2006;104:437–452
28. McLeod SD, Vargas LG, Portney V, Ting A. Synchrony dual-optic accommodating intraocular lens: Part 1: optical and biomechanical principles and design considerations. *J Cataract Refract Surg* 2007;33:37–46
29. Meacock WR, Spalton DJ, Boyce JF, Jose RM. Effect of optic size on posterior capsule opacification: 5.5 mm versus 6.0 mm AcrySof intraocular lenses. *J Cataract Refract Surg* 2001;27:1194–1198
30. Nishi O, Nishi K. Effect of the optic size of a single-piece acrylic intraocular lens on posterior capsule opacification. *J Cataract Refract Surg* 2003;29:348–353

Disclosures: *None of the authors has a financial or proprietary interest in any material or method mentioned.*



First author:

Nathan Ellis, MD

Department of Ophthalmology and Visual Sciences, John A. Moran Eye Center, University of Utah, Salt Lake City

Assessment of the image quality of extended depth-of-focus intraocular lens models in polychromatic light

Yumi Lee, MD, Grzegorz Łabuz, PhD, Hyeck-Soo Son, MD, Timur M. Yildirim, MD, Ramin Khoramnia, MD, FEBO, Gerd U. Auffarth, MD, PhD

Purpose: The use of monochromatic light in the assessment of intraocular lenses (IOLs) has been criticized for not representing the real-world situation. This study aimed to measure and compare the image quality of 3 extended depth-of-focus (EDOF) IOL models in monochromatic and polychromatic light.

Setting: David J Apple Laboratory, Heidelberg, Germany.

Design: In vitro study.

Methods: An optical metrology instrument was used to study image quality metrics of diffractive IOLs with chromatic aberration correction (Symphony and AT Lara) and a refractive lens (Mini Well). The modulation transfer function (MTF) was measured in green and polychromatic light at a 2.0 mm, 3.0 mm, and 4.0 mm aperture. The EDOF IOL's tolerance to defocus was tested against a monofocal lens.

Results: The mean MTF of the EDOF IOL at far distance was decreased in polychromatic compared with monochromatic

light. The largest effect was found in the refractive lens; however, at intermediate distance, only small differences occurred. In their tolerance to defocus, the EDOF IOLs were superior to the monofocal IOL. The diffractive IOL had higher MTFs than that of the refractive IOL at 2 primary foci, the refractive IOL's optical quality varied less with defocus at 3.0 mm. The refractive lens was the most susceptible to changes in aperture size.

Conclusion: The diffractive EDOF IOL was more resistant to chromatic effects than the refractive IOL. The EDOF IOLs provided an extended through-focus performance compared with the monofocal IOL, but differences in optical design, particularly pupil dependency, should be considered when refining IOL selection for patients.

J Cataract Refract Surg 2020; 46:108–115 Copyright © 2019 Published by Wolters Kluwer on behalf of ASCRS and ESCRS

In cataract surgery, removal of the crystalline lens and implantation of a monofocal intraocular lens (IOL) leaves the eye unable to see clearly objects located at various distances. Multifocal IOLs overcome this limitation and enable patients with pseudophakia to achieve good near and far vision.¹ These IOLs usually provide good vision at 2 distinct foci (eg, far and near), but their optical quality decreases in between these separate points.² In addition, multifocal optic designs can generate undesirable photic phenomena such as halos, glare, starbursts, or decreased contrast sensitivity, all of which may limit patient satisfaction.^{1,3} Further development in the field of IOLs led to the introduction of extended depth-of-focus (EDOF) designs.^{4–9} In contrast to traditional multifocal IOLs, the EDOF IOLs aim to preserve good optical quality

continuously across a visual range.¹⁰ This has been associated with a lower incidence rate of photic phenomena such as halo and glare.¹⁰ The literature also shows a high rate of spectacle independence and postoperative satisfaction among patients with EDOF IOLs.^{8–10}

The optics of EDOF lens design has been assessed in in vitro studies.^{4,11} A criticism has been made of those studies^{12,13} that measurements were performed using an aberration-free model cornea, whereas clinical studies demonstrate that the human cornea produces positive spherical aberration.¹⁴ Furthermore, in those studies, optical measurements were performed in monochromatic (green) light, which may be considered a poor indicator of IOL performance in real-life conditions. Instead, the use of polychromatic light has been proposed,^{12,13} as everyday tasks

Submitted: June 11, 2019 | Final revision submitted: July 15, 2019 | Accepted: July 30, 2019

Department of Ophthalmology, the David J Apple Center for Vision Research, University Hospital Heidelberg, Heidelberg, Germany.

Y. Lee and G. Łabuz contributed equally to this work.

Donald J. Munro contributed to the review of the manuscript.

Corresponding Author: Grzegorz Łabuz, PhD, Department of Ophthalmology, University of Heidelberg, Im Neuenheimer Feld 400, Heidelberg 69120, Germany. Email: g.labuz@hotmail.com.

are typically performed in light composed of multiple wavelengths. In the polychromatic light, however, chromatic aberration can limit the imaging quality of an optical system, such as IOLs.¹⁵ Pseudophakic eyes exhibit a different level of chromatic aberration, which besides the intrinsic dispersion of the ocular media also depends on the optical properties of implanted IOLs.¹⁶ Therefore, an *in vitro* IOL assessment using polychromatic light and a corneal lens with a population level of spherical aberration would appear a better approximation of the clinical (*in vivo*) situation.

Our principle research aim was to evaluate the optical quality of 3 EDOF IOLs by measuring the modulation transfer function (MTF) in polychromatic light and with a model cornea with spherical aberration. In addition, the polychromatic and the monochromatic MTF were compared to demonstrate how uncorrected chromatic effects worsen each IOL's optical performance. Last, the IOL's tolerance to tilt and decentration was tested.

METHODS

Intraocular Lenses

The 3 EDOF IOLs studied were the Tecnis Symphony ZXR00 (J&J Vision), AT Lara 829 MP (Carl Zeiss Meditec AG), and Mini Well Ready (SIFI). The tolerance to defocus was compared with a monofocal AcrySof SA60AT (Alcon Laboratories, Inc.): a single-piece spherical IOL made of hydrophobic acrylic material with a 1.55 refractive index and an Abbe number of 37. The *in vitro* analysis was performed at the David J Apple Center for Vision Research, Heidelberg University Eye Hospital, Heidelberg, Germany.

The Symphony is a single-piece lens with an anterior aspheric surface to correct 0.27 μm of corneal spherical aberration. Its posterior diffractive surface has an echelette feature to enhance the range of vision and to compensate chromatic aberration using the opposite chromatic aberration behavior of a refractive and diffractive optical component. It is made of hydrophobic acrylic material with a refractive index of 1.47 and an Abbe number of 55.

Similar to the Symphony, in using diffractive optics, the AT Lara takes advantage of its diffractive design to minimize chromatic aberration effects. It is a single-piece hydrophilic acrylic (25% water content) IOL with a hydrophobic surface. The lens has an aspheric refractive base, which is aberration neutral, and has a refractive index of 1.46 and an Abbe number of 56.5.

The Mini Well is a single-piece IOL manufactured from hydrophilic acrylate (25% water content) with a hydrophobic surface. This lens has 3 circular zones: a central zone with positive spherical aberration, a surrounding zone with negative spherical aberration, and an outer monofocal zone with no induced spherical aberration. According to the manufacturer, the central zone and the middle zone have a diameter of 1.9 mm and 3.0 mm, respectively. The Mini Well's refractive index is 1.46, and the Abbe number is 46.9.

To test the repeatability of the optical quality measurements, each EDOF lens group was comprised of 3 +21 diopter (D) lenses and two +20 D lenses. The monofocal IOL was included solely as a benchmark for the defocus test, thus only one sample with a refractive power of +21 D was used.

Image Quality Assessment

The optical quality of all lenses was evaluated using an optical metrology station (OptiSpheric IOL PRO 2; Trioptics GmbH), which follows the guidelines of the International Standard Organization (ISO 11979-2). The IOLs were measured in a balanced salt solution with a 1.336 refractive index at room temperature. The optical apparatus included an aberrated model cornea that simulated the mean spherical aberration level (0.28 μm) found in the human cornea.¹⁴ A white LED light source and two optical

filters were used. To study the IOL performance in monochromatic light, we used a bandpass filter (10 nm full width at half maximum) with the center wavelength of 546 nm. The polychromatic condition was simulated with a Commission internationale de l'éclairage photopic-response filter. Image quality metrics were primarily determined for a mean photopic pupil size of 3.0 mm.¹⁷ Apertures of 2.0 mm and 4.0 mm sizes were also used to test IOL pupil dependence. The imaging ability of the lens was evaluated objectively by means of the MTF. The optical metrology device measures the MTF with a 2% accuracy and has proven to provide excellent repeatability.¹⁵ MTF measurements were taken at best far and intermediate points and at defocus ranging from -0.5 D to 2.5 D with a 0.25 D increment. The mean MTF (up to 30 cyc/deg), the through-focus MTF at 15 cyc/deg, and the visual Strehl ratio (VSR)¹⁸ were assessed. The VSR was calculated over 30 cyc/deg in the frequency domain and weighted by the neural contrast sensitivity function.¹⁹ In addition, a polychromatic point spread function (PSF), which was an image of a 0.1 mm point source, was recorded through the 3.0 mm aperture for different defocus values. The PSF data were used to visualize the optical performance of IOLs through simulated images of Early Treatment Diabetic Retinopathy Study optotypes. To this end, we used a truncated visual acuity (VA) chart image that covered a range between 0.5 and -0.3 logarithm of the minimum angle of resolution. This image was convoluted with the polychromatic PSF using custom-written software (MATLAB; MathWorks).

IOL tolerance to misalignment was tested by inducing (separately) up to 0.75 mm of decentration and 5° of tilt and calculating the loss of the MTF value at 15 cyc/deg.

RESULTS

Monochromatic vs Polychromatic MTF

Figure 1 shows the comparison between the monochromatic and polychromatic MTF within each lens model. The measurements were performed at the best primary (far) and secondary (intermediate) focus for the 3.0-mm pupil. The position of the secondary focus was 1.90 ± 0.01 D for the AT Lara, 1.76 ± 0.02 D for the Symphony, and 2.20 ± 0.11 D for the Mini Well. The far MTF performance was worse in polychromatic than monochromatic light for all IOLs, as the mean MTF loss was 15% for the AT Lara, 17% for the Symphony, and 26% for the Mini Well. At the secondary focus, the image quality was slightly better for the AT Lara (by 6%) and minimally worse for the Symphony (by 5%) and the Mini Well (by 7%) in polychromatic light. All but one EDOF model demonstrated excellent repeatability regarding MTF measurements, as 5 IOL samples per model were measured. In the Mini Well group, however, the MTF curves differed, particularly between the samples of +20 D and +21 D power.

Polychromatic Image Quality Comparison

Given good repeatability of the MTF in the +21 D IOLs (also in the Mini Well group), only one sample was used in further analysis and comparison of the image quality of the individual models. The polychromatic MTF of the 3 EDOF IOLs and the monofocal control are compared in Figure 2. At far, the SA60AT demonstrated higher MTF levels than those of the EDOF models. The Symphony and the AT Lara presented comparable image quality at the far focus. The Mini Well's MTF was, however, worse than that of the two diffractive lenses at higher spatial frequencies but better up to

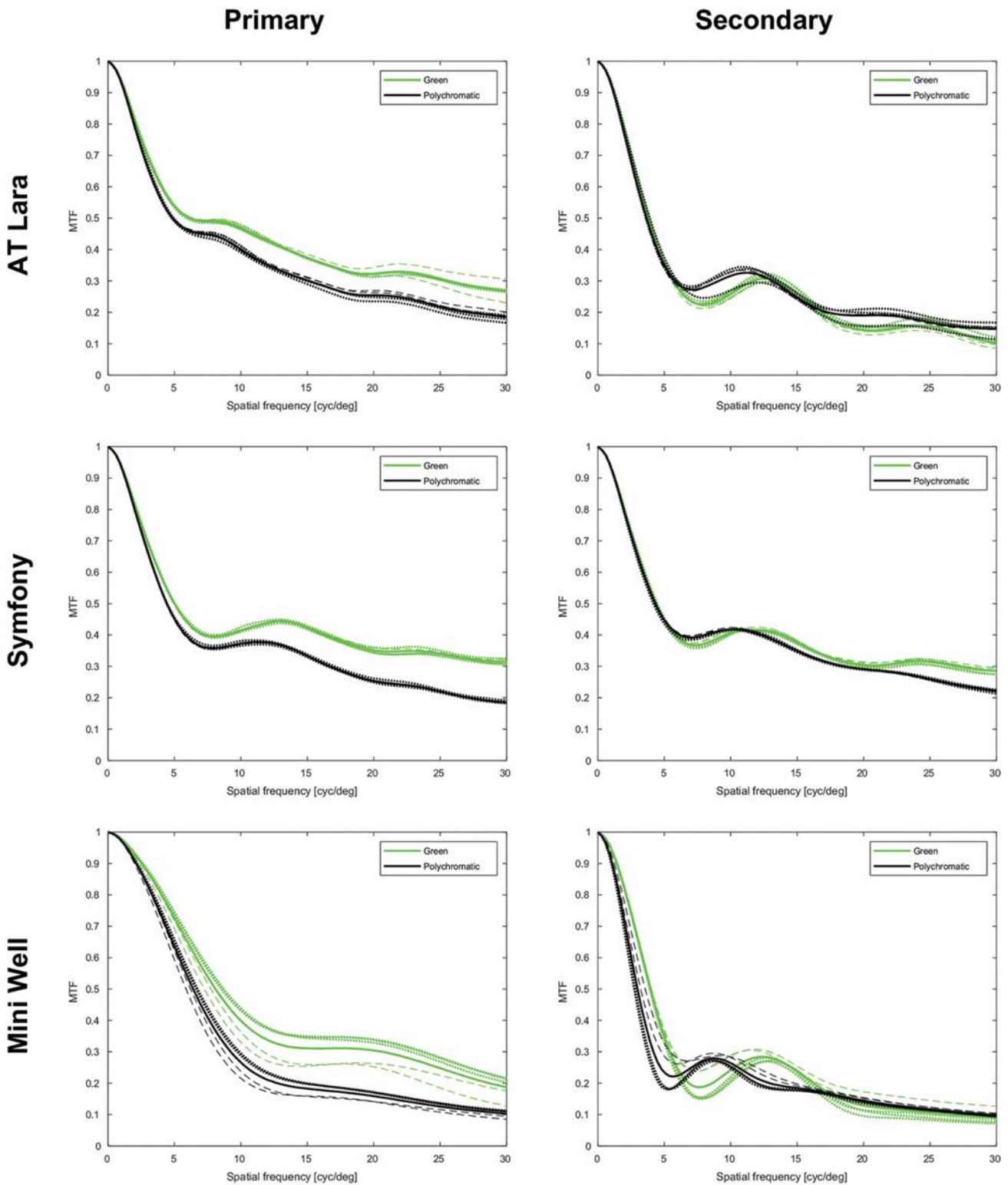


Figure 1. The MTF of the studied IOLs measured in polychromatic (*black lines*) and monochromatic (546 nm; *green lines*) light. The MTF was determined at the best primary (left panels) and secondary (right panels) focus of the IOLs. Five samples of each model were measured, with 3 lenses having +21 D (*dashed lines*) and 2 having +20 D (*dotted lines*). The solid lines refer to the mean MTF curve derived from 5 samples (IOL = intraocular lens; MTF = modulation transfer function).

6 cyc/deg. At the best secondary focus, the Symphony outperformed the two other EDOF models, of which the AT Lara appeared to provide minimally better optical quality

than the Mini Well. Monofocal lens performance at a defocus of 2 D (the average secondary positions of the 3 EDOF IOLs) was inferior to that of the other designs.

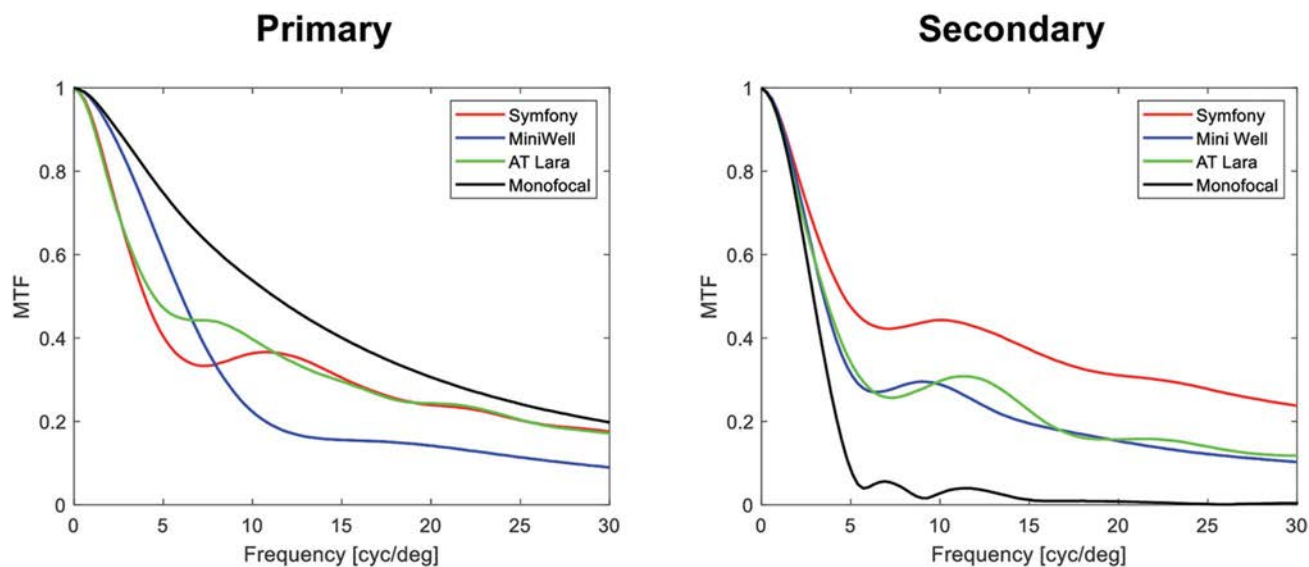


Figure 2. The polychromatic MTF of the AT Lara (green lines), the Symphony (red lines), and the Mini Well (blue lines) IOL measured at the best primary (left panel) and secondary (right panel) focus. For comparison, MTFs of a monofocal IOL (black lines) assessed at zero (left panel) and 2 D (right panel) defocus are shown (IOL, intraocular lens; MTF, modulation transfer function).

Figure 3 presents the VSR over a -0.50 D to 2.50 D defocus range for the 3.0 mm aperture. All 3 EDOF models yielded a lower VSR value than that of the monofocal lens up to approximately 1.0 D. Above this range, the optical quality of the EDOF IOLs provided enhanced optical performance compared with the monofocal one. The Symphony and AT Lara VSR demonstrated 2 clear peaks at 1.75 D and 2 D, respectively, and at zero defocus, with the valley occurring at about 1 D. Although the Mini Well produced lower primary and secondary peaks than the diffractive lenses, its optical performance was nearly

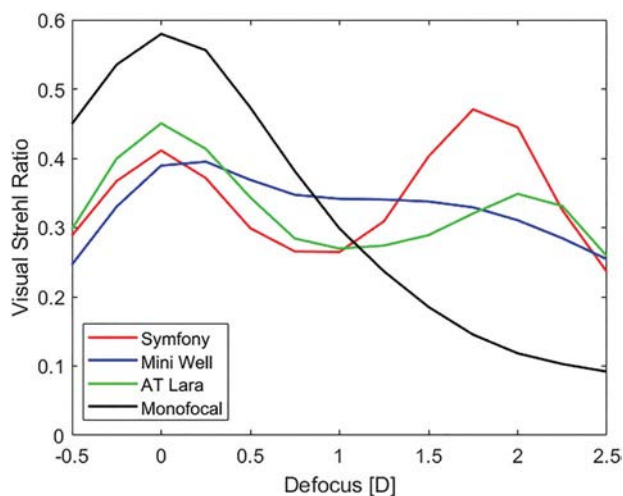


Figure 3. Defocus tolerance of the AT Lara (green line), the Symphony (red line), the Mini Well (blue line), and a monofocal (black line) IOL. The polychromatic modulation transfer function (MTF) was measured for a 3.0 mm aperture with a defocus resolution of 0.25 D starting from the best far focus. The visual Strehl ratio was calculated over 30 cyc/deg (IOL, intraocular lens).

constant for an extended range with a small improvement at far point.

The visual acuity chart simulations that are presented in Figure 4 confirm the MTF results. The monofocal lens provided an excellent image at zero and satisfactory at ± 0.50 D, but it sharply decreased beyond this level. Of the 3 EDOF lenses, at no defocus, the VA prediction of the AT Lara was noticeably better than the Symphony (less intense optotype shadowing) and particularly better than the Mini Well, which appeared blurred. At 1 D, however, the refractive EDOF lens demonstrated a higher image quality than the diffractive ones, which was also better than the AT Lara but worse than the Symphony at 1.5 D. The two diffractive designs proved to be better than the Mini Well at 2 D, of which the Symphony was less affected by shadowing. The simulated resolving power decreases for all the EDOF lenses at 2.5 D, particularly for the Symphony.

The through-focus MTF at 15 cyc/deg was measured for 2.0 mm, 3.0 mm, and 4.0 mm apertures to test how the optical performance changes with the pupil size (Figure 5). The Symphony exhibited only a small effect when changing the aperture, as the MTF values remained high for all conditions. However, the lens appeared to provide slightly better optical quality at the secondary than primary focus for 2.0 mm and 3.0 mm, which was reversed for the 4.0 mm pupil. The Mini Well demonstrated a clear pupil dependency, as the lens was intermediate dominant at 2.0 mm. The refractive lens produced the EDOF effect for the 3.0 mm aperture. However, it became more far dominant at 4.0 mm with an increased primary and decreased secondary peak. Similar to the Symphony, the AT Lara also provided a slightly higher MTF peak at intermediate than zero defocus, but this relationship was reversed for 3.0 mm. Although for the 4.0 mm aperture, the optical quality of the

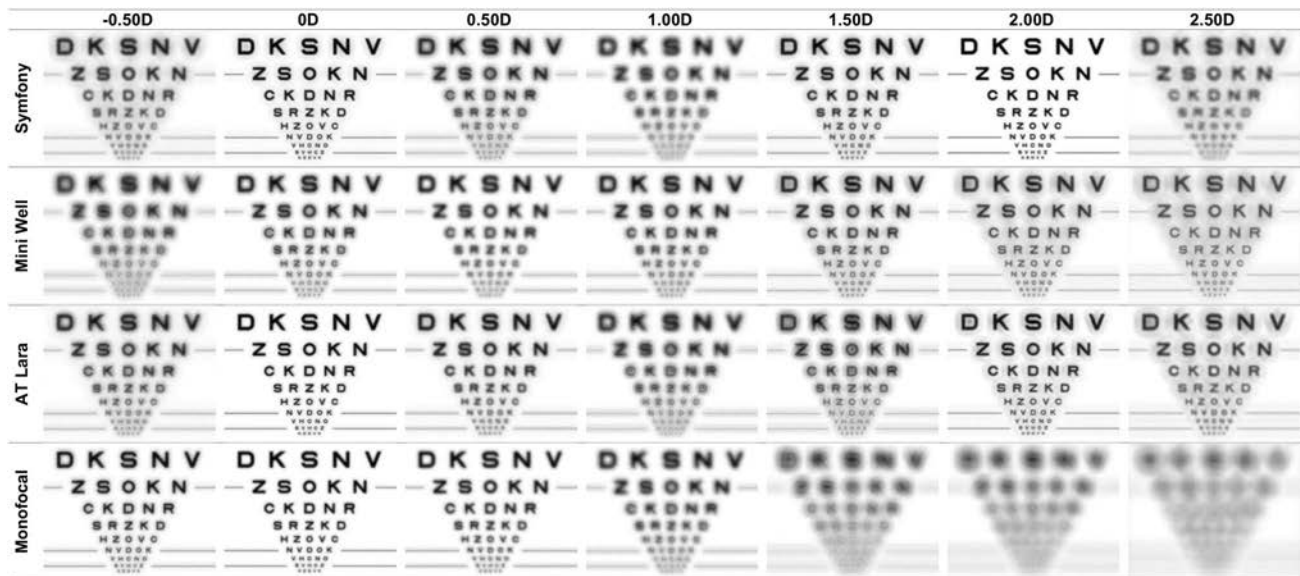


Figure 4. Visual acuity chart simulation at a range of defocus. The chart image, which represents the optotype range from 0.5 to -0.3 logarithm of the minimum angle of resolution, was convoluted with a polychromatic point spread function of the Symphony, Mini Well, AT Lara, and monofocal (SA60AT) lenses.

lens was lower, the MTF value decreased proportionally at the far and intermediate point.

The simulation of IOL tilt up to 5 degrees did not have a major impact on IOL performance; the MTF at 15 cyc/deg decreased by 0.07 for the AT Lara, 0.04 for the Symphony, 0.02 for the monofocal lens, and did not change for the Mini Well. Decentration by 0.75 mm also had a marginal effect on the performance of the AT Lara (Δ MTF = 0.02), the monofocal IOL (Δ MTF = 0.01), and the Mini Well (Δ MTF = 0.01), but the effect was larger for the Symphony (Δ MTF = 0.09).

DISCUSSION

We found that the polychromatic light does indeed affect the optical quality of the IOLs. The EDOF IOLs proved to extend the range of vision compared with the monofocal lens; however, apparent differences between the 3 EDOF models exist.

The comparison between the monochromatic and polychromatic MTF revealed a loss of optical quality in the latter condition. This chromatic effect results from the IOL's internal dispersion of light and the chromatic aberration of the model eye, which is about 1.0 D between 480 nm and 644 nm. The results indicate that the far MTF of the AT Lara and the Symphony decreased less than that of the Mini Well. The material properties may be one factor, as the Mini Well has a lower Abbe number, thus higher dispersion, than that of the diffractive IOLs. Another explanation for better polychromatic image quality of the diffractive IOLs might be that the two models feature the chromatic aberration correction. At the secondary focus, the chromatic effects were lower in all the EDOF lenses. For the AT Lara, we found a small MTF improvement in the polychromatic light. This can be understood as the ability of the lens to correct the chromatic shift and to bring more wavelengths (in contrast

to only one in the monochromatic condition) into focus, which has a constructive effect on the optical quality. The Symphony's chromatic effects were lower at intermediate than far point, but the lens demonstrated a minimal deterioration in the image quality in this in vitro setting. In both diffractive IOLs, the chromatic aberration correction was more effective at the secondary than the primary focus. This can be explained by the diffraction grating design of the EDOF IOLs that use the first and second diffractive orders to diverge the light to far and intermediate point, respectively.⁶ In this design, the chromatic aberration correction is expected to double at the second order (intermediate) as compared to the first order (far).⁶ Interestingly, the Mini Well showed a comparable MTF loss to the Symphony despite its purely refractive design. This may result from an extended intermediate focus of the Mini Well, which did not show a distinct secondary peak so that it may have compensated the chromatic shift at this position.

Although all the studied IOLs share the EDOF principle, a number of key differences in their optical behavior emerge from the study results. At the far focus, the AT Lara had a slightly higher mean MTF than the Symphony with both providing better optical performance than the Mini Well. At the best intermediate focus position, which differed between the IOLs, the Symphony's MTF level was higher than that of the other EDOF lenses and that was followed by the AT Lara and the Mini Well. These differences in the objective optical quality can also be seen in the simulation of the VA chart. Although the measured differences are not likely to affect patients' VA, they may have an impact on the overall quality of vision by creating a ghost (out-of-focus) image of different size and intensity that looks like letter shadowing²⁰ as seen in Figure 4. Although the readability of the 0.0 logarithm of the minimum angle of resolution line is preserved for all the EDOF IOL at

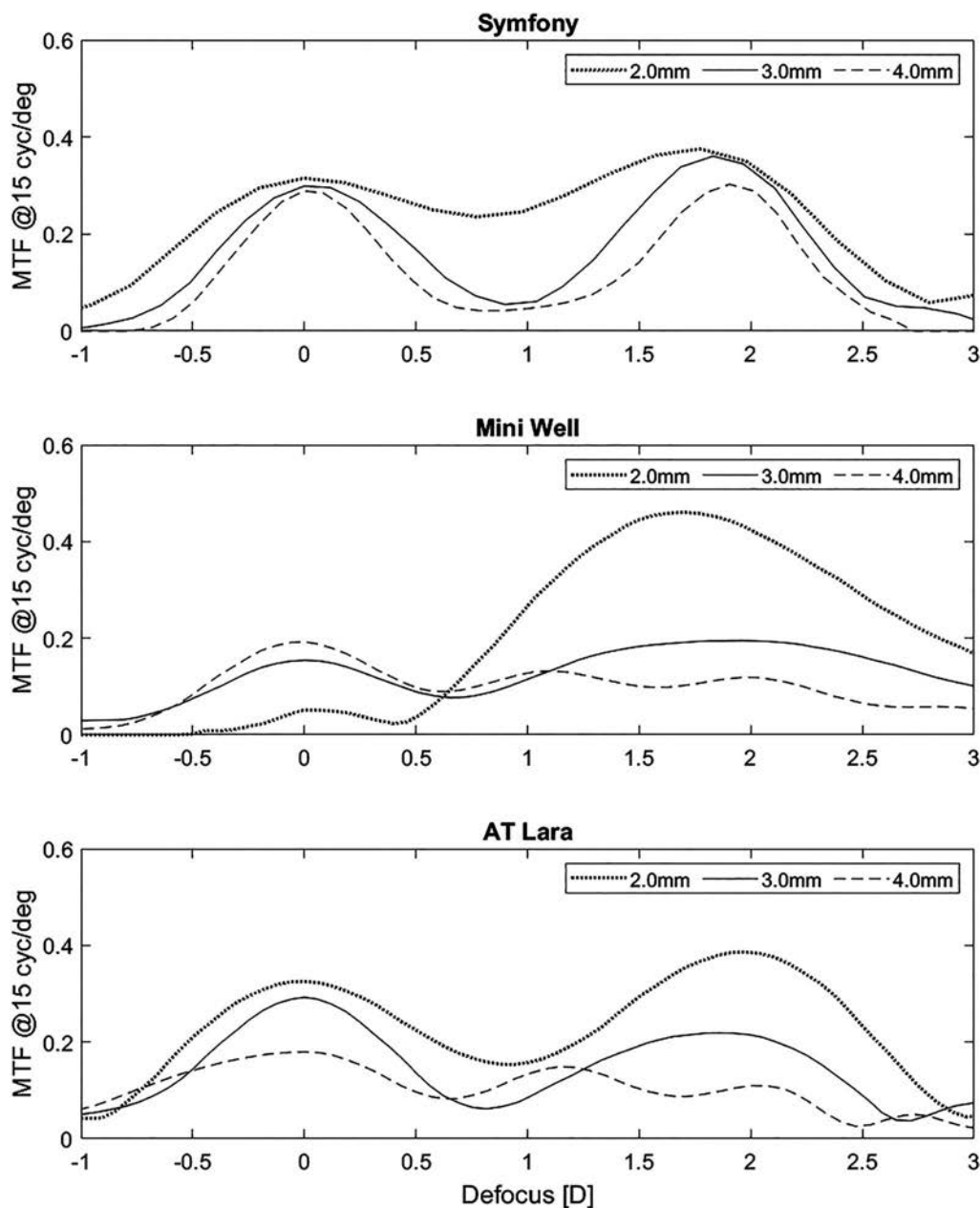


Figure 5. The through-focus modulation transfer function measured at a single frequency of 15 cyc/deg in polychromatic light. The pupil size impact on the image quality was assessed at an aperture of 2.0 mm (dotted lines), 3.0 mm (solid lines), and 4.0 mm (dashed lines).

2 D, the Symphony produces less such shadowing effects than the AT Lara and the Mini Well, which may explain the higher VSR in Figure 3. In addition, the defocus MTF and the VA simulation indicate that the image quality of the diffractive IOLs changes considerably with defocus with two optical points matching the position of their main foci. By contrast, the Mini Well's optical quality is less affected by the defocus change, but none of the optotype images is as good as that of the AT Lara at no defocus or the Symphony at 2 D. Thus, one may conclude that enlarging the depth-of-focus comprises a tradeoff between, on the one hand how far the visual range can be extended and on the other, the optical quality achieved at each point.

The effect of pupil size varied for the studied EDOF IOLs. The diffractive lenses demonstrated minimally better

intermediate than far performance at small apertures; however, it was reversed when the aperture increased. In contrast to the Symphony, the AT Lara's MTF (at 15 cyc/deg) was low through the 4.0 mm pupil. This may result from the difference in the spherical aberration corrections of both IOLs. The Symphony produces $0.27 \mu\text{m}$ of negative spherical aberration to counteract a positive spherical aberration of $0.28 \mu\text{m}$ found in the human cornea.¹⁴ This is similar to the level of spherical aberration in our in vitro model. Given a good match between the spherical aberration of the model cornea and the Symphony, its MTF remains high despite increased pupil size. If a model cornea free of spherical aberration had been used, the Symphony's MTF results at a larger pupil would have deteriorated significantly, as shown in a study by Domínguez-Vicent et al.⁴ This was the

case with the AT Lara, which does not correct corneal spherical aberration, and thus, the MTF level for the 4.0 mm pupil was greatly affected. Figure 5 indicates strong pupil dependency of the Mini Well. At 2.0 mm, the refractive lens demonstrated one extended through-focus MTF peak centered at the intermediate distance (about 1.75 D). For such a small aperture, the first optical zone is dominant. The central area contains positive spherical aberration, which alone would make the eye hyperopic.²¹ For that reason, the first zone has a focus offset that adds refractive power to counter this undesired hyperopic shift.²¹ It appears that for the 2.0 mm pupil, induced spherical aberration and the focus offset are not matched, making the eye slightly myopic. This may result in improving intermediate and the expense of distance vision in patients with small pupils. At 3.0 mm, the IOL MTF increased at far but decreased at intermediate point as the two first zones take part in the image creation providing balanced optical performance for the far–intermediate range. A large pupil (4.0 mm) improved the far but worsened intermediate focus, which could have been expected given the outer monofocal zone of the Mini Well. Similarly to the AT Lara, spherical aberration effects may also affect the performance of the Mini Well as a consequence of the aberration neutral design of the IOL's peripheral zone and the positive spherical aberration of the corneal lens. Domínguez-Vicent et al.⁴ measured the Mini Well using an aberration-free model cornea, which showed MTF (at 15 cyc/deg) = 0.55 with no defocus and a 4.5 mm pupil. In this study, we found a discrete MTF value of 0.19 at 4.0 mm, which illustrates the extent of spherical aberration impact on the image quality. Although Wang et al.¹⁴ have reported the average level of corneal spherical aberration in the normal population as 0.28 μm , that study has also demonstrated a large variability of this parameter ranging from 0.055 to 0.544 μm .¹⁴ Thus, IOL manufacturers and clinicians may expect that aspheric lenses will not function optimally in all patients with larger pupils.

Clinical studies on IOL tilt and decentration have shown highly variable results. The mean decentration value ranges from 0.19 to 0.7 mm, but values greater than 1.0 mm have also been reported.^{22–24} A mean value of 7.8 degrees tilt was shown in one report,²² but in others, it was 3.1 degrees and 2.9 degrees.^{23,24} In this study, we demonstrated that limited tilt does not have an impact on the MTF of all but one IOL, which in principle is in line with results found in the literature.^{5,25} Although the AT Lara was slightly affected by tilt, it proved more robust against decentration. Only a small effect of decentration on MTF was found in the Mini Well IOL, which was comparable to that of the monofocal lens. The MTF (at 15 cyc/deg) loss was 0.01, which is lower than a value reported by Bellucci and Curatolo,⁵ who demonstrated a 0.06 drop under 0.5 mm of decentration in the green light condition. The Symphony's image quality appears to be most sensitive to decentration, which could have been expected, given its high level of spherical aberration correction as shown by Fujikado and Saika.²⁶ In the study by

Yoo et al.⁷ a 15 cyc/deg MTF of the Symphony was reduced by approximately 0.1 at 0.75 mm of decentration, which is close to the 0.09 found in this study.

The repeated measurements of each lens demonstrated a nearly perfect alignment of the MTFs (Figure 1) of different (+20 D and +21 D) samples in the Symphony and the AT Lara groups. This good repeatability was observed at the primary and secondary focus for both lighting conditions (Figure 1). By contrast, the Mini Well showed slight misalignment of the MTF curves measured from the samples of different power. The power difference between the two sets of samples seems to be negligible, as the theoretical cutoff frequency of both differs only by about 1 cyc/deg. Thus, we cannot find a possible explanation for this finding, which should be addressed by the manufacturer.

In conclusion, chromatic and spherical aberration have an essential impact on the in vitro image quality of IOLs. The correction of both aberrations improves IOL MTF, which in turn may improve subjective visual experience.²⁷ The studied EDOF IOLs demonstrated clear potential for enlarging the visual range of patients with pseudophakia. The diffractive IOLs showed a comparable optical behavior, with the main differences being the intermediate optical performance and the management of spherical aberration. The Mini Well's tolerance to defocus proved more robust but yielded lower image quality. In contrast to the diffractive IOLs, the refractive zonal design of the Mini Well exhibits a high level of pupil dependency, which needs to be taken into account in preoperative decision making.

WHAT WAS KNOWN

- Extended depth-of-focus (EDOF) intraocular lens (IOL) models create a continuous range of vision for patients with pseudophakia, but the provided visual quality may differ, given the variety of designs and working principles.

WHAT THIS PAPER ADDS

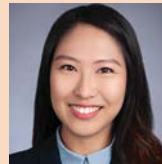
- Although all studied EDOF IOLs proved more tolerant to defocus than a standard monofocal IOL, the key differences lie in their management of chromatic and spherical aberration effects, pupil dependency, and the optical quality at discrete visual points, which may be taken into account to optimize postoperative visual outcomes.

REFERENCES

- de Vries NE, Nuijts RM. Multifocal intraocular lenses in cataract surgery: literature review of benefits and side effects. *J Cataract Refract Surg.* 2013;39:268–278
- Alfonso JF, Fernández-Vega L, Puchades C, Montés-Micó R. Intermediate visual function with different multifocal intraocular lens models. *J Cataract Refract Surg.* 2010;36:733–739
- Jonker SM, Bauer NJ, Makhotkina NY, Berendschot TT, van den Biggelaar FJ, Nuijts RM. Comparison of a trifocal intraocular lens with a+ 3.0 D bifocal IOL: results of a prospective randomized clinical trial. *J Cataract Refract Surg.* 2015;41:1631–1640
- Domínguez-Vicent A, Esteve-Taboada JJ, Del Águila-Carrasco AJ, Ferrer-Blasco T, Montés-Micó R. In vitro optical quality comparison between the Mini WELL Ready progressive multifocal and the TECNIS Symphony. *Graefes Archive Clin Exp Ophthalmol.* 2016;254:1387–1397

5. Bellucci R, Curatolo MC. A new extended depth of focus intraocular lens based on spherical aberration. *J Refract Surg.* 2017;33:389–394
6. Millán MS, Vega F. Extended depth of focus intraocular lens: chromatic performance. *Biomed Opt Exp.* 2017;8:4294–4309
7. Yoo YS, Whang WJ, Byun YS, Piao JJ, Kim DY, Joo CK, Yoon G. Through-focus optical bench performance of extended depth-of-focus and bifocal intraocular lenses compared to a monofocal lens. *J Refract Surg.* 2018;34:236–243
8. Cochener B, Group CS. Clinical outcomes of a new extended range of vision intraocular lens: International Multicenter Concerto Study. *J Cataract Refract Surg.* 2016;42:1268–1275
9. Attia MS, Auffarth GU, Kretz FT, Tandogan T, Rabsilber TM, Holzer MP, Khoramnia R. Clinical evaluation of an extended depth of focus intraocular lens with the Salzburg reading desk. *J Refract Surg.* 2017;33:664–669
10. Savini G, Schiano-Lomoriello D, Balducci N, Barboni P. Visual performance of a new extended depth-of-focus intraocular lens compared to a distance-dominant diffractive multifocal intraocular lens. *J Refract Surg.* 2018;34:228–235
11. Gatinel D, Loicq J. Clinically relevant optical properties of bifocal, trifocal, and extended depth of focus intraocular lenses. *J Refract Surg.* 2016;32:273–280
12. Weeber HA, Canovas C, Alarcon A, Piers PA. Laboratory-measured MTF of IOLs and clinical performance. *J Refract Surg.* 2016;32:211–212
13. Piers PA, Chang DH, Alarcón A, Canovas C. Clinically relevant interpretations of optical bench measurement of intraocular lenses. *J Refract Surg.* 2017;33:64
14. Wang L, Dai E, Koch DD, Nathoo A. Optical aberrations of the human anterior cornea. *J Cataract Refract Surg.* 2003;29:1514–1521
15. Łabuz G, Papadatou E, Khoramnia R, Auffarth GU. Longitudinal chromatic aberration and polychromatic image quality metrics of intraocular lenses. *J Refract Surg.* 2018;34:832–838
16. Vinas M, Dorronsoro C, Garzón N, Poyales F, Marcos S. In vivo subjective and objective longitudinal chromatic aberration after bilateral implantation of the same design of hydrophobic and hydrophilic intraocular lenses. *J Cataract Refract Surg.* 2015;41:2115–2124
17. Koch DD, Samuelson SW, Haft EA, Merin LM. Pupillary and responsiveness: implications for selection of a bifocal intraocular lens. *Ophthalmology* 1991; 98:1030–1035
18. Thibos LN, Hong X, Bradley A, Applegate RA. Accuracy and precision of objective refraction from wavefront aberrations. *J Vis.* 2004;4:9
19. Campbell F, Green D. Optical and retinal factors affecting visual resolution. *J Physiol.* 1965;181:576–593
20. Kollbaum PS, Dietmeier BM, Jansen ME, Rickert ME. Quantification of ghosting produced with presbyopic contact lens correction. *Eye Contact Lens* 2012;38:252
21. Liang J. Methods and Devices for Refractive Treatments of Presbyopia. US patent 8,529,559. 2013.
22. Phillips P, Rosskothén HD, Pérez-Emmanueli J, Koester CJ. Measurement of intraocular lens decentration and tilt in vivo. *J Cataract Refract Surg.* 1988;14:129–135.
23. Lee DH, Shin SC, Joo CK. Effect of a capsular tension ring on intraocular lens decentration and tilting after cataract surgery. *J Cataract Refract Surg.* 2002;28:843–846
24. Baumeister M, Bühren J, Kohnen T. Tilt and decentration of spherical and aspheric intraocular lenses: effect on higher-order aberrations. *J Cataract Refract Surg.* 2009;35:1006–1012
25. Montés-Micó R, López-Gil N, Pérez-Vives C, Bonaque S, Ferrer-Blasco T. In vitro optical performance of nonrotational symmetric and refractive-diffractive aspheric multifocal intraocular lenses: impact of tilt and decentration. *J Cataract Refract Surg.* 2012;38:1657–1663
26. Fujikado T, Saika M. Evaluation of actual retinal images produced by misaligned aspheric intraocular lenses in a model eye. *Clin Ophthalmol* 2014;8:2415.
27. Artal P, Manzanera S, Piers P, Weeber H. Visual effect of the combined correction of spherical and longitudinal chromatic aberrations. *Opt Ex* 2010; 18:1637-1648.

Disclosures: G. U. Auffarth and R. Khoramnia report grants from the Klaus Tschira Foundation, during the conduct of the study; grants, lecture fees, and nonfinancial support from Alcon; grants, lecture fees, and nonfinancial support from Oculentis; grants from Carl Zeiss Meditec; grants, lecture fees, and nonfinancial support from Hoya; grants and nonfinancial support from Kowa; grants and nonfinancial support from Ophtec; grants from Physiol; grants from Powervision; grants, lecture fees, and nonfinancial support from Rayner; grants, lecture fees, and nonfinancial support from SIFI; grants, lecture fees, and nonfinancial support from Johnson & Johnson; grants from AcuFocus; and lecture fees and nonfinancial support from Polytech. None of the other authors has a financial or proprietary interest in any material or method mentioned.



First author:

Yumi Lee, MD

Department of Ophthalmology, The David J Apple Center for Vision Research, University Hospital Heidelberg, Heidelberg, Germany.

Performance of a temperature-controlled shape-memory pupil expander for cataract surgery

Royston K.Y. Tan, PhD, Shamira A. Perera, FRCOphth, Tin A. Tun, MD, Craig Boote, PhD, Michaël J.A. Girard, PhD

Purpose: To perform ex vivo and in vivo validation of a manufactured, optimized shape-memory pupil expander and compare its performance to that of existing devices.

Setting: National University of Singapore and SingHealth Academy.

Design: Prospective randomized blinded assessment.

Methods: Shape-memory expanders were manufactured by overmolding and were inserted into ex vivo porcine eyes and in vivo monkey eyes for validation. The shape-memory expander was compared to the Malyugin ring, OASIS iris expander, and iris hook. After insertion and removal of the devices, the eyes were fixed, and the iris images were analyzed.

Results: The shape-memory expander was successful in pupil expansion for both in vivo and ex vivo experiments. Subsequent

ex vivo device comparison revealed iris pigment epithelial loss in 36.4% of eyes for the iris hooks, 30.8% for the iris expander, and 20.0% for the Malyugin ring. Sphincter tears were observed in 27.3% of eyes for the iris hooks, 0% for the Oasis expander, and 10.0% for the Malyugin ring. No observable tissue irregularities were observed in the shape-memory expander.

Conclusion: The shape-memory expander was optimized to minimize stress exerted onto the iris tissue. The in vivo and ex vivo experimental validation demonstrate efficacy in engineering design and further highlight the translational potential of smart materials in implant development to improve patient healthcare.

J Cataract Refract Surg 2020; 46:116–124 Copyright © 2019 Published by Wolters Kluwer on behalf of ASCRS and ESCRS

Cataract surgery is the most performed surgery worldwide, with this disease affecting more than 20 million people.¹ This number is estimated to increase to over 30 million by 2020^{2,3} driven by an increase in the global elderly population. The surgery is performed by replacing the cloudy crystalline lens with an artificial intraocular lens.⁴ To do so requires a sufficiently large pupil for unobstructed surgical maneuvers. Therefore, pharmacological drugs such as phenylephrine, tropicamide, and cyclopentolate are used to relax the sphincter muscle and constrict the dilator muscle before surgery.^{5,6} Despite this, small pupils may persist due to reduced muscle accommodation from aging or as a result of ingestion of drugs (eg, tamsulosin), long-term miotic drug usage (eg, pilocarpine), and pseudoexfoliation.^{7–10}

To remedy persisting small pupils, surgeons may deploy techniques such as mechanical stretching and sphincter cuts to stretch the iris.^{10–12} Pupil expander devices may also be

deployed to provide external mechanical support. These devices include iris hooks (MicroSurgical Technology), Malyugin ring (Malyugin Ring 2.0' MicroSurgical Technology), Bhattacharjee ring¹⁶ (B-HEX pupil expander, Med Invent Devices), OASIS iris expander (6.25 mm and 7.00 mm, Oasis Medical Inc), Perfect Pupil (Milvella Limited), APX dilator (Assia Pupil Expander, APX Ophthalmology Ltd.), and i-Ring (Beaver-Visitec International, Inc.).^{13–21} They function by engaging the iris margin and providing support to keep the pupil enlarged during cataract surgery.

An issue with many pupil expanders lies in the method of iris margin engagement, where focal points of iris contact induce high stress and potentially increase the risk of iris damage.²² Iris hooks and the APX dilator engage the iris at 4 distinct locations to form a quadrilateral pupil, forming a nonphysiological opening with high localized stresses. The OASIS iris expander, B-HEX pupil expander, and Malyugin

Submitted: June 19, 2019 | Final revision submitted: July 28, 2019 | Accepted: August 23, 2019

From the Department of Biomedical Engineering, Ophthalmic Engineering & Innovation Laboratory (Tan, Tun, Boote, Girard), National University of Singapore, Singapore Eye Research Institute, Singapore National Eye Centre (Perera, Tun, Girard), Duke-NUS Medical School (Perera), Singapore; and Structural Biophysics Research Group, School of Optometry & Vision Sciences (Boote), Cardiff University, Wales, United Kingdom.

Supported by funding from the SNEC-HREF Device R&D fund (R1412/98/2016).

Corresponding Author: Michaël J.A. Girard, PhD, Department of Biomedical Engineering, Ophthalmic Engineering & Innovation Laboratory, National University of Singapore, Engineering Block 4, #04-08, 4 Engineering Drive 3, Singapore 117583. Email: mgirard@nus.edu.sg.

ring also form nonphysiological openings with 6 or 8 contact points that reduce these point forces. The ideal expansion requires full circumferential iris margin engagement, which is only currently adopted by the i-Ring.^{20,23} However, the i-Ring, like the OASIS iris expander, B-HEX pupil expander, and Malyugin ring, requires additional surgical maneuvers for positioning.^{12,16} By stretching the spring-like devices across the anterior chamber at multiple engagement points, large tissue stress beyond the physiological range are generated that could potentially distort and tear the iris tissue.^{20,24} In addition, the need for current mechanical devices to be dragged across the pupil for iris engagement in cases of a small pupil may induce trauma²⁵ and iridodialysis.^{26,27} We previously conducted a theoretical finite element modeling study showing reduced stress on the iris tissue predicted by a uniform circular expansion design.²⁸ In the current study, we applied this design experimentally and developed a novel pupil expander to improve on the cumulative shortcomings of existing devices.

We propose the use of shape-memory technology to enhance the cataract procedure.²⁹ Shape-memory material is able to configure and “memorize” a specific shape at a specific transition temperature. At a lower temperature, this material is flexible and can be compacted. A heat stimulus, such as that from the eye provides the energy for the shape-memory polymer to deform back to its configured shape upon reaching the transition temperature in a controlled manner. Implementing this material in a pupil expander allows for insertion into smaller incisions while retaining its ability to mechanically induce a large pupil. Moreover, expansion of the pupil occurs gradually, slowly stretching the pupil to avoid sudden tissue enlargement.

In this article, we aim to (1) describe the design and construction of an optimized shape-memory material to expand the pupil, (2) validate its performance in ex vivo porcine and in vivo monkey experiments, and (3) compare our pupil expander with commercially available devices using ex vivo porcine eyes.

METHODS

Experiments were conducted at the SingHealth Experimental Medicine Centre at the Singapore Eye Research Institute (SEMC). All experiments were performed in accordance with the Association for Research in Vision and Ophthalmology Statement for the Use of Animals in Ophthalmic and Vision Research and were approved by the Institutional Animal Care and Use Committee of the SEMC located in the SingHealth General Hospital. The SEMC has accreditation by the Association for Assessment and Accreditation of Laboratory Animal Care International.

Molding and Manufacturing the Shape-Memory Pupil Expander

Shape-memory material was purchased from SMP Technologies Inc. (MP Resin and Hardener). To determine the maximum transition temperature allowed, we measured the in vivo anterior chamber temperature in a non human primate (NHP) under surgical conditions using a small custom-made temperature sensor. The measured temperature reading was 34.0°C after filling the anterior chamber with viscosurgical solution.

Our custom shape-memory material was manufactured with a glass transition temperature (T_g) of 30.0°C. Below T_g , the polymer can be folded and physically manipulated into compact shapes. Heating the polymer above T_g will supply the required energy for it to return to its programmed shape. The target shape was set by polymerizing the shape-memory material in a custom mold with the desired shape and dimensions of our pupil expander.

Three-dimensional (3D) printing was used to manufacture molds using MakerBot 2.0 (Stratasys) with acrylonitrile butadiene styrene as the printing material. The mold was 3D printed with a resolution of 50 μm for the center insert and 100 μm for the top and bottom molds. Dimensions of the mold and pupil expander were optimized to minimize the thickness of the device (300 μm) (Figure 1, A, B, and D), while ensuring full engagement at the iris margin and sufficient force for mechanical pupil dilation.

The shape-memory polymer was prepared by potting. The resin and hardener were first placed under vacuum (<200 mTorr) for 1 hour to evaporate the water within the polymers. The resins were then mixed and stirred for approximately 1 minute and placed under vacuum again for 1 minute to remove the effervescence. The final mixture was poured into the mold and left to set overnight. After removal from the mold, the device was trimmed using Vannas scissors (Ref:1-111, Duckworth & Kent Ltd.) to remove the excess material before testing (Figure 1, C).

Ex Vivo Validation in Enucleated Porcine Eyes

Eleven enucleated porcine eyes were purchased from Primary Industries Ltd. (Singapore Food Industries Pte Ltd.). Fresh porcine eyes were transported to the laboratories where experiments were conducted immediately and completed within 6 hours postmortem.

To ensure that the tissues maintained their properties similar to those in vivo, the enucleated eyes were kept in a modified Krebs-Henseleit buffer solution (Product Number K3753; Merck KGaA) similar to the protocol performed by Whitcomb et al.³⁰ The buffer solution was composed of the following: 10.0 mM D-glucose, 1.2 mM MgSO_4 , 1.2 mM KH_2PO_4 , 4.7 mM KCl, 118 mM NaCl, and added with 25 mM NaHCO_3 and 1.25 mM CaCl_2 . The solution was oxygenated with 95% O_2 and 5% CO_2 to maintain a pH of 7.5. This kept the sphincter and dilator muscle tissues active to provide pupil constriction. Thus, we were able to induce pharmacological constriction for small pupil expander insertion to provide validation of our device's function.

Fresh eyes were placed in a warm and moist medium above a rubber heating pad (12 V/10 W Silicone Rubber Flexible Heating Pad, O.E.M Heaters). A temperature sensor was used to maintain a steady temperature of 34.0°C ($\pm 1^\circ\text{C}$) (TE333 Temperature Controller, XCSOURCE) as was measured in vivo. A power transducer (72-10505 DC Bench Power Supply, TENMA Corporation) was used to power the heating pad (10 W) and temperature sensor (9 V, 0.1 A). At the Singapore National Eye Centre, an ophthalmic microscope (OPMI 1 FR Pro, Zeiss) was used to enhance surgical vision, and a DSLR camera (Canon EOS 800D) was used to record the experiments. Pilocarpine was administered to obtain a small pupil (2 drops of 2% Isopto Carpine, Alcon Laboratories, Inc.). The shape-memory pupil expander prototypes were manufactured to provide optimal specifications for the porcine eyes: compact width of under 2.0 mm, expanded circular diameter of 7.0 mm, and 300 μm overall thickness.

Insertion of the shape-memory pupil expander was performed in a similar manner to existing techniques and consisting of several important steps^{9,31} (Figure 2). First, a triangle blade (Ref: 72-2661, Surgical Specialties México) was used to make a 2.65 mm incision at a 30 to 40° angle near the cornea periphery. Viscosurgical solution is usually injected to maintain the shape of the anterior chamber, but was not used in these ex vivo porcine eyes to prevent dilation from its use.

Second, an injector was used to deliver the compacted circular shape-memory pupil expander into the anterior chamber (Figure 2, A). Because we did not have a custom-made injector, we

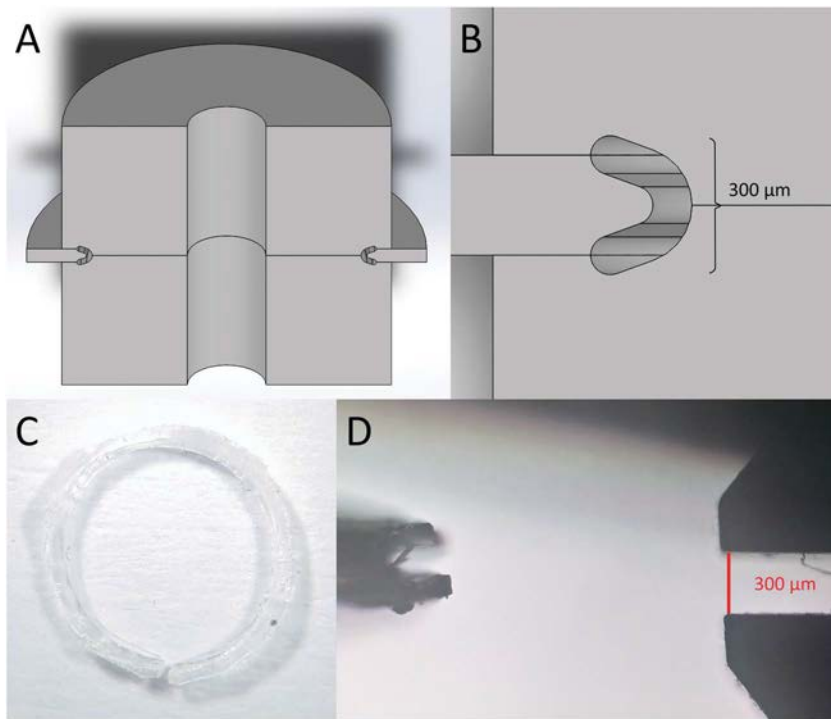


Figure 1. A: Computer-aided design cross-section drawing of the mold design. B: The device is designed to be 300 µm, with the thickness of the device approximately 80 µm. C: Processing of the shape-memory pupil expander after allowing it to set overnight. The polymer is separated from the mold and initially contains excess material. It is manually cut and trimmed down using Vannas scissors until a satisfactory shape is obtained. D: The final thickness of the device is measured to be approximately 300 µm.

used the Malyugin ring injector (Ref: MAL-1002-1, MicroSurgical Technology), although similar injectors from devices such as the OASIS iris expander would perform the same function. Retraction of the circular device flattened it to a hyperellipse shape to fit the injector lumen. The 34.0°C ambient physiological temperature within the anterior chamber provided energy for the flattened device to deform back to a circular shape (Figure 2, B).

Third, a Sinsky hook (Ref: 0105109, John Weiss & Son Ltd.) was used to maneuver and adjust the device into position (Figure 2, C). To engage the iris margin, the Sinsky hook was used

to pull and deform the pupil expander and to push the polymer to enlarge the pupil after iris engagement. This action was performed 3 to 5 times, between 20 to 30 seconds depending on the individual condition of each pupil. Because the device deforms only from user manipulation, the iris tissue would not be overstretched from engagement (Figure 2, D). The result was a 7.0 mm circular expanded pupil that was protected at the iris margin from any external manipulations (Figure 2, E).

Last, the Sinsky hook was used to disengage the pupil expander from the iris margin at the incision site. This was performed by

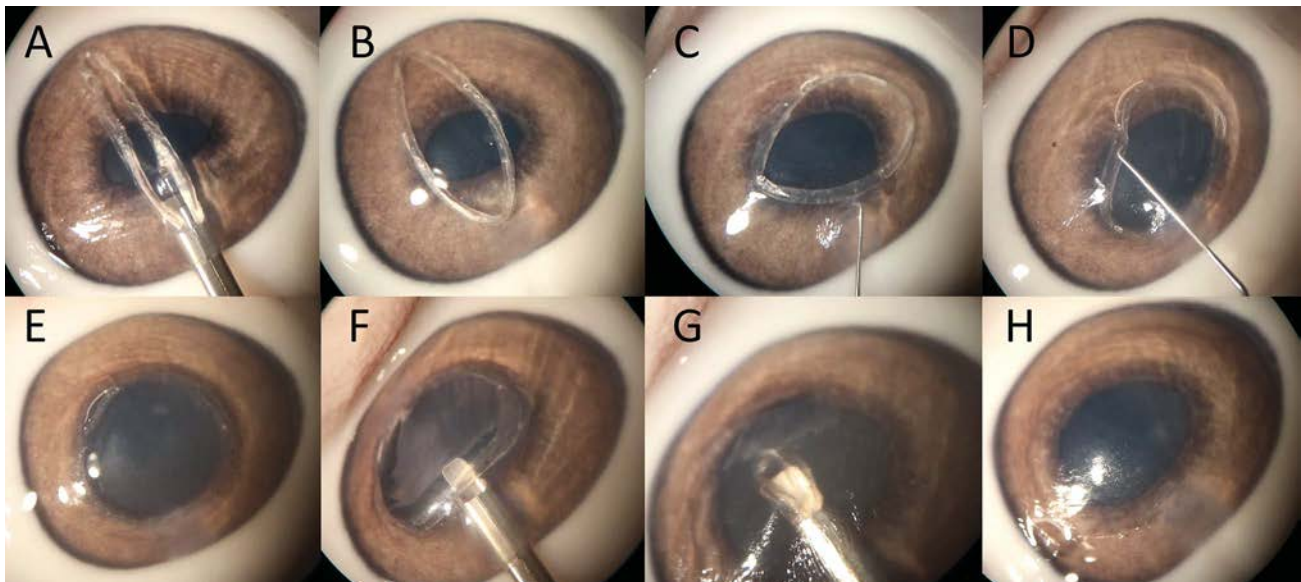


Figure 2. Ex vivo porcine eye validation of the shape-memory pupil expander. A: Insertion of the pupil expander into the anterior chamber using a Malyugin ring injector. B: The ambient temperature slowly opens the device to a more circular shape. C: A Sinsky hook is used to position the device to engage the iris margin. D: The device deforms instead of overstretching the iris for engagement. E: Complete iris margin engagement to provide a 7.0 mm pupil. F–H: Removal of the pupil expander. The Sinsky hook is used to flip up and disengage one section of the device, and the Malyugin ring injector is used to grab and swiftly retract the device, revealing an atraumatic pupil.

run-in to previous paragraph the device at the edge and flipping it upward. The Malyugin ring injector was then inserted to hook the disengaged corner and retract the device. This process was performed swiftly and required no additional surgical maneuvers, leaving an atraumatic pupil (Figure 2, F–H).

In Vivo Validation in NHPs

After optimization and successful validation in ex vivo porcine eyes (Figure 3), the pupil expander was tested in specific pathogen-free NHPs (*Macaca fascicularis*) of approximately 6 to 7 years of age. Because the NHP's eye is significantly smaller, we scaled our device to the following specifications: compacted diameter of 1.5 mm, expanded diameter of 5.0 mm, and 300 μm overall thickness.

Intraoperative optical coherence tomography (OCT) imaging (RESCAN 700; Carl Zeiss Meditec) was used in conjunction with the surgical microscope to validate the position of the device.

The monkeys were anaesthetized with ketamine. The periorcular area was cleaned with povidone-iodine 10%. A wire lid speculum was placed to separate the eyelids, and topical povidone-iodine 5% was instilled onto the ocular surface for a few minutes before the surgery. An operating microscope was positioned over the eye undergoing surgery. The same surgeon (S.A.P.) operated on all the monkeys, using a standardized aseptic surgical technique: two self-sealing wounds were made with a blade into the anterior chamber temporally and for a right-handed surgeon 90 degrees away. The temporal wound allowed insertion of the devices, whereas the other was for manipulation. Viscosurgical solution was injected into the anterior chamber, and the expander device was used to open the pupil to 5.0 mm. The procedure for insertion and deployment in the NHP's eye was identical to that of the ex vivo porcine eye. The compact device was inserted using straight conjunctival forceps (Ref: 2-500-4N, Duckworth & Kent Ltd.) after application of the viscosurgical solution. The choice of forceps was to insert the device into a smaller incision. A Sinskey hook was used, when necessary, to position and adjust the device. After the device was fully deployed, iris cross-sectional images were taken using the intraoperative OCT.

Performance Comparison of Shape-Memory Expander with Commercially Available Devices

To evaluate the efficacies of the shape-memory pupil expander, we selected 3 commercially available pupil expanders for comparison. We selected iris hooks because they are used by surgeons internationally. We also selected the OASIS iris expander and the Malyugin ring expander, the latter being recognized as one of the best devices currently available. In addition to the 11 porcine eyes used for the pupil expander validation, another 34 eyes were purchased for performance comparison from Primary Industries Ltd. (Singapore Food Industries Pte Ltd.). Eyes were placed in the aforementioned Krebs–Henseleit buffer, and pilocarpine was used to obtain a small pupil before pupil expansion. All experiments were conducted within 6 hours postmortem.

Malyugin Ring The technique used for deploying the Malyugin ring was similar to that described in the recent literature.¹² The device was retracted into the injector and delivered into the anterior chamber. Using the Malyugin ring manipulator (Ref: MAL-1003; MicroSurgical Technology), opposite ends of the loops were engaged by flexing and dragging these loops to engage the iris margin to obtain a final pupil diameter of 7.0 mm (Figure 3, A). The reverse procedure was performed for removal of the device from the iris margin, and the injector was used to remove the Malyugin ring from the anterior chamber.

OASIS Iris Expander The technique used for deployment of the OASIS iris expander was similar to the Malyugin ring and described in the provided manual. The injector hooks onto the straight connectors for retraction within the injector lumen. The Sinskey hook was used to engage the opposite ends of the 4 engagement points with the iris margin to obtain a final pupil diameter of 7.0 mm (Figure 3, B). The reverse procedure was performed for removal of the device from the iris margin, and the injector was used to remove the iris expander from the anterior chamber.

Iris Hooks The technique used for deploying the iris hooks was similar to that described in the current literature.¹³ Four stab incisions were made to the cornea, and the hooks were inserted to engage the iris margin. Tightening was performed individually until

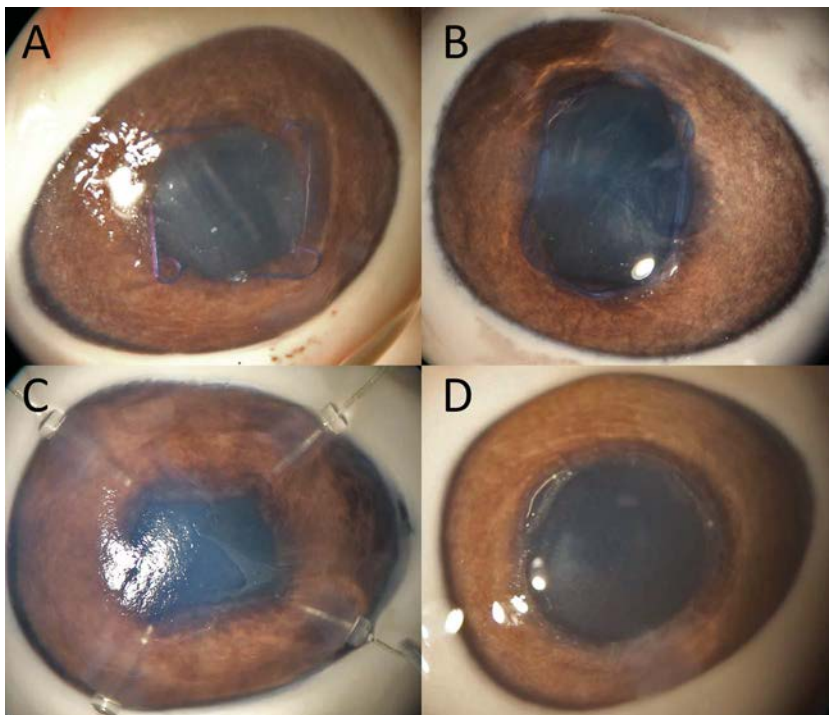


Figure 3. Images from the ex vivo porcine study for each of the devices tested. Fully engaged pupils from the (A) Malyugin ring, (B) OASIS iris expander, (C) iris hooks, and (D) the shape-memory pupil expander. All devices are expanded to a maximal diameter distance of 7.0 mm.

the maximal diameter of the pupil reached 7.0 mm (Figure 3, C). The reverse was performed to remove the iris hooks.

A total of 45 eyes were used for this comparison: 10 eyes for the Malyugin ring, 13 for the iris expander, 11 for the iris hooks, and 11 for the shape-memory pupil expander. After experimentation, the eyes were immersion-fixed in 10% neutral buffered formalin solution for 24 hours. The irides were then isolated under a fume hood and stored again in the 10% neutral buffered formalin solution. All eyes tested were included in the results, without any exclusions.

Images of the fixed irides were taken under a microscope with a DSLR camera and lens (Canon EF-S 10-18mm f/4.5-5.6 IS STM). A primary image of the iris was taken, followed by zoomed in sections of each quadrant of the tissue for a more accurate analysis (Figure 4). To remove bias during results analysis, the iris samples were blind-graded by randomization and evaluated separately by an independent clinician. Analysis was performed by manually marking the areas of tissue affected during the procedure, and image analysis was performed to measure the marked images. Analysis was classified into two complications: iris pigment epithelial (IPE) loss (defined as a section of missing dark pigment of the IPE at the iris margin) and sphincter tear (defined as a discontinuity of the circular shape of the sphincter tissue at the iris margin). Using ImageJ³² (v1.50i, National Institutes of Health), the circumferential lengths of tissue damage at the iris margin were measured (Figure 4, D). The pupil diameters before device insertion were also measured using the smaller radii because the porcine pupil is elliptical rather than circular.

RESULTS

Manufacturing of Shape-Memory Device Prototype

The prototypes were made using potting, requiring custom-designed molds to encase the polymer. Three-dimensional printed molds were successfully manufactured with the 50 μm resolution of the 3D printer. The resultant molds were able to provide the 300 μm overall thickness desired but lacked smoothness in the U-shaped curvature. The cross-sectional thickness of the device was approximately 80 μm , with an opening measuring approximately 140 μm for engagement of the iris margin.

Ex Vivo and In Vivo Validation

The ex vivo porcine iris experiment was performed in accordance with standard cataract surgery protocol. When inserted into the anterior chamber using forceps, the device was able to deform upon reaching the transition temperature within the anterior chamber. This deformation was slow and controlled because of the inherent shape-memory polyurethane properties. This prevented any sudden external forces, which may cause trauma to surrounding tissues. Only a Sinksey hook was needed to manipulate the pupil expander. The device was disengaged from the iris margin with the Sinskey hook and was easily retracted into the injector for all 11 samples tested, leaving the minimally traumatized pupil (Figure 2).

The in vivo experiments were performed by an experienced senior consultant. The device was optimized following the initial experiments with the NHPs. The device was successfully delivered into the anterior chamber and guided to the iris margin with a Sinskey hook. After deployment, we were able to verify that the pupil expander engaged the iris margin using intraoperative OCT (Figure 5). A 6-month follow-up examination showed no complications such as inflammation or ocular hypertension on the primate, indicating biocompatibility using the polyurethane material.

Performance Comparison

Comparison of the 4 pupil expander devices showed mostly IPE loss and minor sphincter tears (Table 1). Sphincter tears are always accompanied with IPE loss at the same location. Iris hooks fared the worst: of the 11 tested samples, 3 exhibited small sphincter tears and 4 exhibited IPE loss. Of the 10 Malyugin ring samples tested, 1 exhibited a small sphincter tear, and 2 exhibited IPE loss. Of the 13 iris expander samples tested, zero exhibited sphincter tears, but 4 exhibited IPE loss. The shape-memory pupil expander

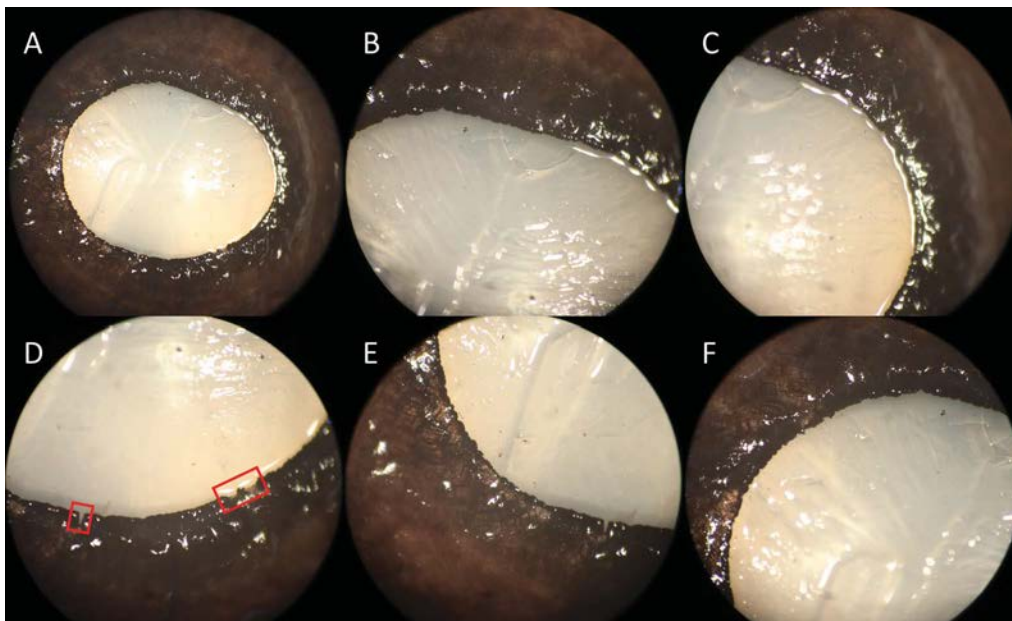


Figure 4. Images of the isolated porcine irides taken from the microscope for processing. (A) First, a x2 zoom image is taken, followed by (B–F) multiple x4.5 zoom images for clear image analysis. (D) Loss of iris pigment epithelium is noted and measured at the locations marked by the red boxes, performed by blind grading. The iris has been isolated from the eye and is therefore not regularly shaped.

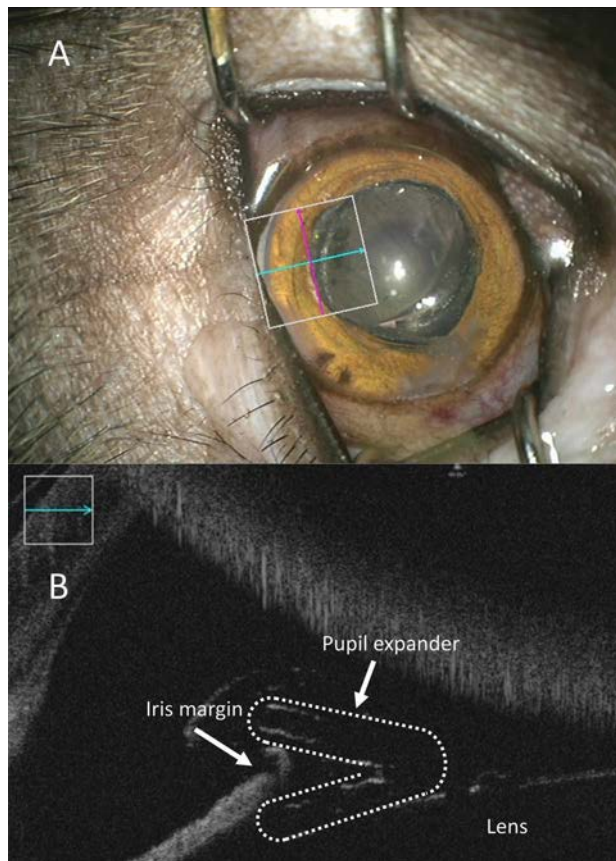


Figure 5. (A) Intraoperative optical coherence tomography image from a monkey undergoing insertion of the pupil expander device. (B) The cross-sectional image of interest is the subimage across the blue arrow. The device successfully engaged the iris margin. The outline of the pupil expander is represented by the white dotted lines.

performed the best, with no observable sphincter tears or IPE loss in the 11 samples tested. The mean pupil diameters before device insertion were 5.50 ± 0.876 mm for the Malyugin ring, 5.35 ± 0.576 mm for the OASIS iris expander, 5.27 ± 0.768 mm for the iris hooks, and 5.10 ± 0.743 mm for the shape-memory expander.

DISCUSSION

Previously, using numerical biomechanical methods,²⁸ we identified the unmet need of a well-optimized pupil

expander for cataract surgery, capable of uniformly engaging the iris margin and smoothly increasing the pupil diameter to avoid potentially deleterious stress and strain on the iris tissue. The present study, to our knowledge, provides the first proof of concept for such a device that uses a shape-memory polymer-based smart material. We demonstrated here its successful application via ex vivo and in vivo experimental testing in porcine enucleated eyes and NHPs. Our novel pupil expander could potentially accommodate even smaller pupil sizes than other commercially available devices.

With devices such as iris hooks and the APX dilator, multiple parts must be deployed individually. For iris hooks, 4 to 5 hooks are inserted, creating high-stress points that greatly increase the risk for tissue tearing.^{14,22,33} Similarly, the scissor-like claws of the APX dilator contact the iris at 4 locations. Although the pupil is enlarged directly, both devices create additional corneal incisions, creating further tissue damage.

In the case of the Malyugin ring, i-Ring, and OASIS iris expander, the opposite issues were observed. Although only requiring the standard primary and secondary corneal incision for cataract surgery, and only deployed into the anterior chamber, there are additional manipulations. Both devices need to engage the iris margin, stretching the iris tissue excessively to engage the opposite ends. Especially when engaging the final corner, the pupil has already been enlarged significantly. Pushing the device to the opposite corner creates significant stress that is clinically suboptimal.

We designed our shape-memory pupil expander to address these two main issues. By adopting a more flexible design, the device is able to deform instead of overstretching the iris tissue. With the U-shaped cross-section, the pupil expander can engage the entire iris margin, exerting uniform stress on the iris tissue while protecting it from external forces such as accidental tears from surgical tool manipulation.³⁴ The circular shape provides minimum distributed stress on the tissues, with full expansion not exceeding the designed maximum diameter, avoiding unnecessary stress.²⁸

Although the type of pupil expansion is important, the speed at which the tissue is stretched also plays a role in determining whether damage is induced.^{22,33} Like most

Iris Comparison	Iris Hooks (n = 11)	Malyugin Ring (n = 10)	OASIS Iris Expander (n = 13)	Shape-memory Expander (n = 11)
Samples with sphincter tear	3	1	0	0
Sphincter tear (µm)	6.16, 11.49, 88.48	10.62	–	–
Samples with IPE loss	4	2	4	0
IPE loss (µm)	8.25, 17.98,* 40.23, 58.18, 88.48	5.92, 12.15	9.93, 14.20, 21.55, 24.32	–

IPE = iris pigment epithelium

*Separate location of IPE loss on a sample also containing sphincter tear

tissues in the human body, the iris tissue behaves in a viscoelastic manner.^{35,36} Fast expansions can create significant stress, which may result in tears. Existing devices mostly use the flexible, spring-like properties of a plastic-like polypropylene. The use of shape-memory material close to the T_g allows for a slower deformation speed that can avoid sudden pupil stretching.

By optimizing the T_g of the polymer, it is possible to control and adjust how fast the device uncoils. Our clinician feedback revealed that the ideal duration to deploy the device is between 20 seconds and 30 seconds after device insertion into the anterior chamber. We designed our shape-memory material to slowly deform over 10 to 20 seconds after insertion; thereafter, simple manipulation is conducted to position the device. The material will remain sufficiently rigid to hold the iris in place for cataract surgery, with stiffness akin to that of a harder silicone rubber.

Femtosecond laser-assisted cataract surgery has been gaining popularity in recent years.³⁷ The use of pupil expanders could enhance the safety of the procedure by maintaining a dilated pupil for extended durations.^{38,39} Before the laser is used, there is a waiting period of about 15 minutes after the pharmacological drug is administered. The drug can wear off in a shorter duration for some patients, resulting in a smaller pupil. Further 1% atropine drops can be administered to limit pupil constriction, but this is not a fail-safe solution.³⁸ With the use of the custom circular pupil expander, an optimal 7.0 mm pupil could be maintained throughout the procedure to ensure patient safety and surgical success. This is not optimal with noncircular devices such as the Malyugin and B-HEX rings, and completely impossible for devices with external protrusions such as iris hooks and the APX dilator because they would interfere with the suction cup placed on the cornea.^{40,41}

In addition, it is believed that the anterior capsulotomy is the main trigger for an increase in prostaglandins in the aqueous with femtosecond laser-assisted cataract surgery. The resulting miosis has been somewhat but not completely mitigated by the use of nonsteroidal anti-inflammatory drugs. The longer the wait between the laser portion and the phase emulsification portion of the surgery, the worse the miosis.⁴² The use of an optimized mechanical device may be helpful in alleviating this problem.

Usually, in a hospital, the variety of pupil expanders available is limited to focus on perfecting the technique in one or two devices. Comparison between multiple devices is therefore uncommon and impractical. The versatility of the current device circumvents some disadvantages of existing alternatives. The method of incision and the size of the small pupil are two areas of concern with currently limited viable solutions.¹⁰ For this study, porcine irides were used to obtain a larger pool sample, and because the pupil expander experiments were all performed by the same person, it is possible to provide an unbiased comparison of the various devices.

Iris hooks take the longest to deploy and remove,¹³ and the small contact points have the greatest potential to damage soft tissue. Although it allows for flexibility in positioning and

varying pupil size, it is less practical in providing a sufficiently large pupil unless the tissue is retracted significantly.⁴³ Multiple stab incisions are not ideal because healing after corneal incisions can be slow and incomplete.^{44–46} More recent devices, including the shape-memory expander, have been more efficient in this regard by eliminating additional incisions.

The OASIS iris expander works similarly to the many variations of ring devices on the market. However, the rigidity in material could be a concern. The connectors between the 4 loops can be weak and break easily, as happened during the first attempt in this study to retract the expander into the retractor. Subsequently, care was taken to assist the device retraction by flattening the sides using forceps. In addition, once in the anterior chamber, the device did not retain its square shape, but remained slightly deformed in a rectangular shape from the bent curved connectors. The material construction is a hard polypropylene that may require excessive force to flex to engage the loops. The hard plastic against the soft iris tissue may have caused iris chafing and IPE loss in several samples. Thus, we chose a soft polymer that can be more easily deformed to reduce the risk for iris-tissue damage.

Although the Malyugin ring may be very popular because of the ease of deployment, removal is significantly more challenging. The OASIS iris expander has specific shielded holes where the Sinsky hook is positioned, and the Malyugin ring relies on a custom manipulator tool to hook onto the expander. The manipulator tool contacts the iris tissue during removal, and it is easy for the iris margin to get caught between the devices. At these 4 loops, the iris tissue may accidentally be dragged and torn. In addition, the Malyugin ring is designed to be a continuous loop glued at the ends. During removal, one of the loops often gets stuck during retraction into the injector. Because it is a one-use device, forceful retraction is possible, but that might bend the device upward or downward, potentially contacting the corneal endothelium and inducing further trauma. Our shape-memory pupil expander encompasses a continuous U-shaped cross-section, eliminating the risk of getting caught by the iris. It is also easily removed, taking less time and effort in comparison to existing methods.

There are several limitations of this study. The intended design consisted of a U-shaped cross-section that can engage the iris margin. However, because of the low resolution of our 3D printer, the curved edges were instead right angled. This resulted in a rectangular cavity for the cross-section. In addition, the surface finish for the completed device was imperfect, with rough edges and surfaces. However, as a first proof-of-principle, this laboratory-made device was successful for both *ex vivo* and *in vivo* testing.

In addition, the polymer used for testing would ideally be manufactured differently from the prototypes tested. We used potting to mold the device individually, whereas injection molding pellets would be better used for large-scale production. With injection molding, the resolution and surface finish for the prototypes would be within acceptable tolerances ($\pm 5 \mu\text{m}$).

Comparison of the various pupil expanders would benefit from a larger sample size. This should allow for a greater pool of data for analysis and an accurate representation of the complication percentages. However, that would require a large number of devices, which is not practical with porcine data.

Finally, because testing of the device was in *ex vivo* porcine and healthy *in vivo* cynomolgus eyes, we have yet to follow-up the procedure with phacoemulsification. Therefore, further studies are needed to ensure that there are no potential complications of our shape-memory pupil expander.

We developed an optimized pupil expansion device designed to minimize and limit the amount of stress exerted onto the iris tissue. The *in vivo* and *ex vivo* experimental validations presented herein provide proof of concept of the device's efficacy and further highlight the translational potential of smart materials in the development of other ophthalmological implants to improve patient healthcare.

WHAT WAS KNOWN

- Current pupil expander devices are made of hard plastic materials, and ring expanders use the tension–spring effect of the plastic during iris engagement, overstretching the iris in the process.
- Removal of pupil expanders can sometimes be more difficult than their deployment.

WHAT THIS PAPER ADDS

- A novel pupil expander that is made of a shape-memory polyurethane could deform to prevent overstretching of the iris tissue during device deployment.
- Experimental validation of pupil expansion devices provided quantitative measurements of iris damage, which may be reduced with optimized devices such as our shape-memory pupil expander.

REFERENCES

1. Foster A. Cataract—a global perspective: output, outcome and outlay. *Eye (Lond)* 1999;13:449–453
2. Taylor HR. Cataract: how much surgery do we have to do? *Br J Ophthalmol* 2000;84:1–2
3. Foster A. Cataract and “Vision 2020—the right to sight” initiative. *Br J Ophthalmol* 2001;85:635–637
4. Desai P, Minassian D, Reidy A. National cataract surgery survey 1997–8: a report of the results of the clinical outcomes. *Br J Ophthalmol* 1999;83:1336–1340
5. Cionni RJ, Barros MIG, Kaufman AH, Osher RH. Cataract surgery without preoperative eyedrops. *J Cataract Refract Surg* 2003;29:2281–2283
6. Amini R, Whitcomb JE, Al-Qaisi MK, Akkin T, Jouzdani S, Dorairaj S, Prata T, Illitchev E, Liebmman JM, Ritch R. The posterior location of the dilator muscle induces anterior iris bowing during dilation, even in the absence of pupillary block. *Invest Ophthalmol Vis Sci* 2012;53:1188–1194
7. Winn B, Whitaker D, Elliott DB, Phillips NJ. Factors affecting light-adapted pupil size in normal human subjects. *Invest Ophthalmol Vis Sci* 1994;35:1132–1137
8. Chang DF, Osher RH, Wang L, Koch DD. Prospective multicenter evaluation of cataract surgery in patients taking tamsulosin (Flomax). *Ophthalmology* 2007;114:957–964
9. Linebarger EJ, Hardten DR, Shah GK, Lindstrom RL. Phacoemulsification and modern cataract surgery. *Surv Ophthalmol* 1999;44:123–147
10. Akman A, Yilmaz G, Oto S, Akova YA. Comparison of various pupil dilatation methods for phacoemulsification in eyes with a small pupil secondary to pseudoexfoliation. *Ophthalmology* 2004;111:1693–1698
11. Chang DF, Campbell JR. Intraoperative floppy iris syndrome associated with tamsulosin. *J Cataract Refract Surg* 2005;31:664–673
12. Malyugin B. Small pupil phaco surgery: a new technique. *Ann Ophthalmol (Skokie)* 2007;39:185–193
13. Novák J. Flexible iris hooks for phacoemulsification. *J Cataract Refract Surg* 1997;23:828–831
14. Merriam JC, Zheng L. Iris hooks for phacoemulsification of the subluxated lens. *J Cataract Refract Surg* 1997;23:1295–1297
15. Santoro S, Sannace C, Cascella MC, Lavermicocca N. Subluxated lens: phacoemulsification with iris hooks. *J Cataract Refract Surg* 2003;29:2269–2273
16. Bhattacharjee S. Pupil-expansion ring implantation through a 0.9 mm incision. *J Cataract Refract Surg* 2014;40:1061–1067
17. Auffarth GU, Reuland AJ, Heger T, Völcker HE. Cataract surgery in eyes with iridoschisis using the Perfect Pupil iris extension system. *J Cataract Refract Surg* 2005;31:1877–1880
18. Kershner RM. Management of the small pupil for clear corneal cataract surgery. *J Cataract Refract Surg* 2002;28:1826–1831
19. Lee BS, Chang DF. Management of small pupils. *Expert Rev Ophthalmol* 2016;11:49–58
20. Tian JJ, Garcia GA, Karanjia R, Lu KL. Comparison of 2 pupil expansion devices for small-pupil cataract surgery. *J Cataract Refract Surg* 2016;42:1235–1237
21. Agarwal A. Visitec® I-Ring® Pupil Expander. *EyeWorld Weekly* 2016;21:77–78
22. Masket S. Avoiding complications associated with iris retractor use in small pupil cataract extraction. *J Cataract Refract Surg* 1996;22:168–171
23. Ha-Eun L, Joon-Young K, Da-Eun L, Jin-Gu K. Two cases of phacoemulsification in the presence of a small pupil using an iris expander. *Turkish J Vet Anim Sci* 2019;43:159–166
24. Chang DF. Use of Malyugin pupil expansion device for intraoperative floppy-iris syndrome: results in 30 consecutive cases. *J Cataract Refract Surg* 2008;34:835–841
25. Mattox C. Management of the small pupil. In: *Cataract Surgery in the Glaucoma Patient*. New York, NY, Springer; 2009:23–34
26. Narang P, Agarwal A. *Small Pupil Phacoemulsification. Step by Step Phacoemulsification*. New Delhi, India, Jaypee Brothers Medical Publishers (P) Ltd; 2015:57
27. Vollman DE, Gonzalez-Gonzalez LA, Chomsky A, Daly MK, Baze E, Lawrence M. Intraoperative floppy iris and prevalence of intraoperative complications: results from ophthalmic surgery outcomes database. *Am J Ophthalmol* 2014;157:1130–1135.e1
28. Tan RKY, Wang X, Perera SA, Girard MJA. Numerical stress analysis of the iris tissue induced by pupil expansion: comparison of commercial devices. *PLoS One* 2018;13:e0194141
29. Huang WM, Yang B, Fu YQ. *Polyurethane Shape Memory Polymers*. Boca Raton, FL: CRC Press; 2012
30. Whitcomb JE, Amini R, Simha NK, Barocas VH. Anterior–posterior asymmetry in iris mechanics measured by indentation. *Exp Eye Res* 2011;93:475–481
31. Minassian DC, Rosen P, Dart JK, Reidy A, Desai P, Sidhu M, Kaushal S, Wingate N. Extracapsular cataract extraction compared with small incision surgery by phacoemulsification: a randomised trial. *Br J Ophthalmol* 2001;85:822–829
32. Abràmoff MD, Magalhães PJ, Ram SJ. Image processing with ImageJ. *Biophotonics Int* 2004;11:36–42
33. Morris B, Cheema RA. Phacoemulsification using iris-hooks for capsular support in high myopic patient with subluxated lens and secondary angle closure glaucoma. *Indian J Ophthalmol* 2006;54:267–269
34. Graether JM. Graether pupil expander for managing the small pupil during surgery. *J Cataract Refract Surg* 1996;22:530–535
35. Zhang K, Qian X, Mei X, Liu Z. An inverse method to determine the mechanical properties of the iris *in vivo*. *Biomed Eng Online* 2014;13:1
36. Jouzdani S. *Biomechanical Characterization and Computational Modeling of the Anterior Eye [dissertation]*. University Of Minnesota, Minneapolis, MN; 2013
37. Roberts TV, Lawless M, Chan CC, Jacobs M, Ng D, Bai SJ, Hodge C, Sutton G. Femtosecond laser cataract surgery: technology and clinical practice. *Clin Exp Ophthalmol* 2013;41:180–186
38. Donaldson KE, Braga-Mele R, Cabot F, Davidson R, Dhaliwal DK, Hamilton R, Jackson M, Patterson L, Stonecipher K, Yoo SH. Femtosecond laser-assisted cataract surgery. *J Cataract Refract Surg* 2013;39:1753–1763
39. Roberts TV, Lawless M, Hodge C. Laser-assisted cataract surgery following insertion of a pupil expander for management of complex cataract and small irregular pupil. *J Cataract Refract Surg* 2013;39:1921–1924

40. Nagy ZZ, Takacs AI, Filkorn T, Kránitz K, Gyenes A, Juhász É, Sándor GL, Kovacs I, Juhász T, Slade S. Complications of femtosecond laser-assisted cataract surgery. *J Cataract Refract Surg* 2014;40:20–28
41. Dick HB, Schultz T. Laser-assisted cataract surgery in small pupils using mechanical dilation devices. *J Refract Surg* 2013;29:858–862
42. Schultz T, Joachim SC, Stellbogen M, Dick HB. Prostaglandin release during femtosecond laser-assisted cataract surgery: main inducer. *J Refract Surg* 2015;31:78–81
43. Birchall W, Spencer AF. Misalignment of flexible iris hook retractors for small pupil cataract surgery: effects on pupil circumference. *J Cataract Refract Surg* 2001;27:20–24
44. Jester JV, Petroll WM, Cavanagh HD. Corneal stromal wound healing in refractive surgery: the role of myofibroblasts. *Prog Retin Eye Res* 1999;18:311–356
45. Ernest P, Tipperman R, Eagle R, Kardasis C, Lavery K, Sensoli A, Rhem M. Is there a difference in incision healing based on location? *J Cataract Refract Surg* 1998;24:482–486
46. Gasset AR, Dohlman CH. The tensile strength of corneal wounds. *Arch Ophthalmol* 1968;79:595–602

Disclosures: Some of the authors have filed a patent application for the device described: “Expander for holding apart an opening in a tissue and method of operating the same” (US20180310929A1, EP3364852A4, WO2017069703A1, and SG11201802973PA).



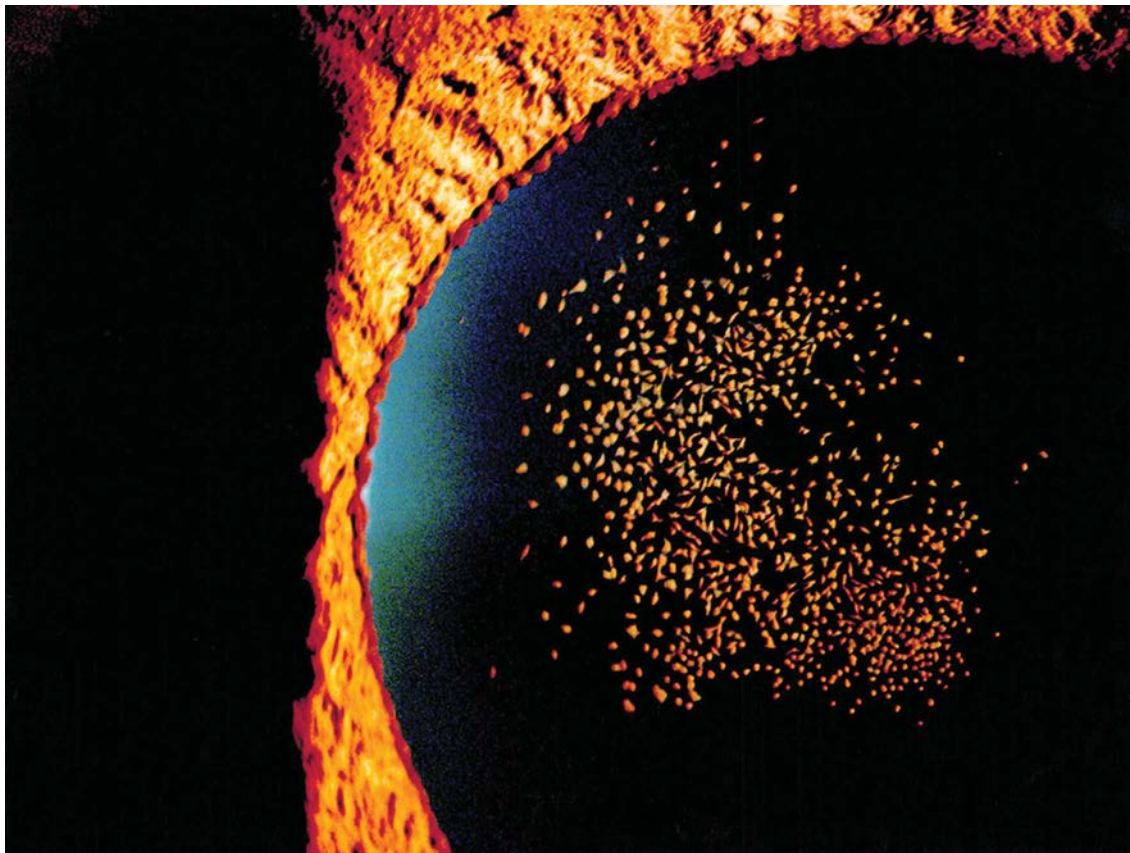
First author:

Royston K.Y. Tan, PhD

*Department of Biomedical Engineering,
Ophthalmic Engineering & Innovation
Laboratory, National University of
Singapore*

Ophthalmic Photographers’ Society Exhibit, May 2019

Category: Eye as Art–Best in Show



Sprinkle of Magic Moon Dust

The OPS annual exhibit, presented during the ASCRS • ASOA Annual Meeting, is sponsored by the ASCRS. Published with the permission of the photographer.

John Leo

*Tun Hussein Onn National Eye Hospital,
Selangor Darul Ehsan, Malaysia*

REVIEW/UPDATE

Middle- and long-term results after iris-fixated phakic intraocular lens implantation in myopic and hyperopic patients: a meta-analysis

Gwyneth A. van Rijn, MD, Zoraida S. Gaurisankar, MD, Antonio P. Ilgenfritz, MD, José Eduardo E. Lima, MD, Geert W. Haasnoot, PhD, Jan-Willem M. Beenakker, PhD, Yanny Y. Y. Cheng, MD, PhD, Gregorius P. M. Luyten, MD, PhD

The iris-fixated phakic intraocular lens (pIOL) has been available for over 25 years. To provide a clear picture of outcomes and risks, for this systematic review and meta-analysis, the literature was searched for reports on middle- and long-term effects. The iris-fixated phakic intraocular lens (pIOL) has been available for over 25 years. To provide a clear picture of outcomes and risks, for this systematic review and meta-analysis, the literature was searched for reports on middle- and long-term effects of iris-fixated pIOLs on myopic and hyperopic eyes with a follow-up of at least 2 to 4 years. Visual and refractive results after implantation for correction of myopia are positive and the complication rate is low. Endothelial cell loss appears to be an

acceptable rate, although the range of endothelial cell change is too wide to draw firm conclusions. Care should be taken when considering an iris-fixated pIOL for hyperopic eyes because complication rates, particularly pigment dispersion, might be higher than those in myopic eyes. More well-designed, long-term studies are needed, especially in hyperopic eyes. The authors advocate for standardized reporting of refractive surgery data. Initiatives proposed by journal authors and editors to achieve uniformity should be supported.

J Cataract Refract Surg 2020; 46:125–137 Copyright © 2019 Published by Wolters Kluwer on behalf of ASCRS and ESCRS

When it comes to the correction of high myopia and hyperopia, the advent of phakic intraocular lens (pIOL) implantation and its improvements in methods and materials were a breakthrough. Inspired by Harold Ridley, Kees Binkhorst, Svyatoslav Fyodorov, and Klaas Otter, among other pioneers in the field of IOLs, Jan Worst introduced an IOL that attached to the iris. In 1978, he implanted the first iris-claw lens for aphakia after cataract surgery. In 1984, an opaque iris-claw lens was implanted in a phakic eye for pupil occlusion to relieve complaints of intractable diplopia. During an ophthalmology meeting in 1986, Worst developed the idea of a “contact lens in the eye.”^A On November 2, 1986, Worst and Fechner implanted the first-generation biconcave iris-fixated pIOL (ref. 209) in a myopic eye of -20 diopter (D).^A The name of the iris-fixated pIOL was changed from Worst iris-claw or lobster-claw lens to Artisan lens. This name was chosen to honor the special skills of Dr. Worst.¹ Despite the

positive visual and refractive results, unacceptable complications occurred and the biconcave Artisan was discontinued.^{1,2} In 1991, a convex-concave-shaped design (ref. 206) to create more distance from the edge of the iris-fixated pIOL to the corneal endothelium was introduced and has been implanted successfully since. The first iris-fixated pIOL for the correction of hyperopia (ref. 203) was released in 1993 and first implanted by Krumeich in April 1993, and Worst in early 1994. In 1997, an iris-fixated pIOL for myopia was developed, with a larger optic diameter (ref. 204) to reduce optic phenomena such as glare and halos.

The modified convex-concave-shaped Artisan iris-fixated pIOL (Ophtec) has been in use since 1998. In 2004, the U.S. Food and Drug Administration approved the use of the Artisan and the identical Verisyse (Abbott Medical Optics, Inc.), and the Artisan/Verisyse iris-fixated IOL has found global acceptance. The iris-fixated pIOL is available in refractive powers ranging from -3.0 to -23.5

Submitted: July 15, 2019 | Final revision submitted: September 23, 2019 | Accepted: September 29, 2019

From the Department of Ophthalmology (van Rijn, Gaurisankar, Ilgenfritz, Lima, Beenakker, Cheng, Luyten), Department of Immunohematology and Blood Transfusion (Haasnoot), Department of Radiology (Beenakker), Leiden University Medical Center, the Netherlands; School of Medicine (Ilgenfritz), Pontifícia Universidade Católica do Paraná, Curitiba, Faculdade de Medicina de Ribeirão Preto (Lima), University of São Paulo, Ribeirão Preto, Brazil.

Supported by Ophtec b.v., Stichting Blindenhulp, and by the following foundations through Uitzicht; ANVVB and LSBS. The funding organizations had no role in the design or conduct of this research.

Corresponding Author: Gwyneth A. van Rijn, MD, Department of Ophthalmology, Leiden University Medical Center, Albinusdreef 2, 2333 ZA Leiden, the Netherlands. Email: g.a.van_rijn@lumc.nl.

D in 1.0 D increments before 1997, and after 1997 in 0.5 D increments. The Artisan Small (ref. 202), which was made available in the year 2000 for eyes with proportionally reduced dimensions of the anterior chamber, is no longer available.

Since the iris-fixated pIOL has been marketed for more than 25 years, an assessment of the long-term effects after implantation of this pIOL for refractive errors seems called for. In this systematic review and meta-analysis, we searched the literature for articles on the middle- and long-term effects (from 2 to 10 years) of the iris-fixated pIOL, to provide a clear picture of the results and risks of implantation.

METHODS

We applied the tenets of the Preferred Reporting Items for Systematic Reviews and Meta-Analyses Statement. The databases PubMed, EMBASE, Web of Science, and Cochrane Library were searched; no time limit was used for the search. Figure 1 shows the eligibility and exclusion criteria. The 4 databases were last searched on the following dates:

1. PubMed on August 3, 2018, yielding 539 references;
2. Web of Science (Thomson Reuters) on August 28, 2018, yielding 476 references;
3. EMBASE on August 28, 2018, yielding 586 references;
4. Cochrane Library on August 28, 2018, yielding 42 references.

Although foldable iris-fixated pIOLs (ie, Artiflex/Veriflex) were an exclusion criterion, the terms “Artiflex” and “Veriflex” were included in the search to avoid missing any relevant articles. Search strings can be found in Appendix 1 (see Supplemental Digital Content 1, available at <http://links.lww.com/JRS/A1>). The search strategy was developed by an information specialist in consultation with the researchers. No restrictions were placed on the levels of evidence required for inclusion in the search because it was expected that most studies would be of observational nature.

All 1643 references were then uploaded in a citation manager (EndNote X7) for organization purposes. After checking for and removing duplicates, a total of 750 unique references remained.

Eligibility criteria

- Implantation of an Artisan/Verisyse IF-pIOL
- Human adults with myopic or hyperopic eyes with no ocular abnormalities other than refractive error
- Reported follow-up of at least 2 years
- Presents at least one of the following categories of outcome: spherical equivalent, endothelial cell change, corrected and uncorrected distance visual acuity, safety index, efficacy index, complications

Exclusion criteria

- Study type (letters, comments, animal trials, in vitro studies, editorial, reviews, and case series and case reports were excluded)
- Studies solely about foldable or toric IF-pIOLs
- Patients operated for problems other than myopia or hyperopia
- Studies in children (< 18 years)
- Follow-up of less than 2 years
- Article not in English
- Publication date before 2000

The title and abstract of every unique publication were analyzed. Two researchers (G.R., A.I.) independently screened and selected the articles retrieved by the search, the results were compared, and disagreements were resolved by discussion; if necessary, a third party was invited to the discussion. References that met any of the established exclusion criteria were excluded. The assessment of the full texts and bibliographies of 137 articles resulted in 32 studies being included in this review and meta-analysis.^{3–35} Relevant articles in which complications were reported as case series but no incidence could be calculated are not listed in the Results section but are still included in the Discussion section.^{35–37}

The bibliography of each eligible reference was searched manually for additional articles that may not have been identified previously by our systematic search. No further articles were found at this stage. However, 1 additional reference that was not included in the databases was found through a simple web search.³⁰ See Figure 2 for the selection process. All relevant information was extracted from each reference and recorded in the spreadsheet software (Microsoft Excel 2010; Microsoft Corp.). Statistics for pooled estimates were performed in IBM SPSS Statistics for Windows software (version 23, IBM Corp.). Studies in which eyes underwent additional corneal refractive surgery were reviewed but were excluded from the meta-analysis for refractive and visual acuity outcome measures. Data on visual acuity were converted to logarithmic of the minimum angle of resolution for calculation purposes. Charts and figures were assembled using either SPSS or Excel.

RESULTS

The selected studies comprised 5523 myopic eyes and 162 hyperopic eyes. The sample sizes in the articles range from 26 to 1140 myopic eyes and from 14 to 136 hyperopic eyes. Twenty-nine articles describe the results after iris-fixated pIOL implantation in myopic eyes.^{3–18,20–32} Four articles describe the results after iris-fixated pIOL implantation in hyperopic eyes.^{19,20,32,33}

In most of the studies, not all participating patients reached the last follow-up visit, and the number of examined patients varies from one follow-up period to another. The

Figure 1. Eligibility and exclusion criteria (IF-pIOL = iris-fixated phakic intraocular lens).

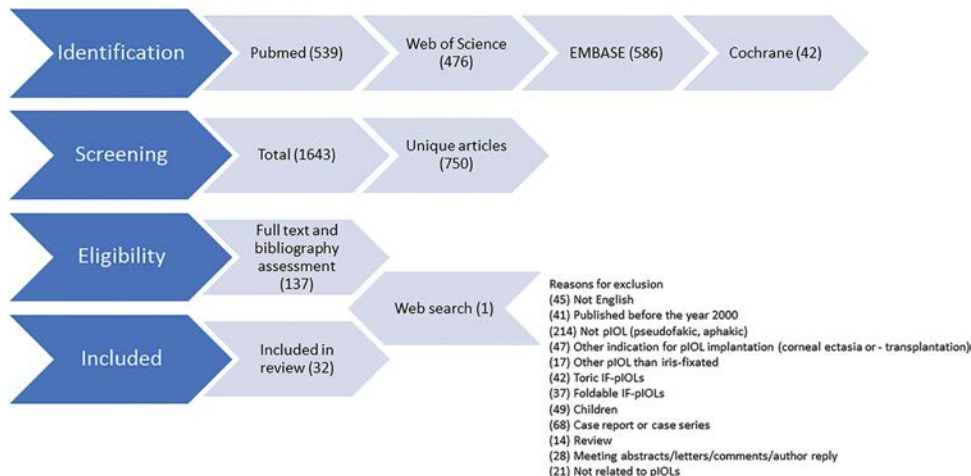


Figure 2. Selection process (IF-pIOL = iris-fixated phakic intraocular lens).

mean age at the time of iris-fixated pIOL implantation ranges from 22 to 51 years in the myopic study groups and from 32 to 44 years in the hyperopic study groups.

All 32 studies were reviewed and are summarized in the Appendices (see Supplemental Digital Content 1 to 5, available at <http://links.lww.com/JRS/A1>, <http://links.lww.com/JRS/A2>, <http://links.lww.com/JRS/A3>, <http://links.lww.com/JRS/A4>, and <http://links.lww.com/JRS/A5>). In two studies, a significant percentage of eyes had additional corneal refractive surgery^{32,33} and were excluded from the pooled estimate calculations for refractive outcome and visual acuity.

Type of Iris-Fixated pIOL

Of all studies selected, 1 study included only the Artisan 6/8.5,³⁰ and 2 studies included only the Artisan 5/8.5.^{3,23} Four studies report on results after the implantation of the Artisan Hyperopia,^{19,20,32,33} and 1 study included the Artisan Myopia Small 5/7.5.¹⁴

Refractive Outcome

Refractive outcome may be presented as changes in the manifest refractive spherical equivalent (MRSE) and deviation in the MRSE from the targeted refraction.

Changes in the MRSE Fifteen studies with a total of 1400 eyes report on changes in the MRSE in myopic eyes. Two studies do not specify the follow-up period of the reported MRSE data. The preoperative pooled MRSE ranges from -18.9 to -10.4 D (median -13.3 D), and the postoperative pooled median MRSE ranges from -0.8 to -0.4 D at various follow-up times (see Table 1). The MRSE per study is summarized in Appendix 2 (see Supplemental Digital Content 2, available at <http://links.lww.com/JRS/A2>).

Two studies report on changes in the MRSE in hyperopic eyes. In the study by Guell et al.,³² 41.4% of the eyes were treated with a combined pIOL implantation and additional corneal refractive surgery. In the study by Saxena et al.,¹⁹ the preoperative MRSE was 6.80 D, and the postoperative MRSE was 0.10 D at 3-year follow-up (see Table 2).

Changes in the MRSE during follow-up periods are described as being not significant. However, only a limited number of studies have statistically proven this.^{4,12,13,15-17,23,28,31} Changes in the MRSE per study are graphically plotted against time in Figure 3.

Deviation in the MRSE From Target Refraction Fourteen studies with a total of 1602 eyes report on the percentage of myopic eyes within 1.0 D of the targeted refraction.

Table 1. Pooled estimates of changes in the MRSE preimplantation vs postimplantation of an iris-fixated phakic IOL in myopic eyes.

Follow-up Time	2 yrs	3 yrs	4 yrs	5 yrs	6 yrs	10 yrs
No. of eyes	534	589	146	341	89	89
Pre-op						
Mean SE (D) \pm SD	-13.6 ± 2.3	-13.7 ± 2.9	-12.4 ± 1.9	-13.9 ± 3.6	-10.4 ± 0	-10.4 ± 0
Range	$-18.9, -11.6$	$-19.8, -11.06$	$-15.0, -11.1$	$-19.8, -11.3$	-10.4	-10.4
Pre-op						
Median SE (D) \pm SD	-12.2 ± 2.3	-13.3 ± 2.9	-11.1 ± 1.9	-12.3 ± 3.6	-10.4 ± 0	-10.4 ± 0
Range	$-18.9, -11.6$	$-19.8, -11.06$	$-15.0, -11.1$	$-19.8, -11.3$	-10.4	-10.4
Post-op						
Mean SE (D) \pm SD	-0.8 ± 0.25	-0.7 ± 0.29	-0.6 ± 0.2	-0.6 ± 0.1	-0.7 ± 0	-0.7 ± 0
Range	$-1.2, -0.4$	$-1.1, -0.3$	$-0.9, -0.4$	$-0.8, -0.4$	-0.7	-0.7
Post-op						
Median SE (D) \pm SD	-0.8 ± 0.25	-0.8 ± 0.29	-0.4 ± 0.2	-0.6 ± 0.1	-0.7 ± 0	-0.7 ± 0
Range	$-1.2, -0.4$	$-1.1, -0.3$	$-0.9, -0.4$	$-0.8, -0.4$	-0.7	-0.7
No. of studies	7	5	2	3	1	1

IOL = intraocular lens; MRSE = manifest refractive spherical equivalent; pre-op = preoperative; post-op = postoperative; SE = spherical equivalent

Table 2. Changes in the MRSE in hyperopic eyes preimplantation vs postimplantation of an iris-fixated phakic IOL in hyperopic eyes.

Study	Eyes (n)	Mean Pre-op SE (D)	Mean Post-op SE (D)	Reported Follow-up Time (yr)
Guell et al. ^{32*}	34	4.92 ± 1.7	-0.11 ± 0.74*	3
	28	4.92 ± 1.7	0.02 ± 0.51*	5
Saxena et al. ¹⁹	15	6.80 ± 1.97	-0.15 ± 0.89	2
	10	6.80 ± 1.97	0.10 ± 0.85	3

IOL = intraocular lens; MRSE = manifest refractive spherical equivalent; pre-op = preoperative; post-op = postoperative; SE = spherical equivalent
 *41.4% additional corneal refractive surgery

Ten studies report on the deviation in the post-operative MRSE from emmetropia; 4 studies report on the deviation from the intended (calculated) correction.

The percentage of eyes within 1.0 D of emmetropia ranges from 55% to 98%. The overall pooled median of eyes within 1.0 D of emmetropia is 94% (all follow-up periods). A slightly smaller range of 65% to 93% of eyes are within 1.0 D of the intended correction. The overall pooled median of eyes within 1.0 D of the intended correction is 78.8% (all follow-up periods). See Tables 3 and 4 and Appendix 2 (see Supplemental Digital Content 2, available at <http://links.lww.com/JRS/A2>). Two studies report on hyperopic eyes combined with additional corneal refractive surgery.^{32,33} Details are given in Appendix 2 (see Supplemental Digital Content 2, available at <http://links.lww.com/JRS/A2>).

Visual Acuity

Uncorrected (UDVA) and corrected (CDVA) distance visual acuity, safety index (SI), and efficacy index (EI) are common parameters to assess the effect of the iris-fixated pIOL on visual acuity; details are in Appendix 3 (see Supplemental Digital Content 3, available at <http://links.lww.com/JRS/A3>).

UDVA and Efficacy Data on UDVA are commonly reported as the cumulative percentage of eyes within a visual acuity range. Efficacy can be described as the percentage of eyes achieving a postoperative UDVA of 20/40 and 20/20 or better. The pooled median of the percentage of myopic eyes with a UDVA of 20/40 or better is 87% and 82% at 2- and 5-year follow-up, respectively. The pooled median of the percentage of myopic eyes with a UDVA of 20/20 or better

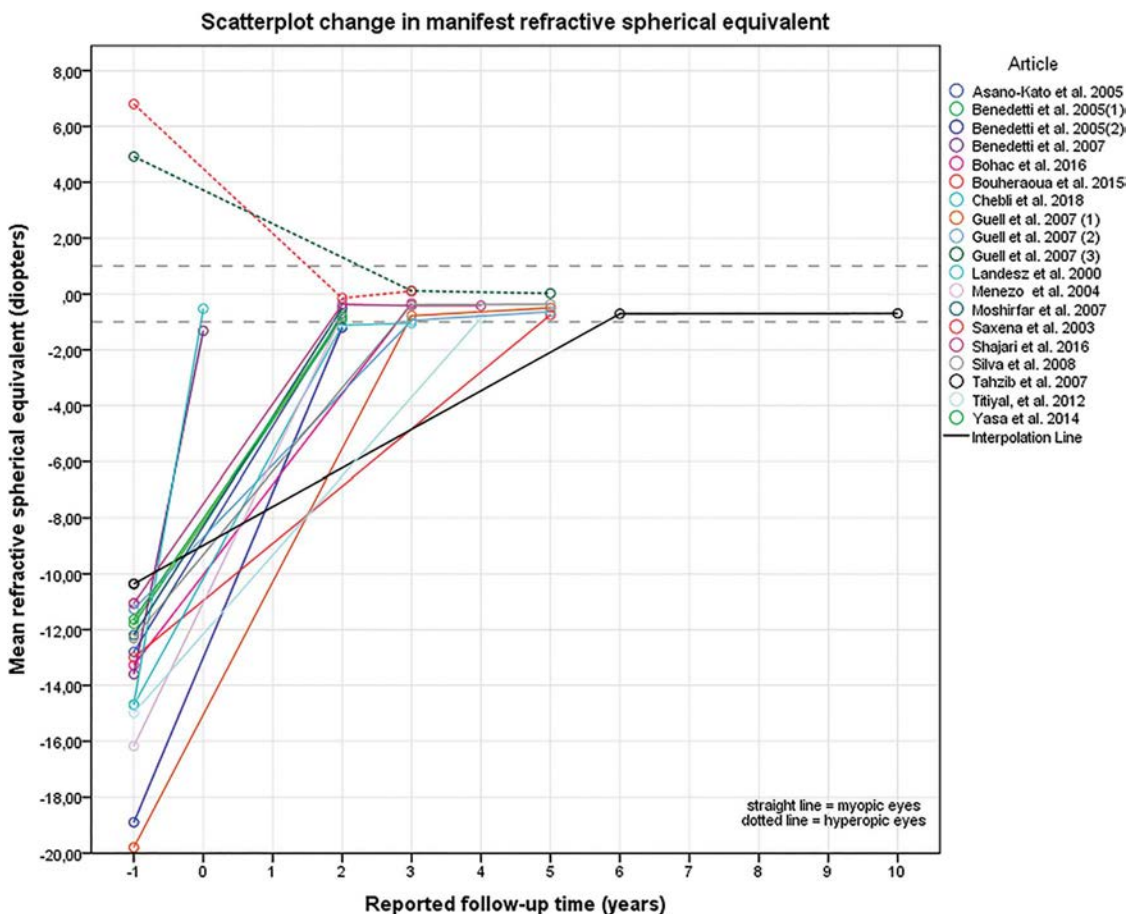


Figure 3. Scatterplot of published data on change in the manifest refractive spherical equivalent.

Table 3. Pooled estimates of the MRSE within the range of emmetropia in myopic eyes (%).

Follow-up	2 yrs		3 yrs		4 yrs		5 yrs		Overall	
	Within 0.5 D	Within 1.0 D	Within 0.5 D	Within 1.0 D	Within 0.5 D	Within 1.0 D	Within 0.5 D	Within 1.0 D	Within 0.5 D	Within 1.0 D
No. of eyes	172	172	505	505	146	146	19	19	909	909
Median	55.0	84.0	85.4	97.7	72.0	94.0	73.7	94.7	73.7	94.0
Mean	53.3	82.1	79.5	94.9	59.2	86.5	73.7	94.7	68.8	89.1
Minimum	33.3	55.0	31.4	74.5	35.3	72.5	73.7	94.7	31.4	55.0
Maximum	68.0	90.0	85.4	97.7	72.0	94.0	73.7	94.7	85.4	97.7
SD	14.1	10.7	16.3	7.3	17.6	10.3	0	0	19.6	10.1
No. of studies	5	5	4	4	3	3	2	2	10	10

% = percentage of eyes; MRSE = manifest spherical equivalent

was 35% and 21% at 2- and 5-year follow-up, respectively (see Table 5).

The EI reflects the ratio between the preoperative CDVA and postoperative UDVA: (mean postoperative UDVA)/(mean preoperative CDVA). The pooled median EI at 2, 5, and 10 years is 0.90, 1.02, and 0.80, respectively (Table 6). Efficacy indices have a wide range from 0.43 to 1.03; only Silva et al.¹⁷ describe an EI of below 0.8. They note a slight undercorrection immediately postoperatively but give no explanation.

Only Qasem et al.³³ report on a small number of hyperopic eyes, with 100% having a UDVA of 20/30 or better at 2- and 3-year follow-up and 28.6% of eyes having additional corneal refractive surgery after iris-fixated pIOL implantation. Efficacy indices are 0.81 and 0.9 at 2 and 5 years, respectively, as reported by Guell et al.,³² with 41.4% of eyes having additional corneal refractive surgery after implantation.

CDVA and Safety Data on CDVA are often reported as the change in visual acuity preimplantation vs post-implantation; 14 studies report on changes in CDVA in myopic eyes (Table 7). All studies report that more than 91% of myopic eyes have a stable or a gain in CDVA. The pooled median postoperative CDVA increased compared with the preoperative CDVA to 0.05, 0.02, and 0.12 logarithmic angle of minimum resolution units at 2, 5, and 10 years of follow-up, respectively, which equals 0.89, 0.96, and 0.76 Snellen (Table 8). Nine studies report on a loss of 2 or more lines of CDVA in up to 4.5% of the

eyes.^{4,5,7,12,13,15,27,28,33} The primary reason for a loss of 2 or more CDVA lines is cataract (9 eyes) (Table 7).

The SI is defined as the ratio of (mean postoperative CDVA)/(mean preoperative CDVA). All reported safety indices for myopic eyes are above 1.0. The pooled median SI at 2, 5, and 10 years of follow-up is 1.19, 1.10, and 1.10, respectively (see Table 6).

Although no specific number is given by Qasem et al.,³³ no hyperopic eye lost a line of CDVA. Saxena et al.¹⁹ describe a CDVA of 0.75 at 3-year follow-up, with 50% of hyperopic eyes having a stable or a gain in CDVA. A SI of 0.95 and 1.25 is reported by Guell et al.³² at 2- and 5-year follow-up, respectively.

EC Loss

Most studies report on EC change from baseline. Other articles report on EC change from 6 months to 1 year after implantation, attempting to describe chronic EC change by excluding the acute EC loss induced by surgery. Some articles only report the yearly percentage of EC loss, some only on absolute EC counts, and others on both. Details per study are in Appendix 4 (see Supplemental Digital Content 4, available at <http://links.lww.com/JRS/A4>).

Various conclusions on EC change are drawn by the different authors, ranging from a gain in EC^{10,23,31} to no significant EC change or a significant EC change over the follow-up period. For the pooled estimates of absolute EC change given in this article, a linear decrease in EC over time is assumed, as in the reviewed articles. Saxena et al.²¹

Table 4. Pooled estimates of the MRSE within the range of intended correction in myopic eyes (%).

Follow-up	3 yrs		5 yrs		6 yrs		10 yrs		Overall	
	Within 0.5 D	Within 1.0 D	Within 0.5 D	Within 1.0 D	Within 0.5 D	Within 1.0 D	Within 0.5 D	Within 1.0 D	Within 0.5 D	Within 1.0 D
No. of eyes	317	317	68	68	89	89	89	89	563	647
Median	57.1	78.8	36.8	70.5	50.5	65.1	43.8	68.8	50.5	78.8
Mean	53.0	76.7	36.8	70.5	50.5	65.1	43.8	68.8	49.2	75.5
Minimum	38.2	69.1	36.8	70.5	50.5	65.1	43.8	68.8	36.8	65.1
Maximum	57.1	78.8	36.8	70.5	50.5	65.1	43.8	68.8	57.1	93.2
SD	7.8	4.0	0	0	0	0	0	0	8.1	5.5
No. of studies	2	2	1	1	1	1	1	1	4	4

% = percentage of eyes; MRSE = manifest refractive spherical equivalent

Table 5. Pooled estimates of UDVA in myopic eyes.

Follow-up Time	2 yrs	3 yrs	4 yrs	5 yrs	6 yrs
No. of eyes	560	733	162	210	89
Mean % UDVA \geq 20/40 (range)	85 (67, 87)	81 (67, 100)	81 (57, 92)	86 (45, 100)	79 (79)
Median % UDVA \geq 20/40 (range)	87 (67, 87)	79 (67, 100)	92 (57, 92)	82 (45, 100)	79 (79)
SD	5.2	8.3	13.3	15.5	0
No. of studies	4	7	3	5	1
No. of eyes	475	733	162	210	—
Mean % UDVA \geq 20/20 (range)	32 (16, 35)	32 (4, 60)	36 (7, 53)	28 (6, 74)	—
Median % UDVA \geq 20/20 (range)	35 (16, 35)	31 (4, 60)	53 (7, 53)	21 (6, 74)	—
SD	5.9	14.7	20.3	20.6	—
No. of studies	3	7	3	5	—

% = percentage of eyes; UDVA = uncorrected distance visual acuity

and Qasem et al.³³ (2- and 3-year follow-up) are excluded from the pooled estimates because the reported EC change in these studies included different types of iris-fixated pIOLs.

Twenty-three articles on myopic eyes report on EC change in the period of 2 to 4 years after implantation, ranging from a small gain of 0.26% to a loss of 14.58%.^{3-7,9-13,15-18,21,22,24,27-30,32} Twelve articles on myopic eyes report on EC change in the period of 5 to 7 years after implantation, with a range of 0% to 15.6% EC loss.^{6,7,12,16-18,21,23,26,29,30,33} Four studies report on a follow-up period of longer than 7 years, with EC loss ranging from 4.9% to 22.5%.^{6,23,26,30} The number of eyes examined at given follow-up periods per study ranges from 6 to 293. Pooled estimates for the percentage of the annual EC change per follow-up period are presented in Table 9. The overall median annual EC loss is 60 cells/mm² (ranging from -96 to 144 cells/mm²). Figure 4 shows a stem-and-leaf plot of the overall annual EC loss and median annual EC change per study.

Two studies on hyperopic eyes report on EC change in the period of 2 to 4 years, ranging from 5.4% to 11.7%.^{19,32} The number of examined eyes ranges from 10 to 35. Pooled estimates for the percentage of the annual EC change per follow-up period are presented in Table 10. In Figure 5, absolute EC counts are plotted against time for both groups. The overall median annual EC loss is 65.5 cells/mm² (ranging from 44 to 93 cells/mm²; see also Figure 4).

A variable minimum anterior chamber depth (ACD) was used as a selection criterion, ranging from 2.6 to 3.2 mm across the various studies. There seems to be no difference in EC loss between the studies that adopted a minimum ACD of 3.0 mm or smaller compared with studies adopting a minimum ACD of greater than 3.0 mm (Figure 4). This may be explained by the fact that the mean ACD is above 3.11 mm in all studies (ranging from 3.11 to 3.87 mm).

Secondary Surgical Intervention

The need for secondary surgical intervention after the iris-fixated pIOL implantation is summarized in Tables 11 and 12 as well as in Figure 6 and specified in more detail in Appendix 5 (see Supplemental Digital Content 1, available at <http://links.lww.com/JRS/A5>).

A total of 23 studies report on secondary surgical intervention in myopic eyes, with a total of 3636 myopic eyes. Secondary surgical intervention was needed in 0% to 27.1% of the myopic eyes. Four studies report on secondary surgical intervention in hyperopic eyes, with a total of 217 eyes. Secondary surgical intervention was needed in 2.2% to 46% of the hyperopic eyes.

Repositioning Repositioning of the iris-fixated pIOL may be necessary due to inadequate surgical fixation or due to inadequate fixation after trauma. Overall, pIOL repositioning or re-enclavation was reported in a total of 59 myopic eyes, of which 23 were due to posttraumatic causes.^{3,5,12,13,15,16,22,27,31,32}

Table 6. Pooled estimates of the efficiency index and safety index in myopic eyes.

Follow-up Time	2 yrs	3 yrs	4 yrs	5 yrs	6 yrs	10 yrs
No. of eyes	153	88	51	87	89	89
Median EI (range)	0.90 (0.83, 0.93)	0.98 (0.43, 0.98)	0.96 (0.96)	1.02 (0.63, 1.02)	0.83 (0.83)	0.8 (0.8)
Mean EI (range)	0.89 (0.83, 0.93)	0.86 (0.43, 0.98)	0.96 (0.96)	0.93 (0.63, 1.02)	0.83 (0.83)	0.8 (0.8)
SD	0.04	0.23	0	0.16	0	0
No. of studies	2	2	1	2	1	1
No. of eyes	153	68	51	68	89	89
Median SI (range)	1.19 (1.12, 1.39)	1.02 (1.02)	1.46 (1.46)	1.10 (1.10)	1.10 (1.10)	1.10 (1.10)
Mean SI (range)	1.19 (1.12, 1.39)	1.02 (1.02)	1.46 (1.46)	1.10 (1.10)	1.10 (1.10)	1.10 (1.10)
SD	0.09	0	0	0	0	0
No. of studies	2	1	1	1	1	1

EI = efficacy index; SI = safety index

Table 7. Safety in myopic eyes, change in lines of CDVA.

Study	Eyes (n)	Follow-up Time	≥Lines (%)	≤2 lines (%)	Notes
Asano-Kato et al. ¹⁴	44	2	95.5	4.5	2 eyes; age-related cataract
Bohac et al. ¹³	166	3	99.5	0.5	1 eye; choroidal neovascularization at 18-mo follow-up
Bouheraoua et al. ¹²	68	5	98.5	0	
Budo et al. ³	249	3	95.8	1.2	3 eyes; 1 eye nuclear cataract and 2 eyes macular myopic degeneration
Landesz et al. ¹¹	67	3	92.5	3	2 eyes cataract and 1 eye unclear reason
Landesz et al. ¹³	78	2	91	2.6	2 eyes nuclear cataract
Qasem et al. ³³	151	5	100	0	
Shajari et al. ⁵	95	4	93	0	
Silva et al. ¹⁷	26	5	—	0	1 eye; progressive cataract at 3-yr follow-up
Stulting et al. ²⁷	355	2	96	0.3	
	228	3	92.5	0.9	2 eyes; 1 eye retinal detachment and macular hole and 1 eye posterior capsular opacification
					3 eyes; 1 eye myopic maculopathy, 1 eye guttate dystrophy, and 1 eye cataract
Tahzib et al. ²³	89	10	—	3.6	
Titiyal et al. ¹⁶	51	4	96.1	1.9	1 eye, reason not specified
Yasa et al. ⁴	62	2	100	0	
Yu an et al. ⁷	84	5	100	0	

% = percentage of eyes; ≤ = loss of 2 or more lines of CDVA; ≥ = stable or gain in lines of CDVA; — = no data available; CDVA = corrected distance visual acuity;

IOL Exchange Iris-fixated pIOL exchange was performed in a total of 20 myopic eyes and in 2 hyperopic eyes reported in 6 studies due to refractive undercorrection or overcorrection.^{3,12,22,27,30,31} In 4 eyes, the pIOL was exchanged because of a pupil diameter exceeding the optic diameter/glare or halo complaints.^{27,31}

Correction of Residual Refractive Error An undesirable amount of residual refractive error can be corrected by exchanging the iris-fixated pIOL either for an iris-fixated pIOL of different dioptric powers or for a different iris-fixated pIOL model. Another way of correcting residual refractive error is to combine the iris-fixated pIOL

Table 8. Pooled estimates of CDVA in myopic eyes.

Follow-up Time	2 yrs	3 yrs	4 yrs	5 yrs	10 yrs
No. of eyes	333	499	84	84	89
Pre-op in logMAR					
Mean CDVA ± SD	0.17 ± 0	0.17 ± 0	0.17	0.17 ± 0	0.16 ± 0
Range	0.17	0.17	0.17	0.17	0.16
Post-op in logMAR					
Median CDVA ± SD	0.17 ± 0	0.17 ± 0	0.17	0.17 ± 0	0.16 ± 0
Range	0.17	0.17	0.17	0.17	0.16
Post-op in logMAR					
Mean CDVA ± SD	0.05 ± 0.02	0.07 ± 0.03	0.02	0.02 ± 0	0.12 ± 0
Range	0.02, 0.06	0.02, 0.11	0.02	0.02	0.16
Post-op in logMAR					
Median CDVA ± SD	0.05 ± 0.02	0.06 ± 0.03	0.02	0.02 ± 0	0.12 ± 0
Range	0.02, 0.06	0.02, 0.11	0.02	0.02	0.16
No. of studies	2	3	1	1	1

CDVA = corrected distance visual acuity; logMAR = logarithmic angle of minimum resolution; pre-op = preoperative; post-op = postoperative

Follow-up Time	2 yrs	3 yrs	4 yrs	5 yrs	6 yrs	7 yrs	8 yrs	9 yrs	10 yrs
No. of eyes	1174	772	610	610	131	45	43	20	222
Median (cells/mm ²)	70.5	78.7	77.0	60.2	13.8	22.1	17.5	23.4	36.8
Mean (cells/mm ²)	81.8	67.6	49.1	46.5	14.5	22.1	17.5	23.4	23.5
SD	39.1	30.5	34.0	25.6	0.9	0.0	0.0	0.0	18.4
Minimum (cells/mm ²)	-96.0	20.3	11.3	16.4	13.8	22.1	17.5	23.4	1.7
Maximum (cells/mm ²)	144.0	107.3	90.8	92.2	15.8	22.1	17.5	23.4	64.2
No. of studies	14	9	6	7	2	1	1	1	3

EC = endothelial cell

implantation with additional corneal refractive surgery, which was performed in 114 myopic eyes and 21 hyperopic eyes.^{3,23,31,32}

IOL Explantation The main reason for explantation of the iris-fixated pIOL in the myopic eye study was due to the formation of significant visual cataract.^{3,8,17,18,23,27,30,31} Patients were between 46 and 62 years at the time of cataract extraction with iris-fixated pIOL removal. Almost all cataracts described were of the nuclear sclerotic type.^{11,17,18,27,32} Cataract formation is overall described as having no direct causative relationship with the iris-fixated pIOL implantation. Only 1 study describes a case that can be attributed to

the surgical procedure, acute glaucoma followed by crystalline lens opacification.²²

Iris-fixated pIOL explantation due to excessive EC loss ranged from 0% to 0.9%.^{3,6,8,16,31} Explantation after traumatic causes was reported in 7 eyes.^{3,15,27} In 3 myopic eyes, the pIOL was explanted because of an inflammatory response.²⁷

Iris-fixated pIOL explantation due to glare/halo complaints or a pupil diameter exceeding the optic diameter was described in 3 eyes.^{3,17,27} The need for retinal repair is reported to be in the range of 0% to 2.4%.^{15,16,27,32,33} The main reason for explantation in hyperopic eyes is the formation of posterior synechiae and pigment cell deposits.^{19,20}

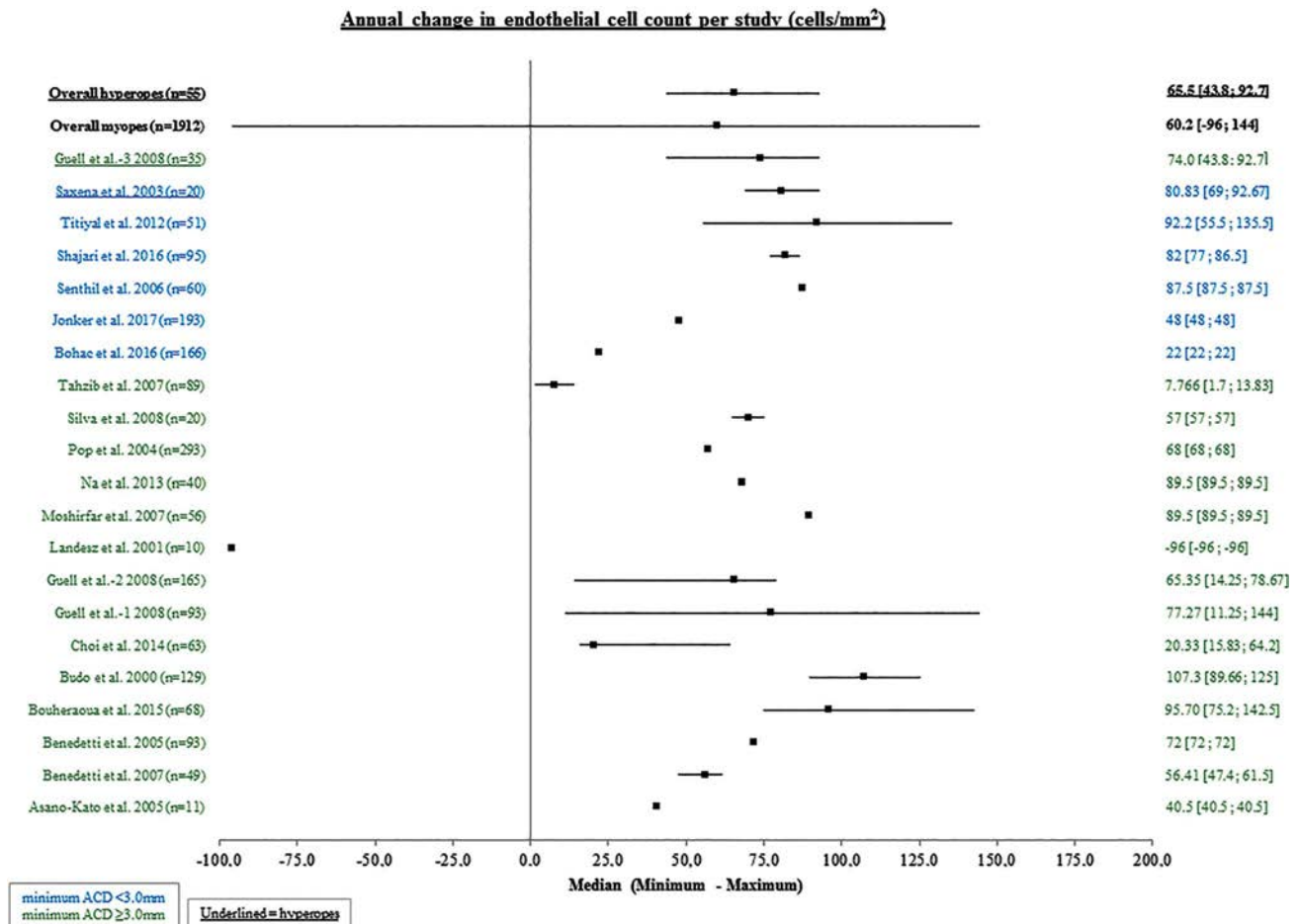


Figure 4. Stem-and-leaf plot annual EC change (ACD = anterior chamber depth; EC = endothelial cell).

Table 10. Pooled estimates of endothelial cell change in hyperopic eyes.

Follow-up Time	2 yrs	3 yrs	4 yrs
No. of eyes	49	44	28
Median (cells/mm ²)	74.0	76.7	43.8
Mean (cells/mm ²)	72.5	80.3	43.8
SD	2.3	6.8	0
Minimum (cells/mm ²)	69.0	76.7	43.8
Maximum (cells/mm ²)	74.0	92.7	43.8
No. of studies	2	2	1

Other Complications

A concern with AC pIOLs is the development of secondary glaucoma due to pigment dispersion, pupillary block, or an uncontrollable inflammatory response. Pigment dispersion is likely to be caused by abnormal pressure on the iris.^{20,38} Baikoff et al.²⁰ describe that of a total of 273 implanted iris-fixated pIOLs (137 myopic and 136 hyperopic eyes), 9 eyes developed pigment dispersion, 8 (5.9%) of which were in hyperopic patients. Although ACs in all eyes were deep enough and irides that were considered too convex were excluded, they found a significant difference in crystalline lens anatomy between the hyperopic and myopic eyes. Saxena et al.¹⁹ report a percentage as high as 15% with pigment dispersion in hyperopic eyes.

To prevent pupillary block, an iridotomy or iridectomy is placed in eyes with iris-fixated pIOLs. There were cases of pupillary block reported in which no iridotomy or

iridectomy was placed or the original iridotomy was closed.²⁷ There was also 1 case of malignant glaucoma for which filtration surgery was needed.¹⁵ However, overall, increased intraocular pressure is uncommon in the long term.

Transient intraocular pressure elevation is mostly described as an early phenomenon arising from corticosteroid use in the early postoperative period. Optic phenomena such as glare and halo complaints can be related to surgical factors of poor centration or cases in which the pupil diameter exceeded the optic.³ Glare/halos were reported to be within a range of 0% to 22.2%. Of the highest percentage reported by Landesz et al.,¹¹ only 2 of 8 patients were disturbed enough by the halos at night that they sometimes used pilocarpine. Moshirfar et al.²² and Titiyal et al.¹⁶ report 2.7% and 3.9% of glare/halo complaints at 2- and 4-year follow-up, respectively. Tahzib et al.²³ scored optic phenomena with a valued questionnaire at 10-year follow-up and reported low scores. Optic phenomena seem to decrease over time and rarely require further action.^{5,7,16}

DISCUSSION

The aim of this systematic review and meta-analysis was to gather all relevant data from the literature on the middle- and long-term effects after implantation of the convex-concave-shaped rigid iris-fixated pIOL (Artisan/Veriseye) for the correction of myopia and hyperopia. After a systematic search, 32 articles were selected and data were collected, reviewed, and summarized in pooled estimates.

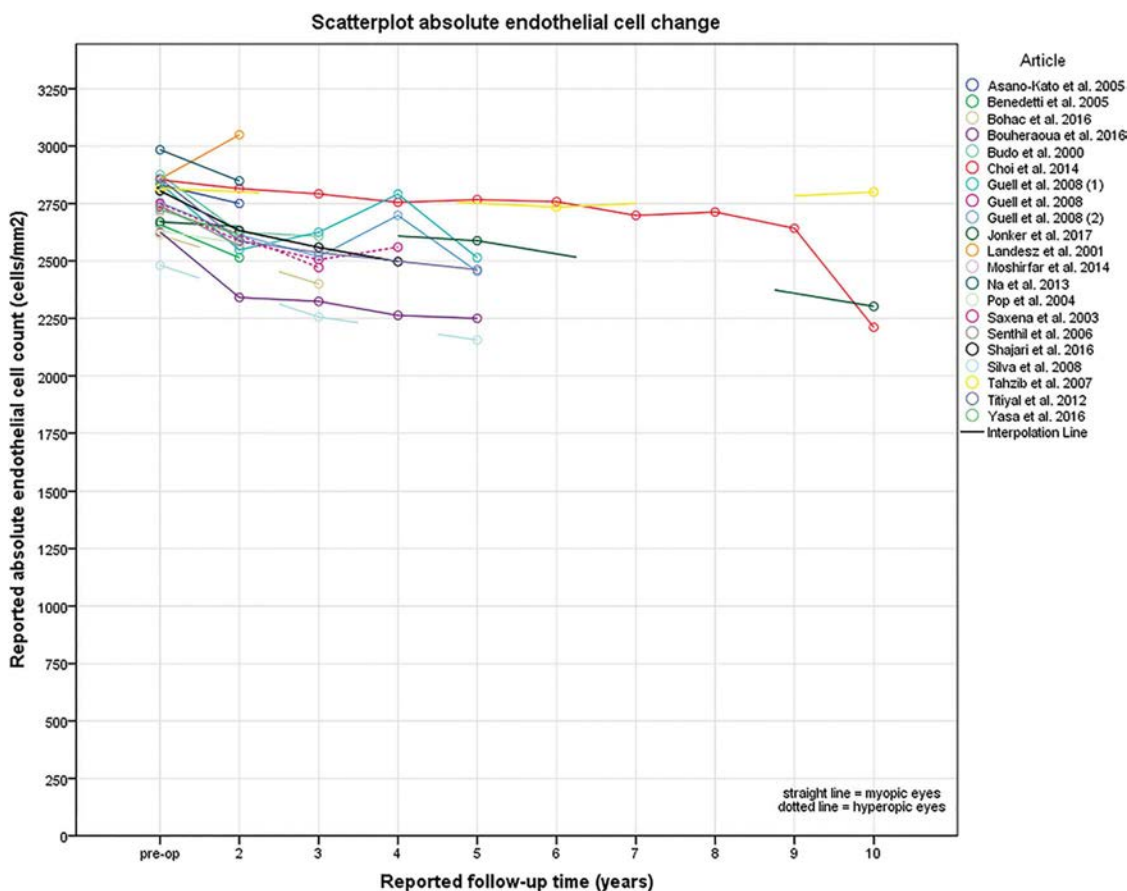


Figure 5. Scatterplot of reported absolute endothelial cell changes.

Secondary Surgical Intervention	Total	Reason	Eyes (count)	Studies (count)
Iris-fixated pIOL explantation	41	Cataract	16	9
		After trauma	7	3
		EC loss	9	5
		Other	9	4
Iris-fixated pIOL repositioning/re-enclavation	59	Inadequate fixation	36	10
		After trauma	23	7
Correction of residual refractive error	134	Iris-fixated pIOL exchange	20	5
		ACRS	114	4
Other	17	Retinal pathology	12	4
		Glare/halo	4	2
		Pigment dispersion	1	1

ACRS = additional corneal refractive surgery; EC = endothelial cell; IF-pIOL = iris-fixated phakic intraocular lens

Refractive Results

A fair to excellent refractive outcome and high stability of the SE over time has been demonstrated by the articles included in this review. Although a wide range of 55% to 98% of eyes is reported to have a deviation within 1.0 D from the targeted refraction, a clear majority of the studies report a mean MRSE within 1.0 D of emmetropia at the last follow-up, without any significant change in the SE over time. When interpreting the results on the deviation of the postoperative SE of targeted refraction, it is important to consider that pure predictability reflects the accuracy of the Van der Heijde formula combined with the surgically induced changes in refraction and is best determined in the period of 3 to 6 months after implantation.²⁴ When describing long-term data on the SE within a certain range, we can only speak of refractive stability because refractive changes due to other reasons might have occurred over time (eg, cataract, progressive elongation of the axial length, and corneal changes).

Visual Outcome

Overall visual outcomes of the iris-fixated pIOL are encouraging, with stable safety indices of above 1.0 in myopic eyes up to 5 years after implantation. Thus, most eyes have a stable or a gain in CDVA. This outcome can be explained by the image magnification effect on the retina with a pIOL in place compared to refractive correction with spectacles, being partly due to the high optical and surface quality of the pIOL.^{39,40} Safety indices in hyperopic eyes are reported to be lower than those in myopic eyes. This can be explained by the retinal minification effect after pIOL implantation compared with spectacles. Most studies report less than 1% of the eyes losing 2 or more lines of CDVA. In eyes with a loss of 2 or more Snellen lines of CDVA, the authors claim that the main reasons are age-related cataract formation or

the nature of myopic eye disease and not directly related to the implantation of the iris-fixated pIOL. In terms of efficacy, a significant gain in UDVA preimplantation vs post-implantation is reported by all authors, with all pooled estimates of the EI being above 0.8.

Corneal Endothelium

Accelerated EC loss has been, and still is, a great concern after any type of intraocular surgery, especially with the implantation of any type of AC IOL. Multiple pIOLs have been withdrawn from the market because of an unacceptable EC loss. The extent of EC change varies widely among the different studies involving the iris-fixated pIOL, ranging from a loss to a gain in ECs. The general trend, demonstrates a decrease in the EC density over time, with a comparable result between the myopic and hyperopic eyes. Pooled estimates reveal an annual decrease of 60 cells/mm² in myopic eyes and 65.5 cells/mm² in hyperopic eyes.

In clinical trials, corneal specular microscopy (CSM) is used to noninvasively study the EC layer of the cornea. The evaluation of the corneal ECs with CSM is susceptible to various errors. Internal CSM errors may arise from different sources, such as the accuracy of operator–software interaction, software imprecision, specular reflection limitations generating low-quality images, versatility for acquiring endothelial images, and sampling processes.⁴¹ It has also been shown that different brands of CSM cannot be interchanged reliably.^{42–44} Protocols to evaluate the corneal endothelium are not consistent among the studies included in this review and are mostly not described in detail. The long follow-up time generates additional errors in which changes, updates, or repairs of CSMs may have taken place, and new insights into how to perform and evaluate the corneal endothelium might lead to updates and adjustments

Secondary Surgical Intervention	Total	Reason	Eyes (count)	Studies (count)
Iris-fixated pIOL explantation	5	Pigment dispersion	5	2
Correction of residual refractive error	23	ACRS	21	2
		Iris-fixated pIOL exchange	2	1

ACRS = additional corneal refractive surgery; IF-pIOL = iris-fixated phakic intraocular lens

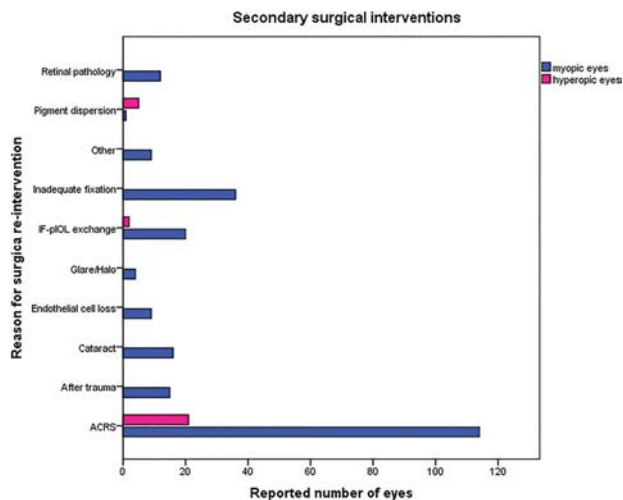


Figure 6. Reasons for secondary surgical intervention (ACRS = additional corneal refractive surgery; IF-pIOL = iris-fixed phakic intraocular lens).

in evaluation methods. Other reasons for a wide range of EC change may be due to surgical experience, patient selection criteria, characteristics of the patient population (eg, race and distribution of age in cohorts), the method of calculating and reporting EC change, a selection bias, the multicenter nature of the study, or reasons still unknown. There is no definite explanation for the wide range reported by the various authors. It may be multifactorial, and in this case, the extent to which each factor may contribute to the wide range in EC change also remains unknown. This fact emphasizes the need for regular follow-up visits and well-controlled prospective and comparative studies and studies with a long follow-up period. Guidelines on how to perform accurate analysis of the corneal endothelium and how to minimize the variability of CSM measurements should be encouraged.^{41,45}

Cataract Formation

Most cataracts reported after iris-fixed pIOL implantation in myopic eyes were of the nuclear type and were the main reason for iris-fixed pIOL explantation. In hyperopic eyes implanted with iris-fixed pIOLs, cataract formation has not been described, but the study population is far smaller and the follow-up time far shorter compared with studies concerning myopic eyes. In their meta-analysis, Chen et al. report an incidence of cataract formation after Artisan/Verisyse pIOL implantation of 1.11% and 0.32% in myopic and hyperopic eyes, respectively, with half of the new onset of cataracts being of the nuclear sclerotic type.³⁴ The mean time to cataract development was 37.65 months. Alio et al.³⁵ describe the reasons for the explantation of various types of pIOLs in one of the largest consecutive case series. They report that almost half of the cases of iris-fixed pIOL explantation were due to nuclear cataract formation. The mean time between iris-fixed pIOL implantation and cataract development was 9.19 years, and the time between iris-fixed pIOL implantation and explantation was 9.55 years. Menezo et al.³⁷ also report a case series of 7 out of 231 eyes (3%) that developed nuclear cataract after the

implantation of an iris-fixed pIOL after a mean period of 4.7 years and, in which cataract extraction was performed, after a mean period of 11.4 years. Although 20% of the eyes were reported as being implanted with the older type of the biconcave Worst-Fechner iris-fixed pIOL, the type of cataract formation and time to cataract extraction is comparable to Alio et al. and the articles analyzed in this review.

Cataract formation is a potential complication of any surgical intraocular procedure, although a direct relationship between cataract formation and the iris-fixed pIOL has not been clearly shown. In cases in which iris-fixed pIOLs are implanted in highly myopic eyes, it is unclear whether cataract formation is due to the implantation procedure (complexity of the procedure and surgical experience) or related to the pIOL itself (material, metabolic effects, and intermittent touch), patient risk factors (trauma, medications, other diseases, and genetic predisposition), or high myopia. Data reported in long-term follow-up studies appear to support author claims that cataract development does appear to be directly related to iris-fixed pIOL implantation. Evidence in long-term, population-based follow-up studies has been provided to support the hypothesis that myopia and hyperopia itself may increase the risk of cataract development, especially of the nuclear type, compared with emmetropic eyes.^{46,47} However, more in-depth studies are needed to prove such statements and to clarify what factors contribute, and to what extent, to possibly earlier cataract development after pIOL implantation.

Glare/Halo

Optical phenomena, such as glare and halo may be caused by various factors such as a scotopic pupil size that exceeds the size of the lens optic, false light through a too large or not adequately located peripheral iridectomy or iridotomy, or a lens that is not stable and/or not adequately centered over the pupil entrance. The surgical procedure of enclavating an iris-fixed pIOL requires skill and practice and has a steep learning curve. A certain amount of enclavated iris tissue is required to ensure proper, stable, and well-centered enclavation. Greater surgical experience increases the ability to accurately enclavate the proper amount of the iris and center the iris-fixed pIOL over the pupil, which will lower the rate of re-enclavations.^{3,48} Although no standardized method is used to evaluate these subjective visual complaints in the various studies, optic phenomena seem to decrease over time and rarely require secondary surgical intervention.^{5,7,16}

Other Complications

The factors mentioned as contributing to an increased risk of spontaneous subluxation include the quality and quantity of enclavated iris tissue at the initial implantation, the amount of iris manipulation during surgery, iris color, anatomy and architecture, and the amount of atrophy and depigmentation at the enclavation site.^{16,36,48} In addition to the articles studied in this review, Moran et al.³⁶ have published a retrospective case series in which 2% of 609 eyes required re-enclavation with a follow-up of 11 years

after Artisan or Artiflex implantation, which globally seems in line with the articles included in this review.

Reported rates of the need for retinal repair are low, ranging between 0% and 1.3%. However, there is no consistent protocol among the studies reviewed concerning prophylactic treatment of the retina; in one study, prophylactic panretinal laser photocoagulation was performed in all treated eyes.¹⁵ A higher risk for retinal detachment after pIOL implantation has been associated with an axial length of greater than 30 mm.^{35,49} In comparison with refractive clear lens exchange (RCLE), an alternative option to correct high refractive errors, Nanavaty and Daya⁵⁰ state that pIOL implantation for the correction of myopic refractive errors may be a safer option than RCLE because retinal detachment in myopic eyes is a concern after RCLE, with incidences reported up to 8%.

Other complications, such as secondary glaucoma or other retinal problems, are rarely reported in myopic eyes. In hyperopic eyes though, severe pigment dispersion seems to present a problem, with an incidence rate of up to 15%.¹⁹ Moreover, the main reason for iris-fixated pIOL explantation in hyperopic eyes is the formation of pigment deposits and posterior synechiae formation. In a short-term study on iris-fixated pIOL implantation in primary and secondary hyperopia, Alio et al.³⁸ also reported that 5% of eyes developed posterior synechiae. It is believed that a convex-shaped iris increases the incidence of pigment dispersion.^{20,38} To decrease the risk Baikoff et al.²⁰ suggested adding the objective measurement of a crystalline lens rise to the safety criteria, instead of using the subjective observation of a convex iris configuration. Prospective or comparative studies to verify a reduction in the incidence of severe pigment dispersion in hyperopic eyes when considering the crystalline lens rise are unfortunately not available.

In conclusion, most articles in the literature present the results on myopic eyes with a medium-term follow-up of 2 to 4 years. Only a few studies present the results from a follow-up of 7 years or longer.

Main findings of our meta-analysis are:

1. Visual and refractive results after the implantation of an iris-fixated pIOL for the correction of myopia are positive.
2. The complication rate is low. Age-related cataract is the main reason for iris-fixated pIOL explantation. Endothelial cell loss seems acceptable, or perhaps better said incalculable, although the range of EC change is too wide to draw firm conclusions.
3. Great care should be taken when considering implanting an iris-fixated pIOL in hyperopic eyes because complication rates, particularly pigment dispersion, might be higher than those in myopic eyes.
4. More well-designed long-term studies are needed, especially in hyperopic eyes.

To provide more evidence for the long-term safety of the iris-fixated pIOL and other IOLs, and to enable proper comparison of different pIOLs and other methods to correct

refractive errors, we advocate for standardized reporting methods for refractive surgery data. Initiatives proposed by journal authors and editors to achieve uniformity should be supported.^{26,51,52}

REFERENCES

1. Fechner PU, Haubitz I, Wichmann W, Wulff K. Worst-Fechner biconcave minus power phakic iris-claw lens. *J Refract Surg* 1999;15:93–105
2. Perez-Santonja JJ, Bueno JL, Zato MA. Surgical correction of high myopia in phakic eyes with Worst-Fechner myopia intraocular lenses. *J Refract Surg* 1997;13:268–281;discussion 281–284
3. Budo C, Hessloeh JC, Izak M, Luyten GP, Menezo JL, Sener BA, Tassignon MJ, Termote H, Worst JG. Multicenter study of the Artisan phakic intraocular lens. *J Cataract Refract Surg* 2000;26:1163–1171
4. Yasa D, Ağca A, Alkin Z, Çankaya KI, Karaküçük Y, Coşar MG, Yılmaz İ, Yıldırım Y, Demirok A. Two-year follow-up of Artisan iris-supported phakic anterior chamber intraocular lens for correction of high myopia. *Semin Ophthalmol* 2016;31:280–284
5. Shajari M, Scheffel M, Koss MJ, Kohnen T. Dependency of endothelial cell loss on anterior chamber depth within first 4 years after implantation of iris-supported phakic intraocular lenses to treat high myopia. *J Cataract Refract Surg* 2016;42:1562–1569
6. Chebli S, Rabilloud M, Burillon C, Kocaba V. Corneal endothelial tolerance after iris-fixated phakic intraocular lens implantation: a model to predict endothelial cell survival. *Cornea* 2018;37:591–595
7. Yuan X, Ping HZ, Hong WC, Yin D, Ting Z. Five-year follow-up after anterior iris-fixated intraocular lens implantation in phakic eyes to correct high myopia. *Eye (Lond)* 2012;26:321–326
8. Moshirfar M, Imbomoni LM, Ostler EM, Muthappan V. Incidence rate and occurrence of visually significant cataract formation and corneal decompensation after implantation of Verisyse/Artisan phakic intraocular lens. *Clin Ophthalmol* 2014;8:711–716
9. Pop M, Payette Y. Initial results of endothelial cell counts after Artisan lens for phakic eyes: an evaluation of the United States Food and Drug Administration Ophtec Study. *Ophthalmology* 2004;111:309–317
10. Na KS, Jeon S, Joo CK. Effect of intraoperative manipulation during iris-claw phakic IOL implantation on endothelium. *Can J Ophthalmol* 2013;48:259–264
11. Landesz M, Worst JGF, Van Rij G. Long-term results of correction of high myopia with an iris claw phakic intraocular lens. *J Refractive Surg* 2000;16:310–316
12. Bouheraoua N, Bonnet C, Labbé A, Sandali O, Lecuen N, Ameline B, Borderie V, Laroche L. Iris-fixated phakic intraocular lens implantation to correct myopia and a predictive model of endothelial cell loss. *J Cataract Refract Surg* 2015;41:2450–2457
13. Bohac M, Anticic M, Draca N, Kozomara B, Dekaris I, Gabric N, Patel S. Comparison of Verisyse and Veriflex phakic intraocular lenses for treatment of moderate to high myopia 36 months after surgery. *Semin Ophthalmol* 2017;32:725–733
14. Asano-Kato N, Toda I, Hori-Komai Y, Sakai C, Fukumoto T, Arai H, Dogru M, Takano Y, Tsubota K. Experience with the Artisan phakic intraocular lens in Asian eyes. *J Cataract Refract Surg* 2005;31:910–915
15. Senthil S, Reddy KP. A retrospective analysis of the first Indian experience on Artisan phakic intraocular lens. *Indian J Ophthalmol* 2006;54:251–255
16. Titiyal JS, Sharma N, Mannan R, Pruthi A, Vajpayee RB. Iris-fixated intraocular lens implantation to correct moderate to high myopia in Asian-Indian eyes: five-year results. *J Cataract Refract Surg* 2012;38:1446–1452
17. Silva RA, Jain A, Manche EE. Prospective long-term evaluation of the efficacy, safety, and stability of the phakic intraocular lens for high myopia. *Arch Ophthalmol* 2008;126:775–781
18. Menezo JL, Peris-Martínez C, Cisneros AL, Martínez-Costa R. Phakic intraocular lenses to correct high myopia: Adatomed, Staar, and Artisan. *J Cataract Refract Surg* 2004;30:33–44
19. Saxena R, Landesz M, Noordzij B, Luyten GP. Three-year follow-up of the Artisan phakic intraocular lens for hypermetropia. *Ophthalmology* 2003;110:1391–1395
20. Baikoff G, Bourgeon G, Jodai HJ, Fontaine A, Lellis FV, Trinquet L. Pigment dispersion and Artisan phakic intraocular lenses: crystalline lens rise as a safety criterion. *J Cataract Refract Surg* 2005;31:674–680
21. Saxena R, Boekhoorn SS, Mulder PG, Noordzij B, van Rij G, Luyten GP. Long-term follow-up of endothelial cell change after Artisan phakic intraocular lens implantation. *Ophthalmology* 2008;115:608–613.e1
22. Moshirfar M, Holz HA, Davis DK. Two-year follow-up of the Artisan/Verisyse iris-supported phakic intraocular lens for the correction of high myopia. *J Cataract Refractive Surg* 2007;33:1392–1397

23. Tahzib NG, Nuijts RM, Wu WY, Budo CJ. Long-term study of Artisan phakic intraocular lens implantation for the correction of moderate to high myopia: ten-year follow-up results. *Ophthalmology* 2007;114:1133–1142
24. Van Der Heijde GL. Some optical aspects of implantation of an IOL in a myopic eye. *J Implant Ref Surg* 1989;1:245–248
25. Aerts AA, Jonker SM, Wielders LH, Berendschot TT, Doors M, De Brabander J, Nuijts RM. Phakic intraocular lens: two-year results and comparison of endothelial cell loss with iris-fixed intraocular lenses. *J Cataract Refract Surg* 2015;41:2258–2265
26. Jonker SMR, Berendschot TTJM, Ronden AE, Saelens IEY, Bauer NJC, Nuijts RMMA. Long-term endothelial cell loss in patients with Artisan myopia and Artisan toric phakic intraocular lenses: 5- and 10-year results. *Ophthalmology* 2018;125:486–494
27. Stulting RD, John ME, Maloney RK, Assil KK, Arrowsmith PN, Thompson VM; U.S. Verisyse Study Group. Three-year results of Artisan/Verisyse phakic intraocular lens implantation. Results of the United States Food and Drug Administration clinical trial. *Ophthalmology* 2008;115:464–472.e1
28. Benedetti S, Casamenti V, Marcaccio L, Brogioni C, Assetto V. Correction of myopia of 7 to 24 diopters with the Artisan phakic intraocular lens: two-year follow-up. *J Refract Surg* 2005;21:116–126
29. Benedetti S, Casamenti V, Benedetti M. Long-term endothelial changes in phakic eyes after Artisan intraocular lens implantation to correct myopia: five-year study. *J Cataract Refract Surg* 2007;33:784–790
30. Choi BJ, Lee JK, Lee JS. Ten-year long-term endothelial cell changes after iris-fixed phakic intraocular lens implantation in Korean patients. *J Clin Exp Ophthalmol* 2014;5:1–5
31. Landesz M, van Rij G, Luyten G. Iris-claw phakic intraocular lens for high myopia. *J Refract Surg* 2001;17:634–640
32. Guell JL, Morral M, Gris O, Gaytan J, Sisquella M, Manero F. Five-year follow-up of 399 phakic Artisan-Verisyse implantation for myopia, hyperopia, and/or astigmatism. *Ophthalmology* 2008;115:1002–1012
33. Qasem Q, Kirwan C, O'Keefe M. 5-year prospective follow-up of Artisan phakic intraocular lenses for the correction of myopia, hyperopia and astigmatism. *Ophthalmologica* 2010;224:283–290
34. Chen LJ, Chang YJ, Kuo JC, Rajagopal R, Azar DT. Meta-analysis of cataract development after phakic intraocular lens surgery. *J Cataract Refract Surg* 2008;34:1181–1200
35. Alio JL, Toffaha BT, Peña-García P, Sádaba LM, Barraquer RI. Phakic intraocular lens explantation: causes in 240 cases. *J Refract Surg* 2015;31:30–35
36. Moran S, Kirwan C, O'Keefe M, Leccisotti A, Moore T. Incidence of dislocated and subluxed iris-fixed phakic intraocular lens and outcomes following re-enclavation. *Clin Exp Ophthalmol* 2014;42:623–628
37. Menezo JL, Peris-Martínez C, Cisneros-Lanuza AL, Martínez-Costa R. Rate of cataract formation in 343 highly myopic eyes after implantation of three types of phakic intraocular lenses. *J Refract Surg* 2004;20:317–324
38. Alio JL, Mulet ME, Shalaby AM. Artisan phakic iris claw intraocular lens for high primary and secondary hyperopia. *J Refract Surg* 2002;18:697–707
39. Artigas JM, Peris C, Felipe A, Menezo JL, Sánchez-Cortina I, López-Gil N. Modulation transfer function: rigid versus foldable phakic intraocular lenses. *J Cataract Refract Surg* 2009;35:747–752
40. Kohnen T, Baumeister M, Magdowski G. Scanning electron microscopic characteristics of phakic intraocular lenses. *Ophthalmology* 2000;107:934–939
41. Abib FC, Holzchuh R, Schaefer A, Schaefer T, Godois R. The endothelial sample size analysis in corneal specular microscopy clinical examinations. *Cornea* 2012;31:546–550
42. Garza-Leon M. Corneal endothelial cell analysis using two non-contact specular microscopes in healthy subjects. *Int Ophthalmol* 2016;36:453–461
43. Goldich Y, Marcovich AL, Barkana Y, Hartstein M, Morad Y, Avni I, Zadok D. Comparison of corneal endothelial cell density estimated with 2 noncontact specular microscopes. *Eur J Ophthalmol* 2010;20:825–830
44. Gasser L, Reinhard T, Bohringer D. Comparison of corneal endothelial cell measurements by two non-contact specular microscopes. *BMC Ophthalmol* 2015;15:87
45. McCarey BE, Edelhauser HF, Lynn MJ. Review of corneal endothelial specular microscopy for FDA clinical trials of refractive procedures, surgical devices, and new intraocular drugs and solutions. *Cornea* 2008;27:1–16
46. Kanthan GL, Mitchell P, Rohtchina E, Cumming RG, Wang JJ. Myopia and the long-term incidence of cataract and cataract surgery: the Blue Mountains Eye Study. *Clin Exp Ophthalmol* 2014;42:347–353
47. Wong TY, Klein BE, Klein R, Tomany SC, Lee KE. Refractive errors and incident cataracts: the Beaver Dam Eye Study. *Invest Ophthalmol Vis Sci* 2001;42:1449–1454
48. Titiyal JS, Sharma N, Mannan R, Pruthi A, Vajpayee RB. Outcomes of re-enclavation of subluxated iris-fixed phakic intraocular lenses: comparison with primary surgery outcomes. *J Cataract Refract Surg* 2010;36:577–581
49. Ruiz-Moreno JM, Montero JA, de la Vega C, Alió JL, Zapater P. Retinal detachment in myopic eyes after phakic intraocular lens implantation. *J Refract Surg* 2006;22:247–252
50. Nanavaty MA, Daya SM. Refractive lens exchange versus phakic intraocular lenses. *Curr Opin Ophthalmol* 2012;23:54–61
51. Dupps WJ Jr, Kohnen T, Mamalis N, Rosen ES, Koch DD, Obstbaum SA, Waring GO III, Reinstein DZ, Stulting RD. Standardized graphs and terms for refractive surgery results. *J Cataract Refract Surg* 2011;37:1–3
52. Stulting RD, Dupps WJ, Kohnen T, Mamalis N, Rosen ES, Koch DD, Obstbaum SA, Waring GO, Reinstein DZ. Standardized graphs and terms for refractive surgery results. *Cornea* 2011;30:945–947

OTHER CITED MATERIAL

A. Penning Y, Worst-van Dam A. *An Eye on OPHTEC, Focus on Perfection*. Scholtema druk, 2014

Disclosures: *None of the authors has a financial or proprietary interest in any material or method mentioned.*

Severe corneal melting after cataract surgery in patients prescribed topical postoperative NSAIDs and dexamethasone/neomycin combination therapy

Emily Cabourne, FRCOphth, Nicola Lau, FRCOphth, Declan Flanagan, FRCOphth, Julie Nott, BSc, Jill Bloom, FRPharms, Romesh Angunawela, FRCOphth

Three patients using a postoperative combination of topical ketorolac (Acular) and neomycin/polymyxin B sulfate/dexamethasone (Maxitrol) were diagnosed with atypical keratopathy soon after routine cataract surgery. An immediate retrospective analysis of hospital patients who had used this topical drug combination in the previous year identified 10 other patients who also had significant corneal pathology after uneventful cataract surgery. Five of the 13 affected patients had corneal melting and 1 patient had corneal perforation and endophthalmitis. At the last recorded follow-up appointment, 8 of the 13

patients had a visual acuity of 6/36 or worse. Corneal melting is a rare complication of topical nonsteroidal anti-inflammatory drugs (NSAIDs). We propose that the combined use of topical NSAIDs and other agents, such as neomycin and benzalkonium, that further compromise the corneal epithelium, should be used with vigilance and increased awareness of potential keratopathy and permanent visual morbidity.

J Cataract Refract Surg 2020; 46:138–142 Copyright © 2019 Published by Wolters Kluwer on behalf of ASCRS and ESCRS

It has been widely reported that nonsteroidal anti-inflammatory drugs (NSAIDs) are effective in the prevention and treatment of macular edema after cataract surgery.¹ In addition, the ESCRS PREvention of Macular EDema study has recently shown that the combination of a topical corticosteroid and a NSAID is more effective than when either agent is used alone to reduce the risk for developing cystoid macular edema after cataract surgery in nondiabetic patients.^A Complications related to topical NSAIDs are relatively uncommon; however, punctate keratitis, infiltrative keratitis, persistent epithelial defect, corneal ulceration, corneal melting, and corneal perforation have all been reported with NSAID use.^{2,3} Corneal melting has been associated with diclofenac, ketorolac, bromfenac, and nepafenac, mostly when local or systemic factors predisposed the patient to develop corneal melting.^{2–10}

We report a series of patients who developed visually significant corneal complications after the combined use of topical ketorolac (Acular) and neomycin/polymyxin B sulfate/dexamethasone (Maxitrol) after uneventful cataract surgery and, in some cases, without any identifiable predisposing factor.

CASE REPORTS

Three patients presented to our eye casualty over a period of several months, each complaining of eye pain and reduced vision in the early postoperative period after uneventful cataract surgery, after which they had routinely been prescribed topical ketorolac and neomycin/polymyxin B sulfate/dexamethasone. Two patients had corneal melting and 1 had an atypical keratopathy. A retrospective investigation of 32 hospital sites in London identified 970 patients who had used this medication combination during the preceding year and, of those, 13 patients (14 eyes [1.3%]) developed severe corneal complications. Five patients developed corneal melting and 8 patients developed prolonged corneal epitheliopathy, which comprised irregular epithelial hypertrophy and punctate epithelial staining. The UK Medicines and Healthcare products Regulatory Agency was immediately informed, as well as relevant pharmaceutical companies, the Royal College of Ophthalmologists, and the UK Ophthalmic Pharmacists Group.

Table 1 shows the patient demographics, corneal complication, eyedrop regimen, and medical background. All patients had surgery completed between January 2015 and March 2016 and ranged in age from 72 to 99 years. Three

Submitted: December 10, 2017 | Final revision submitted: August 9, 2019 | Accepted: August 16, 2019

From the Moorfields Eye Hospital, London, United Kingdom.

Presented at the XXXIV Congress of the ESCRS, Copenhagen, Denmark, September 2016, and the Oxford Ophthalmological Congress, Oxford, England, July 2017.

Corresponding author: Romesh Angunawela, FRCOphth, Moorfields Eye Hospital, City Rd, London EC1V 2PD, United Kingdom. Email: r.angunawela@nhs.net.

Table 1. Summary of all affected cases.

Patient (age/sex/eye)	Corneal Complication	Drug Regimen Until Complication (days)	Surgical Complication	Ophthalmic History	Medical History
1 (85/M/L)	Corneal melt	ketorolac TDS (20) Maxitrol QDS (20)	None	POAG	IHD Atrial fibrillation
2 (84/F/R)	Prolonged epitheliopathy	ketorolac TDS (17) Maxitrol QDS (17)	None	Dry eyes	IHD Hypertension Osteoarthritis GERD Asthma
3 (94/F/L)	Corneal melt	ketorolac TDS (17) Maxitrol QDS (24)	None	None	Hypertension Rheumatoid arthritis Raynaud disease Hypothyroidism
4 (78/M/L)	Corneal melt	ketorolac TDS (7) Maxitrol QDS (7)	Anterior capsule tear	None	None
5 (81/F/R)	Corneal melt	ketorolac QDS (7) Maxitrol QDS (7)	None	Blepharitis	Hypertension
6 (74/F/R)	Prolonged epitheliopathy	ketorolac QDS (14) Maxitrol QDS (14)	None	None	Hypertension Raised cholesterol
7 (72/F/R)	Corneal melt	ketorolac TDS (8) Maxitrol QDS (8)	None	None	Osteoarthritis Thrombocytopenia Asthma
8 (86/F/L)	Prolonged epitheliopathy	ketorolac QDS (20) Maxitrol QDS (20)	None	None	Hypertension GERD Osteoarthritis
9 (74/F/R)	Prolonged epitheliopathy	ketorolac TDS (17) Maxitrol QDS (17)	None	Dry AMD	Asthma Epilepsy Hypothyroidism
9 (74/F/L)	Prolonged epitheliopathy	ketorolac TDS (24) Maxitrol QDS (24)	Epithelial defect and iris trauma	None	Raised cholesterol
10 (78/M/R)	Prolonged epitheliopathy	ketorolac TDS (17) Maxitrol QDS (22)	None	None	Osteoarthritis Spinal spondylosis Raised cholesterol BPH
11 (81/F/R)	Prolonged epitheliopathy	ketorolac TDS (17) Maxitrol QDS (17)	None	Dry eyes Left BRVO	Rheumatoid arthritis, raised cholesterol, bowel and ovarian cancer
12 (72/F/L)	Prolonged epitheliopathy	ketorolac TDS (21) Maxitrol QDS (21)	None	None	Rheumatoid arthritis, DVT, breast cancer, raised cholesterol
13 (99/F/R)	Prolonged epitheliopathy	ketorolac TDS (31) Maxitrol QDS (24)	None	None	Hypertension IHD

AMD = age-related macular degeneration; BPH = benign prostatic hypertrophy; BRVO = branch retinal vein occlusion; DVT = deep vein thrombosis; GERD = gastroesophageal reflux disease; IHD = ischemic heart disease; L = left eye; POAG = primary open-angle glaucoma; QDS = 4 times a day; R = right eye; TDS = 3 times a day

patients were men and 10 were women. Patients were managed by different doctors during their initial presentation to eye casualty, which led to some variation in the initial treatment they received. Those patients who developed corneal melting are discussed in further detail later.

Blood tests were performed, where possible, to screen for any underlying autoimmune process that might have impacted the development of the adverse effect; [Table 2](#) shows the blood test results for 12 patients. One patient did not consent for further investigation. Ten patients were positive for both herpes simplex virus and varicella zoster virus immunoglobulin G on serological testing, and 1 patient was positive for varicella zoster virus alone. Owing to the high

rate of positive serology in the general population, we considered these results as insignificant in relation to the pathogenesis of reported adverse effects. Patient 4, who had a 50% inferior corneal melt, had a mildly raised rheumatoid factor and positive antinuclear antibody despite no known medical diagnoses. Two other patients had a positive antinuclear antibody test; 1 developed a corneal melt and 1 had prolonged epitheliopathy. No negative controls were tested.

Patient 1

An 85-year-old man with primary open-angle glaucoma, ischemic heart disease, and atrial fibrillation underwent uneventful cataract surgery in the left eye. The preoperative

visual acuity was 6/36. He had been prescribed a routine postoperative combination of Acular three times a day and neomycin/polymyxin B sulfate/dexamethasone 4 times a day for 4 weeks. Postoperatively, he withheld the Latanoprost eyedrops that he was using at night for his glaucoma. On day 20, he attended the eye clinic complaining of discomfort and blurred vision. Examination confirmed stromal thinning and an epithelial defect of the left cornea. The topical medications at this initial review were changed to preservative-free dexamethasone 0.1% and chloramphenicol 0.5%, both 4 times a day. At last follow-up at 3 months postoperatively, this patient remains on long-term ocular lubricants and has a visual acuity of 6/36.

Patient 3

A 94-year-old woman with rheumatoid arthritis, hypothyroidism, and Raynaud disease underwent uneventful left eye cataract surgery. Her preoperative visual acuity was counting fingers. She had been prescribed a routine postoperative combination of ketorolac 3 times a day and neomycin/polymyxin B sulfate/dexamethasone 4 times a day for 4 weeks. On day 11, she presented to the eye clinic with a sore red eye and was diagnosed with a large corneal epithelial defect and stromal thinning. On day 43, the cornea was debrided and she continues on preservative-free topical dexamethasone 0.1%, moxifloxacin, and long-term ocular lubricants. Her visual acuity at 3 months was 6/60. Blood tests showed a raised erythrocyte sedimentation rate of 52, which could be attributable to her age and rheumatoid arthritis.

Patient 4

A 78-year-old man with no systemic or ocular history underwent cataract surgery in the left eye, during which there was an anterior capsule tear. There were no further sequelae of this surgical complication, and an intracapsular posterior chamber intraocular lens was inserted as planned. He had been prescribed a routine postoperative combination of ketorolac 3 times a day and neomycin/polymyxin B sulfate/dexamethasone 4 times a day for 4 weeks. On day 6 postoperatively, he

presented to the eye clinic with a large corneal epithelial defect and an 80% stromal melt (Figures 1, A, B, and C). The loose corneal epithelium was debrided at that time. Topical medication was changed to preservative-free dexamethasone 0.1%, moxifloxacin, and ocular lubricants. Three days later, a 4-week course of oral doxycycline and a reducing regimen of oral prednisolone were prescribed. This man continued on ocular lubricants and has a visual acuity of counting fingers. His preoperative corrected visual acuity was 6/12.

Patient 5

An 81-year-old woman with a history of blepharitis and hypertension had uneventful right eye cataract surgery. Her preoperative visual acuity was 6/12. She had taken 3 months of oral lymecycline preoperatively to control her blepharitis. She had been prescribed a routine postoperative combination of ketorolac 4 times a day and neomycin/polymyxin B sulfate/dexamethasone 4 times a day for 4 weeks. Four days postoperatively, she attended the eye clinic with pain and blurred vision. At this time, she was diagnosed with a corneal epithelial defect. Medication was changed to hourly topical moxifloxacin, ganciclovir ointment 0.03%, 400 mg oral acyclovir 5 times a day, and ocular lubricants. Over the course of 9 months, this patient had recurrent filamentary keratitis requiring debridement and corneal stromal melt (Figure 2). Fourteen months after the initial surgery, her visual acuity remains counting fingers and she remains on ocular lubricants, preservative-free dexamethasone 0.1% once daily, and acetylcysteine 5% 4 times a day.

Patient 7

A 72-year-old woman with osteoarthritis, thrombocytopenia, and asthma had uneventful right eye cataract surgery. Her preoperative visual acuity was 6/9. She had been prescribed a routine postoperative combination of ketorolac 3 times a day and neomycin/polymyxin B sulfate/dexamethasone 4 times a day for 4 weeks. Eight days postoperatively, she presented to the eye clinic with a 4-day history of blurred vision. She was immediately diagnosed

Table 2. Serology of affected cases.

Patient	Rheumatoid Factor	Antinuclear Antibody	ESR	Varicella zoster IgG	Herpes simplex IgG
1	Negative	Negative	12	Negative	Negative
2	Negative	Weakly positive	*	Positive	Positive
3	Negative	Negative	52	Positive	Positive
4	Mildly raised	Positive	*	Positive	Negative
5	Negative	Positive	*	Positive	Positive
6	Negative	Negative	32	Positive	Positive
7	Negative	Negative	5	Positive	Positive
8	Negative	Negative	32	Positive	Positive
9		Negative	2	Positive	Positive
10	Negative	Negative	3	Positive	Positive
11	Negative	Negative	1	Positive	Positive
12	Negative	Negative	16	Positive	Positive
13	†	†	†	†	†

ESR = erythrocyte sedimentation rate; IgG = immunoglobulin G

*Blood tests not performed

†Patient 13 did not consent to further blood testing

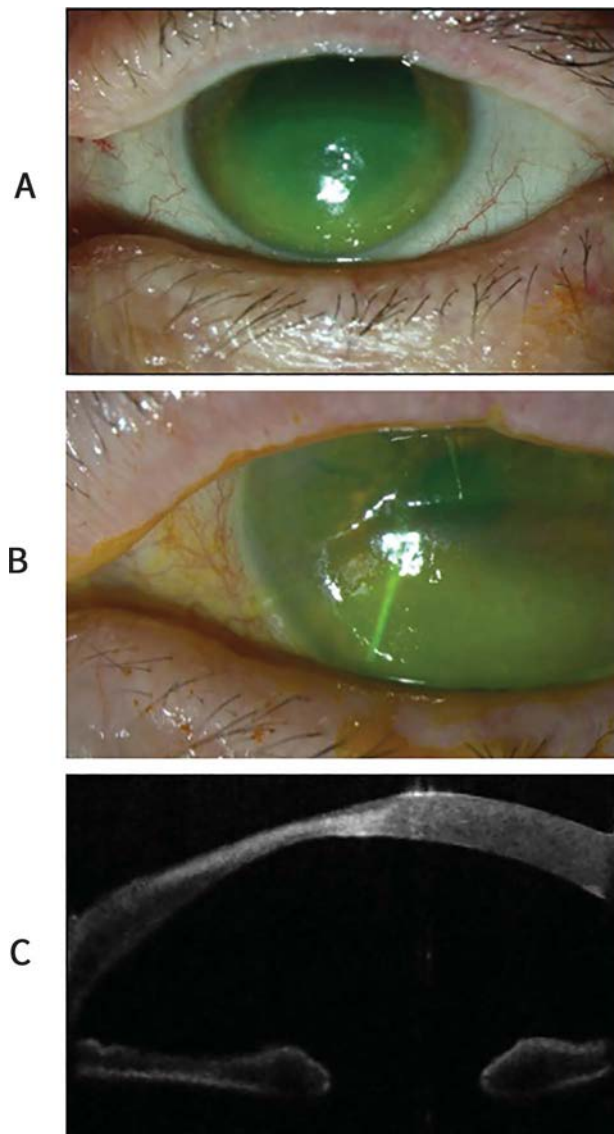


Figure 1. A and B: Color photographs of Patient 4 with an inferior corneal melt and (C) anterior segment optical coherence tomography showing the extensive degree of corneal melting.

with a corneal melt and central corneal perforation, which was sealed using standardized corneal gluing techniques. Four days later, the right eye became more painful, and she was diagnosed with endophthalmitis. A tectonic corneal graft was performed alongside routine endophthalmitis management. Her final visual acuity is perception of light.

DISCUSSION

This case series highlights the risk of drug-related complications following the use of routine medications after uneventful cataract surgery.

NSAIDs reduce inflammation through the inhibition of cyclooxygenases, reducing the synthesis of prostaglandins. In 1999, the ASCRS surveyed its members to investigate any complications that were associated with topical NSAID use postoperatively.^B The results of this survey demonstrated

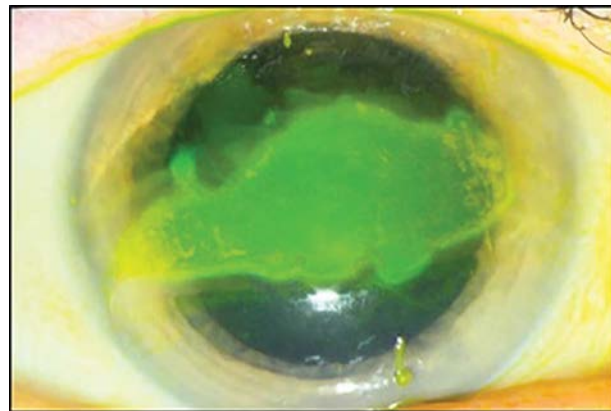


Figure 2. Patient 5 with a central corneal melt and epithelial loss.

that generic diclofenac was mostly associated with either corneal melting or punctate epitheliopathy.^B Varying degrees of keratitis were reported with the use of Acular in that report, but no cases of corneal melting.^B

Although the exact mechanisms leading to corneal melting with NSAIDs are not clearly identified, a proposed mechanism is the upregulation of matrix metalloproteinases that have proteolytic and collagenolytic activity and destroy the corneal extracellular matrix.^{2,11} It has also been reported that topical NSAIDs reduce corneal sensation through their effect on the corneal nociceptor response, which, though helping postoperative pain, can also result in delayed wound healing and re-epithelialization.²

It is well documented that some topical antibiotics and preservatives can be toxic to the corneal epithelium. Lazarus et al.¹² studied ophthalmic preparations and the associated epithelial toxicity to the cornea. On reviewing antibiotic preparations, gentamicin and neomycin were significantly more toxic than tobramycin. With regard to preservatives, benzalkonium chloride (BAK) was the most toxic. Relevant to our case series, Acular contains both ketorolac and BAK, whereas Maxitrol contains neomycin and BAK.

In a rheumatology population, Maxitrol has been reported to be an independent causative factor in the development of corneal melts after cataract surgery.¹³ This highlights that when used even as a single agent, these topical medications can lead to adverse effects on the cornea. In our reported series, 3 patients had rheumatoid arthritis, 1 of whom developed corneal melting. A deficient tear film also has been reported as a risk factor for developing corneal melting if a precipitating factor such as a topical NSAID is used.¹⁴ Two patients in our case series had a diagnosis of dry-eye disease, and another patient used long-term preserved glaucoma eyedrops, which can independently adversely affect the quality of the ocular surface, specifically the corneal epithelium. Marcon et al. report a case of sterile corneal melting in a 78-year-old man with dry eyes who presented 2 months after cataract surgery.¹⁰ The patient had been using a combination of ketorolac and tobramycin/dexamethasone (Tobradex) 4 times daily. Other ocular and systemic risk factors recognized to predispose the cornea to NSAID-related

adverse effects have been reported including keratoconjunctivitis sicca, limbal stem cell deficiency, neurotrophic keratitis, persistent epithelial defects, rosacea, Sjögren syndrome, and erythema multiforme, none of which were identified in our cohort of patients.^{5–7}

Given the variety of patients in our cohort and across the literature, we conclude that the risk of developing adverse effects, including corneal melting, with the use of topical NSAIDs is multifactorial. This case series suggests that there may be a combined toxic effect on the cornea when using topical neomycin/polymyxin B sulfate/dexamethasone with ketorolac after cataract surgery. We recognize that these topical medications are widely and successfully used for a variety of clinical indications; hence, further experimental studies would need to be performed to investigate any potential mechanisms or causal relationships. In the meantime, we propose that the combined use of topical NSAIDs and other agents such as neomycin and benzalkonium should be considered with added caution, especially in populations at risk, to prevent the rare event of corneal melting and the associated permanent visual morbidity.

REFERENCES

- Hoffman RS, Brage-Mele R, Donaldson K, Emerick G, Henderson B, Kahook M, Mamalis N, Miller K, Realini T, Shorstein NH, Stiverson RK, Wirostko B. Cataract surgery and nonsteroidal anti-inflammatory drugs. *J Cataract Refract Surg* 2016;42:1368–1379
- Prasher P. Acute corneal melt associated with topical bromfenac use. *Eye Contact Lens* 2012;38:260–262
- Asai T, Nakagami T, Mochizuki M, Hata N, Tsuchiya T, Hotta Y. Three cases of corneal melting after instillation of a new nonsteroidal anti-inflammatory drug. *Cornea* 2006;25:224–227
- Lin J, Rapuano C, Laibson P, Eagle R, Cohen E. Corneal melting associated with use of topical nonsteroidal anti-inflammatory drugs after ocular surgery. *Arch Ophthalmol* 2000;118:1129–1134
- Flach A. Topically applied nonsteroidal anti-inflammatory drugs and corneal problems: an interim review and comment. *Ophthalmology* 2000;107:1224–1226
- Guidera A, Luchs J, Udell I. Keratitis, ulceration, and perforation associated with topical nonsteroidal anti-inflammatory drugs. *Ophthalmology* 2001;108:936–944
- Montes-Mollon M, Perez-Rico C, Beckford-Tongren C, Castro M, Pareja-Esteban J, Romero-Garcia A. Corneal melting and topical nonsteroidal anti-inflammatory drug (NSAID). A case report. *Arch Soc Esp Oftalmol* 2009;84:311–314
- Khalifa Y, Mifflin M. Keratitis and corneal melt with ketorolac tromethamine after conductive keratoplasty. *Cornea* 2011;30:477–478.
- Mian S, Gupta A, Pineda R. Corneal ulceration and perforation with ketorolac tromethamine (Acular®) use after PRK. *Cornea* 2006;25:232–234
- Marcon A, Rapuano C, Tabas J. Tissue adhesive to treat 2-site corneal melting associated with topical ketorolac use. *J Cataract Refract Surg* 2003;29:393–394
- Brejchova K, Liskova P, Cejkova J, Jirsova K. Role of matrix metalloproteinases in recurrent corneal melting. *Exp Eye Res*. 2010;90:583–590
- Lazarus HM, Imeria PS, Botti RE, Mack RJ, Lass JH. An in vitro method which assesses corneal epithelial toxicity due to antineoplastic, preservative and antimicrobial agents. *Lens Eye Toxic Res* 1989;6:59–85
- Lockington D, Sharma R, Mantry S, Ramaesh K. Maxitrol-induced corneal melts after routine cataract surgery in rheumatology patients. *Clin Exp Ophthalmol* 2015;43:188–189
- Flach A. Corneal melts associated with topically applied nonsteroidal anti-inflammatory drugs. *Trans Am Ophthalmol Soc* 2001;99:205–212

OTHER CITED MATERIAL

- "Prevention of Macular Edema After Cataract Surgery (PREMED) study," presented at ESCRS Congress, Lisbon, Portugal, *Journal of Cataract and Refractive Surgery*, 2017
- NSAID Adverse Reaction Report (Press release): American Society of Cataract and Refractive Surgery, USA, 1999

Disclosures: None of the authors has a financial or proprietary interest in any material or method mentioned.



First author:

Emily Cabourne, FRCOphth

Moorfields Eye Hospital, London, United Kingdom

CASE REPORT

Transient corneal ectasia after phacoemulsification in an eye with femtosecond intrastromal presbyopic treatment

Tommy C.Y. Chan, MD, Jason C.K. Chan, MBBS, Nai-Man Lam, MBBS, John S.M. Chang, MD

We report a case of transient corneal ectasia developed after phacoemulsification in an eye previously treated with INTRACOR. There was a myopic refractive surprise after cataract surgery. Corneal tomography showed an increase in keratometry and elevation profile compared with preoperative examination. Soft contact lenses and intraocular pressure-lowering medications were prescribed as interim treatment. Clinical improvement was

seen gradually, and the resolution of myopia and ectasia was achieved at 3 months. We believe that high intraocular pressure during phacoemulsification and the weakening effect of femtosecond intrastromal presbyopic treatment can be the culprits.

J Cataract Refract Surg 2020; 46:143–146 Copyright © 2019 Published by Wolters Kluwer on behalf of ASCRS and ESCRS

The procedure INTRACOR (Technolas Perfect Vision GmbH) uses the femtosecond laser to create intrastromal cuts to correct presbyopia. It aims to induce a local reorganization of biomechanical forces and steepening of the central cornea to improve near vision. Good visual outcomes and safety profiles have been reported.^{1,2} There are 4 reports in the literature showing corneal ectasia associated with the procedure. Three patients had laser in situ keratomileusis (LASIK) performed before or after INTRACOR.^{3–5} In one patient ectasia developed with no history of additional refractive surgery.⁶ Here, we report a case of transient corneal ectasia after phacoemulsification cataract surgery in an eye with INTRACOR, which had been stable for 8 years.

CASE REPORT

A 55-year-old woman underwent an uneventful INTRACOR procedure for her left eye at a private eye clinic for the correction of presbyopia. She enjoyed satisfactory distant and near uncorrected vision after the procedure. At 8 years postoperatively, she experienced progressive blurring of vision in the left eye. In our clinic, her uncorrected visual acuity was 6/18 for distant and N5 for near in the left eye. Slitlamp examination revealed the presence of nuclear sclerotic cataract, and fundus examination was unremarkable.

Phacoemulsification and insertion of an intraocular lens (IOL) with a target spherical equivalent refraction

of -1.0 diopter (D) was performed. The surgery was uneventful. At 1 week postoperatively, we noted a refractive surprise of -3.00 diopter sphere (DS)/ -1.50 diopter cylinder (DC). Uncorrected vision was 6/90 for distance and N14 for near. Slitlamp examination revealed a clear cornea, mild anterior chamber reaction, and the presence of the posterior chamber IOL. Intraocular pressure (IOP) was 12 mm Hg.

At 1 month postoperatively, uncorrected visual acuities remained the same with a manifest refraction of -3.75 DS/ -1.50 DC. Slitlamp and fundus examination were unremarkable. Intraocular pressure was 10 mm Hg. Corneal tomography (Pentacam HR, OCULUS Optikgeräte GmbH) of the left eye showed an increase in the average keratometry from 46.5 D preoperatively to 50.1 D postoperatively. Maximum keratometry increased from 49.4 D to 65.4 D. Increase in the anterior and posterior corneal elevation was also noted postoperatively (Figures 1 and 2). Soft contact lenses and IOP-lowering medications, including a 2-week course of oral acetazolamide and a 4-week course of topical beta-blocker, were given in view of her presumed corneal ectasia.

At 3 months, the patient reported significant improvement in vision. Uncorrected distant and near visual acuity was 6/9 and N4, respectively. Manifest refraction was -1.50 DS/ -1.00 DC. Corneal tomography showed reduction in the average and maximum keratometry value to 46.9 D and 51.0 D, respectively.

Submitted: August 7, 2019 | Accepted: August 16, 2019

From the Department of Ophthalmology, Hong Kong Sanatorium & Hospital (T.C.Y. Chan, Chang); Department of Ophthalmology and Visual Sciences, The Chinese University of Hong Kong (T.C.Y. Chan, J.C.K. Chan, Lam, Chang); and Hong Kong Eye Hospital (C.K. Chan, Lam), Hong Kong, China.

Corresponding Author: Tommy C.Y. Chan, MD, Department of Ophthalmology and Visual Sciences, The Chinese University of Hong Kong, 147K Argyle St, Kowloon, Hong Kong, China. Email: tommychan.me@gmail.com.

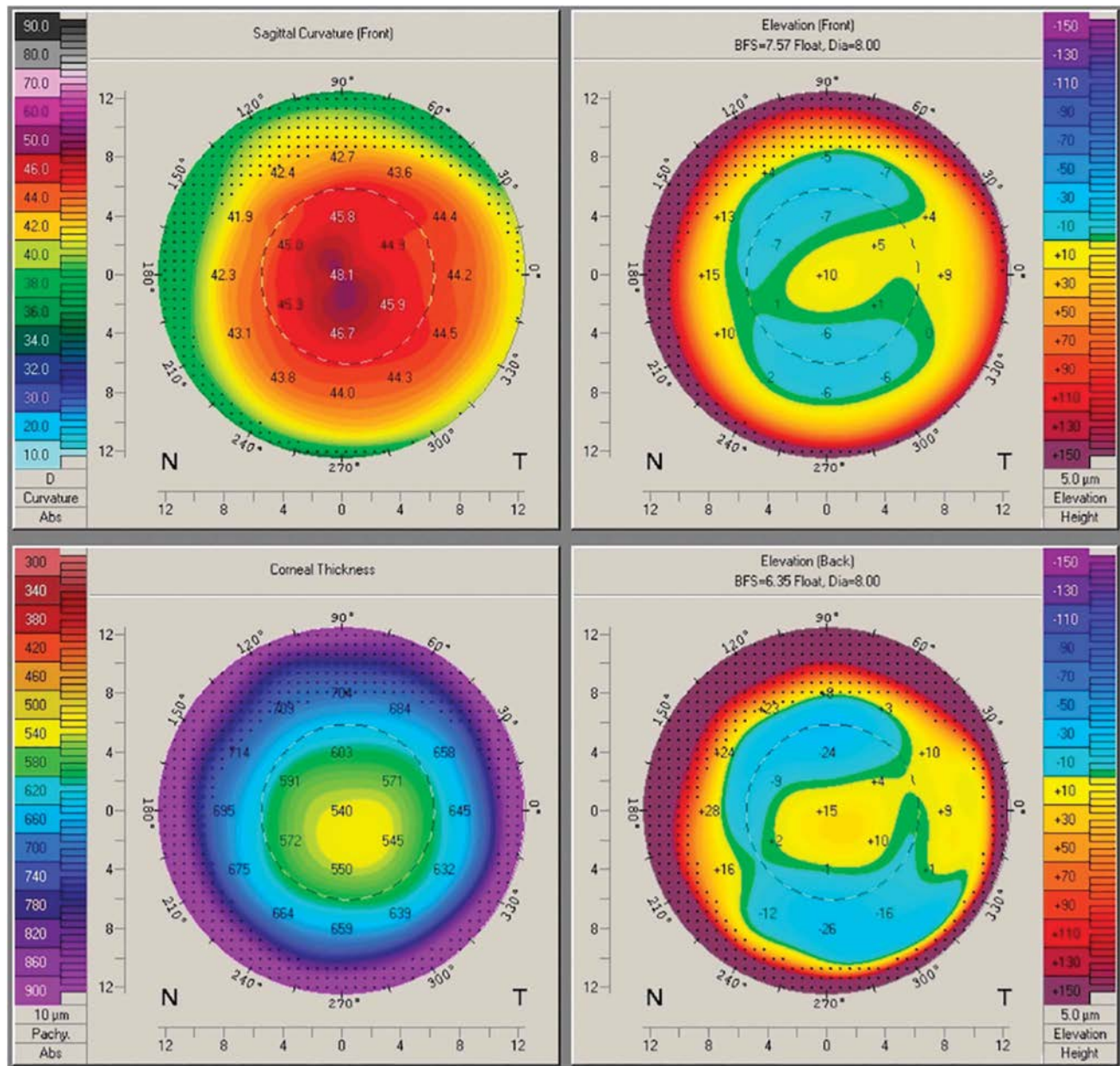


Figure 1. Corneal tomography of the patient's eye with INTRACOR before phacoemulsification.

Significant reduction in the elevation profile was also noted. Corneal thickness remained similar to preoperative values (Figure 3).

DISCUSSION

This case illustrated transient bulging of the cornea that was previously treated with INTRACOR after phacoemulsification. The ectasia was transient as demonstrated by the resolution of myopic refractive surprise, keratometry, and elevation profile in corneal tomography. The high IOP (up to 60 mm Hg) during phacoemulsification could lead to excessive forward shifting of the central cornea,⁷ which is weakened intentionally by the femtosecond intrastromal presbyopic treatment. The basic pattern of INTRACOR is a series of femto-disruptive

cylindrical rings that are delivered within the stroma, sparing the Bowman layer, Descemet membrane, and endothelium.¹ Transient ectasia and increased myopia have been reported in association with elevated IOP after high myopic LASIK correction.^{8,9} In these cases, reduction in the IOP improved the myopic shift and forward bulging of the cornea. We also tried to lower the IOP after ectasia was detected. In our patient, the biomechanical property of the cornea was still sufficient to resume its original shape at 3 months after phacoemulsification following treatment.

Although good visual outcomes and safety profiles have been reported with INTRACOR, the relaxing effect on corneal biomechanical property remained unknown. There were some cases of corneal ectasia reported after the

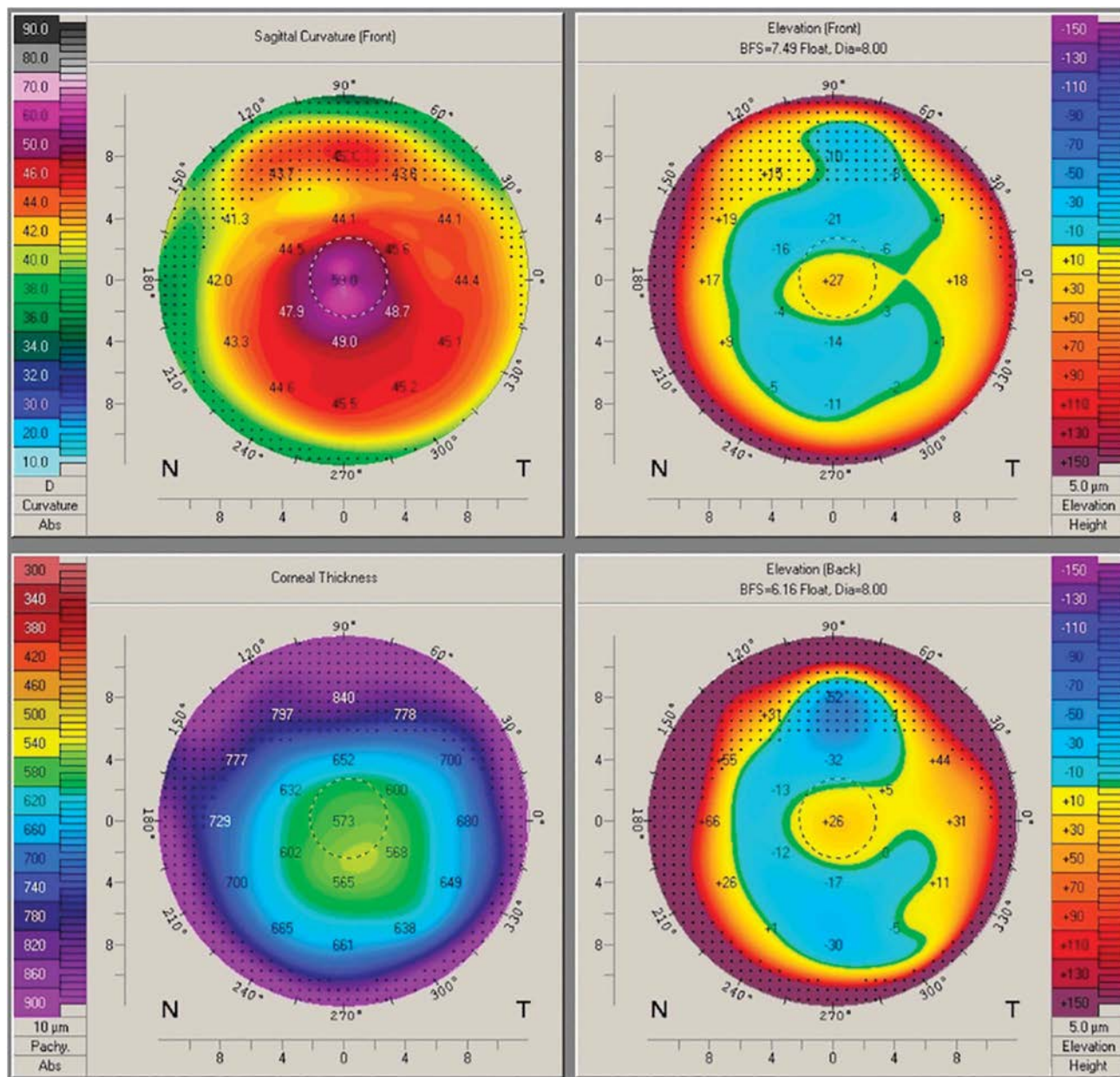


Figure 2. Corneal tomography of the patient's eye with INTRACOR at 1 month after phacoemulsification.

femtosecond intrastromal presbyopic treatment. Saad et al.³ described a case of bilateral ectasia after INTRACOR in a patient who had received multiple hyperopic LASIK treatments. The tomographic pattern was suggestive of isolated anterior corneal protrusion without corneal thinning. Courjaret et al.⁴ reported another case of bilateral ectasia after INTRACOR in a patient who had hyperopic LASIK twice in both eyes. Central corneal protrusion was also demonstrated in tomography. Histology of the corneal button in one eye after keratoplasty revealed stromal bed dehiscence at the intrastromal incision. Taneri and Oehler⁵ reported a case of ectasia in an eye with INTRACOR followed by Supracor (Technolas Perfect Vision GmbH) LASIK enhancement 2 years later. The tomographic changes were limited to the

treated area of INTRACOR. These cases illustrated that the combined weakening effect of Supracor and LASIK, which disrupt the Bowman layer and anterior stroma, may predispose a normal cornea to develop ectasia. A recently published report described a case of postoperative ectasia 5 years after INTRACOR with no history of additional refractive surgery.⁶ However, no preoperative tomography was available for risk determination of ectasia in the report.

This case illustrated that the high IOP during phacoemulsification could lead to forward bulging of the cornea in an eye which had undergone INTRACOR. Future studies are warranted to determine the long-term effect of this observation.

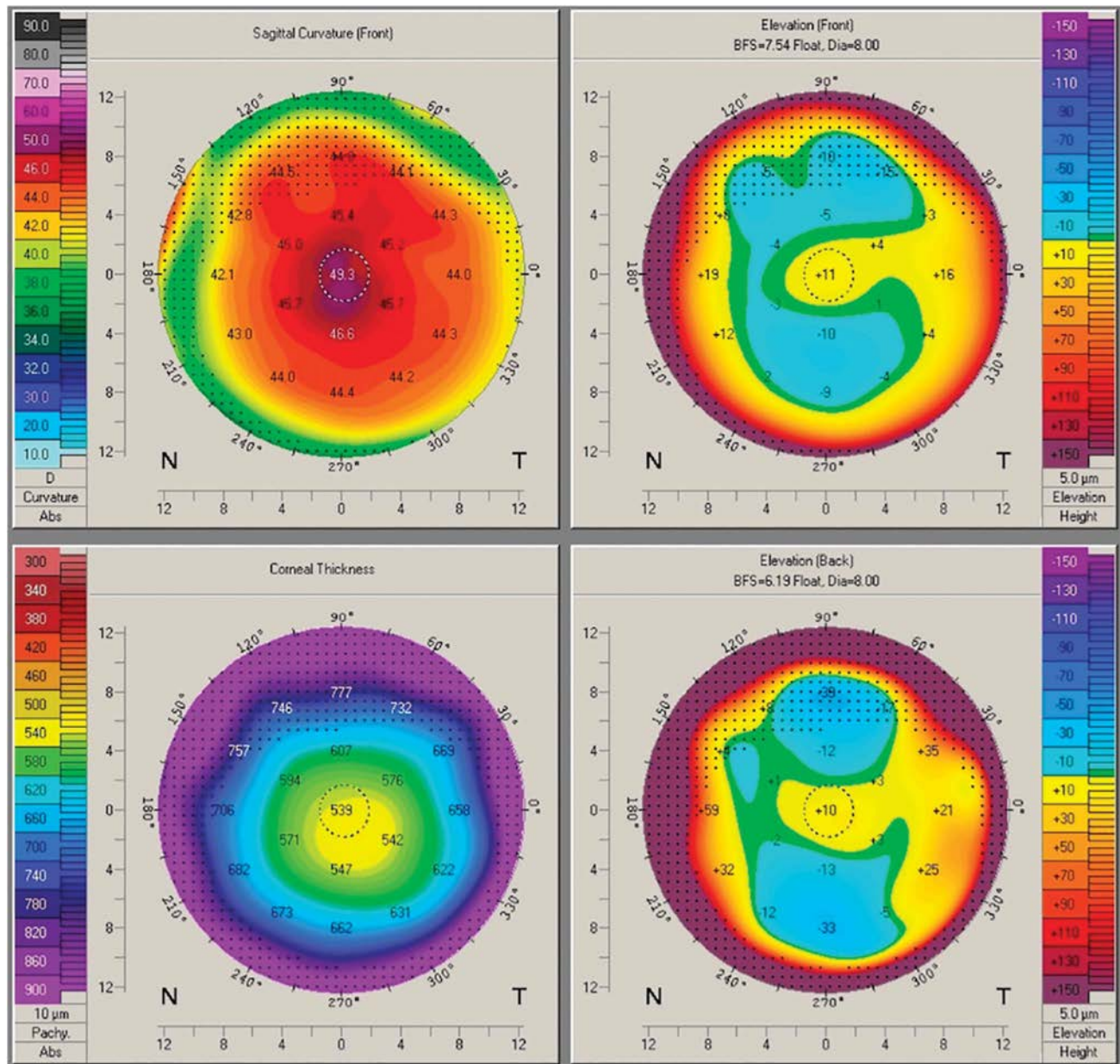


Figure 3. Corneal tomography of the patient's eye with INTRACOR at 3 months after phacoemulsification.

REFERENCES

- Ruiz LA, Cepeda LM, Fuentes VC. Intrastromal correction of presbyopia using a femtosecond laser system. *J Refract Surg* 2009;25:847–854
- Holzer MP, Knorz MC, Tomalla M, Neuhann TM, Auffarth GU. Intrastromal femtosecond laser presbyopia correction: 1-year results of a multicenter study. *J Refract Surg* 2012;28:182–188
- Saad A, Grise-Dulac A, Gatinel D. Bilateral loss in the quality of vision associated with anterior corneal protrusion after hyperopic LASIK followed by intrastromal femtosecond laser-assisted incisions. *J Cataract Refract Surg* 2010;36:1994–1998
- Courjaret JC, Matonti F, Savoldelli M, D'Hermies F, Legeais JM, Hoffart L. Corneal ectasia after intrastromal presbyopic surgery. *J Refract Surg* 2013;29:865–868
- Taneri S, Oehler S. Keratoectasia after treating presbyopia with INTRACOR followed by SUPPRACOR enhancement. *J Refract Surg* 2013;29:573–576
- Lun K, Ray M. Keratoectasia after presbyopia treatment with INTRACOR. *Eye Contact Lens* 2018;44:S333–S336
- Khng C, Packer M, Fine IH, Hoffman RS, Moreira FB. Intraocular pressure during phacoemulsification. *J Cataract Refract Surg* 2006;32:301–308
- Toshino A, Uno T, Ohashi Y, Maeda N, Oshika T. Transient keratoectasia caused by intraocular pressure elevation after laser in situ keratomileusis. *J Cataract Refract Surg* 2005;31:202–204
- Katbab A, Pooyan S, Salouti R, Reza H, Hosseini J. High IOP as a cause of sudden increased myopia after LASIK. *J Cataract Refract Surg* 2005;31:2031–2032

Disclosures: None of the authors has a financial or proprietary interest in any material or method mentioned.

CORRESPONDENCE

Binocular Goldmann visual field testing of negative dysphotopsia

Two previous reports have disclosed that Goldmann perimetry can define a scotoma induced by negative dysphotopsia (ND).^{1,2} The findings of the two studies are somewhat similar; however, we used the Haag-Streit model 900 perimeter, whereas Makhotkina et al² used a traditional Goldmann perimeter.¹ We also reported that contralateral monocular occlusion reduces symptoms and visual field (VF) defects associated with ND in the fellow eye by a mean of 65% in approximately 80% of cases.¹ Furthermore, we noted that blocking temporal light in the contralateral eye with a peripherally opaque contact lens was also effective in reducing the ND symptoms of the fellow eye.¹ This led us to conclude that the central nervous system (CNS) plays a role in ND, irrespective of the causal intraocular mechanism, the latter remaining unclear. The CNS findings were novel and remain unexplained. Among other aspects of our prior Correspondence,¹ unlike patients with VF defects due to glaucoma, retinal, or neurologic disease, the patient with ND tends to be significantly more symptomatic. However, we were unable to achieve a long-term therapeutic effect with contralateral occlusion by either a patch or a peripherally opaque contact lens, in part due to poor treatment tolerance. This differs from a case report in which a recent post-operative patient with ND required eyelid surgery after injury and noted improved ND after ipsilateral ocular occlusion during healing.³

Using a contact lens with an opaque periphery for partial contralateral occlusion (Figure 1), we expanded our previous study to investigate the VF of patients with



Figure 1. Peripherally opaque contact lens with a 7.0 mm clear central zone.

ND under binocular conditions. To our knowledge, this is the first report concerning binocular Goldmann VF testing of ND. In the present pilot investigation, patients with either monocular or binocular chronic ND (symptoms persistent beyond 3 months) were queried as before regarding improvement in ND with contralateral occlusion under ambient lighting conditions (543 lux).¹ All reported improvement of ND with occlusion and all eyes were physically normal (except for uncomplicated pseudophakia), and no patient had any condition that could induce a VF defect other than ND.

Subsequently, patients had binocular Goldmann VF testing using the V4e target. To plot a scotoma, they were asked to identify when the target, moving from the periphery centrad, was first noted, when/if it became obscured or abnormal, and then when it normalized again as the target moved centrad. Next, a soft contact lens with a 7 mm central clear zone (Kontour) was applied to the fellow eye and the VF study repeated in the same fashion. The pupil size was measured before and after instillation of the contact lens using the Colvard pupillometer.

As can be observed in Figure 2, the ND scotoma is far greater in extent when both eyes are fully open than when a peripherally occluding contact lens is applied to the fellow eye. This phenomenon offers an understanding of why patients with ND may be more symptomatic than can be explained by the ND scotoma under monocular vision testing with full occlusion of the contralateral eye. However, under binocular VF testing, one can easily note that the scotoma is large enough to interfere with visual function in the temporal field of the involved eye(s). All previous reported VF studies of ND have been under monocular conditions.¹⁻³ We have observed this VF phenomenon in 3 of 4 tested patients. The one negative test occurred in a patient with vastly improved ND over time. For this case, we could not discern a scotoma.

From the present investigation and from our previously reported study, it would appear that ND has CNS manifestations that are, as of yet, poorly understood.¹ Why should blockage of temporal light in the fellow eye (contralateral) improve ND symptoms? One potential explanation could be alteration in the pupil size. However, we found no consistent change in the pupil aperture after the application of the specialized contact lens. In some eyes, there was no change, in others it was larger by 0.5 mm, whereas it was smaller by 0.5 mm in others. Therefore, we doubt that the change in the pupil size could account for our observations. Future investigations regarding functional magnetic resonance imaging studies are planned, and we anticipate that other centers will investigate binocular Goldmann VFs to corroborate and help explain our findings.

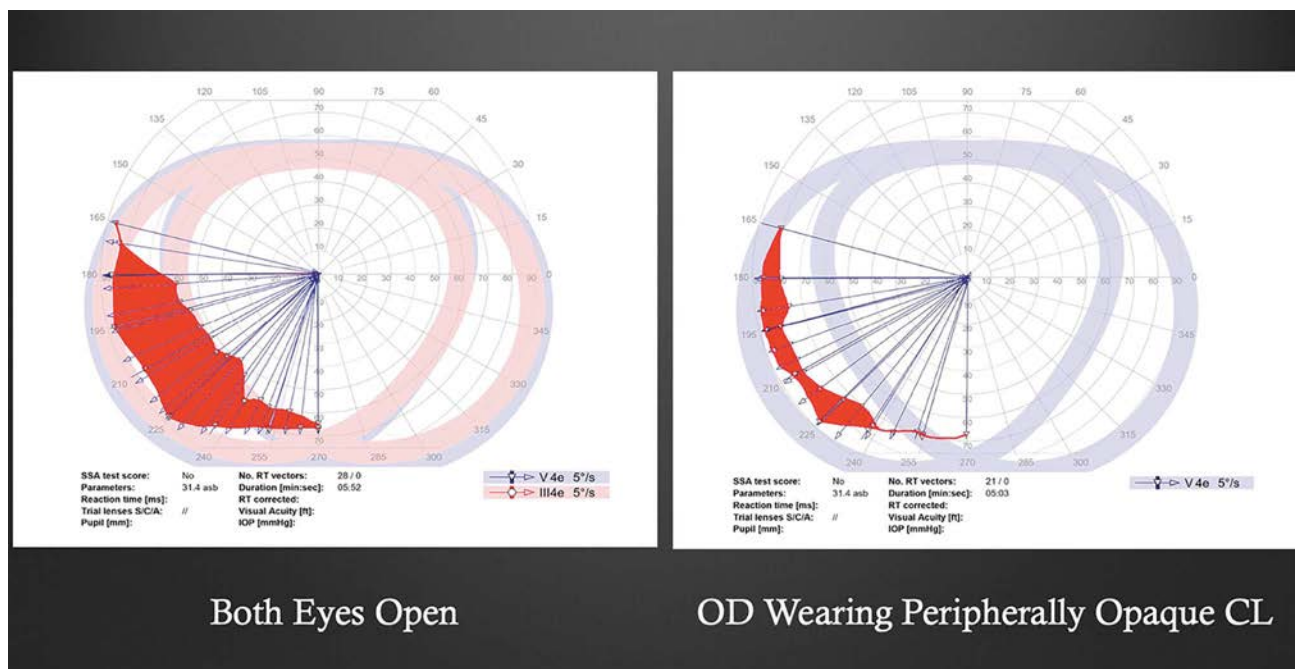


Figure 2. Binocular Goldmann visual field study in patients with ND involving only the left eye. On the left side is the field study with both eyes fully opened. Note the large inferotemporal scotoma (in red). On the right side, the visual field study was repeated with a peripherally opaque contact lens on the contralateral right eye, after which one can observe a marked reduction of the ND scotoma (in red) (Please note that by technician error 1 meridian was recorded with the III4e target for the study on the left side.) (CL = contact lens; ND = negative dysphotopsia).

Samuel Masket, MD
Zsófia Magdolna Rupnik, MD
Nicole R. Fram, MD
Ryan J. Vikesland, OD

- Makhotkina NY, Berendschot TT, Nuijts RM. Objective evaluation of negative dysphotopsia with Goldmann kinetic perimetry. *J Cataract Refract Surg* 2016;42:1626–1633
- Wenzel M, Langenbucher A, Eppig T. Causes, diagnosis and therapy of negative dysphotopsia [in German]. *Klin Monbl Augenheilkd* 2019;236:767

REFERENCES

- Masket S, Rupnik Z, Fram NR. Neuroadaptive changes in negative dysphotopsia during contralateral eye occlusion. *J Cataract Refract Surg* 2019;45:242–243

Disclosures: *None of the authors has a financial or proprietary interest in any material or method mentioned.*

CORRESPONDENCE

Resurgence of inflammatory giant-cell deposits in modern surface-modified intraocular lenses

Intraocular lenses (IOLs) have continually evolved over the years to enhance their biocompatibility, minimize posterior capsular opacification (PCO), and provide optimal clarity. Rigid poly(methyl methacrylate) IOLs have given way to present-day foldable hydrophobic acrylic IOLs.^{1,2}

Amon³ described the concepts of capsular and uveal biocompatibility, wherein capsular biocompatibility was assessed in terms of lens epithelial cell (LEC) outgrowth and the opacification of anterior or posterior capsules. Uveal biocompatibility was assessed in terms of foreign-body giant-cell reactions on the IOL surface. Blood–aqueous barrier breakdown after phacoemulsification results in the release of protein and macrophages, which get adsorbed on the IOL surface and promote cell adhesion.^{3–5} Inflammatory giant-cell deposits (IGCDs) have typically been observed with poly(methyl methacrylate) IOLs and, to some extent, with silicone IOLs, and their incidence in modern hydrophobic acrylic IOLs is minimal.^{6,7}

Various techniques of surface modification of IOLs have been used to enhance IOL biocompatibility, including surface coating, surface-grafted modification, plasma surface modification, photochemical immobilization, and layer-by-layer self-assembly.^{8–10} Tan et al.⁹ covalently grafted a hydrophilic copolymer-P on the surface of a hydrophobic acrylic IOL using plasma technology and observed decreased protein adsorption and cell adhesion on the IOL surface. Biological functional coatings such as hyaluronic acid–lysozyme composites may reduce LEC adhesion in addition to their bactericidal properties.¹⁰

Vivinex XY1 (Hoya Surgical Optics, Inc.) is an aspheric hydrophobic acrylic IOL with enhanced square edge design and surface modification (ultraviolet [UV]/ozone treatment) to minimize the formation of PCO.² UV/ozone surface modification is performed by irradiating the IOL

with UV light to generate ozone and reactive oxygen species on the IOL surface. Both the anterior and posterior optic surfaces undergo UV/ozone modification, which leads to increased surface composition of hydroxyl and carboxyl functional groups resulting in enhanced fibronectin and LEC on the IOL surface.² This promotes posterior capsule (PC) adhesion to the posterior IOL surface and prevents PCO.²

The Vivinex XY1 IOL was implanted after clear corneal phacoemulsification in 72 eyes with immature senile cataract. Written informed consent was obtained from all patients, and the study adhered to the tenets of the Declaration of Helsinki. Patients with ocular comorbidities (corneal disorders, glaucoma, uveitis, retinopathies, etc.), white cataract, and complicated cataract; systemic comorbidities such as diabetes, uncontrolled hypertension, and connective tissue disorders; and pregnant and nursing females were excluded. Patients with prior ocular surgery and inability or unwillingness to follow-up were excluded. Postoperatively, all patients were prescribed topical moxifloxacin 0.5% 3 times a day for 4 weeks, prednisolone phosphate 1% 4 times a day tapered over 4 weeks, nepafenac 0.1% 3 times a day for 8 weeks, and tropicamide 1% 2 times a day for 2 weeks. Follow-up was performed on postoperative day 1 and at 1, 3, 6, and 12 months.

IGCDs were observed in 11 (15.3%) of 72 eyes implanted with the Vivinex XY1 IOL (Figures 1 and 2). The mean age of patients developing IGCDs was 54.2 ± 8.9 years (range 45 to 72 years). There were 7 males and 4 females, and all patients had immature senile cataract with Grades 2 to 4 nuclear sclerosis (Lens Opacities Classification System III).

IGCDs were detected 1 to 6 months after uneventful phacoemulsification (3 eyes, 1 month; 6 eyes, 3 months; 2 eyes, 6 months). IGCDs were observed on the anterior IOL surface, concentrated just within the capsulorhexis edge with a relative sparing of the visual axis. They were quantified on a 0 to 6 scale.⁵ The grading was performed using slitlamp biomicroscopy after dilating the pupil to at

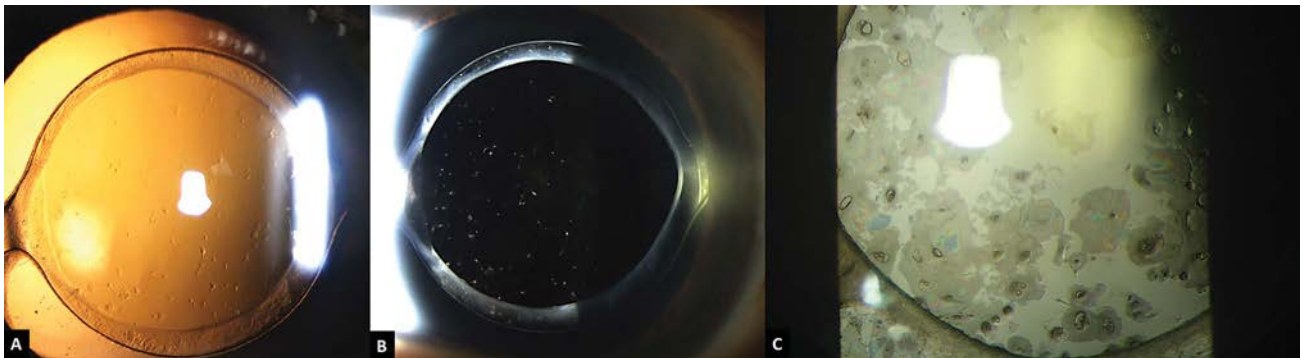


Figure 1. Slitlamp biomicroscopy images of IGCDs on the anterior surface of a hydrophobic acrylic intraocular lens with ultraviolet/ozone surface modification. A: Retroillumination image showing a relatively clear pupillary region. B: Low-magnification photograph of IGCDs concentrated just within the capsulorhexis margin with a relatively clear pupillary region. C: High-magnification image showing clumps of multinucleated giant cells (IGCD = inflammatory giant-cell deposit).

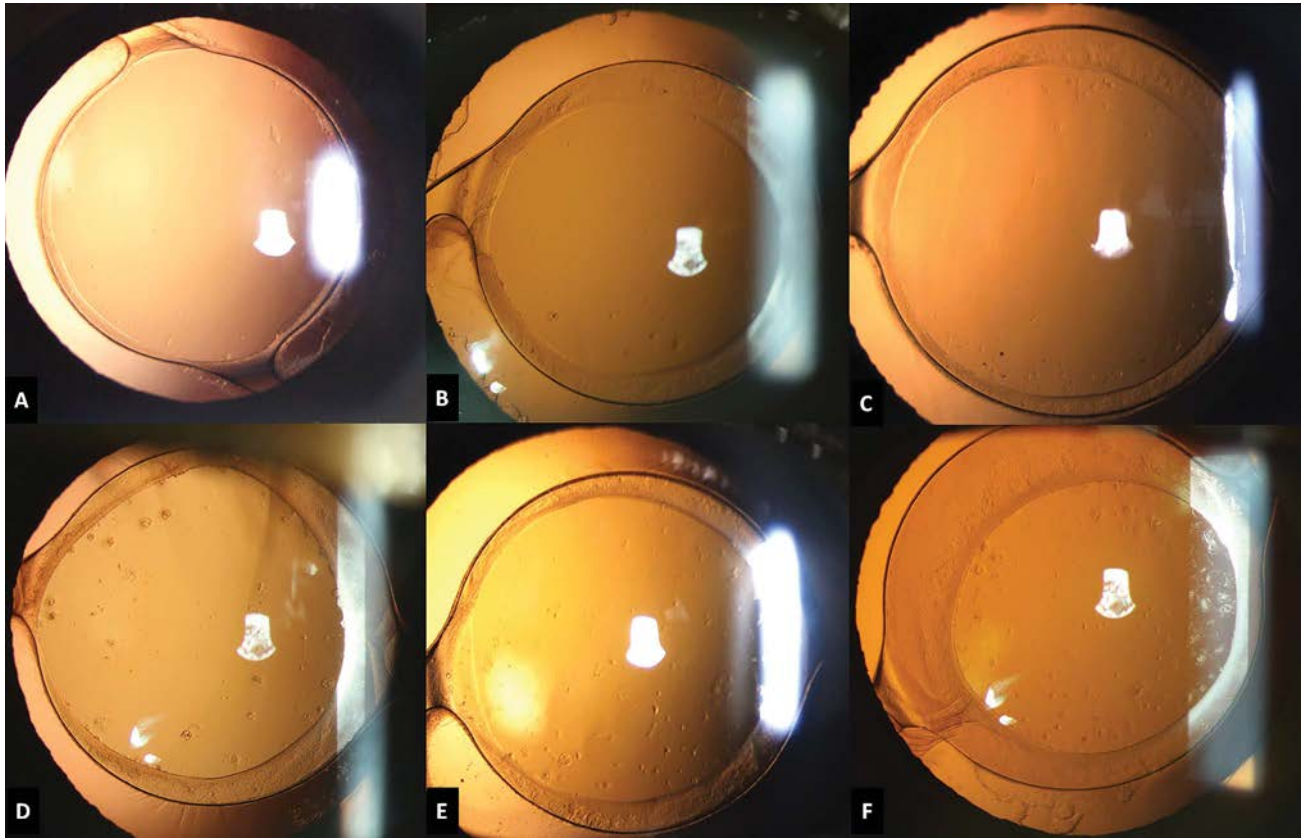


Figure 2. Severity of IGCDs in cases implanted with a hydrophobic acrylic intraocular lens with ultraviolet/ozone surface modification. A: Grade 1 IGCDs. B: Grade 2 IGCDs. C: Grade 3 IGCDs. D: Grade 4 IGCDs. E: Grade 5 IGCDs. F: Grade 6 IGCDs; (IGCD = inflammatory giant-cell deposit).

least 6 mm, so that the entire IOL optic was visible. The grading was performed by a single surgeon (M.K.) and verified by a second surgeon (J.S.T.) in all cases. On initial detection, 3 eyes had mild deposits of Grades 1 to 2, 6 eyes had moderate deposits of Grades 3 to 4, and 2 eyes had severe deposits of Grades 5 to 6. IGCDs progressed in 8 eyes, and at 1 year, 1 eye had mild Grade 1 to 2 deposits, 6 eyes had moderate Grade 3 to 4 deposits, and 4 eyes had severe Grade 5 to 6 deposits. No patient had a spontaneous resolution of IGCDs.

Phacoemulsification was uneventful in all patients with no complications, such as iris prolapse, posterior capsular rupture, vitreous loss, or wound leak. All patients had a continuous curvilinear capsulorhexis with 360-degree coverage of the IOL optic with a rhexis margin. All cases had a minimal anterior capsular opacification of Grades 0 to 1.¹¹ We did not observe capsular shrinkage and significant fibrosis in any patient. No excessive postoperative inflammation was observed. The anterior chamber flare was 5.5 ± 0.9 ph/ms at postoperative Day 1 and 2.2 ± 1.2 ph/ms at 1 year. No abnormality was detected in macular optical coherence tomography findings, and no patient developed PCO. The magnitude of cellular reaction is influenced by the IOL material, inflammatory response during surgery, the presence of pre-existing inflammation, and postoperative therapy.⁵⁻⁷ IGCDs in our series were

likely related to an abnormal surface interaction rather than increased inflammation.

We did not observe a drop in visual acuity associated with the development of these surface deposits, and all patients had uncorrected distance visual acuity of 20/32 or better. There were no subjective complaints by the patients regarding a decrease in the quality of vision or dysphotopic symptoms. This may be attributed to relative sparing of the central visual axis as the intensity of deposits decreased from the capsulorhexis edge inward.

Cellular proliferation on the IOL surface is a marker of biocompatibility of the IOL material.³ IGCDs have rarely been reported with modern hydrophobic IOLs, usually in association with other ocular comorbidities or combined surgical procedures.^{6,7} UV/ozone surface modification is intended to enhance the capsular biocompatibility of the IOLs and promote PC adhesion to the posterior IOL surface to prevent PCO. We believe that surface modification may also promote the proliferation of inflammatory cells on the anterior IOL surface, leading to the characteristic IGCDs observed in our series.

Jeewan S. Titiyal, MD
Manpreet Kaur, MD
Farin Shaikh, MD
Jyoti Rawat, BSc(H)

REFERENCES

1. Tetz M, Jorgensen MR. New hydrophobic IOL materials and understanding the science of glistenings. *Curr Eye Res* 2015;40:969–981
2. Matsushima H, Iwamoto H, Mukai K, Obara Y. Active oxygen processing for acrylic intraocular lenses to prevent posterior capsule opacification. *J Cataract Refract Surg* 2006;32:1035–1040
3. Amon M. Biocompatibility of intraocular lenses. *J Cataract Refract Surg* 2001;27:178–179
4. Miyake K, Asakura M, Kobayashi H. Effect of intraocular lens fixation on the blood-aqueous barrier. *Am J Ophthalmol* 1984;98:451–455
5. Ravalico G, Baccara F, Lovisato A, Tognetto D. Postoperative cellular reaction on various intraocular lens materials. *Ophthalmology* 1997;104:1084–1091
6. Samuelson TW, Chu YR, Kreiger RA. Evaluation of giant-cell deposits on foldable intraocular lenses after combined cataract and glaucoma surgery. *J Cataract Refract Surg* 2000;26:817–823
7. Hollick EJ, Spalton DJ, Ursell PG, Pande MV. Biocompatibility of poly(methylmethacrylate), silicone, and AcrySof intraocular lenses: randomized comparison of the cellular reaction on the anterior lens surface. *J Cataract Refract Surg* 1998;24:361–366
8. Huang Q, Cheng GP, Chiu K, Wang GQ. Surface modification of intraocular lenses. *Chin Med J (Engl)* 2016;129:206–214
9. Tan X, Zhan J, Zhu Y, Cao J, Wang L, Liu S, Wang Y, Liu Z, Qin Y, Wu M, Liu Y, Ren L. Improvement of uveal and capsular biocompatibility of hydrophobic acrylic intraocular lens by surface grafting with 2-methacryloyloxyethyl phosphorylcholine-methacrylic acid copolymer. *Sci Rep* 2017;7:40462
10. Wang B, Lin Q, Jin T, Shen C, Tang J, Han Y, Chen H. Surface modification of intraocular lenses with hyaluronic acid and lysozyme for the prevention of endophthalmitis and posterior capsule opacification. *RSC Adv* 2015;5:3597–3604
11. Werner L, Pandey SK, Apple DJ, Escobar-Gomez M, McLendon L, Macky TA. Anterior capsule opacification: Correlation of pathologic findings with clinical sequelae. *Ophthalmology* 2001;108:1675–1681

Disclosures: *None of the authors has a financial or proprietary interest in any material or method mentioned.*

Should routine testing in patients undergoing cataract surgery be avoided?

There is increasing evidence that routine preoperative nonophthalmic medical testing is not necessary among patients undergoing eye surgery.¹⁻³ Preoperative medical screening, which includes medical visits, chest X-rays, laboratory tests, and electrocardiograms, is very costly. Moreover, the tests might need to be repeated if they do not fit into the 30-day window preceding surgery.² Routine preoperative testing does not increase the safety of cataract surgery.³ Instead, self-administered health questionnaires are a cost-effective substitute for physical examinations to identify those at an increased risk of adverse events due to cataract surgery.³ The abandonment of low-value services related to preoperative screening in routine cataract surgery could yield substantial savings. Despite this evidence, such examinations commonly take place before cataract surgery and other ambulatory procedures in different parts of the world.⁴

According to the American Academy of Ophthalmology-preferred practice pattern for cataract surgery in adults, routine preoperative laboratory testing in association with history-taking and physical examination is not indicated. On the other hand, in Europe, there exists a variety of practice patterns regarding preoperative cataract screening. We contacted key opinion leaders and expert cataract surgeons in several European countries to evaluate practice patterns regarding preoperative cataract screening. Several European countries such as Spain, the Czech Republic, France, and the Nordic countries do not have any particular recommendations regarding this issue, and no medical screening is performed routinely.^{A,B} In the Czech Republic, a patient is asked to provide a certificate from his or her general practitioner, who decides whether to perform any medical screening. The German Ophthalmological Society recommends additional preoperative screening and the involvement of the general practitioner alone in patients with systemic illnesses.^C On the other hand, in Italy and Poland, an anesthetic consultation is recommended preoperatively in all cases.^D In the United Kingdom, preoperative testing is not common. Although re-routing of patients through general practitioners was primarily believed to ensure the appropriateness of preoperative screening, currently it is believed that optometrists rather than general practitioners may be better placed to help patients decide whether or not they wish to be referred for cataract surgery.^E Moreover, according to the Royal College of Ophthalmologists, 21% of patients were preoperatively

interviewed by an optometrist or nurse practitioner and saw the ophthalmologist solely on the day of surgery.^E We could not find any evidence of medical benefits associated with any of the aforementioned approaches.

Globally, there is a cultural tendency to treat every patient as an individual and with the best treatment available. However, physicians should be challenged to prioritize appropriately.⁵ The presented data could generate discussion about the requirement of preoperative testing and address inefficiencies of such screening, reducing costs without sacrificing quality in the case. Importantly, it is estimated that the impact of unnecessary tests might reach about 30% of total healthcare expenditures.¹ With that, using evidence-based guidelines should be supported by the reimbursement system.⁶ On the other hand, in some environments, there might be advantages associated with preoperative medical screening. In remote areas, testing before cataract surgery might be the only chance for some patients to undergo basic laboratory tests such as a full blood count, blood glucose, or cholesterol level monitoring.

We believe that a change in unnecessary practice patterns, although not easy, is possible. For example, for many years, elderly patients using antiplatelet or anticoagulant treatments were believed to manifest a higher risk for complications during cataract surgery and were requested to modify their anticoagulant treatment before any such operation. This resulted in additional consultations and tests, both being cost-consuming and bothersome for patients. Currently, with advances made in the field is known that such surgery performed with a topical anesthesia through a clear corneal incision does not cause an increased risk for ocular hemorrhagic events; thus, anticoagulant therapy does not need to be modified.⁷ We believe that there is a need for updated European recommendations on routine preoperative nonophthalmic medical testing in cataract surgery.

Andrzej Grzybowski, MD, PhD, MBA
Piotr Kanclerz, MD, PhD
Raimo Tuuminen, MD, PhD, FEBO

REFERENCES

1. Parke DW II, Coleman AL, Rich WL III, Lum F. Choosing Wisely: five ideas that physicians and patients can discuss. *Ophthalmology* 2013;120:443-444
2. Chen CL, Clay TH, McLeod S, Chang HYP, Gelb AW, Dudley RA. A revised estimate of costs associated with routine preoperative testing in Medicare cataract patients with a procedure-specific indicator. *JAMA Ophthalmol* 2018;136:231-238

Partially funded by the Institute for Research in Ophthalmology, Foundation for Ophthalmology Development, Poznan, Poland.

Dr. Matteo Piovella, Medical Director, Centro Microchirurgia Ambulatoriale, Monza, Italy, and the current president of the Italian Society of Ophthalmology; Dr. Pavel Rozsival, the Director of the Ophthalmology Clinic of the Charles University, Hradec Kralove, the Czech Republic and the former President of the Czech Ophthalmological Society; Dr. Catherine Creuzot-Garcher, University Hospital of Dijon, France; and Rafael I. Barraquer from the Barraquer Ophthalmology Center, Barcelona, Spain, helped collect the national guidelines.

3. Keay L, Lindsley K, Tielsch J, Katz J, Schein O. Routine preoperative medical testing for cataract surgery. *Cochrane Database Syst Rev* 2019;1:CD007293
4. Ganguli I, Lupo C, Mainor AJ, Raymond S, Wang Q, Orav EJ, Chang CH, Morden NE, Rosenthal MB, Colla CH, Sequist TD. Prevalence and cost of care cascades after low-value preoperative electrocardiogram for cataract surgery in fee-for-service Medicare beneficiaries. *JAMA Intern Med* [Epub ahead of print June 3, 2019.]
5. Tuulonen A. Is more always better? *Acta Ophthalmol Scand* 2004;82:377–379
6. Kessel L, Emgaard D, Flesner P, Andresen J, Hjortdal J. Do evidence-based guidelines change clinical practice patterns? *Acta Ophthalmol* 2017;95:337–343
7. Grzybowski A, Ascaso FJ, Kupidura-Majewski K, Packer M. Continuation of anticoagulant and antiplatelet therapy during phacoemulsification cataract surgery. *Curr Opin Ophthalmol* 2015;26:28–33
- B. Cataract (adults)—Current Care Recommendations. <https://www.kaypa-hoito.fi/hoi50035?tab=suositus>. Accessed August 24, 2019.
- C. Guideline No 19. Cataract in Adults. <https://www.dog.org/wp-content/uploads/2009/09/Leitlinie-Nr.-19-Katarakt-Grauer-Star-im-Erwachsenenalter.pdf>. Accessed August 23, 2019.
- D. Recommendations of the Polish Ophthalmic Society—Surgical Treatment of Cataract. <https://pto.com.pl/storage/guidelines/14/8eca57bb8d03-be309702b8c0d7c7a57b.pdf>. Accessed August 23, 2019.
- E. The Royal College of Ophthalmologists. The Way Forward. Options to help meet demand for the current and future care of patients with eye disease. <https://www.rcophth.ac.uk/wp-content/uploads/2015/10/RCOphth-The-Way-Forward-Cataract-300117.pdf>. Accessed May 10, 2019.

OTHER CITED MATERIALS

- A. Danish Health and Medicines Authority. National clinical guidelines for the treatment of age-related cataracts. <https://www.sst.dk/-/media/Udgi-velser/2013/Publ2013/NKR-for-behandling-af-aldersbetiget-gra-staer.aspx?la=da&hash=D703A562737C7F7F86573207715CCCCDEA362A46D>. Accessed August 23, 2019.
- Disclosures:** Dr. Grzybowski reports nonfinancial support from Alcon, Topcon, Carl Zeiss Meditec AG, Pfizer, Inc., and Novartis and personal fees and nonfinancial support from Santen, Bausch Health Companies Inc., Thea, and Polpharma. Dr. Kanclerz reports nonfinancial support from Visim and Optopol Technologies. Dr. Tuuminen reports nonfinancial support from Bayer and Thea Laboratoires and personal fees from Alcon, Allergan, and Novartis.

Cataract, glaucoma, possible Marfan syndrome, and conception aspirations

Edited by Thomas W. Samuelson, MD

A 36-year-old highly myopic woman was referred for management of both cataract and glaucoma. Her ocular history included retinal detachment repair in each eye, 9 years earlier in the right eye and 7 years earlier in the left eye. Although the patient did not remember specific details of the retinal surgery, she recalled that she had a “gas bubble” postoperatively in the right eye, but not the left eye. She also had a very dense nuclear cataract in the right eye, but only mild nuclear sclerosis in the left eye.

At presentation, the patient’s corrected distance visual acuity (CDVA) was 20/125 in the right eye, with a large myopic shift ($-18.25 + 2.00 \times 175$). Her CDVA in the left eye was 20/20 ($-11.00 + 1.00 \times 20$). It is notable that she is contact lens-intolerant.

Her angle was wide open in each eye, and each optic nerve had severe myopic saucerization and cupping. The axial length was 28.5 mm and 28.7 mm in the right eye and left eye, respectively.

The intraocular pressure (IOP) at presentation was 18 mm Hg in the right eye and 20 mm Hg in the left eye; each eye was treated with a topical β -blocker, α -2 agonist, and a prostaglandin. The highest IOP measurements before treatment were 27 mm Hg and 25 mm Hg in the right eye and left eye, respectively. The pachymetry was 545 μ m in the right eye and 540 μ m in the left eye.

Her visual fields and nerve fiber layers on optical coherence tomography (OCT) are shown in [Figures 1](#) and [2](#), respectively.

Cataract surgery was scheduled along with a coincident glaucoma procedure. It is noteworthy that intraoperatively, the right capsular bag was very loose. Indeed, the capsular bag

could not be penetrated with the cystotome, which only dimpled the capsule severely but would not penetrate it. Accordingly, a super-sharp, #15 blade was used to pierce the capsule and initiate the capsulotomy.

Whereas the zonule was obviously loose, the remainder of the procedure was completed without incident and the intraocular lens (IOL) placed in the capsular bag with perfect centration. It was unclear whether the loose zonule was a consequence of the patient’s vitreoretinal surgery or whether there was a systemic cause for her zonulopathy. Although it was not suspected before the surgery, in retrospect, this patient had the classic body habitus of Marfan syndrome. Moreover, subsequent surgery in the fellow left eye found the zonule to be quite loose, but not as severe as in the right eye.

How would you manage this patient’s glaucoma? Given the finding of very loose zonular fibers, would you initiate a workup for Marfan syndrome? Certain microinvasive glaucoma surgery (MIGS) procedures are labeled for mild-to-moderate glaucoma. How strictly do you adhere to such labeling? Do you ever use a MIGS device in severe glaucoma?

J Cataract Refract Surg 2020; 46:154–161 Copyright © 2019 Published by Wolters Kluwer on behalf of ASCRS and ESCRS

 [Online Video](#)

Sameh Mosaed, MD

Irvine, California, USA

Treatment of advanced primary open-angle glaucoma (POAG) in a young patient, where the stakes are much higher than in the typical POAG patient, involves complex consideration. For this 36-year-old female, we must consider the fact that she already has severe disease encroaching on fixation in the right eye and involving fixation in the left eye. Prompt and consistent IOP control is imperative if she is to keep her remaining vision for her lifetime. Given that she is in her childbearing years, we also must consider methods to eliminate or reduce medication reliance.

She is presenting with progressive field loss despite IOP in the high teens. Typically, MIGS procedures will only lower IOP into the mid-teens, usually with continued medication reliance. Additionally, MIGS procedures often have a waning effect over time; hence, it may not represent

an adequately robust or enduring alternative for this young patient. Because she does not have low-tension glaucoma and likely does not require IOP in the high single digits, I would defer a trabeculectomy or other bleb-reliant procedure at this time. A reasonable goal IOP would be somewhere in the low teens, and a reliable procedure to deliver this is the placement of a Baerveldt glaucoma implant (Johnson & Johnson Vision Care, Inc.). While medication reliance may still be necessary, it is typically lower than with valved tube shunts or with any of the MIGS procedures.

MIGS procedures are generally low-risk and it would not be unreasonable to offer them to this patient to ascertain her individual response. When deciding on the appropriateness of a MIGS procedure, I use the goal IOP as the determining factor: if the goal is in the mid-teens, then I think the MIGS procedures are appropriate, regardless of disease severity. The trabecular bypass procedures using the goniotomy code have broad indications and likely would all have a similar effect here, and one could not discriminate among them. There are many real-

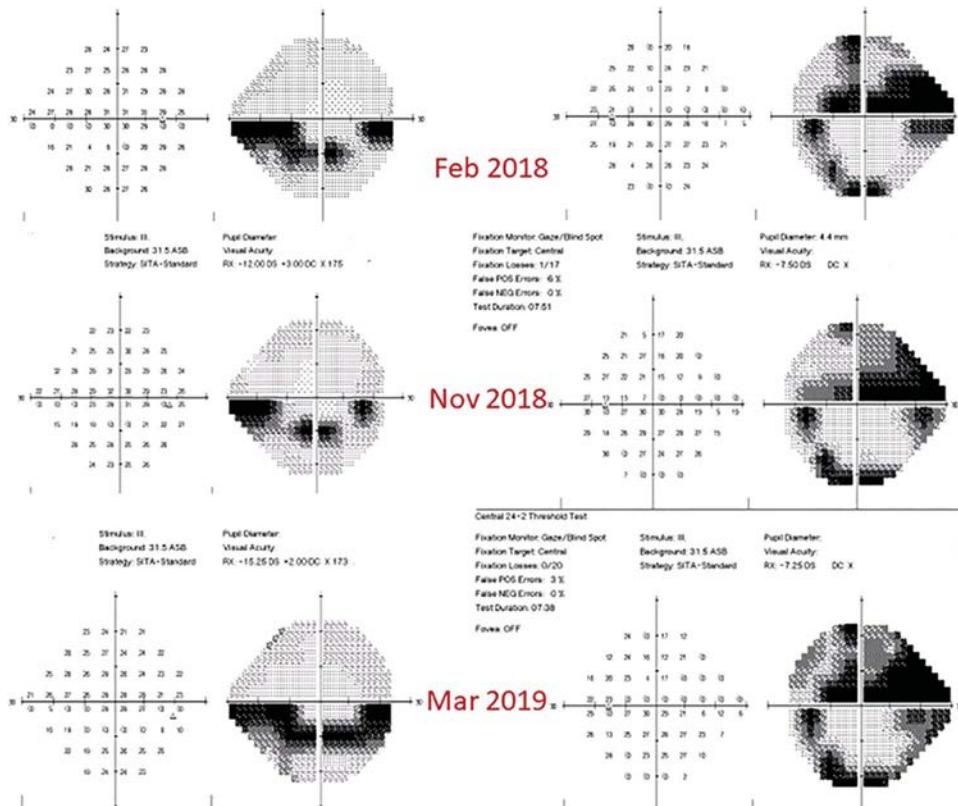


Figure 1. Visual fields from the previous year (2018) and the current visual field (2019).

world studies showing that patients with advanced disease can benefit greatly from trabecular bypass surgeries, as they typically have profound IOP reductions into the mid-teens from a high baseline. In contrast, the Schlemm canal implants are indicated only for mild-to-moderate disease. However, if the target IOP is in the mid-teens, then I would consider off-label use as reasonable in patients with more advanced glaucoma.

Given the body habitus and ocular signs of possible Marfan syndrome, referral for workup would allow for earlier detection of potentially life-threatening aortic aneurysms and other cardiovascular abnormalities. It would also provide information to the patient for consideration for family planning.

While this patient represents a tough case for the clinician considering the high risks involved, I would opt for placement of the Baerveldt glaucoma implant 101 to 350 in each eye. This is more predictable, higher-yield, and definitive than MIGS, and would hopefully result in a one-and-done surgical intervention for this patient.

Disclosures: The author does not have a financial or proprietary interest in any material or method mentioned.

Jacob W. Brubaker, MD
Sacramento, California, USA

There are many key points in this case to consider. Since initially the zonular laxity was unknown, at consideration is a young patient with advanced glaucoma with bilateral

cataract status post retinal detachment surgery. To complicate matters she wishes to conceive and thus a reduced medication burden would be ideal.

With increasing adjunctive glaucoma surgical options at the time of cataract surgery becoming available, more precisely tailoring therapy to individual patients is now a reality. Options for this patient include trabecular stenting, ablating, or bypass. When treating with stents we are often constrained by insurance coverage based on their labeling for mild-to-moderate glaucoma. In my practice, I have found success in using trabecular stents to reduce medication burden if patients are well controlled on medications. This is independent of the glaucoma stage. The case at hand, however, shows a patient that is not well controlled and is in fact progressing on multiple medications. In addition, this patient is quite young and likely has a component of juvenile open-angle glaucoma (JOAG). The primary dysgenesis in these patients is located at the trabecular meshwork. Therefore, similar to a recent paper by Grover et al., I have found that that 360-degree goniotomy in this demographic is quite successful.¹ Alternatively one could consider a subconjunctival microstent. In this situation, however, I would reserve this as a future consideration. Given her uncontrolled glaucoma, likely diagnosis of JOAG, and high myopia, I would have discussed and elected to proceed with 360-degree goniotomy at the time of her cataract surgery.

The discovery of zonular laxity as well as consideration for Marfan syndrome does change the discussion considerably. From an ocular standpoint, her glaucoma

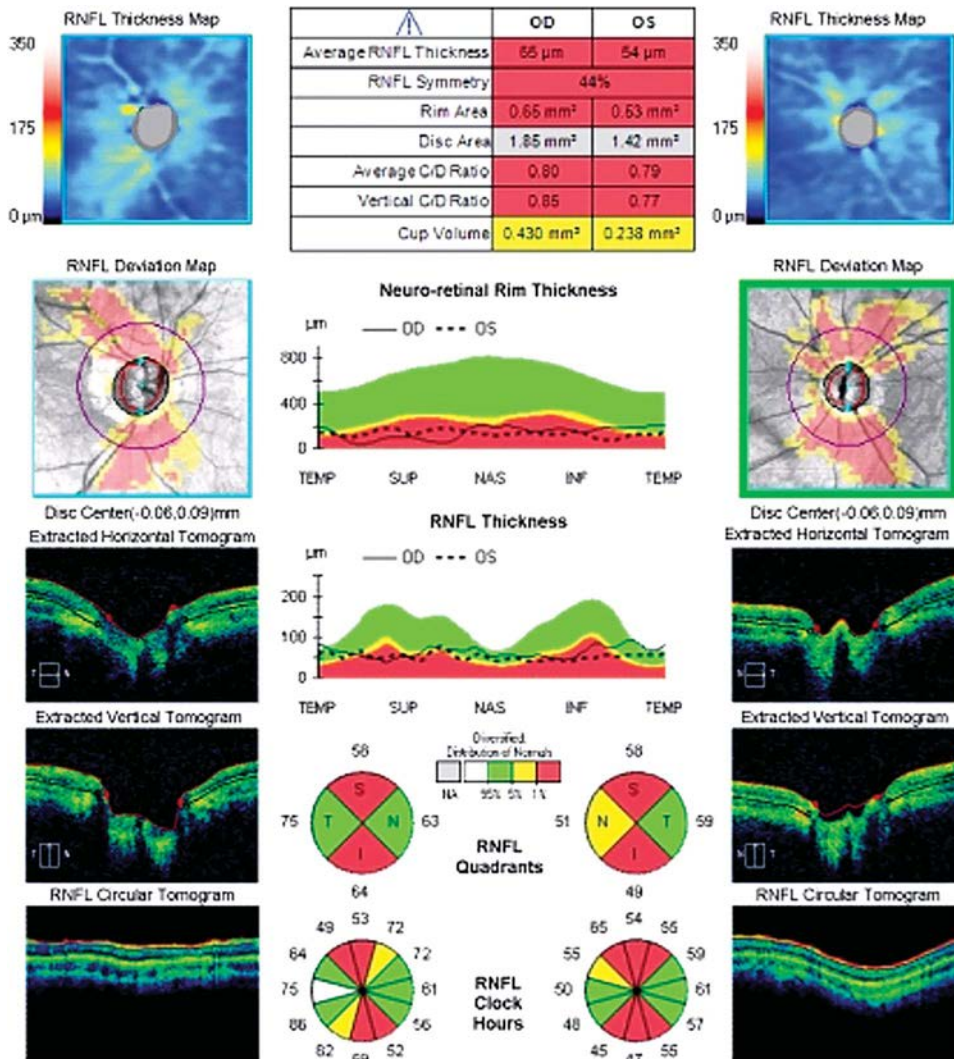


Figure 2. Nerve fiber layers in the right and left eyes.

mechanism would need to be more fully determined. One paper looking at the rate of glaucoma in patients with Marfan syndrome² showed that nearly half of those that developed glaucoma had POAG, with the minority having acute angle closure due to lenticular subluxation. The other half had post-surgical glaucoma, either post lens extraction or scleral buckle. Since secondary pigmentary glaucoma can develop due to IOL laxity, proper scleral fixation would need to be ensured.

More importantly, the possibility of Marfan syndrome needs to be investigated due to the high rate of aortic aneurysms. Given her desire to conceive, she would need to be informed and monitored, not only due to the increased risk of aortic dissection during pregnancy but also so she can be informed about the risk of passing this condition to her offspring. Although mechanical valve replacement is becoming less common in these patients, the risk of requiring long-term anticoagulants could potentially persuade against the use of a 360-degree goniotomy. If this diagnosis were confirmed, after consulting with her cardiologist, I would consider a trabecular stent if future blood thinners may be warranted as I feel the risk of future blood

reflux into the anterior chamber is less common with these devices.

Disclosures: Neither author has a financial or proprietary interest in any material or method mentioned.

REFERENCES

1. Grover DS, Smith O, Fellman RL, Godfrey DG, Butler MR, Montes de Oca I, Feuer WJ. Gonioscopy assisted transluminal trabeculotomy: an ab interno circumferential trabeculotomy for the treatment of primary congenital glaucoma and juvenile open angle glaucoma. *Br J Ophthalmol* 2015;99:1092–1096
2. Izquierdo NJ, Traboulsi EI, Enger C, Maumenee IH. Glaucoma in the Marfan syndrome. *Trans Am Ophthalmol Soc* 1992;90:111–122

Sarah Maki, MD

Christine L. Larsen, MD

Minneapolis, Minnesota, USA

There are several factors that are noteworthy when evaluating further surgical intervention in this patient. In the context of this patient's young age, the severity of her glaucomatous loss is concerning. Under the

assumption that the IOP measurements were similar over the last year to those at the time of referral, the visual fields demonstrate a clear worsening of deficits despite multiple topical medications and an IOP of 18 and 20 in the right eye and left eye, respectively. It is apparent that the patient requires additional pressure lowering from her current baseline, which is further complicated by the fact that topical therapeutic options may be limited in the near future due to her desired pregnancy. In addition, and not an inconsequential consideration, are her previous history of retinal detachment repairs, which may limit surgical options. Because of these aforementioned factors we recommend fairly aggressive IOP control.

Regarding her left eye, her visual field changes in addition to her OCT scan demonstrating little nerve fiber layer reserve, would classify the stage of her glaucoma as severe. In this case, we would recommend careful evaluation for MIGS procedures, such as goniotomy. One could consider assessment for a primary tube shunt; however, given the risk of hypotony maculopathy in this young, highly myopic female, we would recommend MIGS, which would provide a superior safety profile. We would advise a thorough discussion with the patient regarding the aforementioned risks, and the possibility of requiring some topical medications after surgery. It should be noted that some topical medications classified as category C could likely be continued during her pregnancy without consequence if adequate IOP control was not achieved with goniotomy alone. Although her glaucomatous damage would be classified as severe, this case makes an indisputable argument that use of MIGS is best assessed by clinical context and not stage severity.

In surgical planning for the patient's right eye, there is again progression of her visual field with significant glaucomatous loss shown on her OCT scan, although not to the degree of her left eye. In this situation, we would again consider the use of MIGS. Specifically, we would recommend the use of larger canal microstent devices and goniotomy/viscodilation procedures involving the trabecular meshwork. We feel confident that this would best mitigate the surgical risk of more invasive glaucoma procedures such as trabeculectomy or tube shunt in the setting of less advanced visual field changes.

An important final point is that the patient's ocular pathology, including retinal detachments, high myopia, zonulopathy, and glaucoma, in addition to body habitus, are worrisome for Marfan syndrome. Given the significant comorbidities associated with this diagnosis, most notable thoracic aortic aneurysm and dissection, we believe it is imperative to work in conjunction with the patient's primary care provider for further evaluation and workup of this disease.

Disclosures: Dr. Sheybani is a consultant for Allergan, Inc. The other author does not have a financial or proprietary interest in any material or method mentioned.

Erin Sieck MD

Arsham Sheybani MD

St. Louis, Missouri, USA

This case presents a difficult position for glaucoma providers while treating women of childbearing age. Brimonidine, an alpha agonist, is the only category B topical antiglaucoma medication approved for use in pregnant women by the U.S. Food and Drug Administration. All other glaucoma-directed medications are category C and pose a potential teratogen to the fetus.¹ In addition to her currently taking 2 category C medications, she has clear progression in her IOP in both eyes over the last year on her Humphrey Visual Field test. Given the severity of impact and IOP progression, and her young age, she needs a surgical intervention that has the potential to achieve an IOP below episcleral venous pressure.

At the time of cataract surgery, one could still consider a trabecular meshwork procedure, but a canal-based procedure will likely not get her IOP into the low teens without medication. I do consider MIGS procedures for severe glaucoma if the patient is near their IOP goal, has multiple comorbidities, and/or is of advanced age. This is not the case for this patient. Although a 360-degree ab interno trabeculotomy might be very reasonable in a young patient who may have a patent distal outflow system, in this case, the post-vitreotomized eye and weak zonules may mean she is at increased risk for a hyphema that may spill into the posterior segment.

To obtain an ideal IOP without medication, the patient needs subconjunctival surgery. Given her high myopia and the long axial length, I would avoid a traditional trabeculectomy. A tube shunt is unlikely to achieve goal IOPs because of the starting presurgical IOP. At this time, I would recommend a subconjunctival microshunt, such as the XEN stent (Allergan, Inc.). The implant could be placed ab interno without dissecting conjunctiva, especially if the conjunctiva is thin, or ab externo placed below Tenon and conjunctiva after ensuring a broad posterior dissection. The gel stent implant offers the best chance for lowering the IOP but minimizes the chance of chronic hypotony, for which she is at high risk. If she were to need bleb needling during her pregnancy, we would discuss the risk and benefits of using an antimetabolite during that procedure.

I would not initiate a workup for Marfan syndrome if she had a negative family history unless she had classic systemic findings such as arachnodactyly, pectus excavatum, pectus carinatum, or scoliosis. Zonular pathology can be seen following vitrectomy with or without gas placement. In addition, high myopes may have zonulopathy either with a normal axial length (microspherophakia) or a long axial length (as in this case).

Disclosures: Dr. Sheybani is a consultant for Allergan, Inc. The other author does not have a financial or proprietary interest in any material or method mentioned.

REFERENCE

1. Razeghinejad MR. Glaucoma medications in pregnancy. *Oman J Ophthalmol* 2018;11:195–199

Antonio Maria Fea, MD, PhD

Torino, Italy

This case presents several challenges: the patient has glaucoma, high myopia, a monolateral cataract, and progressive visual field damage despite maximal medical therapy, and an IOP in the high teens. Furthermore, she is contact lens-intolerant and the future use of medications may be limited due to her desire to conceive a child.

Considering her progression and her myopia, a lower-target IOP may be advisable; the need for maximal reduction of medical therapy excludes the option of a combined surgery with a trabecular/Schlemm canal procedure. Potential alternatives are phaco-trabeculectomy, phaco-sclerectomy or phacoemulsification combined with a subconjunctival MIGS device (ie, XEN stent, PreserFlo microshunt [Santen]). I would certainly opt for a combined MIGS procedure. Phaco-trabeculectomy, even with lower or no mitomycin-C, may carry a significant risk of early postoperative hypotony, and both phaco-trabeculectomy and sclerectomy would limit future potential options. Either phaco-MIGS procedure may be advisable, but I would probably opt for a phacoemulsification combined with the Preserflo microshunt, because this may result in a lower final pressure and definitely in a lower number of adjunctive procedures. I would implant in the nasal quadrant in order to have the temporal and possibly the superior quadrant untouched in case surgery may be necessary in the future. For an IOL, I would probably choose a monovision option.

The findings of bilateral loose zonules and Marfan syndrome habitus would certainly suggest more investigation, specifically genetic and cardiological workups.

I do not limit the use of MIGS to mild-to-moderate glaucoma. The variables I take into consideration are the age, general health, and tolerance of topical therapy of the patient. Elderly patients with precarious health conditions are certainly included in my MIGS scenario; the choice between trabecular/Schlemm canal procedures vs subconjunctival procedures will mainly depend on the opportunity of adding topical therapy after the surgical procedure if needed. Another factor that plays a role in the decision-making is the starting IOP, the pharmaceutical load, and the need to combine with cataract surgery. In elderly patients with reasonable medical therapy (1 to 2 compounds), with moderately elevated IOP and with concomitant, combo trabecular/Schlemm canal surgery would certainly be an option. I would also consider MIGS in cases with previous complicated glaucoma surgery in the fellow eye; these patients, due to their previous unlucky experience, frequently refuse any further surgery but the offer of a less invasive surgery can be accepted and

sometimes open the road for further surgery if necessary. I do use a MIGS device in severe glaucoma cases.

Disclosures: *The author does not have a financial or proprietary interest in any material or method mentioned.*

Manjool Shah, MD

Ann Arbor, Michigan, USA

There are several interesting and relevant points to review in this case. The choice of an adjunctive glaucoma procedure is important in ideally achieving relative medication independence in this young female patient of childbearing age. It is first important to recognize the relationship between previous vitrectomy and the development of elevated IOP independent of preexisting ocular hypertension.¹ Oxidative stress causing progressive damage to the conventional outflow system has been proposed as a mechanism of this observation.² Furthermore, the patient's young age suggests the possibility of a JOAG pathophysiology, which also may point to a trabecular meshwork and conventional outflow-centered disease. Both observations suggest the possibility of trabecular meshwork bypass procedures as a treatment of choice. In choosing between Schlemm canal-based procedures, there may be a beneficial role in a microstent as opposed to incisional techniques, as incisional goniotomy and trabeculotomy tend to result in greater earlier postoperative hyphema. Because of the zonulopathy and the fact that the patient has had a vitrectomy, there is a greater chance of posterior segment spillover of the hyphema, resulting in significant delay in return to visual function. While Schlemm canal microstents are labelled for use with only mild-to-moderate glaucoma, a strong case for improved predictability and patient safety can certainly be made in this context, and I would favor pushing back against payors as much as possible to do what is best for the patient. I would delay the use of a subconjunctival procedure, reserving it for a later stage if additional IOP or medication reduction is required to achieve the patient's goals. The presence of previous vitreoretinal surgery may have resulted in some conjunctival scarring, which may preclude subconjunctival MIGS procedures, but conventional subconjunctival approaches, such as tube shunts, may be indicated. That being said, MIGS devices in general can certainly have a role in all levels of glaucoma severity, as the disease severity itself may not be as relevant as the desired IOP goal and medication reduction requirements.

In terms of working up the patient for Marfan syndrome given her zonulopathy, it is important to recognize that the patient already has numerous other risk factors for zonular weakness and laxity, namely her history of vitrectomy and her axial myopia. However, because of the Marfan syndrome habitus, the likelihood of a congenital predisposition to zonulopathy may exist. Again, as the patient is thinking about having a child, genetic testing

with appropriate counseling may be helpful for this patient and her growing family.

Disclosures: *The author does not have a financial or proprietary interest in any material or method mentioned.*

REFERENCES

1. Chang S. LXII Edward Jackson lecture: open angle glaucoma after vitrectomy. *Am J Ophthalmol* 2006;141:1033–1043
2. Siegfried CJ, Shui YB, Holekamp NM, Bai F, Beebe DC. Oxygen distribution in the human eye: relevance to the etiology of open-angle glaucoma after vitrectomy. *Invest Ophthalmol Vis Sci* 2010;51:5731–5738

Davinder S. Grover, MD, MPH

Dallas, Texas, USA

Angle surgeries tend not to work well in patients with POAG who are highly myopic. I am not sure whether this finding is due to my personal selection bias or due to stretching of the downstream episcleral venous plexus that impairs outflow, or if it is possibly due to other reasons. For this concern alone, I hesitate to consider angle surgery in this case. If the patient were opposed to any more invasive filtration surgery, I may consider a gonioscopy-assisted transluminal trabeculectomy (GATT); however, I would not expect a GATT surgery or any angle surgery to get her off all glaucoma medications. Of note, zonular weakness puts patients at high risk of a vitreous hemorrhage after angle surgery.

Given her young age, she may be on the JOAG spectrum; however, the myopia and prior retina surgery are confounding this picture. If she were a JOAG patient, I would lean heavily toward a GATT surgery. But because of the prior retina surgery and high myopia, I think there is more going on than just impaired trabecular outflow.

Given the patient's advanced glaucoma stage (the cataract is likely affecting her visual field) and young age, my target IOP would be the low teens. She needs a surgery that will definitively get her IOP in the low teens on as few drops as possible.

My first choice for this patient is cataract surgery and a XEN45 gel stent augmented with 60 mcg of mitomycin-C, but the zonular weakness changes things. If I were to experience intraoperative zonular issues, I would be concerned of dislocating the lens during ab interno implantation of the gel stent. I may consider an ab externo gel stent to avoid excessive anterior chamber manipulation, but this patient will likely need subsequent surgeries for a potential dislocated IOL or additional retinal detachment, and such surgery could possibly cause the stent to fail. Therefore, I may consider a 250-nonvalved implant as this would provide more resilience with subsequent eye surgeries, and I would augment the tube with low-energy cilioablation if the IOP is not at target.

Because of the finding of very loose zonular fibers, connective tissue disorders could have implications for the patient and her future children. Therefore, I would recommend a workup for Marfan syndrome.

MIGS limitations based on staging are due to insurance-imposed limitations and pertain to devices (stents).

Goniotomy and GATT are not tied to a specific staging of disease and can be used more flexibly. For POAG, I use stenting procedures in very mild glaucoma on 1 or 2 drops. I use a goniotomy procedure for mild-to-moderate disease on several drops. I use GATT on moderate-to-advanced disease on several drops when I need significant pressure lowering. I do not typically use angle surgeries for advanced POAG. In secondary open-angle glaucomas, I use GATT in relatively advanced cases as they tend to do well. I will consider either goniotomy or GATT in severe secondary open-angle glaucomas. I do not use stenting procedures in advanced glaucoma unless the patient cannot be taken off blood thinners.

Disclosures: *The author does not have a financial or proprietary interest in any material or method mentioned.*

Sarah H. Van Tassell, MD

New York City, New York, USA

We are presented with a young woman of childbearing age with JOAG in both eyes; she is hoping to conceive a child soon.

The right eye has moderate glaucoma with concern for progression over the last year to an IOP of 18 mm Hg, with the patient on 3 topical IOP-lowering medications. She will likely need incisional surgery in her lifetime, but it is worth it to attempt an angle surgery, particularly because eyes with JOAG can be exquisitely sensitive to the effects of angle surgery. I would perform gonioscopy-assisted transluminal trabeculectomy or goniotomy with a dual blade (Kahook, New World Medical, Inc.); additional angle surgery approaches might also be successful. True surgical success would reduce her IOP as well as her medication burden, so her treatment regimen could be better tailored to her pregnancy and postpartum needs.

For the left eye, I have the option of assessing the early response to angle surgery in the first eye before finalizing a surgical plan. If her IOP reduction in the first eye was substantial, I would repeat the same surgery in the left eye despite the severe glaucoma. Failure of early response in the first eye would point me away from angle surgery in the second eye. Given the patient's axial myopia and young age, I would avoid trabeculectomy. Although one could consider placement of a gel stent, cataract extraction together with placement of a glaucoma drainage implant is my preferred plan. It is worth bearing in mind that her timeline for attempting pregnancy may result in limited opportunities for surgery in the years ahead. Cataract extraction with placement of a glaucoma drainage implant has a high likelihood of IOP and medication reduction with little need for anti-fibrotic injections, needling, revisions, or additional surgery.

It is rare in ophthalmology to have the opportunity to save a person's life, but identifying undiagnosed Marfan syndrome is precisely such an opportunity. This patient has Marfanoid body habitus, high myopia, zonular weakness, glaucoma, and a history of retinal detachments, all of which are more common in patients with Marfan syndrome.^{1,2} Discussing the possibility of Marfan syndrome with this young woman is

prudent. Pregnancy and the postpartum period are high-risk for aortic dissection and rupture in women with Marfan syndrome, and such a diagnosis would be important for her family planning and pregnancy risk management.³ In the absence of a Marfan syndrome diagnosis, I would strongly consider JOAG genetic testing, which may have implications for family planning and monitoring of her children.

Severe glaucoma describes a heterogeneous population of eyes,⁴ and many eyes with severe glaucoma can benefit from the “moderate risk, moderate reward” paradigm of MIGS. As an example, eyes with nasal steps in both hemifields routinely do beautifully following a variety of MIGS; it is unfortunate to arbitrarily exclude eyes such as in this case that may benefit from MIGS. I generally avoid MIGS in eyes with fixation-threatening visual field defects, although there are cases in which MIGS can be appropriate in such eyes, as described above.

Disclosures: *Dr. Van Tassell is a speaker for New World Medical, Inc.*

REFERENCES

1. Esfandiari H, Ansari S, Mohammad-Rabei H, Mets MB. Management strategies of ocular abnormalities in patients with Marfan syndrome: current perspective. *J Ophthalmic Vis Res* 2019;14:71–77
2. Maumenee IH. The eye in the Marfan syndrome. *Trans Am Ophthalmol Soc* 1981;79:684–733
3. Cauldwell M, Steer PJ, Curtis SL, Mohan A, Dockree S, Mackillop L, Parry HM, Oliver J, Sterrenberg M, Wallace S, Malin G, Partridge G, Freeman LJ, Bolger AP, Siddiqui F, Wilson D, Simpson M, Walker N, Hodson K, Thomas K, Bredaki F, Mercaldi R, Walker F, Johnson MR. Maternal and fetal outcomes in pregnancies complicated by Marfan syndrome. *Heart Br Card Soc* 2019;105:1725–1731
4. American Academy of Ophthalmology, American Glaucoma Society. ICD-10 glaucoma reference guide. American Academy of Ophthalmology AAOE Practice Management website. Available at: <https://www.aao.org/Assets/5adb14a6-7e5d-42ea-af51-3db772c4b0c2/636396205914600000/glaucoma-quick-reference-guide-update-8-29-17-pdf?inline=1>. Revised June 2018. Accessed December 2, 2019

Thomas Patrianakos, DO

Chicago, Illinois, USA

The management of this patient’s glaucoma and coexisting cataracts requires multiple considerations due to her complex ocular history. She has documented progression on her visual fields, which means her IOP control has been sub-optimal and needs to be lowered. She is also hoping to conceive in the near future, which will limit her use of topical medications. In addition, she is a high myope, which can make traditional glaucoma filtration surgery (GFS) more complicated due to an increased risk of choroidal effusion/hemorrhage. Her previous retina surgery poses additional surgical challenges secondary to scarring of the conjunctiva.

The safest option would be to perform a nonincisional surgical procedure, such as a transscleral micropulse laser procedure. However, the pressure-lowering effects may be short-lived and therefore the patient should be counseled that further surgical intervention may be required. A more definitive approach would be an ab interno viscodilation of Schlemm canal, goniotomy, or both combined with cataract

extraction. The combined viscodilation and goniotomy would be my preferred procedure as I feel, in my hands, it would be the safest and most efficacious procedure to achieve her target IOP.

MIGS is traditionally not as efficacious as GFS and therefore reserved for mild-to-moderate glaucoma. However, the risk for devastating complications with traditional GFS in this patient with severe glaucoma would make me favor the use of the safer MIGS procedure. More invasive surgeries, such as tube shunts or a Schocket procedure, with greater rates of complications, can be reserved for later in the disease process if needed.

The patient also should be tested for Marfan syndrome as she exhibits many ocular signs of the disorder, including cataracts, loose zonules, retinal detachment, and glaucoma. Arguably, testing for Marfan syndrome is even more paramount in her case as there is an increased risk of a dissecting aortic aneurysm occurring during delivery. The future parents should also be counseled on the genetic probability of passing the disease on to their children.

Disclosures: *The author does not have a financial or proprietary interest in any material or method mentioned.*

EDITOR’S COMMENT

Thomas W. Samuelson, MD

Minneapolis, Minnesota, USA

As uniformly expressed by the panel of expert consultants, there are many important considerations to address in this case. The panel has outlined them beautifully. Consistent with the times, our consultants were quite varied in their recommendations. In 2020, we have a luxury of riches with numerous different glaucoma procedure options from which to select. While the array of options can be confusing indeed, it helps to frame the portfolio of incisional glaucoma surgical options into two broad classifications: those procedures that augment physiological outflow, and those that create a novel and new outflow pathway. The former class of procedures involves canal-based surgery, while the latter represents transscleral surgery. Of course, each of these broad classes have numerous subdivisions. Five of 9 consultants chose a canal-based glaucoma surgery for this patient while 4 recommended transscleral procedures. As an aside, it would be interesting to know how many would have opted for a supraciliary device had that been available. I suspect some would have; endothelial matters related to Cypass notwithstanding. Of those opting for canal surgery, 3 consultants preferred incisional goniotomy with or without canal dilation, while 2 planned on placing a canal stent. Of the 5 consultants preferring transscleral surgery, 1 recommended a long tube, while 3 preferred one of the newer, device-assisted transscleral outflow procedures, such as Xen or PreserFlo. Note, while PreserFlo has the Conformité Européenne mark, it is not yet available to U.S. surgeons. In this particular case, axial myopia and the patient’s aspirations to conceive a child were critical considerations. As emphasized by the expert panel, this case also poignantly demonstrates that procedure selection is far more complex than the device labelling would suggest. While device labelling is based primarily on disease staging, procedure selection is very nuanced. In addition to disease severity, one must consider disease velocity, desired IOP target, anticoagulation status, axial length, availability of glaucoma medications postoperatively, longevity, and perhaps most importantly, likelihood of future progression.

This was my patient and I after considerable discussion she elected to proceed with phacoemulsification combined with the Hydrus microstent (Ivantis, Inc.) (Video 1, available at <http://links.lww.com/JRS/A20> and

Video 2, available at <http://links.lww.com/JRS/A21>). We viewed her pending pregnancy as an important impediment to medication use requiring purposeful utilization of punctal occlusion and careful drug selection, but not an absolute contraindication and not necessarily a reason to take on significant additional surgical risk. Indeed, we did not expect, nor did we achieve, a medication-free result, at least thus far. Two months

postoperatively, her IOP is 15 mm Hg and 16 mm Hg, respectively, while using latanoprost each evening and timolol each morning. Her uncorrected visual acuity is 20/20 in the right eye and 20/70 J1 in the left eye with "mini-monovision." The patient is quite pleased with her outcome yet remains well aware that she may need transscleral surgery at some point should her field progress.

Injection volume and intracameral moxifloxacin dose

We read with interest the recently published article of Shorstein and Gardner,¹ which highlights the importance of adequate intracameral (IC) moxifloxacin dosing and injection protocols in achieving consistent bactericidal levels for postoperative endophthalmitis prophylaxis in cataract surgery.¹ In their study, mathematical models of the anterior chamber (AC) concentrations of moxifloxacin and its elimination rates were calculated following laboratory experimentation with 3 concentrations/injected volumes (0.5%/0.05 mL, 0.5%/0.10 mL, and 0.15%/0.50 mL). Two different AC volumes representing the human pseudophakic eye (0.19 mL and 0.33 mL) for each dosing method were used for their calculations. They concluded that larger injection volumes yielded more reliable aqueous concentrations.

In our recent publication,² we share the authors' viewpoint that larger injection volumes, with similar total dosing, offer greater precision and reliability. We concluded that an IC injection dose of 600 µg moxifloxacin in 0.4 mL (yielding an AC concentration of about 1200 µg/mL), replacing most of the AC and intracapsular volume as the final step of surgery, enables more consistent antibiotic delivery into the AC. Our proposed IC injection method, after hydration of the main incision to avoid leakage, also enables slight adjustments of the intraocular lens position while injecting. It is important to understand that with IC injection, the IC drug concentration continuously accumulates within the AC by logarithmic growth throughout the injection, gradually approaching the injected solution's concentration as aqueous is replaced, rather than providing a complete exchange or wash, an overly simplistic concept.

We chose our injection technique, because our research led us to results somewhat divergent from those of

Shorstein and Gardner.¹ Their model's assumption of the human pseudophakic AC volume of 0.19 mL and 0.33 mL was derived from Kanellopoulos and Asimellis,³ whose Scheimpflug imaging measurements were taken 3 months after cataract surgery. This is long after postsurgical equilibration (ie, fibrosis and closure of the capsular bag) has taken place.³ Our calculation of 0.5 mL volume of the AC and a just-evacuated capsular bag after phacoemulsification was derived by summing the preoperative anterior and posterior chamber volumes with that of the mean preoperative capsular bag.²

As a result of smaller AC volume estimates, Shorstein and Gardner¹ arrived at a half-life elimination of moxifloxacin from the AC of 1.2 hours. This differs from our calculation⁴ of 2.89 hours, as illustrated in Figure 1, which is consistent with the literature.^{5,6} At our calculated abatement rate, the IC moxifloxacin does not dilute to below the bactericidal level of minimum inhibitory concentration greater than 64 µg/mL (the minimum inhibitory concentration of 90% of strains tested of the most moxifloxacin-resistant endophthalmitis pathogens, published in the ARMOR [Antibiotic Resistance Monitoring in Ocular Microorganisms] study) until 7.4 hours (with efficacy to 10.4 hours due to the postantibiotic effect of fluoroquinolones) after injection. This compares favorably with Shorstein and Gardner's¹ estimation of 5.4 hours for moxifloxacin levels to fall to the same level.

Practical and ethical limitations preclude frequent postoperative AC sampling of antibiotic levels in humans. Improved understanding of moxifloxacin's complex pharmacokinetics as clinical and bacteriological data accumulate will help us refine mathematical models representing IC abatement profiles. We arrived at greater immediate postphacoemulsification AC volume and IC moxifloxacin half-life than Shorstein and Gardner.¹

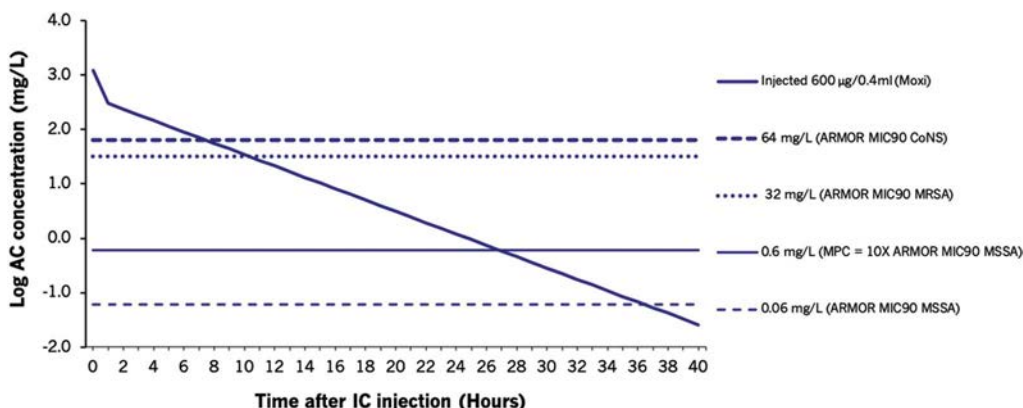


Figure 1. Abatement rate of intracameral moxifloxacin 600 µg in 0.4 mL against the background of the MIC₉₀s for the indicated strains from the ARMOR study. The calculated abatement of the concentration of moxifloxacin in the AC shows that the AC level will not fall below the ARMOR-reported MIC₉₀ of MSSA, the most frequent pathogen, for almost 37 hours, or below its mutant prevention concentration for 27 hours. Even for

the most resistant strains ever reported, ARMOR CoNS MIC₉₀ = 64 and ARMOR MRSA MIC₉₀ = 32 mg/L, the level of moxifloxacin exceeds those MICs for 7.4 and 10.4 hours, respectively (AC = anterior chamber; ARMOR = Antibiotic Resistance Monitoring in Ocular Microorganisms; CoNS = coagulase-negative *Staphylococcus*; MIC = minimum inhibitory concentration; MIC₉₀ = minimum inhibitory concentration of 90% of strains tested; MPC = mutant prevention concentration = 10× MIC for dose-dependent fluoroquinolones; MRSA = methicillin-resistant *Staphylococcus aureus*; MSSA = methicillin-sensitive *Staphylococcus aureus*).

However, we agree that larger volume IC injection with similar total dose is a more precise and reliable method to achieve consistent antibiotic delivery.

Steve A. Arshinoff, MD, FRCSC
Ontario, Canada

Milad Modabber, MD, MSc, FRCSC
Sacramento, California, USA

REFERENCES

1. Shorstein NH, Gardner S. Injection volume and intracameral moxifloxacin dose. *J Cataract Refract Surg* 2019;45:1498–1502
2. Arshinoff SA, Modabber M. Dose and administration of intracameral moxifloxacin for prophylaxis of postoperative endophthalmitis. *J Cataract Refract Surg* 2016;42:1730–1741
3. Kanellopoulos AJ, Asimellis G. Clear-cornea cataract surgery: pupil size and shape changes, along with anterior chamber volume and depth changes. A Scheimpflug imaging study. *Clin Ophthalmol* 2014;8:2141–2150
4. Arshinoff SA, Felfeli T, Modabber M. The aqueous level abatement profiles of intracameral antibiotics: a comparative mathematical model of moxifloxacin, cefuroxime and vancomycin with determination of relative efficacies. *J Cataract Refract Surg* 2019;45:1568–1574
5. Asena L, Akova YA, Gokta MT, Bozkurt A, Yaşar U, Karabay G, Demiralay E. Ocular pharmacokinetics, safety and efficacy of intracameral moxifloxacin 0.5% solution in a rabbit model. *Curr Eye Res* 2013;38:472–479
6. Libre PE, Mathews S. Eye diseases and conditions—endophthalmitis; researchers from Norwalk hospital describe findings in endophthalmitis (endophthalmitis prophylaxis by intracameral antibiotics: in vitro model comparing vancomycin, cefuroxime and moxifloxacin). *Health Med Week* 2017;43:1441

Disclosures: None of the authors has a financial or proprietary interest in any material or method mentioned.

Reply: Arshinoff and Modabber⁵ call into question two assumptions of our mathematical model describing the residence times of moxifloxacin in the anterior segment with two different intracameral injection strategies.¹ The authors of the letter agree with us on the underlying principle of our publication but disagree on the volume of the anterior chamber (AC) and the half-life of antibiotics.

We selected two representative mean pseudophakic AC volumes (0.19 mL and 0.33 mL), substantiated by the literature,^{2,3} to demonstrate the principle that injecting the same dose of antibiotics (eg, 500 µg) into ACs with varying volumes produces varying concentrations of antibiotics within the total aqueous humor volume. The larger volume of 0.33 mL of Matsuura was derived from aqueous humor sampling immediately after intracameral injection in humans, before any possible fibrosis of the capsule. Libre and Mathews⁴ also agree with this volume. Arshinoff and Modabber's⁵ estimation of 0.5 mL is based on a mean phakic AC volume in the human eye of 0.25 mL; however, measurements of the AC volume in the elderly phakic eye average only 0.15 mL.^{6,7} With this experimentally derived volume, Arshinoff's estimation of the mean pseudophakic aqueous volume would be 0.4 mL, close to Matsuura and Libre's reported value of 0.33 mL.

The AC size is known to vary from patient to patient, which cataract surgeons recognize when operating on smaller eyes and myopic eyes with longer axial lengths and

larger chambers. Therefore, attempting to replace the aqueous contents with an antibiotic solution of known concentration will achieve the more consistent final concentration of drug, irrespective of the patient's pseudophakic AC volume. This same principle would have been demonstrated had we chosen two different AC volumes.

There is a wide variation in the reported half-life elimination of antibiotics in the AC. Generally speaking, interdrug variation in elimination times, especially in the eye, may be due to factors such as differences in the drug molecular size, tissue binding, active pump mechanisms, and obstructions or reductions to outflow and drug elimination. Asena obtained antibiotic half-lives between 1.2 hours and 13 hours in rabbits, depending on which time points were used⁸; Lipnitzki et al.⁹ found between 0.64 hours and 1.8 hours in rabbits. Matsuura et al.^{3,10} demonstrated a half-life in rabbits and humans that averaged 1.2 hours over most time points. We chose 1.2 hours as it agrees with the 1% per minute aqueous turnover rate noted by Goel et al.¹¹ The varied measures of the intradug half-life elimination time of moxifloxacin and other antibiotics in the AC may be due to imprecision in injection and sampling techniques, pharmacokinetics that are not single compartment, and variations in individual subject anatomy and physiology. We would caution against the speculation of postantibiotic effects in regard to half-life because efficacy should be related to the target microorganism.¹² Furthermore, principles that apply to the multidose administration of antibiotics in the treatment of systemic infections should not be presumptively applied to the scenario of single-dose intraocular injection without empirical evidence.

Our study used two different and substantiated aqueous volumes and demonstrated that injecting small volumes of an agent can result in unequal final drug concentrations in the AC. Given the patient-to-patient variations, the “flushing” or large-volume injection technique should offer some degree of standardization and assurance of a more uniform final drug concentration in the pseudophakic AC as compared with smaller-volume-injected aliquots, thereby minimizing the interpatient variable of AC volume differences during cataract surgery.—*Neal H. Shorstein, MD,*
Susanne Gardner, D Pharm

REFERENCES

1. Shorstein NH, Gardner S. Injection volume and intracameral moxifloxacin dose. *J Cataract Refract Surg* 2019;45:1498–1502
2. Kanellopoulos AJ, Asimellis G. Clear-cornea cataract surgery: pupil size and shape changes, along with anterior chamber volume and depth changes. A Scheimpflug imaging study. *Clin Ophthalmol* 2014;8:2141–2150
3. Matsuura K, Suto C, Akura J, Inoue Y. Comparison between intracameral moxifloxacin administration methods by assessing intraocular concentrations and drug kinetics. *Graefes Arch Clin Exp Ophthalmol* 2013;251:1955–1959
4. Libre PE, Mathews S. Endophthalmitis prophylaxis by intracameral antibiotics: in vitro model comparing vancomycin, cefuroxime, and moxifloxacin. *J Cataract Refract Surg* 2017;43:833–838

5. Arshinoff SA, Modabber M. Dose and administration of intracameral moxifloxacin for prophylaxis of postoperative endophthalmitis. *J Cataract Refract Surg* 2016;42:1730–1741
6. Fontana ST, Brubaker RF. Volume and depth of the anterior chamber in the normal aging human eye. *Arch Ophthalmol* 1980;98:1803–1808
7. He W, Zhu X, Wolff D, Zhao Z, Sun X, Lu Y. Evaluation of anterior chamber volume in cataract patients with swept-source optical coherence tomography. *J Ophthalmol* 2016;2016:8656301
8. Asena L, Akova YA, Goktaş MT, Bozkurt A, Yaşar Ü, Karabay G, Demiralay E. Ocular pharmacokinetics, safety and efficacy of intracameral moxifloxacin 0.5% solution in a rabbit model. *Curr Eye Res* 2013;38:472–479
9. Lipnitski I, Ben Eliahu S, Marcovitz AL, Ezov N, Kleinmann G. Intraocular concentration of moxifloxacin after intracameral injection combined with presoaked intraocular lenses. *J Cataract Refract Surg* 2014;40:639–643
10. Matsuura K. Pharmacokinetics of subconjunctival injection of moxifloxacin in humans. *Graefes Arch Clin Exp Ophthalmol* 2013;251:1019–1020
11. Goel M, Picciani RG, Lee RK, Bhattacharya SK. Aqueous humor dynamics: a review. *Open Ophthalmol J* 2010;4:52–59
12. Boswell FJ, Andrews JM, Wise R. Pharmacodynamic properties of BAY 12-8039 on gram-positive and gram-negative organisms as demonstrated by studies of time-kill kinetics and postantibiotic effect. *Antimicrob Agents Chemother* 1997;41:1377–1379

Supported by a grant: R01 EY027329.

Endolenticular pressure gradient vs capsule grasping

We read the article by Kodavoor et al.¹ with some dismay. They describe a cannula-vacuum continuous curvilinear capsulorhexis technique that demonstrates one way a surgeon can hold onto a loose capsular flap. Their suggestion that it provides a safer mechanism for capsulorhexis belies the currently accepted understanding of the physical mechanisms of capsulorhexis extension or runoff, known as the Argentinian flag sign as described in Figueiredo et al.² The Argentinian flag sign results from rapid decompression of a capsular bag with a high endolenticular pressure. This pressure occurs when lens proteins denature and break down into smaller proteins, increasing the number of osmotically active particles in the bag. This osmotic gradient draws fluid into the bag, which is a semipermeable membrane, until the hydrostatic pressure within the bag balances the osmotic pressure. Kodavoor et al.¹ seemingly misconceive the pathophysiology as the surgeon inducing posterior mechanical pressure on the lens by misdirection of a capsulorhexis forceps. They describe first piercing the capsule with a cystotome, then a capsular extension may occur immediately, based on the degree to which the anterior chamber has been pressurized with the ophthalmic viscosurgical device (OVD), relative to the endolenticular pressure. We advocate piercing the central capsule with a 25-gauge needle first so that the surgeon can immediately decompress the liquid cortex from the capsular bag before switching to another instrument. The mechanism by which the capsule is held—vacuum or mechanical friction within the jaws of a forceps—is irrelevant. In fact, one might posit that if the vacuum device is activated but the capsular flap is not rapidly engaged into the port, the anterior chamber pressure could drop, increasing the risk of a meridional extension. Kodavoor et al.¹ further suggest that aspirating cortical fluid that leaks out of the capsular bag into the OVD

as an additional advantage of their technique; however, we discourage surgeons from aspiration from the anterior chamber before completing the capsulorhexis and depressurizing the capsular bag because, by doing so, the surgeon might inadvertently also aspirate some amount of the OVD and depressurize the anterior chamber. Instead, to improve visualization, the surgeon should clear the central area view by injecting more OVD and pushing the liquefied cortex to the periphery.

The authors do accurately state the importance of maintaining a pressurized anterior chamber throughout the procedure. Many reusable coaxial manual capsulorhexis forceps are now available that can similarly access the anterior chamber through a paracentesis, thus avoiding OVD leakage from a primary wound. The cost per use of such forceps is negligible.

The low 1.5% rate of capsulorhexis extension in Kodavoor et al.'s study may be attributable to pressurization of the anterior chamber before creating the cystotome entry and surgical dexterity, rather than the vacuum capsulorhexis.¹ The reader should not be deceived to think that the described device has any logical benefit on risk reduction in the intumescent lens. We would encourage readers to review the lessons of the landmark article by Figueiredo et al.², which the authors of vacuum capsulorhexis proudly cite, but sadly ignore.

Michael E. Snyder, MD
Kavitha R. Sivaraman, MD
Cincinnati, Ohio, USA
Gabriel B. Figueiredo, MD
Rio Preto, Brazil

REFERENCES

1. Kodavoor SK, Deb B, Ramamurthy D. Cannula-vacuum continuous curvilinear capsulorhexis: inexpensive technique for intumescent total cataract. *J Cataract Refract Surg* 2019;45:899–902
2. Figueiredo CG, Figueiredo J, Figueiredo GB. Brazilian technique for prevention of the Argentinian flag sign in white cataract. *J Cataract Refract Surg* 2012;38:1531–1536

Ketorolac used to control pain after photorefractive keratectomy

In their study on pain management after photorefractive keratectomy (PRK), Shetty et al.¹ found that a bandage silicone hydrogel contact lens soaked in preservative-free ketorolac 0.45% solution and used as a drug depot reduced pain after transepithelial PRK in patients who also received ketorolac 0.45% eyedrops 2 times on the day of surgery. Our first question is when were the 2 eyedrops applied?

In addition, in Table 1, the authors showed pain scores at the immediate postoperative period and 3 days postoperatively. However, the exact time used for determining the immediate postoperative period is not indicated. As Sobas et al.² have shown, patients report pain after PRK as soon as 30 minutes after the procedure, with the peak intensity being approximately 24 hours postoperatively. In their group of 32 patients who received a cold patch for 15 minutes, topical

cold dexamethasone, and oral alprazolam (and topical cyclopentolate and oral tramadol/paracetamol as rescue medications for unbearable pain), Sobas et al.² found great variability among patients in the intensity of pain experienced during the early postoperative period. However, there was a tendency for the pain level to increase during the first 9 hours postoperatively, reaching its peak at 24 hours and then being mostly stable until 36 hours, when it started to diminish until 96 hours postoperatively. Therefore, regarding the study by Shetty et al.,¹ it is critical to know how much time had elapsed at the time of the evaluation of the immediate pain score and also whether the evaluation was performed at the same time postoperatively in all cases. It would also be important to know the pain level 24 hours postoperatively.

Finally, the authors mentioned that topical moxifloxacin 0.5% eyedrops and lubricating eyedrops (sodium hyaluronate 0.1%) were administered. Did the patients receive topical corticosteroids or oral analgesics?

Virgilio Galvis, MD
Alejandro Tello, MD
Manuel Andrés Alfonso, MD
Néstor I. Carreño, MD
Ruben D. Berrospi, MD
Camilo A. Niño, MD
Floridablanca, Colombia

REFERENCES

1. Shetty R, Dalal R, Nair AP, Khamar P, D'Souza S, Vaishnav R. Pain management after photorefractive keratectomy. *J Cataract Refract Surg.* 2019;45:972–976
2. Sobas EM, Videla S, Vázquez A, Fernández I, Maldonado MJ, Pastor JC. Pain perception description after advanced surface ablation. *Clin Ophthalmol.* 2017;11:647–655

Disclosures: *Drs. van Rijn and Ilgenfritz received support from Ophtec b.v., Stichting Blindenhulp and through Uitzicht; ANVVB and LSBS. The funding organizations had no role in the design or conduct of this research. None of the other authors has a financial or proprietary interest in any material or method mentioned.*

40. Nagy ZZ, Takacs AI, Filkorn T, Kránitz K, Gyenes A, Juhász É, Sándor GL, Kovacs I, Juhász T, Slade S. Complications of femtosecond laser-assisted cataract surgery. *J Cataract Refract Surg* 2014;40:20–28
41. Dick HB, Schultz T. Laser-assisted cataract surgery in small pupils using mechanical dilation devices. *J Refract Surg* 2013;29:858–862
42. Schultz T, Joachim SC, Stellbogen M, Dick HB. Prostaglandin release during femtosecond laser-assisted cataract surgery: main inducer. *J Refract Surg* 2015;31:78–81
43. Birchall W, Spencer AF. Misalignment of flexible iris hook retractors for small pupil cataract surgery: effects on pupil circumference. *J Cataract Refract Surg* 2001;27:20–24
44. Jester JV, Petroll WM, Cavanagh HD. Corneal stromal wound healing in refractive surgery: the role of myofibroblasts. *Prog Retin Eye Res* 1999;18:311–356
45. Ernest P, Tipperman R, Eagle R, Kardasis C, Lavery K, Sensoli A, Rhem M. Is there a difference in incision healing based on location? *J Cataract Refract Surg* 1998;24:482–486
46. Gasset AR, Dohlman CH. The tensile strength of corneal wounds. *Arch Ophthalmol* 1968;79:595–602

Disclosures: Some of the authors have filed a patent application for the device described: “Expander for holding apart an opening in a tissue and method of operating the same” (US20180310929A1, EP3364852A4, WO2017069703A1, and SG11201802973PA).



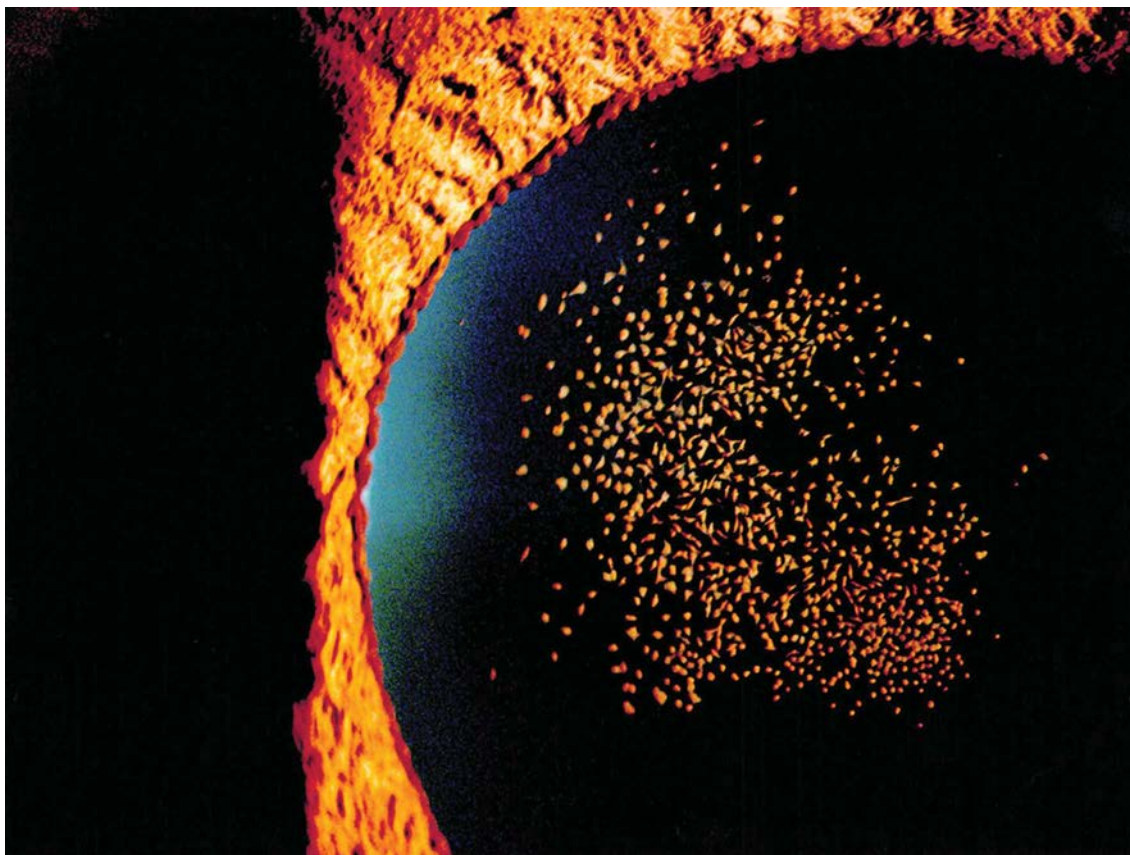
First author:

Royston K.Y. Tan, PhD

*Department of Biomedical Engineering,
Ophthalmic Engineering & Innovation
Laboratory, National University of
Singapore*

Ophthalmic Photographers’ Society Exhibit, May 2019

Category: Eye as Art–Best in Show



Sprinkle of Magic Moon Dust

The OPS annual exhibit, presented during the ASCRS • ASOA Annual Meeting, is sponsored by the ASCRS. Published with the permission of the photographer.

John Leo

*Tun Hussein Onn National Eye Hospital,
Selangor Darul Ehsan, Malaysia*